# An Investigation of Multibody System Modelling and Control Analysis Techniques for the Development of Advanced Suspension Systems in Passenger Cars

in Two Volumes

Volume 1

**by**

**Ann Susan Cherry**

*A thesis submitted for the degree of Doctor of Philosophy*

*Engineering Department*

*University of Warwick*

*Rover Group Advanced Technology Centre*

*December 1992*

*with much love and thanks to*

*Roger and Rosie*

It is good to have an end to journey towards;

but it is the journey that matters in the end.

Ursula K Leguin.

# Summary

The subject of this thesis is the investigation of multibody system modelling and control analysis techniques for the development of advanced suspension systems in passenger cars. A review of the application of automatic control to all areas of automotive vehicles illustrated the important factors in such developments, including motivating influences, constraints and methodologies used. A further review of specific applications for advanced suspension systems highlighted a major discrepancy between the significant claims of theoretical performance benefits and the scarcity of successful practical implementations. This discrepancy was the result of idealistic analytical studies producing unrealistic solutions with little regard for practical constraints. The predominant application of prototype testing methods in implementation studies also resulted in reduced potential performance improvements.

This work addressed this gap by the application of realistic modelling and control design techniques to practical realistic suspension systems. Multibody system modelling techniques were used to develop vehicle models incorporating realistic representations of the suspension system itself, with the ability to include models of the controllers, and facilitate control analysis tasks. These models were first used to address ride control for fully active suspension systems. Both state space techniques, including linear quadratic regulator and pole placement and frequency domain design methods were applied. For the multivariable frequency domain study, dyadic expansion techniques were used to decouple the system into single input single output systems representing each of the sprung mass modes. Both discretely and continuously variable damping systems were then addressed with a range of control strategies, including analytical solutions based on the active results and heuristic rule-based approaches. The controllers based on active solutions were reduced to satisfy realistic practical limitations of the achievable damping force. The heuristic techniques included standard rule-based controllers using Boolean logic for the discretely variable case, and fuzzy logic controllers for the continuously variable case.

# Acknowledgements

The author would like to acknowledge Rover Group for supporting this research. Special thanks go to Dr. R.P. Jones for his invaluable help and guidance as academic supervisor for the project.

Thanks are also due to the staff of the Engineering Department, University of Warwick, and Rover's Advanced Technology Centre.

Finally thanks go to friends and family for their love and support through all.

# Table of Contents

# List of Tables

# List of Figures

# Chapter 1 : Introduction

## 1.1 Automotive Vehicle Control

One of the most exciting developments in automotive vehicle design over recent years has been the increasing trend towards the application of automatic control to all areas of the vehicle. Today most passenger cars have some form of control system fitted, ranging from the small inexpensive vehicle with the simplest form of fuelling control, to top of the range luxury vehicles incorporating the full complement of control systems available covering every area of the vehicle. The most prolific users of electronic control systems in automotive vehicles are the Japanese manufacturers.

The most common application of electronic control systems in automotive vehicles is in engine management systems that regulate fuelling or ignition. Automatically controlled braking systems are also widely available especially on larger, more expensive vehicles. A few manufacturers are even fitting controlled suspension and steering systems to their luxury and sports models. A wide variety of ancillary functions also involve automatic control in modern passenger cars, such as heating and ventilation and security systems.

In order to discuss the use of automatic control in automotive vehicles, it is important to understand the overall driving forces and constraints of the automotive industry. The most important constraint shared by all commercial manufacturers is that all product development and change must be led by customer expectation and market influences. The first and most direct of these market influences is that of continually increasing customer requirements in terms of levels of vehicle performance and specification. Customer expectations

also come indirectly from other external influences, notably economic conditions, such as new road taxation, insurance, ownership and running costs including petrol and parking etc. These economic factors usually lead to increased customer requirements in terms of fuel efficiency and overall value for money. Other important market influences include automotive legislation, either direct legislation such as safety standards or emissions regulation, or indirect legislation as seen in product liability. New product liability legislation means that meeting legislative standards is not necessarily sufficient, especially in safety related functions of the vehicle. If higher levels of safety are met by other manufacturers or can be reasonably expected, then it is indirectly also a product liability requirement. All developments in automotive vehicle design, including the application of automatic control, will be in direct response to a change in one or more of these market requirements.

Once a vehicle change has been initiated by suitable market influences, the other automotive industry constraints have to be recognised. One of the most important constraints is that of cost, a significant factor of which is component cost. This obviously depends on the type of vehicle, but component costs are usually in the order of tens of pounds. This is in direct contrast with other control engineering fields such as process control or aircraft flight control systems, where very expensive sensors, processors and other electronic equipment are commonly used. Reliability including safety are also vital considerations since any failure will cause at best minor customer annoyance reducing the possibility of future sales, and at worst accidents causing injury, for safety critical failures in systems such as steering and braking. There are significantly different conditions surrounding the reliability and safety issues

for the automotive industry compared with other control engineering fields. All vehicle systems must be completely fail safe and idiot proof, due to the manufacturing methods widely used especially by large volume producers, and to the service requirements of the vehicles. The vehicles and subsystems have to assembled easily and quickly on partly automated production lines. Assembly process times are in the order of minutes for individual components and subassemblies. Once in the field, passenger cars may be serviced and maintained by a wide variety of skilled or unskilled people, ranging from highly trained and specialised garage mechanics, to the amateur enthusiast or completely unskilled owner. The vehicle is also driven by a wide range of virtually untrained and unpredictable drivers with little or no knowledge of the vehicle dynamics or its systems. Despite the variabilities between vehicles and conditions arising from these factors, every car must be completely safe and reliable.

From a control engineering point of view the automotive control application presents different problems compared to other more traditional areas of control engineering. The vehicle or plant is a complex non-linear system with fast time constants. For most automotive vehicle systems it is not sufficient to control the steady state behaviour, as control of the transients are essential, especially in safety critical areas such as suspension, steering and braking. The control objectives have a different emphasis for automotive applications since in most vehicle systems the basic uncontrolled plant is essentially stable. Moreover in most areas of the vehicle the conventional mechanical system to be replaced is very well developed and achieves good performance. Any application of a control system must offer significant benefits

with regard to customer requirements in order to justify the added complexity and cost. The objective of the automatic control in this case therefore is performance improvement, with any induced instability or even marked oscillation being intolerable.

The automotive design processes most commonly used within the industry also warrant consideration. Even today with the availability of a wide range of predictive analytical techniques, a large part of vehicle design is achieved by building prototypes and testing. This design process is costly and time consuming and with the increasing pressure to reduce the lead times for new models, these design methods must be improved. Recently this has been changing and analytical and predictive techniques have been introduced into the early design stages, leading to the reduced requirement for prototype testing. However there is still room for improvement.

This development led approach to vehicle system design was also widely adopted for the earliest implementations of automatic control in automotive vehicles. The early controlled vehicle systems were designed using heuristic methods, without the use of any theoretical control analysis techniques. In fact the majority of applications of automatic control found on passenger cars today were developed using these techniques. Again this is changing and most automotive research projects currently underway are utilising mathematical modelling of vehicle systems and control design and analysis techniques.

For the discussion of automotive applications of control engineering, the total vehicle system has been split into four main areas of concern:

- propulsion
- steering
- suspension
- ancillaries

The first three of these areas are concerned with the primary function of the vehicle. Propulsion is concerned with the longitudinal dynamics of the vehicle including engine, transmission, braking and acceleration, suspension is concerned with the vertical, pitch and roll dynamics, and steering involves the lateral and yaw dynamics. These three subsystems are interconnected at the tyre to form the complete vehicle system as shown in figure 1.1. The fourth vehicle function contains all the ancillary functions that are not primarily concerned with the basic function of the vehicle as a mode of transport, but with creating the desirable environment for travelling.

### 1.1.1 Propulsion Control

The first area to be discussed is propulsion control, concerned with the control of the longitudinal dynamics of the vehicle via the torque at the wheels. Therefore propulsion control will include control of the engine, transmission, braking and acceleration systems.

The recent interest in the automotive application of automatic control began in the USA in the early 1970's as a direct response to the oil crisis. This sudden increase in the cost of motoring created a demand for improved fuel economy. The automotive industry responded to this demand with the development of the first generation of microprocessor based engine control systems. The second major driver for the improvement of the propulsion system

was the introduction of emissions legislation firstly in California and subsequently throughout the USA and Europe. The problem of vehicle emissions was addressed in two ways, firstly by the second generation of engine control to further improve the efficiency of the engine and thus reduce the production of exhaust gases. The introduction of exhaust after treatment in the form of catalytic converters also addressed the emissions problem by preventing the offending gases from reaching the atmosphere once produced. The use of 3-way catalysts also provides a need for more accurate combustion control, as the required oxidant and reduction processes require tight regulation of the output gases.

The early engine management systems were designed using heuristic techniques based on empirical data from laboratory testing. They involved open loop static calibration maps for various engine parameters produced by steady state engine measurements taken during controller laboratory engine testing [4, 108, 109, 113]. The majority of engine management systems available on passenger cars today use this type of steady state engine map.

More recently studies have been published in which the control of transients is addressed and the application of modern model-based control techniques is discussed. A review of engine control and modelling techniques was presented by Sweet [108]. Athans [4] described the improvement of traditional static calibration maps by the use of multivariable control theory. The extension of engine control systems to include transient maps for the dynamic control of fuelling etc was also addressed. The importance of modelling was emphasised in order to utilised the full potential of modern control techniques. Toyoda et al [113] also illustrated the limitations of static

calibration maps and examined the application of advanced strategies to engine control. This included both steady state and transient control for fuel injection and ignition timing, with adaptive control for air/fuel ratio regulation. Sweet investigated idle speed control with the use of classical feedback and adaptive control techniques [109]. Hrovat & Powers [57] and Kiencke [46] also discussed the application of modern model-based control techniques to engine control, including modelling, parameter and state estimation and adaptive and robust control techniques [57].

Environmental legislation, however, is constantly being tightened until in California at least there will be zero emissions legislation for some inner city areas within the next few years. Unless there is some major technological breakthrough, any zero emission vehicle will be electrically powered. Since the zero emission legislation will probably only apply to inner city areas at first, the use of hybrid vehicles is a further possibility.

Electric vehicles are by no means a new concept, in fact during the first two decades of automotive developments electric propulsion was a serious opponent to internal combustion (IC) engines. Increasing performance requirements in terms of acceleration, top speed and range, together with improved product life led to the emergence of IC engines as the preferred propulsion method. The majority of automotive manufacturers have been renewing their interest in electric propulsion methods recently in order to meet the proposed legislation [12, 15, 58]. Hybrid vehicles are also attracting some interest, and this provides the control challenge of determining the propulsion source to be used under any set of conditions [108, 51].

The second area included under the heading of propulsion control is the

automatic control of transmissions. The motivator behind the early investigation into advanced transmissions and transmission control was also the fuel economy requirement created by the oil crisis. Electronically controlled transmissions can be used to improve not only fuel economy, but also performance and drivability by selecting the most suitable gear shift strategy. These transmissions can be divided into two types, discrete and continuous. Hrovat & Powers [46] described the control of a discrete transmission for both shift scheduling and execution, using closed loop control for shift execution. Continuously variable transmissions (CVT) have also been discussed by Christensen et al [20], and Ironside & Stubbs [47]. Both studies investigate the use of optimal fuel consumption maps for the control of CVT's. Ironside & Stubbs [47] describe the development of the CVT map plus subsequent evaluation by the use of a test rig. Christensen et al [20] in contrast utilise modelling techniques to evaluate the CVT performance. The use of modelling and analytical techniques for the design of a CVT controller has also been addressed by Jones et al [49, 50].

The third and final area contained within the heading of propulsion control is concerned with wheel control during acceleration and braking manoeuvres. As vehicles were designed to achieve greater performance in terms of acceleration and speed, the braking system also improved steadily, until almost optimal braking was achieved providing stable braking on uniform road surfaces assuming no excessive braking. However under excessive braking or poor road conditions wheel lock may occur, causing the vehicle to become unsteerable and even unstable, and increasing the braking distances achieved. Anti-slip braking systems (ABS) were developed in order to overcome this safety

issue [13, 61, 62]. These systems are designed to control the brake pressure to ensure maximum braking force without wheel locking. A related development was in anti-slip regulation (ASR), or traction control which is concerned with obtaining the maximum acceleration force without the wheel slipping. Most ABS and ASR systems involve rule-based controllers again developed using heuristic methods. The Bosch system as described by Leiber & Czinczel [61, 62] is typical and involves comparing the inputs of wheel deceleration and wheel slip against thresholds and switching the braking pressure accordingly. More recently the application of modelling and analytical control techniques to traction control has been addressed by Crossley et al [28], Crossley & Cook [29].

Further developments in all areas of propulsion control include the replacement of the mechanical and hydraulic actuation systems with electronic systems, for example throttle by wire, braking by wire etc., as in the aircraft industry. The major prohibitive factors currently are the conflicting safety and cost requirements. However all electric vehicles involve electric acceleration and braking actuation and with time these systems will appear on other vehicles.

### 1.1.2 Suspension Control

Over the past twenty years there has been large interest shown in the potential for electronically controlled suspension systems to significantly improve automotive vehicle ride and handling performance. Conventional suspension system performance is dependent upon a difficult compromise between the conflicting ride and handling requirements, largely determined by the choice of spring and damper characteristics. Throughout the life of this suspension system design the ride and handling performance achieved has been

continuously improving until this compromise became the limiting factor. Any further requirements for improvement would only be possible by adopting a new design concept. The application of electronic feedback control to a suspension system appeared to provide the ability to vary the suspension force characteristics as the road and driving conditions vary.

There have been a large number of investigations into advanced suspension systems and these will be discussed in detail later. They have been reviewed, however, by Goodall & Kortum [36], and Sharp & Crolla [98, 99]. The majority of these were theoretical studies using simple linear modelling techniques based on hand derived equations of motion. They have considered ideal active suspension systems and have designed controllers by the use of modern linear state space control techniques.

The two most notable practical implementations were the fully active suspension system developed by Lotus for their Formula One racing car in 1983 [81, 116], and more recently the active anti-roll system developed by Citroen [5]. For these two applications fully active systems are feasible since the cost constraints for a Formula One vehicle are completely different to those for a production vehicle, and the hydro-pneumatic suspension system of Citroens facilitates the implementation of an active systems without the need for major suspension system redesign.

The majority of other automotive manufacturers have shown interest in the simplest advanced suspension systems such as variable rate damping systems [39, 44, 45, 77, 89]. The controllers used for these systems were heuristic rule-based controllers, and traditional testing and vehicle development tuning methods were used to achieve the required levels of performance.

### 1.1.3 Steering Control

One of the more recent applications of automatic control has been in the area of steering, with the development of four wheel steering (4WS) systems, providing significant improvements in vehicle lateral dynamics as described by Nakaya & Oguchi [83]. The two major vehicle improvements achieved are high speed steering stability, and low speed manoeuvrability. These improvements provide a safety requirement for vehicles with increasing performance in terms of speed and acceleration, plus drivability especially for large passenger cars. As with many of the advanced vehicle systems using automatic control, Japanese manufacturers have shown the most interest.

The early 4WS systems used feedforward control to produce anti-phase rear wheel steering at low speeds for large steering inputs, and same-phase rear wheel steering for high speed and small steering inputs [94, 103, 110]. Takiguchi et al [110], Sano et al [94], and Shibahata et al [103] described the various techniques used to develop the feedforward strategy, mostly based empirically on test data.

More recent studies have shown the use of advanced control techniques for the control of 4WS systems. Braess & Thompson [13] described the use of multivariable classical techniques with decoupling to improve the conventional feedforward controllers. Nagai [82] considered the use of a combination of feedforward control to provide accurate steering angle control, and feedback control to reduce the sensitivity to external disturbances such as wind. In this study optimal state space control techniques were used to provide the feedback control. Yamamoto et al [117] again considered feedback control, but in this

case a practical system without the measurement difficulties associated with full state feedback was investigated by analysis of the system dynamics. Senger & Kortum [97] addressed the measurement difficulties of optimal feedback control by the use of various state space observers.

Again, as for propulsion control, a possible future development would by steering by wire systems in which the mechanical and hydraulic actuation systems are fully replaced by electronics. In fact one such study has been reported by Haynes et al [42] for an electronic steering system for disabled drivers. The controller described uses conventional proportional and integral (PI) controller.

### 1.1.4 Ancillaries

Apart from the main functionality of an automotive vehicle as a mode of transport, many other areas of the modern passenger car utilise electronic control of some form. Various ancillaries such as heating and ventilation [34], security systems, etc., require simple automatic control.

One ancillary area attracting significant interest from automotive manufacturers currently is traffic management. The external influence driving this research is the worldwide traffic congestion problem especially in and around city centres. One solution being considered is to develop intelligent highways and smart cars with the ability to communicate traffic and other information and allow the efficient control of traffic. This advanced traffic management concept was discussed by Rivard [91], and a specific example of a guidance system based on radio transmission was described by Becker et al [9]. The development of a communication infrastructure in automotive vehicles

would provide the means to the first step towards automatic pilots for passenger cars. The systems currently under investigation include collision avoidance, convoy driving, parking assistance etc, all of which improve safety and traffic efficiency on our roads.

The type of communication between vehicles and road systems under discussion require cross vehicle and indeed cross continent compatibility. As a result these areas of research have attracted large collaborative projects. In Europe, PROMETHEUS is a collaboration program involving all leading European owned car companies, over one hundred suppliers, and seventy research institutions and universities. The aim of the program is the gradual development of the automobile from an individually guided vehicle to one which operates as an integral part of a more efficient and safe traffic network [38].

### 1.1.5 Vehicle Control

The design and implementation of these control systems to date has been carried out in a piecemeal fashion. The obvious question that arises out of this vehicle development method is that of system interaction and therefore the need for integration. The ideal aim would be for the vehicle to have one central processor that controls all of the subsystems and thus the full range of vehicle dynamic behaviour with full consideration of the interactions between systems. Costa & Jones [22 - 25] have described the need for vehicle motion control and have discussed the modelling and control analysis environment required for this type of integrated control.

Theoretically there is no limit to these control applications in the field of automotive vehicle design and traffic infrastructure. In fact the trend is closely

following the aircraft industry towards fully automated passenger cars, as described by Rivard [91]. The entire vehicle may be automatically controlled incorporating full drive by wire systems and automatic pilots, with automatic communications to the road network and infrastructure providing traffic, guidance and weather information for the vehicle systems. With these possible automotive developments the use of extensive modelling and advanced control techniques would become essential.

## 1.2 Aims of Thesis

The area of automotive vehicle control addressed in this thesis is the control of advanced suspension systems for modern passenger cars. Despite a large amount of interest from both academic circles and the automotive industry for more than 20 years, there are still relatively few successful practical implementations on vehicles currently. Another aspect of advanced suspension systems control worth noting relates to the significant differences in approach adopted by academic and automotive industry research. Academic studies have tended to address the ideal active suspension control problem with simple linear models and modern control theory. In contrast practical investigations have used practically realistic suspension systems and heuristic control design techniques. The objective of this thesis is to bridge this gap by addressing practical advanced suspension control problems with analytical control techniques.

The major aim of this study was to investigate various analytical techniques with regard to their suitability for the design of a suspension system utilising automatic control. This involved the use of both vehicle modelling, and

control design and analysis techniques. The objective was not, however, to produce a purely academic study, but to show the applicability of modern analytical techniques to a practical design problem. Throughout this work emphasis was placed on realistic, validated models and practical control solutions. To support the modelling, real vehicle experiments were carried out to provide correlation data for model validation.

In order to use analytical techniques as far as possible in the suspension design process, some form of vehicle model had to be developed and used in place of the prototype vehicles traditionally involved in the development led design process. The vehicle model had to be sufficiently complex to realistically represent the vehicle behaviour under a variety of driving conditions, but also be simple enough to provide a usable tool for control system design and analysis. An essential feature for the models involved in the work was that they were fully validated against real vehicles for the range of operating conditions under consideration.

It was not anticipated that a single vehicle model would be developed for all control studies, but that a range of models would be developed with each being specifically tailored to a particular application, to ensure all possible simplification is achieved. The modelling therefore was to be in a modular form to allow models to be developed and extended quickly and easily.

Throughout the investigation described in this thesis, one important factor was that the techniques developed had to be suitable for future use within the automotive vehicle design process. Emphasis therefore had to be placed upon ease of use by automotive design engineers with relatively new experience in the field of control engineering. With regard to the control design,

practically feasible suspension systems within the usual automotive constraints described had to be considered. The design process had as far as possible to account for practical limitations of the system under investigation including actuator sensor and processor dynamics.

The aim of the work was to consider a range of different advanced suspension system types and thus a variety of different control system design techniques also required investigation.

## 1.3 Discussion of Content

As an introduction to the area of suspension control the thesis will begin with a discussion of the conventional suspension system, its function, and design. This will lead into the motivation behind the application of automatic control to automotive suspension design. A detailed discussion of the recent interest in electronically controlled suspension systems will follow, including practical implementations by the automotive industry as well as academic studies describing analytical modelling and design techniques. The work described in this thesis will then be motivated by the significant differences in these two approaches to the design of electronically controlled suspension systems. This will indicate the need for the gap to be bridged if any further progress is to be made in practical implementations of advanced suspension systems.

Vehicle modelling is not a new field by any means, however to date the suspension modelling involved in control studies has used simple linear models derived by hand. The motivation behind a more comprehensive approach to vehicle modelling for suspension system control studies will be discussed. In

order to illustrate the modelling approach and also to provide an initial look at the suspension control problem, a simple pilot study was undertaken. The simplest useful study involved the use of a validated quarter car model to address ride control for a fully active suspension system. For this study a range of linear control techniques were applied including both state space and frequency domain methods.

Once confidence had been gained in the modelling, a full vehicle model was developed and validated against test data. The active ride control study was then repeated using this full vehicle model, with the same range of linear control techniques. For the frequency domain study the multivariable full vehicle system was decoupled by the application of dyadic expansion techniques. This study provided further insight into automotive vehicle ride control, and also illustrated the uses for the two levels of model.

The second half of the work described in this thesis was concerned with the more practical advanced suspension system type, involving variable damping. Firstly the full vehicle model was extended to include the variable rate damper characteristics, some sensor dynamics and models of the discrete controllers designed. Both discretely and continuously variable damping systems were considered, and various controllers were designed for each system. Two design methods were used, the first used the ideal active system controllers designed previously and reduced these to suit the practical limitations of the actuators under consideration. The second involved direct control system design using heuristic techniques, rule-based control for the discretely variable case, and fuzzy logic for the continuously variable case. The results of all of the controllers designed were discussed and some interesting

conclusions drawn with regard to the modelling and control design techniques applied to suspension control.

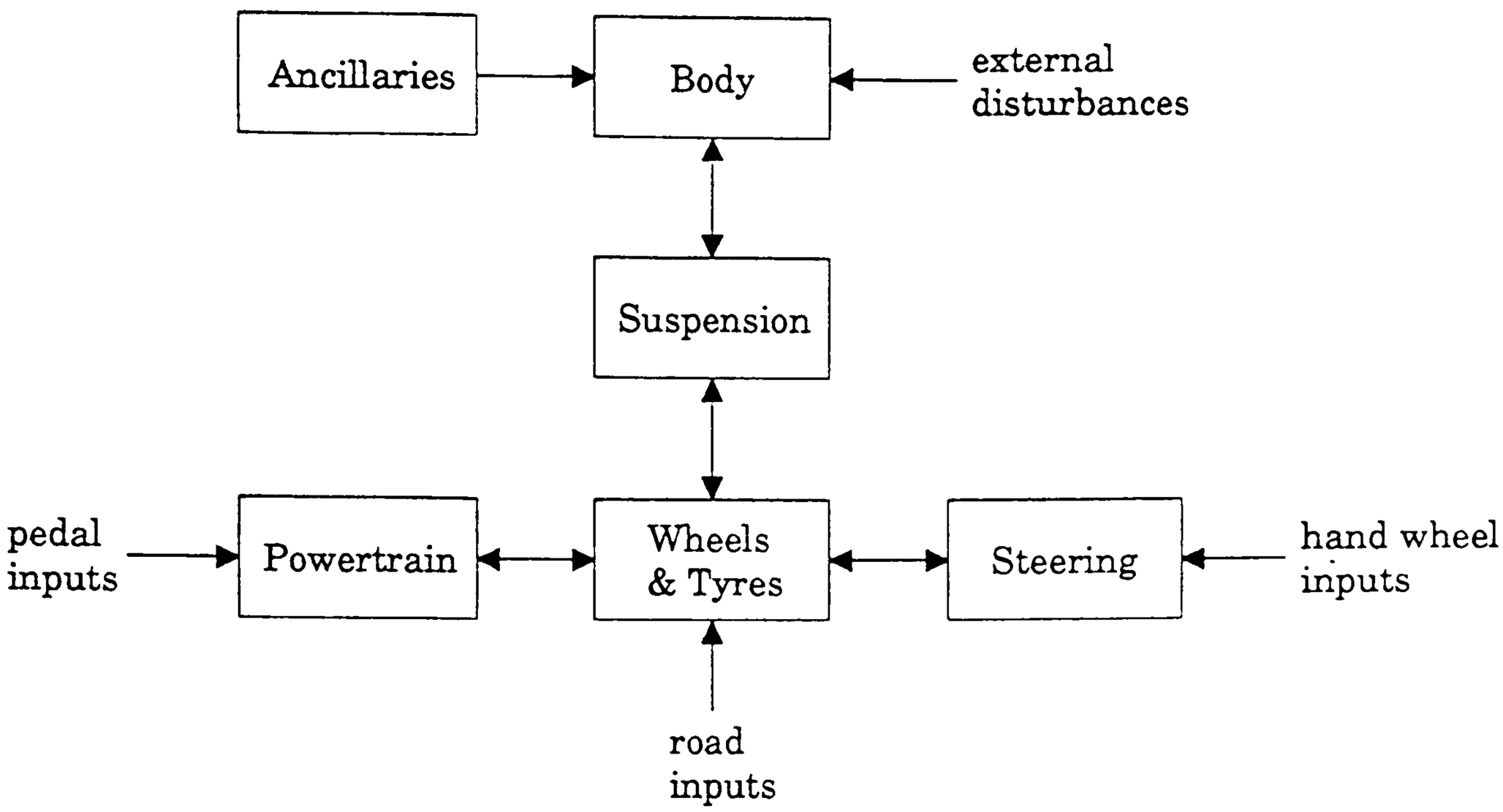


Figure 1.1 : Vehicle Systems Integration

# Chapter 2 : Suspension Control in Automotive Vehicles

## 2.1 Introduction

The application of automatic control to passenger car suspension systems is a very exciting new development. From the very first automotive vehicles the basic design principles of the suspension system really have not changed conceptually until very recent times. That is not to say that over the years there have not been dramatic improvements in automotive suspension performance. On the contrary, today's conventional vehicles have reached very high levels of rid and handling performance. However recently this process of continuous improvement has reached the performance limit of the design concept.

In order for suspension performance to improve further a radical change to this design concept is required, and the interest in the use of electronic control to provide that potential has grown as a result. At first glance the possibilities for performance improvement using automatic control appear limitless. However the real objective for any electronically controlled suspension system to meet is to provide significant vehicle performance improvements that will justify the additional cost and complexity of the system.

Before any consideration of advanced suspension systems can be motivated it is necessary to fully understand conventional suspension system designs and the reasons behind their performance limitations.

## 2.2 Automotive Suspension Systems

The primary function of an automotive vehicle suspension system is to

provide isolation of the sprung mass from disturbances induced by road or driver inputs to the vehicle via the wheels and tyres. The major concern is reducing passenger compartment vibration, although any load carrying area of the vehicle or equipment and components would also benefit from reduced disturbances. This isolation is usually referred to as ride quality, and is a measure of passenger comfort. More specifically the ride quality of a passenger car is concerned with vibrations transmitted to the sprung mass at frequencies between 0-25 Hz. Above 25 Hz, the vibrations are usually referred to as noise or harshness, and are predominantly related to body structural or powertrain modes and road noise.

The vehicle ride quality is usually split into two areas, known as primary and secondary ride. Primary ride is the low frequency, 0-5 Hz, vibrations of the sprung mass as a rigid body, including three modes of oscillation, heave, pitch and roll. Figure 2.1 shows the vehicle coordinate system as used within Rover and illustrates these modes of vibration. Heave or bounce is the translational motion of the sprung mass in the direction of the vehicle z-axis, and usually occurs at the lower end of the primary ride frequency range, around 1 Hz. Road inputs are the predominant excitation for the heave oscillations. The pitch mode involves a rotational motion about the y-axis of the vehicle, and is excited by road inputs and driver inputs such as braking and acceleration. Finally roll is a rotational motion about the vehicle x-axis, and again this mode can be excited by road inputs, although the predominant excitation is driver steering inputs. Both pitch and roll occur at a higher frequency than heave, around 2 Hz.

Secondary ride is also concerned with vibration of the sprung mass, but

as a flexible body in this case, and usually involves the frequency range 5-25 Hz. Secondary ride vibrations can be excited by a range of different inputs, notably the oscillations of the unsprung masses. Wheel hop is the vertical oscillatory motion of the unsprung masses between the road surface and the sprung mass. Parallel hop refers to a pair of wheels oscillating in phase and tramp refers to out of phase wheel hop. Brake hop and power hop are wheel hop oscillations induced by braking and acceleration of the vehicle. Since secondary ride is concerned with sprung mass vibrations, the transmission of these unsprung mass vibrations to the sprung mass is also an important consideration.

The frequency range 5-25 Hz can also include engine vibration on its mounts, steering systems modes, and axle oscillatory behaviour. At the lower end of this frequency range the mode in which the whole vehicle vibrates on the stiffness of the tyres with the suspension friction-locked also occurs. This mode is independent of the suspension design under consideration here and so will not be discussed further in this thesis.

The isolation objective of the suspension system, however, is subject to the general constraint that other areas of vehicle performance should not deteriorate significantly. The most important consideration here is vehicle stability or drivability, although other factors such as packaging constraints such as suspension travel are also important. Vehicle stability is primarily concerned with the control of the vehicle response to driver inputs such as steering, braking and acceleration. The response of the vehicle to steering inputs is described in terms of handling characteristics, and involves the lateral and yaw dynamic behaviour. Longitudinal stability is similarly concerned with

the vehicle response to acceleration and braking inputs. To a lesser extent vehicle stability is also concerned with the response of the vehicle to other external disturbances such as wind gusts etc. The essential requirements for vehicle stability is to maintain good tyre road contact under all driving and road conditions.

The suspension objective of sprung mass isolation without loss of vehicle stability as described has been achieved to date with a variety of suspension system design concepts [6]. Independent suspension is more popular for light vehicles including passenger cars, whereas for heavier trucks and off-road vehicles live axles are predominant. Combinations of the two usually involve independent front suspension with a rear axle. There are several standard design types including double wishbone, MacPherson strut, trailing arm, multi-link etc., with many modern suspension systems using hybrid designs.

All of these suspension systems have the same essential constituent parts, including some form of springing and damping elements. The major differences are in the suspension linkage layouts, and even here some basic design rules are generally adhered to. All of these constituent parts of the overall suspension system have some influence on the ride and handling performance of the vehicle.

The suspension geometry defines the relative motion of the sprung and unsprung masses and this affects both the ride and handling characteristics of the vehicle. The actual geometry of the suspension system influences the vehicle handling and stability most significantly, by defining the important suspension angles, such as king pin inclination, castor, camber and toe angles, together with the variation of these angles with the relative movement of the wheel and

vehicle body. The suspension linkage and mounting systems also play an important role in the secondary ride characteristics of the vehicle. They have little effect in controlling the unsprung mass oscillations, but define the method of transmission of the vibrations to the passenger compartment.

The function of the suspension springing systems is two fold, supporting the weight of the sprung mass and providing sprung mass isolation. In most passenger cars today, coil springs provide this function, whereas for heavier vehicles leaf springs are used. An alternative is to use hydro-pneumatic systems such as that fitted by Citroen, and the hydrogas units used on the Rover Metro. In these cases the pneumatics provide the springing element. In order to address the packaging constraint, restrictions to the allowable suspension travel in both directions are included in the form of a bump and rebound stop. The rebound stop is usually a simple rubber stop, whereas frequently a spring aid or small non-linear rubber spring is placed in series with the spring, providing a progressive spring rate and a bump restriction. Figure 2.2 shows a schematic diagram of the resultant suspension springing arrangement, producing a typical overall force displacement characteristic as shown in figure 2.3.

The final element of the suspension system is some form of damper to control the resonant vibrations of both the sprung and unsprung masses introduced by the compliance of the springs and tyres. Automotive suspensions use viscous dampers in parallel with the suspension spring either as separate shock absorbers or MacPherson struts, or as part of a combined spring and damper system as in the case of hydro-pneumatic suspensions. The damper rates are inherently non-linear and in most applications the rates are different in bump and rebound.

Consequently the design of the suspension system is a difficult compromise between the conflicting requirements of ride quality and vehicle stability, including good handling behaviour. The spring rate choice balances the need for good isolation, requiring a soft rate, with vehicle sprung mass support for the full range of laden conditions and vehicle stability, requiring a firm rate. Similarly the damper rate should be soft for sprung mass isolation and firm for resonant oscillation control and vehicle stability. The bias of the resultant compromise will depend upon the type of vehicle under consideration and its potential customer and market requirements. The design of the suspension system characteristics around this compromise has been reported in several studies [10, 88, 111].

## 2.3 Potential for Control

Throughout the life of these conventional suspension systems, automotive vehicle designers have constantly improved the overall ride and handling performance by fine tuning of this design compromise. Recently the performance limits of the design dictated by this compromise have been rapidly approached, until any future improvement would necessitate a conceptual change in suspension system design. However customer expectations of vehicle performance in terms of ride and handling are always increasing, and so a method of reducing the inherent ride and handling compromise was required.

The obvious way around the design compromise was to design a suspension system in which the performance characteristics could vary depending upon the current driving conditions. The application of automatic control to the suspension system would facilitate this achievement.

Over recent years there have been major advances in electronic technology, including microprocessors and sensors, both in terms of capability, size and cost. Similar technology had been utilised within the automotive industry in the development of advanced powertrain design throughout the 1970's and 1980's. Alongside these developments suspension component design had also advanced, leading to the availability and reduction in cost of variable rate springs and dampers and other suitable actuators. As a result the concept of electronically controlled suspension systems became a feasible development of conventional suspension systems. This ability to regulate the ride and handling characteristics of a vehicle in real time depending on the road and driving conditions offers the potential for improving or even removing the need for the inherent suspension design compromise. The result would be significant potential improvement in vehicle ride and handling performance.

There is a wide range of possible types of advanced suspension system involving different levels of control. Most of these have been considered to some extent either in academic studies, on prototypes, and more recently on production vehicles, with varying levels of success. Before discussing the development of suspension control it is important to clarify the terminology to be used with regard to the different types of system.

Conventional systems using springs and dampers with a single fixed rate as described earlier are referred to as passive systems, and provide the base for comparison purposes. The simplest utilisation of control is seen in self-levelling suspensions in which vehicle ride height is maintained in response to variations in vehicle static loading. These systems involve the input of external power to the system, but are very slow with time constants in the order of seconds.

Semi-active systems have the ability to dissipate energy only, but provide variability in the rate of dissipation. Typically this involves the use of variable rate springs and/or dampers in place of the passive components. The rate variation of these actuators can either be discrete, allowing two or three fixed rate settings, or continuously variable between a maximum and minimum allowable rate. Figure 2.4 illustrates the possible arrangements for semi-active suspension systems. Adaptive systems refer to semi-active systems with relatively slow characteristic variation.

Finally active systems use actuators with the ability to input external power to and dissipate energy from the suspension system. The active actuator can either replace or supplement the passive spring and/or damper, depending upon the actuator and system under consideration. If the actuator locks solid when no force is demanded, it would be placed in series with a passive spring, whereas if it has compliance for zero demanded force a passive spring in parallel would support the vehicle weight. This arrangement also reduces the power requirement form the actuator. Figure 2.5 illustrates the possible arrangements. Slow-active systems are essentially active systems with a low bandwidth allowing control of the sprung mass modes only. Active anti-roll systems are a specialised form of active control providing sprung mass roll control only.

## 2.4 Review of Suspension Control

Since the early 1970's there has been widespread interest in the application of automatic control to automotive suspension systems as described in several reviews [36, 98, 99]. Large numbers of theoretical studies have been

reported claiming significant potential improvements in vehicle ride performance [2, 7, 8, 16, 26, 31, 33, 35, 40, 55, 59, 64, 66, 69, 70, 71, 73, 79, 90, 100, 101, 102, 115].

Analytical techniques have been applied to the control design for these systems, including simple vehicle modelling together with linear control techniques. The majority of the authors of these theoretical studies have used quarter car models representing one corner of a vehicle for both the control design and resultant ride performance evaluation. These models varied from a single degree of freedom model concerned with the sprung mass heave dynamics only [55, 69, 70, 71, 72, 80, 105]. Models incorporating the sprung and unsprung mass heave degrees of freedom are the most common [11, 17, 26, 31, 40, 43, 54, 59, 73, 101, 102, 115], and some authors extended to three degrees of freedom, by including the seat dynamics [44]. This allows control of the heave dynamics of the vehicle only and on application to a full vehicle takes no account of the coupling between modes. Some authors have subsequently extended their quarter car models to include pitch first [33, 69, 79, 90], shortly followed by roll [2, 7, 8, 16, 35, 64, 66, 100]. Malek & Hedrick [66] considered the coupling between modes directly and designed controllers to decouple the modes and provide improved ride performance. Fruhauf et al [35] included Pade approximations to the time delays between front and rear wheels in order to accurately model the dependence between road inputs to the tyres. The majority of these simple linear vehicle  models were hand derived from first principles, although Karnopp and Margolis describe the use of bond graph techniques [54, 55, 69, 71].

The most popular starting point for these investigations has been a

study of ideal active systems in which an ideal force generator is used to represent the active actuator. This is a fictional device that is assumed to have the ability to generate a force with any magnitude and direction instantaneously. This theoretically ideal system provides the least restrictions and thus allows the best possible performance improvements to be illustrated.

The majority of theoretical active suspension studies have adopted one of two control strategies. The first to consider here is the concept of the skyhook damper introduced by Crosby & Karnopp [27] in the early 1970's. In this system the passive suspension is replaced with a passive spring in parallel with an ideal force generator. The skyhook damping concept uses an active control law that represents a fictional inertial damper as illustrated in figure 2.6. The actuator is controlled to generate a force proportional to the absolute sprung mass velocity with the opposite sign. Many authors have subsequently used this control strategy and the results for vehicle heave dynamics have shown that inertial damping provides very good sprung mass isolation, with only limited unsprung mass control [69 - 72].

The second and most popular active suspension control design technique considered has been linear optimal control producing state variable feedback. In these studies authors who have considered active suspension only have replaced the passive spring and damper with an ideal force generator otherwise they have tended to use a passive spring in parallel with the force generator. In this way an easy and comparable transition from active to semi-active is achieved. However since the state variable feedback solution will involve terms proportional to sprung and unsprung mass displacements and velocities, a variety of implementations may result from the same solution.

The linear optimal control design technique involves the minimisation of a performance index equating to the overall suspension system's objectives. This usually takes the form of a weighted sum of sprung mass acceleration and tyre load variation, although in some studies the performance index has included a measure of suspension travel requirements. The best results are obtained when full state feedback is used, but this involves the road profile as part of the state. Some studies have considered road preview to be a feasible development [33, 59, 87], although the majority of authors consider road profile measurement to be a luxury that is far from practical. In response to this state availability problem many studies have considered the use of limited state feedback control and estimation techniques [2, 35, 115]. Foag [33] describes a different approach to active feedback design and feed-forward preview by the use of conventional control design techniques together with parameter optimisation. Pilbeam & Sharp [87] used road preview for feedforward control of the rear suspension from information measured at the front.

The resultant optimal state variable feedback controllers produce significant ride performance benefits. The sprung mass isolation is greatly superior to passive systems, but marginally worse than systems using the skyhook damper. However state variable feedback leads to improved unsprung mass control, since this is addressed directly in the control design performance index. More recently Gordon & Marsh [37] have discussed the use of non-linear state variable feedback control strategies for active suspension systems. This applies the usual quadratic regulator theory, with higher order terms in the performance index, again with significant performance benefits claimed. Truscott & Wellstead [114] and Lizell [64] extended the usual techniques to

include adaptation to allow the controller to adjust for variations in driving conditions.

Active suspension systems however have been shown to present several limitations both practical and theoretical. Karnopp [54] first described the theoretical limitations inherent in active suspension systems, by illustrating that even with full state variable feedback control there will still be a design compromise. Hedrick & Butsuen [43] and Lee & Hedrick [60] described this limitation in terms of invariant points in the sprung mass acceleration and suspension rattle space transfer functions.

The major practical limitation of fully active systems is the large power requirement and Crolla & Nour [26] included a power measure in the performance criterion for a study comparing various active systems. Cech [16] has partially addressed the problem by using a slow-active system with a passive spring and damper in series with the active actuator and second passive spring in parallel, as shown in figure 2.7. The control uses slow actuation and addresses sprung mass control only to reduce the power consumption of the system. Lizell [64] similarly reduces the power requirements by the use of a slow-active suspension system to control the sprung mass modes.

Active anti-roll systems have attracted less interest in academic fields, although Sharp & Pan [100] have reported successful application of conventional control techniques to the problem of active roll control.

Despite the widespread interest in fully active suspension systems and the claims of significant performance benefits in their application to automotive vehicles, the implementations of such systems have been restricted to two manufacturers, Lotus and Citroen [5, 81, 116]. The main reasons for this

reticence are the cost and complexity of a system in which significant external power is required. For the majority of automotive manufacturers the implementation of a fully active system would involve the complete redesign of their conventional passive suspension system with large cost implications. Lotus and Citroen both provided specialised circumstances in which these considerations were overcome.

Probably the best known active suspension system on a vehicle today is the Lotus system [81, 116]. This was initially developed as a prototype on an Esprit, and subsequently fitted to a Formula One racing car. After further development the system has also been successfully introduced onto the production Esprit. The system utilises electro-hydraulic actuators at each wheel, specialised Moog servovalves, a variety of electronic sensors located on the sprung and unsprung parts of the vehicle, and on-board computer control. The control algorithm was developed in a subjective manner by the use of testing and tuning. The motivation for the development of this system was in the dramatic increase in aerodynamic down loads experienced by Formula One racing vehicles due to ground effect. In order to maintain the required performance characteristics of a racing car under these circumstances the suspension stiffnesses were extremely high. This led to very high mode frequencies and so an extremely harsh ride, and a significant increase in injuries. The solution was the development of an active ride system that enabled the suspension to achieve the required handling performance and still maintain a reasonable ride. For racing applications the cost constraints are radically different to a volume production vehicle, and even for the production vehicle application the cost issues are not insurmountable for a small volume

manufacturer of specialised vehicles.

The only other motor manufacturer to have considered active suspension is Citroen [5]. However their system, fitted to the XM, is not truly active as the Lotus system. Instead it is a development of the automatic height control of their hydro-pneumatic suspension system, incorporating computer control, together with slow active roll control. The usual prohibitive cost associated with active suspensions is reduced for Citroen since their suspension systems are already hydro-pneumatic. As a result a complete redesign is not required and in fact active systems can be incorporated relatively easily.

Consequently, although active suspension systems offered significant potential ride performance improvements, the power requirements and prohibitive cost and complexity led to the requirement for an alternative approach to advanced suspensions. The use of semi-active systems was seen as a more practically viable alternative and many theoretical studies addressed the question of relative ride performance of continuous semi-active compared with active systems. Again for these studies an ideal semi-active force generator was considered in which any dissipative force can be generated instantaneously. The most popular control strategies were based upon the equivalent active control law using skyhook damping or state variable feedback with the dissipation constraint imposed [69, 71, 102]. That is the semi-active force was simply set to equal the desired active force, and was set to zero if this required external power input to the system. This was achieved by a comparison of the sign of the relative velocity of the sprung and unsprung mass with the desired active force. This is illustrated in figure 2.8.

Several studies have undertaken a direct comparison of active and semi-

active systems against conventional passive systems [26, 69, 70, 101]. The ride performance results have shown that both systems offer large improvements over passive systems, but that active systems are not dramatically better that their semi-active counterpart. Margolis [69] extended this comparison to cover active and semi-active systems using both skyhook damping and state variable feedback control strategies.

Margolis & Goshtasbpour [72] modified their skyhook damping semi-active strategy to reduce the chatter of on/off systems by only switching when the relative velocity across the actuator changes sign. Karnopp & Margolis [55] suggested a different design method using the slow adaption of damper and spring rates to obtain the desired ride performance. A method of experimental simulation to obtain the optimum choice of rates was discussed.

A further simplification of controlled suspension systems has also been discussed in which the passive damper is replaced by a discretely variable damper providing two fixed rate settings, soft and firm, and the ability to switch between them. The most popular reported method of defining the control strategy is to refer again to the principle of inertial damping [17, 39, 63]. For a switchable damper the strategy is to chose the firm setting when the relative velocity across the damper has the same sign as the absolute sprung mass velocity, and to chose soft otherwise, as shown in figure 2.9. For switched damper systems several other strategies have been considered with varying levels of success.

Rajamani & Hedrick have described an alternative strategy similar to this simplification of skyhook damping, in which the damper rate giving a damping force closest to the desired skyhook damping force is chosen. This

control law achieved very similar results to the traditional skyhook strategy with marginally improved performance in the intermediate frequency range between the sprung and unsprung modes. A very simple adaptive strategy controlling a damper with three fixed rate settings by vehicle speed alone has also been described by Mastinu [73]. Charalambous et al [17] considered several switching strategies, including skyhook damping together with one based upon the minimisation of sprung mass acceleration and an empirical rule-based controller. The acceleration minimisation strategy switched the dampers according to the relative signs of the velocity and displacement across the damper as shown in figure 2.10. Frequency dependent strategies have also been considered by several authors [44, 63], whereby the range of frequencies of interest is split into four sections, including sprung mass modes, intermediate, unsprung mass modes and high frequency noise. The damper is switched to give the best rate for each frequency range. Lizell [63] combined this frequency dependent approach with skyhook damping for the sprung mass modes and an empirical strategy based on thresholds for the unsprung mass modes. The softest damper rate was chosen for the other two frequency ranges. Many practical implementations of discretely variable damping systems have also considered heuristic rule-based controllers [45]. However since these have tended to be commercially sensitive prototypes developed by automotive manufacturers, very little has been published.

The majority of these studies have been theoretical using the simple modelling techniques previously described with ideal actuators with no account for the practical limitations of such systems. Some authors have, however, partially addressed this problem. Margolis [70] considered the effect of

measurement dynamics on the performance improvements possible with active and semi-active systems. Doi et al [31] at Toyota and Rajamani & Hedrick [90] have included a first order lag to represent the damper switching dynamics in their vehicle models. Besinger [11], and Miller [80] carried out studies to determine damper characteristic requirements for discrete semi-active systems in terms of switching times, minimum and ratio of damper rates required and valve dynamics. However this is only a small step and there are more significant vehicle non-linearities and practical system limitations that will have large effects on ride performance that have yet to be addressed.

For automotive manufacturers, semi-active systems offered a significantly more attractive proposition than the previously described active systems. These systems allowed the simple replacement of passive springs and dampers from a conventional suspension system with variable rate elements. The addition of sensors and control systems then completed the system, and yet significant performance benefits were still claimed.

The restriction on the implementation of these systems has predominantly been the availability and cost of the components especially continuously variable rate dampers. As a result the interest has concentrated on the discrete semi-active system. Recently, however continuously variable rate dampers have become available, although the costs still present a hurdle, and the possibility of electro-rheological fluids for damper variability have also been considered [105].

The development of these discrete semi-active systems has been led by component manufacturers, mostly by damper suppliers, and the control of the overall system tailored to a specific vehicle manufacturer. Many suppliers and

manufacturer have been involved and have production vehicles fitted with simple systems, some of which have been compiled by Hennecker & Zeiglmeier [44]. The control strategies vary from heuristic rule based algorithms based on ride and handling expertise, to similar strategies described in academic literature based on the skyhook principles.

Armstrong [45, 89] have developed a system using dampers with two or three fixed rate settings and an empirical controller. The control strategy is split into different vehicle operational modes, ride, handling, acceleration, braking and levelling. Various measured vehicle responses are then compared to preset threshold values and the damper rate is switched accordingly. Hine & Pearce [77] described two specific applications for a General Motors Corvette and a Ford Granada. The semi-active control strategy reported by Lizell [39, 63] utilising a combination of empirical, skyhook damping and frequency dependent control as described earlier was developed by Monroe. Ford have successfully applied this system to a vehicle in the USA. Similarly BMW were involved in the frequency dependent semi-active system described by Hennecke & Zieglmeier [44]. Boge [77] have also reported a semi-active controller developed with BMW again using an empirical rule-based control algorithm. In this system the switching is based on measurements of sprung mass acceleration, brake pressure, steering angle, throttle angle, load and road speed. As before preset thresholds are used to determine the required damper rates. The system developed by Bosch [30] uses variable rate springs as well as dampers to provide greater ride control. In this case the control strategy is based upon the skyhook damping concept previously described. Cadillac produce a very simple adaptive system using a three stage damper. The control strategy chooses the

damper setting by vehicle speed alone, with the added capability for anti-lift and anti-dive.

Many other systems are available including a large number of Japanese manufacturers, all of which use the type of control algorithms already described.

The simplest form of suspension control is self-levelling, and has attracted widespread application by automotive industry, but very little academic interest. They are very simple systems providing a minimum of control, however real performance benefits are achieved at low cost. Citroen's hydro-pneumatic height control system provides the capability to adjust the ride height depending on the vehicle load conditions. Many other manufacturers also offer self-levelling by means of self-levelling struts or air springs.

## 2.5 Proposed Design Approach

From this discussion it can be seen that the application of automatic control systems to automotive suspensions have been approached from two very different standpoints. Large numbers of theoretical studies have been reported over the past twenty years claiming significant potential improvements in vehicle ride performance. These studies have used simplistic vehicle modelling techniques together with linear control techniques to address the ride control of ideal active and semi-active suspension systems. In contrast the response from automotive manufacturers and component suppliers has been much slower and, with two notable exceptions, has concentrated on the simplest systems. Discretely variable damping systems have attracted the most interest and the majority of the implementations of such systems have involved heuristic rule-

based controllers developed by traditional subjective testing and evaluation methods.

In order for any further developments to be made in the field of suspension control in terms of effective implementation, a design methodology must be developed that bridges the gap that exists between academic studies and practical implementations. The use of predictive techniques for any design process reduces both project cost and lead time by reducing the need for prototype parts and testing. Simulation results are repeatable and less susceptible to external disturbances that may invalidate results, again reducing design times and errors. However heuristic prototype testing methods offer the advantage of dealing with the complete system without approximations that may lead to errors.

The aim of the work described in this thesis is to bridge the gap between the two current design approaches and introduce realistic analytical techniques to practical suspension control investigations. The analytical techniques involved in this study fall into two parts, vehicle modelling and control design and analysis.

### 2.5.1 Modelling Techniques

The modelling involved in any form of suspension design process consists of three areas, realistic inputs, vehicle model and objective response evaluation. The choice for each part depends on the specific application under consideration. For the study of advanced suspension ride control the inputs will be road profile inputs as well as driver inputs such as acceleration, braking and steering inputs. The response evaluation will be measures of the sprung and

unsprung mass responses.

Road profile modelling can take two basic forms, stochastic frequency domain models or time histories of isolated road disturbances. The majority of the suspension control studies have used stochastic road profile models for use in the control design process and subsequent evaluation, as described by Hac [40] and Barak & Hrovat [7]. This essentially represents the road surface by its frequency content and allows the frequency response of the vehicle to be evaluated. In this way the effect of different road surface roughnesses on the vehicle ride can be evaluated.

However for automotive suspension design another very important road input affecting vehicle ride are isolated disturbances such as potholes, sleeping policemen and hump back bridges. In fact in terms of passenger comfort the response of the vehicle to these severe disturbances would be more important than the small amplitude vibrations caused by road surface roughness on the majority of roads. This is especially true of modern passenger cars whose basic ride characteristics are very good, such that significant improvements will only be possible in the severe disturbance response. Similarly the sprung mass pitch response to acceleration and braking manoeuvres, known as squat and dive, together with the roll response to steering inputs, are more significant ride performance characteristics than other small amplitude oscillations. These severe large amplitude disturbances cause some difficulty in that the vehicle non-linearities cannot be ignored for inputs of this type.

The method of objective evaluation of vehicle ride performance is obviously dependent upon the type of input under consideration. For stochastic road profile models it is common practice to use root mean square (rms)

measures of the sprung mass acceleration. The use of frequency dependent weightings allows the evaluation to account for human sensitivity to certain frequency ranges and modes of oscillation [48]. For isolated time domain inputs objective evaluation is less simple, but again would involve sprung mass accelerations together with displacements and orientations.

For both input modelling and performance evaluation a combination of methods could be used for any type of application. In this way the vehicle or system is examined for the full range of operating conditions, and a better overall result would be achieved. The vehicle modelling approach itself is very much more dependent upon the specific application under consideration.

Vehicle models are used for a wide range of tasks from fuel consumption studies, steering and suspension kinematics to passenger cabin acoustic investigation. As a result the model has to be application specific in order to keep it manageable. However it is also important not to over simplify and ignore important influences.

The majority of automotive modelling for suspension system studies to date has fallen into two categories. The first of these involves the use of simple linear models, as used for published suspension control studies described earlier. These models are usually hand derived from first principles, although bond graph modelling techniques have also been applied. They use lumped mass representations incorporating rigid bodies representing the sprung and unsprung masses, linear compliance and damping elements for the suspension and linear compliance for the tyres. The most commonly used vehicle model used in these suspension control studies was a quarter car model representing one corner of the vehicle. This method directly addresses the heave dynamics,

and by considering each corner separately, the other sprung mass modes are also indirectly addressed. However this does not allow for the coupling between modes which plays an important part in vehicle dynamic performance. Half and full vehicle models have also been developed and used for suspension control, allowing the control of heave pitch and roll sprung mass modes together with their interactions.

This simple modelling technique has been used with some success for various suspension control studies, however there are some serious limitations. The first is the inherent non-linearity of automotive suspension systems which is absent from this type of modelling. For stochastic ride investigations where small amplitude road inputs are considered this is not such a significant approximation. However for the consideration of large amplitude isolated road inputs together with steering and braking inputs, the linear representation is unacceptable. The second limitation is in the omission of the suspension system components. These provide a direct link between the sprung and unsprung masses and as a result the suspension spring and damper alone do not provide complete isolation. The suspension geometry provides a direct transmission path for the road inputs to the passenger compartment. A representation of the suspension system is also essential when simulating the vehicle response to driver inputs such as steering and braking, or the interactions between such vehicle modes.

In contrast, vehicle modelling techniques used in other areas of automotive suspension system design are significantly more complex and realistic. Multibody system (MBS) modelling techniques are widely used within the industry for all areas of vehicle chassis simulation. MBS vehicle models are

used throughout the complete design process including kinematics for suspension packaging, prediction of loads induced by the suspension system, and dynamic ride and handling predictions. These vehicle models are developed with large generic MBS modelling packages that involve numerical solution of computer generated code. Several such MBS packages are commercially available, including ADAMS, which is currently one of the most popular [84].

The types of vehicle models developed using ADAMS are comprehensive vehicle representations including the complete suspension and steering systems with all compliances including bushes. This results in a very accurate predictive tool for non-linear vehicle analysis, but would be too large and complex for control analysis studies.

Sohoni et al [104] have described the use of MBS modelling techniques for control design studies, however the model only involved the vertical unsprung mass motion, and the full motion of the sprung mass. As a result the use of MBS techniques provides no advantage over the hand derived models used elsewhere. MBS techniques were also applied to control system design models by Costa [22 - 25]. In contrast this study uses a model with realistic representation of the unsprung mass motion due to suspension geometry.

The modelling approach used for the work described in this thesis is aimed at the middle ground between these two methods, addressing the major limitations and drawbacks of both. The objective was to enable MBS representations to be included in vehicle models for control analysis investigations. The approach used had to facilitate the application of a variety of control design methods including linear control techniques and heuristic methods. The other important consideration to be made regards the ease of use,

as these techniques should be suitable for use within the conventional vehicle design process in industry.

A combination of SD/FAST, a MBS modelling package, and ACSL, a simulation language, was used to achieve the modelling requirement described. SD/FAST has several advantages over other MBS packages for all suspension modelling and specifically suspension control studies. Kane's formulation is used to generate the equations of motion, and symbolic manipulation subsequently simplifies the model, resulting in very efficient code [52, 53, 92]. The equations of motion together with various other utilities are generated in the form of subroutines, allowing flexibility in the choice of simulation environment. A limited range of simulation facilities is provided with the new version of the software, however for this application ACSL was chosen to provide a simulation environment better suited to control studies.

ACSL provides comprehensive simulation capabilities including continuous and discrete time [3]. This allows a discrete model of the controller to be included into a continuous model of the vehicle suspension system allowing accurate evaluation of control strategies. The linearisation facility together with the direct interactive link to MATLAB provides a comprehensive control design and analysis capability [3, 74 - 76].

Despite the widespread use of ADAMS within Rover, this was not a suitable choice for this study since at the beginning of the project the control capabilities were negligible. This has recently been partially addressed by a linearisation facility and a link to MATRIX-X, however a discrete modelling capability is still unavailable.

### 2.5.2 Control Design Techniques

As previously mentioned the control design discussed in the literature varies greatly between academic studies and practical implementations. The academic studies have heavily utilised analytical techniques with very few practical considerations. Ideal actuators have been assumed with the ability to generate any demanded force instantaneously. One or two reported studies have discussed practical issues with regard to variable damper requirements, however these have not been incorporated into the design or evaluation processes. Damper switching dynamics were included in vehicle models in a couple of studies by the use of first order lags. As a result despite claims of significant performance benefits, there must be questions over the realistically achievable results on a real implementation.

In contrast industrial implementations tend to rely heavily on empirical design methods using prototype testing and development. This ensures that the true non-linear plant is considered, although it does have serious drawbacks in terms of the costs and lead times involved with prototypes and the limits on achievable results. For advanced suspensions to be viable they have to offer significant performance improvements, and so these development techniques are seriously limited.

The control design methods described in this thesis will attempt to incorporate analytical techniques, without losing sight of practical constraints and vehicle experience available within industry. In this way the advantages of both approaches are utilised, analytical formality together with heuristic experience to produce realistic solutions.

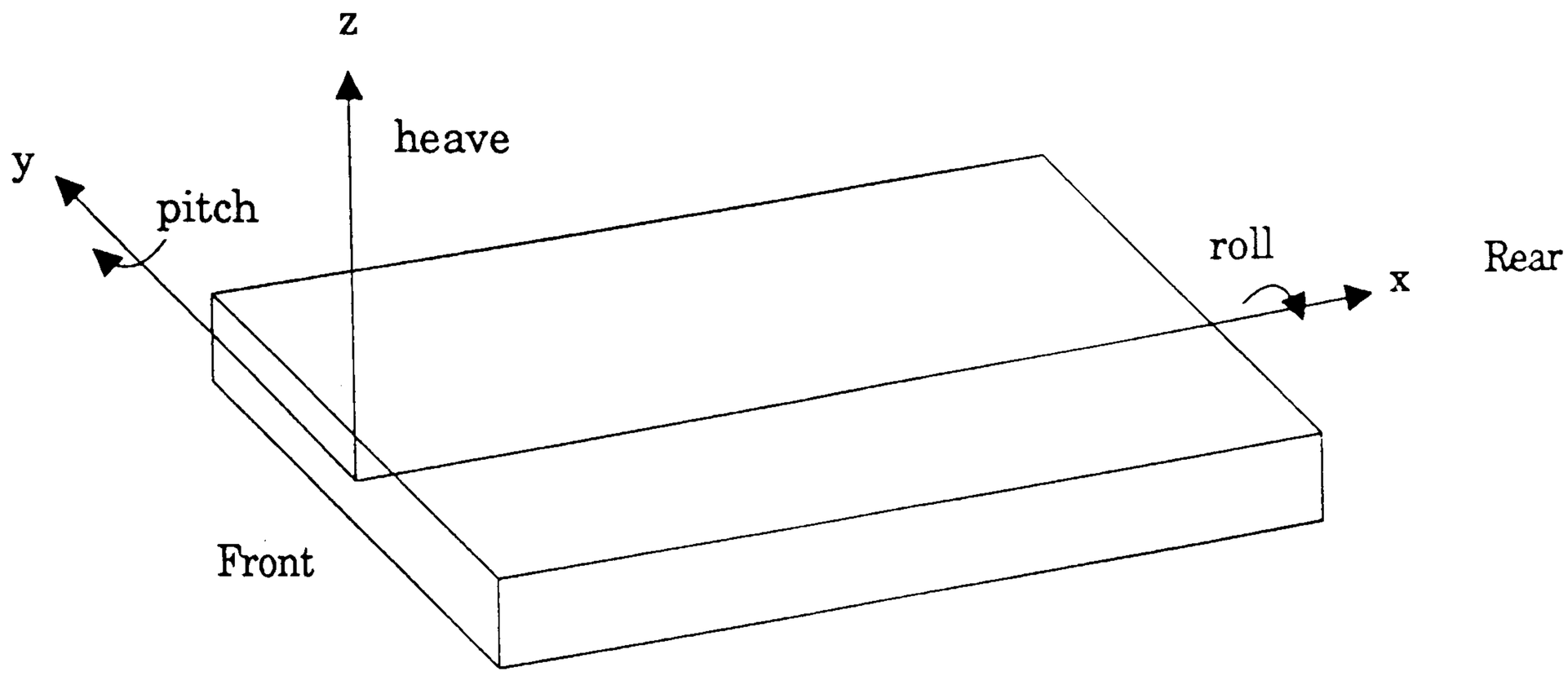


Figure 2.1 : Primary Ride Modes and Vehicle Coordinate System

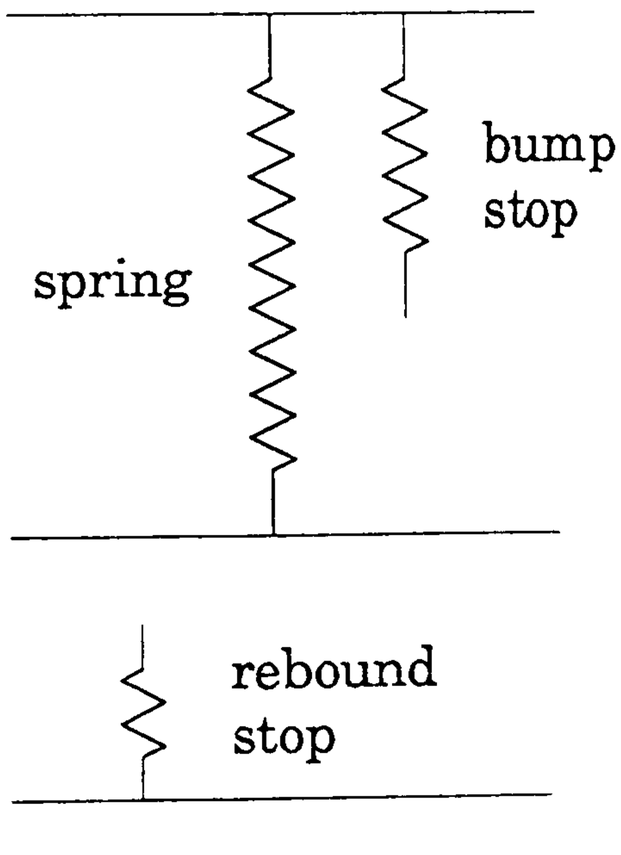


Figure 2.2 : Suspension Compliance

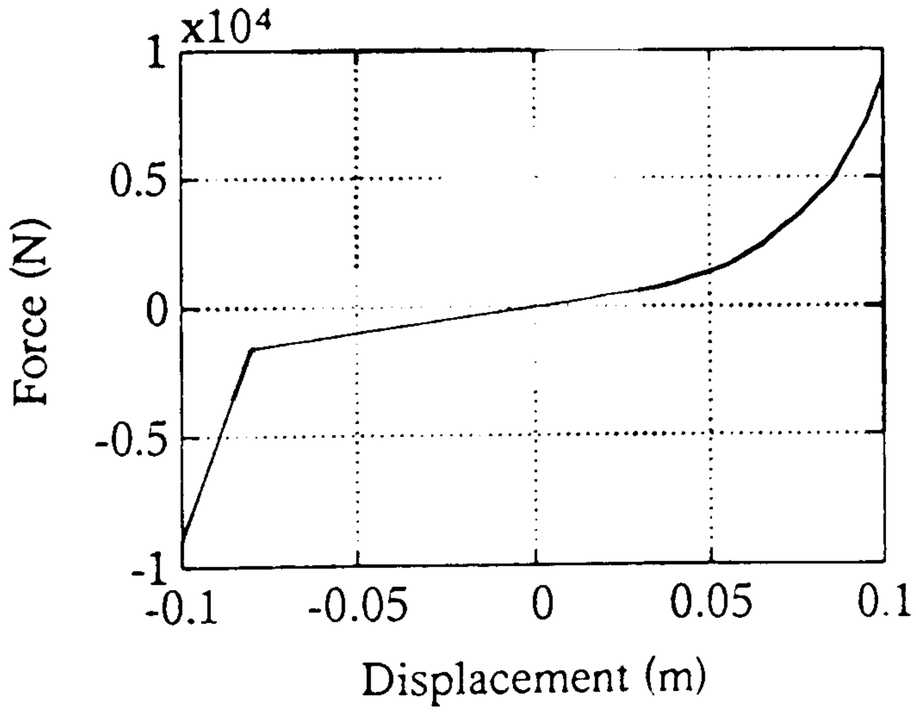


Figure 2.3 : Typical Force Characteristic

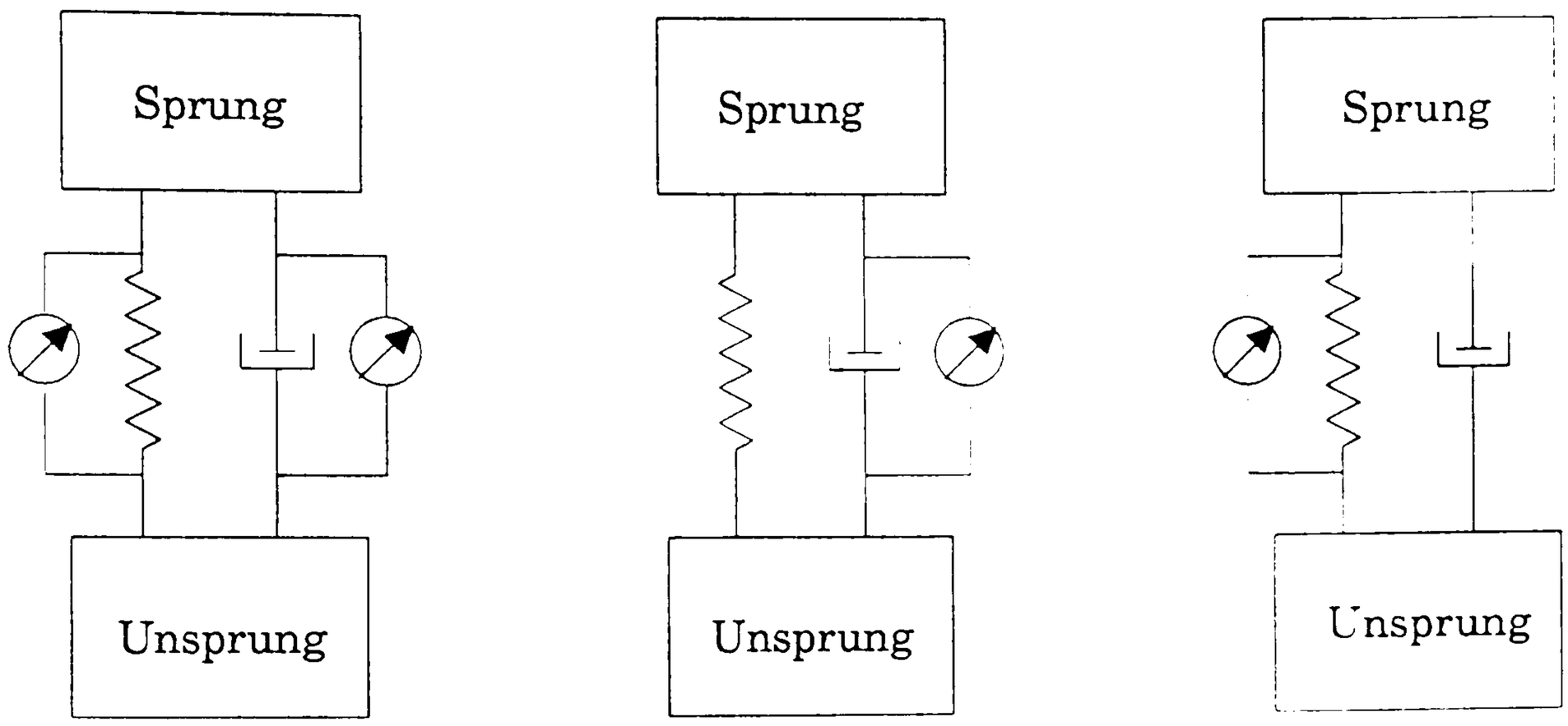


Figure 2.4 : Semi-Active Arrangements

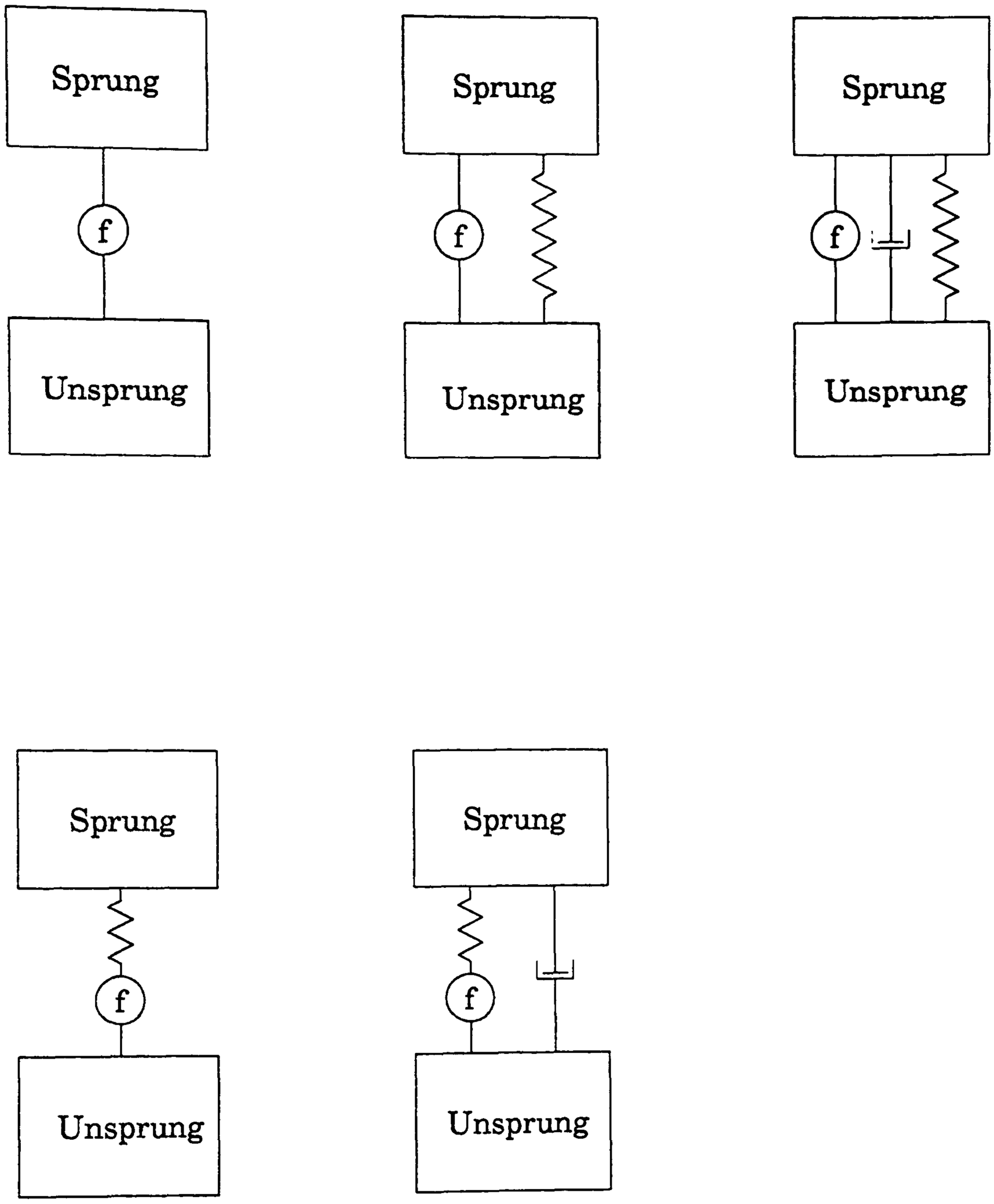


Figure 2.5 : Active Arrangements

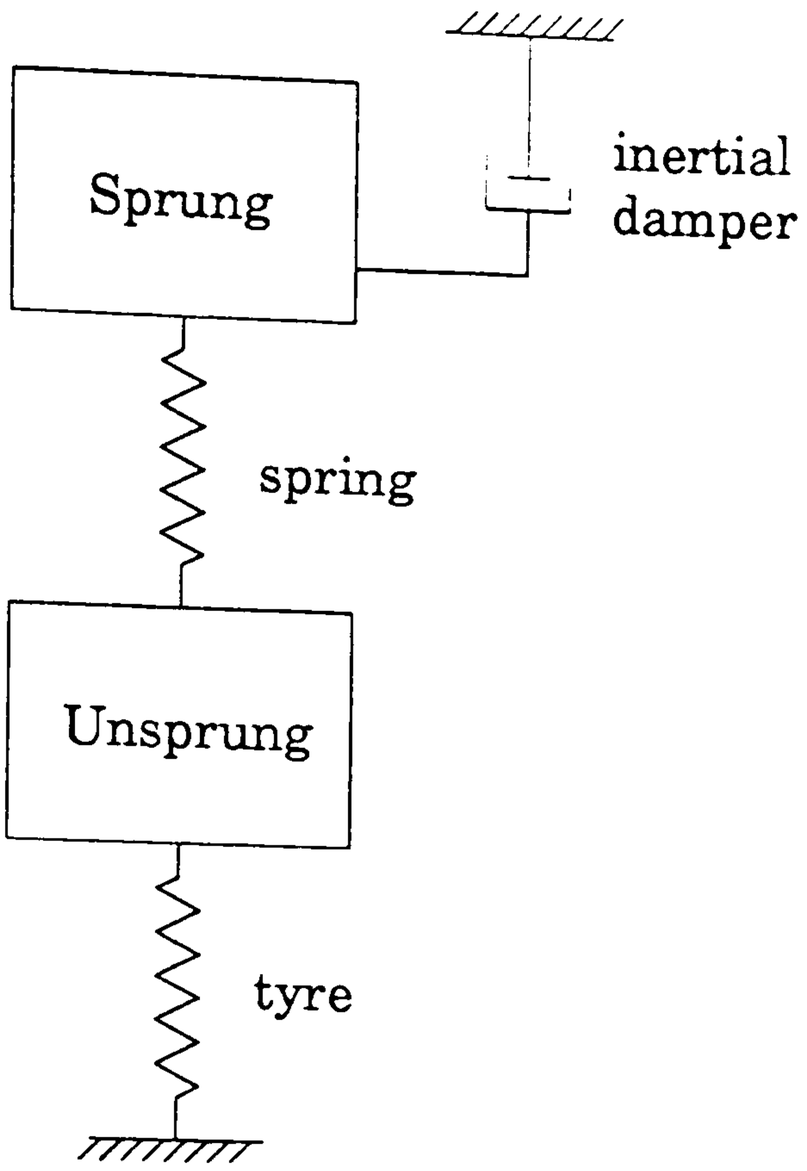


Figure 2.6 : Inertial Damper

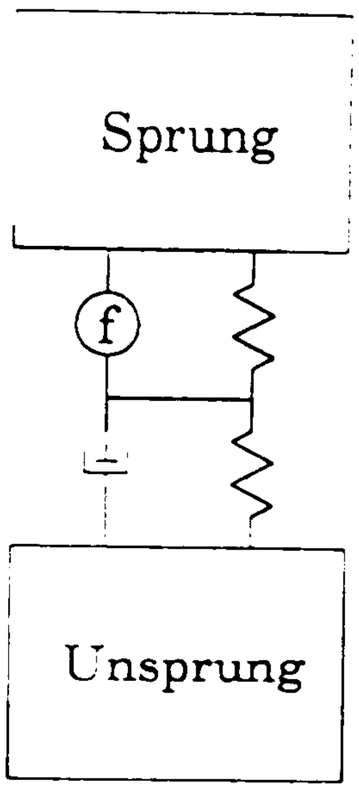


Figure 2.7 : Slow Active Arrangement

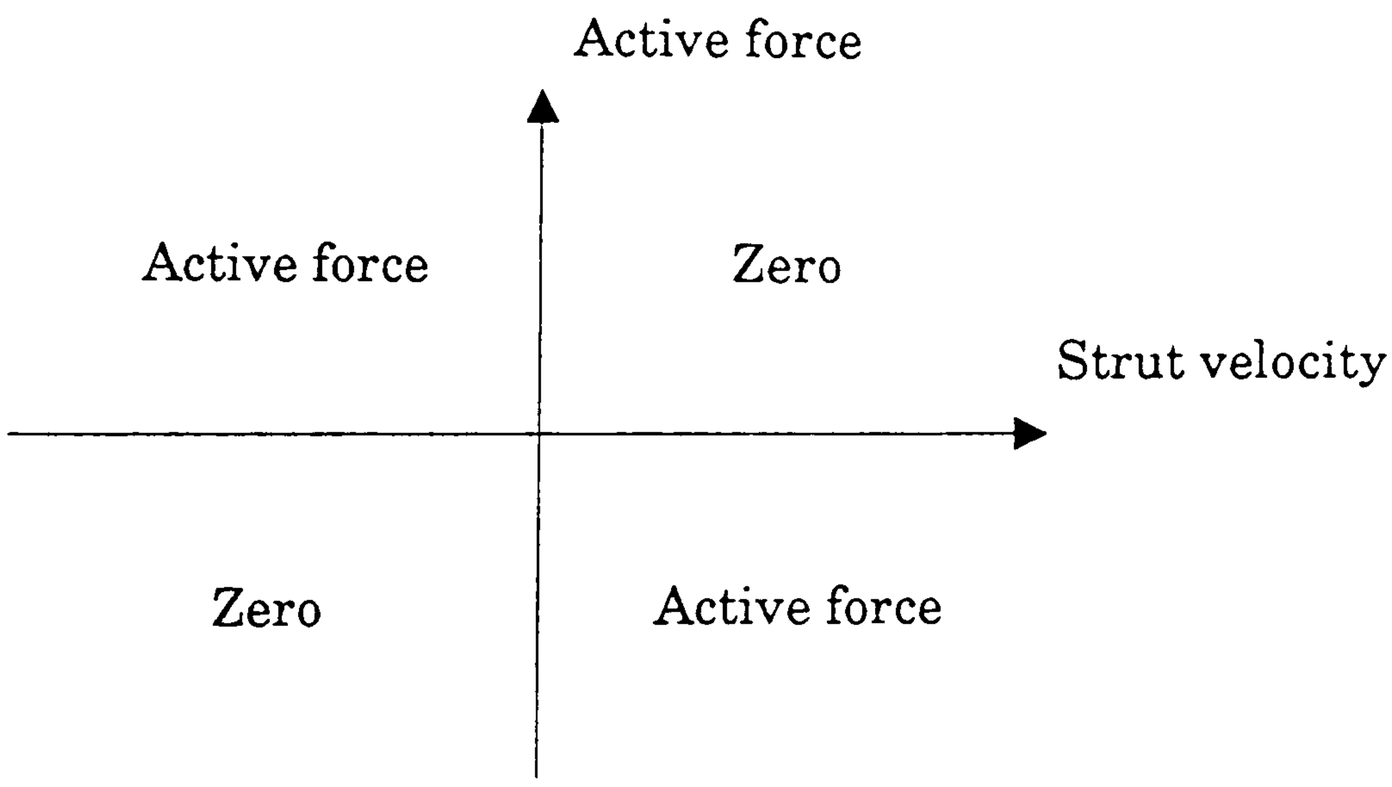


Figure 2.8 : Semi-Active Skyhook Damping

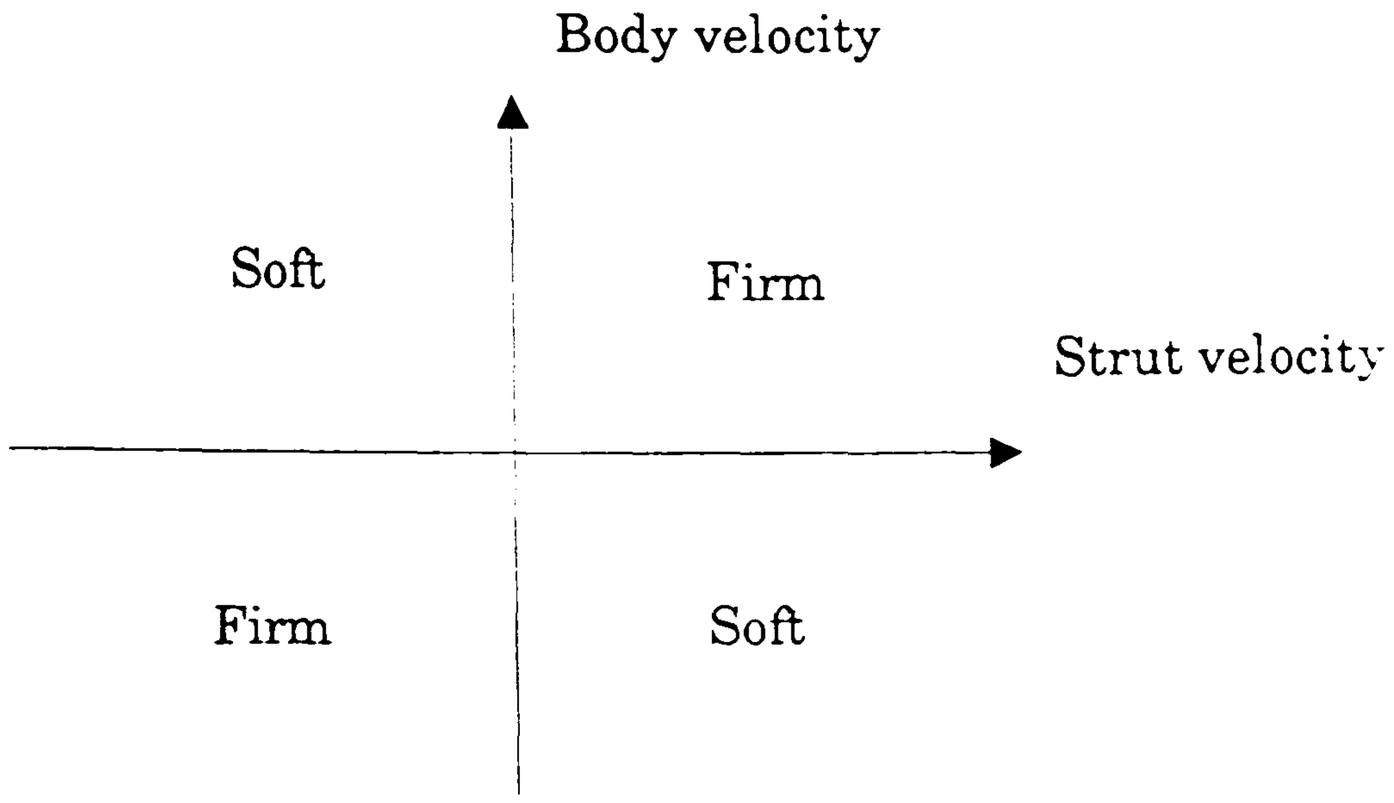


Figure 2.9 : Skyhook Damping Switching Strategy

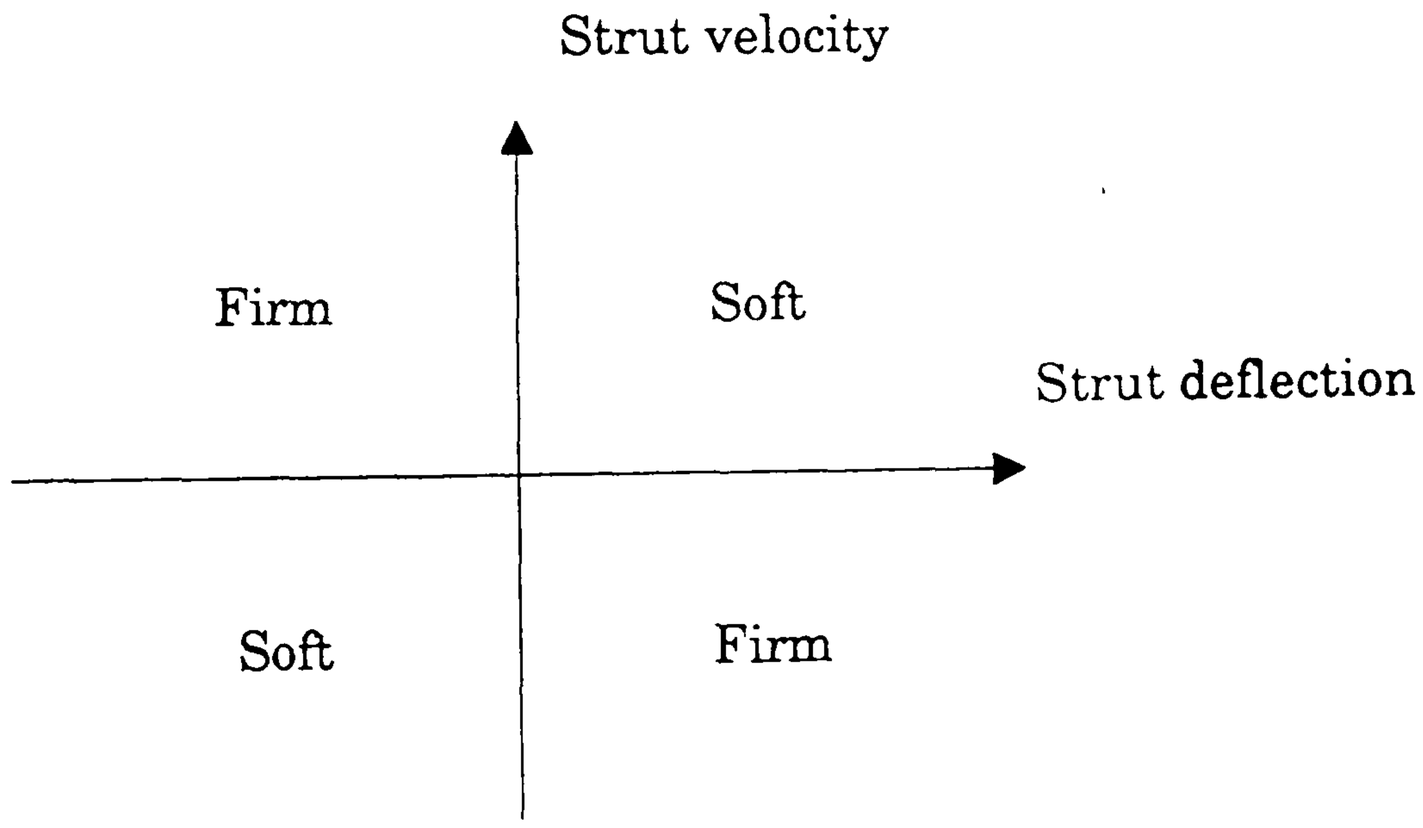


Figure 2.10 : Minimum Acceleration Switching Strategy

# Chapter 3 : Modelling and Analysis of a Quarter Car Suspension

## 3.1 Introduction

This chapter describes the first vehicle model developed using the MBS modelling techniques discussed in the previous chapter, together with a study using this model to address an automotive suspension control problem. This pilot study was aimed at providing a realistic evaluation of both the modelling and control design and analysis techniques as applied to vehicle suspension systems. At the same time an initial study of the problems associated with and possible solutions to the suspension control problem was achieved. The example chosen for this purpose was the most widely addressed area of suspension control to date, ride control for a fully active system, using a quarter car model and linear control techniques. By investigating this well known problem, a simple yet informative and comparative pilot study was defined that would meet the initial objectives.

The quarter car model used for this pilot was based on the two degree of freedom linear model described extensively in the literature, with the addition of a multibody representation of the suspension system. Realistic non-linear characteristics of the primary suspension compliance and damping forces were also included. The resultant model had two unconstrained degrees of freedom, the sprung mass vertical motion and the unsprung mass motion following a realistic arc defined by the suspension geometry. Once completed, this model was validated against real vehicle data, obtained from a quarter car suspension

test rig. Although the quarter car model is limited in terms of full vehicle dynamic behaviour, it provides a simple but useful tool for ride control studies.

The fully active suspension system under consideration here incorporated an ideal active force generator in parallel with the passive suspension spring, in place of the conventional passive spring and damper. Thus the spring carries the vehicle weight, and the force generator supplies body motion controlling forces. For the pilot study under discussion, practical actuator and sensor dynamics were ignored in order to first evaluate the methods proposed, and gain insight into the area of suspension control.

Vehicle ride control has two major objectives, that of isolating the sprung mass from road and driver inputs for passenger comfort, and maintaining good tyre contact with the road for vehicle stability. These objectives were addressed with a variety of linear control techniques including both state space and frequency domain methods.

This chapter will conclude with a discussion of the pilot study results in terms of ride performance obtained, but more importantly, the suitability of the modelling and control techniques used.

## 3.2 Modelling

The model used for the active ride control study described in this chapter was a quarter car model representing the front corner of a current production vehicle. Much of the ride control work described in the literature [11, 17, 26, 31, 40, 43, 54, 59, 73, 101, 102, 115] used simple linear quarter car models similar to that shown in figure 3.1. This diagram shows the sprung mass $m_b$, and unsprung mass $m_w$, connected by a linear spring with stiffness $K_s$, and a linear

damper with rate $b$. In these studies the tyre was commonly represented by a linear spring with stiffness $K_t$. This model has two degrees of freedom, the vertical displacements of the sprung mass $x_b$ and the unsprung mass $x_w$, with a single input, the vertical road displacement, $d$. The equations of motion for this model are easily derived from first principles giving,

$$\begin{aligned} m_b\ddot{x}_b &= K_s(x_w - x_b) + b(\dot{x}_w - \dot{x}_b) \\ m_w\ddot{x}_w &= K_t(d - x_w) - K_s(x_w - x_b) - b(\dot{x}_w - \dot{x}_b) \end{aligned} \tag{3.1}$$

The quarter car model used for the pilot study was based on this simple two degree of freedom model, with two important additions. In order to provide a more accurate connection between the sprung and unsprung masses, a representation of the suspension geometry was included. The kinematic connection involving rigid links and joints was modelled without bush compliance, as this would significantly increase the model complexity for only minor advantages. Bushes affect ride harshness and noise, but have very little effect on the sprung and unsprung mass modes of vibration of interest in ride control studies.

The second model addition improved the vehicle dynamic representation by the use of realistic non-linear characteristics for the suspension compliance and damping forces. These non-linearities are important, providing a progressive spring rate, suspension travel restriction for large amplitude inputs, and also realistic representation of the non-linear viscous effects at low velocities.

Figure 3.2 shows a schematic diagram of the resultant quarter car model. The sprung mass was represented by a single rigid body with one vertical translational degree of freedom as in the earlier model. The suspension

then included five rigid bodies representing the upper and lower arms or wishbones, steering track rod and two strut bodies, strut and yoke, with a further rigid body for the unsprung mass. The ball joints between the unsprung mass and upper and lower arms are left as three rotational degree of freedom joints, and the bushes between these arms and the sprung mass are replaced by joints with a single rotational degree of freedom in the axial direction of the bush. This connection of the sprung and unsprung masses by the lower and upper arms as shown on the diagram determine the locus of allowable wheel travel. As a result the unsprung mass also has one degree of freedom, however it is not purely vertical as in the earlier model, but follows a realistic arc.

The steering track rod to sprung mass connection was modelled as a two rotational degree of freedom joint, and again the ball joint to the unsprung mass as a three rotational degree of freedom joint. This direct connection without any steering rack motion was included to prevent the wheel steering. In future full vehicle models, however, this could be included to allow steering inputs and simulate cornering manoeuvres.

The final suspension link involves the strut and yoke bodies, and the bush connecting the strut to the sprung mass was replaced by a three rotational degree of freedom joint, and the yoke to lower arm bush by a single rotational degree of freedom joint. The motion between the yoke and strut bodies is represented by a single translational degree of freedom joint.

The suspension compliance and damping forces are then applied between these two bodies constituting the strut, labelled strut and yoke in figure 3.2. These forces included four suspension components, a linear road spring and rebound stop, together with a spring aid or bump stop and damper. For this

quarter car model the tyre was simply represented by a linear spring acting on the unsprung mass in a vertical direction.

A combination of two software packages was used to model the arrangement shown in figure 3.2, the MBS modelling package, SD/FAST, and the Simulation Language, ACSL, as discussed in the previous chapter. The input to SD/FAST, consists of the mass and inertial properties of the rigid bodies together with the geometrical description of their kinematic connections, and any gravitational forces acting on the system. SD/FAST provides as output, subroutines containing the dynamic equations of motion plus utilities that facilitate the various calculations required including forces and prescribed motions. The simulation model was completed with an ACSL model in which all internal and external forces, excluding gravitational forces, and prescribed motions were calculated. These calculations included spring and damper forces, for the passive case, control algorithm and actuator forces for the controlled active case, plus the tyre force and road inputs. The ACSL simulation environment including integration algorithms and various analysis capabilities, linked with the SD/FAST subroutines then provides a complete simulation model.

### 3.2.1 SD/FAST Multi-body Model

A MBS model in SD/FAST has to be defined in terms of a basic tree structure of rigid bodies and joints, together with constraints, either geometrical loop constraints, prescribed motion constraints, or general user defined constraints [96]. Figure 3.2 clearly shows that the suspension system under consideration did not exhibit such a tree topology, but instead formed a

collection of complete loops. In order to reduce the quarter car model described into the required tree structure, the loops had to be broken and the joints replaced by geometric constraints to maintain the correct suspension connectivity.

The efficiency of the resultant SD/FAST model is dependent on a variety of factors including branch length, number of bodies and degrees of freedom, number of constrained degrees of freedom. In this case the loops were all chosen to be at joints with three degrees of freedom, ie. lower arm to unsprung mass and upper arm and strut to sprung mass. In this way each loop involves constraining three translational degrees of freedom, thus minimising the number of constraints, without significantly increasing any of the other factors. A diagram of the resultant tree and constraint topology is shown in figure 3.3 showing the arrangement of the bodies and connections between them.

A similar model was also set up, in which three further massless bodies were added between the unsprung mass and ground providing the full six degrees of freedom, three translational and three rotational. In effect this introduces joints representing the wheel position and orientation relative to ground, without altering the kinematics or dynamics of the resultant model. The main advantage is that since SD/FAST joint displacements orientations and velocities become the states in the ACSL model, the wheel position, orientation and velocity will be available as part of the state vector for use in the suspension control studies. For this case the resultant tree and constraint topology is formed by connecting the unsprung mass to ground with three massless bodies and six degrees of freedom, and replacing the joint between the unsprung mass and the lower arm with a loop constraint, as shown in figure

3.4. However since the SD/FAST model has three extra bodies, albeit massless, and three extra constraints, the resultant simulation code becomes more complex, and less efficient.

Once the tree and constraint topology for the model was finalised, the SD/FAST input file was prepared. SD/FAST uses an ASCII, keyword oriented input which consists of the mass and inertial properties of each body, any gravitational forces acting on the system, plus a geometrical description of the topology. The mass and inertial properties of the bodies involved in the quarter car model are given in table 3.1. The sprung mass inertial properties have been set to zero, as the only allowable motion of this body is vertical translational motion. A gravitational force was also applied to the system in the negative z direction. In the simple two degree of freedom models used in the literature the gravity term cancelled with the static forces in the suspension spring and tyre. However with this more complex model the gravitational forces for each body are not collinear with the suspension spring and tyre forces and as a result this cancellation does not apply.

The geometrical description of the SD/FAST model is required in terms of two vectors describing the position of the joint relative to the centres of mass of the connected bodies (keywords 'inbtojoint', 'bodytojoint'), plus unit vectors representing the direction of the joint axes (keyword 'pin'). Tables 3.2 and 3.3 give details of body centre of masses and joint positions, from which the vectors required by SD/FAST can be calculated. For all of the data quoted in this thesis the coordinate system used is the vehicle coordinate system with origin at a position in front of and above the front bumper as shown in figure 2.1. As an illustration, the SD/FAST input file for the model shown in figure 3.4, is given

in table 3.4.

The resultant input files were then submitted to the SD/FAST program which generates up to four output files. In order to achieve compatibility with ACSL, Fortran was chosen as the output language for the SD/FAST subroutines. The dynamics file contains source code relating to the dynamic model including all equations of motion and utilities that facilitate the internal and external force calculation. The analysis file is also source code and contains a selection of analysis routines such as assembly, initial velocity, static analysis, motion analysis and steady state analysis. For this work, however, ACSL was used to provide the simulation environment, and as a result this file was not required. The two final files include source code for a library of general functions that are independent of the specific model, together with a text file containing details of the model topology, for reference. The resultant SD/FAST model had 13 joints and 26 degrees of freedom, including joint displacements, orientations and velocities.

### 3.2.2 ACSL Model

The quarter car simulation model was completed with the ACSL model of all internal and external forces, excluding gravitational forces, prescribed motions and details of inputs and output calculations. For the model under consideration the forces included the suspension compliance and damping forces plus the tyre force. Any prescribed motions required would also be defined in the ACSL code. Prescribed motion can be used to define inputs such as steering wheel angles, however the road inputs included in this pilot study were defined in terms of the tyre force, and as a result the ACSL code contained no

prescribed motions.

#### 3.2.2.1 Suspension Forces

The suspension forces consisted of compliance and damping forces in the strut. Three separate elements, a road spring, a spring aid or bump stop, and a rebound stop, all acting in parallel, combine to provide the primary suspension compliance. The spring aid and rebound stop are effectively suspension travel restrictions and as a result only act after a certain amount of strut deflection in bump or rebound. The damping forces all arise from the damper in the strut and also act in parallel with the suspension compliance forces. This arrangement is illustrated in figure 3.5.

These forces are all functions of the relative translational displacement or velocity between the two bodies representing the strut, labelled yoke and strut in figure 3.2. The equations of motion contained in the SD/FAST subroutines are expressed in terms of the joint displacements or orientations, and velocities, and these in turn form the state vector in ACSL. As a result the strut relative displacement and velocity are simply elements in the state vector, greatly simplifying the force calculations.

The road spring was represented by a linear function of the strut displacement $\boldsymbol{x_s}$, with stiffness $\boldsymbol{K_s}$ given in table 3.5, as

$$F_{spring} = - K_s x_s \tag{3.2}$$

The spring aid used was more than a suspension travel restriction, providing a progressive spring rate and a bump restriction. It was modelled as a non-linear function of strut displacement that begins to act after the strut has compressed by an amount, ***salim***, given in table 3.5,

$$F_{spaid} = SAC(x_s + salim) \qquad x_s < -salim \tag{3.3}$$

where ***SAC*** is the force displacement characteristic shown in figure 3.6. The rebound stop was simply represented by a very stiff linear spring which acts when the extension of the strut exceeds an amount ***rslim***, given in table 3.5, giving

$$F_{reb} = -K_r (x_s - rslim) \qquad x_s > rslim \tag{3.4}$$

where $K_r$ is the rebound stop stiffness, again given in table 3.5.

The damping force was similarly a non-linear function of the strut velocity given by

$$F_{damp} = DC(\dot{x}_s) \tag{3.5}$$

and is modelled by the force velocity characteristic ***DC*** shown in figure 3.7.

The model was defined at static equilibrium and SD/FAST sets all joint displacements orientations and velocities to be zero at the defined configuration [96]. As a result the suspension forces are all zero at static equilibrium, yet the gravitational forces are acting. To overcome this discrepancy a static spring force, $F_{sstat}$ was calculated, as given in table 3.5, and included in the total strut force.

All of the strut forces described were then summed to give a total suspension force as follows

$$F_s = F_{spring} + F_{spaid} + F_{reb} + F_{damp} + F_{sstat} \tag{3.6}$$

which was then applied as a hinge force to the strut slider joint. The result is an equal and opposite force acting in the direction of the strut translational

joint on the two bodies that constitute the strut, strut and yoke.

#### 3.2.2.2 Tyre Forces

For this quarter car model for ride control studies, the tyre was represented by a linear spring with stiffness $K_t$, given in table 3.5. In reality the tyre characteristics are highly non-linear and poorly understood. However for this study the effects of the primary suspension on vehicle ride performance are under consideration, and so this simple model is sufficient for comparison purposes. Thus the tyre force $F_t$ was a linear function of vertical tyre deflection $x_w$, with a discontinuity as the tyre loses contact with the ground. Vertical road inputs were incorporated into this by representing the road profile as a vertical displacement against time characteristic $x_0$,

$$F_t = -K_t (x_w - x_0 - x_{tstat}) \qquad x_w - x_0 - x_{tstat} < 0.0 \tag{3.7}$$

As for the suspension forces a static tyre force had to be included to allow the joint displacements and velocities to be zero at static equilibrium position, however in this case it was achieved by the use of a static deflection $x_{tstat}$ in order to simplify the tyre force discontinuity. This static tyre deflection is given in table 3.5.

For the second model whose topology is shown in figure 3.4, with joints representing the six degrees of freedom between the unsprung mass and ground, the tyre force is calculated directly using the vertical translational joint, and applied as a hinge force as for the suspension forces.

For the original model with no joint directly representing the vertical displacement of the wheel, with topology shown in figure 3.3, the tyre deflection had to be calculated from absolute body positions using the SD/FAST utility

subroutines that facilitate this type of calculation. The resultant tyre force was then applied in a vertical direction to the centre of mass of the unsprung mass as an external force.

The resultant ACSL model for the topology in figure 3.4 and SD/FAST input as given in table 3.4, is included in table 3.6 by way of an illustration of a typical input file. This model had 26 states relating to the SD/FAST joint deflections, orientations and velocities.

For all of the work described in this chapter, the model illustrated in figure 3.4 with massless bodies providing joints between the unsprung mass and ground was used, with SD/FAST and ACSL inputs as given in tables 3.4 and 3.6. The advantages in tyre force calculation and simplification of the linear analysis as previously mentioned were sufficient to justify the increase in complexity of the SD/FAST code caused by the extra bodies and constraints.

## 3.3 Model Simulation and Validation

Validation is an essential part of any modelling process, and all of the vehicle models involved in this work were correlated against vehicle test data. Before describing the model validation process used here, some non-linear simulations were performed with the quarter car model to obtain an understanding of the model itself. These simulations involved various isolated large amplitude road inputs and provided illustration of the kinematic behaviour of the bodies and joints, and the dynamic response of the vehicle.

Four such road inputs were chosen, a step input, two bump inputs one corresponding to the heave primary ride frequency, and a ramp input. The response of the non-linear passive model to these inputs are shown in figures

3.8. The vehicle response is illustrated in terms of the sprung mass heave response (solid line), the wheel vertical response (dashed), and the road input is also included (dotted).

These results illustrate the typical response of the passive vehicle to various road inputs. The suspension damping ensures the sprung mass oscillations induced by road inputs are damped out after one full oscillation for the standard passive damping. The unsprung mass response involves a little more oscillation, but overall the vehicle response was quite good.

In order to illustrate the effects of the vehicle non-linearities on the ride performance, the second bump input simulation was repeated with varying input amplitudes. These simulations included positive inputs corresponding to a bump, and negative inputs corresponding to a pothole. The results of these simulations are shown in figure 3.9 including the sprung and unsprung mass vertical displacements and the corresponding road inputs.

These results show that for a bump input the vehicle response is significantly non-linear even for small amplitude inputs. In contrast for pothole inputs up to 0.06 m amplitude the response is approximately linear. This is due to the major non-linearity seen at small amplitude inputs being in the damping force, and this is only significant for the low velocities in extension. For the bump input the strut is in extension after the initial input when the damper velocity is relatively low. In contrast the pothole input causes the damper to be in extension for the initial input phase when the damper velocities are relatively high. As a result the damper non-linearities would affect the bump input significantly more than the equivalent pothole input.

For the control studies described in this chapter, a linear ideal active

actuator replaces the damper, and so the damper non-linearities are of reduced importance. In order to investigate the effects of the other more important non-linearities, the simulations were repeated using a linear damping force. These results are given in figure 3.10, and clearly show that the model is approximately linear for bump and pothole inputs with amplitudes up to 0.06 m. The reason for this is that the predominant non-linearities are the spring aid and rebound stop, and these only have a large effect at large strut deflections. The spring aid acts for small deflections, but the effective suspension rate is progressive, and the effects are only noticed for larger inputs. The final non-linearity is related to the suspension geometry, but again this has negligible effect on the overall linearity of the model.

### 3.3.1 Experimental Work

An important emphasis of the work described throughout this thesis has been the use of realistic models that have been validated against real vehicle test data. Extensive experimental work was not included as a major part of the project, instead use was made of existing test facilities within Rover, and of existing test results.

In order to validate the quarter car model, an electro-hydraulic single station suspension test rig was used. The rig was previously built for suspension development purposes at the Rover test centre, Gaydon, and is shown in figure 3.11. The rig comprised of a vertical actuator with a wheel pan connected to the piston on which the wheel rests. The vehicle front suspension system was then assembled and mounted at the normal body mounting positions to a large mass representing the sprung mass. This mass was

attached to ground by two large 'z' frames as seen in figure 3.11, allowing virtually vertical motion of the sprung mass representation. The correct sprung mass was achieved by the addition of extra weights as required.

The actuator used was an in-house 10 kN actuator, and an analogue servo control system was used to control the actuator response to a drive signal representing the road input.

When the test rig was first commissioned and built, an extensive correlation exercise was undertaken to validate the suspension response achieved on the test rig against the suspension response installed on a vehicle. This correlation involved the complete response of the sprung and unsprung mass together with the major suspension components.

For the correlation of the ACSL quarter car model under consideration, sine sweep tests were undertaken. The suspension system on the rig was first instrumented with accelerometers mounted on the sprung and unsprung mass in a vertical direction. The actuator was then driven with a sine wave input in which the frequency is swept through the frequency range of interest with related amplitude variations. The sine sweep covered the range of ride frequencies up to 25 Hz. This sine sweep test provides the frequency response of the quarter car representation.

The body and wheel hub vertical acceleration measurements were recorded and averaged to give root mean square acceleration values across the frequency range. The resonant frequencies were read off the resultant graphs and are tabulated in table 3.7. More extensive experimental work for model validation was not possible due to availability of the test rig. This was not a major problem as the full vehicle model subsequently developed was also to be

validated.

### 3.3.2 Model Validation

In order to correlate the quarter car model against these sine sweep test results, a modal analysis was required. In order to perform such an analysis a linearised representation of the ACSL model was required.

The ACSL quarter car model described earlier is a non-linear representation in the form

$$\dot{x} = f(x,d) \tag{3.8}$$

where $\boldsymbol{x}$ is the 26x1 state vector containing the joint displacements or orientations and velocities, and $\boldsymbol{d}$ the 1x1 road disturbance. In order to undertake a modal analysis and determine natural frequencies and mode shapes of the system, and also for any linear control design or analysis, a linear representation of the model was required. ACSL provides the capability to find a static equilibrium position and linearise about this operating position, to give a linear model of the form

$$\begin{aligned} \dot{x} &= J\,x \\ J &= \frac{\partial f}{\partial x} \end{aligned} \tag{3.9}$$

where $\boldsymbol{J}$ is the jacobian used for modal analysis [3]. The road input, $\boldsymbol{d}$, is treated as a disturbance and ignored for the modal analysis.

In the first instance the non-linear ACSL model was linearised about the static equilibrium position giving the modes and frequencies shown in the first entry of table 3.8. In addition to these modes, the analysis also produced several modes with unity frequency and damping factor. These modes related to the

SD/FAST loop constraints.

SD/FAST uses Baumgarte stabilisation routines for the convergence and stability of constraints [96], and so the modes related to these constraints have natural frequency and damping ratio determined by the Baumgarte constants chosen. This choice is a compromise between the requirement for constraint stability, and for the eigenvalues to be small relative to the dominant system eigenvalues in order to minimise the effects on the other system eigenvalues. For this modal analysis the Baumgarte constants were chosen to be $2a$, $a^2$, $a=1.0$, giving good constraint stabilisation for non-linear simulations and minimum effects on the other system eigenvalues. For this modal analysis these modes will be ignored.

A comparison of the frequencies of the first set of modes given in table 3.8 with the test results given in table 3.7 shows a discrepancy in both natural frequencies, with the modal results being significantly lower. This discrepancy can be explained by examination of the vehicle non-linearities not considered in the linear modal analysis, together with an evaluation of their effects on the modal results.

The linearisation for the modal analysis was performed about the static equilibrium position, and as a result two major approximations were made to the original non-linear ACSL model. At static equilibrium position there is no spring aid or rebound stop forces, and as a result the suspension compliance would have been approximated to the linear spring alone. In contrast for the sine sweep tests the strut deflections would have caused the spring aid to be acting for a significant part of the test, especially around the resonant frequencies. The rebound stop only acts under extreme road inputs, and would

not have influenced the test results.

The second approximation involved the non-linear damping force. Again linearisation around the static equilibrium position would result in a linear damping force with the equivalent damping rate for low velocities. Figure 3.7 shows that this part of the force velocity characteristic exhibits a larger rate than the majority of the curve. Again under the test conditions the strut velocities would have resulted in a lower average damping rate.

In order to evaluate the effects of these approximations to the modal analysis results, the analysis was repeated with different spring stiffnesses equivalent to the influence of the spring aid forces, and different damping rates. These results are also included in table 3.8. The first of these results show that a reduction in the suspension damping rate results in a small increase in the unsprung mass resonant frequency and a small decrease in the sprung mass frequency. These effects are small in comparison with the discrepancy to be explained.

The spring stiffness changes, however, had a more significant effect on the modal results. An increase in the spring stiffness, equivalent to the action of the spring aid, resulted in an increase in both resonant frequencies. In fact the discrepancy between the test and analytical results for the sprung mass resonant frequency can be explained by this single approximation. The non-linear ACSL model, however, includes a full non-linear representation of the spring aid and so these results validate the sprung mass response from this model.

The further discrepancy in the unsprung mass response can be similarly explained by the simplified linear tyre model used. In reality the tyre

characteristics would be non-linear and would include some damping. In order to confirm this, and complete the correlation, the modal analysis was again repeated with varying tyre stiffnesses and damping levels. The results are given in table 3.8, and they illustrate the same trends, with the damping having minor influence, and an increase in the tyre stiffness causing an increase in the unsprung mass frequency. Again this approximation would account for the discrepancy between test and model results. However in this case the ACSL model only uses this simplified tyre model.

As a result the ACSL non-linear model produces good correlation with test results for the sprung mass response, and reasonable unsprung mass correlation within the limitations of the tyre model. For the work described in this thesis, the control studies are primarily concerned with the sprung mass response, and thus the model was satisfactorily validated for the studies under consideration.

## 3.4 Suspension Control

The objectives of the pilot study were to address ride control for an ideal active suspension system with a quarter car model and a variety of linear control techniques, including both state space and frequency domain techniques. The validated quarter car model with passive suspension was easily adapted to an ideal active system by replacing the conventional passive damper with an ideal active force generator. This force was then used in subsequent investigations as the control variable. As discussed fully in the previous chapter, the objectives of ride control are to isolate the sprung mass from disturbances and maintain tyre road contact, which equates to minimising the

sprung mass acceleration and tyre load variations.

The passive model non-linearities, as discussed, are found in the damper characteristics at low velocities, and in the suspension compliance for large displacements. For the active system with an ideal actuator replacing the passive damper, the suspension travel restrictions provide the only relevant non-linearities. As a result, if relatively small amplitude road inputs are assumed, the ride control problem can be considered linear. Having made this approximation, however, it is important to investigate the behaviour of any resultant controller for all possible inputs, especially those that render the assumptions invalid.

In order to address the ride control problem with linear control techniques, a linear representation of the quarter car model was required. ACSL provides the facility to linearise models in two ways, one of which has already been described and given in equation 3.9. Alternatively by defining the control inputs $\boldsymbol{u}$ and measured outputs $\boldsymbol{y}$ required, the non-linear system given in equation 3.8 will be of the form

$$\dot{x} = f(x,u,d) \tag{3.10}$$

This model can then be linearised about static equilibrium to give a standard state space representation of the form

$$\dot{x} = Ax + Bu \tag{3.11}$$

$$y = Cx + Du$$

where $\boldsymbol{A}$, $\boldsymbol{B}$, $\boldsymbol{C}$, $\boldsymbol{D}$ are the system matrices, with the road input $\boldsymbol{d}$ as a disturbance [3]. These system matrices can then be read directly into MATLAB, a matrix manipulation package, for any subsequent control design and analysis.

For the active ride control study the control variable was chosen to be the ideal active force $\boldsymbol{f}$, and the vertical road input, $\boldsymbol{d}$ was considered to be a disturbance. The first four system outputs were chosen to be the sprung and unsprung mass vertical displacements and velocities for vehicle response evaluation purposes. The strut deflections and velocities together with the vertical tyre deflection and wheel velocity were also chosen as system outputs in order to facilitate the required feedback solution as described later.

The linearisation of the ACSL quarter car model then gives a single input multi-output (SIMO) system governed by the following equation

$$\begin{aligned} \dot{x} &= Ax + Bf + Gd \\ y &= Cx + Df + Hd \end{aligned} \tag{3.12}$$

where $\boldsymbol{x}$ is the 26x1 state vector containing the joint displacements or orientations and velocities, $\boldsymbol{u}$ is the 1x1 input vector, $\boldsymbol{d}$ the 1x1 road disturbance and $\boldsymbol{y}$ is the 7x1 output vector, and the state space matrices are $\boldsymbol{A}$, $\boldsymbol{B}$, $\boldsymbol{G}$, $\boldsymbol{C}$, $\boldsymbol{D}$ & $\boldsymbol{H}$ the first three of which are given in table 3.9, with assumed accuracy of two decimal places.

These matrices constitute a poorly scaled system with the elements of $\boldsymbol{B}$ being an order of magnitude of 10000 less than $\boldsymbol{A}$, $\boldsymbol{H}$.

In order to illustrate the reason for this, first consider the two degree of freedom example defined by equation 3.1. Replacing the passive damping force with the ideal active force, $\boldsymbol{f}$, gives

$$\begin{aligned} m_b\ddot{x}_b &= K_s(x_w - x_b) + f \\ m_w\ddot{x}_w &= K_t(d - x_w) - K_s(x_w - x_b) - f \end{aligned} \tag{3.13}$$

which can be rewritten in the required state space form

$$\frac{d}{dt}\begin{pmatrix} x_b \\ x_w \\ \dot{x}_b \\ \dot{x}_w \end{pmatrix} = \begin{pmatrix} 0 & 0 & 1 & 0 \\ 0 & 0 & 0 & 1 \\ -\frac{K_s}{m_b} & \frac{K_s}{m_b} & 0 & 0 \\ \frac{K_s}{m_w} & -\frac{(K_t + K_s)}{m_w} & 0 & 0 \end{pmatrix} \begin{pmatrix} x_b \\ x_w \\ \dot{x}_b \\ \dot{x}_w \end{pmatrix} + \begin{pmatrix} 0 \\ 0 \\ \frac{1}{m_b} \\ -\frac{1}{m_w} \end{pmatrix} f + \begin{pmatrix} 0 \\ 0 \\ 0 \\ \frac{K_t}{m_w} \end{pmatrix} d \qquad (3.14)$$

Reference to the mass and stiffness values given in tables 3.1 & 3.5 indicate the differences in magnitude between the elements of the matrices ***A, B & G***. Although the matrices for the full ACSL linearisation are more complex, the basic structure and magnitude of elements would be similar, giving rise to the same scaling problems. Thus to avoid numerical problems the actuator force was scaled to give following system, with a new control variable ***u***

$$\begin{aligned} \dot{x} &= Ax + Bu + Gd \\ y &= Cx + Du + Hd \\ u &= 1e{-}4f \end{aligned} \qquad (3.15)$$

### 3.4.1 State Space

In order to apply state space control techniques, including linear quadratic regulator and pole placement, to the linear model given in equation 3.14, some manipulation of the state space description was required. In this study the method reported by Wilson et al [115] was closely followed, in which the road input displacement ***d*** was included in the state vector to allow the performance index to incorporate a measure of tyre load variation. This is also reasonable since in equation 3.14, ***d*** appears to be a disturbance and yet the ride objectives do not require all road inputs to be rejected. In fact some large

amplitude low frequency road inputs should be tracked.

In order to illustrate the required manipulation of the state space representation, the two degree of freedom example will again be considered first. In order to include $\boldsymbol{d}$ in the state vector and retain a fully controllable system of equations, the state vector was redefined by replacing the absolute wheel position $\boldsymbol{x_w}$ with the tyre deflection $\boldsymbol{x_w}$ - $\boldsymbol{d}$, the absolute body displacement $\boldsymbol{x_b}$ with relative body to wheel deflection $\boldsymbol{x_b}$ - $\boldsymbol{x_w}$ and similarly for the body velocity. In this case the new system of equations becomes

$$\frac{d}{dt}\begin{pmatrix} x_b - x_w \\ x_w - d \\ \dot{x}_b - \dot{x}_w \\ \dot{x}_w \end{pmatrix} = \begin{pmatrix} 0 & 0 & 1 & 0 \\ 0 & 0 & 0 & 1 \\ -K_s\left(\frac{1}{m_b} + \frac{1}{m_w}\right) & \frac{K_t}{m_w} & 0 & 0 \\ \frac{K_s}{m_w} & -\frac{K_t}{m_w} & 0 & 0 \end{pmatrix} \begin{pmatrix} x_b - x_w \\ x_w - d \\ \dot{x}_b - \dot{x}_w \\ \dot{x}_w \end{pmatrix} + \begin{pmatrix} 0 \\ 0 \\ \frac{1}{m_b} + \frac{1}{m_w} \\ -\frac{1}{m_w} \end{pmatrix} 1e4u + \begin{pmatrix} 1 \\ 0 \\ 0 \\ 0 \end{pmatrix} w \quad (3.16)$$

where the road velocity, $\boldsymbol{w}$, was then treated as a disturbance

For the ACSL linearisation of the quarter car model a similar manipulation was required, but in this case the strut deflection and velocity were already states since they were SD/FAST joint degrees of freedom. The road input, $\boldsymbol{d}$, was included in the state vector as described, by replacing the absolute vertical wheel displacement with the relative tyre deflection. As expected this system gives the same number of controllable modes as the simple example, body heave and wheel hop with the rest of the modes in the large system being related to loop constraints.

The SD/FAST Baumgarte stabilisation constants chosen to be $\boldsymbol{2a}$, $\boldsymbol{a^2}$ $\boldsymbol{a=1.0}$, give eigenvalues with unity frequency and damping factor relating to the

loop constraints. These are then small enough relative to the dominant system eigenvalues to be cancelled without affecting the resultant system dynamics significantly. In order to obtain the smallest realisation of the vehicle ride model, these roots were therefore cancelled from the linear state space model. This was achieved within MATLAB, leaving a controllable reduced order model suitable for state space control techniques, of the form

$$\begin{aligned} \dot{p} &= \hat{A}p + \hat{B}u + \hat{G}w \\ y &= \hat{C}p + \hat{D}u + \hat{H}w \\ u &= 1e\text{-}4f \end{aligned} \tag{3.17}$$

where $\boldsymbol{p}$ is the 4x1 transformed state vector, $\boldsymbol{u}$ is the 1x1 input vector, $\boldsymbol{w}$ the 1x1 road velocity disturbance and $\boldsymbol{y}$ the 7x1 output vector. For the state space design methods, the disturbances are assumed to be zero in this system of equations.

### 3.4.1.1 Linear Quadratic Regulator

The ride control objectives stated earlier can be re-posed to fit in with the linear quadratic regulator concept of minimising a performance index, by taking the performance index $\boldsymbol{J}$, to be a weighted combination of body acceleration $\boldsymbol{acc}$, tyre load variation $\boldsymbol{tlv}$, and control effort $\boldsymbol{u}$, as below

$$J = \int [\rho_1 (acc)^2 + \rho_2 (tlv)^2 + \rho_3 u^2] dt \tag{3.18}$$

The performance index is then expressed in the required matrix form by substituting expressions for body acceleration and tyre load variation from the linearised system of equations 3.15, and rearranging to give

$$J = \int (p' \;\; u') \begin{pmatrix} Q & N \\ N' & R \end{pmatrix} \begin{pmatrix} p \\ u \end{pmatrix} dt \qquad (3.19)$$

where $\boldsymbol{Q}$, $\boldsymbol{N}$ and $\boldsymbol{R}$ are weighting matrices.

Again using the example given in equation 3.16 as an illustration, with the disturbances assumed to be zero, the expression for the sprung mass acceleration is

$$\ddot{x}_b = -\frac{K_s}{m_b}(x_b - x_w) + \frac{1}{m_b} 1e4u \qquad (3.20)$$

and so the quadratic terms for equation 3.18 are given by

$$\begin{aligned} acc^2 &= \frac{K_s^2}{m_b^2}(x_b - x_w)^2 - 2\frac{K_s}{m_b} 1e4(x_b - x_w)u + \frac{1}{m_b^2} 1e8u^2 \\ tlv^2 &= (x_b - x_w)^2 \end{aligned} \qquad (3.21)$$

Rearranging these equations into the form of equation 3.19 using the state given in equation 3.16, gives the following weighting matrices for the performance index $\boldsymbol{J}$.

$$Q = \begin{pmatrix} \frac{K_s^2}{m_b^2}\rho_1 & 0 & 0 & 0 \\ 0 & \rho_2 & 0 & 0 \\ 0 & 0 & 0 & 0 \\ 0 & 0 & 0 & 0 \end{pmatrix}, \quad N = \begin{pmatrix} \frac{-K_s 10^4}{m_b^2}\rho_1 \\ 0 \\ 0 \\ 0 \end{pmatrix}, \quad R = \frac{10^8}{m_b^2}\rho_1 + \rho_3 \qquad (3.22)$$

The quadratic performance index for the linearised ACSl model given in equation 3.17 was similarly obtained by substituting the expression for the sprung mass acceleration.

Optimal regulator theory was then applied to the system of equations

given in 3.17 to provide an optimum state variable feedback solution of the form

$$u = -Kp \tag{3.23}$$

where $\boldsymbol{K}$ is the 1x4 vector of feedback gains, for the set of performance index weightings chosen. The control design process then involved several iterations to find the set of weightings providing the required vehicle response. During this iterative process it was found that the performance index weightings required were of significantly different orders of magnitude. The reason for this is made clear by inspection of the weighting matrices for the two degree of freedom example shown in equation 3.22. In order to achieve comparable influence over the solution, the first weight will need to be of a larger order of magnitude.

### 3.4.1.2 Pole Placement

Linear optimal control techniques have provided the most popular solution to ride control to date. In this study, however, the objectives were to consider a variety of different control design techniques, and pole placement was the second state space techniques to be applied. Pole placement is based on the same system of equations 3.17 and produces the same state variable feedback solution of the form given in equation 3.23, however an alternative method of designing the feedback matrix $\boldsymbol{K}$ is involved. In pole placement the gains are obtained by selecting the desired s-plane pole locations for the resultant closed loop system. This involved the placement of two pairs of complex poles related to the two modes. This method, however, takes no account of the control effort required to achieve a response, and optimum feedback solutions are not obtained.

The ride control problem under consideration in this pilot study was addressed using pole placement techniques. Again for this method an iterative design process was required to obtain the required vehicle ride performance characteristics.

### 3.4.1.3 Estimation

Both of the state space techniques described use full state feedback solutions, and since the system state includes the tyre deflection, road profile is a required measured output. Although the use of road preview has been described in various theoretical studies in the literature [33, 59, 87], it is not a practical proposition for real implementations. State estimation techniques can be used to calculate this quantity from the measured outputs that are available, removing the road preview requirement. These techniques can also be used in systems where measurement or process noise is a major problem. Many reported studies have successfully applied state estimation techniques and used limited state variable feedback solutions with negligible degradation in performance [2, 35, 115]

Assuming the full system with a linear state space controller is as below

$$\begin{aligned} \dot{p} &= \hat{A}p + \hat{B}u + \hat{G}w \\ y &= \hat{C}p + \hat{D}u + v \\ u &= -Kp \end{aligned} \tag{3.24}$$

where $w$ is the process noise and $v$ is the measurement noise. The degradation in performance of the resultant system using an estimation for $d$ is dependent on $w$ and $v$. However for this pilot study noise and sensor dynamics were being neglected and since for small $v$ the performance degradation due to this estimation was negligible, estimation will not be discussed further.

### 3.4.2 Frequency Domain

In order to investigate a variety of different approaches to the ride control design for an automotive suspension system, frequency domain techniques were also considered. The applicability of frequency domain techniques was indicated by the frequency dependence of the required vehicle response to road disturbances. Although the sprung mass is to be isolated from road disturbances, some large amplitude low frequency inputs should be followed, illustrating the possible advantage of frequency domain compensation.

In standard frequency domain theory the system under consideration is as shown in figure 3.12 in which the compensator designed to achieve both stability of the plant, and rejection of all disturbances. For suspension ride control however, not all disturbances are to be rejected, as the road input constitutes in part a disturbance to be rejected, but also a reference signal to be tracked. For the sprung mass, rejection of high frequency disturbances is of prime importance for isolation purposes, but the body must follow long term road profile changes. For the unsprung mass response tracking the road input is more important than disturbance rejection in order to maintain good road tyre contact. Thus standard frequency domain techniques are not ideally suited to this application, however a brief investigation of frequency dependent compensation was undertaken for this pilot study.

In order to apply frequency domain techniques the state space description of the ACSL linearised model had to be converted into transfer function form. This conversion can be illustrated simply by referring to the two degree of freedom example used previously, with equations of motion given in

equation 3.13. Taking Laplace transforms of this system of equations gives the following

$$\begin{aligned} m_b x_b s^2 &= K_s(x_w - x_b) + f \\ m_w x_w s^2 &= K_t(d - x_w) - K_s(x_w - x_b) - f \end{aligned} \tag{3.25}$$

The equations were manipulated to produce the block diagram shown in figure 3.13. By further equation manipulation the systems can be decoupled into an equivalent block diagram form given in figure 3.14, suitable for frequency domain compensation design.

For the linearised ACSL quarter car model, a reduced order transfer function model has to be obtained, in which the modes related to the topological constraints are removed, as previously discussed for the state space study. This was achieved in MATLAB, with the state space representation given in equation 3.15 as a starting point. For the conversion to a transfer function block diagram of the form given in figure 3.14, the road input was considered to be a second input as opposed to a state. In order to allow feedback compensation of the body, strut and wheel displacements and velocities, the output equation was modified to include these variables.

Again this state space representation was reduced to remove the modes related to the SD/FAST loop constraints by the MATLAB function minreal [75]. The resultant reduced order state space model was then converted into reduced order transfer function representations for both of the inputs by the use of ss2tf in MATLAB [75], resulting in a system with block diagram structure as shown in figure 3.15. Each of the transfer functions have a common denominator of order four, with second order numerators, with coefficients given in table 3.10.

For the application of frequency domain techniques the SIMO system was considered as separate SISO systems for each of the chosen outputs.

A brief study was undertaken to look at a range of proportional, integral, derivative and lead-lag compensators on a variety of outputs, and combinations of outputs. Stability criteria were first applied to determine which range of frequency domain compensators on which outputs ensured stability, and then performance was achieved by varying the compensator parameters.

Feed-forward control using road preview information was a possibility also considered, and was achieved by replacing the wheel displacement output with tyre deflection. Frequency domain compensation of this output would then involve road preview.

## 3.5 Discussion of Results

Each of the control design methods described was applied to this ride control problem, involving iterative tuning processes to achieve the desired ride performance characteristics. In order to evaluate each intermediate closed loop system designed, a step input was used for the road displacement and a linear simulation performed in MATLAB. The results of these step responses can be seen in figures 3.16-3.18, and the vehicle response is illustrated in terms of the sprung mass displacement (solid line), the unsprung mass vertical displacement (dashed line) together with the control effort required, given in terms of the actuator forces $\boldsymbol{f}$. For the frequency domain results in figures 3.18 the strut deflection is also included (dotted line).

Once the best solutions were obtained, a full non-linear evaluation was undertaken by the using the ACSL model to simulate various road inputs.

Isolated large amplitude road inputs were considered here as opposed to the more usual small amplitude frequency domain road spectra. The reason for this is that these are considered to illustrate more important aspects of vehicle ride characteristics from the customers' point of view as discussed in the previous chapter. For a passive system comparison, the same simulations were performed using the non-linear model with representative linear damping rates, in order to provide a fair comparison for a system with linear feedback control. These non-linear simulation results are included in figures 3.19-3.21, and illustrate the sprung mass displacement (solid line), the unsprung mass vertical displacement (dashed line), and the road input (dotted line), together with the required control force or passive damping force.

### 3.5.1 State Space

For the state space study control solutions were provided in the state variable feedback form shown in equation 3.23. However since the state $\boldsymbol{p}$ was a transformation of the original state, the controller is not a physically meaningful feedback solution as it stands. Conversion back to a function of the original state would produce a feedback involving all joint displacements or orientations and velocities, and this would involve significant measurement difficulties. The two degree of freedom example described earlier was reduced to a minimum order model with strut deflection, strut velocity, tyre deflection, and wheel velocity as states. From this experience, the difficulty arising from the ACSL linearised model was overcome by choosing these outputs from equation 3.17 giving

$$y = \hat{C}p \qquad (3.26)$$
$$u = Kp$$

where $y$ is now the new 4x1 output vector. By inverting this new output equation, the solution can be transformed into a physically meaningful linear combination of strut deflection and velocity, tyre deflection and wheel velocity

$$u = K\hat{C}^{-1}y \qquad (3.27)$$

The resultant closed loop systems were then obtained by substituting this equation for the control variable $u$ in equation 3.15.

### 3.5.1.1 Linear Quadratic Regulator

For the linear optimal techniques, the feedback design consisted of choosing the weighting parameters in equation 3.18 to obtain the desired performance. This choice was not a trivial task and resulted in an iterative design procedure. As previously explained the orders of magnitude of the performance index weights were significantly different and care was required in the iterative tuning of the control design.

The ride performance was tuned firstly to damp out any sprung and unsprung mass oscillation, and secondly to achieve the desired response in terms of overshoot, response time etc. Some of the resultant closed loop system step responses obtained in this procedure are shown in figures 3.16a-g, with the weighting used for each solution given in table 3.11, and resultant feedback solutions given in table 3.12. A comparison of these results illustrates the effects of the individual weightings on vehicle ride characteristics. The effects of increasing the body acceleration weighting as seen from figures 3.16a,b,c is a small reduction in sprung mass acceleration as expected, together with

increased oscillations in the wheel response. In fact the improvements in the sprung mass response are insignificant compared with the deterioration in unsprung mass response, and the resultant response soon becomes unacceptable due to these wheel oscillations as seen in figure 3.16c.

Figures 3.16a,d,e show the effect of increasing the tyre deflection weighting, improving the wheel response to achieve almost exact tracking of the road input with minimal overshoot and no oscillation. However this also results in a much slower body response with increasing overshoot, which is not the most suitable sprung mass response and which in turn implies a large control effort requirement. By increasing both the body acceleration and tyre deflection weightings and effectively reducing the control effort weighting, a similar trend can be seen, figures 3.16f,a,g. The wheel response can be tuned to almost exact tracking of the road input, whereas control of the body response is more complicated.

The main reason for this is explained by the over simplified specification of ride performance objectives in terms of the performance index. The term relating to minimisation of tyre load variation is sufficient for the unsprung mass control as indicated by the results discussed. However the sprung mass control objective of minimising acceleration is shown to be an oversimplification. For a road input such as a bump or pothole, the body response is required to completely reject it as a disturbance. However for a road profile change such as a step, the body must track the input to a certain extent whilst also minimising the passenger compartment acceleration. The performance index used here only achieves the required response for pure disturbance inputs as expected. The design method does not easily allow for the inclusion of the complete

performance requirements.

### 3.5.1.2 Pole Placement

Pole placement gives the same feedback solution as above but provides a method of choosing the gain $\boldsymbol{K}$ in terms of modes, which may be more intuitive for vehicle design engineers. The feedback solution is defined in terms of the required closed loop poles, allowing the specification of the frequency and damping of the vehicle ride modes. This method was also approached in an iterative fashion, and some step responses of resultant closed loops are shown in figures 3.17a-j, with the relevant pole locations given in table 3.13, and corresponding feedback gains given in table 3.14. The original open loop system had no damping, since the passive damper was replaced by the force actuator, and so the first step in the pole placement study was to introduce some damping to both vehicle modes, as shown in the step response in figure 3.17a. From this point the pole locations were tuned to give the best achievable ride response.

For the pole placement design procedure, sprung mass response was addressed first, and figures 3.17b,c show the effects of increasing and decreasing the frequency of the body mode, with an increase having the effect of reducing the body overshoot and flattening the response. Figures 3.17d,e,f then show the added effect of increasing the damping for the first three results, providing a reduction of body overshoot and a minor increase of wheel overshoot. In the limit this increase of damping removes all body overshoot, as seen in figure 3.17e. However, using this pole placement method of specifying the feedback solution $\boldsymbol{K}$ does not allow the speed of body response to be altered easily.

Using the poles for the best sprung mass response achieved as seen in figure 3.17e, the techniques were then used to obtain the desired unsprung mass response, with the results given in figures 3.17g,h,i. Figures 3.17g,h illustrate the effects of increasing and decreasing the frequency of the wheel hop mode from the system illustrated by figure 3.17e, and figures 3.17i increasing the damping over figure 3.17g. Again speed of response seems to be an attribute not easily defined by pole locations. Also it appears that the required wheel hop mode is more difficult to express in terms of pole positions, than in terms of a quadratic performance measure, whilst the sprung mass performance is better with pole placement techniques.

Pole placement takes no account of the control effort required, and for some of the responses shown here, where there is no body overshoot, this effort would be large in the initial stages of a road input change.

### 3.5.2 Frequency Domain

The use of frequency domain control techniques in this ride control study caused several difficulties, one of which was the fact that the problem does not fit standard theory very well. However a study of various frequency domain compensators was undertaken and some reasonable results were achieved.

Stability criteria were first applied to the open loop system in order to determine which range of compensators on which outputs ensured stability of the closed loop system. For each of these cases an iterative procedure was used to tune the compensator parameters and achieve the desired vehicle response characteristics. It is interesting to note that the proportional feedback of the sprung mass absolute velocity produces the widely used skyhook damping

control. This iterative process resulted in the combination of outputs and compensators given in table 3.15 being evaluated.

This design process indicated that for the range of outputs and compensators ensuring system stability, only strut displacement and velocity compensation provided acceptable ride performance characteristics as illustrated by the linear model step response. The major problem was that designing a controller for one output may achieve good control for that output, however poor control, if any, over the other outputs was the result. Frequency domain compensation of the sprung or unsprung mass led to excessive oscillation or even instability in the response of the other output. A combination of sprung and unsprung displacement or velocity compensation feedback has the potential to address this problem, however such a design would be based on trial and error methods only. This illustrates a significant drawback of frequency domain techniques in that they provide no insight into how the control using one output will affect the others, nor into how a combination of feedback loops might interact.

One other problem associated with the feedback of sprung or unsprung mass displacement feedback was again due to good disturbance rejection being achievable, with poor tracking for road profile changes. For the unsprung mass case this can be overcome by using the tyre deflection as the feedback signal, resulting in good tracking response. However the sprung mass feedback problem is less obvious and presents the same problem as in the state space study of specification of the sprung mass response requirements.

One possible method of achieving a good design using compensation of one output is to consider strut displacement or velocity as the feedback, since

then some control over both sprung and unsprung mass responses are obtained. However again for this case there were design difficulties in the definition of good ride characteristics in terms of strut response, since the standard design objectives of feedback systems, ie rejection of disturbances and tracking of the reference, are not exactly applicable.

As described, the study of frequency domain compensation was undertaken using strut displacement and velocity as feedback signals and the desired ride performance achieved by tuning of the compensator parameters, with some reasonable result. Figures 3.18a-c show the closed loop step responses for some systems with the strut displacement as controlled output, figures 3.18d-g with strut velocity, and figures 3.18h,i with a combination of the two, and details of the relevant compensators are given in table 3.15.

The use of frequency domain techniques produced solutions that were stable and well damped, however tuning the body and wheel responses as desired was difficult. The best response achieved was simply the system with least sprung and unsprung mass oscillation as shown in figures 3.18c,h,i. For this design method the responses were difficult to tune separately, simply because only the strut feedback was used, resulting in the same response characteristic being achieved for both the sprung and unsprung mass. Again this method takes no account of the control effort required.

### 3.5.3 Evaluation of solutions in the non-linear model

Finally the best of the linear active feedback solutions were evaluated on the non-linear ACSL model. The passive damping force was therefore simply replaced by the active feedback control force and the four road input

simulations used for the passive model were performed. For each of the three control design methods applied in the study, the best solution achieved was selected and evaluated as described, and the results are included in figures 3.19-3.21. The active solutions used had linear responses given in figures 3.16b for the linear quadratic regulator solution, 3.17i for pole placement and figure 3.18a for the frequency domain results.

The evaluation simulations for the best regulator solution is shown in figure 3.19, with linear response as in figure 3.16b. A comparison of these results shows a significant deterioration in the sprung mass response caused by the model non-linearities. The spring aid has a general effect on all of the simulations since it acts for the majority of the simulations. However since the force is effectively a continuous progression of the linear road spring, the effect is a general deterioration in the response in terms of increased overshoot and an increase in the frequency of sprung mass response. In contrast the rebound stop has a more dramatic effect on the response in isolated cases involving large suspension rebound travel. The majority of the deterioration in the sprung mass response to the bump inputs was caused by the rebound stop non-linearity, since the active solutions tend to use more rattle space. The unsprung mass response was not affected by the model non-linearities significantly.

Figures 3.20, 3.21 show the non-linear response of the pole placement and frequency domain results, with corresponding linear results given in figures 3.17i, 3.18a. In both of these cases similar trends to those described for the regulator study can be seen.

The ramp input can produce poor vehicle responses in some state space studies due to the inclusion of the absolute wheel vertical velocity in the

feedback control. However for these solutions this term in the controller had relatively small gains, although this still resulted in the frequency domain results producing superior ramp response compared with both state space methods.

As a result the active solutions are only marginally affected by the vehicle non-linearities for the majority of small road inputs, however for large bump inputs, the suspension travel restriction would cause significant degradation of performance.

## 3.6 Conclusions

The pilot study described in this chapter addressed ride control for ideal active suspension systems with the use of a quarter car model and various linear control techniques. As a result a simple yet useful study was undertaken using the modelling techniques proposed in the previous chapter to investigate the specific concerns relating to suspension control and conventional control techniques.

The work described has shown the modelling approach to be suitable for the range of requirements discussed in chapter two, including full non-linear simulation and linear control design and analysis. As a result the control design procedure can account for the suspension linkage influence on ride performance, and controllers can be evaluated on realistic non-linear models without the need for prototypes.

With regard to the ride control problem under consideration, the major difficulty encountered with all design methods was in the specification of the sprung mass response requirements. However the details of the design

difficulties varied between methods together with the level of achievable performance despite these design problems.

Both state space techniques gave good resultant vehicle ride performance characteristics, with linear quadratic regulator providing superior unsprung mass responses, and pole placement achieving the best sprung mass characteristics. The state space methods also provided a well-defined iterative design procedure, again a significant advantage. The major disadvantages with both methods was in defining the performance objectives in the required terms, sprung mass performance in terms of a performance index to be minimised, and unsprung mass characteristic in terms of mode frequency and damping. Pole placement results were also compromised by the difficulty in dealing with the interactions between modes. However it is important to note the major difference between the two state space methods was that pole placement techniques impose no restriction on the allowable control effort.

In comparison frequency domain techniques did not suit the problem in hand very well, and thus the design method was heavily based on trial and error, although some reasonable results were obtained. Again the major difficulties were found in the control objectives and interaction between modes. The obvious way for improving the results obtained with frequency domain techniques was to use a combination of output compensation terms. However in this case the design becomes difficult.

In summary the state space techniques achieved the best vehicle ride performance, with the linear quadratic regulator providing the best unsprung mass response, and pole placement the best sprung mass response. However all methods encountered difficulties in some respect with the specification of the

ride performance objectives.

As a result the pilot study achieved the aims set of gaining experience of the modelling approach and control design techniques, plus insight into the problems associated with suspension control.

| Body | Mass (kg) | Ixx (kg $m^2$) | Iyy (kg $m^2$) | Izz (kg $m^2$) |
|---|---|---|---|---|
| Sprung | 391.65 | 0.0 | 0.0 | 0.0 |
| Lower arm | 6.112 | 0.052525 | 0.187495 | 0.23857 |
| Yoke | 4.446 | 0.0658 | 0.0658 | 0.000889 |
| Strut | 2.152 | 0.01255 | 0.01255 | 0.00269 |
| Upper arm | 2.088 | 0.004188 | 0.004211 | 0.008398 |
| Track rod | 0.75 | 0.005636 | 0.000021 | 0.005636 |
| Unsprung | 41.333 | 0.448 | 0.827 | 0.448 |

Table 3.1 : Front Corner Mass and Inertia Properties

| Body | x coord (m) | y coord (m) | z coord (m) |
|---|---|---|---|
| Sprung | 0.973 | 0.325 | 0.400 |
| Lower arm | 0.9025 | 0.4975 | 0.0947 |
| Yoke | 0.9681 | 0.5592 | 0.3011 |
| Strut | 0.9571 | 0.5143 | 0.4827 |
| Upper arm | 1.066 | 0.53 | 0.55 |
| Track rod | 1.1256 | 0.53295 | 0.1839 |
| Unsprung | 0.973 | 0.745 | 0.167 |

Table 3.2 : Centre of Mass of Front Corner Bodies

| Inboard | Outboard | x coord (m) | y coord (m) | z coord (m) |
|---|---|---|---|---|
| Sprung | Lower arm | 1.05 | 0.34825 | 0.137 |
| Lower arm | Yoke | 0.99043 | 0.61537 | 0.10749 |
| Yoke | Strut | 0.96973 | 0.55263 | 0.34 |
| Sprung | Upper arm | 1.073 | 0.47335 | 0.5463 |
| Sprung | Track rod | 1.145 | 0.392 | 0.196 |
| Track rod | Unsprung | 1.1062 | 0.6739 | 0.1718 |
| Unsprung | Lower arm | 0.9621 | 0.70309 | 0.09071 |
| Upper arm | Unsprung | 0.98655 | 0.63934 | 0.57208 |
| Sprung | Strut | 0.9459 | 0.4804 | 0.6077 |

Table 3.3 : Front Corner Joint Positions

```
# front quarter car model with joints between unsprung mass and ground

# preamble

grounded
gravity = 0   0   -9.807

# tree structure

body = sprung    joint = slider
mass = 391.65
inertia = 0   0   0
bodytojoint = 0   0   -0.528
pin = 0   0   1

body = lowarm    inb = sprung     joint = pin
mass = 6.112
inertia = 0.052525   0.187495   0.238570
inbtojoint = 0.077   0.02325   -0.263
bodytojoint = 0.1475   -0.14925   0.0423
pin = 0.96169539426633   0.23080421413801   0.14788976767535

body = yoke      inb = lowarm     joint = pin
mass = 4.446
inertia = 0.0658   0.0658   0.000889
inbtojoint = 0.08793   0.11787   0.01279
bodytojoint = 0.02233   0.05617   -0.19361
pin = 0.96169539426633   0.23080421413801   0.14788976767535

body = strut     inb = yoke       joint = slider
mass = 2.152
inertia = 0.01255   0.01255   0.00269
inbtojoint = 0.00163   -0.00657   0.0389
bodytojoint = 0.01263   0.03833   -0.1427
pin = -0.08563305318152   -0.25955295728520   0.96192475930673

body = uparm     inb = sprung     joint = pin
mass = 2.088
inertia = 0.0041876   0.0042108   0.0083984
inbtojoint = 0.1   0.14835   0.1463
bodytojoint = 0.007   -0.05665   -0.0037
pin = 0.8740443162851 5   0.4855316176964   -0.01748088632570

body = track     inb = sprung     joint = ujoint
mass = 0.75
inertia = 0.005636   0.000021   0.005636
inbtojoint = 0.172   0.067   -0.204
bodytojoint = 0.0194   -0.14095   0.0121
pin = 1   0   0
pin = 0   0   1

body = lat       inb = $ground    joint = slider
mass = 0
inertia = 0   0   0
inbtojoint = 0   0   0
bodytojoint = 0   -0.42   0
pin = 0   1   0
```

Table 3.4 : Front Quarter Car SD/FAST Model

```
body = faft      inb = lat        joint = slider
mass = 0
inertia = 0   0   0
inbtojoint = 0   0   0
bodytojoint = 0   0   0
pin = 1   0   0

body = trans     inb = faft       joint = slider
mass = 0.0
inertia = 0   0   0
inbtojoint = 0   0   0.295
bodytojoint = 0   0   0
pin = 0   0   1

body = unsprung inb = trans      joint = gimbal
mass = 41.333
inertia = 0.448   0.827   0.448
inbtojoint = 0   0   0
bodytojoint = 0   0   0
pin = 0   0   1
pin = 0   1   0
pin = 1   0   0

# loop constraints

body = unsprung inb = track      joint = gimbal
inbtojoint = -0.0194   0.14095   -0.0121
bodytojoint = 0.1332   -0.0711   0.0048
pin = 0   0   1
pin = 0   1   0
pin = 1   0   0

body = unsprung   inb = lowarm   joint = gimbal
inbtojoint = 0.0596   0.20559   -0.00399
bodytojoint = -0.0109   -0.04191   -0.07629
pin = 0   0   1
pin = 0   1   0
pin = 1   0   0

body = strut     inb = sprung    joint = gimbal
inbtojoint = -0.0271   0.1554   0.2077
bodytojoint = -0.0112   -0.0339   0.125
pin = 0   0   1
pin = 0   1   0
pin = 1   0   0

body = unsprung inb = uparm      joint = gimbal
inbtojoint = -0.07945   0.10934   0.02208
bodytojoint = 0.01355   -0.10566   0.40508
pin = 0   0   1
pin = 0   1   0
pin = 1   0   0
```

Table 3.4 (continued)

| Variable | Value |
|---|---|
| $K_s$ | 37050 N/m |
| salim | 0.008 m |
| $K_r$ | 10000000 N/m |
| rslim | 0.038 m |
| $F_{sstat}$ | 5535.10645 N |
| $K_t$ | 215000 N/m |
| $x_{tstat}$ | 0.02046 m |

Table 3.5 : Front Corner ACSL Variable Values

```
PROGRAM FRONT QUARTER CAR MODEL

"-------------------------------------------------------------------"
" This is the ACSL model for the front quarter vehicle model with    "
" joints between the unsprung mass and ground                        "
"                                                                    "
" Fortran subroutines are used to convert to double precision       "
"-------------------------------------------------------------------"

INITIAL

        ARRAY     JTDIS(13), JTVEL(13), JTDISD(13), JTVELD(13)
        ARRAY     DISIC(13), VELIC(13), PERRS(12), VERRS(12)
        ARRAY     LQ(12), LU(12), LQDOT(12), LUDOT(12)

        INTEGER   I, INPUT, STRUT, WHEEL, SDINDX

        "-------------- Model Parameters ---------------------------"

        CONSTANT  KT = 215000, KS = 37050, KRS = 10000000
        CONSTANT  SALIM = 0.008, RSLIM = 0.038, TYRLIM = 0.028
        CONSTANT  TSTATD = 0.0204592728
        CONSTANT  SSTATF = 5535.1064453125
        CONSTANT  STRUT = 4, WHEEL = 9
        CONSTANT  HEIGHT = 0.0, SPEED = 0.0

        "-------------- Constraint Stabilisation Constant ----------"

        CONSTANT  A = 1.0

        "-------------- Simulation Parameters ----------------------"

        CONSTANT  SIMLEN = 0.999
        ALGORITHM IALG = 9
        CINTERVAL CINT = 0.01
        NSTEPS    NSTP = 100
        MAXTERVAL MAXT = 1E10
        MINTERVAL MINT = 1E-10

        "-------------- Damping and spring aid curves --------------"

        TABLE     CCOMP, 1, 9/0, 0.052, 0.075, 0.131, 0.262, 0.393 ...
                  , 0.524, 1, 1.5, 0, 165, 180, 220, 295, 385, 500 ...
                  , 1000, 1650/

        TABLE     CEXT, 1, 9/0, 0.052, 0.075, 0.131, 0.262, 0.393 ...
                  , 0.524, 1, 1.5, 0, 480, 1000, 1310, 1620, 1820 ...
                  , 2000, 2600, 3280/

        TABLE     SPRAID, 1, 11/0, 0.01, 0.02, 0.03, 0.04, 0.05 ...
                  , 0.055, 0.06, 0.062, 0.06974, 0.08886, 0, 98 ...
                  , 294, 490, 883, 1960, 3300, 5890, 7848, 20000 ...
                  , 50000/

        "-------------- Road inputs --------------------------------"

        TABLE     RBUMP, 1, 9/-100, 0.2, 0.4, 0.6, 0.8, 1.0, 1.2  ...
                  , 1.4, 100, 0, 0, 0.5, 0.866, 1, 0.866, 0.5, 0, 0/

        TABLE     RSTEP, 1, 5/-100, 1, 2, 5, 100, 0, 0, 1, 1, 1/

        TABLE     RRAMP, 1, 6/0, 1, 8, 15, 100, 200 ...
                  , 0, 0, 0.5, 1.0, 1.0, 1.0/

        "-------------- Initialisation -----------------------------"
```

Table 3.6 : Front Quarter Car ACSL Model

```
      DO L10 I = 1, 13

            DISIC(I) = 0.0
            VELIC(I) = 0.0

L10..CONTINUE

      DO L20 I = 1, 12

            PERRS(I) = 0.0
            VERRS(I) = 0.0

L20..CONTINUE

            INPUTD = 0.0
            DAMP = 0.0
            INPUT = 0
            LASTME = 0.0
            VEHSPD = SPEED*1.6093/3.6

            CALL INITIALISE(A)

END $ "of initial"

DYNAMIC

DERIVATIVE

            "--------------- Set SD/FAST states -------------------------"

            CALL SETSTATE(T, JTDIS, JTVEL)

            "--------------- Calculate road input -----------------------"

            INPUTD = HEIGHT*RSTEP(VEHSPD*T)

            "--------------- Calculate suspension spring force ----------"

            SPRF = -KS*JTDIS(SDINDX(STRUT ,1))

            "--------------- Calculate spring aid force -----------------"

            SADEFL = -SALIM - JTDIS(SDINDX(STRUT ,1))
            BUMP = RSW((SADEFL .LE. 0.0), 0.0, SPRAID(SADEFL))

            " ------------- Calculate rebound stop force ---------------"

            RSDEFL = JTDIS(SDINDX(STRUT ,1)) - RSLIM
            REB = RSW((RSDEFL .LE. 0.0), 0.0, -KRS*(RSDEFL))

            "--------------- Calculate total spring forces --------------"

            SUSPF = SPRF + BUMP + REB + SSTATF

            "--------------- Calculate suspension damping force ---------"

            STRVEL = JTVEL(SDINDX(STRUT ,1))
            ABSVEL = ABS(STRVEL)
            CS = RSW((STRVEL .GE. 0.0), CEXT(ABSVEL) , CCOMP(ABSVEL))
            DAMP = -SIGN(CS, STRVEL)

            " ------------- Calculate tyre force -----------------------"

            TYRED = JTDIS(SDINDX(WHEEL ,1)) - TSTATD - INPUTD
            TYREF = RSW((TYRED .LE. 0.0), -KT*TYRED, 0.0)
```

Table 3.6 (continued)

```
"-------------- Calculate derivatives ----------------------"

CALL CALCDERIVS(JTDISD, JTVELD, LQ, LU, LQDOT, LUDOT  ...
        = SUSPF, DAMP, TYREF, STRUT, WHEEL)

"-------------- Integrate to obtain states -----------------"

JTDIS = INTVC(JTDISD, DISIC)
JTVEL = INTVC(JTVELD, VELIC)

"-------------- Calculate maximum constraint errors ---------";

 PROCEDURAL(PERRS, VERRS, MAXERR = JTDIS, JTVEL)

          MAXERR = 0.0
          CALL CONCHECK(VERRS, PERRS = )
          DO L30 I = 1, 12
          IF(ABS(VERRS(I)) .GT. MAXERR) MAXERR = ABS(VERRS(I))
     L30..CONTINUE
          DO L40 I = 1, 12
          IF(ABS(PERRS(I)) .GT. MAXERR) MAXERR = ABS(PERRS(I))
     L40..CONTINUE

        END $ "of procedural"

END $ "of derivative"

"--------------------- Calulate maximum constraint error -----------"

IF(MAXERR .GT. LASTME) LASTME = MAXERR

"---------------------- Terminate ----------------------------------"

TERMT(T .GE. SIMLEN)

END $ "of dynamic"

END $ "of program"
        subroutine initialise(a)
C-----------------------------------------------------------------
C This subroutine initialises the SD/FAST variables and sets the
C stabilisation constant
C-----------------------------------------------------------------
        real a
        real*8 ad
        ad = a
        call sdinit
        call sdstab(2.0d0*ad, ad*ad)
        return
        end
        subroutine setstate(t, q, u)
C-----------------------------------------------------------------
C This subroutine sets the SD/FAST states from the last integration
C interval
C-----------------------------------------------------------------
        real t, q(13), u(13)
        real*8 td, qd(13), ud(13)
        integer i
        td = t
        do 50 i = 1, 13
                qd(i) = q(i)
                ud(i) = u(i)
   50   continue
        call sdstate(td, qd, ud)
        return
        end
```

Table 3.6 (continued)

```
      subroutine calcderivs(suspf, damp, tyref, strut, wheel
     +  , qdot, udot, lq, lu, lqdot, ludot)
C-----------------------------------------------------------------
C This subroutine applies the forces and calculates the state
C derivatives, ie velocities and accelerations
C-----------------------------------------------------------------
      real suspf, damp, tyref, qdot(13), udot(13)
      real lq(12), lu(12), lqdot(12), ludot(12)
      real*8 suspfd, dampd, tyrefd, qdotd(13),udotd(13)
      real*8 lqd(12), lud(12), lqdotd(12), ludotd(12)
      integer i, strut, wheel
      suspfd = suspf
      dampd = damp
      tyrefd = tyref
      call sdpseudo(lqd, lud)
      call sdpsqdot(lqdotd)
      call sdhinget(strut, 1, suspfd)
      call sdhinget(strut, 1, dampd)
      call sdhinget(wheel, 1, tyrefd)
      call sdderiv(qdotd, udotd)
      call sdpsudot(ludotd)
      do 60 i = 1, 13
            qdot(i) = qdotd(i)
            udot(i) = udotd(i)
60    continue
      do 70 i = 1, 12
            lq(i) = lqd(i)
            lu(i) = lud(i)
            lqdot(i) = lqdotd(i)
            ludot(i) = ludotd(i)
70    continue
      return
      end
      subroutine concheck(verrs, perrs)
C-----------------------------------------------------------------
C This subroutine calculates the constraint errors
C-----------------------------------------------------------------
      real verrs(12), perrs(12)
      real*8 verrsd(12), perrsd(12)
      integer i
      call sdverr(verrsd)
      call sdperr(perrsd)
      do 80 i = 1, 12
            verrs(i) = verrsd(i)
            perrs(i) = perrsd(i)
80    continue
      return
      end
```

Table 3.6 (continued)

| Mode | Frequency (Hz) | Frequency (rad/s) |
|---|---|---|
| Body Heave | 1.4 | 10.68 |
| Wheel Hop | 14.0 | 87.97 |

Table 3.7 : Sine Sweep Test Results

| Condition | Body Heave Frequency (rad/s) | Wheel Hop Frequency (rad/s) |
|---|---|---|
| Non-Linear Damping | 7.14855 | 67.0344 |
| Linear Damping 1200/2000 N/m | 6.81358 | 70.33 |
| Increased Suspension Stiffness by 500 N | 7.93867 | 71.5998 |
| Increased Suspension Stiffness by 2000 N | 9.18503 | 73.3518 |
| Linear Tyre Damping 5000 N/m | 6.7968 | 70.5036 |
| Increased Tyre Stiffness by 35000 N/m | 6.85382 | 75.3968 |

Table 3.8 : Modal Analysis Results

$$A = \begin{pmatrix} 0 & I \\ A1 & A2 \end{pmatrix}$$

A1 =

| | | | | |
|---|---|---|---|---|
| 2.5575e+00 | -2.4764e-01 | -3.6078e+00 | -6.7336e+01 | -9.4081e-04 |
| -6.7130e+01 | 5.4129e+00 | 9.1379e+01 | 1.7061e+03 | 3.0076e-02 |
| 5.5173e+01 | -5.2707e+00 | -7.6104e+01 | -1.4022e+03 | -2.4719e-02 |
| 1.7401e+01 | -1.6624e+00 | -2.3687e+01 | -4.4324e+02 | -7.7962e-03 |
| -1.2472e+02 | 1.1914e+01 | 1.6977e+02 | 3.1696e+03 | -9.4412e-01 |
| -7.8595e+01 | 7.5082e+00 | 1.0699e+02 | 1.9974e+03 | 3.5213e-02 |
| -1.1289e+01 | 1.0785e+00 | 1.5368e+01 | 2.8692e+02 | 5.0580e-03 |
| -1.3723e+00 | 1.3109e-01 | 1.8680e+00 | 3.4875e+01 | 6.1481e-04 |
| 3.3176e+00 | -3.1693e-01 | -4.5160e+00 | -8.4315e+01 | -1.4864e-03 |
| -2.0989e+01 | 2.0973e+00 | 2.9806e+01 | 5.5650e+02 | 1.0057e-02 |
| -1.0450e+00 | 9.9847e-02 | 1.4226e+00 | 2.6559e+01 | 4.6821e-04 |
| -1.2665e+01 | 1.2098e+00 | 1.7239e+01 | 3.2186e+02 | 5.6740e-03 |
| -9.8948e+00 | 9.4525e-01 | 1.3469e+01 | 2.5147e+02 | 4.4331e-03 |

| | | | | |
|---|---|---|---|---|
| 8.2629e-04 | -1.1945e-03 | -3.7973e+00 | 4.9339e+00 | 9.8457e+00 |
| -1.4963e-02 | 3.0263e-02 | 9.6203e+01 | -1.2500e+02 | -1.2391e+04 |
| 1.2298e-02 | -2.4873e-02 | -7.9069e+01 | 1.0274e+02 | 1.0184e+04 |
| 3.8787e-03 | -7.8449e-03 | -2.4938e+01 | 3.2402e+01 | 3.2120e+03 |
| -2.7799e-02 | 5.6225e-02 | 1.7873e+02 | -2.3223e+02 | -2.3021e+04 |
| -1.0175e+00 | 3.5432e-02 | 1.1263e+02 | -1.4635e+02 | -1.4508e+04 |
| -2.5163e-03 | -9.9491e-01 | 1.6179e+01 | -2.1022e+01 | -2.0839e+03 |
| -3.0587e-04 | 6.1865e-04 | 9.6658e-01 | -2.5552e+00 | -2.5330e+02 |
| 7.3948e-04 | -1.4956e-03 | -4.7544e+00 | 5.1775e+00 | 6.1238e+02 |
| -4.6450e-03 | 9.8715e-03 | 3.1380e+01 | -4.0773e+01 | -4.5221e+03 |
| -2.3294e-04 | 4.7112e-04 | 1.4977e+00 | -1.9459e+00 | -1.9290e+02 |
| -2.8229e-03 | 5.7095e-03 | 1.8149e+01 | -2.3582e+01 | -2.3377e+03 |
| -2.2055e-03 | 4.4608e-03 | 1.4180e+01 | -1.8425e+01 | -1.8264e+03 |

| | | |
|---|---|---|
| -2.7545e-02 | -1.5906e-01 | 1.6769e-01 |
| 6.9784e-01 | 4.0298e+00 | -4.2483e+00 |
| -5.7355e-01 | -3.3120e+00 | 3.4916e+00 |
| -1.8089e-01 | -1.0446e+00 | 1.1012e+00 |
| 1.2965e+00 | 7.4868e+00 | -7.8927e+00 |
| 8.1702e-01 | 4.7180e+00 | -4.9739e+00 |
| 1.1736e-01 | 6.7770e-01 | -7.1445e-01 |
| 1.4265e-02 | 8.2376e-02 | -8.6843e-02 |
| -3.4488e-02 | -1.9915e-01 | 2.0995e-01 |
| 2.2763e-01 | 1.3144e+00 | -1.3857e+00 |
| -9.8914e-01 | 6.2743e-02 | -6.6132e-02 |
| 1.3165e-01 | -2.3975e-01 | -8.0147e-01 |
| 1.0286e-01 | 5.9398e-01 | -1.6262e+00 |

Table 3.9 : State Space Matrices

A2 =

| | | | | |
|---|---|---|---|---|
| 4.7690e-03 | 4.8811e-03 | -1.2212e-03 | 1.0376e-02 | 2.9126e-04 |
| -4.7901e+00 | -1.8456e+00 | -1.5362e-02 | -2.9011e-02 | 5.1022e-03 |
| 3.9370e+00 | -1.2688e-01 | -1.9874e+00 | 2.3844e-02 | -4.1934e-03 |
| 1.2417e+00 | -4.0016e-02 | 3.9822e-03 | -1.9925e+00 | -1.3226e-03 |
| -8.8994e+00 | 2.8680e-01 | -2.8541e-02 | -5.3898e-02 | -1.9905e+00 |
| -5.6083e+00 | 1.8074e-01 | -1.7986e-02 | -3.3966e-02 | 5.9736e-03 |
| -8.0558e-01 | 2.5961e-02 | -2.5835e-03 | -4.8789e-03 | 8.5805e-04 |
| -9.7920e-02 | 3.1556e-03 | -3.1403e-04 | -5.9304e-04 | 1.0430e-04 |
| 2.3673e-01 | -7.6291e-03 | 7.5922e-04 | 1.4337e-03 | -2.5215e-04 |
| 2.5323e-01 | 6.1327e-02 | -6.8385e-03 | -2.3253e-04 | 2.1569e-03 |
| -7.4571e-02 | 2.4032e-03 | -2.3916e-04 | -4.5163e-04 | 7.9425e-05 |
| -9.0370e-01 | 2.9123e-02 | -2.8982e-03 | -5.4731e-03 | 9.6257e-04 |
| -7.0606e-01 | 2.2754e-02 | -2.2644e-03 | -4.2762e-03 | 7.5205e-04 |

| | | | | |
|---|---|---|---|---|
| 1.9132e-04 | -4.6209e-05 | -1.1849e-02 | 2.8647e-02 | -4.7690e-03 |
| 7.0952e-03 | 1.1707e-03 | 3.0020e-01 | -7.2576e-01 | 4.7901e+00 |
| -5.8315e-03 | -9.6218e-04 | -2.4673e-01 | 5.9650e-01 | -3.9370e+00 |
| -1.8392e-03 | -3.0347e-04 | -7.7817e-02 | 1.8813e-01 | -1.2417e+00 |
| 1.3182e-02 | 2.1750e-03 | 5.5772e-01 | -1.3484e+00 | 8.8994e+00 |
| -1.9917e+00 | 1.3706e-03 | 3.5147e-01 | -8.4972e-01 | 5.6083e+00 |
| 1.1932e-03 | -1.9998e+00 | 5.0485e-02 | -1.2205e-01 | 8.0558e-01 |
| 1.4504e-04 | 2.3931e-05 | -1.9939e+00 | -1.4836e-02 | 9.7920e-02 |
| -3.5065e-04 | -5.7856e-05 | -1.4836e-02 | -1.9641e+00 | -2.3673e-01 |
| 2.7857e-03 | 3.8186e-04 | 9.7920e-02 | -2.3673e-01 | -2.5323e-01 |
| 1.1045e-04 | 1.8226e-05 | 4.6734e-03 | -1.1298e-02 | 7.4571e-02 |
| 1.3386e-03 | 2.2086e-04 | 5.6635e-02 | -1.3692e-01 | 9.0370e-01 |
| 1.0458e-03 | 1.7256e-04 | 4.4249e-02 | -1.0698e-01 | 7.0606e-01 |

| | | |
|---|---|---|
| -9.7807e-05 | -2.1880e-03 | -9.2606e-04 |
| 2.4779e-03 | 5.5433e-02 | 2.3462e-02 |
| -2.0366e-03 | -4.5560e-02 | -1.9283e-02 |
| -6.4231e-04 | -1.4369e-02 | -6.0817e-03 |
| 4.6036e-03 | 1.0299e-01 | 4.3588e-02 |
| 2.9011e-03 | 6.4901e-02 | 2.7469e-02 |
| 4.1673e-04 | 9.3224e-03 | 3.9456e-03 |
| 5.0653e-05 | 1.1332e-03 | 4.7960e-04 |
| -1.2246e-04 | -2.7395e-03 | -1.1595e-03 |
| 8.0826e-04 | 1.8081e-02 | 7.6528e-03 |
| -2.0000e+00 | 8.6296e-04 | 3.6524e-04 |
| 4.6748e-04 | -1.9895e+00 | 4.4262e-03 |
| 3.6524e-04 | 8.1707e-03 | -1.9965e+00 |

Table 3.9 (continued)

$$B = \begin{pmatrix} 0 \\ B1 \end{pmatrix}, \qquad G = \begin{pmatrix} 0 \\ G1 \end{pmatrix}$$

| B1 = | G1 = |
|---|---|
| 1.8176e+01 | -1.2403e+01 |
| -4.6049e+02 | 1.2458e+04 |
| 3.7848e+02 | -1.0239e+04 |
| 1.1937e+02 | -3.2294e+03 |
| -8.5553e+02 | 2.3146e+04 |
| -5.3914e+02 | 1.4586e+04 |
| -7.7443e+01 | 2.0952e+03 |
| -9.4134e+00 | 2.5467e+02 |
| 2.2758e+01 | -6.1570e+02 |
| -1.5021e+02 | 4.5431e+03 |
| -7.1688e+00 | 1.9395e+02 |
| -8.6876e+01 | 2.3504e+03 |
| -6.7876e+01 | 1.8363e+03 |

Table 3.9 (continued)

| | $s^4$ | $s^3$ | $s^2$ | s | 1 |
|---|---|---|---|---|---|
| Denominator | 1.0 | 0.0 | 5022.1 | 0.0 | 229630 |
| Numerator $D_b$ | 0.0 | 0.0 | -12.403 | 0.0 | 229630 |
| Numerator $D_s$ | 0.0 | 0.0 | -3229.4 | 0.0 | 229630 |
| Numerator $D_w$ | 0.0 | 0.0 | 4543.1 | 0.0 | 229630 |
| Numerator $G_b$ | 0.0 | 0.0 | 18.176 | 0.0 | 80713 |
| Numerator $G_s$ | 0.0 | 0.0 | 119.37 | 0.0 | 57218 |
| Numerator $G_w$ | 0.0 | 0.0 | -150.21 | 0.0 | 0.0 |

Table 3.10 : Transfer Function Coefficients

| Solution | $acc^2$ | $tlv^2$ | $u^2$ |
|---|---|---|---|
| a | 1 | $10^7$ | $10^3$ |
| b | 1 | $10^8$ | $10^3$ |
| c | 1 | $10^6$ | $10^2$ |
| d | 1 | $10^5$ | 10 |
| e | 1 | $10^9$ | $10^3$ |
| f | 1 | $10^7$ | $10^4$ |
| g | 1 | $10^7$ | $10^2$ |

Table 3.11 : Performance Index Weightings

| Solution | Strut Defl. | Tyre Defl. | Strut Vel. | Wheel Vel. |
|---|---|---|---|---|
| a | -0.53381 | -63.713 | 1.1124 | -0.04092 |
| b | -0.53381 | -248.41 | 2.1474 | -0.11409 |
| c | -2.0787 | -27.929 | 0.66542 | -0.095253 |
| d | -3.3254 | -4.4143 | 0.32627 | -0.012054 |
| e | -0.53379 | -840.34 | 3.9274 | -0.22495 |
| f | -0.06495 | -14.162 | 0.55109 | 0.0025971 |
| g | -2.0787 | -127.48 | 1.2058 | -0.35134 |

Table 3.12 : Linear Quadratic Regulator Feedback Gains

| Solution | Body Mode Pole Position | Wheel Mode Pole Position |
|---|---|---|
| Undamped | 0.0 +/- 6.793i | 0.0 +/- 70.54i |
| a | -4.0 +/- 5.496i | -40.0 +/- 58.08i |
| b | -6.0 +/- 8.000i | -40.0 +/- 58.08i |
| c | -2.0 +/- 3.000i | -40.0 +/- 58.08i |
| d | -6.0 +/- 3.195i | -40.0 +/- 58.08i |
| e | -9.0 +/- 4.359i | -40.0 +/- 58.08i |
| f | -3.4 +/- 1.200i | -40.0 +/- 58.08i |
| g | -9.0 +/- 4.359i | -55.0 +/- 80.00i |
| h | -9.0 +/- 4.359i | -30.0 +/- 45.00i |
| i | -9.0 +/- 4.359i | -60.0 +/- 70.00i |
| j | -9.0 +/- 4.359i | -50.0 +/- 70.00i |

Table 3.13 : Pole Positions

| Solution | Strut Defl. | Tyre Defl. | Strut Vel. | Wheel Vel. |
|---|---|---|---|---|
| a | 0.0028755 | -4.2411 | 0.75994 | 0.018064 |
| b | 4.6785 | -3.0139 | 1.1828 | 0.3275 |
| c | -2.8833 | -4.1833 | 0.36585 | -0.26849 |
| d | 0.0030502 | -6.3714 | 1.1076 | 0.26773 |
| e | 4.6786 | -6.2095 | 1.7043 | 0.70199 |
| f | -2.8833 | -5.6746 | 0.60922 | -0.09373 |
| g | 12.459 | -33.259 | 3.1572 | 1.6569 |
| h | 1.0988 | 6.9789 | 1.025 | 0.2953 |
| i | 10.842 | -29.584 | 2.8837 | 1.3729 |
| j | 8.9198 | -21.392 | 2.5027 | 1.2033 |

Table 3.14 : Pole Placement Feedback Gains

| Solution | Strut Defl. Compensation | Strut Vel. Compensation |
|---|---|---|
| a | 100(s + 1)/(s + 100) | - |
| b | (s + 10) | - |
| c | (s + 1) | - |
| d | - | 0.01(s + 100) |
| e | - | 0.02(s + 100) |
| f | - | (s + 10)/s |
| g | - | 0.01(s + 10)(s + 100)/s |
| h | 50(s + 1)/(s + 100) | 0.005(s + 100) |
| i | 0.5(s + 1) | 0.005(s + 100) |

Table 3.15 : Frequency Domain Compensators

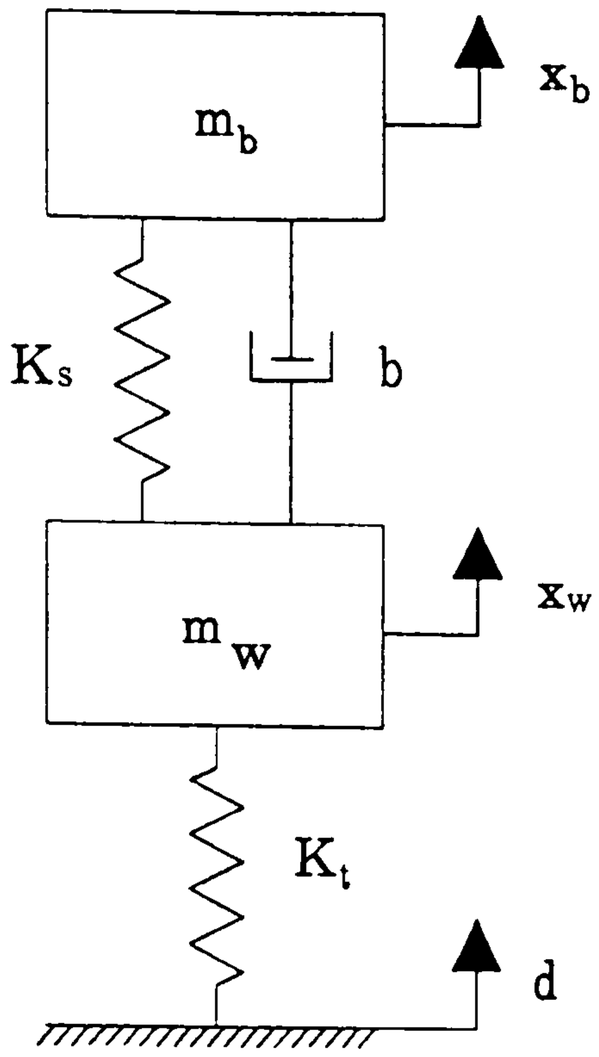


Figure 3.1 : Two Degree of Freedom Quarter Car Model

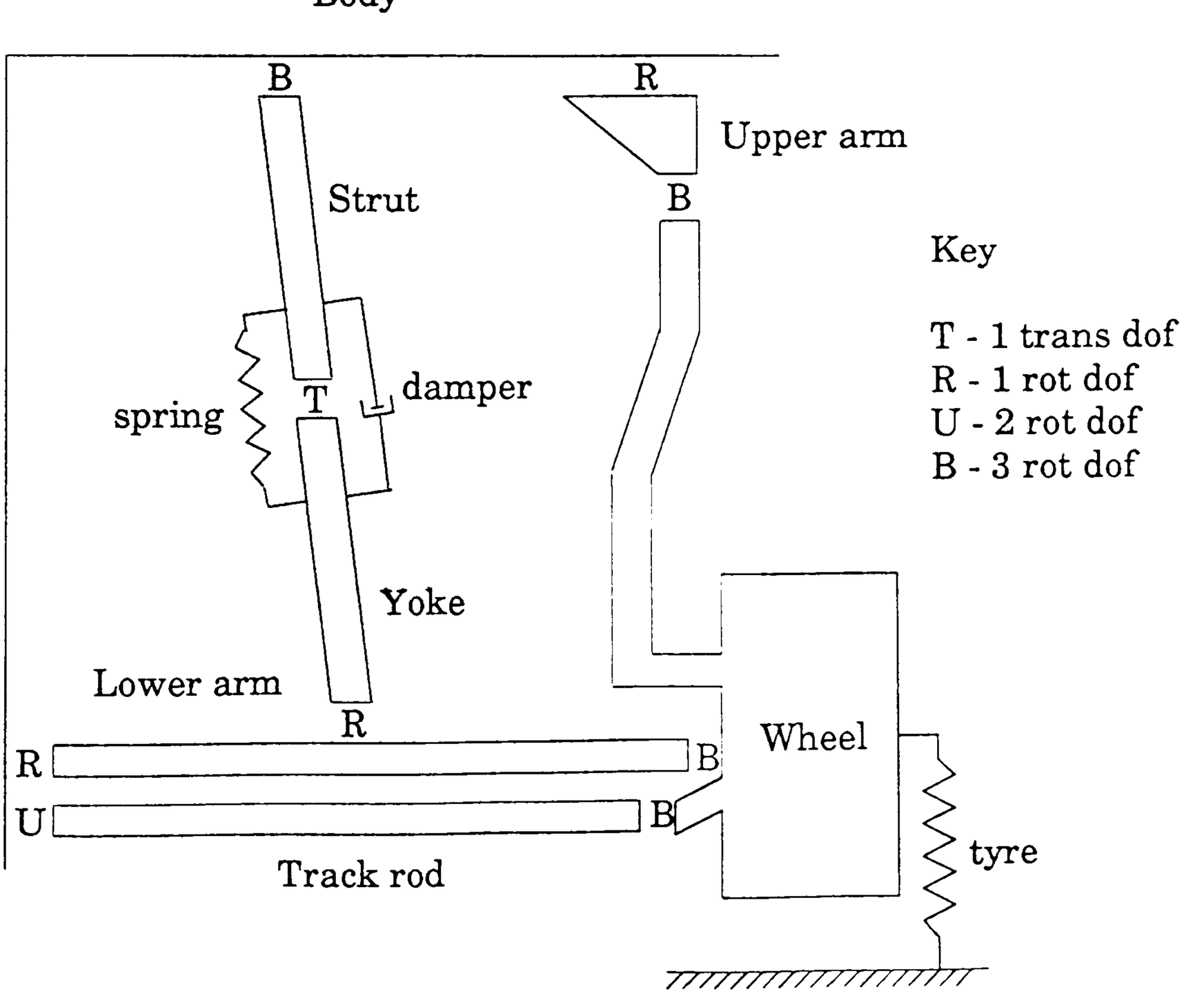


Figure 3.2 : Front Quarter Car Model

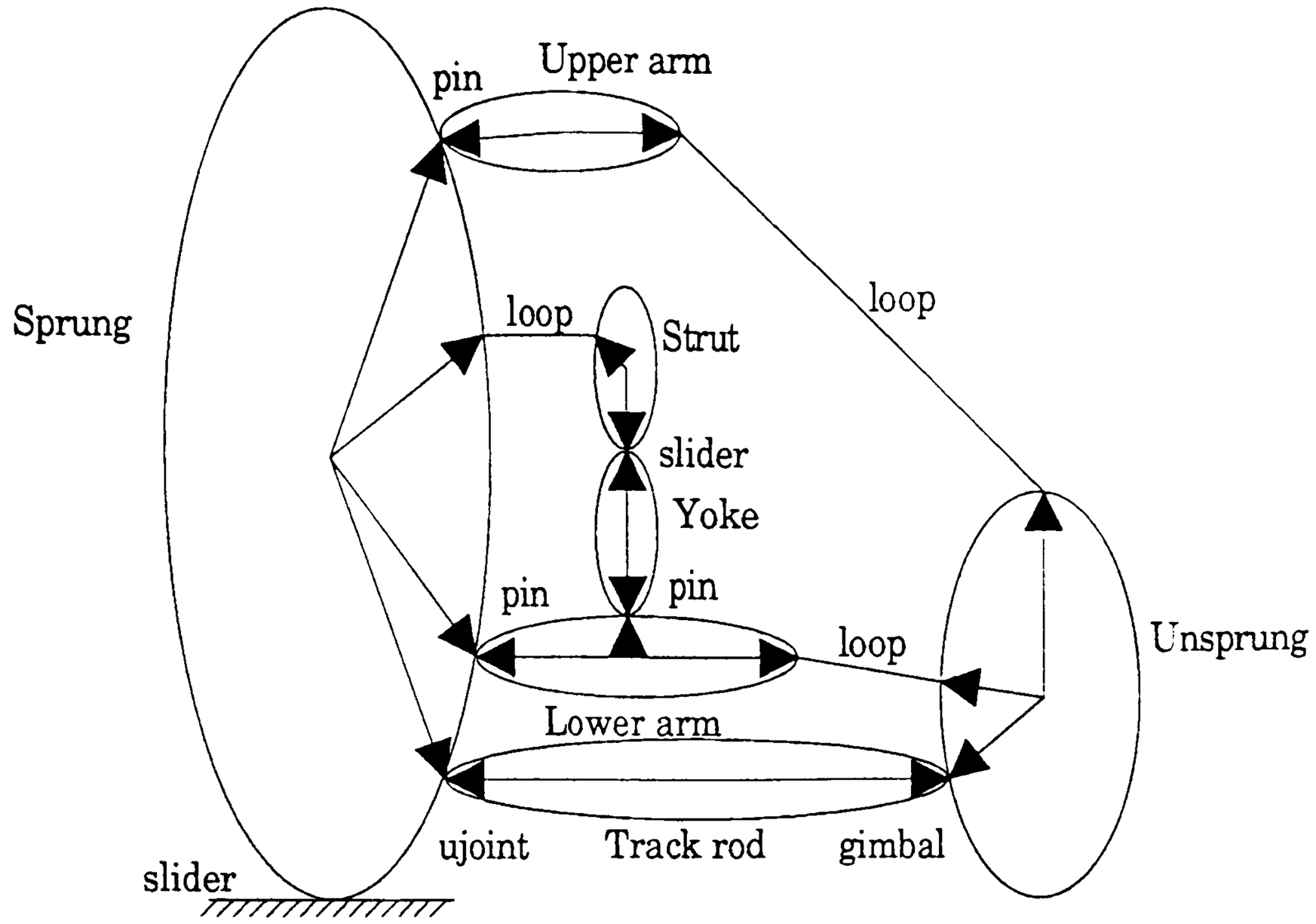


Figure 3.3 : Tree and Constraint Topology

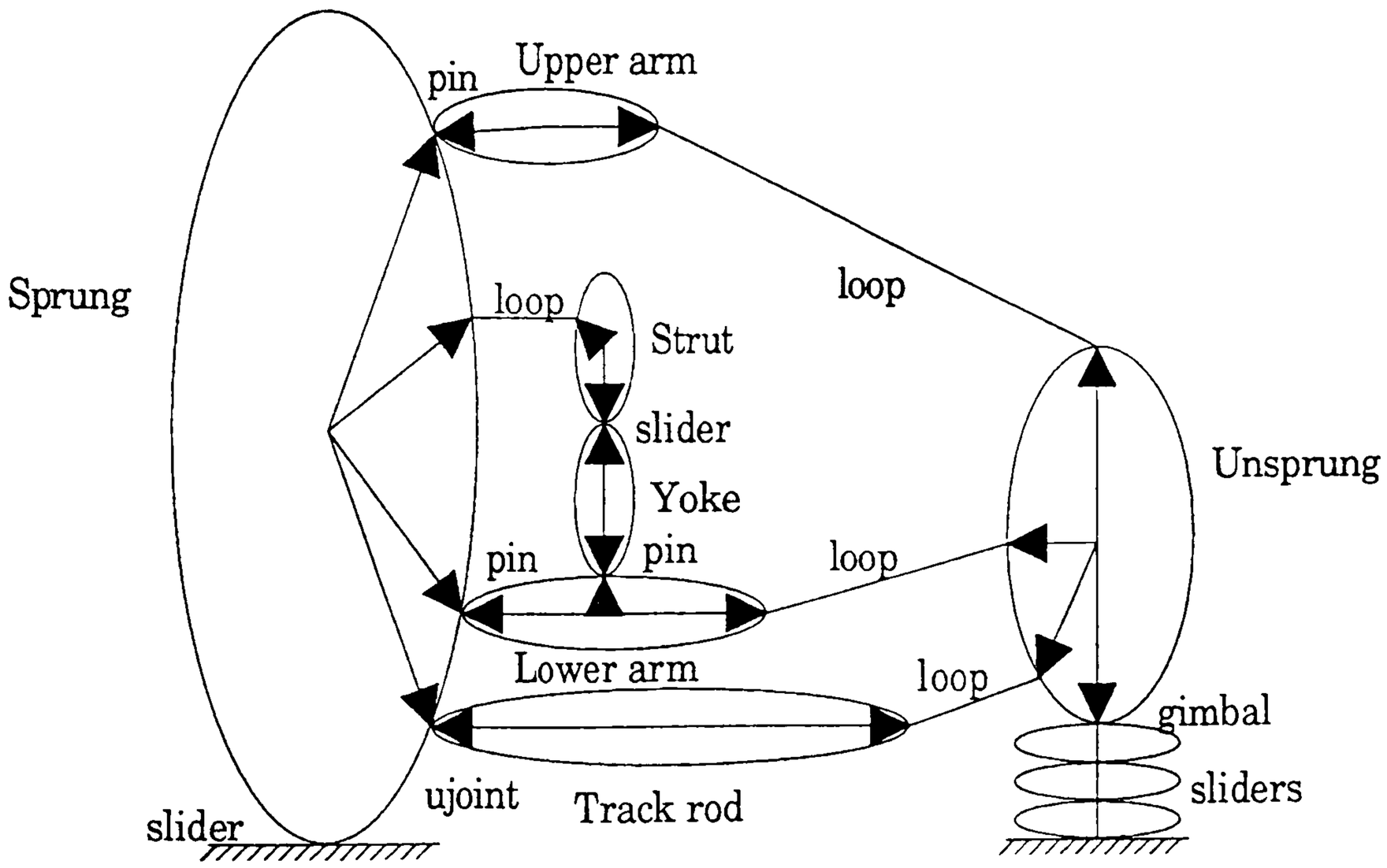


KEY

| | |
|---|---|
| pin | - 1 rot. dof. joint |
| ujoint | - 2 rot. dof. joint |
| gimbal | - 3 rot. dof. joint |
| slider | - 1 trans. dof. joint |
| loop | - 3 rot. dof. constraint |

Figure 3.4 : Topology with Extra Joints to Ground

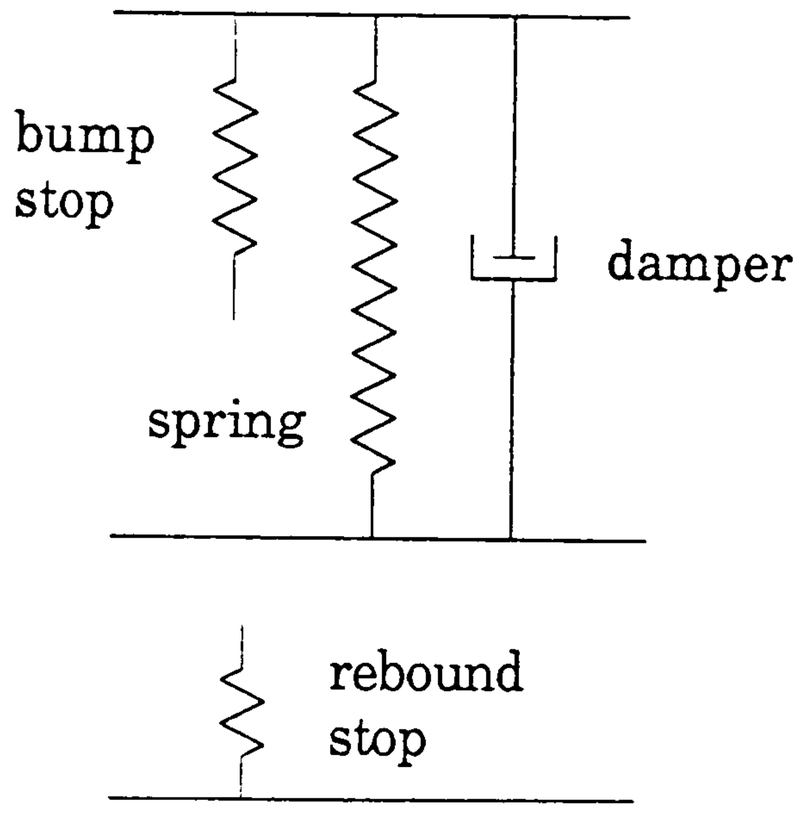


Figure 3.5 : Suspension Compliance and Damping

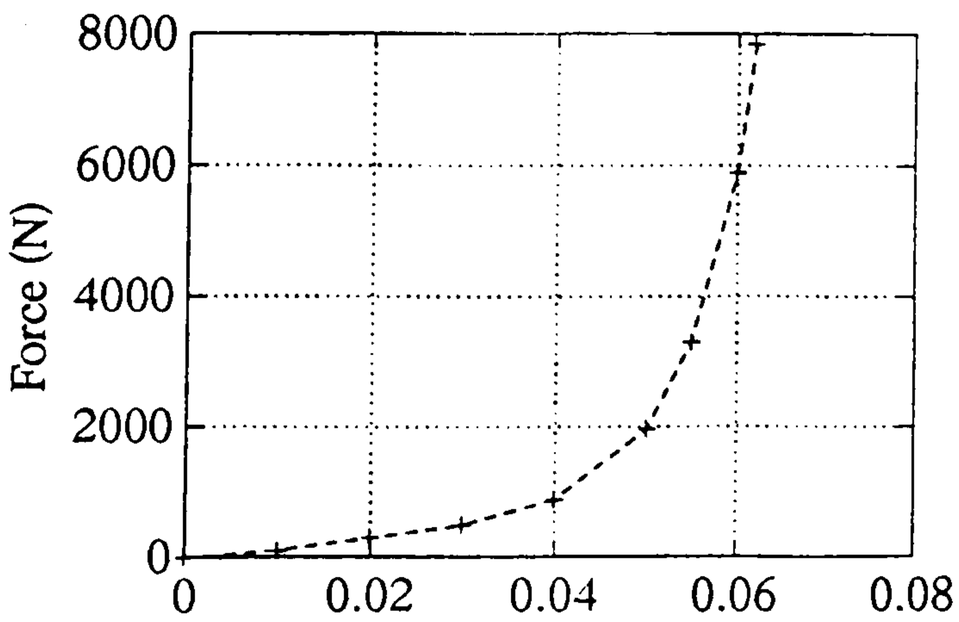


Figure 3.6 : Front Spring Aid Characteristic

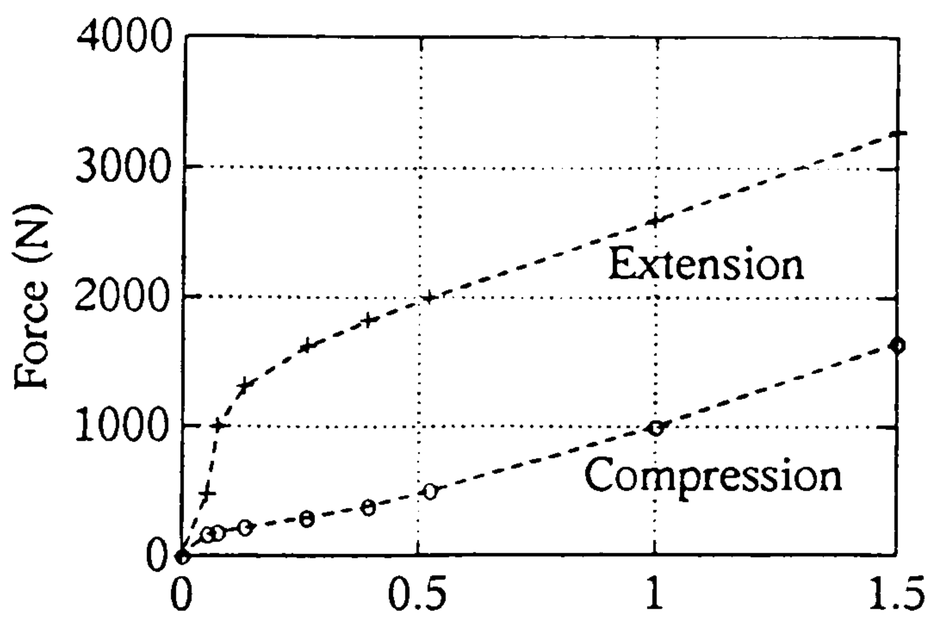


Figure 3.7 : Front Damping Characteristic

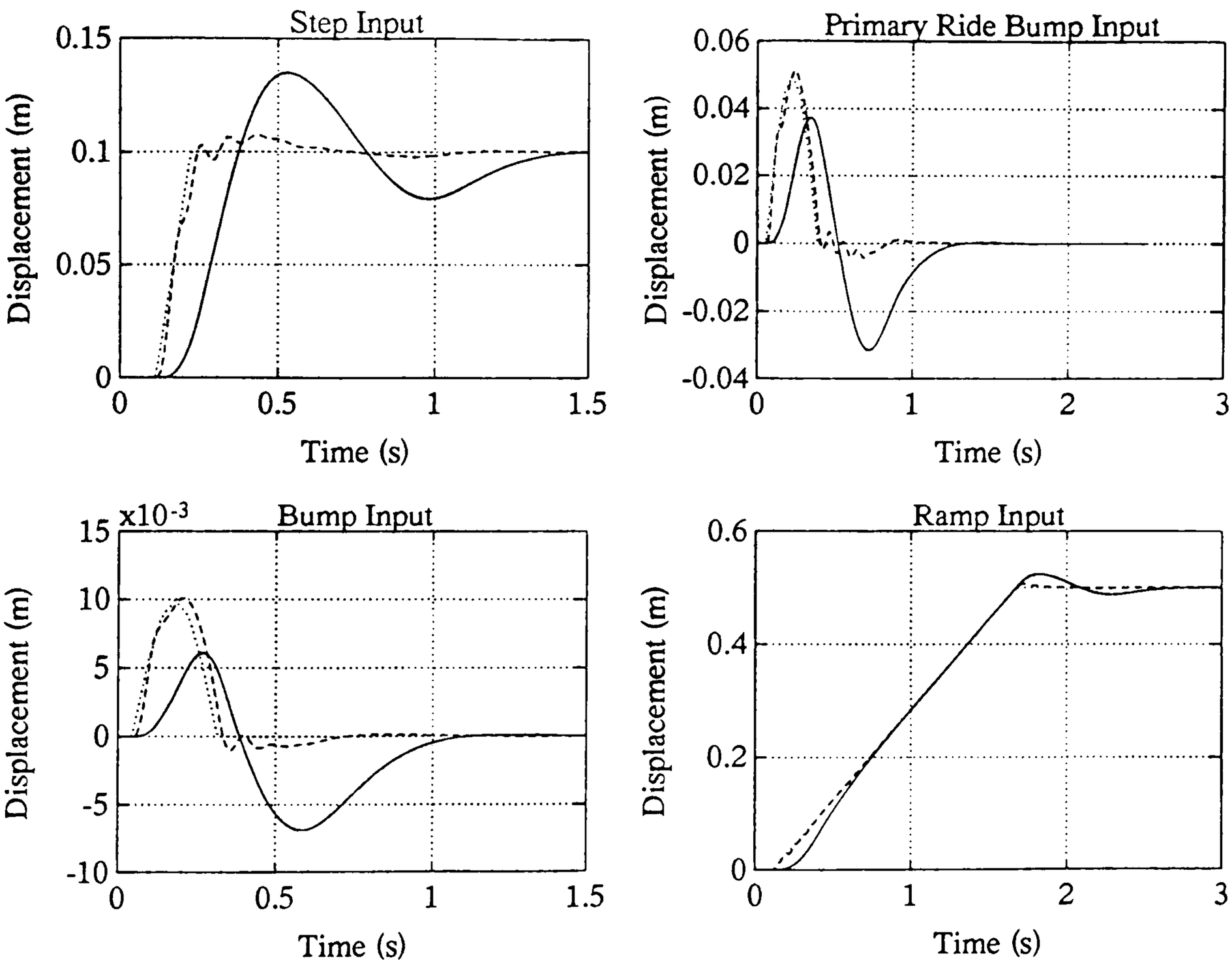


Figure 3.8 : Non-Linear Passive Model Ride Simulations

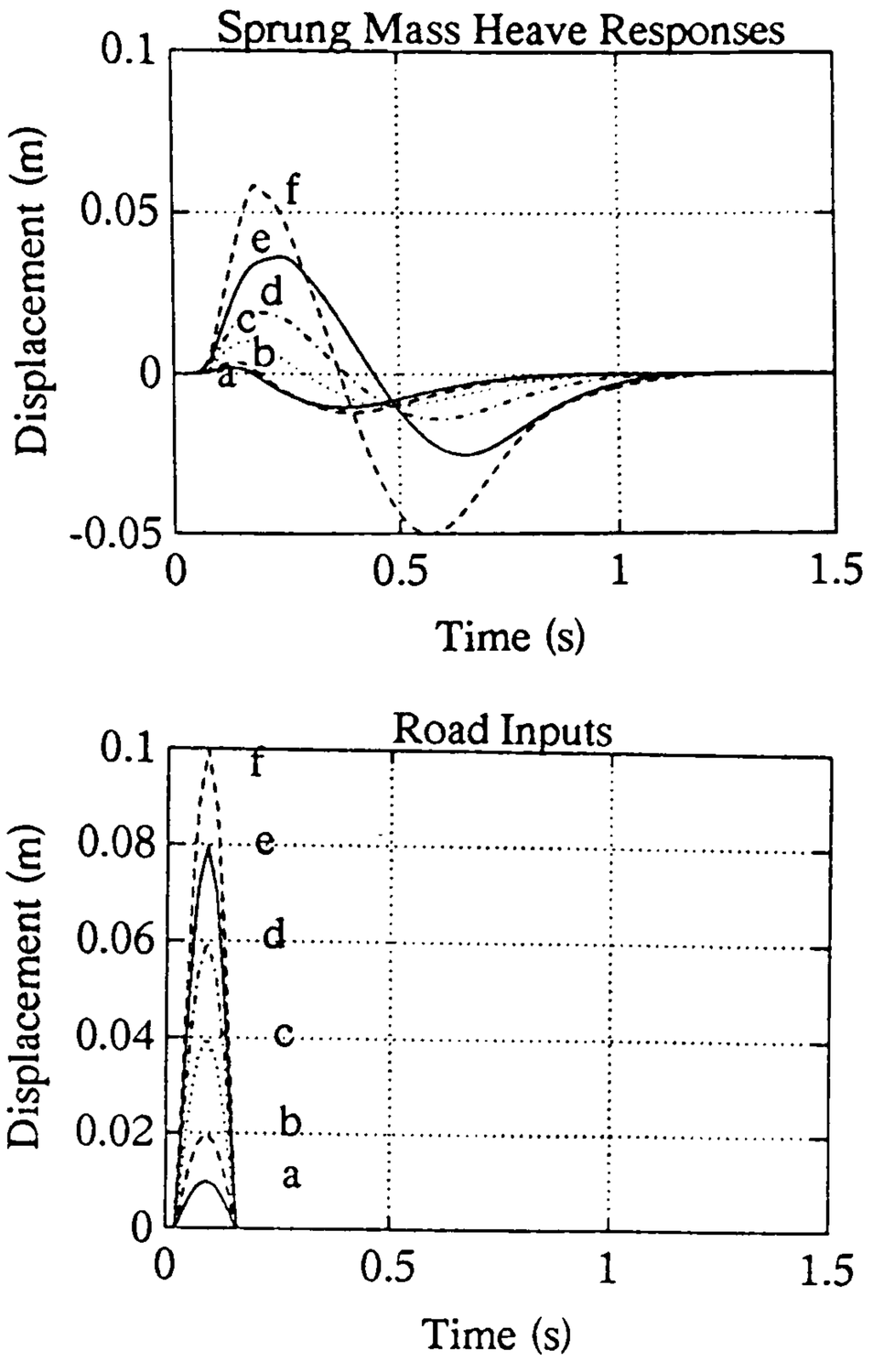


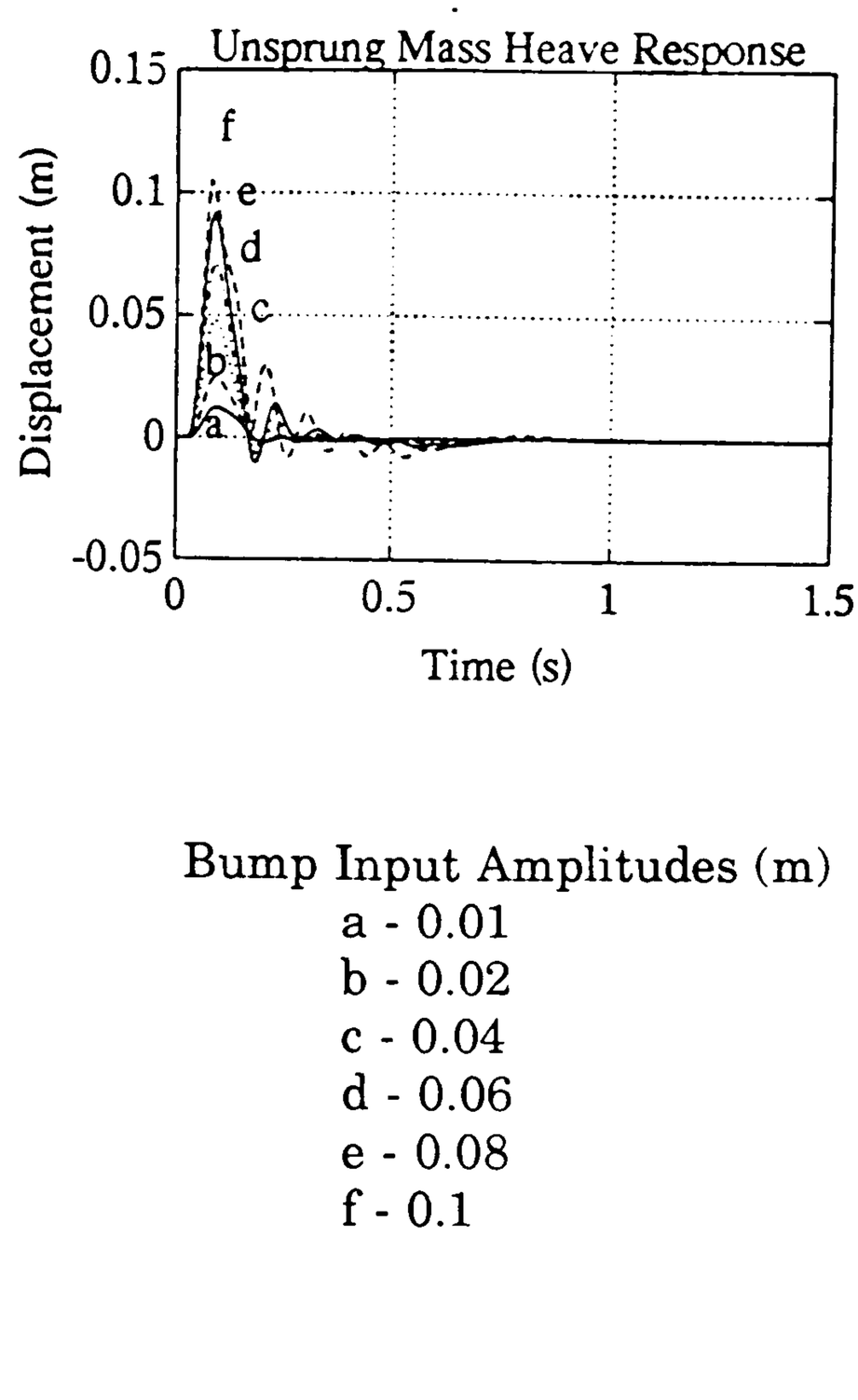


Bump Input Amplitudes (m)

a - 0.01
b - 0.02
c - 0.04
d - 0.06
e - 0.08
f - 0.1

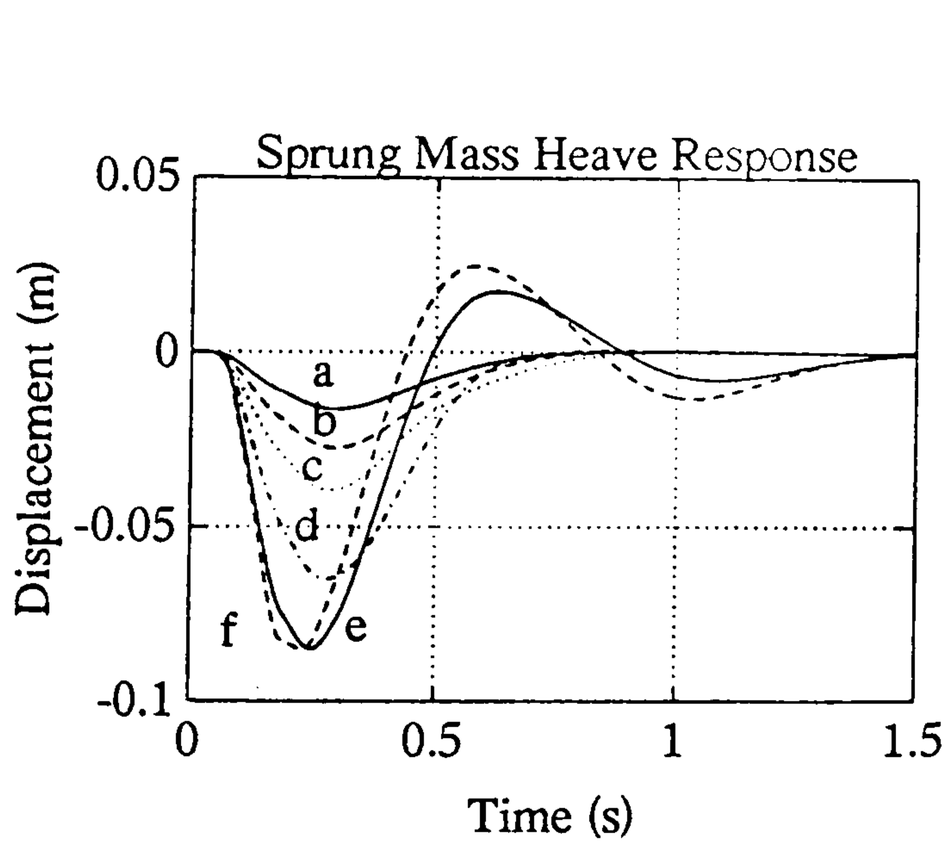


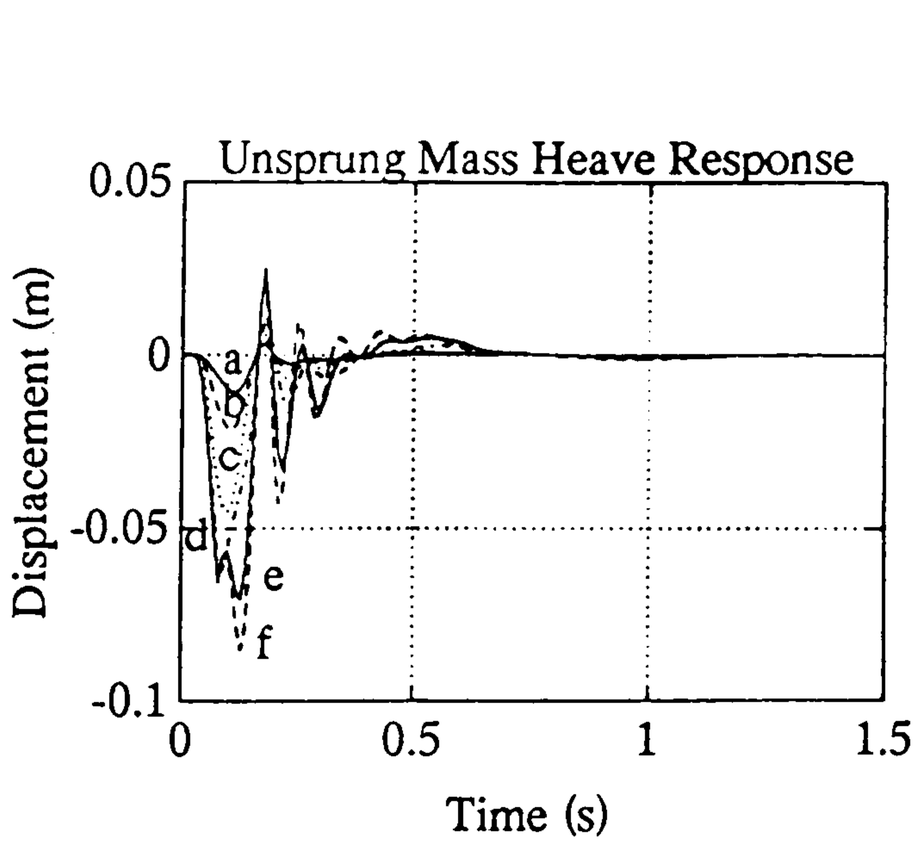


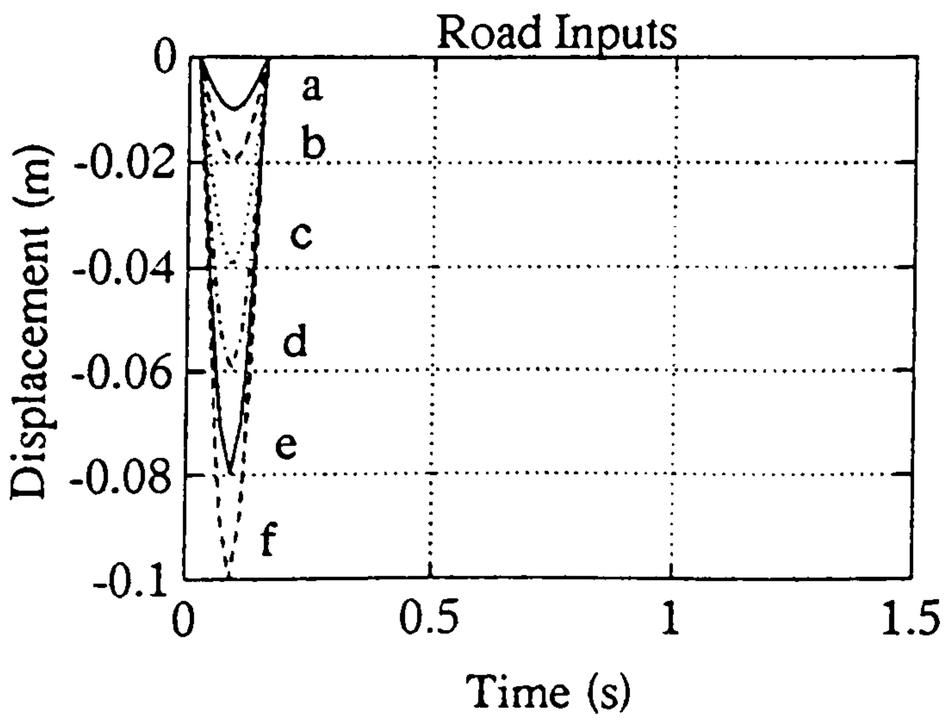


Pothole Input Amplitudes (m)

a - 0.01
b - 0.02
c - 0.04
d - 0.06
e - 0.08
f - 0.1

Figure 3.9 : Model Linearity Results with Non-Linear Damping

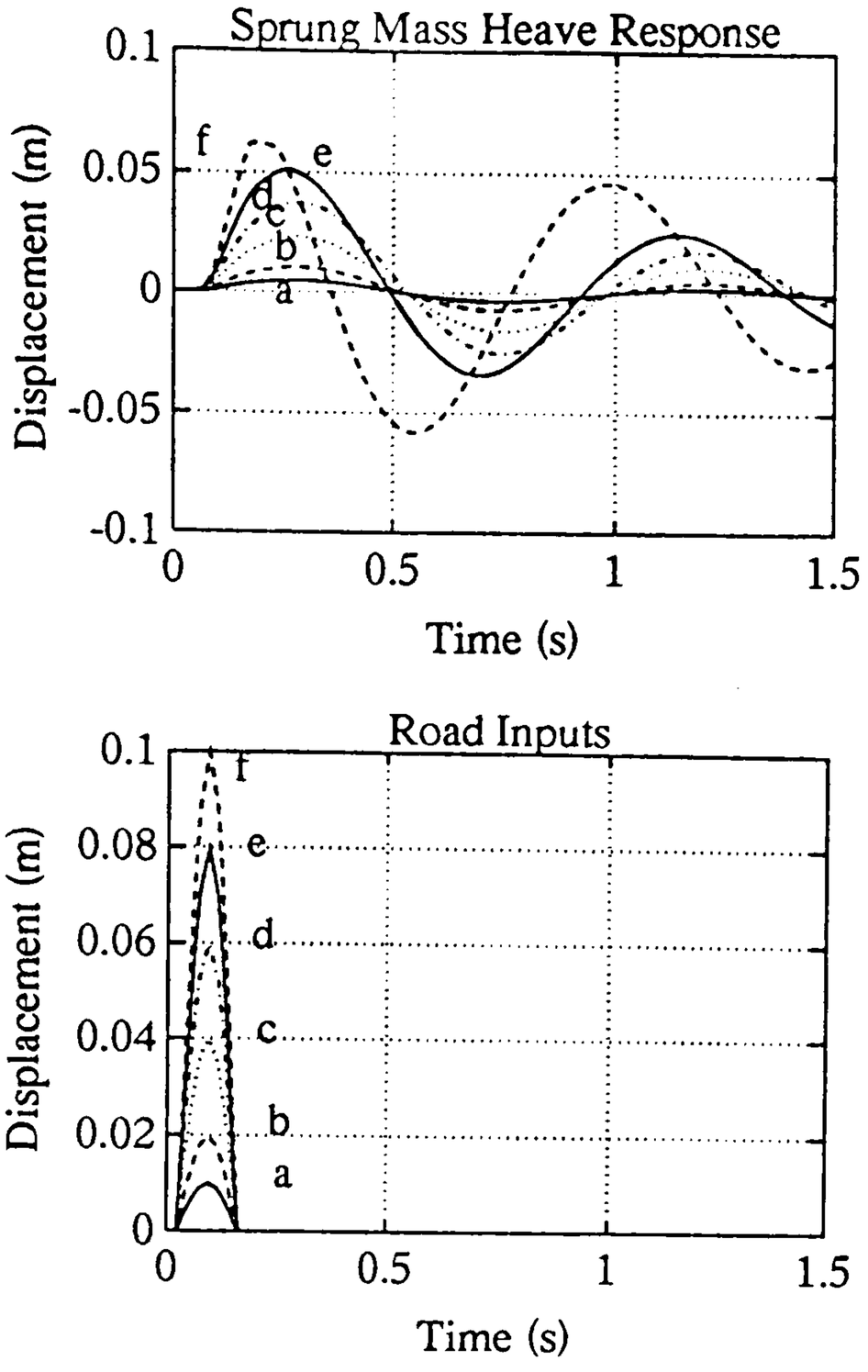


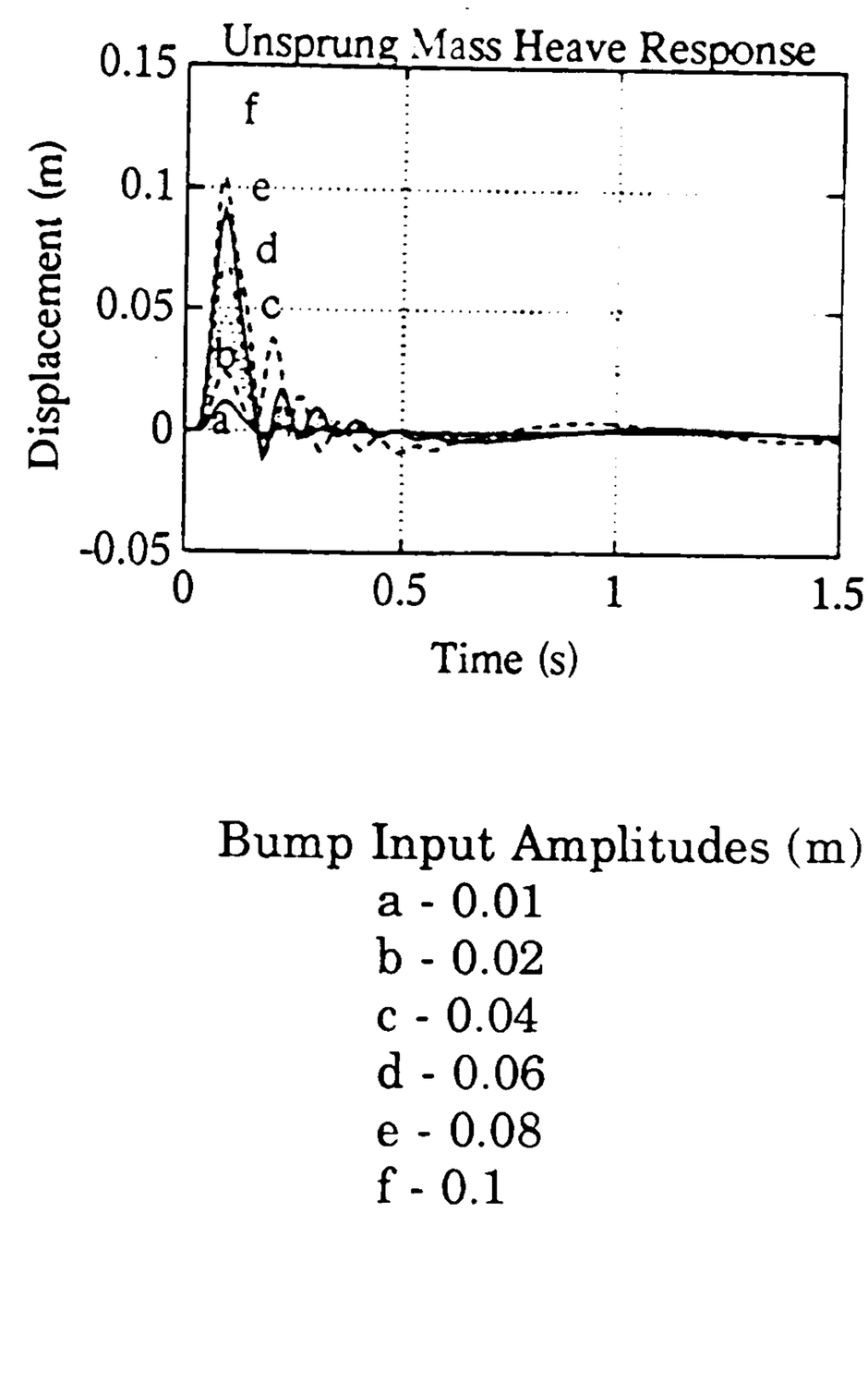


Bump Input Amplitudes (m)

a - 0.01
b - 0.02
c - 0.04
d - 0.06
e - 0.08
f - 0.1

Pothole Input Amplitudes (m)

a - 0.01
b - 0.02
c - 0.04
d - 0.06
e - 0.08
f - 0.1

Figure 3.10 : Model Linearity Results with Linear Damping

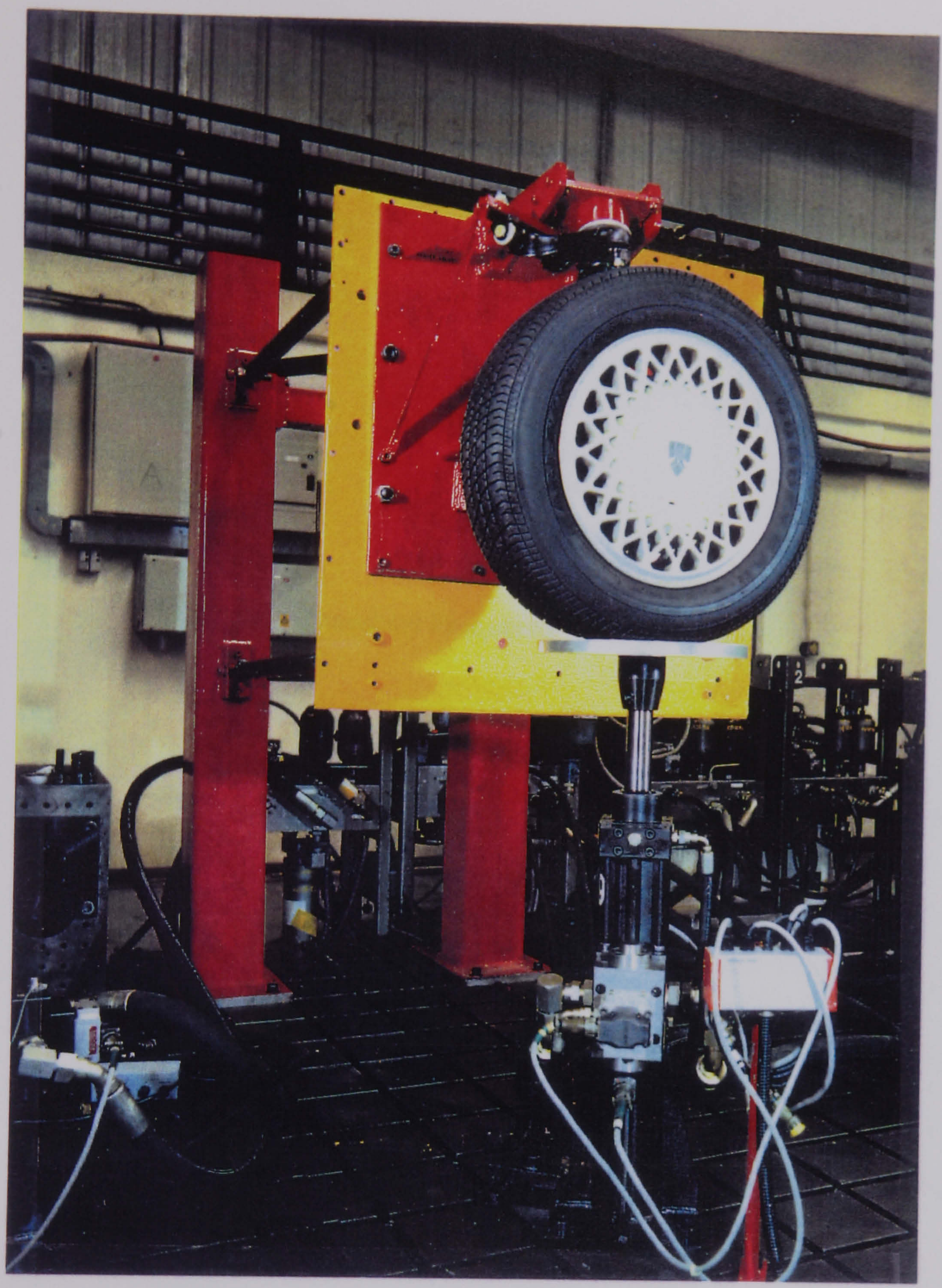

Figure 3.11 : Suspension Test Rig

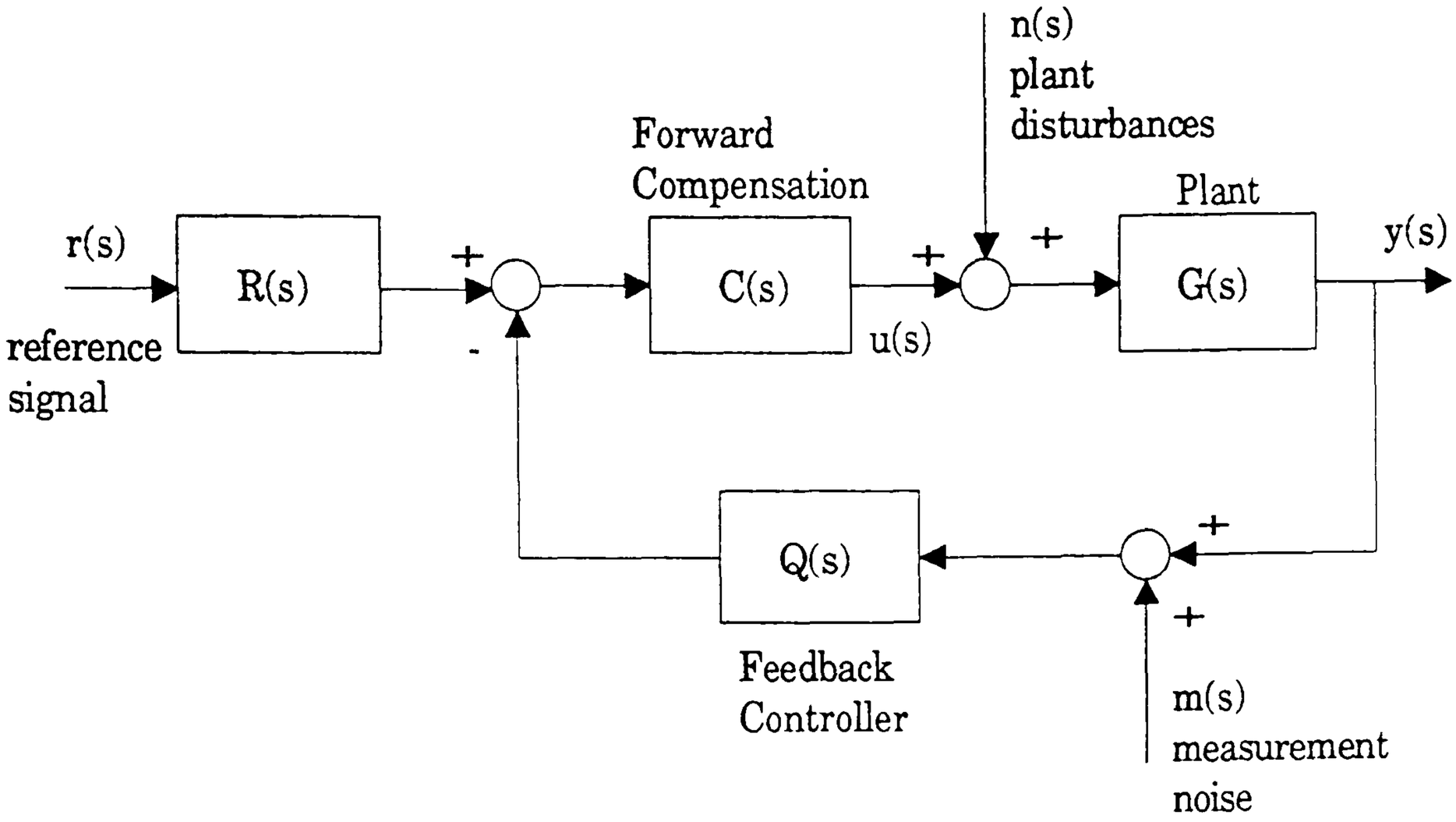


Figure 3.12 : Standard Frequency Domain System

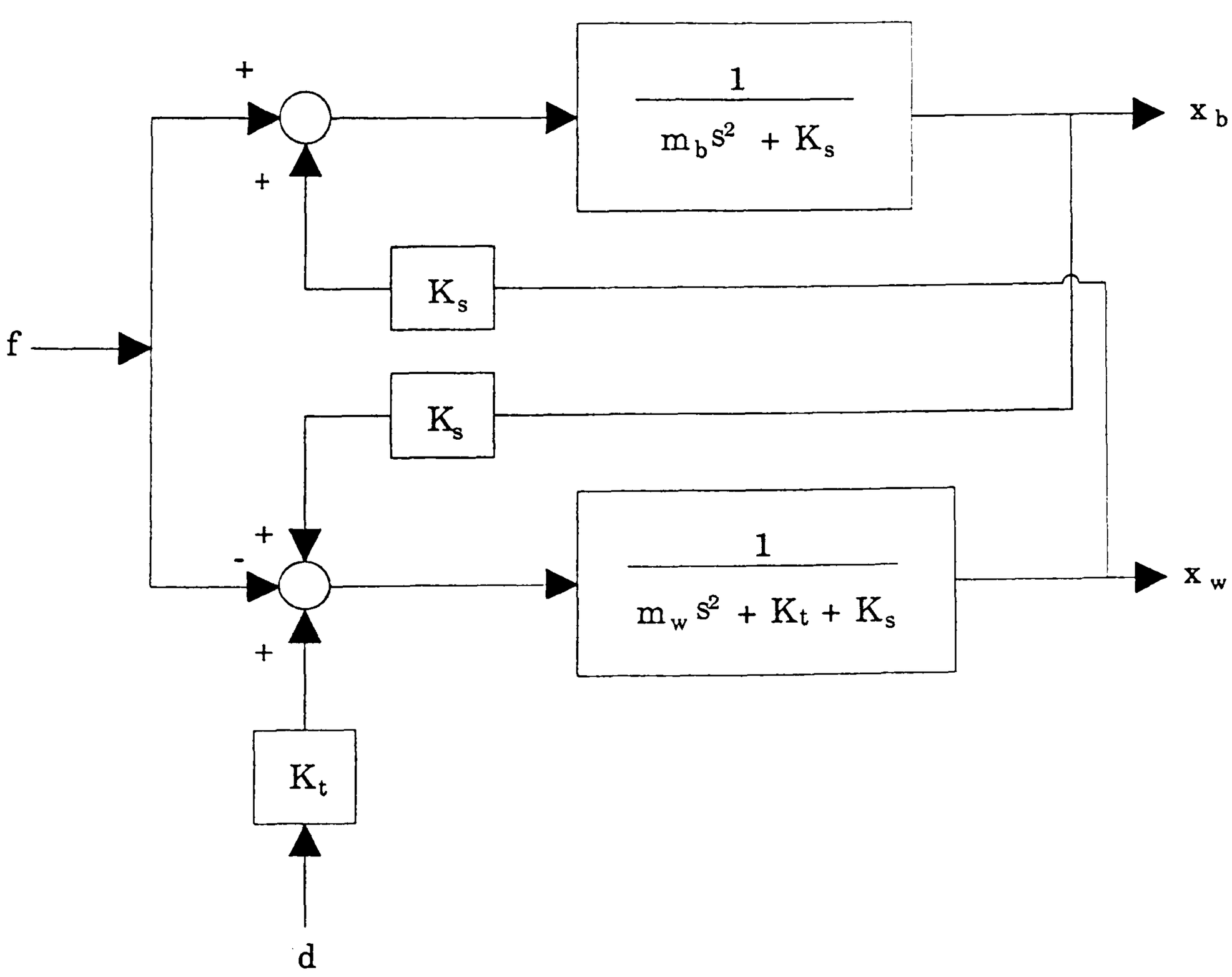


Figure 3.13 : Block Diagram for Two Degree of Freedom Model

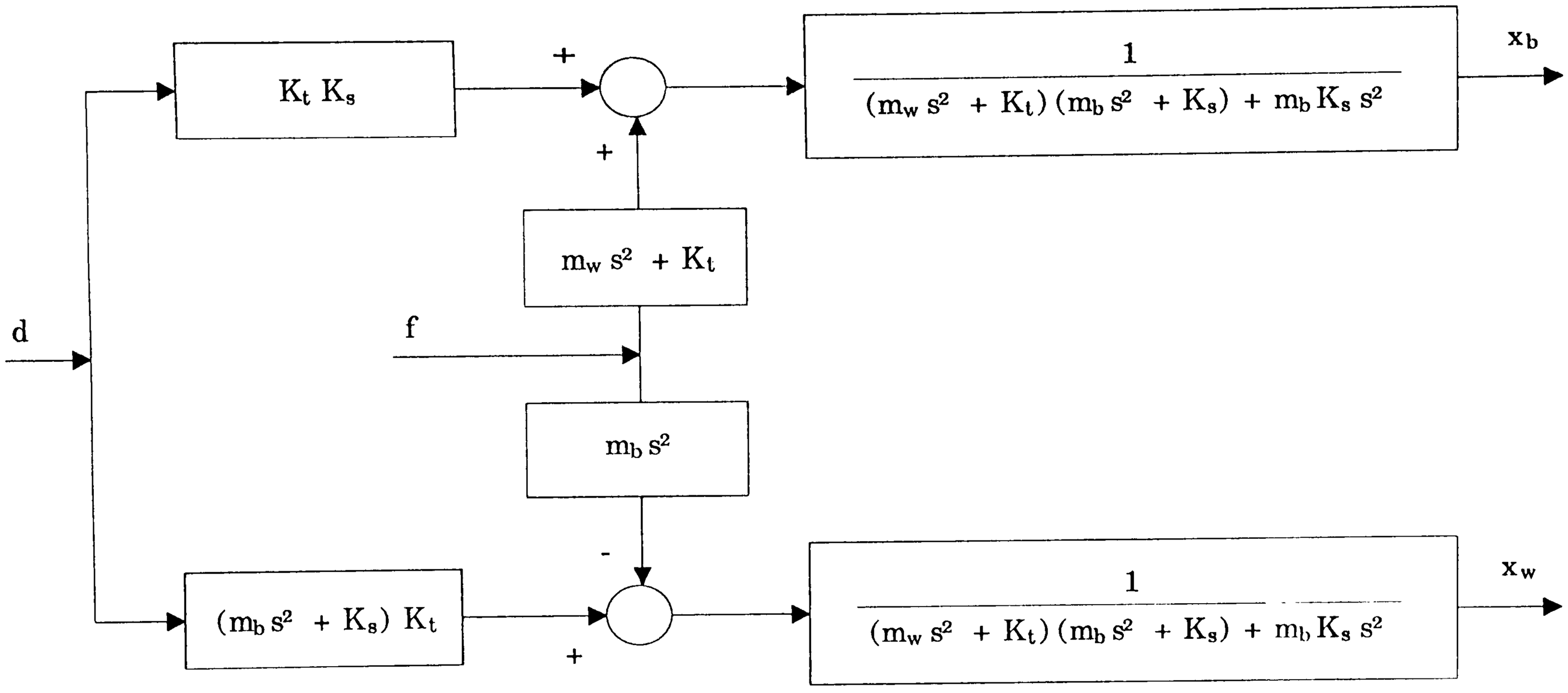


Figure 3.14 : Equivalent Block Diagram Structure

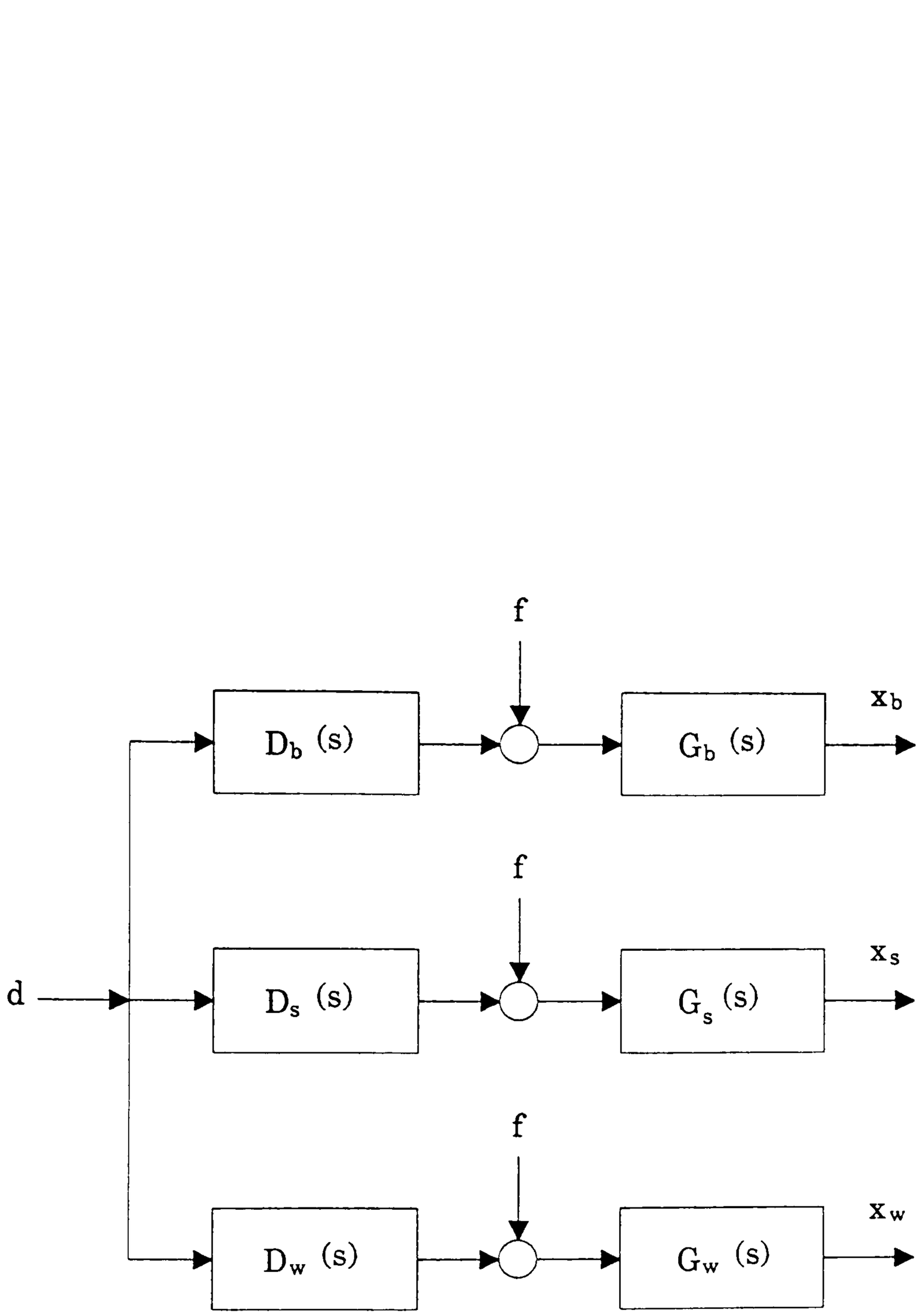


Figure 3.15 : Block Diagram for Front Quarter Car Model

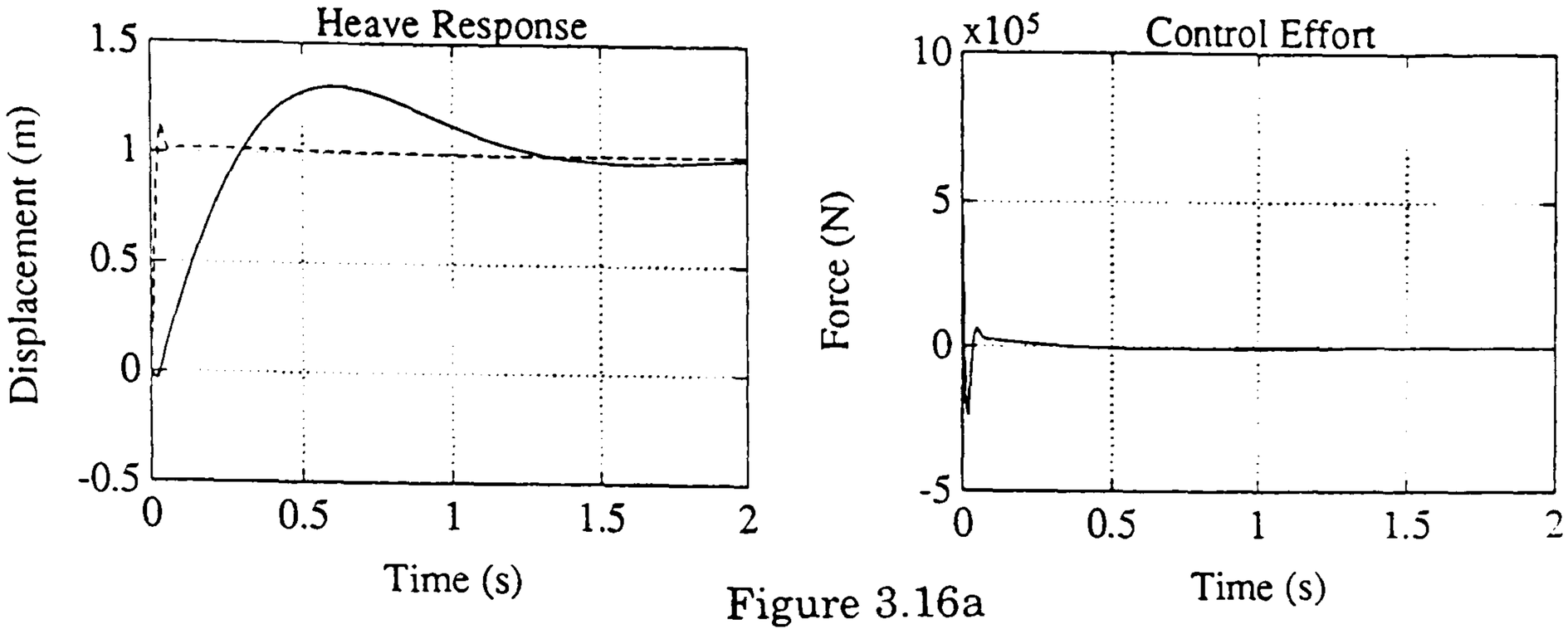


Figure 3.16a

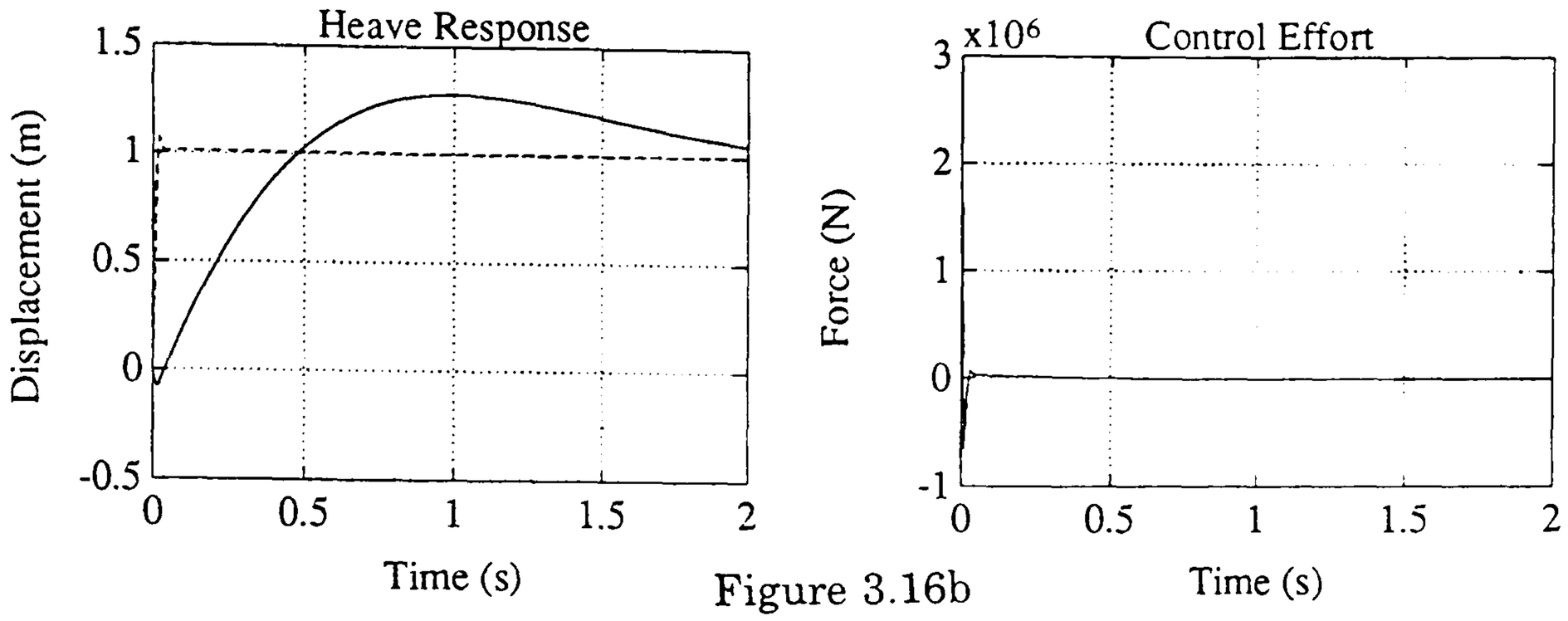


Figure 3.16b

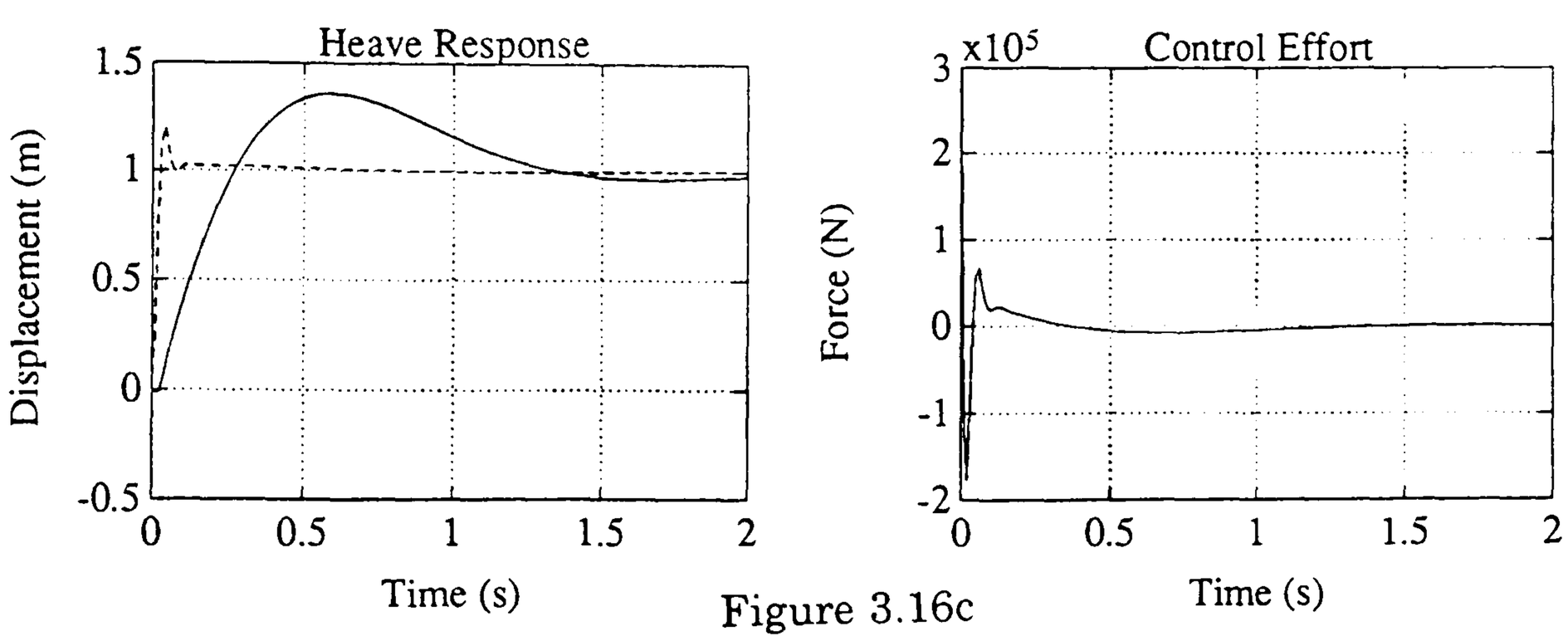


Figure 3.16c

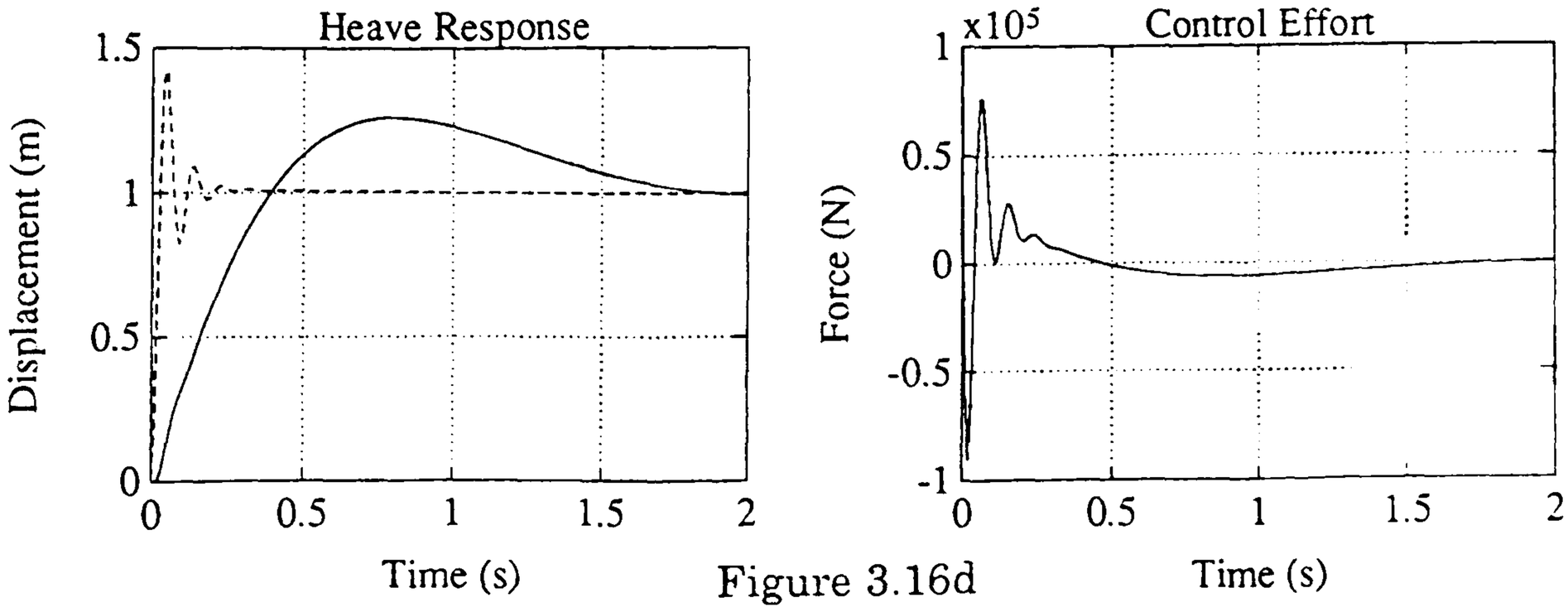


Figure 3.16d

Figure 3.16 : Linear Quadratic Regulator Solutions

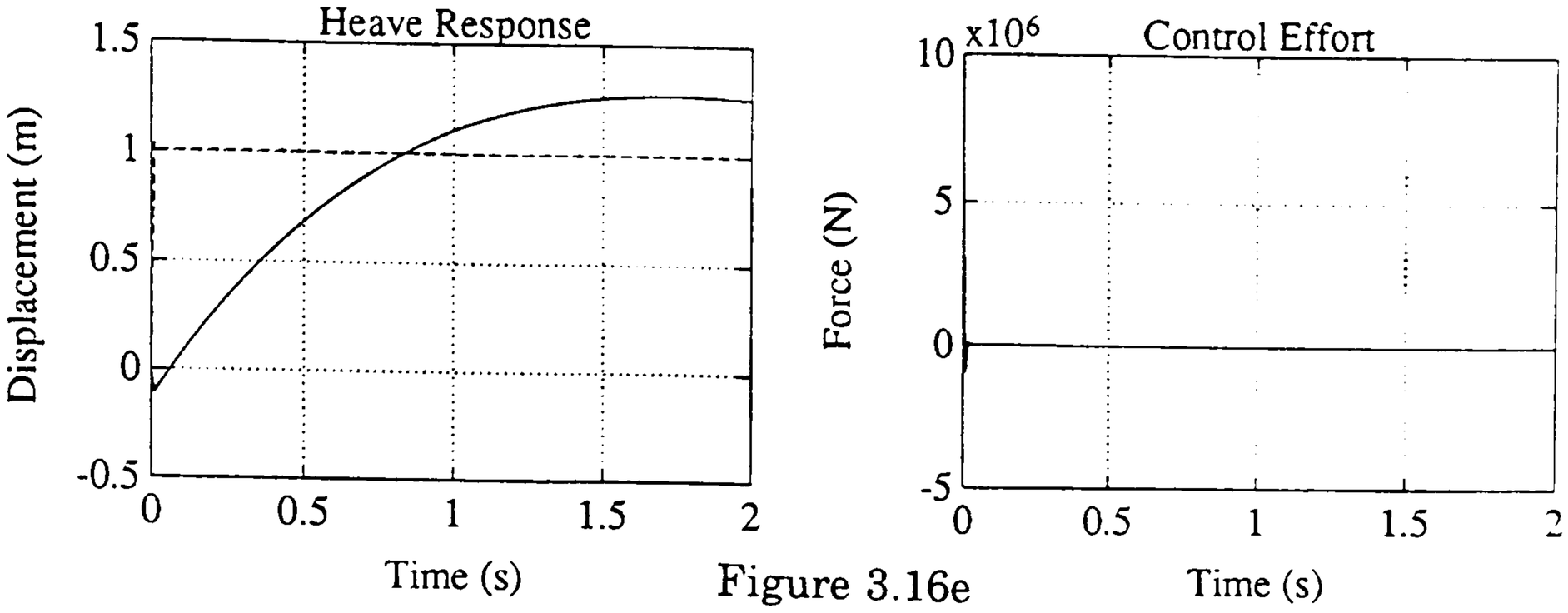


Figure 3.16e

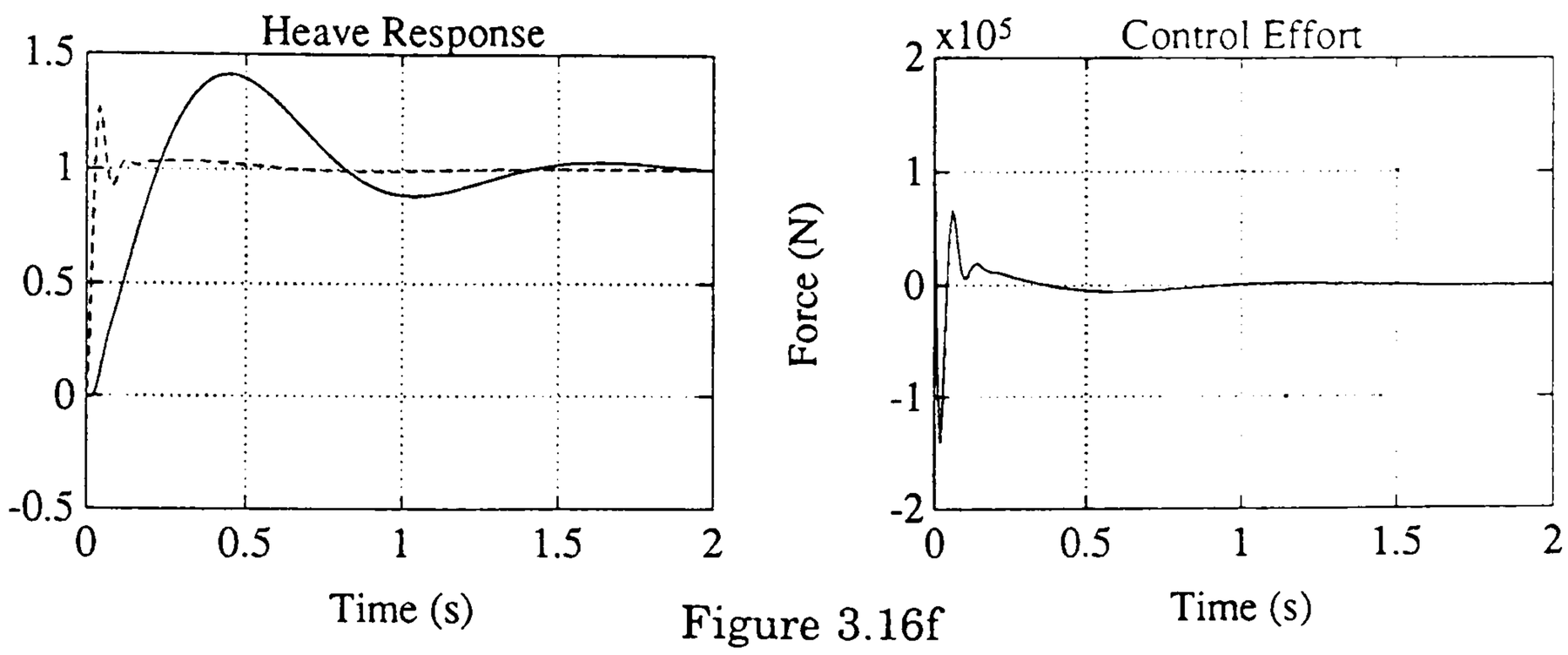


Figure 3.16f

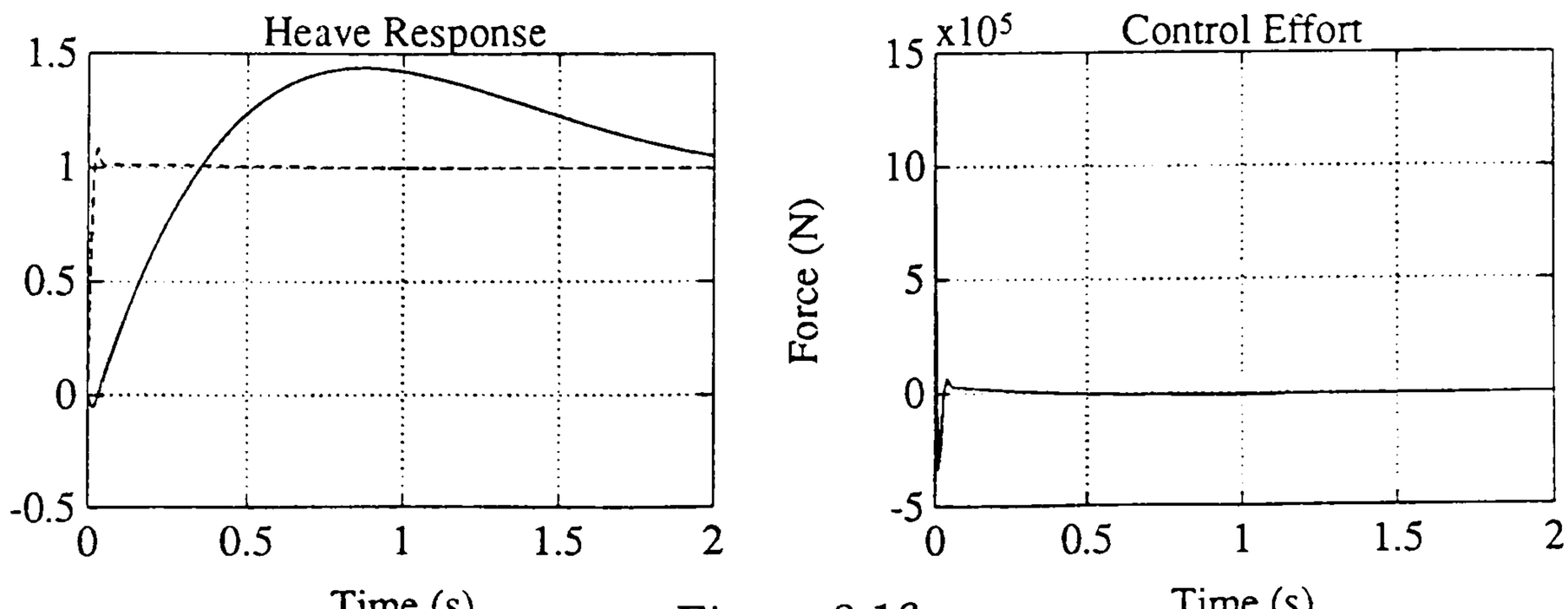


Figure 3.16g

Figure 3.16 (continued)

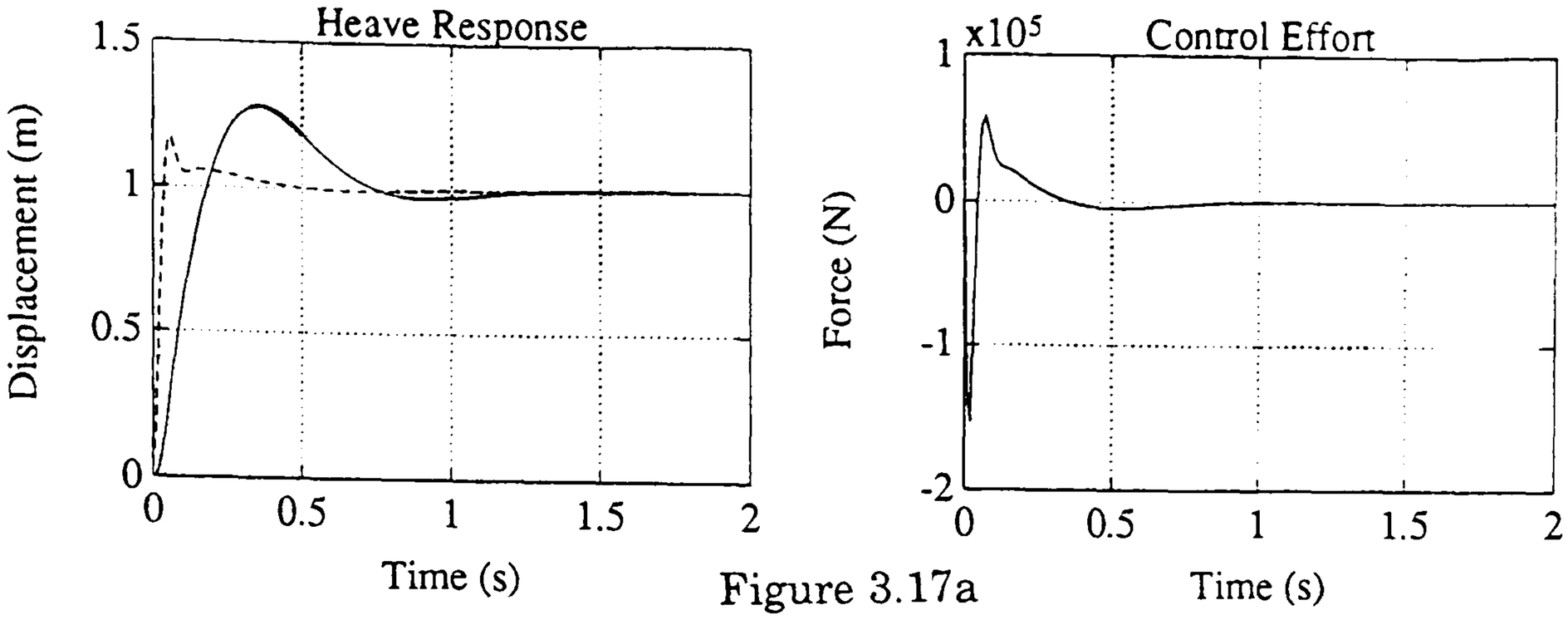


Figure 3.17a

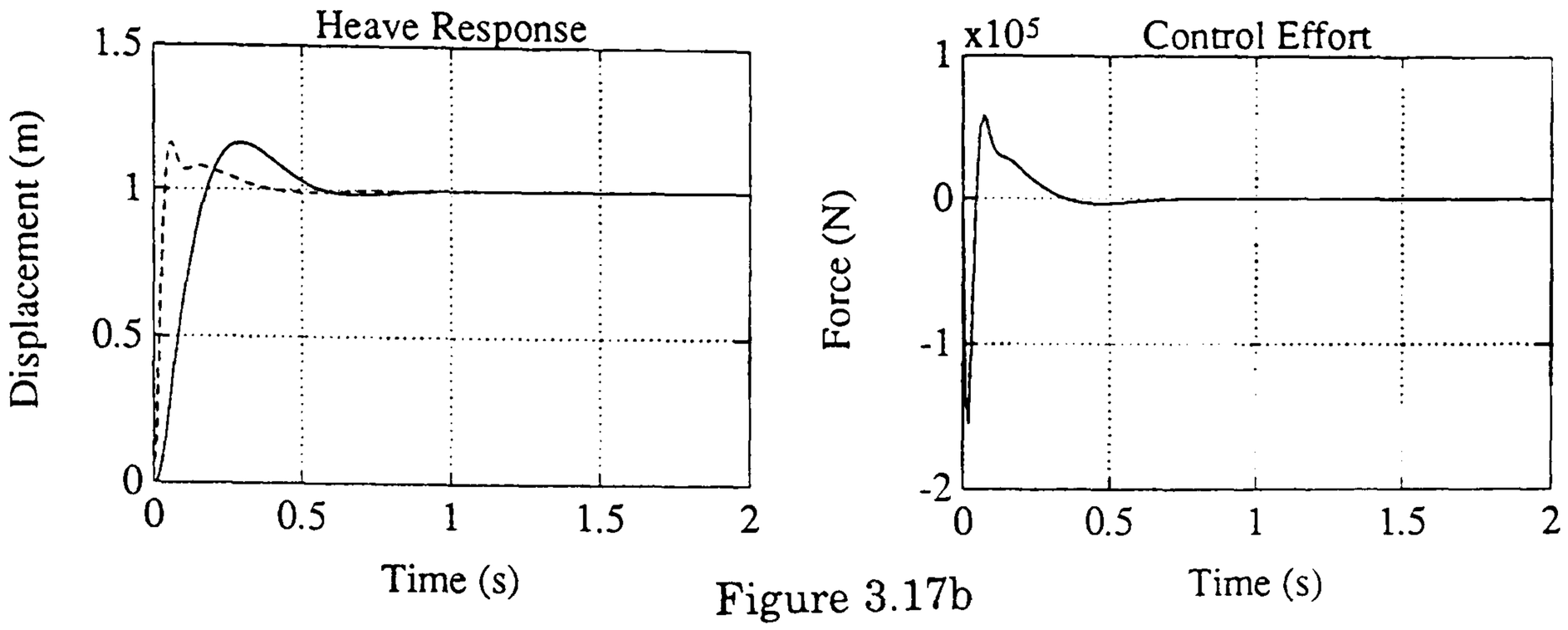


Figure 3.17b

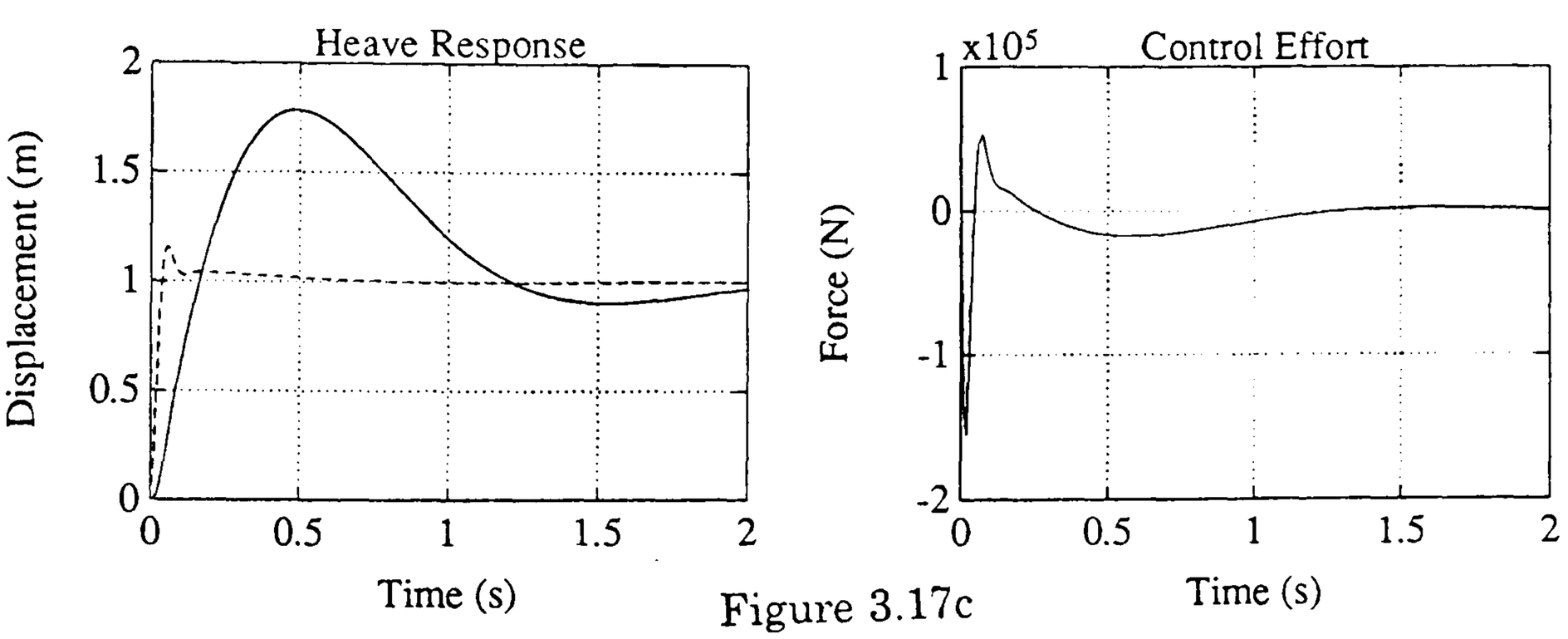


Figure 3.17c

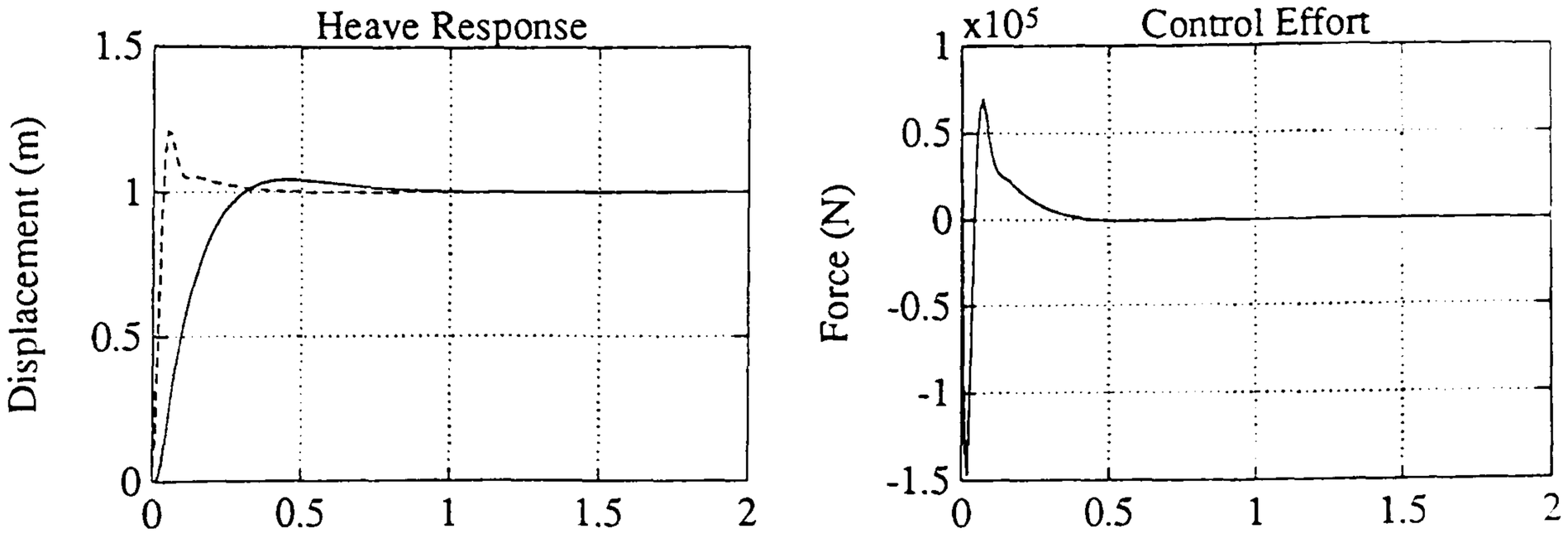


Figure 3.17d

Figure 3.17 : Pole Placement Solutions

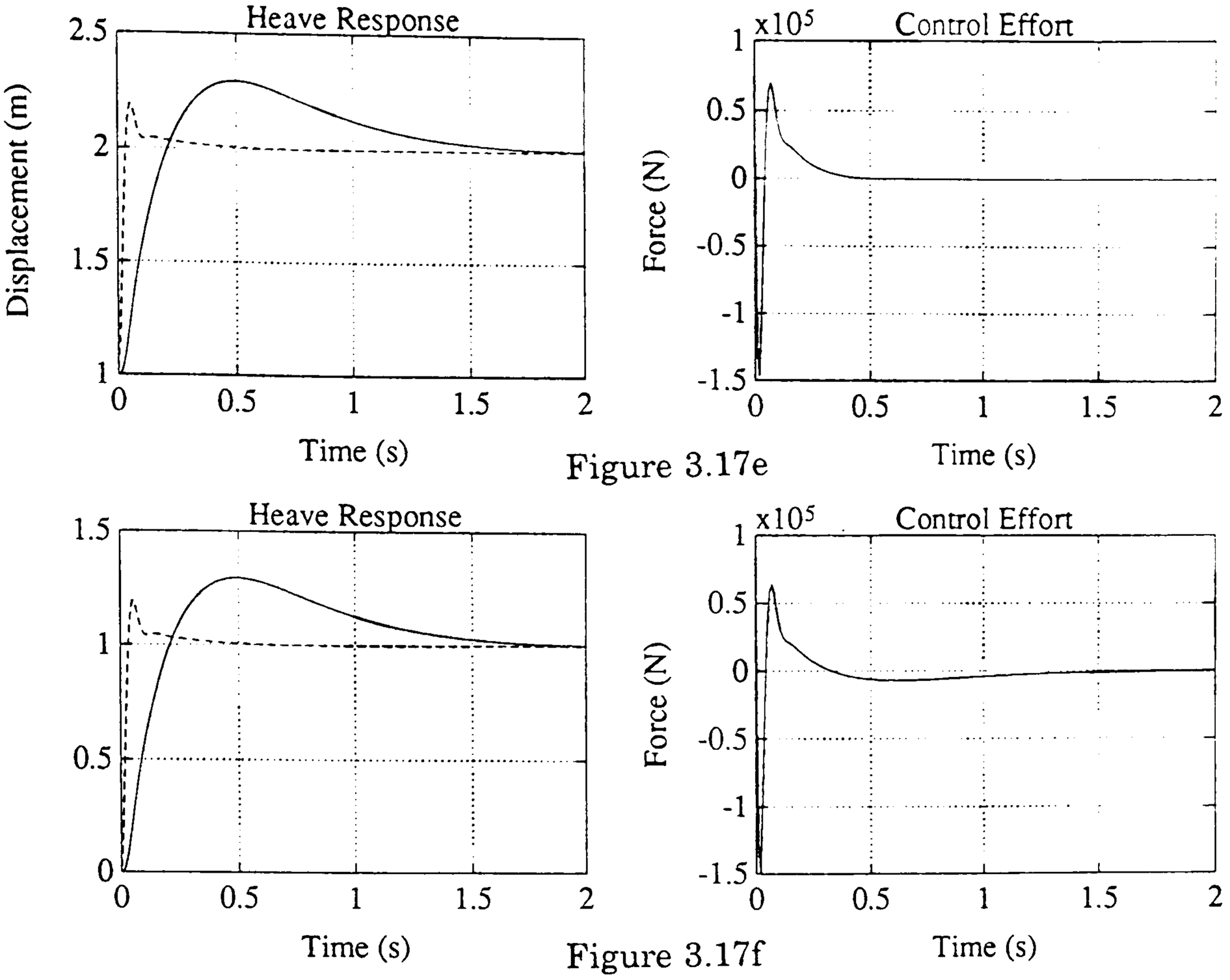


Figure 3.17e




Figure 3.17f

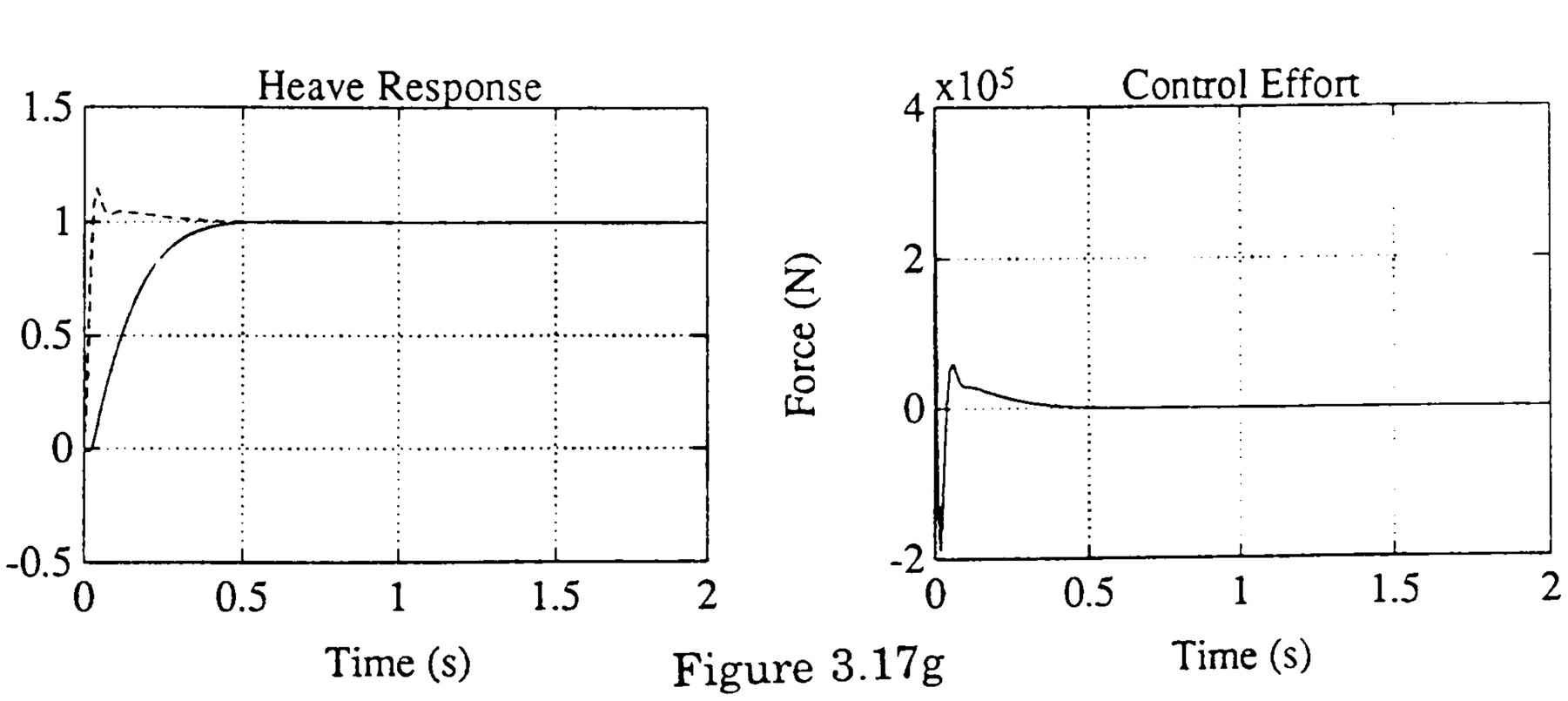


Figure 3.17g

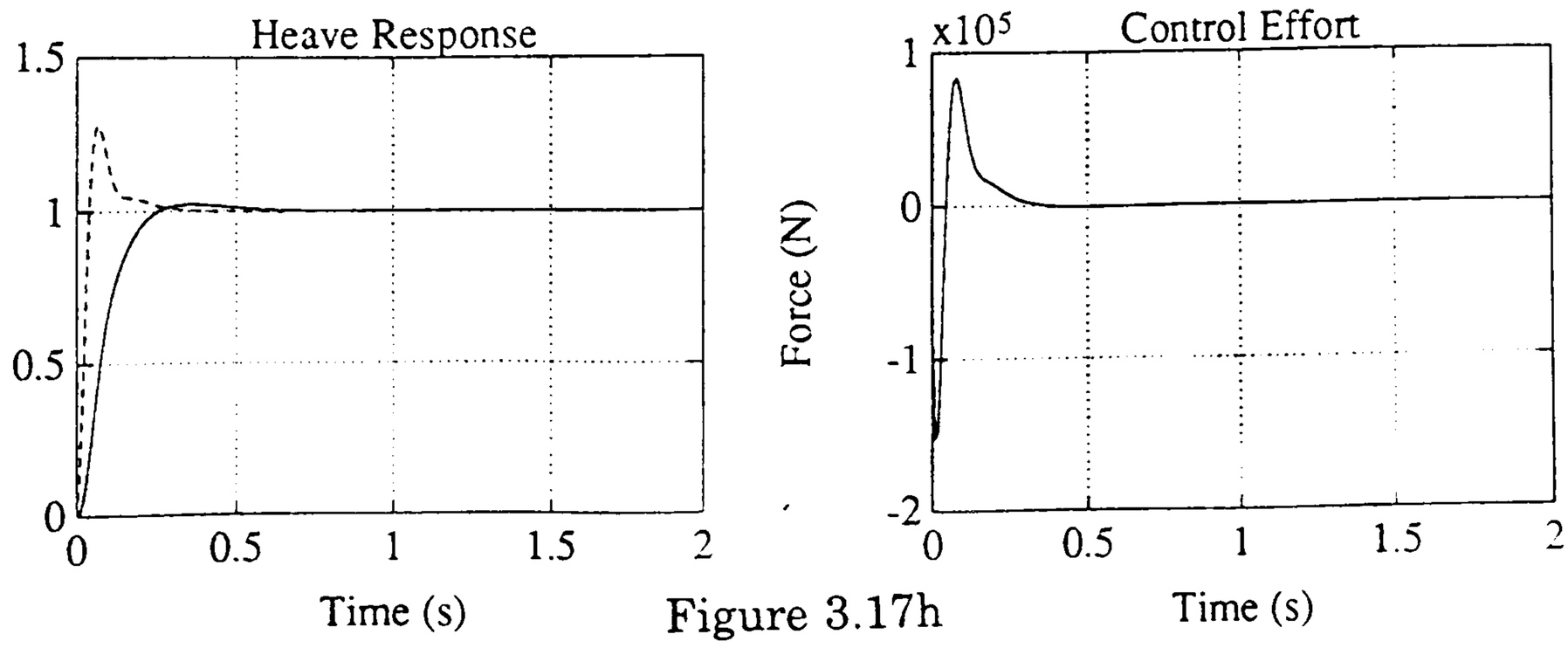


Figure 3.17h

Figure 3.17 (continued)

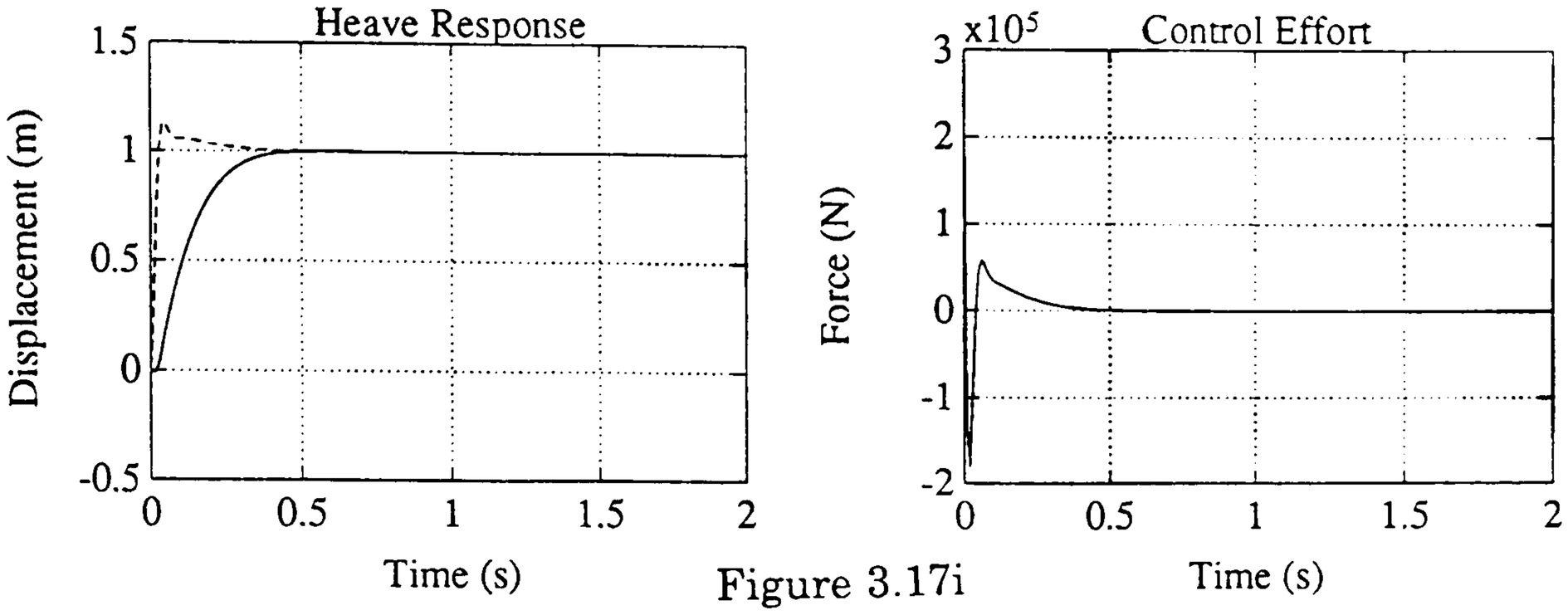


Figure 3.17i

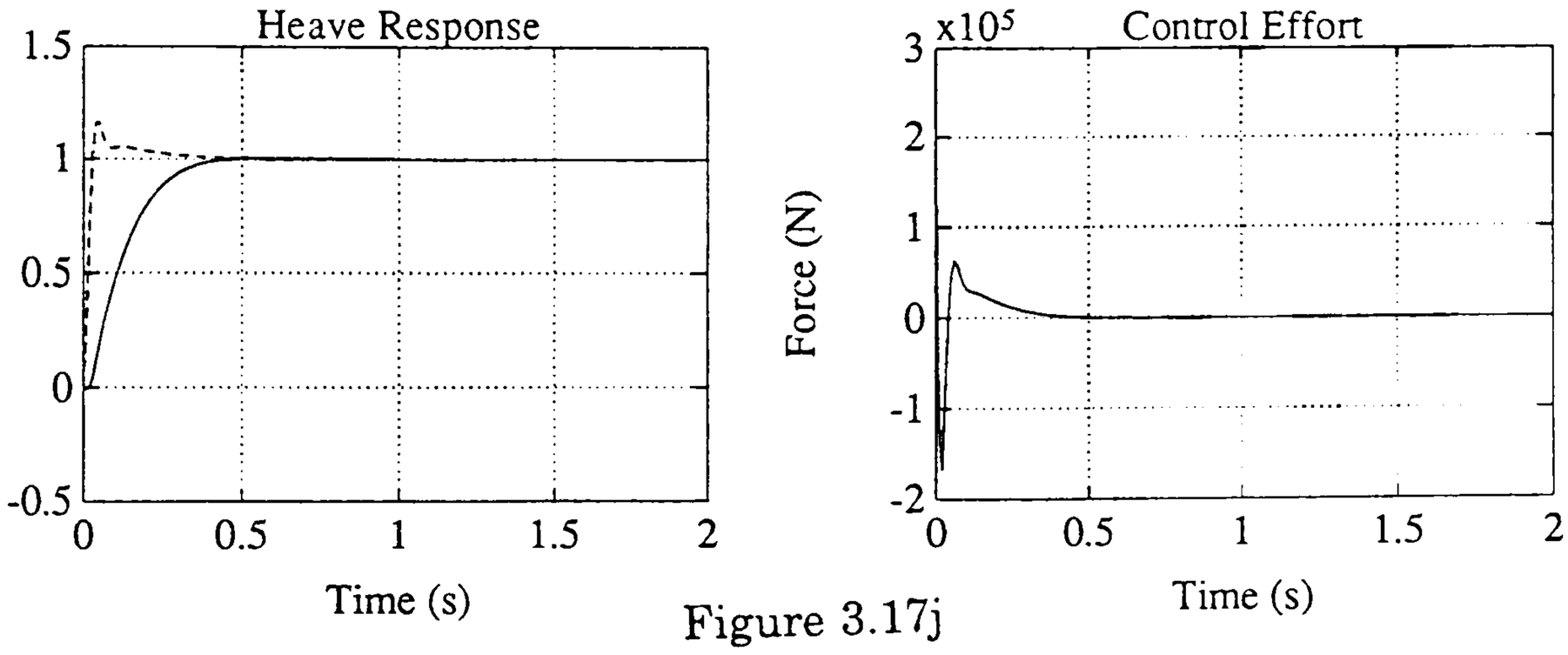


Figure 3.17j

Figure 3.17 (continued)

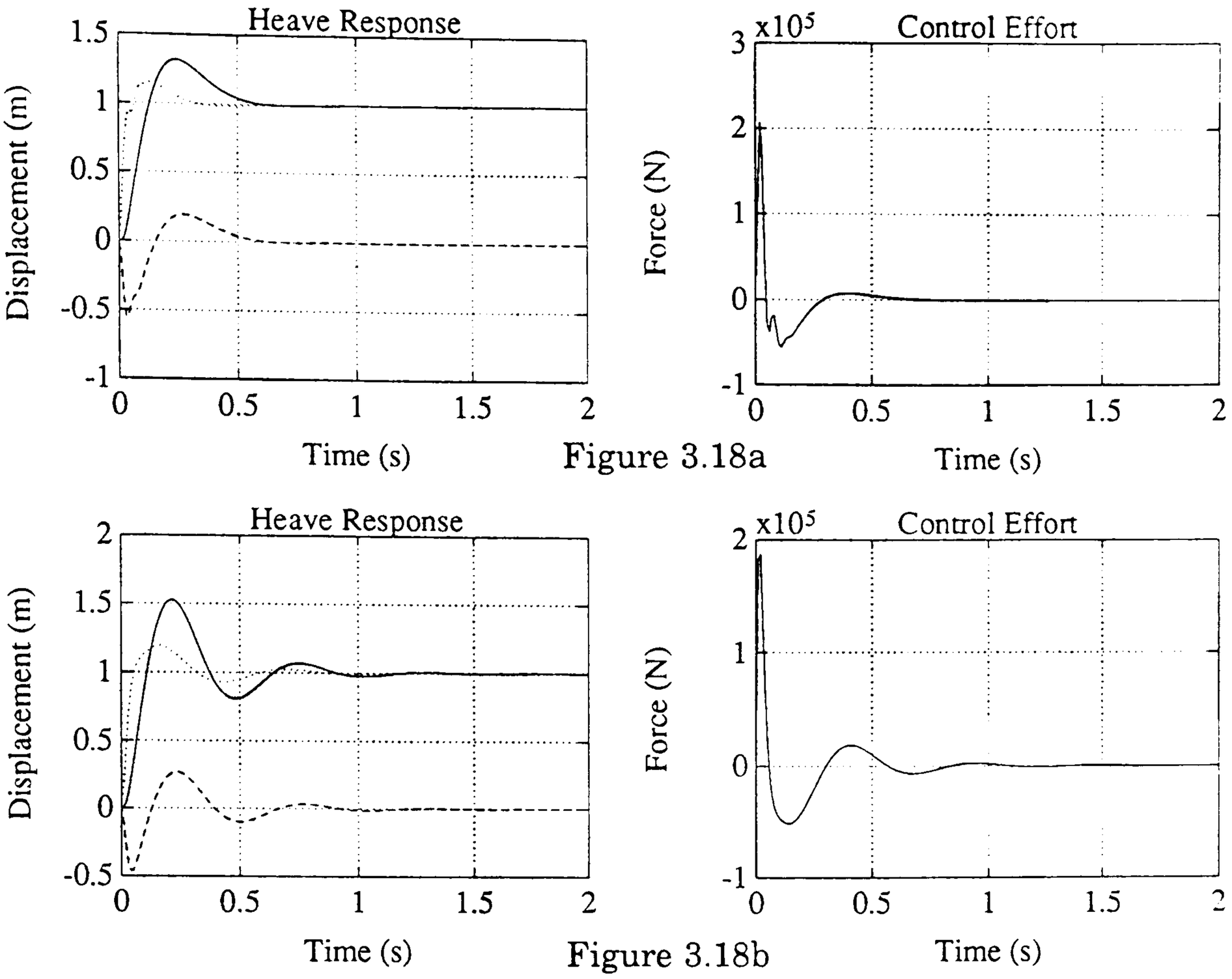


Figure 3.18a




Figure 3.18b

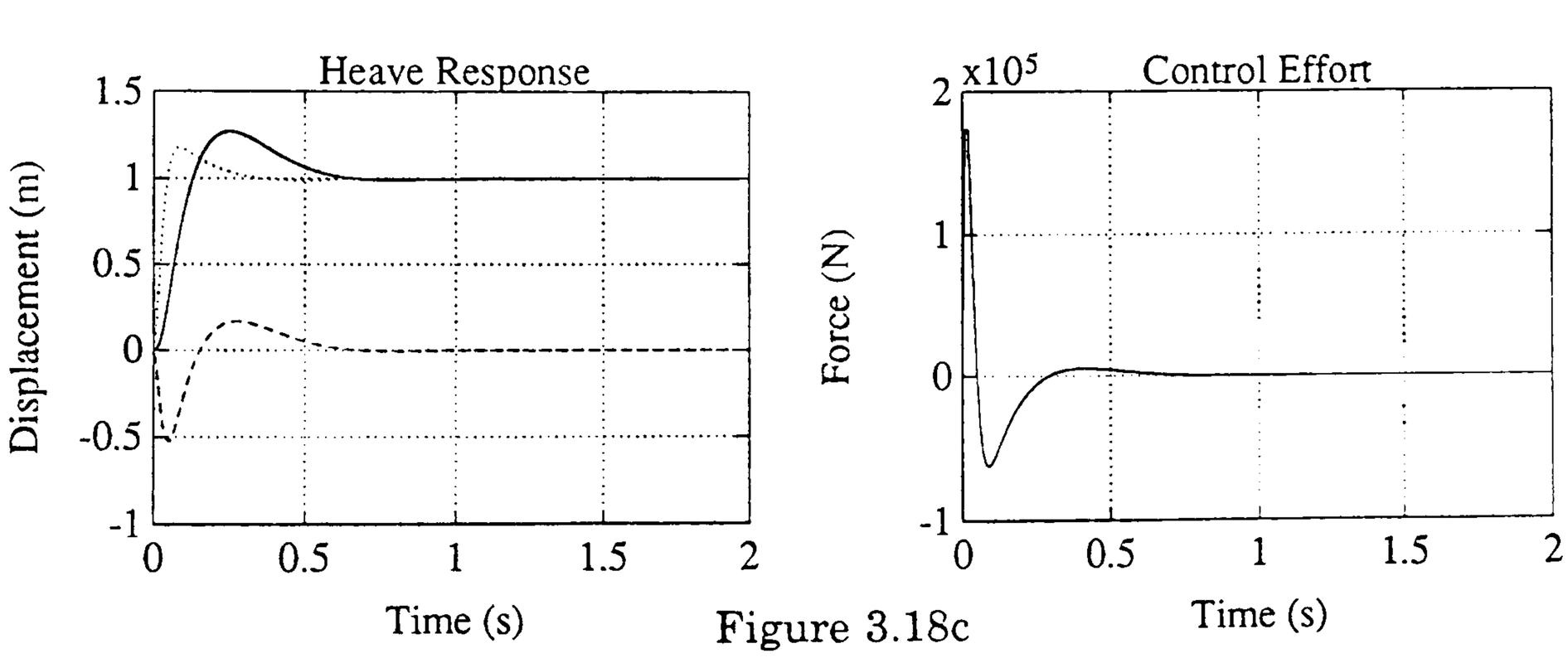


Figure 3.18c

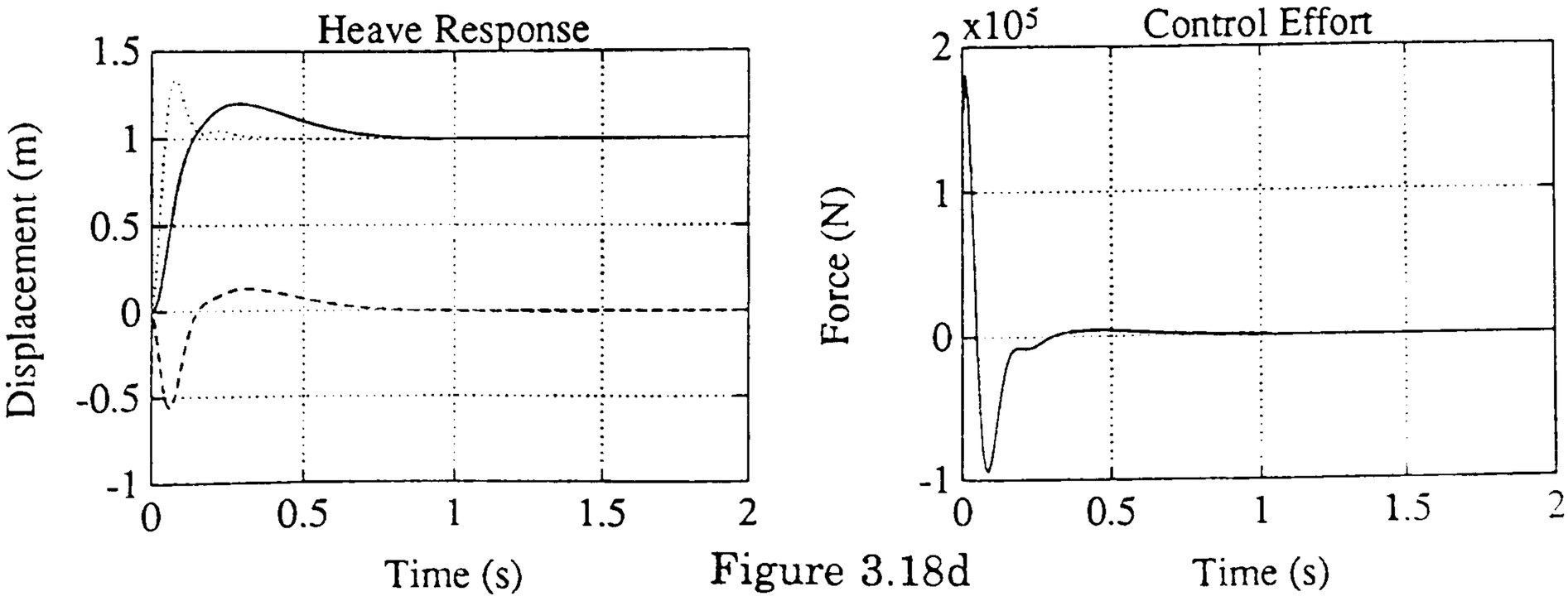


Figure 3.18d

Figure 3.18 : Frequency Domain Solutions

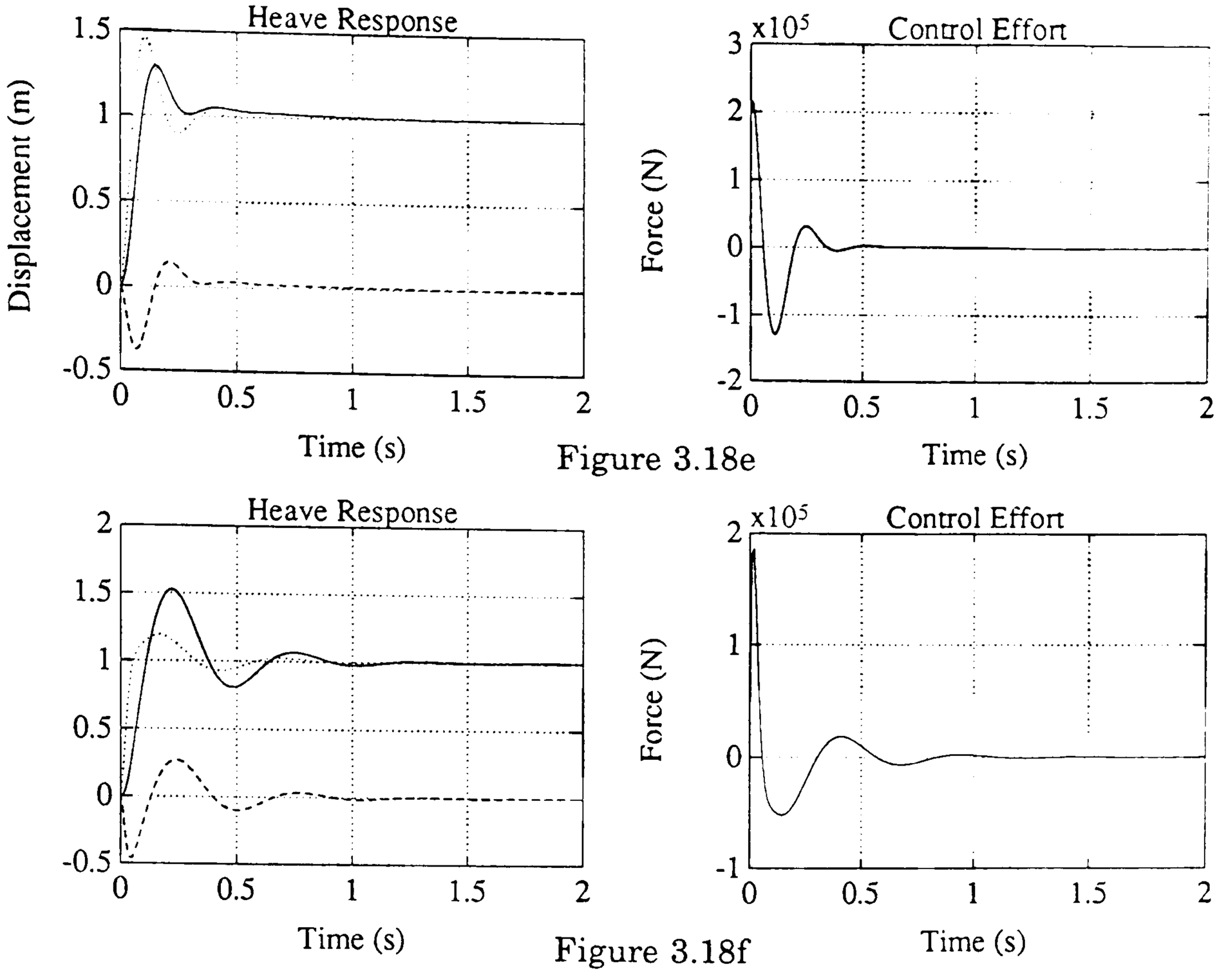


Figure 3.18e




Figure 3.18f

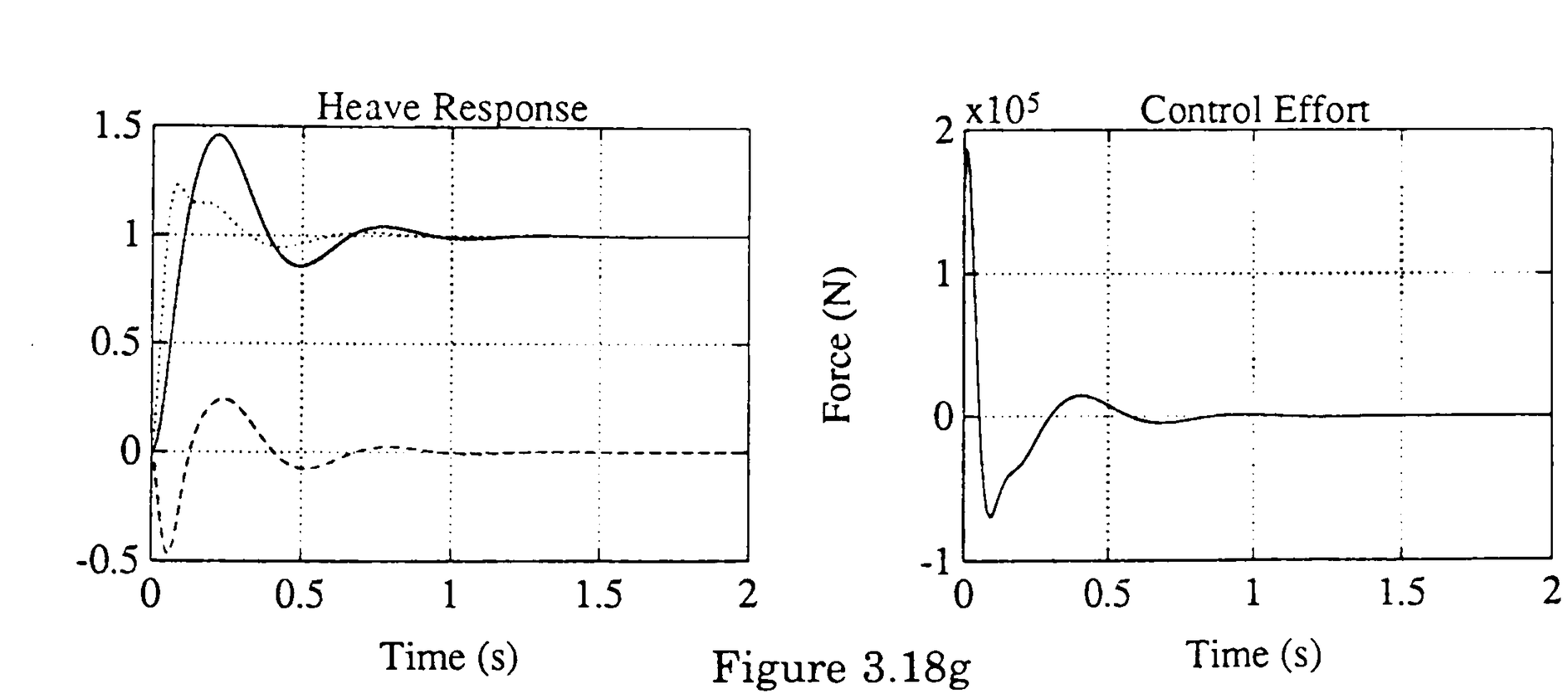


Figure 3.18g

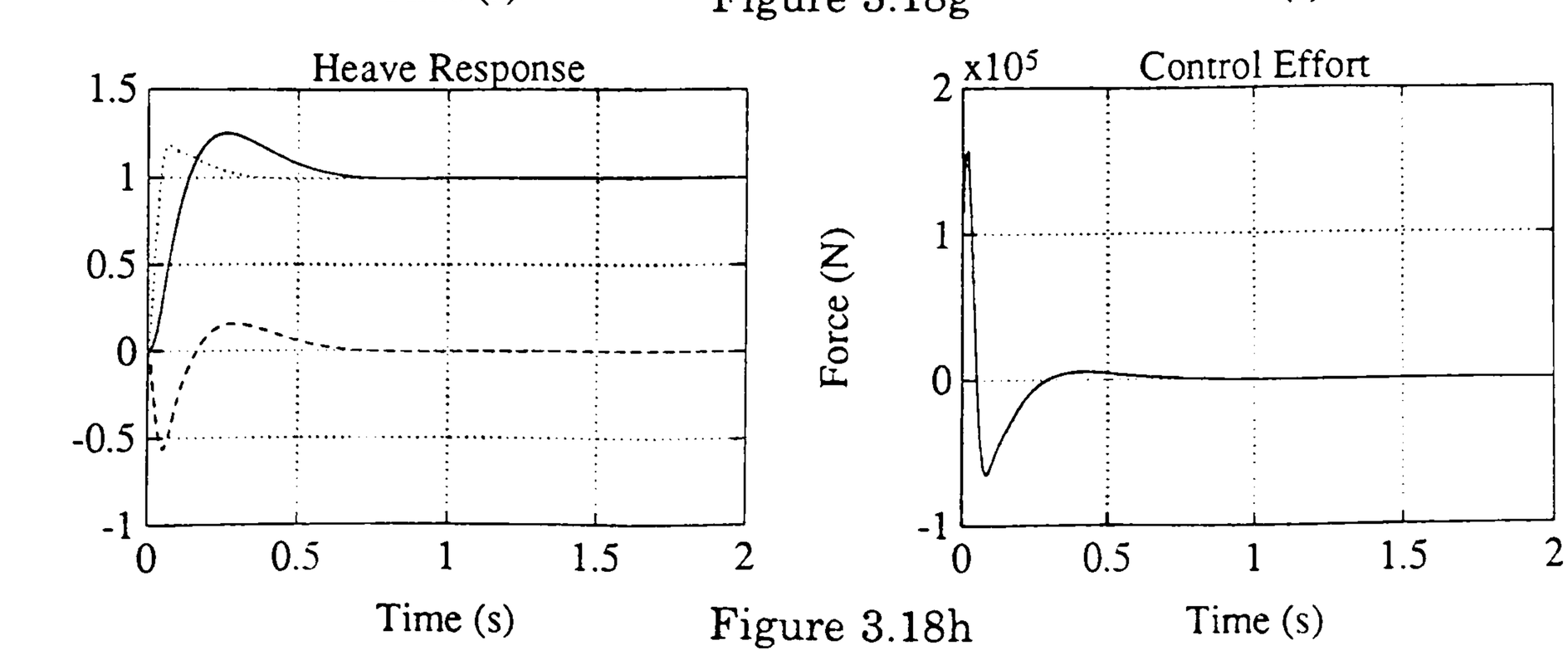


Figure 3.18h

Figure 3.18 (continued)

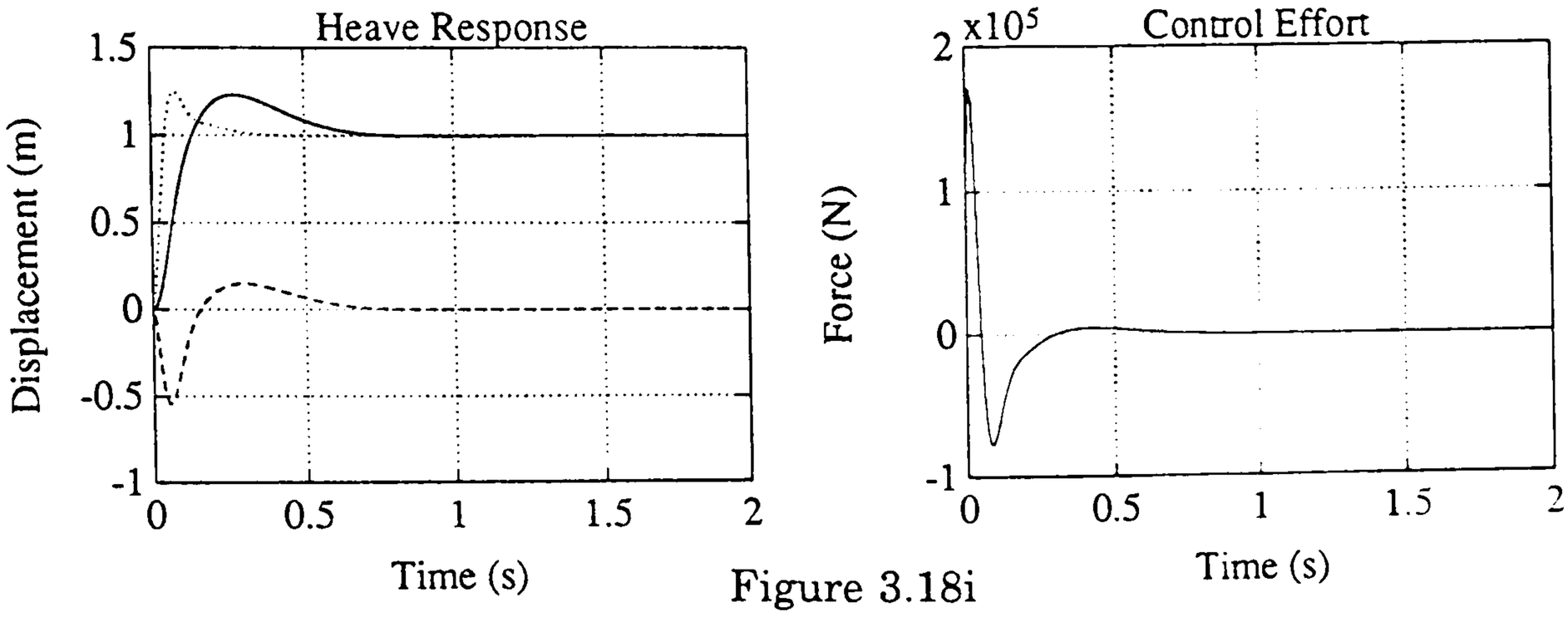


Figure 3.18i

Figure 3.18 (continued)

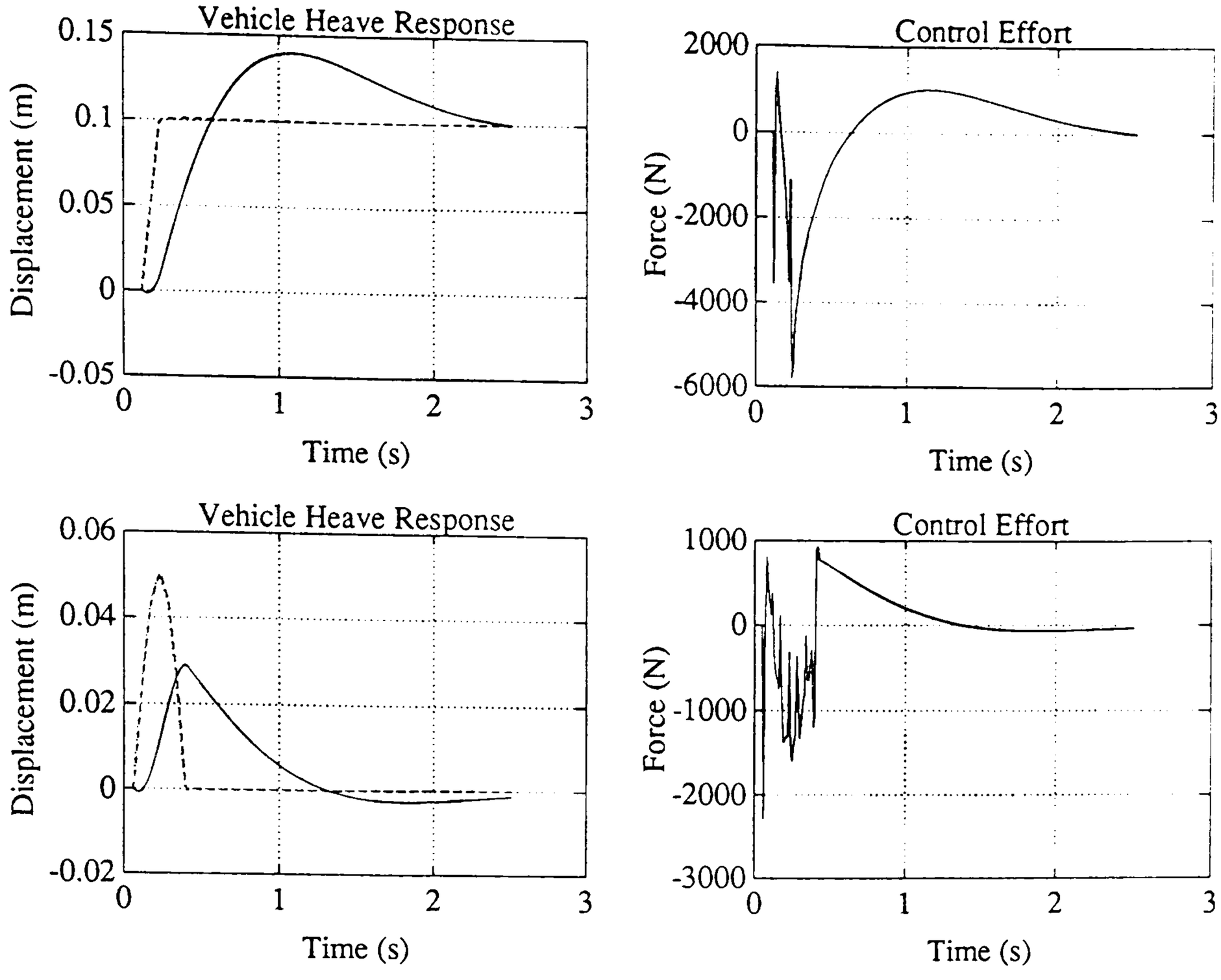


Figure 3.19 : Non-Linear Simulations of Best Regulator Result

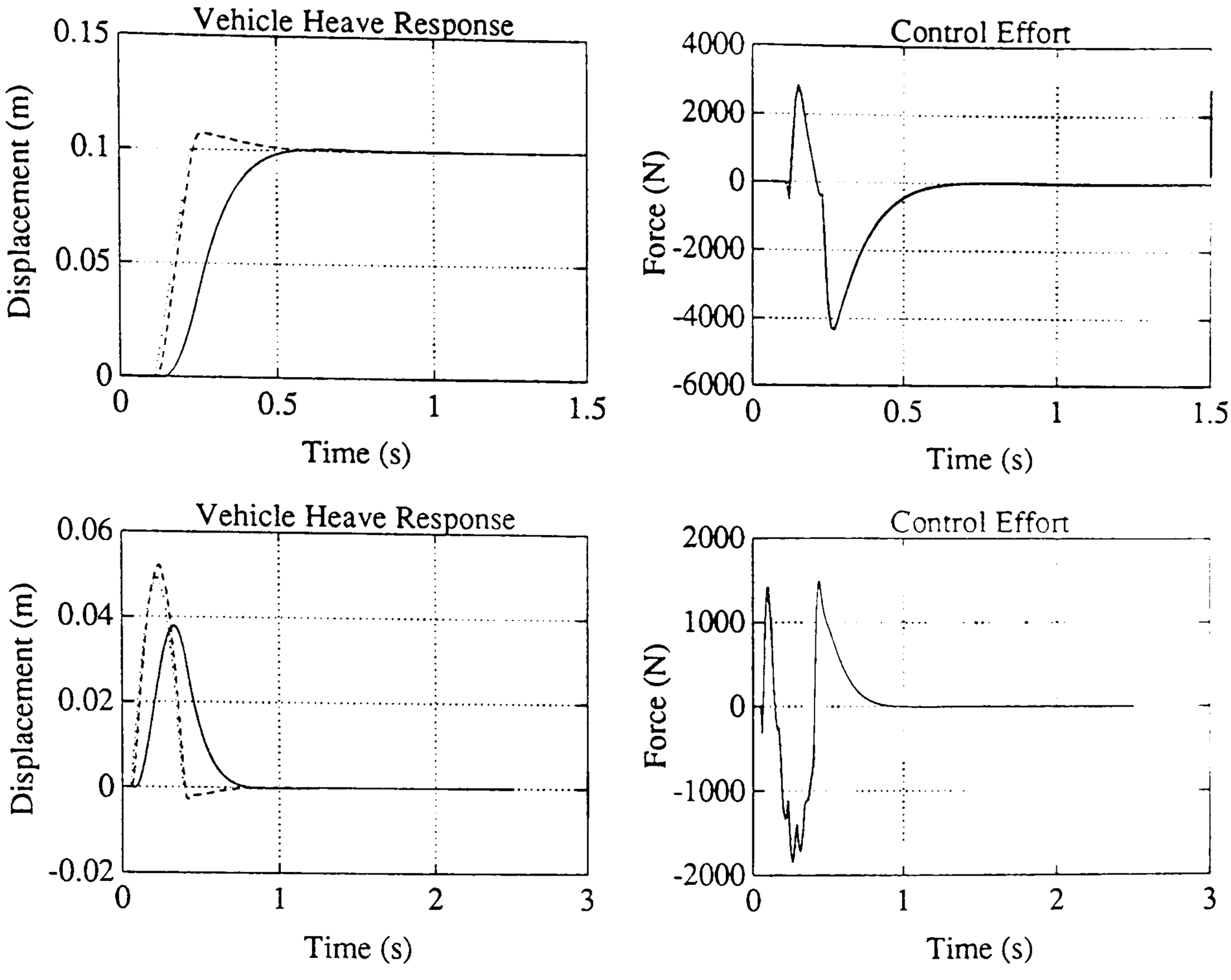


Figure 3.20 : Non-Linear Simulations of Best Pole Placement Result

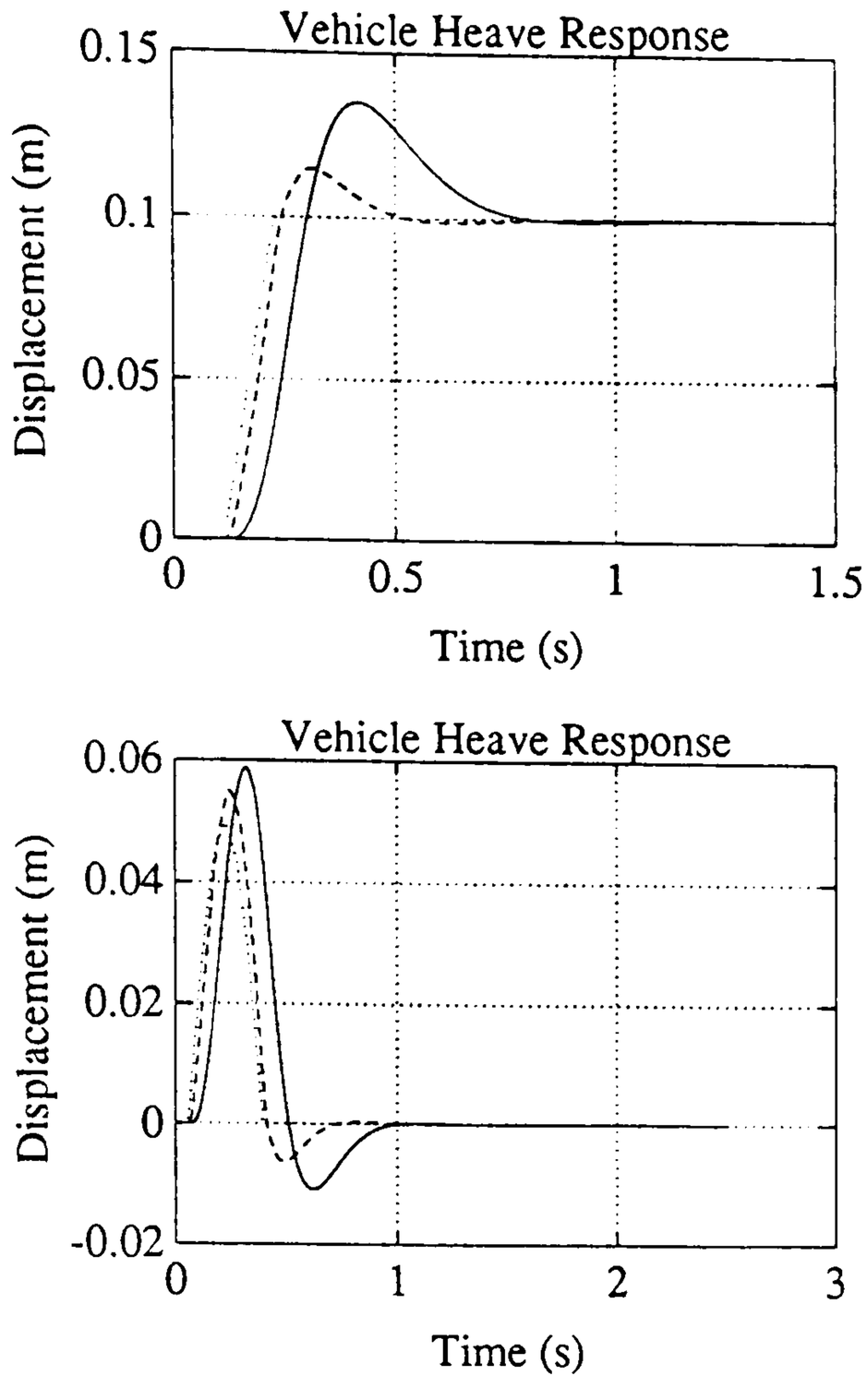


Figure 3.21 : Non-Linear Simulations of Best Frequency Domain Result

# Chapter 4 : Modelling and Analysis of a Full Vehicle Suspension System

## 4.1 Introduction

The use of quarter car models for automatic ride control of passenger car suspension systems provides a good starting point for initial feasibility studies. However these simplistic models have major limitations in terms of the complete vehicle ride performance as described in chapter two. The predominant limitation arises from the resultant solutions achieving independent control of each corner of the vehicle with no consideration of coupling. In these quarter car studies both the coupling between the corners of the vehicle by the sprung mass and anti roll bars, and the coupling between vehicle ride modes are ignored.

The work described in this thesis was to concentrate predominantly on full vehicle models, with the previous quarter car model used simply for a pilot study looking at the techniques and suspension control problem.

Following the success of the pilot study, a full vehicle model was similarly developed using the same modelling approach and tools as described in the previous chapter. This full vehicle representation was achieved by building an equivalent quarter car model of the rear suspension system, and using symmetry, reflecting about the vehicle longitudinal axis. The full vehicle model was then completed with modified sprung mass properties representing the complete body and anti-roll bars coupling the unsprung masses. The resultant full vehicle model was subsequently validated against real vehicle test

data obtained from experimental work using a four poster electro-hydraulic rig.

In order to evaluate the relative advantages and difficulties related to the use of this comprehensive model for suspension control, an equivalent study of ride control for an ideal active system using the full vehicle model was undertaken and reported in this chapter. Again both state space and frequency domain techniques were utilised, and a comparison of the resultant ride performance achieved was discussed. In order to compare the results obtained by the quarter car based study with those generated by the full vehicle study, the linear control study described in chapter three was similarly applied to the rear suspension system. The ride performance was then evaluated for a controller with the relevant quarter car control independently applied to each corner of the vehicle.

## 4.2 Development of Full Vehicle Model

The full vehicle model used for the ride control study described in this chapter was developed using the same modelling approach illustrated in the pilot study, with a representation of the suspension linkage and non-linear suspension compliance and damping characteristics. The model was based on the current production vehicle used in chapter three.

This model could have been generated straight from the front quarter model in one step. However in this work it was advantageous to split this process into two separate stages, development of a similar quarter car model representing the rear suspension, followed by the combination of both front and rear models to form the full vehicle model. Modular development always provides advantages in terms of debugging and validation, however it also

facilitated the rear quarter linear control study for the comparison of quarter car and full vehicle based design methods.

### 4.2.1 Rear Quarter Model

A schematic diagram illustrating the rear suspension model used for this study is shown in figure 4.1. As for the front quarter model, the sprung mass was represented by a single rigid body with one vertical translational degree of freedom. The rear suspension linkage then consisted of two rigid bodies representing the lower arm and the strut, with a further rigid body for the unsprung mass. The bushes between the lower arm and the sprung and unsprung masses were replaced by joints with a single rotational degree of freedom in the axial direction of the bush. The strut was then connected to the unsprung mass by a single translational degree of freedom joint, and the bush mounting the strut to the sprung mass was replaced by a three rotational degree of freedom joint.

In order to provide the tyre deflection as an ACSL state to simplify the tyre force calculation and facilitate the use of this state in the state space control study, dummy massless bodies were again used to provide six degrees of freedom between the unsprung mass and ground.

In contrast to the front suspension system, the rear road spring does not act at the strut, but further inboard, between the sprung mass and lower arm as shown in figure 4.1. For simplicity the spring is not represented by two rigid bodies connected by a single translation degree of freedom joint. Instead the mass of the spring is split between the sprung mass and lower arm, and the force is applied as an external force to both bodies. The spring aid, rebound

stop, damping and tyre forces are as for the front quarter model with different rate characteristics.

The SD/FAST multibody model was then prepared by rearranging the body connections to produce the required tree and constraint topology as shown in figure 4.2. For this model the loops were broken at the three degree of freedom joint between the sprung mass and strut, and at the single degree of freedom joint between the unsprung mass and the lower arm, and constraints included to regain the correct suspension topology. The choice was again a compromise between branch length and the number of constrained degrees of freedom justifying the choice of three degree of freedom constraint. Breaking the loop at the three degree of freedom joint between the massless dummy bodies and the unsprung mass would minimise the constrained degrees of freedom, however the resultant dynamics would be incorrect due to a massless body being at the end of a branch.

The mass and inertia properties, together with the geometrical data required for this SD/FAST model are given in tables 4.1 - 4.3. The coordinate system used for this model data was again the vehicle coordinate system, with its origin at a position in front of and above the front bumper and with the orientation shown in figure 2.1. The resultant SD/FAST model had 9 joints with 18 degrees of freedom including displacements, orientations and velocities.

The ACSL code for the rear quarter car model was also similar to the front, with one exception, and that is the calculation and application of the spring force. As was seen from the topological diagram shown in figure 4.2, there was no joint representing the spring in the rear model, and so the relative displacement is not automatically available in the state vector. As a result the

relative displacement in the spring was calculated via an SD/FAST function giving absolute positions of points on bodies, applied to the spring connection points on the sprung mass and lower arm. The spring force was then a linear function of the relative deflection as before, with stiffness as given in table 4.4. A static spring force was similarly calculated, as given in table 4.4, and was included in the spring force. This overall spring force was then applied as an equal and opposite external force to both bodies at the spring fixing positions. The damping, spring aid and rebound stop forces are calculated exactly as previously, and applied as internal forces in the joint representing the strut. The non-linear characteristics for the rear spring aid and damper are shown as force deflection and force velocity curves in figures 4.3, 4.4. A large linear stiffness was used to represent the rebound stop and this is given in table 4.4, together with the deflections required in the strut before the spring aid and rebound stop begin to act. The tyre force was modelled exactly as for the front, with the same stiffness as given in table 3.5. A static tyre deflection was similarly included, and is given in table 4.4. The resultant rear quarter car ACSL model had 18 states.

### 4.2.2 Full Vehicle Model

With both front and rear quarter car models complete, the full vehicle model was a simple combination of these with a couple of minor modifications. In order to complete the full vehicle geometrical model in SD/FAST, symmetry was assumed and the front and rear quarter models were reflected about the vehicle longitudinal axis, shown in figure 2.1 as the x axis. The four sprung masses were replaced with a single rigid body with representative mass and

inertia properties together with a new centre of mass position as given in tables 4.5 - 4.6.

For this model the sprung mass required full motion relative to ground. This can be achieved automatically in SD/FAST by choosing a free flying system or manually by connecting the sprung mass to ground by massless dummy bodies providing six degrees of freedom in a similar manner to that used for the unsprung masses in the quarter car models. Both methods are valid, however defining these six joints specifically provides the option of directly choosing both the order and type of the joints used. The free flying system uses three single translational degree of freedom joints and a ball joint providing three rotational degrees of freedom. SD/FAST ball joints use Euler parameters and no joint axes [96]. By specifying the joints manually and choosing a gimbal joint to provide the three rotational degrees of freedom, the axes of rotation can be specified with any direction and in any order. In this way a choice of order vertical z, lateral y, longitudinal x provides the correct yaw, pitch and roll angles of the sprung mass.

The final modification to complete the full vehicle SD/FAST model was the redefinition of the vectors relating to the joint positions to the new vehicle body centre of mass. The resultant full vehicle SD/FAST model consisted of 46 joints resulting in 92 degrees of freedom including displacements, orientations and velocities.

Once the SD/FAST model of the geometry and mass and inertia properties was complete, the ACSL model including internal and external forces was also extended to represent the full vehicle. This simply involved the inclusion of representations of the front and rear anti-roll bar stiffnesses, and

modification of the static spring force and tyre deflections to suit the new sprung mass. The anti-roll bars were modelled as linear functions of the relative displacement of the two relevant unsprung masses,

$$F_{arb} = K_{arb}(x_r - x_l) \tag{4.1}$$

where $x_r$ and $x_l$ are the left and right unsprung mass absolute vertical displacements, and the front and rear stiffnesses $K_{arb}$ are given in table 4.7. These forces were applied as equal and opposite external forces to each of the front and rear unsprung masses, in a similar manner to that used for the rear spring force. Finally the static spring force and tyre deflections were modified for the new sprung mass to provide static equilibrium at the defined configuration with all joint displacements and orientations equal to zero. These are given in table 4.7. The resultant full vehicle ACSL model had 92 states relating to the joint displacements, orientations and velocities.

The completed model described is a full non-linear representation of a vehicle suitable for ride studies, allowing vertical road inputs to each wheel and full sprung mass motion including heave, pitch and roll modes. The road inputs could be left independent, or alternatively realistic correlation between the road inputs could be incorporated. For small amplitude road surface models, the road input correlation is approximately represented by a time delay for front to rear dependence defined by the vehicle speed and wheelbase, and equality for left to right dependence. However for large amplitude isolated road disturbances such as potholes and sleeping policemen, the inputs should be independent. In order to maintain the required flexibility the road inputs were left independent with the option to introduce the required correlation subsequently if required.

## 4.3 Model Validation and Simulation

An essential part of any form of modelling, whether for prediction, analysis or design, is validation. In this work the emphasis has been placed on realistic vehicle models that have been correlated against real vehicle test data. This involved obtaining relevant vehicle test data and then producing equivalent results from the model using simulation and analysis techniques.

### 4.3.1 Experimental Work

The experimental work involved in the correlation of the full vehicle model was not carried out specifically for this project. Instead, existing test results previously produced as part of the standard design and development process within Rover were used. The experimental results used for the correlation were produced from tests carried out on a four poster road simulator, used extensively for vehicle validation purposes. The use of such a simulator allows vehicle testing to be performed under controlled and repeatable conditions.

Figure 4.5 shows a photograph of the four poster rig concerned. This road simulator can be seen to consist of four vertically oriented high performance hydraulic actuators. Attached to each of the actuator pistons are dishes into which the vehicle tyres are located. The motion of each of the actuators is then controlled by electrical signals supplied by a mini computer and conditioned by analogue servo controllers.

Two types of test results were used for validation of the full vehicle model. The first type was similar to those used for the quarter car model, namely sine sweeps. This involved all four actuators following the same signal

of a sine wave sweeping through a specified range of frequencies, with the amplitude varying accordingly. Again the ride frequency range was chosen for this correlation exercise. The use of sine sweep tests provide information relating to the frequency response of the vehicle. The second set of test results related to rig simulations of real road profile inputs allowing the evaluation of the vehicle ride performance to realistic road inputs.

These road inputs were generated from road load data collected during vehicle road test by a techniques known as remote parameter control (RPC). A fully instrumented vehicle is driven over road profiles of interest, and a full set of vehicle response data is recorded. The vehicle is then transferred onto the road simulator rig, and the actuators are driven with generated inputs obtained from the test data. RPC is then an iterative process that tunes the actuator drive signals to replicate the vehicle response to the road inputs on the rig. For this model correlation exercise, road inputs corresponding to the Fossway at 50 mph were used.

For both sets of tests the vehicle response was measured by the use of accelerometers mounted in the vertical direction on the sprung and unsprung masses. The vertical acceleration of each wheel hub was recorded, together with the sprung mass vertical acceleration at each suspension tower. The results from the sine sweep tests are again presented in terms of resonant frequencies as given in table 4.8. For the Fossway road profile test results, the vehicle response is given in terms of power spectrum densities for each of the outputs, and these are shown in figure 4.6.

### 4.3.2 Model Correlation

Once all of the test data was collected, the model was then used to replicate the results. The sine sweep results were again reproduced from a modal analysis of the linearised version of the full vehicle ACSL model. In order to validate the response of the model to real road inputs, the linear model was again used, and the required power spectrum outputs obtained within MATLAB. As a result for both sections of the correlation exercise, the starting point was to achieve a linear model.

The full vehicle ACSL model was linearised in the same way as the quarter car model in chapter three, with the only exceptions relating to the size of the system matrices and vectors. Equation 3.9 gave the linearised form required for the modal analysis, with a 92x1 state vector in this case. For the road input correlation, the alternative linear representation of the form given in equation 3.11 was required. For this study the inputs were the four road displacement inputs, and the outputs were chosen to include the sprung mass heave, pitch and roll accelerations, together with the unsprung mass and sprung mass suspension tower vertical accelerations.

#### 4.3.2.1 Sine Sweep Results

The correlation procedure for the sine sweep results began with a modal analysis of the model with representative linear damping rates, in place of the non-linear rates. The experience from the quarter car study showed that the suspension damping non-linearity made negligible difference to the modal results, however for the full vehicle model, it reduced the linearisation errors. The results obtained from this analysis are included in table 4.9.

Again the results obtained from the linear modal analysis gave lower resonant frequencies compared with the test results, although the sprung mass results did not show such a marked difference as the unsprung mass modes. Again the discrepancy can be explained by examination of the effects of the non-linearities, by repeating the modal analysis with increased spring and tyre stiffnesses. The effects of introducing tyre damping was also ignored from the quarter car results. This allows the effects of compliance non-linearities to be evaluated. These results are also included in table 4.9. Again an increase in the suspension stiffness equivalent to the spring aid effect resulted in an increase in the sprung mass modes. In this way the ACSL model that includes the spring aid and other non-linearities is validated for the sprung mass responses.

The tyre approximations in the model also account for the correlation discrepancy, with table 4.9 showing an increase in tyre stiffness results in an increase of the sprung mass mode frequencies. The ACSL model is therefore limited in its tyre representation, but is adequate for the comparative evaluation of controllers for this primarily sprung mass control study.

#### 4.3.2.2 Fossway Road Input Results

The linear model for the road input correlation study was read into MATLAB, together with the road input information in the form of a power spectrum. The road input used for the test results and analysis is given in figure 4.7. The model response was found by first approximating the road input to be equal for the right and left inputs, and for the rear wheels to see a delayed version of the front. The frequency response of the model to these road inputs was then calculated in MATLAB [74, 76], and the resultant power spectrums for each of the outputs are given in figures 4.8.

A comparison of the analytical responses with the test results shows good correlation. The frequencies relating to the resonant peaks are again higher for the test results, and again this discrepancy can be explained by the compliance non-linearities. The differences in the magnitude values can also be explained by the use of different averaging techniques. Otherwise the frequency response predicted by the model correlates well with the actual vehicle response to this road input.

The overall model correlation results show that the ACSL non-linear model forms a good representation for the vehicle under consideration, with the limitation in the unsprung mass response due to the simplified tyre model. However for the study under consideration the sprung mass response is of primary importance, and the model is sufficient for any comparison between controllers.

## 4.4 Suspension Control

As for the quarter car study, the suspension control problem under consideration here is ride control, including in this case all three sprung mass ride modes, heave, pitch and roll, and the four wheel hop modes. The fully active system under consideration was as before, with the passive damper replaced by an ideal force generator at each corner of the vehicle. Although the model described could be developed to provide the opportunity for lateral and longitudinal dynamics, in order to ensure a direct comparison with the quarter car ride control study, road inputs were the only disturbance inputs considered. Again a range of control design and analysis techniques were applied, including both state space and frequency domain.

The full vehicle ride controller design could have been achieved in two distinct ways. Firstly by basing the controller on the quarter car feedback solutions obtained front both front and rear corner systems and simply applying each to the relevant vehicle corner, as previously described. The design task is then split into two (front and rear) SISO, for frequency domain, or SIMO, for state space, design tasks as illustrated in chapter three. This design method equates to controlling the heave motion of each corner of the sprung mass separately with no account taken of the coupling between vehicle corners or between the sprung mass modes. The second method of ride control design would be to use the techniques used in the quarter car study, and apply these to the full vehicle model. This would result in the control of all sprung and unsprung mass modes with full account of all interactions. The full vehicle model, however, would result in a multi-input multi-output (MIMO) system.

The differences between these two methods in terms of ease of design and resultant achievable performance depend heavily on the technique involved. With regard to achievable performance the influencing factor would be the coupling between vehicle modes, and as a result the design method based on the full vehicle model would be expected to provide better ride control. The resulting differences will be discussed fully later. The ease of design, however, is totally dependent on the specific control design technique under consideration.

The application of state space techniques to the full vehicle model would present very little noticeable difference, since state space techniques apply equally to SISO and MIMO systems. The only real difference would be in the performance index, which would include the minimisation of the sprung mass

acceleration for each mode, and the tyre load variation and control effort at each corner. Thus the only possible difficulty in extending the techniques to the full vehicle case would be the increase in complexity, size and possible numerical problems that may result.

In contrast frequency domain techniques would involve significantly more effort to address the MIMO problem, as standard frequency domain techniques apply to SISO systems only. Despite the quarter car model being a SIMO system, the control design was satisfactorily addressed by considering this as separate SISO systems by controlling one output at a time. However, in order to address the full vehicle ride control task with full account taken of the coupling, the full MIMO system must be considered. The first step in addressing MIMO systems with the use of frequency domain techniques is to find a method of removing the interaction with some form of decoupling technique. In this way the MIMO system is reduced to several independent SISO systems and standard frequency domain techniques can then be applied to each SISO system individually. This decoupling is usually a difficult and time consuming task, and as a result, if the combination of quarter car results provided good results, this method would be significantly more attractive for its simplicity and ease of design.

For the full vehicle ride control study described, both methods were considered and a full comparison undertaken. In order to consider the case with separate quarter car based controllers at each corner, the quarter car design study described in chapter three was repeated for the rear suspension. The methods were exactly the same with the only variations being in the number of states involved in the original state space system. The resultant reduced order

model actually used in the design process involved matrices and vectors of the same dimensions. Again all three design techniques, linear quadratic regulator, pole placement and frequency domain were utilised.

In this chapter the application of linear control techniques to the ride control using the full vehicle model directly is described in detail.

### 4.4.1 State Space

The application of state space control techniques to the full vehicle model followed the same procedure used for the quarter car model with the only difference being in the size of the state space and performance index matrices and vectors. The linearisation process was exactly the same producing a system of equations of the form given in equation 3.12 with a 92x1 state vector, $\boldsymbol{x}$, a 4x1 input vector of actuator forces, $\boldsymbol{f}$, and a 4x1 road input vector, $\boldsymbol{d}$. For the full vehicle model the outputs chosen included the sprung mass heave, pitch and roll displacements, orientations and velocities, and the absolute wheel vertical displacement and velocity for evaluation purposes. The strut deflections and velocities together with the tyre deflections were also included for obtaining the feedback solution in the required form as described later.

As for the quarter car study the control variables were scaled by 10000 to avoid the scaling problems illustrated for the two degree of freedom model. The wheel displacements in the state vector were similarly replaced by tyre deflections, and an equivalent reduced order model obtained of the form given in equation 3.17, with a 14x1 transformed state vector, $\boldsymbol{p}$, a 4x1 scaled input vector, $\boldsymbol{u}$, and a 4x1 road velocity disturbance, $\boldsymbol{w}$. The linear control design techniques used in chapter three were then applied to this resultant linear

model.

For the linear quadratic regulator design the major difference was that the performance index included the minimisation of heave, pitch and roll accelerations of the sprung mass, together with the four tyre load variations and four control forces. For simplicity only three performance index weights were used, thus assuming equal weighting for all three sprung mass accelerations, all four tyre load variations and all four control efforts. As a result the performance index was of the form given in equation 3.18 with

$$\begin{aligned} acc^2 &= hacc^2 + pacc^2 + racc^2 \\ tlv^2 &= tlv_1^2 + tlv_2^2 + tlv_3^2 + tlv_4^2 \\ u^2 &= u_1^2 + u_2^2 + u_3^2 + u_4^2 \end{aligned} \tag{4.2}$$

where ***pacc, hacc, racc*** are the sprung mass accelerations in the heave, pitch and roll directions, $tlv_i$, $u_i$ are the tyre load variations and control efforts at the $i^{th}$ corner. Otherwise the design procedure was exactly the same as previously. The application of pole placement techniques was also very similar except that there were seven pairs of imaginary poles of the uncontrolled plant to be placed. For both methods the resultant state variable feedback solution was of the form given in equation 3.23 with a 4x14 matrix $K$ of gains.

### 4.4.2 Frequency Domain

The full vehicle ride control problem is a MIMO problem, with four actuator forces as control variables, four road inputs as disturbances, and for this study the four strut deflections were chosen as outputs from the experience gained from the quarter car design results. In order to apply frequency domain techniques to this ride control problem, the state space description of the

linearised ACSL model was converted into transfer function form. This was achieved by a similar method to that employed in the quarter car study, by first obtaining a state space reduced order model with both the road inputs and actuator forces as inputs. This was then converted to transfer function form in MATLAB [75] by the use of the multivariable function mvss2tf for the full vehicle model. The resultant multivariable transfer function matrix has eight inputs including road input and actuator forces and four strut deflection outputs as shown in figure 4.9. The common denominator polynomial was of order fourteen with order twelve numerators.

For the frequency domain design the road inputs are considered disturbances, and the transfer function matrix can be partitioned, as illustrated in the diagram, into a matrix relating to road disturbances and one to control inputs. Alternatively this can be illustrated in the block diagram form shown in figure 4.10. The control design study is then concerned with the plant transfer function matrix, $\boldsymbol{G(s)}$, and $\boldsymbol{G_d(s)}$ is present for the evaluation of the response to road inputs.

The application of multivariable frequency domain techniques to such a MIMO system can be addressed using a variety of techniques, as discussed by Maciejowski [65]. Each of these approaches ultimately replaces the MIMO system under consideration by a set of SISO design problems. These techniques involve some assumption as to the structure of the system in terms of pairing inputs with outputs, and in terms of the interactions.

For the ride control study of the full vehicle model under consideration here, the approach based on the quarter car results assumed no interactions. This comparative study was aimed at taking full account of the interactions. As

a result a frequency design approach that involved two stages was adopted. Firstly a process of decoupling the MIMO system into independent SISO systems was undertaken, followed by the application of standard frequency domain techniques to each of the SISO systems and combining to obtain the resultant multivariable controller.

#### 4.4.2.1 Decoupling

The method chosen for decoupling the system was dyadic expansion as described by Owens [85]. This dyadic expansion technique achieves specific decoupling into the sprung mass ride modes, heave, pitch, roll and flexure. Thus producing a technique for removing the interactions between modes, and also resulting in individual SISO systems relating to each of these modes for separate control, as seen later.

The diagonalisation objective for this frequency domain study was to decouple $G(jw)$ at least for a range of frequencies of interest, including the natural frequencies of the vehicle. For the application of the decoupling technique the resonant frequencies of the transfer function matrix under consideration play an important role, and these are given in table 4.10. The dyadic expansion was then achieved by first choosing a frequency of interest, $w_o$, and post multiplying the frequency response matrix $G(jw)$ by the value of its inverse evaluated at the chosen frequency, to give

$$G(jw)G^{-1}(jw_o) \tag{4.3}$$

This results in a transformed transfer function matrix with the interactions removed and with unity gain at the chosen frequency $w_o$. Having achieved diagonalisation at this specific frequency, the process was then aimed at

achieving this property for a range of frequencies. In order to do this the transformed transfer function matrix is expressed in the form

$$G(jw)G^{-1}(jw_0) = I + (w - w_0)L(jw) \tag{4.4}$$

We now choose a second frequency of interest, $w_1$, and define the transfer function matrix $L(jw)$ to be

$$L(jw_1) = \lim_{w \to w_1} \frac{1}{(w - w_0)}(G(jw)G^{-1}(jw_0) - I) \tag{4.5}$$

Computing $V$, the 4x4 matrix whose columns are the eigenvectors of $L(jw_1)$ gives the property

$$V \quad st \quad L(jw_1)V = diag(lamda)V = V\, diag(\lambda) \tag{4.6}$$

resulting in the ability to diagonalise $L(jw_1)$ by pre-multiplying by the inverse of the matrix of eigenvectors

$$V^{-1}L(jw_1)V = diag(\lambda) \tag{4.7}$$

resulting in the diagonal matrix with system eigenvalues on the diagonal. By way of an illustration the matrix, $V$, for $w_o = 12.07$, $w_1 = 7.2$ was found to be

$$V = \begin{pmatrix} 0.58437 & -0.41444 & -0.44449 & -0.23555 \\ 0.58437 & 0.41444 & 0.44451 & -0.23556 \\ 0.39814 & -0.57292 & 0.54991 & 0.66672 \\ 0.39814 & 0.57292 & -0.54995 & 0.66672 \end{pmatrix} \tag{4.8}$$

From this example it can be seen that this matrix of eigenvectors relate to the four modes of the sprung mass, heave, pitch, roll and flexure.

Finally by post-multiplying the transfer function matrix given in equation 4.3 by $V$ and pre-multiplying by its inverse, the following transformed

transfer function matrix is obtained

$$V^{-1}\ G(jw)G^{-1}(jw_0)V = I + (w - w_0)\ V^{-1}\ L(jw)V \qquad (4.9)$$

Now since the transfer function matrix in equation 4.4 is diagonal at $w_o$, and the transfer function matrix in equation 4.7 is diagonal at $w_1$, then the equation given above shows that the overall transfer function matrix is diagonal at both chosen frequencies $w_o$, $w_1$. In fact the application of this dyadic expansion techniques to the full vehicle linear system under consideration here results in the above transfer function matrix being diagonal for a range of frequencies dependent on the two chosen values for $w_o$, $w_1$. The details of this will be discussed later.

This resultant transfer function matrix is illustrated in block diagram form in figure 4.11, and this diagram shows how, due to the eigenvector structure of $V$, the inputs and outputs related to individual vehicle corners are transformed into inputs and outputs related to the sprung mass modes. As a result the dyadic expansion actually decouples the MIMO system into the four individual SISO systems related to each of the sprung mass modes, heave, pitch, roll and flexure. The subsequent application of standard frequency domain control techniques to these SISO systems involves the individual control of each sprung mass mode.

Applying this dyadic expansion technique to the linearised ACSL transfer function model under consideration led to numerical problems arising from the transfer function polynomials having seven double roots, with frequencies as given in table 4.10, resulting in very large polynomial coefficients. This numerical problem can be overcome by diagonalising the

numerator alone and taking the denominator out as a scaling factor. This keeps the polynomial coefficients reasonable, as it scales the system by the value of the denominator of $G(jw_o)$.

Incorporating the decoupled transfer function matrix given in equation 4.9 and shown in figure 4.11, results in the block diagram form illustrated in figure 4.12. Now in order to arrange each of the decoupled SISO systems in the same form achieved for the quarter car study, this block diagram structure was rearranged to give the new structure shown in figure 4.13. The disturbance transfer function $\boldsymbol{D}$, shown in this diagram, was derived from the original matrix, $G_d(jw)$ by preserving the overall transfer function of strut outputs to road inputs. Inspection of the equivalent block diagram form shown in figures 4.12 and 4.13 then gives

$$G(jw)G^{-1}(jw_o)V\ D = G_d \tag{4.10}$$

Pre-multiplying this equation with the inverse of the matrix $\boldsymbol{V}$ of eigenvectors results in

$$V^{-1}G(jw)G^{-1}(jw_o)V\ D = V^{-1}G_d \tag{4.11}$$

and the required disturbance transfer function matrix $\boldsymbol{D}$ can be found by noting that we have

$$G_{diag}(jw)D = V^{-1}G_d \tag{4.12}$$

where $G_{diag}(jw)$ is the resultant decoupled transfer function matrix.

Now the system illustrated in figure 4.13 consists of four SISO systems, one for each of the body modes, heave, pitch, roll, and flexure. Standard frequency domain control design techniques were then applied to each of these

systems separately, and then combined in a diagonal controller as illustrated. The flexure mode was left uncontrolled by including a zero feedback compensator term at the relevant diagonal, since the non-linear model was developed assuming a rigid sprung mass.

The resultant decoupled SISO transfer functions obtained from the diagonal terms in the transformed transfer function matrix had a very similar structure, including zero and pole positions, to the quarter car transfer functions described in chapter three. As a result the same forms of compensators ensured system stability and gave the best performance results. Thus the best compensator for the study in chapter three was applied and the desired vehicle response for each mode was achieved by tuning the compensator parameters in an iterative procedure for each SISO system.

## 4.5 Discussion of Results

For the state space control design techniques used throughout this design process, the resultant state variable feedback solutions were evaluated on the linear model within MATLAB. Primarily a road heave input consisting of a vertical step input at each of the four wheel inputs was considered, with a subsequent look at the response to pitch and roll step inputs for some of the better results. For all of these linear results presented, the vehicle ride performance is illustrated in terms of the heave (solid line), pitch (dashed) and roll (dotted) responses of the sprung mass, the vertical displacement of all four wheels. The required control effort in terms of the equivalent actuator forces, $\boldsymbol{f}$, is also given for each corner of the vehicle. For the wheel responses and the control efforts, the results for the front corners are shown with solid and dashed

lines, and the rear by dotted and dashed and dotted lines. By way of an illustration one state space controller was evaluated on the full non-linear ACSL model and for these results a plot of the road input is also included.

For the frequency domain techniques both the linear model in MATLAB and the non-linear ACSL model were used for evaluation purposes. The linear MATLAB model was used to evaluate the system decoupling achieved with the dyadic expansion techniques, together with the intermediate frequency domain results for each of the individual SISO systems. However for these intermediate evaluations the inputs and outputs are measures of heave, pitch and roll inputs and outputs as opposed to specific vehicle parameter values. These results are illustrated by considering step inputs to the SISO systems and evaluating the sprung mass mode outputs. Finally the resultant diagonal controllers were evaluated on the non-linear ACSL model in order to consider the ride performance achieved by the decoupling procedure and the resultant frequency domain control. For these non-linear simulations the same response parameters were plotted as for the state space case.

For both the state space and frequency domain studies, the results for the direct design process based on the full vehicle model are discussed first, followed by a comparison of the best of these results with the best results achieved for the quarter car studies.

### 4.5.1 State Space

For the state space solutions obtained in the form given by equation 3.23, the feedback control had to be transformed into a suitable form as described in the previous chapter. This was achieved for the full vehicle case by

selecting the output equations relating to the strut deflections and velocities, tyre deflections and absolute wheel vertical velocities. The required transformation of the matrix of feedback gains is then given by equation 3.27. In MATLAB the pseudo inverse can be found for non-square matrices, and this was used to invert $\boldsymbol{C}$.

For the linear quadratic regulator study an iterative process of varying the performance index weights was used to achieve some good results, showing similar trends to those described in the quarter vehicle studies. Figures 4.14a-g show the linear model responses to a heave input for the linear quadratic regulator design process, with performance index weights used for each given in table 4.11 and resultant feedback gains for the best solution given in table 4.12. An increase in the tyre load variation weight, gave a reduction in body and wheel response oscillation, together with a decrease in the speed of response of the body, and an increase in speed of response for the wheel. This trend can be seen in figures 4.14a-d. An increase in the sprung mass heave, pitch and roll accelerations weight had very little effect on the overall vehicle response, however overshoot was marginally reduced in both the body and wheel response, as shown in figures 4.14g,c,f. As expected, an increase in the control effort weight produced a deterioration in both body and wheel response, in terms of oscillation and overshoot as illustrated in figures 4.14g,b,e.

The best of these regulator results was then used to show the equivalent response to a pitch and roll input. The heave response of the best solution chosen is shown in figure 4.14d, and the corresponding pitch and roll responses are given in figures 4.14h,i. These results show that a control design achieving a good vehicle heave response, also provides good pitch and roll responses, with

similar characteristics in terms of levels of overshoot, oscillation and speed of response. This can be explained by the use of equal performance index weights for each of the sprung mass modes of acceleration.

For the pole placement study an iterative process as described in chapter three was similarly undertaken and good results were obtained with trends as expected intuitively. Figures 4.15a-h show the heave results for this pole placement study, with pole positions used given in table 4.13, and resultant feedback gains for the best solution given in table 4.14. The effect of increasing the damping in the body modes was a reduction in the primary ride frequency oscillations in both the response of the sprung and unsprung masses, as shown in figures 4.15a-c. Similarly, increasing the damping in the unsprung mass modes reduced the oscillation at secondary ride frequencies in both responses, shown in figures 4.15d-f. However combining the best sprung mass mode poles locations with the best unsprung mass mode poles, did not result in the equivalent combination of responses. By way of an example, figure 4.15f contains the same body mode poles as in figure 4.15b, and wheel mode poles in figure 4.15e. The explanation for this is in the inability of pole placement methods to account for the interactions between modes.

Altering the frequencies of the modes also improves the resultant ride performance. Decreasing the frequency of the sprung mass modes, whilst increasing the frequency for the unsprung mass modes, yielded the best results. Figure 4.15g illustrates that these modal frequency changes improve the wheel response in terms of both overshoot and oscillation, however it also increases the body overshoot and oscillations. After further study it was found that due to interactions, the ideal solution of minimal overshoot and oscillations was

unobtainable. Figure 4.15h shows the response for the best frequencies for all modes as found above, with maximum damping, which would be expected to give the best overall ride performance. However, the vehicle response can be seen to be significantly worse than previous results, in terms of both the sprung and unsprung mass responses.

Again the best result from these heave results, as given in figure 4.15c, was subjected to a pitch and roll input. The results shown in figures 4.15i,j were again good, with similar characteristics to the heave response. The reason in this case is not so obvious, but comes from similar modifications to pole positions being made for all three sprung mass modes.

As a comparison the best results from the individual quarter car state space studies, using both linear quadratic regulator and pole placement design methods, were then evaluated on the full vehicle linear model with results given in figures 4.16a-f. The corresponding control design parameters and feedback solutions for these quarter car results are given in tables 4.15-4.18. Figures 4.16a,b show the heave response for the best regulator and pole placement solutions achieved, showing very good sprung and unsprung mass responses, which are in no way inferior even to the best full vehicle result. For the vehicle heave response this could be expected as the quarter car models are a valid simplification for the full vehicle heave problem, in which the cross corner coupling has insignificant effect. Similarly, however, the pitch and roll responses seen in figures 4.16c-f are very good for the quarter vehicle results, in some cases better than the full vehicle results.

This can be explained for the regulator study by considering the comparison of performance indexes. For the full vehicle model the heave, pitch

and roll accelerations of the sprung mass were minimised with equal weights. The tyre load variation minimisation also had a single weight for all four corners, as did the control effort. However the dynamic characteristics of the front and rear quarters are in fact significantly different. In contrast, for the individual quarter car studies, a separate performance index was used for the front and rear, resulting in more effectively independent weightings. Thus the equivalent minimised performance measure involved two independent weightings for the sprung mass accelerations, two for the tyre load variations and two for the control efforts. This could similarly be achieved for the full vehicle direct design method by including more independent performance index weightings, but this would lead to further complication of an already complex system.

For the pole placement study the quarter car results were also significantly better than the full vehicle based design results, in that good sprung and unsprung mass responses are achieved simultaneously. Again a possible explanation is that the quarter car results involved the placement of eight pairs of poles, two per corner, whereas the full vehicle techniques only placed seven pairs.

Finally one example full vehicle linear result was taken and evaluated on the non-linear model, in order to see the effects of the non-linearities on the performance. The best linear quadratic regulator result was chosen, with linear response shown in figure 4.14d, and the equivalent non-linear evaluation is shown in figure 4.17. It can be seen that there is negligible degradation of performance, with the sprung mass overshoot marginally increasing and the unsprung mass overshoot decreasing. This regulator solution was chosen for

non-linear evaluation since the linear heave response involved the greatest strut compression leading to the greatest effect of the spring aid non-linearity. This solution would therefore be expected to cause the greatest performance deterioration. This result validates the linear approximation assumed in this ride control study.

### 4.5.2 Frequency Domain

The dyadic expansion technique was applied as described using various values for the chosen frequencies $w_o$ and $w_1$ with the aim of achieving diagonalisation of the system transfer function matrix for the complete range of ride frequencies of interest here. However, after an extensive study, no pair of values was found to give this level of diagonalisation. By choosing both $w_o$ and $w_1$ to be two of the three sprung mass natural frequencies, however, decoupling was achieved for the range of primary ride frequencies. The best decoupling was in fact obtained by choosing $w_o = 12.07$, and $w_1 = 7.2$, which correspond to the sprung mass roll and heave resonant frequencies as shown in table 4.10. The resultant decoupling matrices were then found to be

$$V^{-1} = \begin{pmatrix} 0.68963 & 0.68963 & 0.24365 & 0.24365 \\ -0.56979 & 0.56979 & -0.46055 & 0.46055 \\ -0.59361 & 0.59361 & 0.42941 & -0.42940 \\ -0.41184 & -0.41180 & 0.60446 & 0.60443 \end{pmatrix} \qquad (4.13)$$

$$VG^{-1}(jw_0) = \begin{pmatrix} 2.2618E8 & 8.1795E8 & -3.1877E2 & -2.6343E6 \\ 2.2618E8 & -8.1795E8 & 3.1878E2 & -2.6343E6 \\ 7.9971E7 & 6.5517E8 & 2.2760E2 & 3.8758E6 \\ 7.9971E7 & -6.5317E8 & -2.2770E2 & 3.8759E6 \end{pmatrix} \quad (4.14)$$

In order to illustrate the level of diagonalisation achieved with dyadic expansion, measures of the column and row dominance ratios are given by

$$col\ dom = \frac{\sum_j abs(F(j,i)) - abs(F(i,i))}{abs(F(i,i))} \quad (4.15)$$

$$row\ dom = \frac{\sum_j abs(F(i,j)) - abs(F(i,i))}{abs(F(i,i))} \quad (4.16)$$

where $F(i,j)$ are the component frequency response matrices. These measures for the system under consideration are plotted in figures 4.18. These results showed good column dominance was achieved with significantly poorer row dominance. By simply scaling the columns of the new transfer function, the column dominance is left unaltered, whilst the row dominance can be improved. This scaling effectively scales each of the individual SISO systems, and will provide a scaling factor for the feedback compensation used. Figures 4.19. show the resultant column and row dominance measures for the scaled system, with the scaling matrix given by

$$Scale = \begin{pmatrix} 1 & 0 & 0 & 0 \\ 0 & 1 & 0 & 0 \\ 0 & 0 & 1000 & 0 \\ 0 & 0 & 0 & 10 \end{pmatrix} \quad (4.17)$$

Figures 4.20 show bode plots for the resultant diagonalised transfer function

matrix with block diagram as given in figure 4.13, and these results also illustrate the level of decoupling achieved.

The frequency domain design was then performed individually for each of the heave, pitch and roll SISO systems in the same way as for the quarter car studies described in chapter three. As the structure of the SISO transfer functions in terms of poles and zeros were so similar to the quarter car transfer function, the same compensator was chosen, and the parameters tuned by a similar iterative process to obtain the desired system response. Figures 4.21a-k show the frequency domain design results for the heave, pitch and roll SISO systems, with the compensator details as given in table 4.19 used with the scaled diagonalisation described. These figures show the trend in mode response as the parameters are varied. The best solutions for each mode with linear response given in figures 4.21c,g,j were chosen to be the middle result for each.

The combined diagonal controller, with the flexure mode left uncontrolled with zero feedback compensation, was subsequently evaluated on the non-linear ACSL model. Figure 4.22a shows the vehicle response to a road input including heave and pitch, and 4.22b used a road input with heave, pitch and roll constituents. The results show reasonable vehicle responses, with negligible oscillation but some overshoot.

Finally the best quarter car frequency domain results were applied independently to each corner of the vehicle and the resultant controller evaluated on the non-linear ACSL model as a comparison to the full vehicle results already seen. Table 4.20 gives the feedback compensation used for these results. A road input consisting of heave and pitch components was used, and the response is shown in figure 4.23. In contrast to the state space study, the

frequency domain quarter car results achieved very poor vehicle ride performance, with significant levels of overshoot and oscillation in both sprung and unsprung mass responses. This is as expected and is explained by the effects of coupling between the four corners of the vehicle and between the ride modes of the vehicle.

## 4.6 Conclusions

The objectives of the full vehicle ride control study were to investigate the achievable performance limitations incurred by designing the control strategy with quarter car model, together with the level of additional complexity involved in designing the controllers directly with the full vehicle model. To this end the ride control study for an ideal active system was repeated using a full vehicle model. This involved the development of such a model using the same techniques and tools previously described, with the intermediate step of a rear quarter car representation. Again both state space and frequency domain design methods were applied and the resultant ride performances achieved were discussed. These results were the  compared to the performance achieved by applying the quarter car feedback solutions independently to each corner of the vehicle.

The conclusions drawn from the results discussed are two fold. Firstly the state variable feedback controllers achieved better heave, pitch and roll performance for the quarter car based designs. The directly designed full vehicle results were good, but the additional complexity involved in the design did not offer any potential performance improvements, and so was not justified.

The major reason for this unexpected result related to the number of

independent design parameters involved on the two different design methods. The designs based on the quarter car model involved more independent performance index weightings in the regulator design, and more pole locations in the pole placement techniques. Thus the full vehicle model based results could be improved by increasing these parameters, but at the cost of increased complexity. For both state space methods the interactions ignored in the quarter car designs had negligible effects on the resultant ride performance.

In contrast, for frequency domain techniques the quarter car results gave very poor results for heave, pitch and roll inputs. The full vehicle study produced reasonable results, but at a cost in terms of an increase in design process complexity due to the decoupling requirement. The dyadic expansion procedure was complex, with some numerical problems, and only provided diagonalisation around the sprung mass resonant frequencies. However this was sufficient to provide some good ride control results, although these were still inferior to the state space results.

The decoupling achieved by the dyadic expansion techniques, however, provide other significant advantages and opportunities in the area of suspension control. Valuable insight into the vehicle coupling characteristics was gained throughout this exercise. One advantage could be gained by the application of the decoupling system forming the first stage of any suspension controller. Subsequently the control of the different vehicle modes could be addressed independently. This provides the ability to specify different control objectives for the heave, pitch and roll modes, which is inherently advantageous as these modes are very different in terms of passenger requirements.

The decoupling of the system as a first control step also allows the use of

a variety of different control design techniques for the different requirements of each mode, not just frequency domain techniques as described in this study. Model-based and heuristic techniques could be easily combined and implemented together, allowing the most suitable choice to be made for individual modes.

| Body | Mass (kg) | Ixx (kg $m^2$) | Iyy (kg $m^2$) | Izz (kg $m^2$) |
|---|---|---|---|---|
| Sprung | 234.124 | 0.0 | 0.0 | 0.0 |
| Lower arm | 4.795 | 0.02558 | 0.001214 | 0.02558 |
| Strut | 2.884 | 0.00552 | 0.00552 | 0.000225 |
| Unsprung | 38.958 | 0.422 | 0.779 | 0.422 |

Table 4.1 : Rear Corner Mass and Inertia Properties

| Body | x coord (m) | y coord (m) | z coord (m) |
|---|---|---|---|
| Sprung | 3.732 | 0.325 | 0.400 |
| Lower arm | 3.743 | 0.4709 | 0.1267 |
| Strut | 3.707 | 0.542 | 0.534 |
| Unsprung | 3.732 | 0.725 | 0.167 |

Table 4.2 : Centre of Mass of Rear Corner Bodies

| Inboard | Outboard | x coord (m) | y coord (m) | z coord (m) |
|---|---|---|---|---|
| Sprung | Lower arm | 3.743 | 0.496 | 0.084 |
| Lower arm | Unsprung | 3.747 | 0.706 | 0.1095 |
| Strut | Sprung | 3.7012 | 0.525 | 0.6062 |
| Unsprung | Strut | 3.7044 | 0.5377 | 0.5714 |

Table 4.3 : Rear Corner Joint Positions

| Variable | Value |
|---|---|
| $K_s$ | 58550 N/m |
| salim | 0.028 m |
| $K_r$ | 5000000 N/m |
| rslim | 0.0624 m |
| $F_{sstat}$ | 4360.478 N |
| $K_t$ | 215000 N/m |
| $x_{tstat}$ | 0.012807 m |

Table 4.4 : Rear Corner ACSL Variable Values

| Body | Mass (kg) | Ixx (kg $m^2$) | Iyy (kg $m^2$) | Izz (kg $m^2$) |
|---|---|---|---|---|
| Sprung | 1247.257 | 244.6 | 946.16 | 1190.76 |

Table 4.5 : Full Vehicle Sprung Mass and Inertia Properties

| Body | x coord (m) | y coord (m) | z coord (m) |
|---|---|---|---|
| Sprung | 2.000 | 0.0 | 0.400 |

Table 4.6 - Full Vehicle Sprung Centre of Mass

| Variable | Value |
|---|---|
| $K_{arb}$ front | 11600 N/m |
| $K_{arb}$ rear | 4920 N/m |
| $F_{sstat}$ front | 5533.9020 N |
| $F_{sstat}$ rear | 4323.9196 N |
| $x_{tstat}$ front | 0.0204553 m |
| $x_{tstat}$ rear | 0.0127127 m |

Table 4.7 : Full Vehicle ACSL Variable Values

| Mode | Frequency (Hz) | Frequency (rad/s) |
|---|---|---|
| Sprung Mass | 1.5 - 1.8 | 9.425 - 11.31 |
| Unsprung Mass | 15.0 - 17.0 | 94.25 - 106.81 |

Table 4.8 : Sine Sweep Test Results

| Condition | Body Modes Frequency (rad/s) | | Wheel Modes Frequency (rad/s) | |
|---|---|---|---|---|
| Linear Damping 1500 N/m Front 1000 N/m Rear | 7.2295 | Heave | 70.3746 | Front In Phase |
| | 11.8296 | Pitch | 73.6526 | Front Anti-Phase |
| | 12.1903 | Roll | 74.7622 | Rear In Phase |
| | | | 76.6788 | Rear Anti-Phase |
| Increased Suspension Stiffness by 23000 N/m Front | 7.9676 | Heave | 71.4157 | Front In Phase |
| | 12.1517 | Pitch | 74.6593 | Front Anti-Phase |
| | 13.1104 | Roll | 74.7547 | Rear In Phase |
| | | | 76.6462 | Rear Anti-Phase |
| Increased Suspension Stiffness to 33000 N/m Front 12500 N/m Rear | 8.5920 | Heave | 72.2146 | Front In Phase |
| | 13.1486 | Pitch | 75.3322 | Front Anti-Phase |
| | 14.1548 | Roll | 75.4294 | Rear In Phase |
| | | | 77.177 | Rear Anti-Phase |
| Increased Tyre Stiffness by 35000 N/m | 7.2710 | Heave | 75.4415 | Front In Phase |
| | 11.8842 | Pitch | 78.4952 | Front Anti-Phase |
| | 12.2463 | Roll | 80.2697 | Rear In Phase |
| | | | 82.0758 | Rear Anti-Phase |

Table 4.9 : Modal Analysis Results

| Mode | Frequency (rad/s) |
|---|---|
| Body Heave | 7.2026 |
| Body Pitch | 11.7066 |
| Body Roll | 12.0725 |
| Front Wheel Hop In Phase | 70.6522 |
| Front Wheel Hop Anti-Phase | 73.9524 |
| Rear Wheel Hop In Phase | 75.5306 |
| Rear Wheel Hop Anti-Phase | 77.1124 |

Table 4.10 : Undamped Pole Frequencies

| Solution | $acc^2$ | $tlv^2$ | $u^2$ |
|---|---|---|---|
| a | 1 | $10^5$ | $10^3$ |
| b | 1 | $10^6$ | $10^3$ |
| c | 1 | $10^7$ | $10^3$ |
| d | 1 | $10^8$ | $10^3$ |
| e | 1 | $10^6$ | $10^4$ |
| f | 1 | $10^8$ | $10^4$ |
| g | 1 | $10^6$ | $10^2$ |

Table 4.11 : Performance Index Weightings

| | | | | |
|---|---|---|---|---|
| Strut Deflection Gains | 40.491 | -40.831 | 32.814 | -32.886 |
| | -40.831 | 40.491 | -32.886 | 32.814 |
| | 35.562 | -35.60 | 28.761 | -28.809 |
| | -35.60 | 35.562 | -28.809 | 28.761 |
| Tyre Deflection Gains | -219.16 | -47.549 | -18.271 | -0.93791 |
| | -47.549 | -219.16 | -0.93791 | -18.271 |
| | -5.4283 | -5.2407 | -197.60 | -36.391 |
| | -5.2407 | -5.4282 | -36.391 | -197.60 |
| Strut Velocity Gains | 1.4994 | 0.5293 | 0.1237 | 0.15566 |
| | 0.52932 | 1.4994 | 0.15566 | 0.12369 |
| | 0.12354 | 0.08987 | 0.80526 | 0.05975 |
| | 0.08987 | 0.12354 | 0.05975 | 0.80525 |
| Wheel Velocity Gains | -0.55223 | 0.34756 | -0.13661 | 0.284 |
| | 0.34757 | -0.55224 | 0.28401 | -0.13661 |
| | -0.10816 | 0.17384 | -0.52105 | 0.07573 |
| | 0.17384 | -0.10816 | 0.07573 | -0.52106 |

Table 4.12 : Feedback Gains for the Best Regulator Solution d

| Solution | Body Mode Pole Positions | Wheel Mode Pole Positions |
|---|---|---|
| a | -2.0 +/- 6.919i | -20.0 +/- 67.762i |
| | -3.0 +/- 11.316i | -20.0 +/- 67.671i |
| | -4.0 +/- 11.347i | -20.0 +/- 72.835i |
| | | -20.0 +/- 72.840i |
| b | -6.0 +/- 3.985i | -20.0 +/- 67.762i |
| | -10.0 +/- 6.087i | -20.0 +/- 67.671i |
| | -10.05 +/- 5.873i | -20.0 +/- 72.835i |
| | | -20.0 +/- 72.840i |
| c | -7.0 +/- 1.696i | -20.0 +/- 67.762i |
| | -11.0 +/- 4.007i | -20.0 +/- 67.671i |
| | -11.5 +/- 3.535i | -20.0 +/- 72.835i |
| | | -20.0 +/- 72.840i |
| d | -2.0 +/- 6.919i | -50.0 +/- 49.917i |
| | -3.0 +/- 11.316i | -50.0 +/- 49.794i |
| | -4.0 +/- 11.347i | -55.0 +/- 51.768i |
| | | -55.0 +/- 51.775i |
| e | -2.0 +/- 6.919i | -60.0 +/- 37.306i |
| | -3.0 +/- 11.316i | -60.0 +/- 37.141i |
| | -4.0 +/- 11.347i | -65.0 +/- 38.470i |
| | | -65.0 +/- 38.480i |
| f | -6.0 +/- 3.985i | -60.0 +/- 37.306i |
| | -10.0 +/- 6.087i | -60.0 +/- 37.141i |
| | -10.5 +/- 5.873i | -65.0 +/- 38.470i |
| | | -65.0 +/- 38.480i |

Table 4.13 : Pole Positions

| Solution | Body Mode Pole Positions | Wheel Mode Pole Positions |
|---|---|---|
| g | -2.5 +/- 1.000i | -50.0 +/- 69.000i |
| | -5 .0 +/- 2.500i | -50.0 +/- 68.000i |
| | -5 .5 +/- 3.000i | -55.0 +/- 70.000i |
| | | -55.0 +/- 71.000i |
| h | -3.0 | -85.0 |
| | -5.5 | -84.0 |
| | -6.0 | -86.0 |
| | | -87.0 |

Table 4.13 (continued)

| | | | | |
|---|---|---|---|---|
| Strut Deflection Gains | 4.0329 | -11.715 | -6.3481 | 9.8188 |
| | -1.3636 | 14.393 | 8.6602 | -7.7902 |
| | 4.6202 | -9.6623 | -6.587 | 7.5911 |
| | -0.22493 | 8.7532 | 5.7033 | -6.1382 |
| Tyre Deflection Gains | 3.0243 | -8.4722 | -8.7378 | 6.1782 |
| | -5.0863 | 5.5761 | 8.8014 | -5.0011 |
| | 4.9040 | -6.6051 | -9.3742 | 5.7437 |
| | -4.8076 | 9.8138 | 7.2768 | -6.1740 |
| Strut Velocity Gains | 0.21312 | 0.00097 | 0.21244 | 0.30910 |
| | 0.98289 | 1.2806 | 0.20711 | 0.02047 |
| | -0.36221 | -0.17131 | 0.40876 | 0.13028 |
| | 0.63103 | 0.39664 | -0.01454 | 0.31671 |
| Wheel Velocity Gains | -0.09097 | -0.02728 | 0.17673 | 0.29904 |
| | 0.69024 | 0.69803 | 0.20411 | -0.005655 |
| | -0.2497 | -0.14927 | 0.1859 | 0.12996 |
| | 0.45424 | 0.30345 | -0.00551 | 0.09646 |

Table 4.14 : Feedback Gains for the Best Pole Placement Solution c

| Corner | $acc^2$ | $tlv^2$ | $u^2$ |
|---|---|---|---|
| Front | 1 | $10^8$ | $10^3$ |
| Rear | 1 | $10^8$ | $10^3$ |

Table 4.15 : Performance Index Weightings for the Best Quarter Car Solution

| | | | | |
|---|---|---|---|---|
| Strut Deflection Gains | -0.53381 | 0.0 | 0.0 | 0.0 |
| | 0.0 | -0.53381 | 0.0 | 0.0 |
| | 0.0 | 0.0 | -0.78492 | 0.0 |
| | 0.0 | 0.0 | 0.0 | -0.78492 |
| Tyre Deflection Gains | -248.41 | 0.0 | 0.0 | 0.0 |
| | 0.0 | -248.41 | 0.0 | 0.0 |
| | 0.0 | 0.0 | -181.64 | 0.0 |
| | 0.0 | 0.0 | 0.0 | -181.64 |
| Strut Velocity Gains | 2.1474 | 0.0 | 0.0 | 0.0 |
| | 0.0 | 2.1474 | 0.0 | 0.0 |
| | 0.0 | 0.0 | 0.80489 | 0.0 |
| | 0.0 | 0.0 | 0.0 | 0.80489 |
| Wheel Velocity Gains | -0.11409 | 0.0 | 0.0 | 0.0 |
| | 0.0 | -0.11409 | 0.0 | 0.0 |
| | 0.0 | 0.0 | -0.43 | 0.0 |
| | 0.0 | 0.0 | 0.0 | -0.43 |

Table 4.16 : Feedback Gains for the Best Regulator Quarter Car Solution

| Corner | Body Mode Pole Position | Wheel Mode Pole Position |
|---|---|---|
| Front | -9.0 +/- 4.359i | -60.0 +/- 70.00i |
| Rear | -11.0 +/- 5.440i | -70.0 +/- 78.60i |

Table 4.17 : Pole Positions for the Best Quarter Car Solution

| | | | | |
|---|---|---|---|---|
| Strut Deflection Gains | 10.842 | 0.0 | 0.0 | 0.0 |
| | 0.0 | 10.842 | 0.0 | 0.0 |
| | 0.0 | 0.0 | 7.1155 | 0.0 |
| | 0.0 | 0.0 | 0.0 | 7.1155 |
| Tyre Deflection Gains | -29.584 | 0.0 | 0.0 | 0.0 |
| | 0.0 | -29.584 | 0.0 | 0.0 |
| | 0.0 | 0.0 | -31.037 | 0.0 |
| | 0.0 | 0.0 | 0.0 | -31.037 |
| Strut Velocity Gains | 2.8837 | 0.0 | 0.0 | 0.0 |
| | 0.0 | 2.8837 | 0.0 | 0.0 |
| | 0.0 | 0.0 | 1.4725 | 0.0 |
| | 0.0 | 0.0 | 0.0 | 1.4725 |
| Wheel Velocity Gains | 1.3729 | 0.0 | 0.0 | 0.0 |
| | 0.0 | 1.3729 | 0.0 | 0.0 |
| | 0.0 | 0.0 | 0.82953 | 0.0 |
| | 0.0 | 0.0 | 0.0 | 0.82953 |

Table 4.18 : Feedback Gains for the Best Pole Placement Quarter Car Solution

| Mode | Compensation |
|---|---|
| Heave | 2.5E-7(s + 1)/(s + 100) |
| Flexure | 0 |
| Roll | 5.0E-7(s + 1)/( s + 100) |
| Pitch | 7.5E-5(s + 1)/(s + 100) |

Table 4.19 : Feedback Compensation

| Corner | Strut Defl. Compensation |
|---|---|
| Front | 100(s + 1)/(s + 100) |
| Rear | 50(s + 1)/(s + 100) |

Table 4.20 : Feedback Compensation for the Best Quarter Car Solution

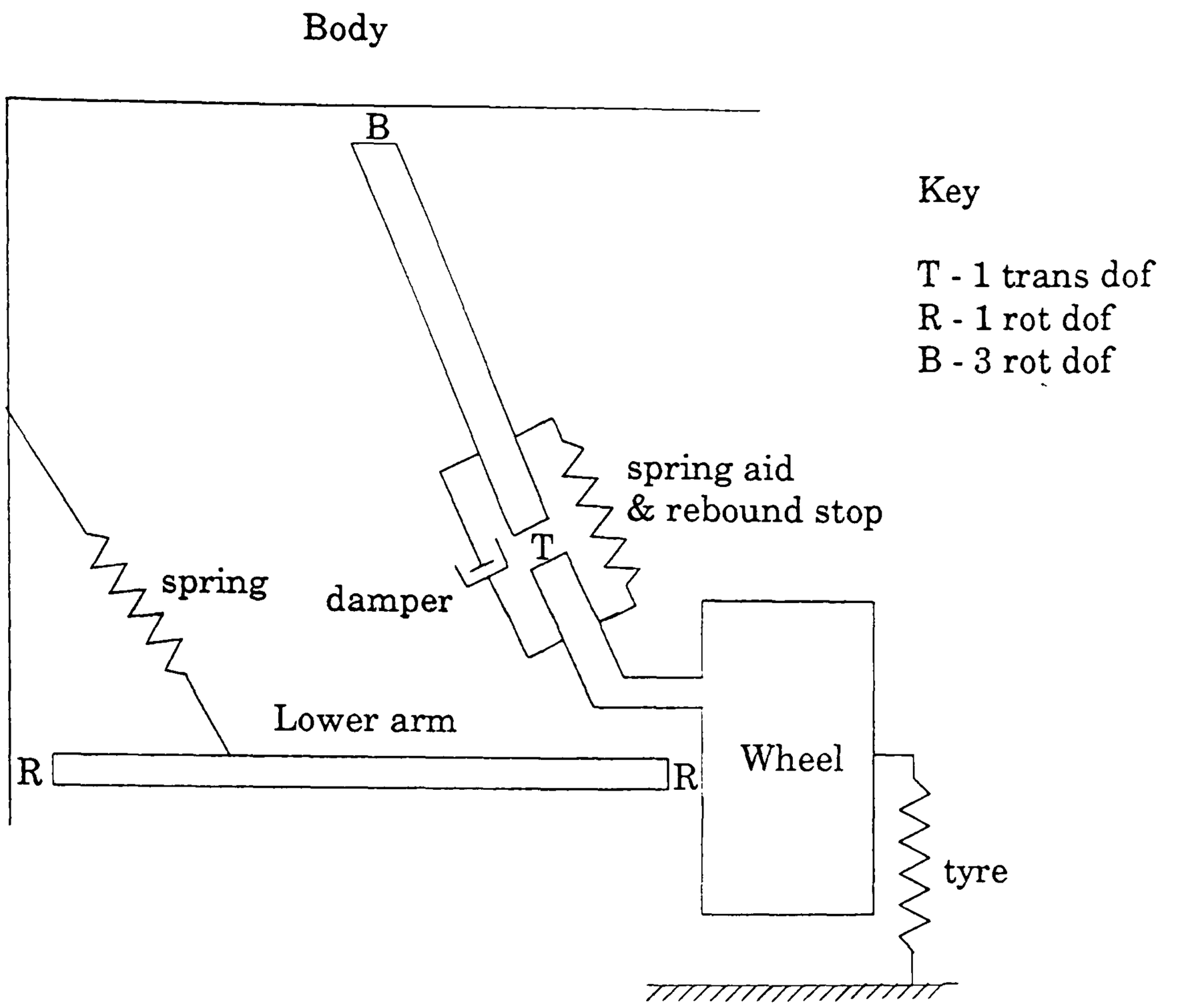


Figure 4.1 : Rear Quarter Car Model

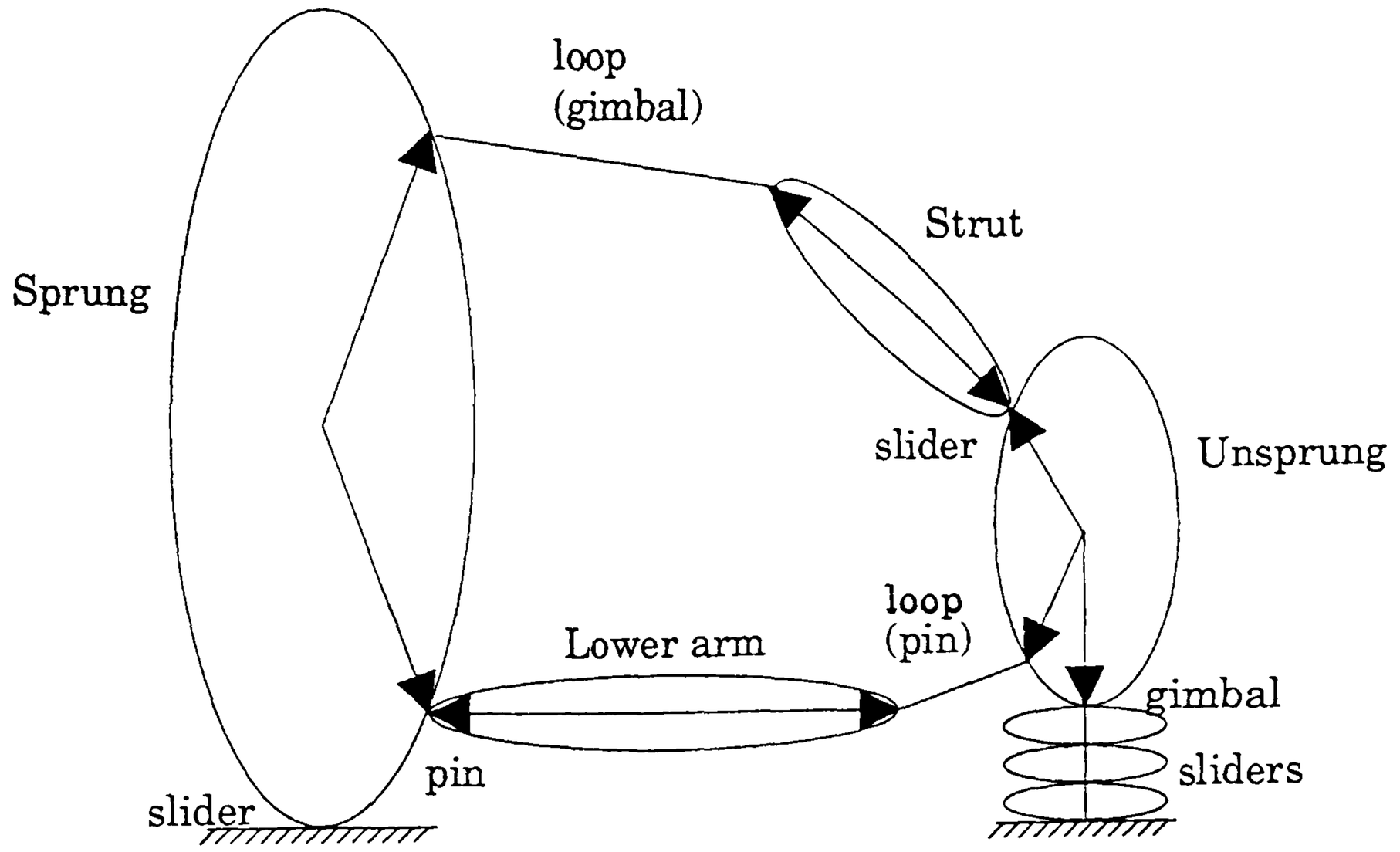


Figure 4.2 : Tree and Constraint Topology

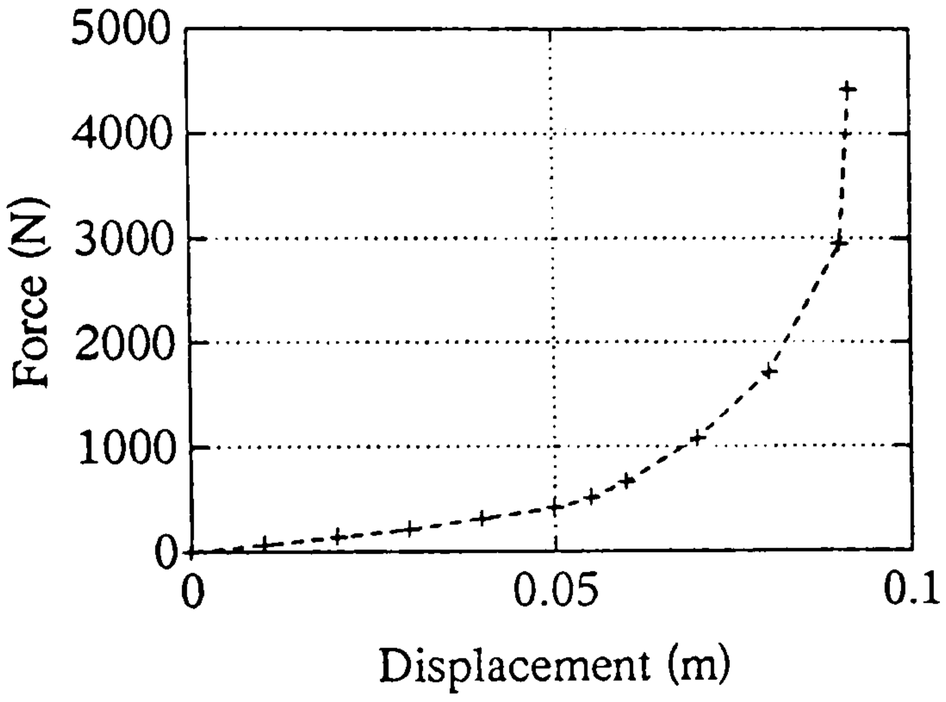


Figure 4.3 : Rear Spring Aid Characteristic

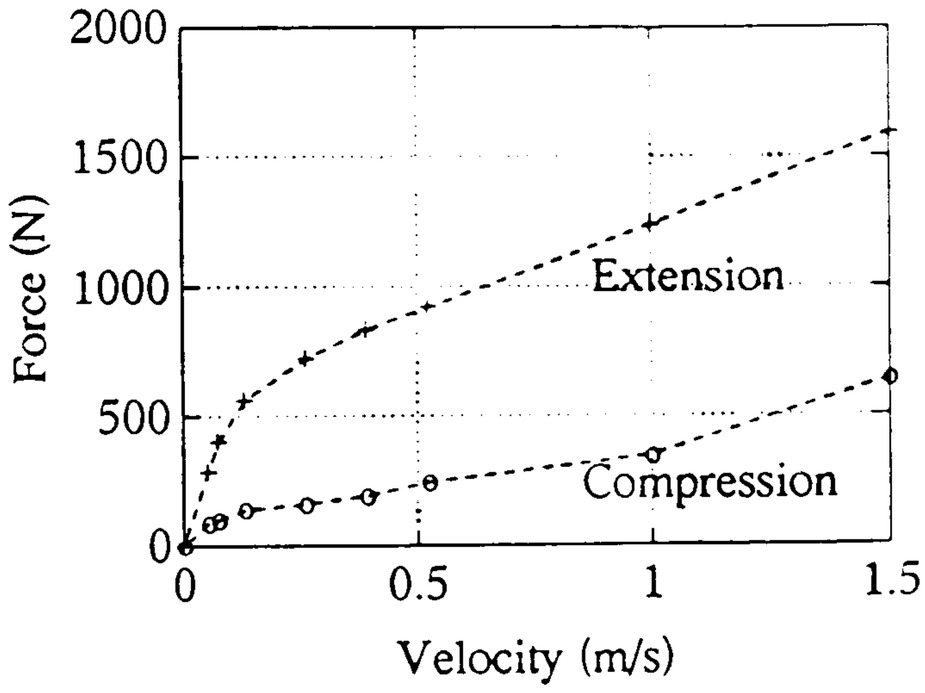


Figure 4.4 : Rear Damping Characteristic

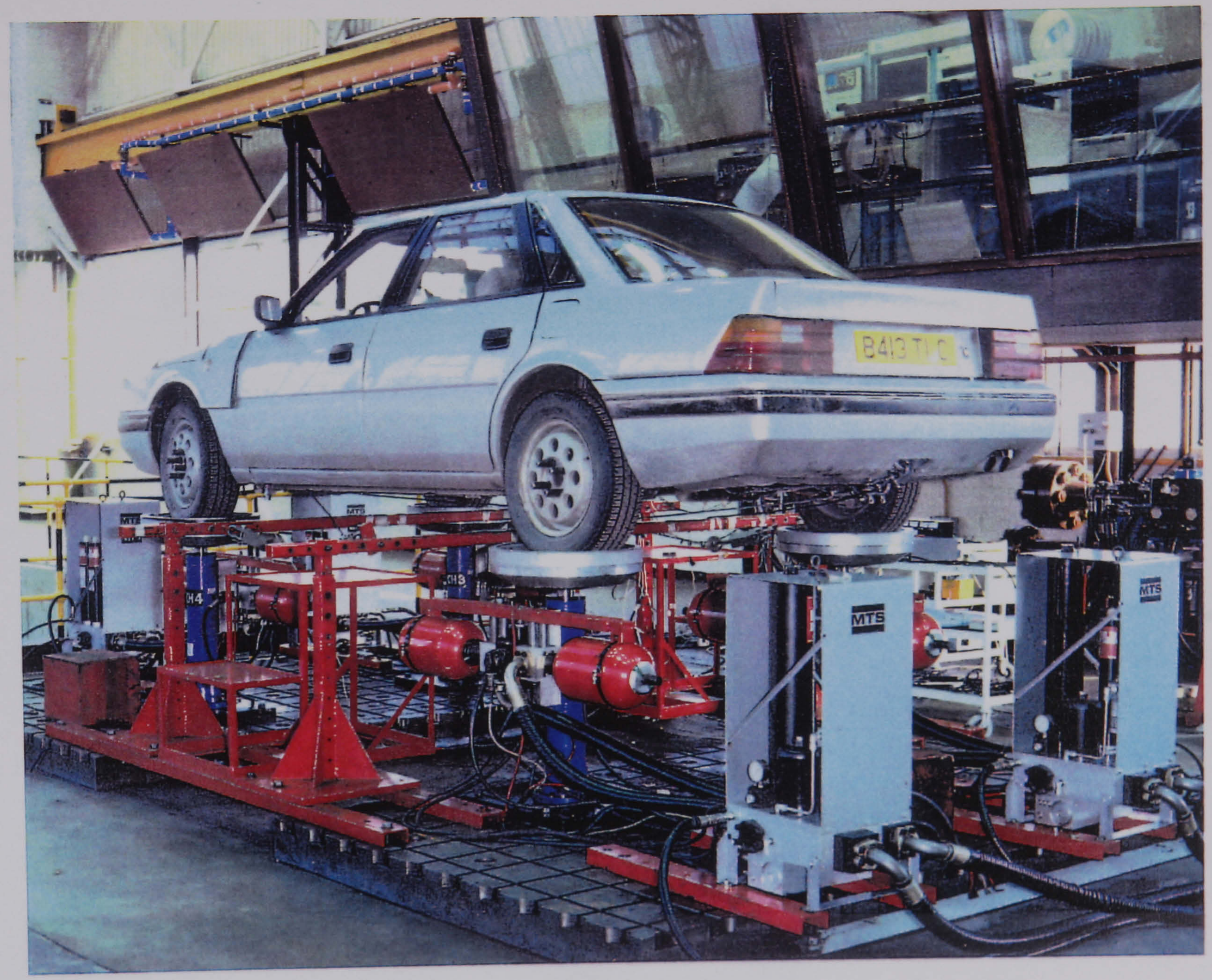


Figure 4.5 : Four Poster Road Simluator

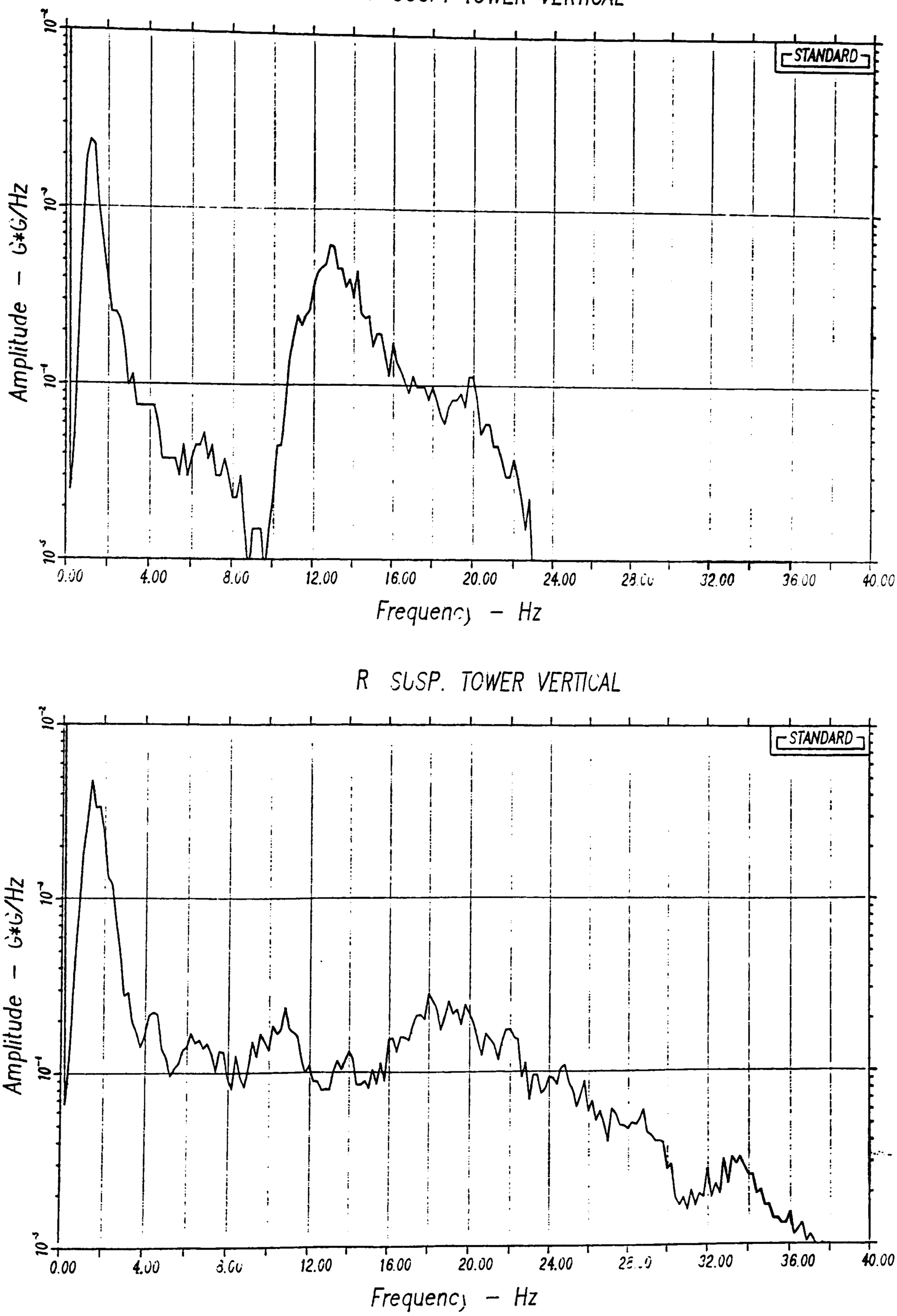


Figure 4.6 : Fossway Road Input Test Results

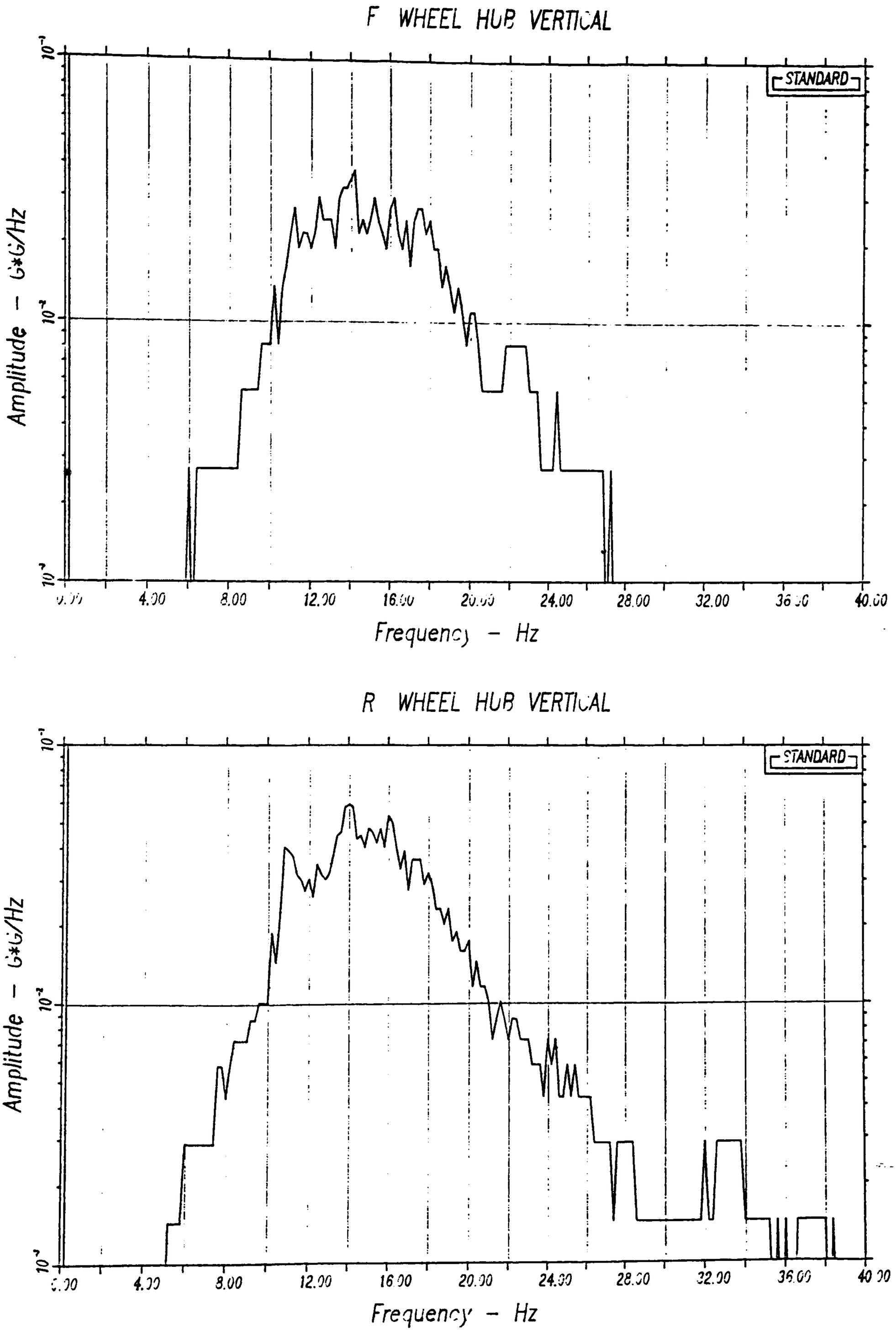


Figure 4.6 (continued)

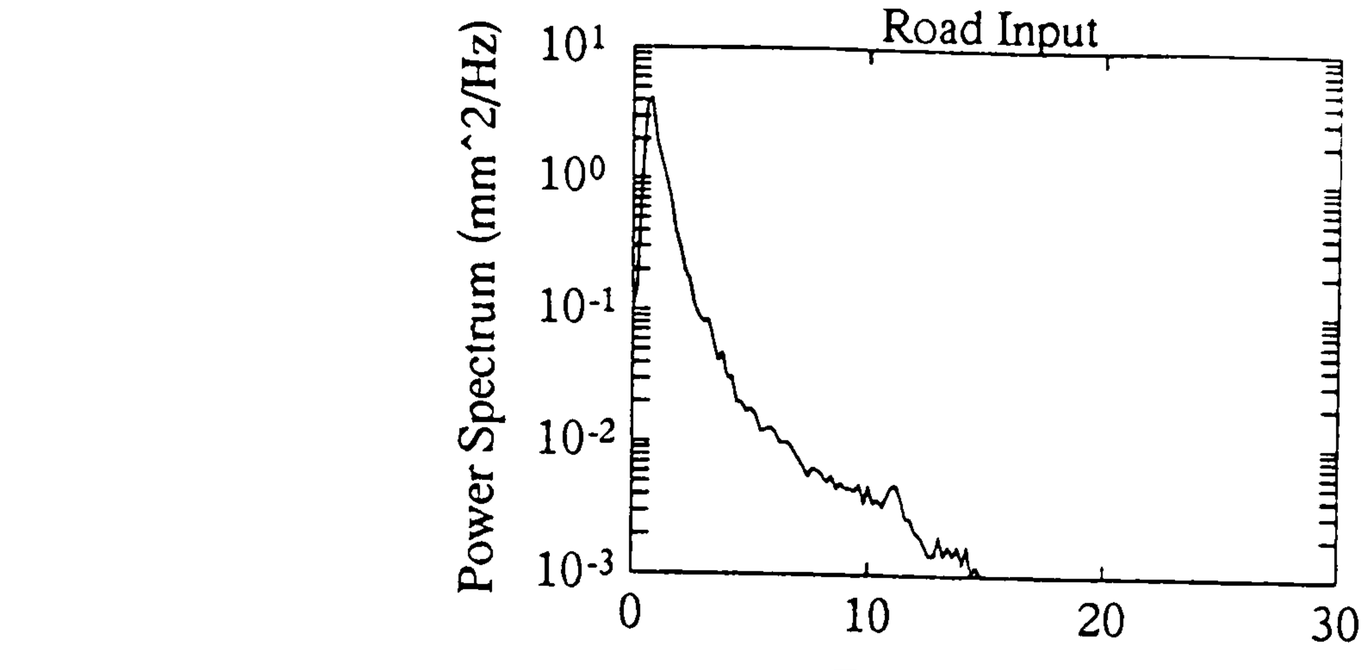


Figure 4.7 : Fossway Road Input

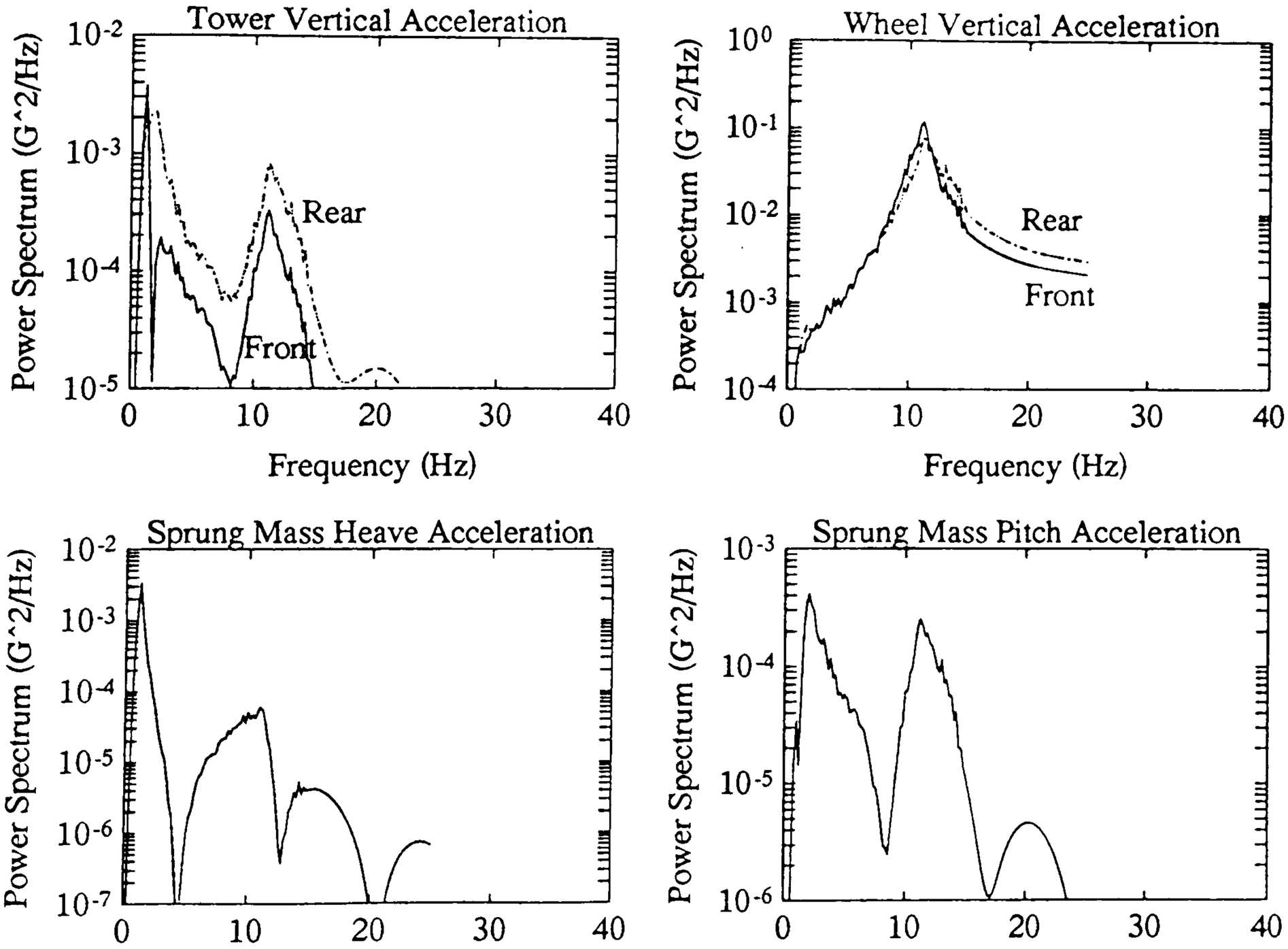


Figure 4.8 : Fossway Road Input Analysis Results

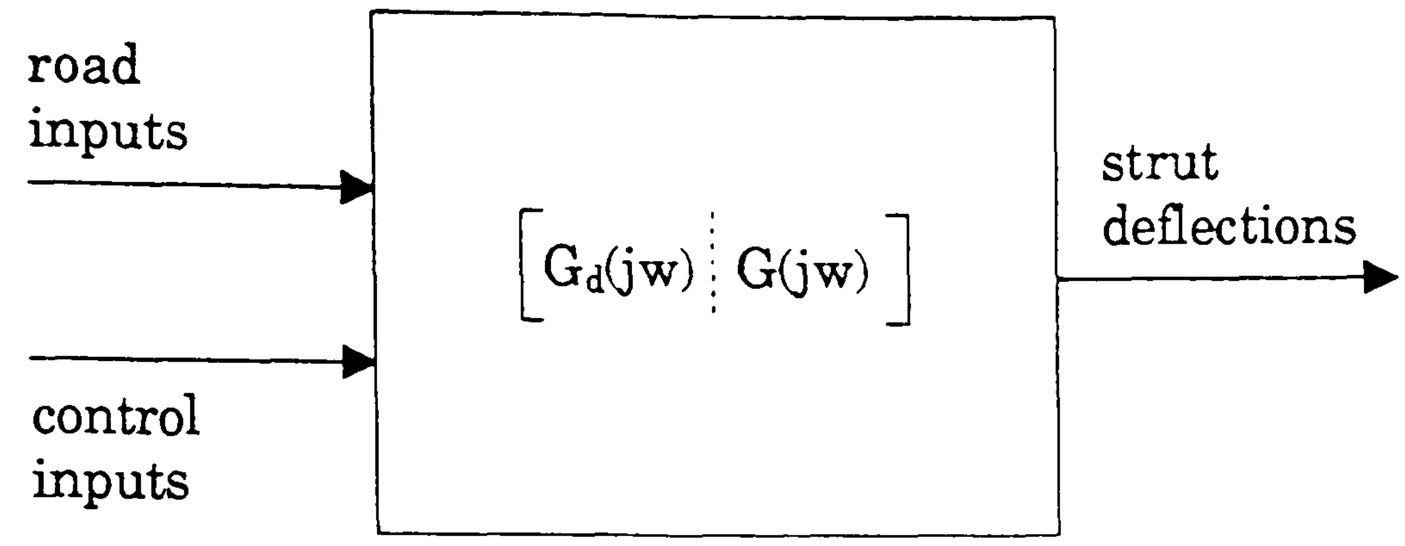


Figure 4.9 : Multivariable Full Vehicle Transfer Function

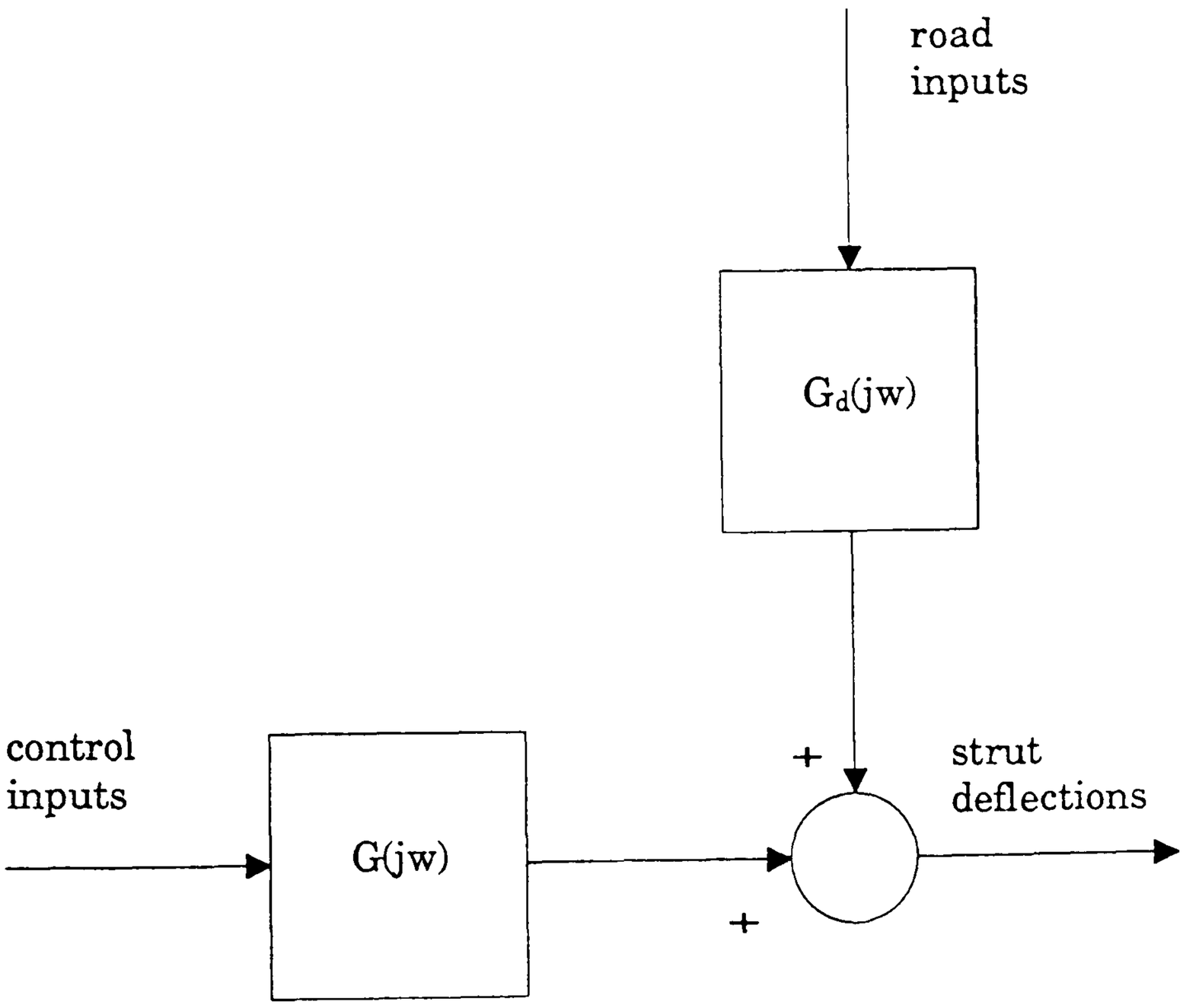


Figure 4.10 : Block Diagram of Full Vehicle

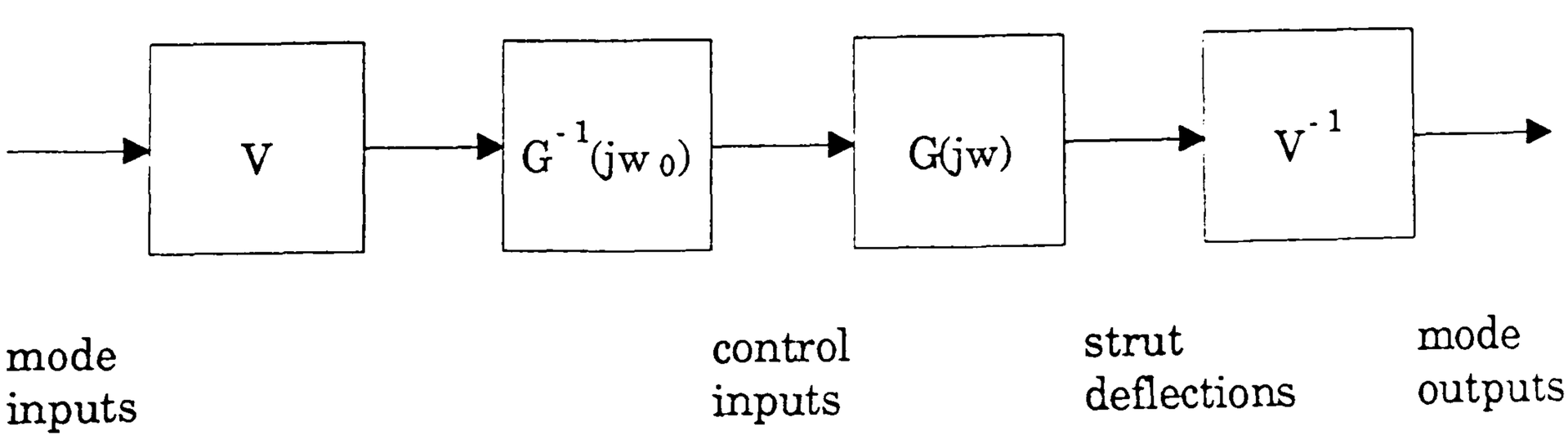


Figure 4.11 : Decoupled Transfer Function

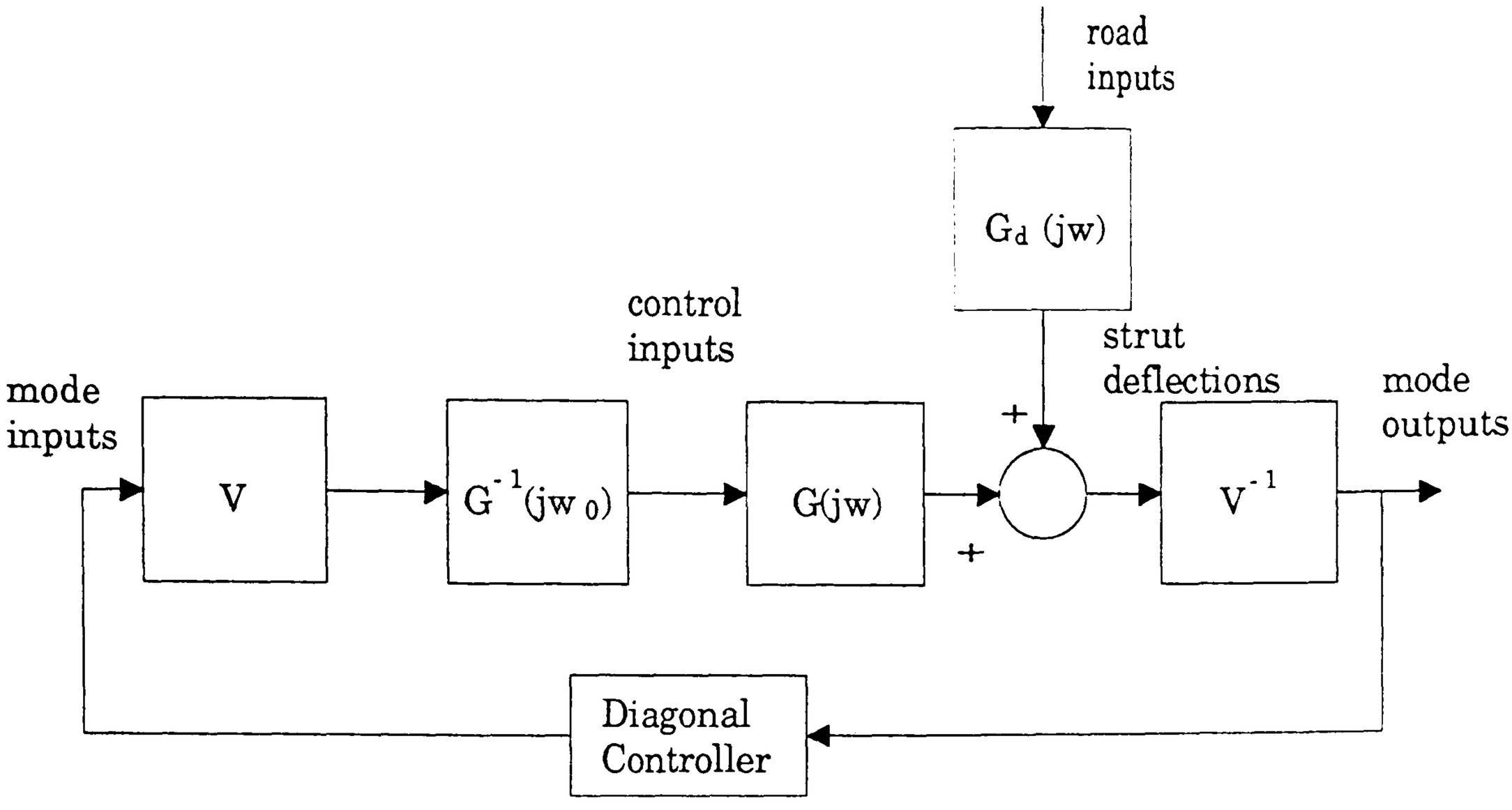


Figure 4.12 : Block Diagram of Decoupled System

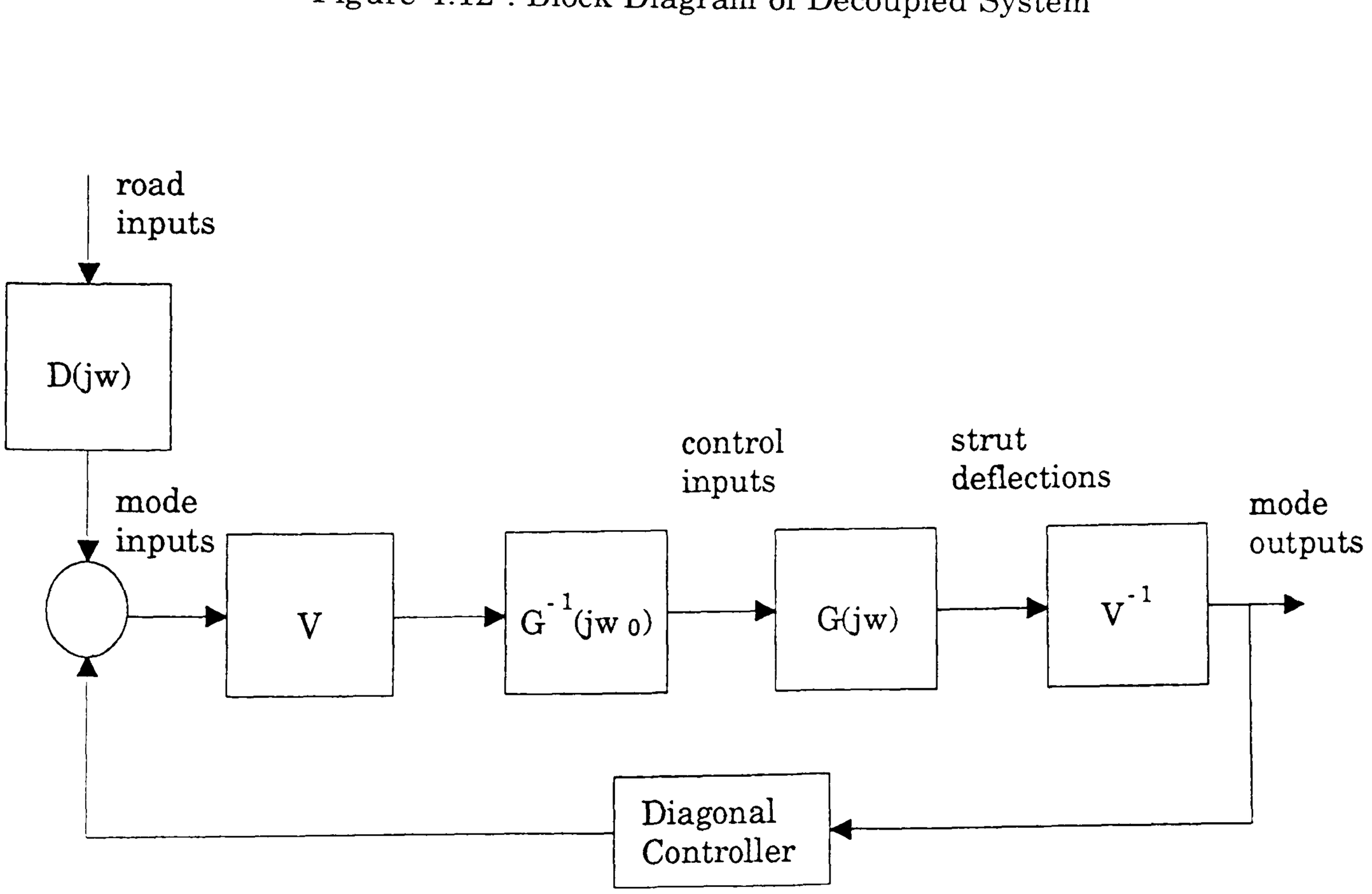


Figure 4.13 : Equivalent Block Diagram Structure

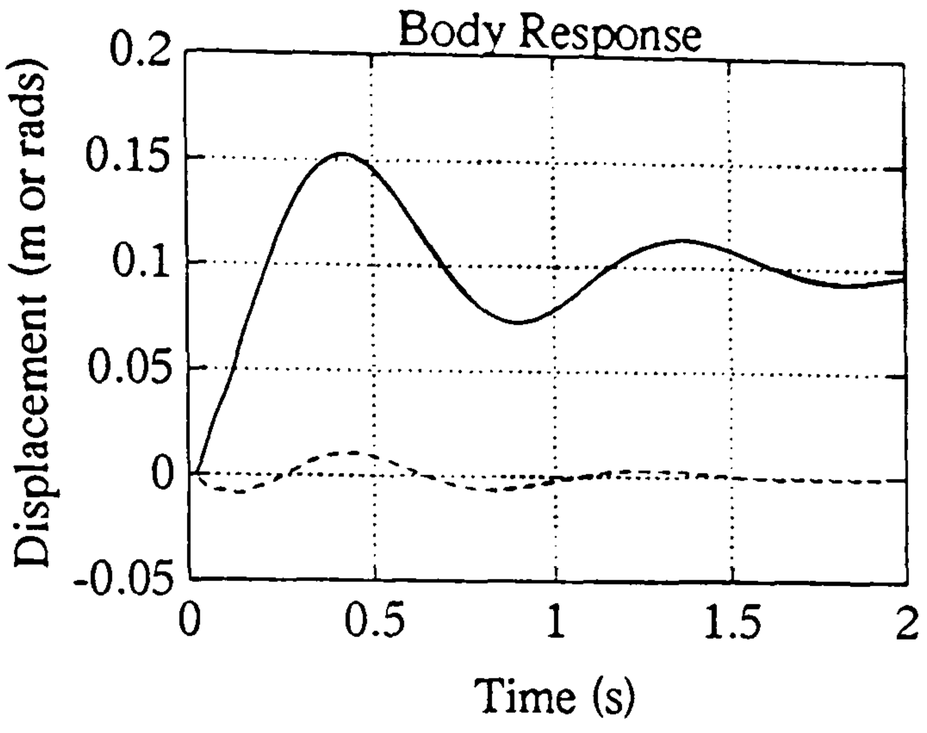


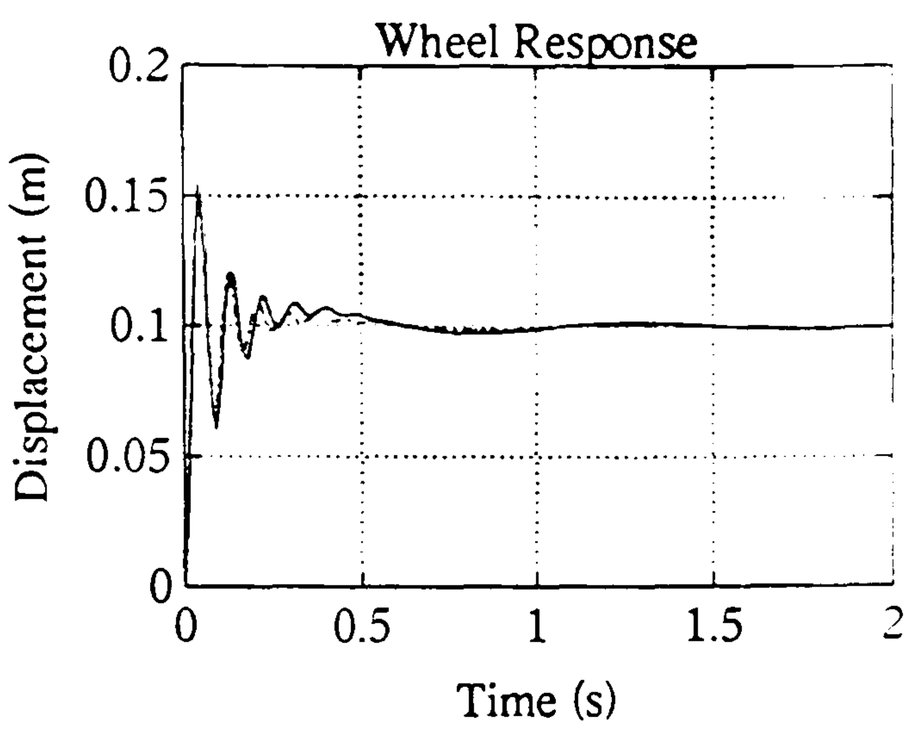


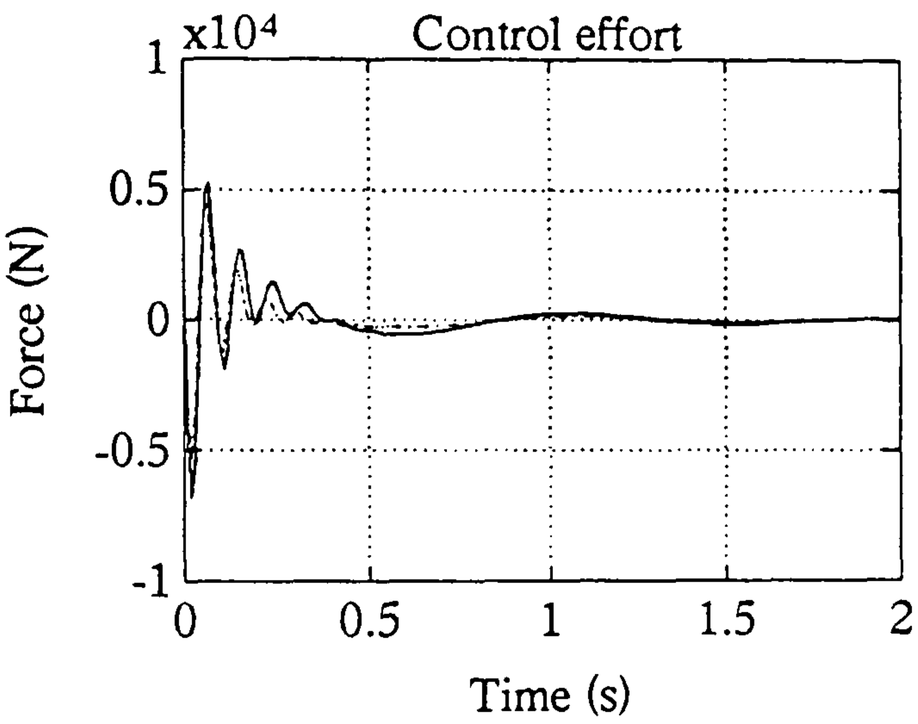


Figure 4.14a : Heave Response

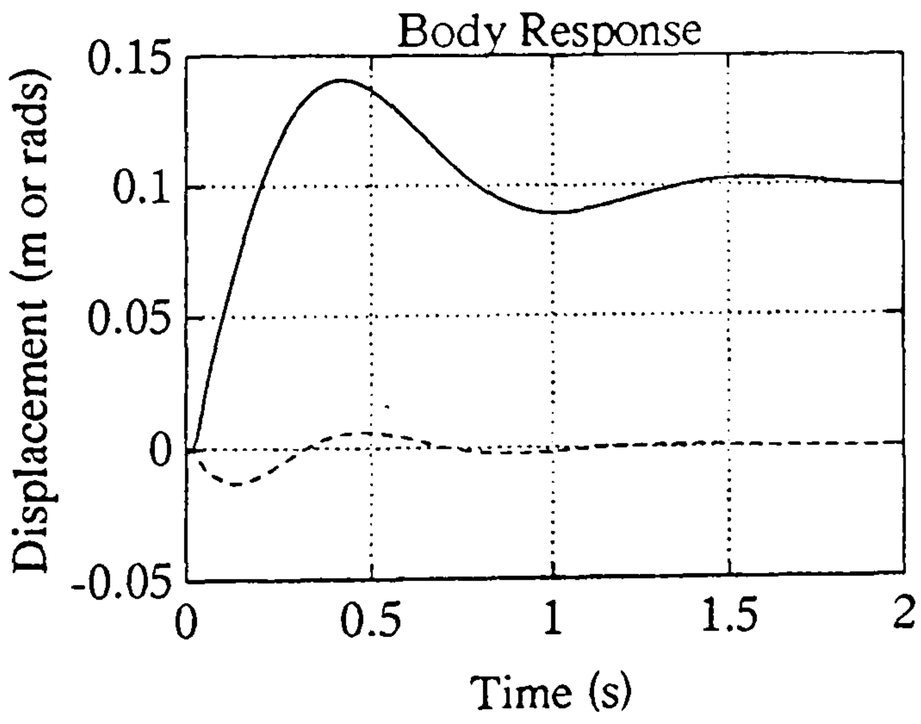


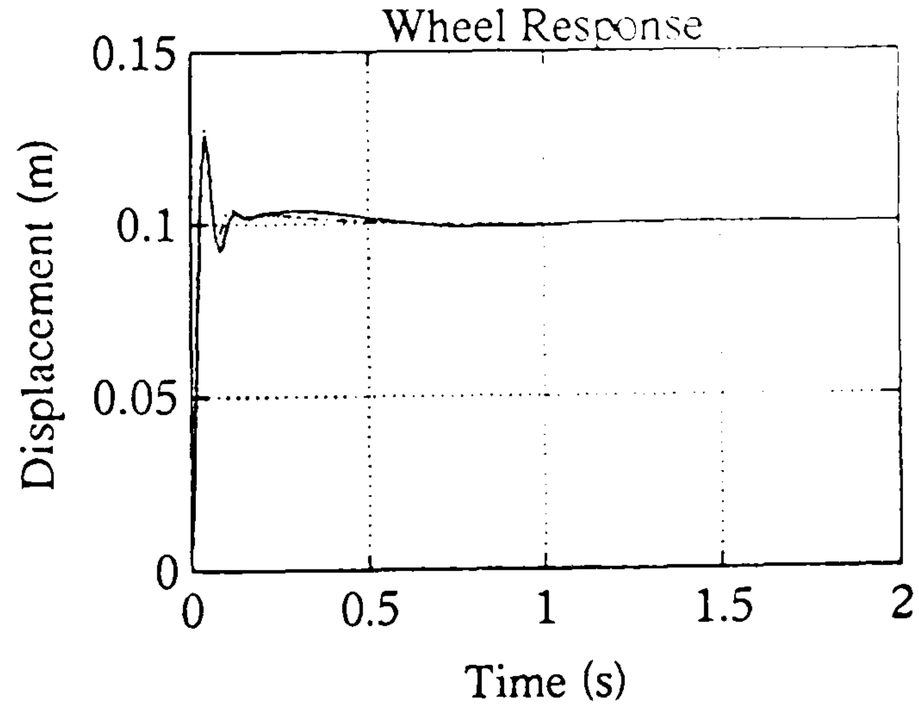


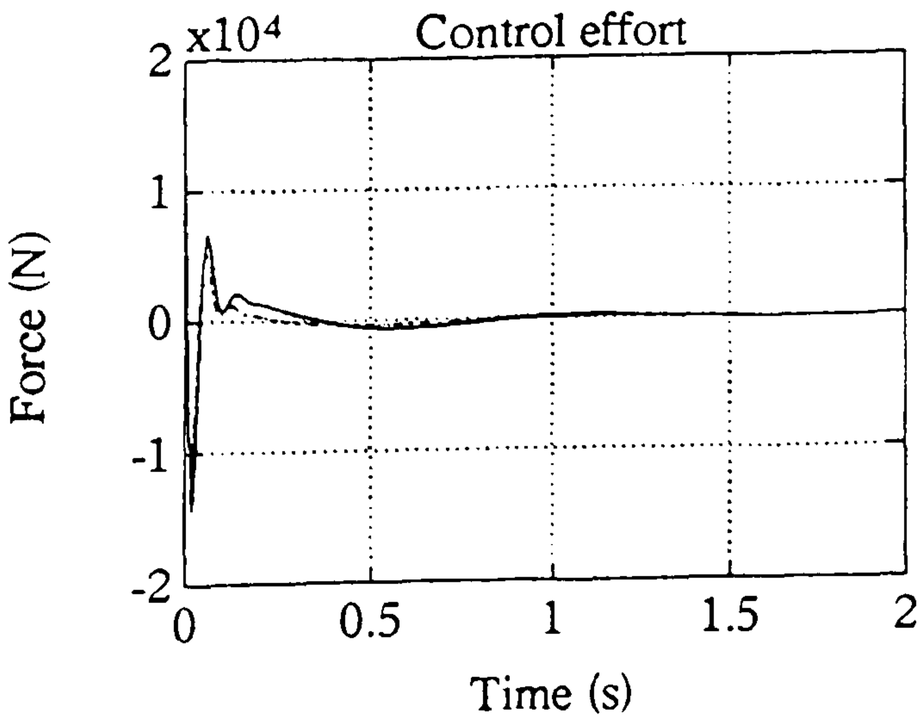


Figure 4.14b : Heave Response

Figure 4.14 : Linear Quadratic Regulator Solutions

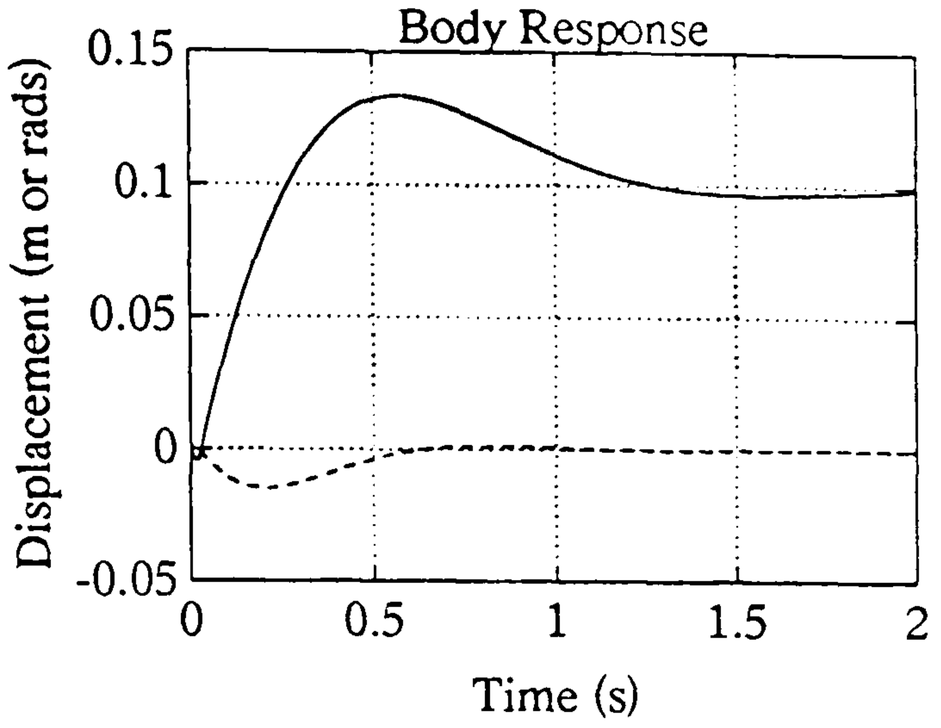


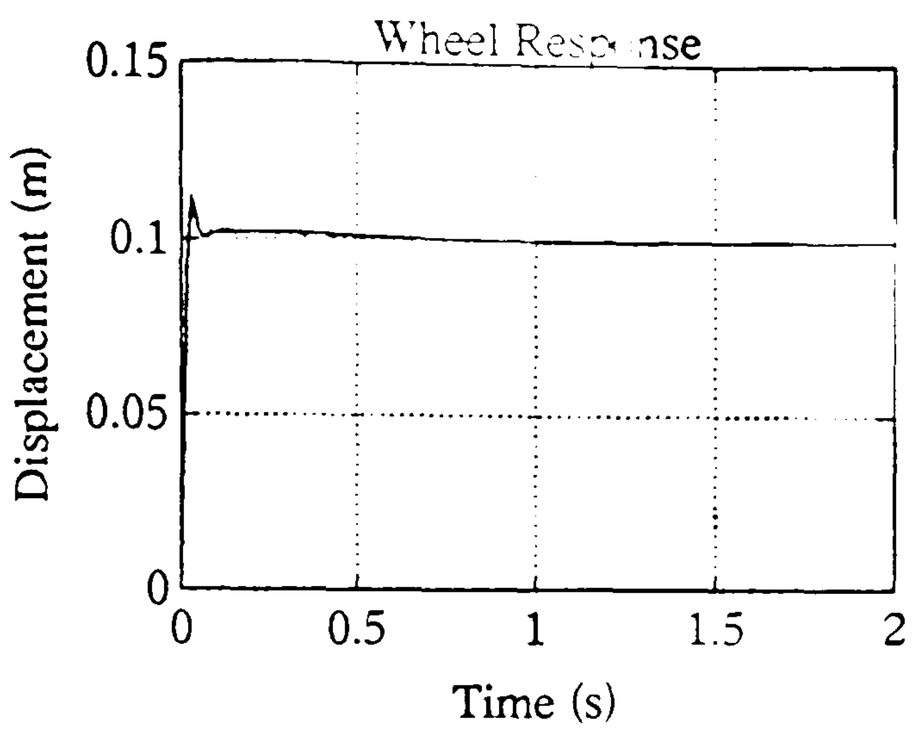


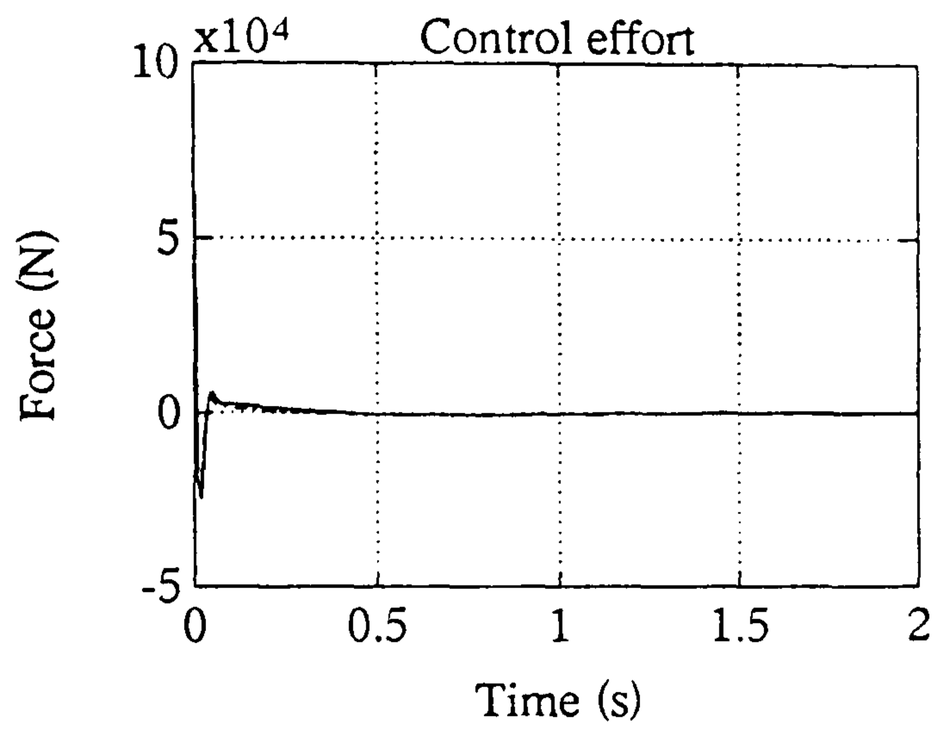


Figure 4.14c : Heave Response

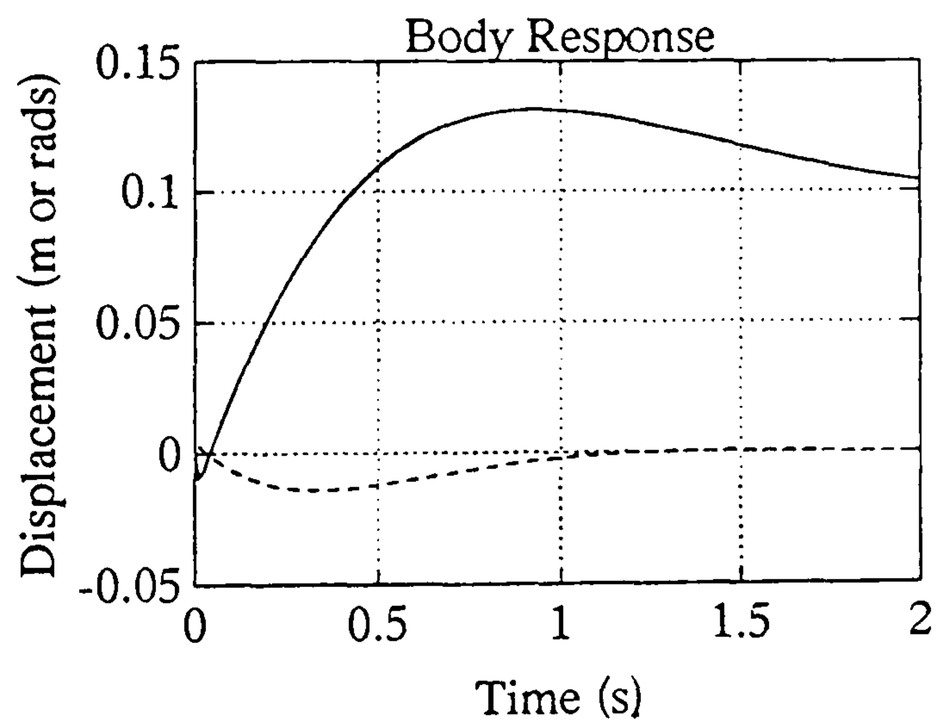


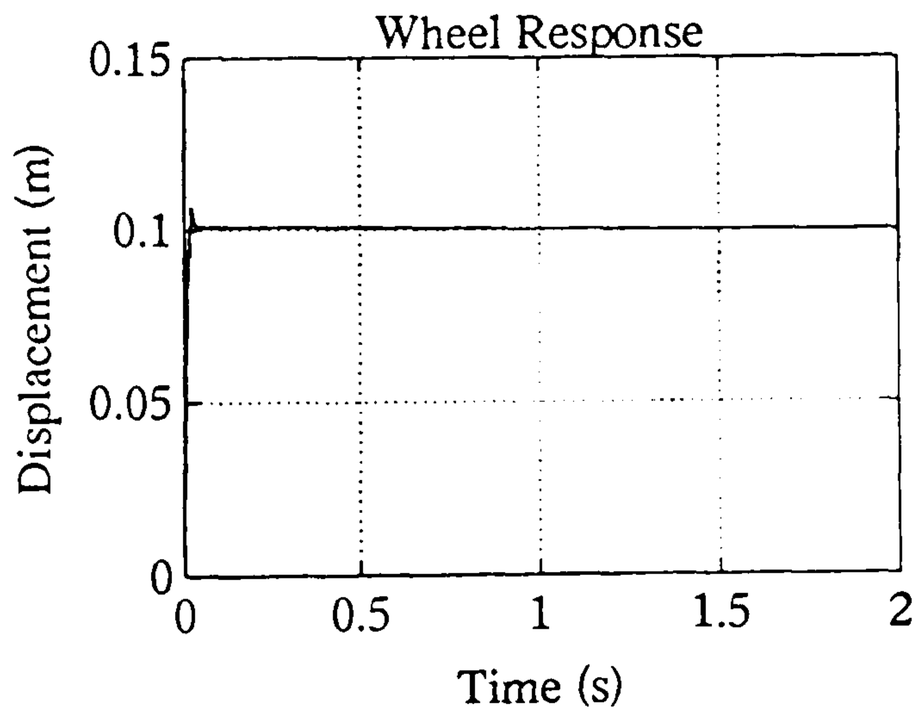


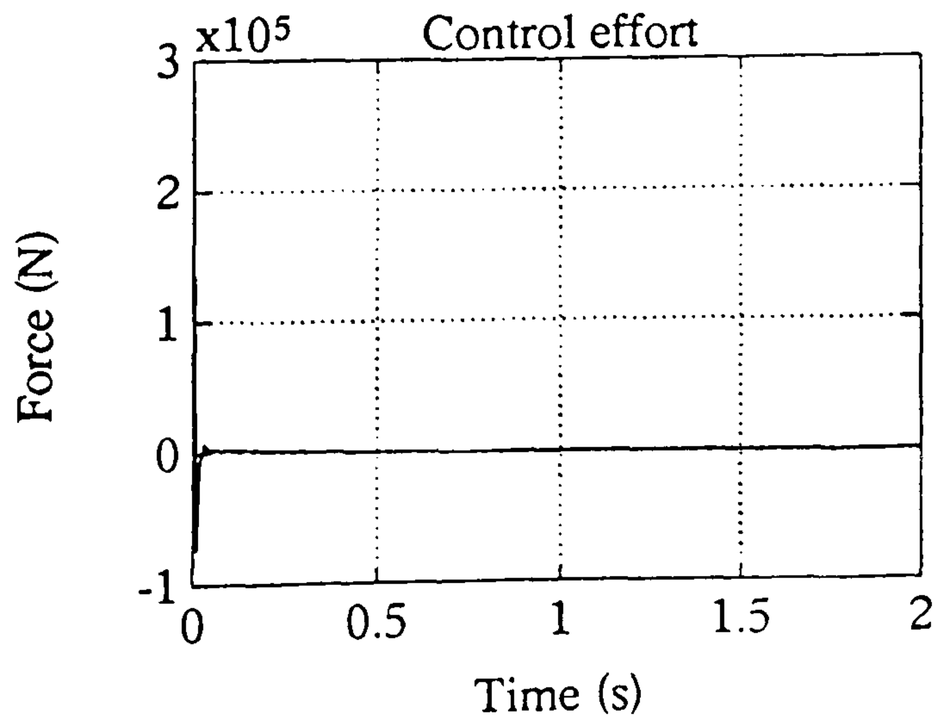


Figure 4.14d : Heave Response

Figure 4.14 (continued)

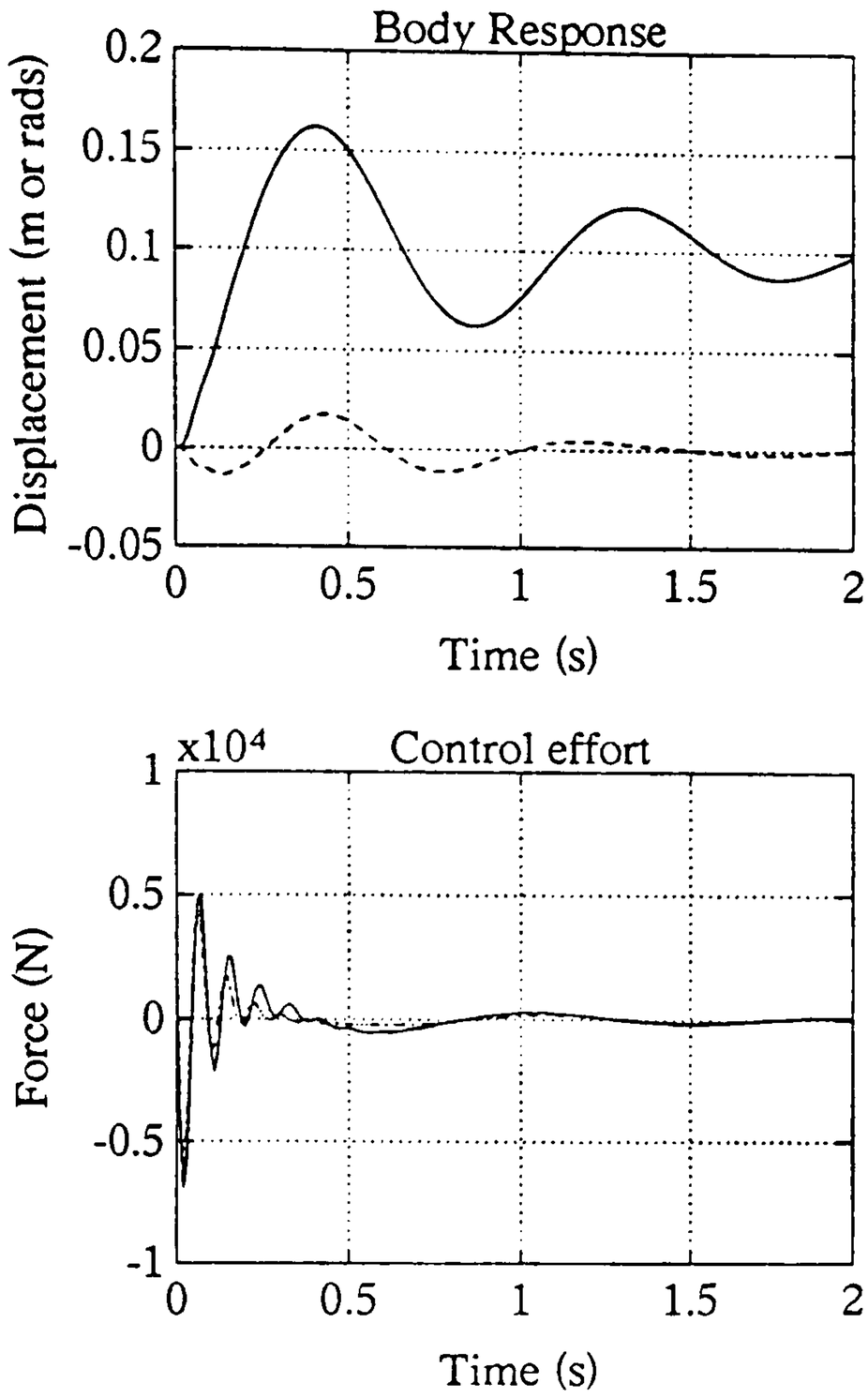


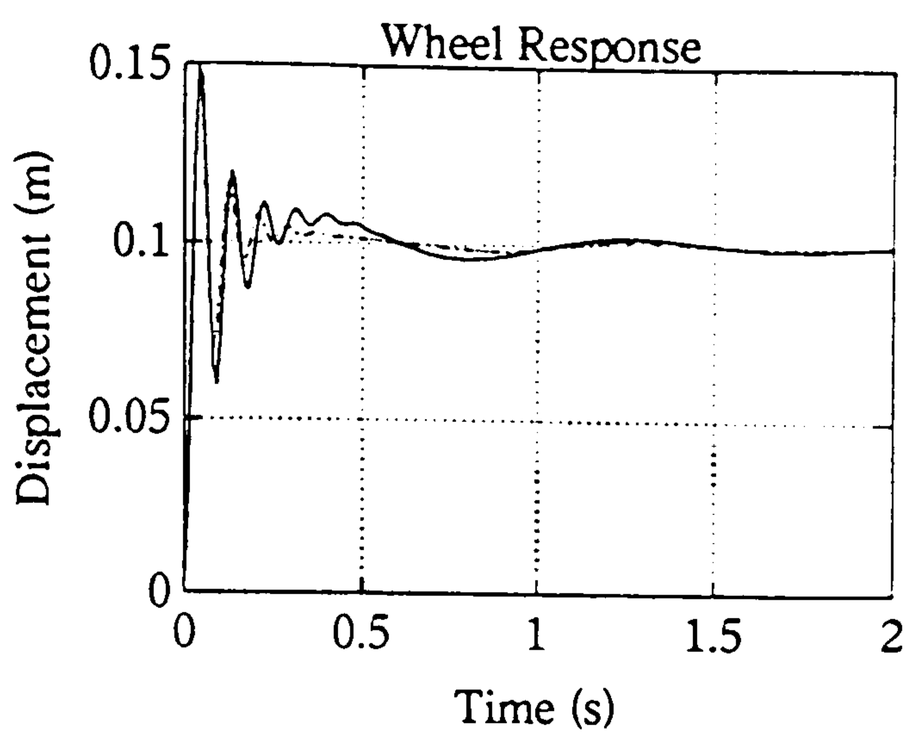


Figure 4.14e : Heave Response

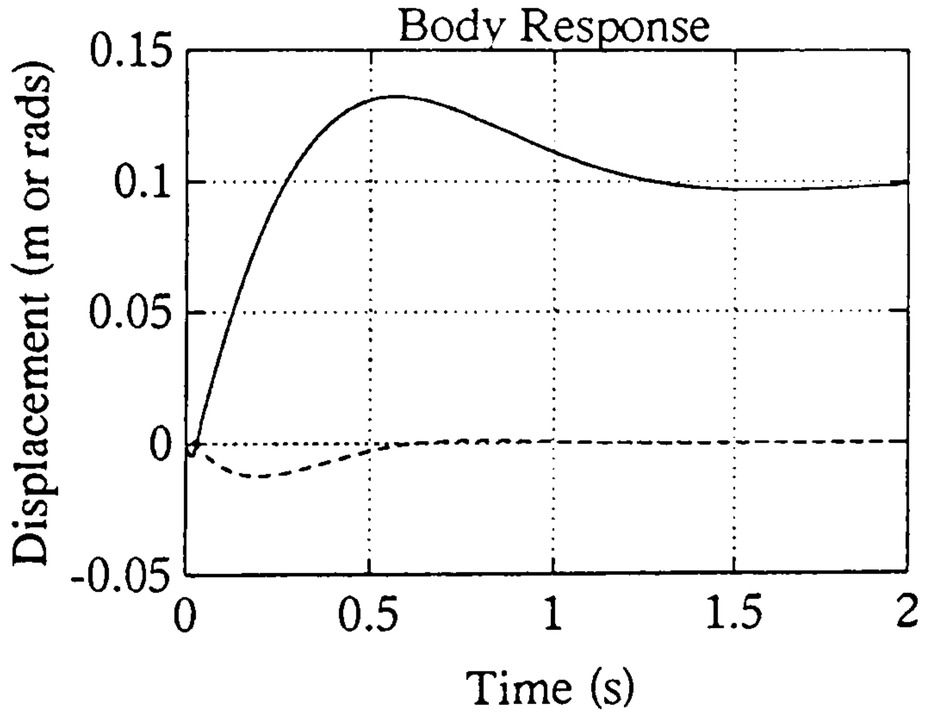


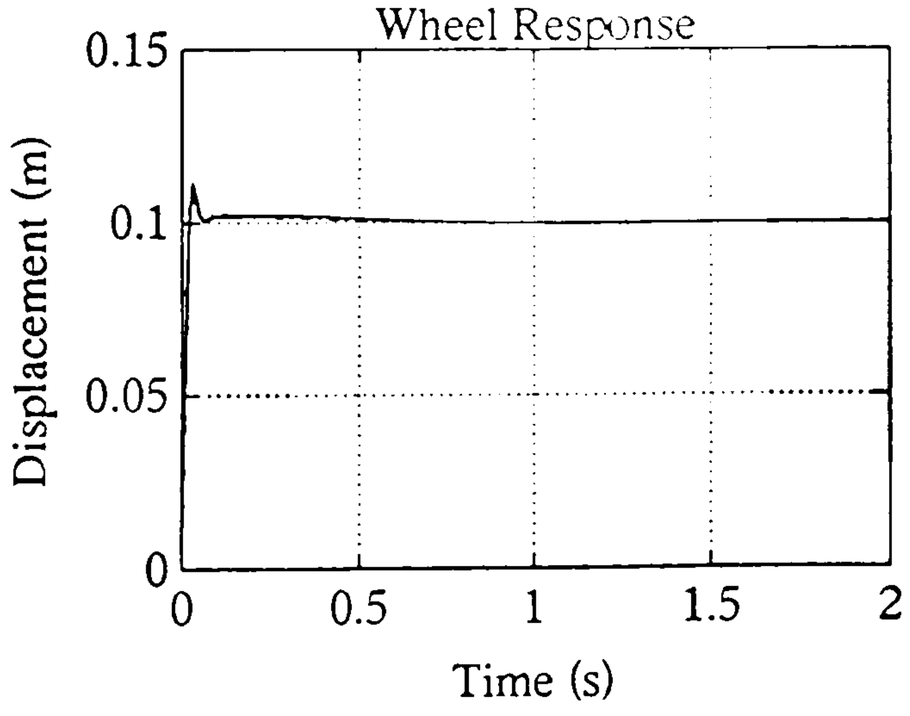


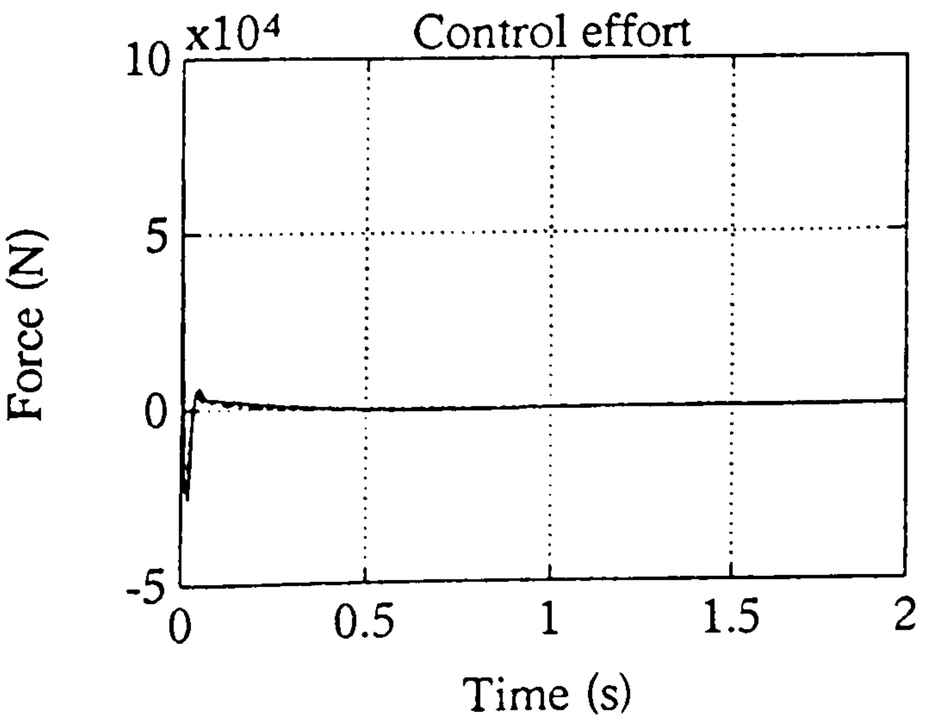


Figure 4.14f : Heave Response

Figure 4.14 (continued)

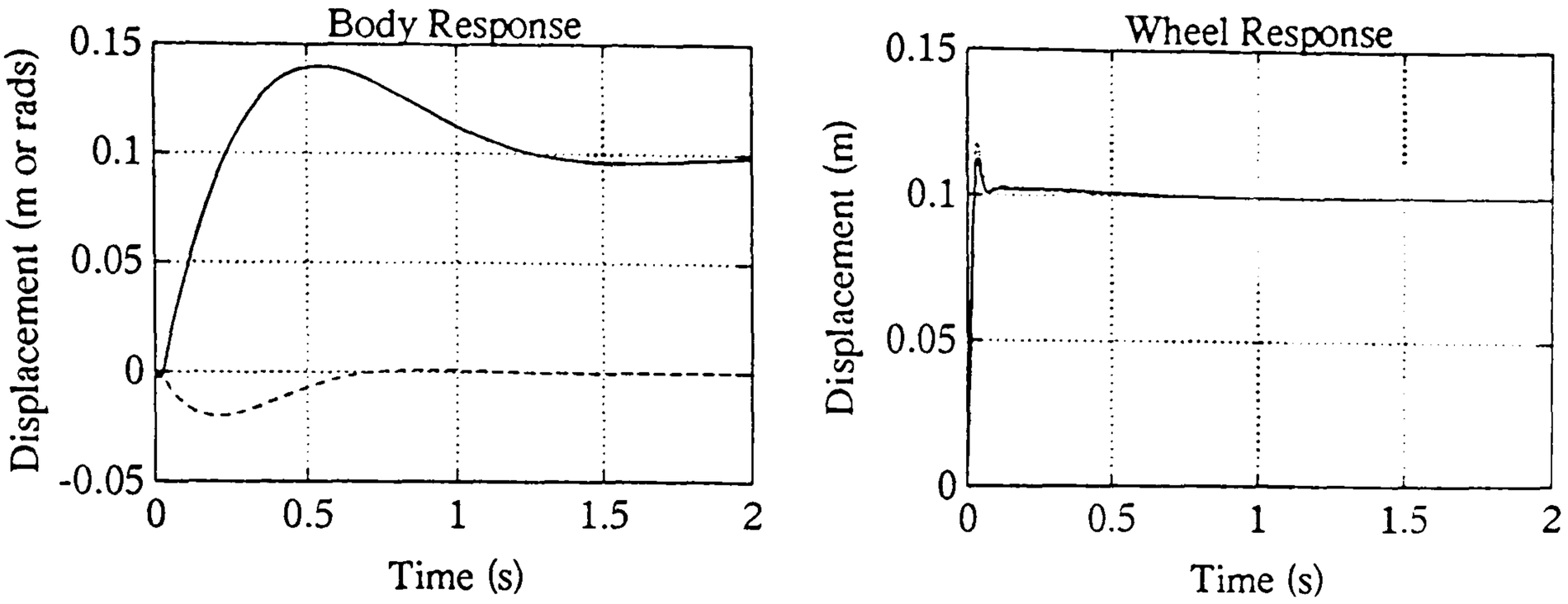


Figure 4.14g : Heave Response

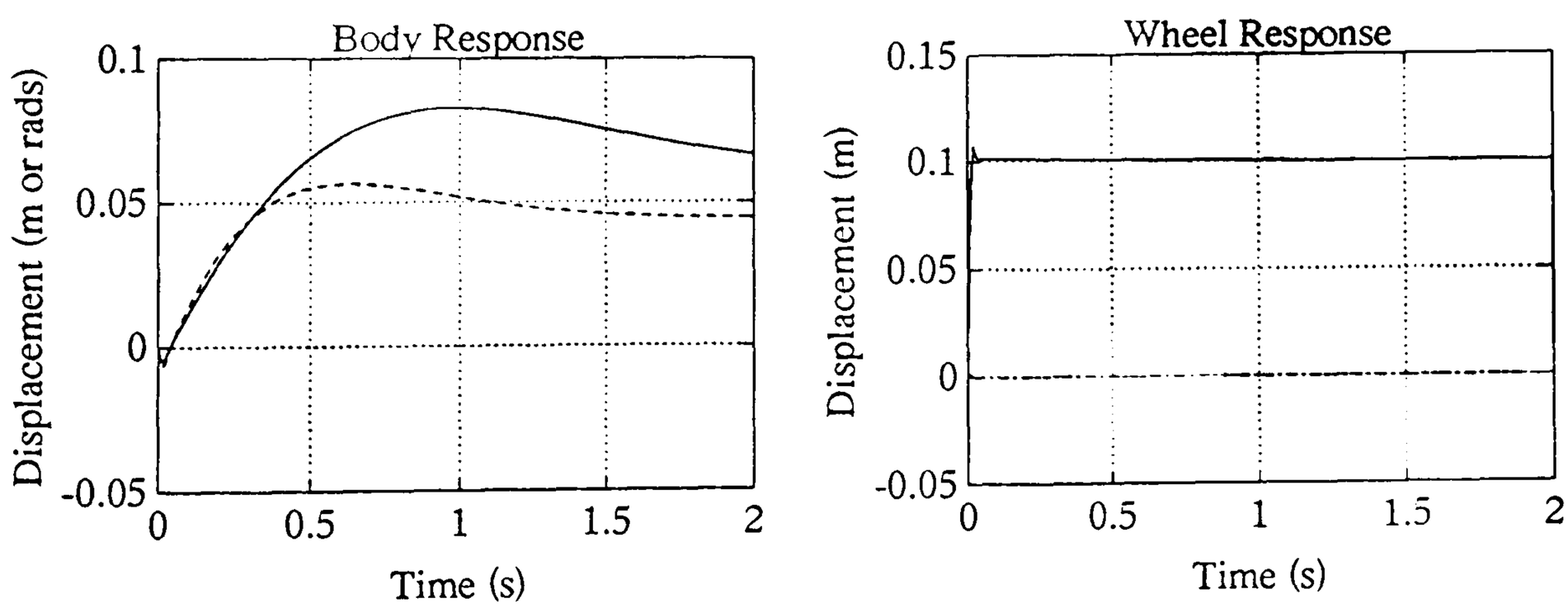


Figure 4.14h : Pitch Response

Figure 4.14 (continued)

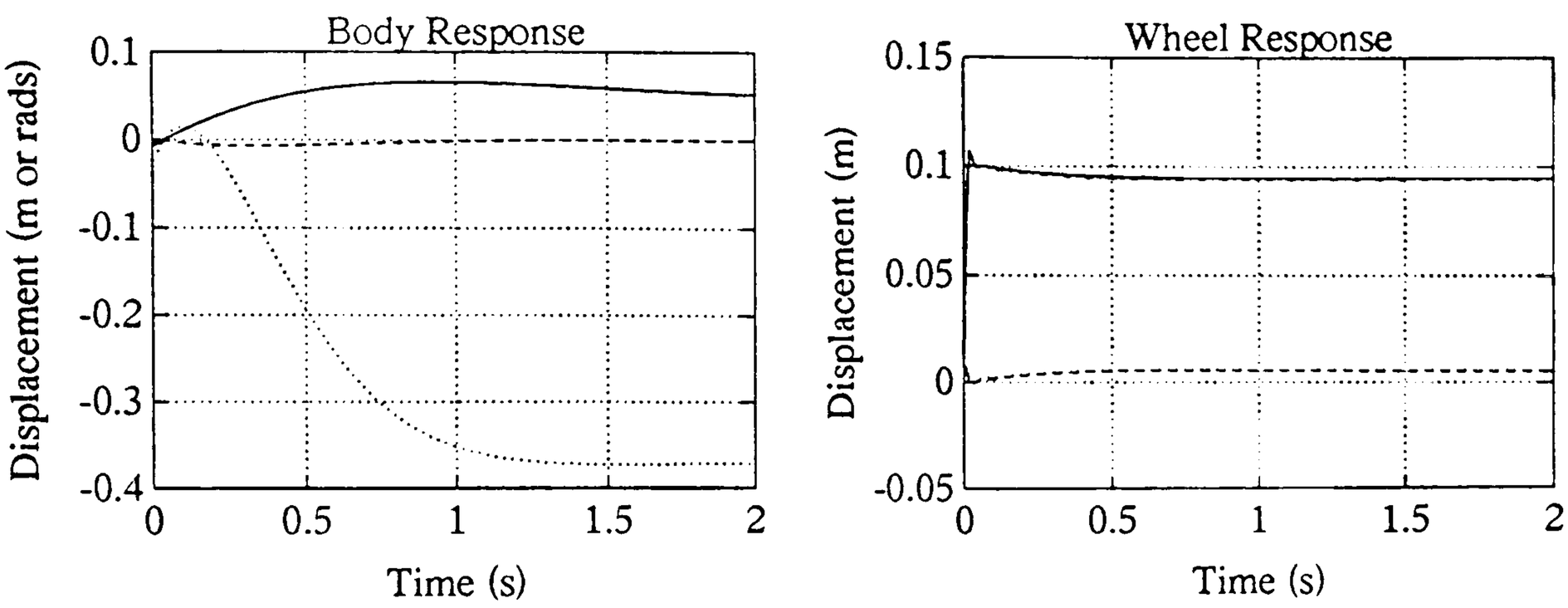


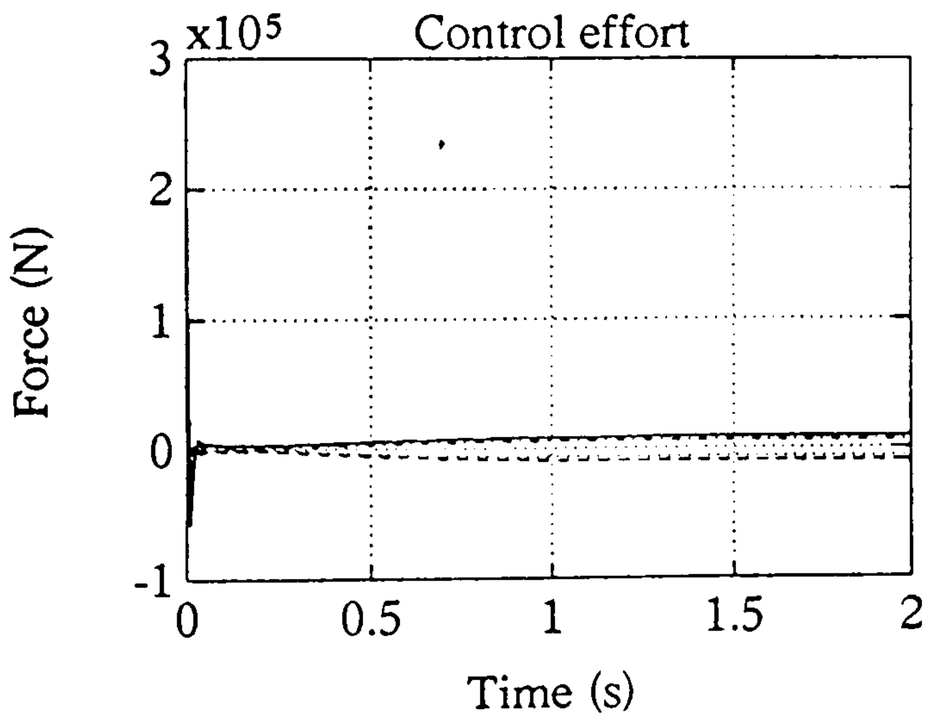


Figure 4.14i : Roll Reponse

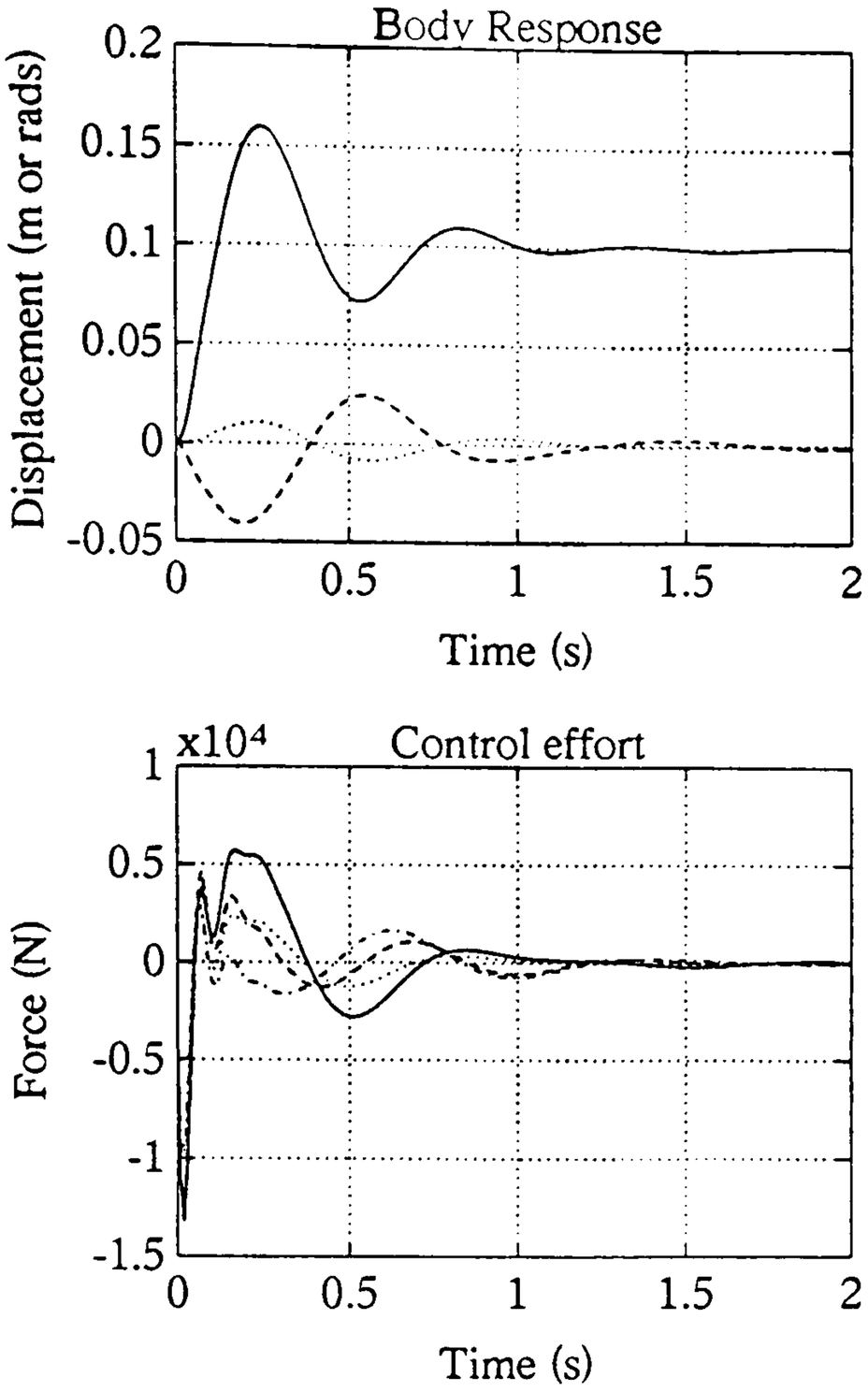


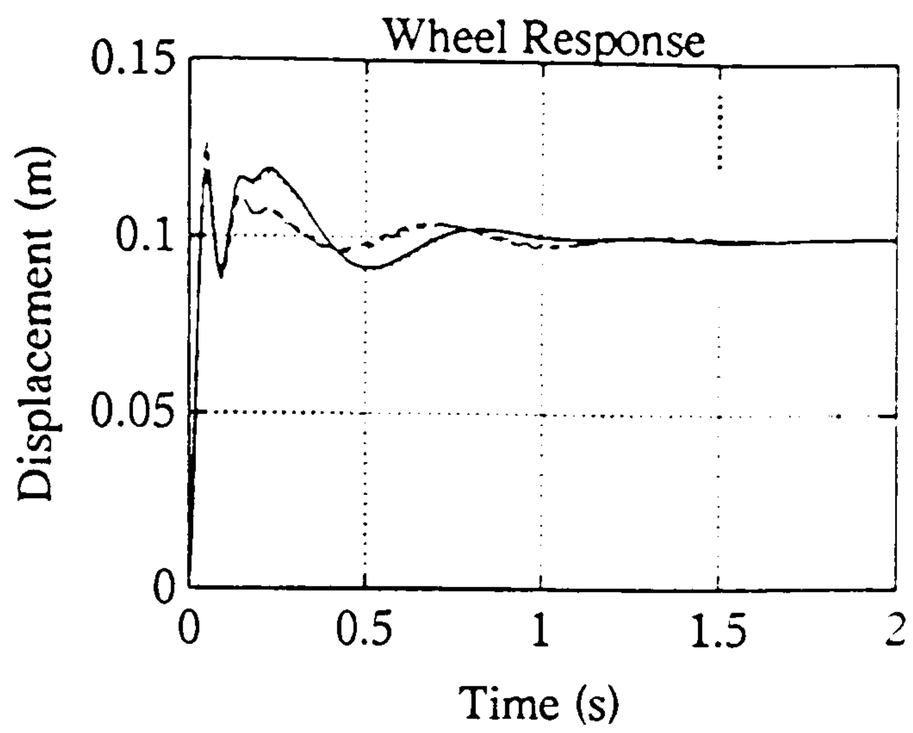


Figure 4.15a : Heave Response

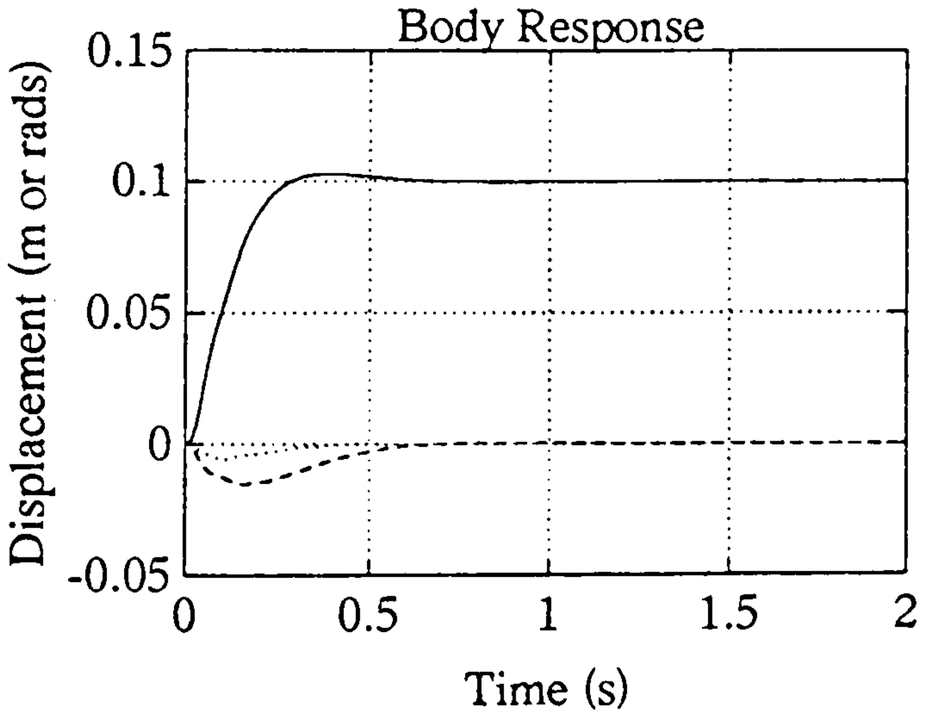


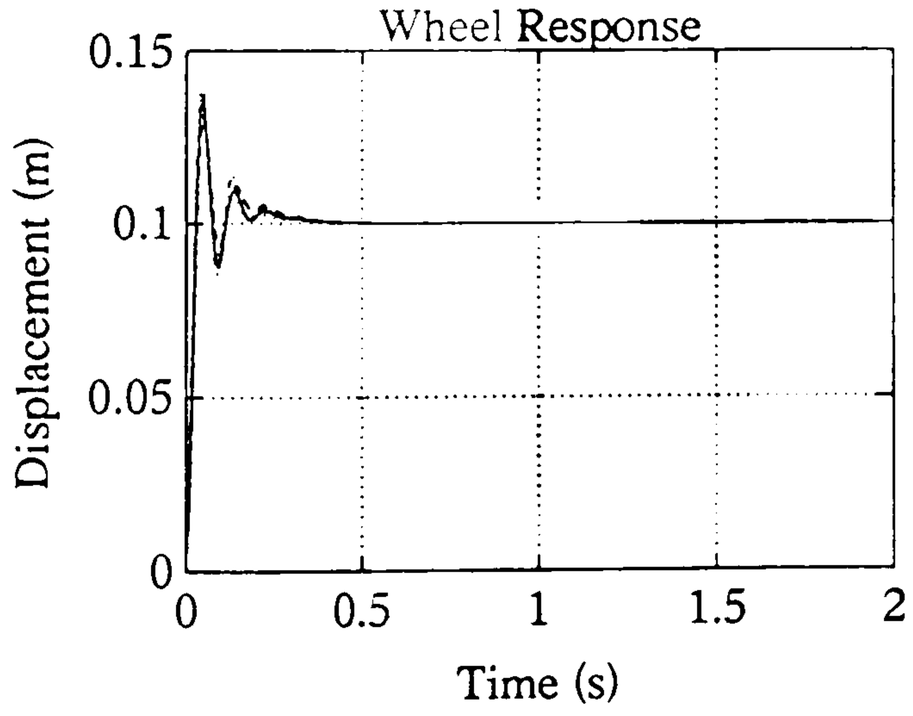


Figure 4.15b : Heave Response

Figure 4.15 : Pole Placement Solutions

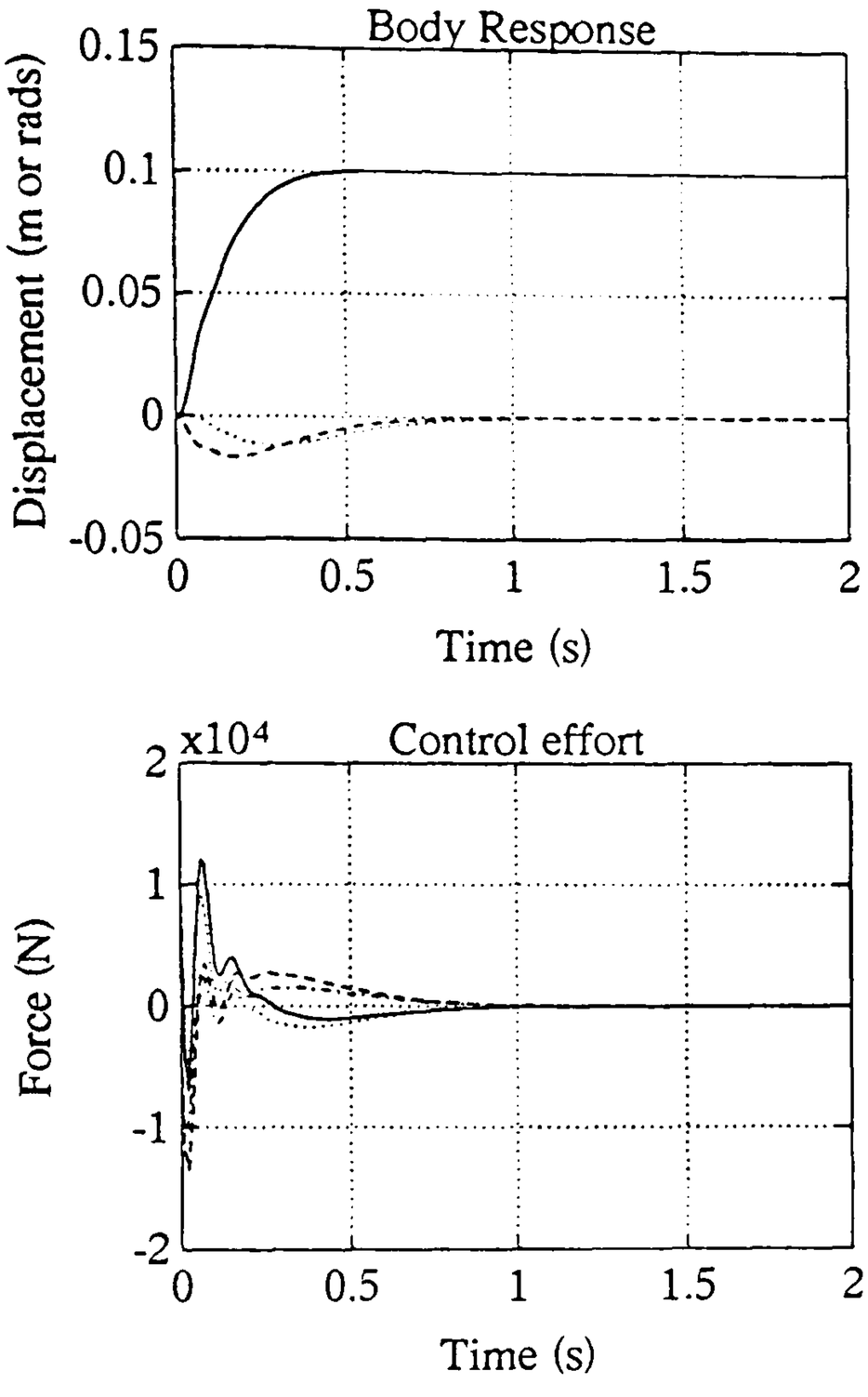


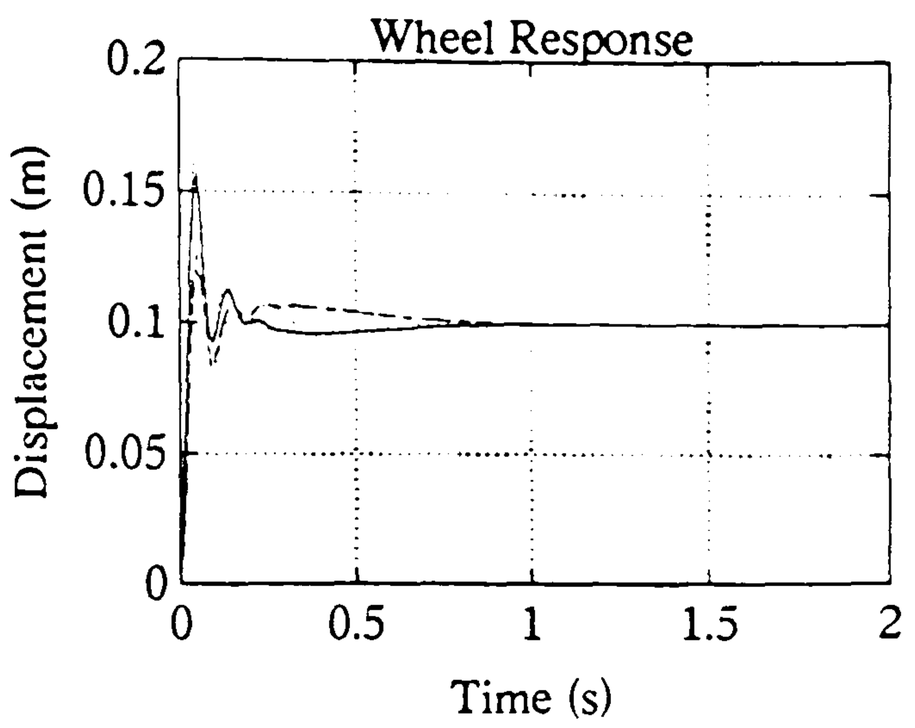


Figure 4.15c : Heave Response

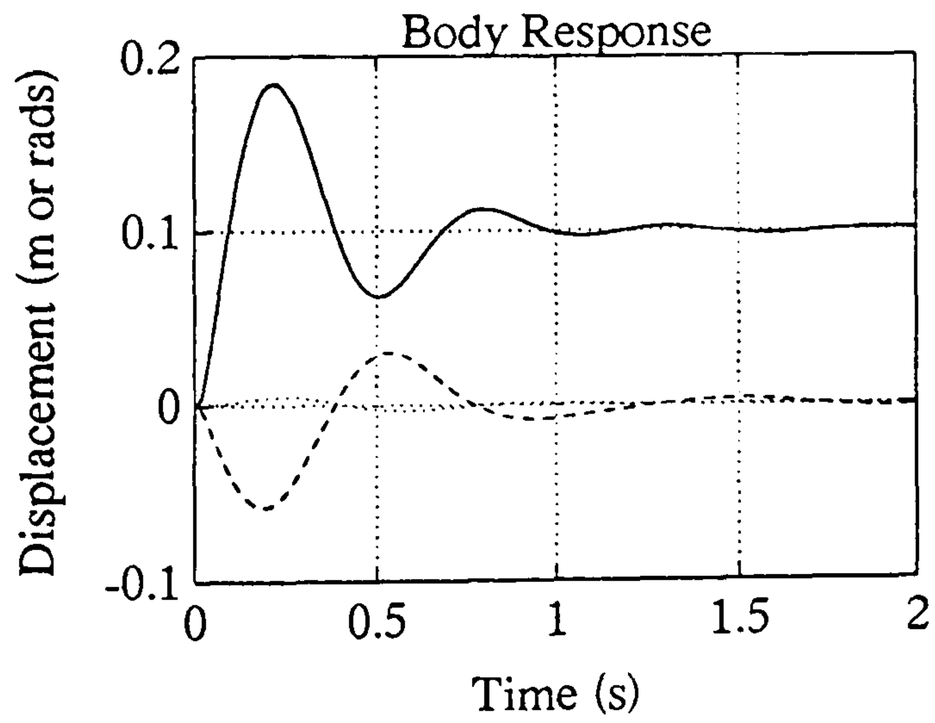


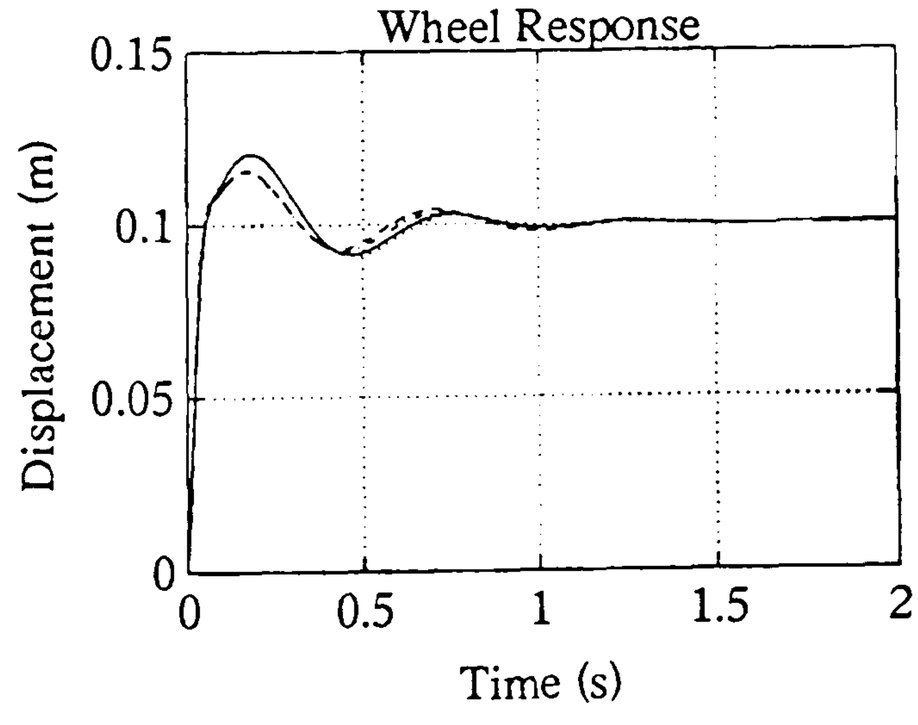


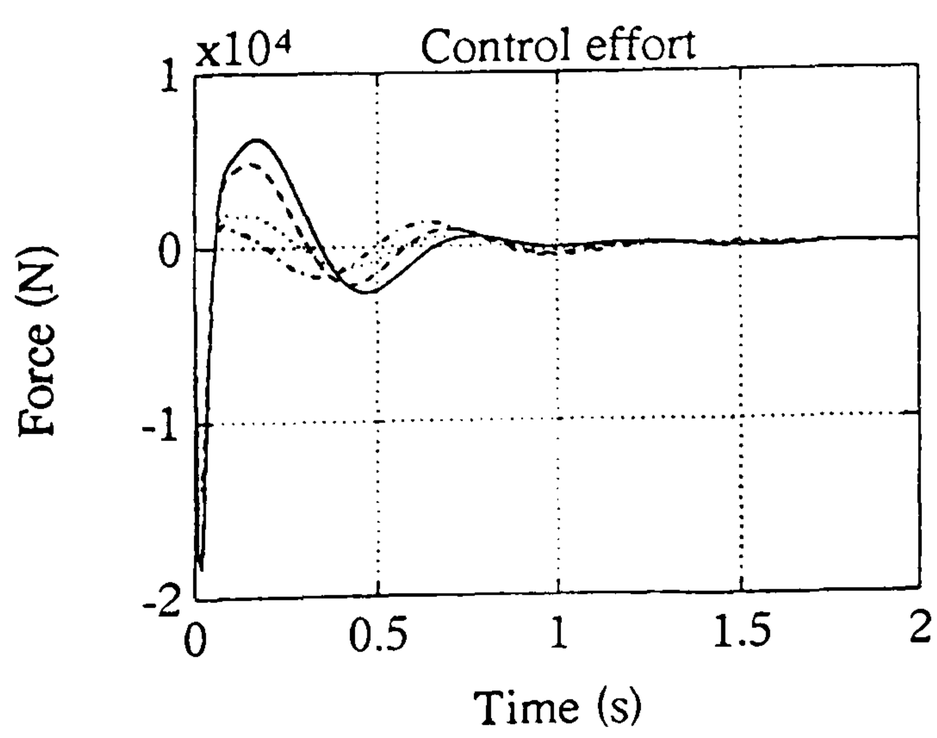


Figure 4.15d : Heave Response

Figure 4.15 (continued)

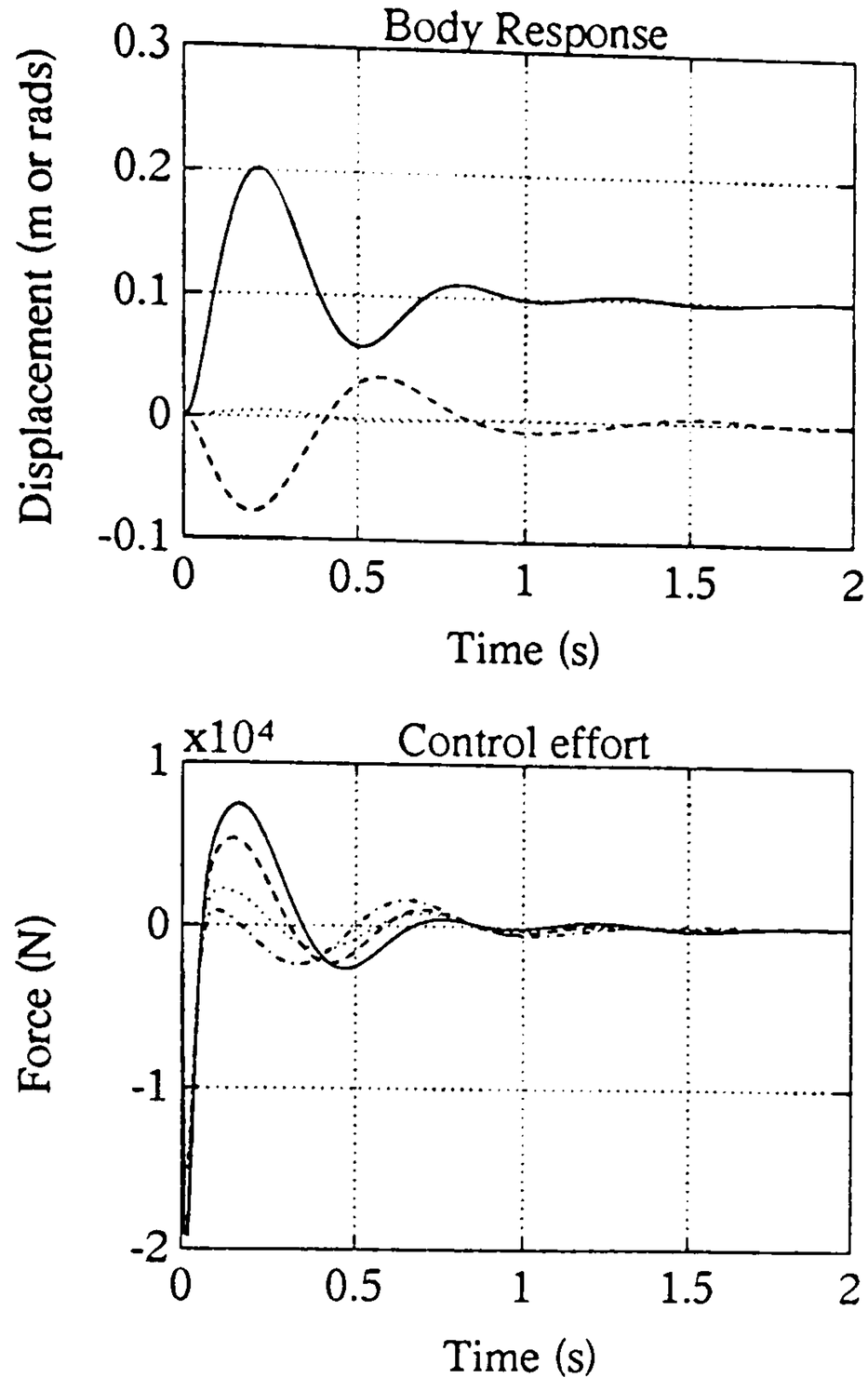


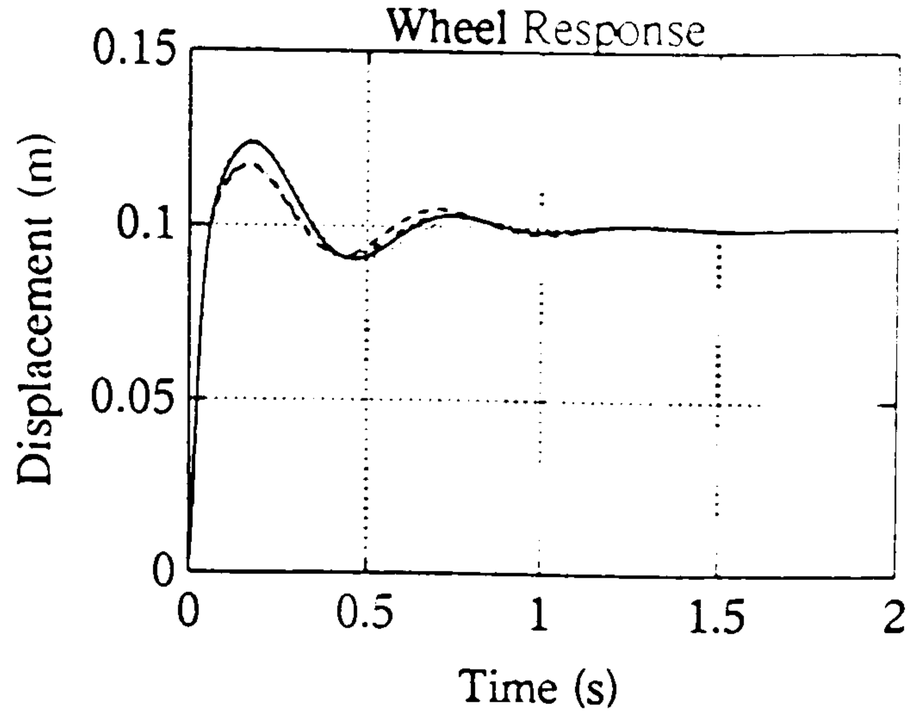


Figure 4.15e : Heave Response

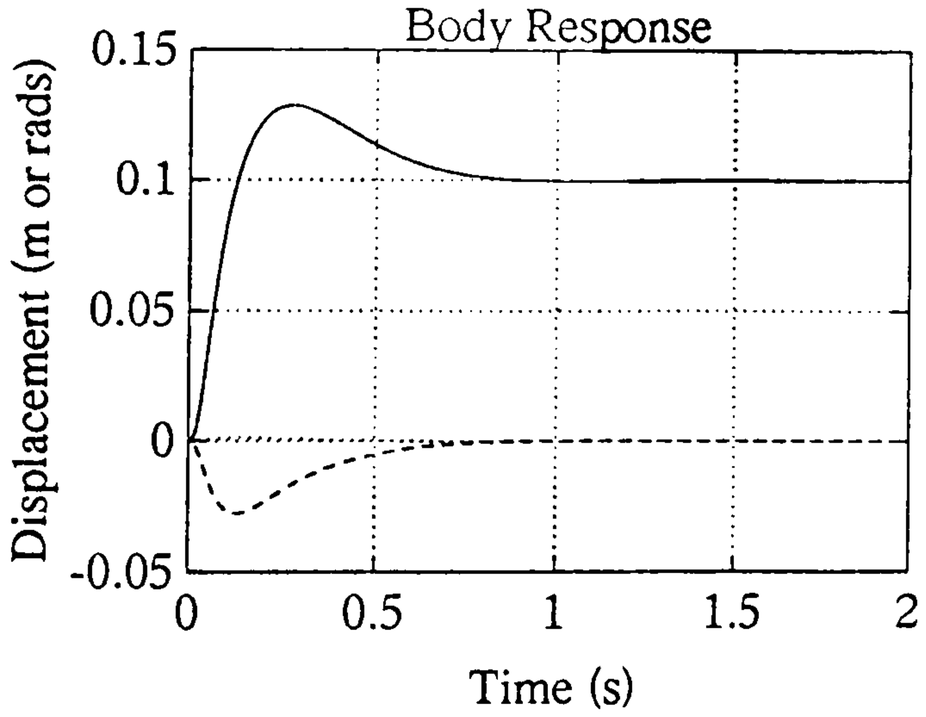


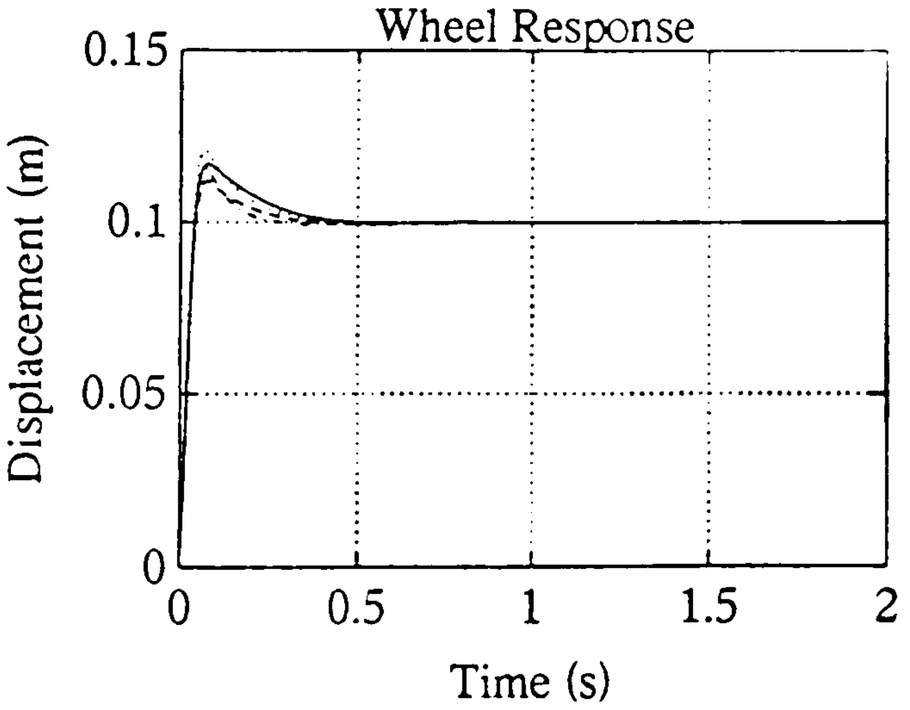


Figure 4.15f : Heave Response

Figure 4.15 (continued)

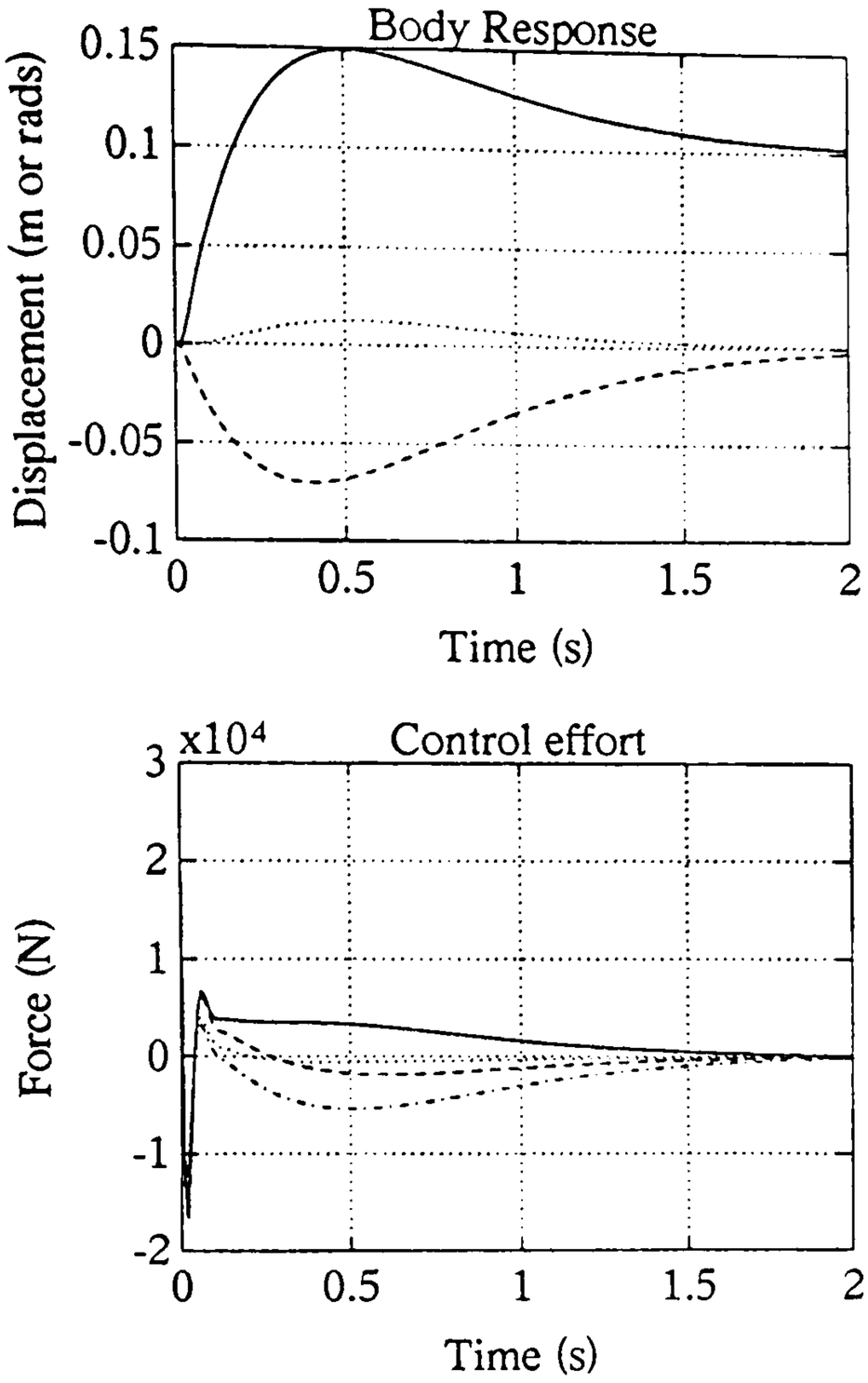


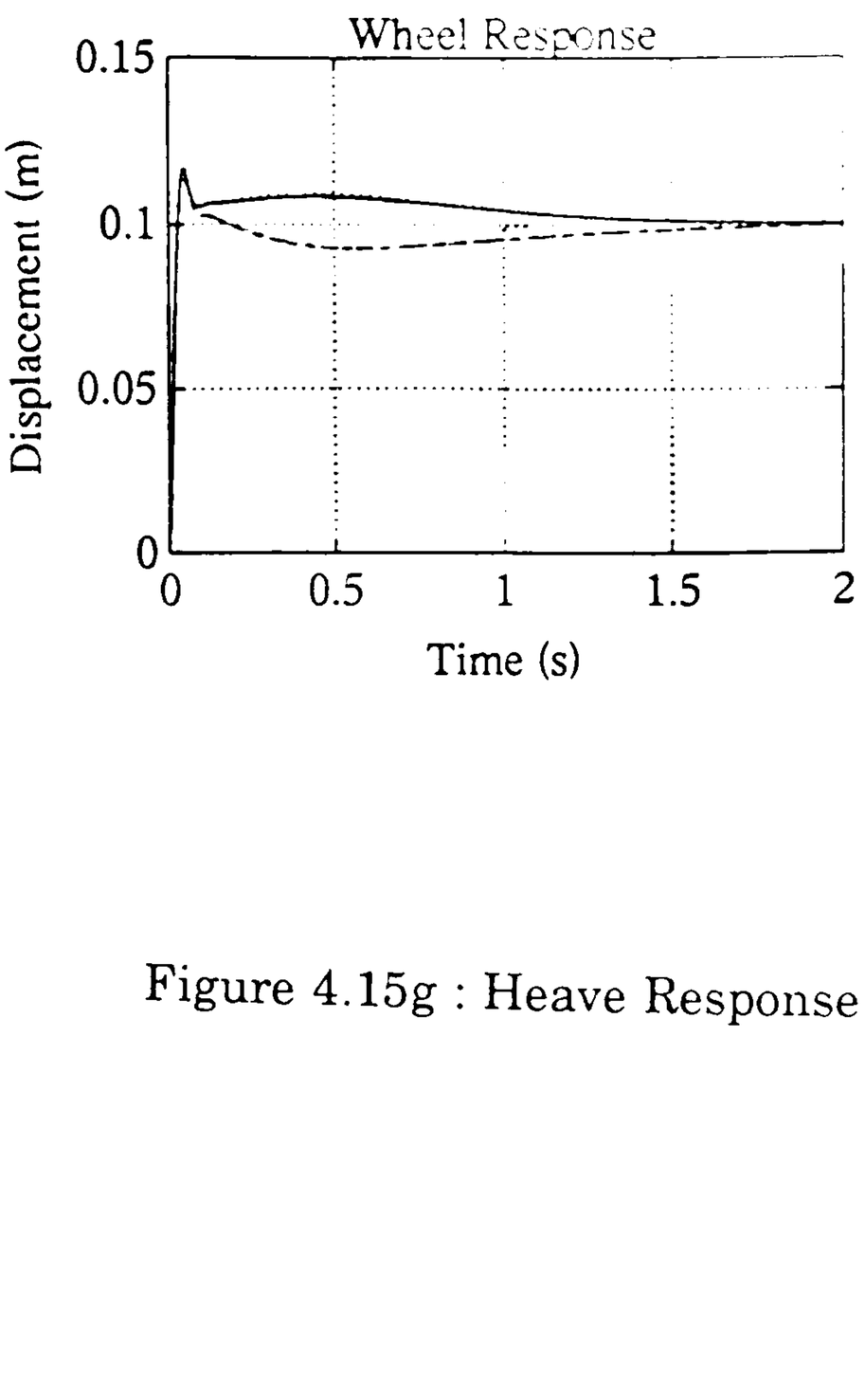


Figure 4.15g : Heave Response

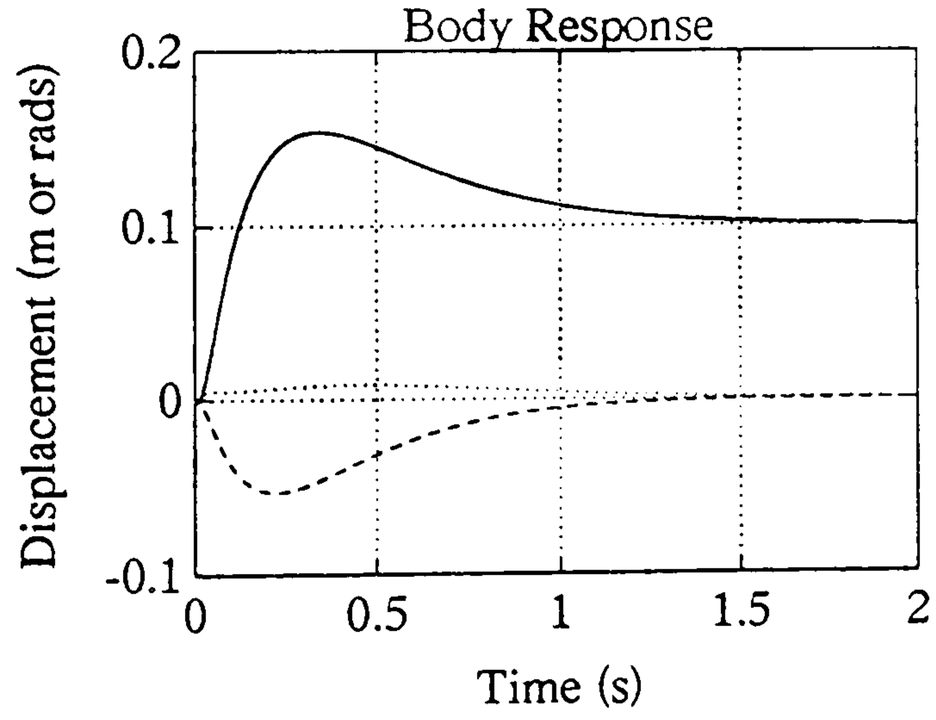


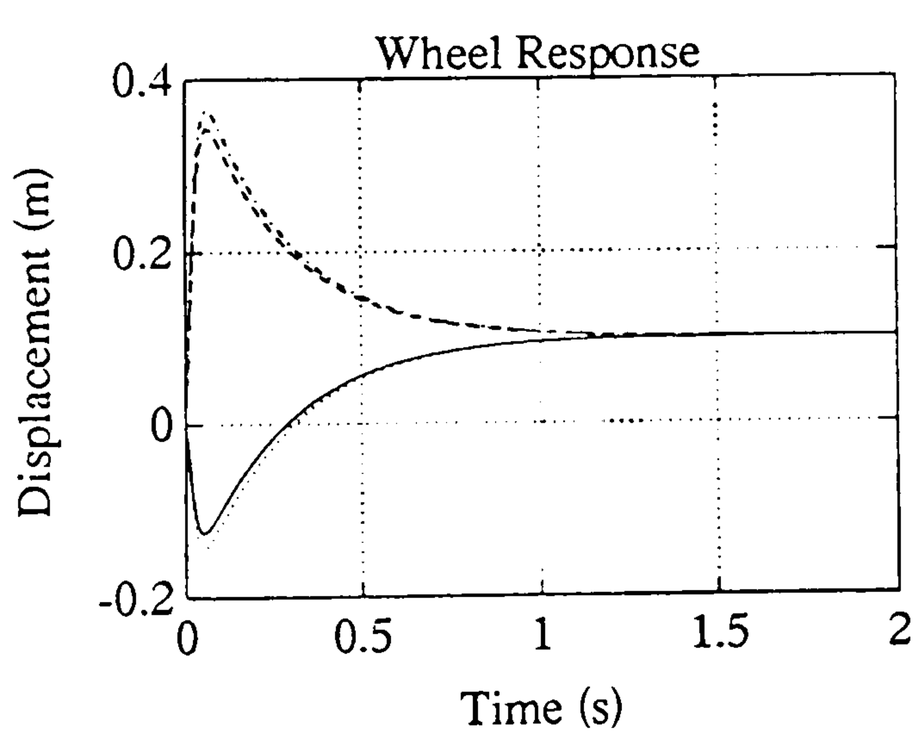


Figure 4.15h : Heave Repsonse

Figure 4.15 (continued)

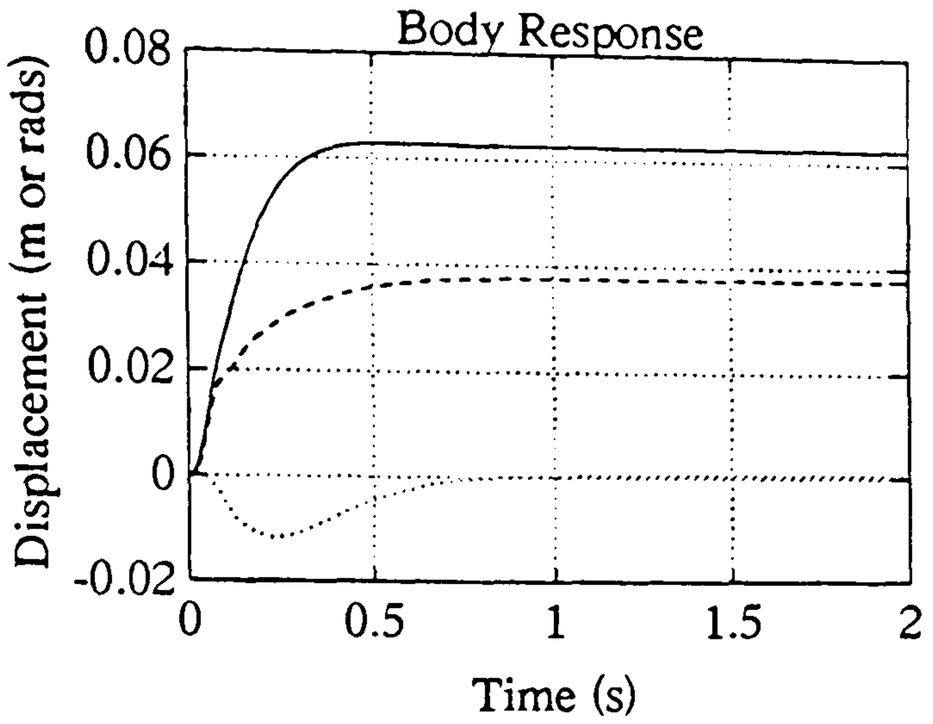


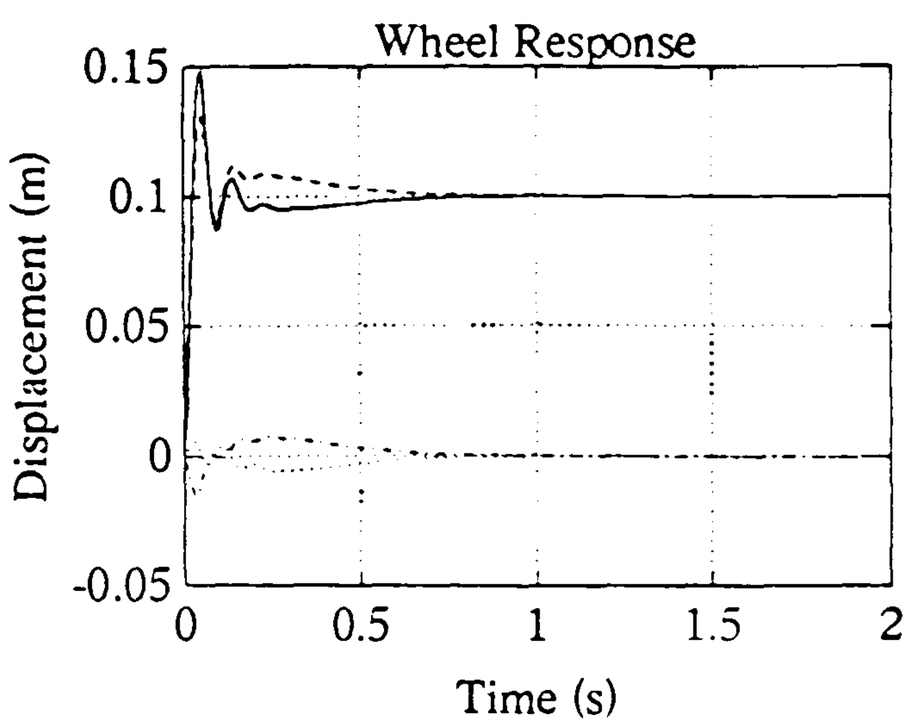


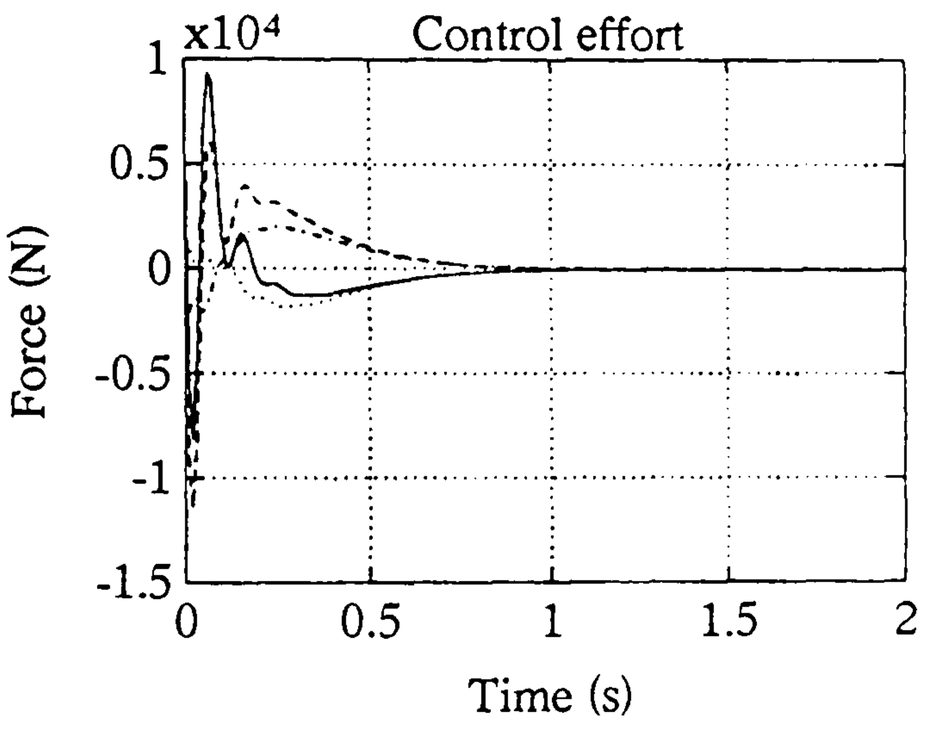


Figure 4.15i : Pitch Response

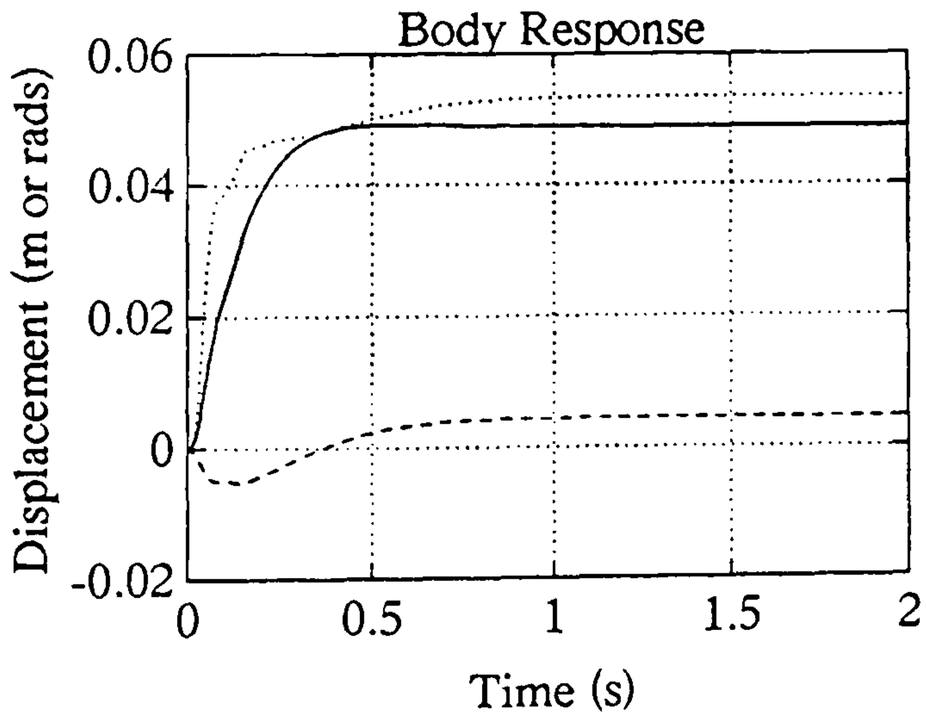


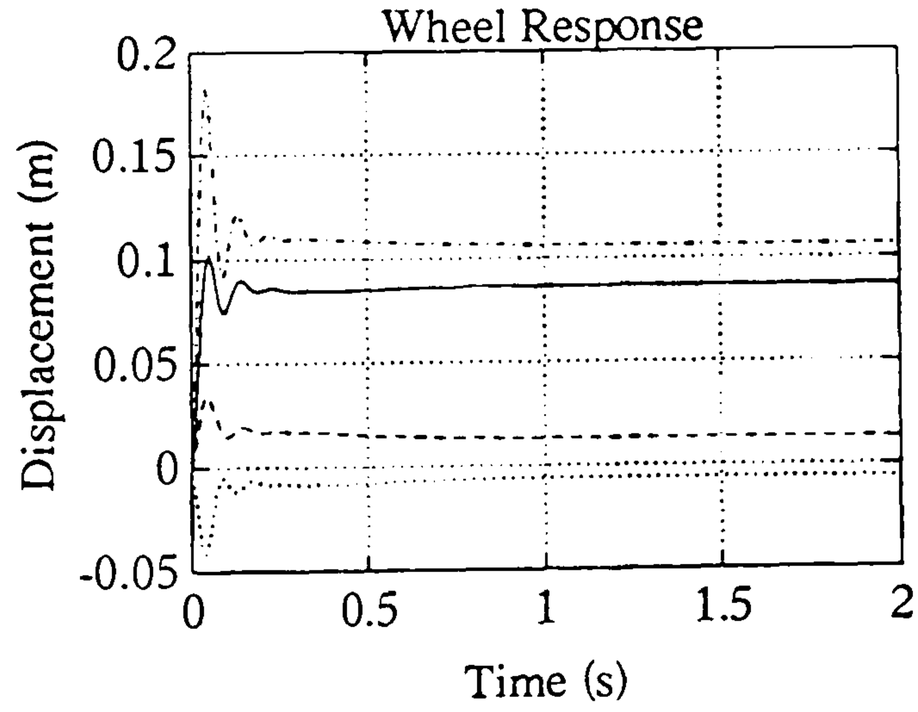


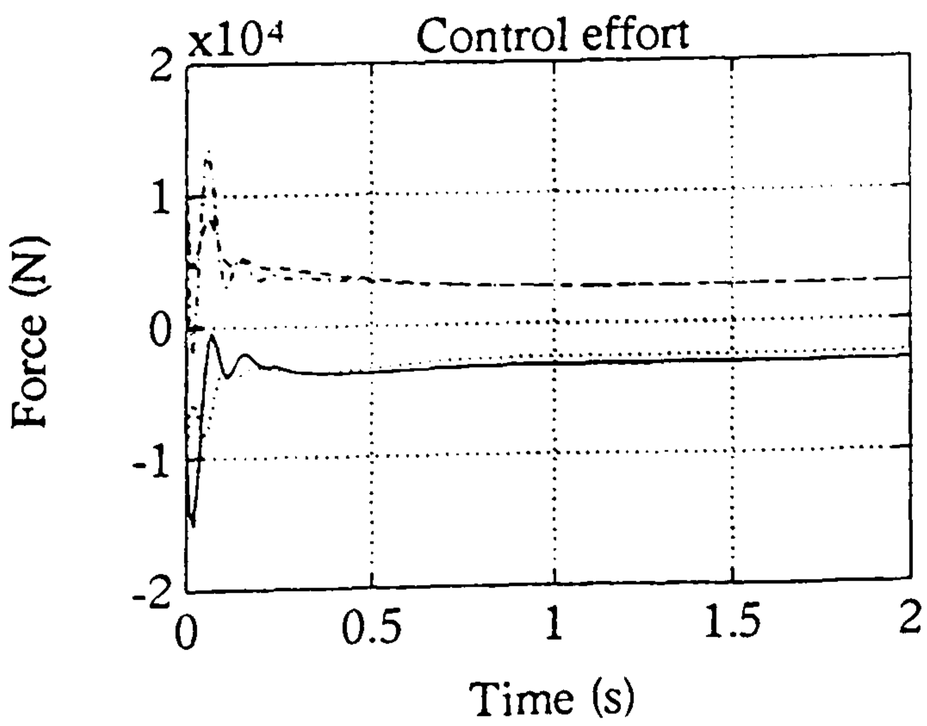


Figure 4.15j : Roll Reponse

Figure 4.15 (continued)

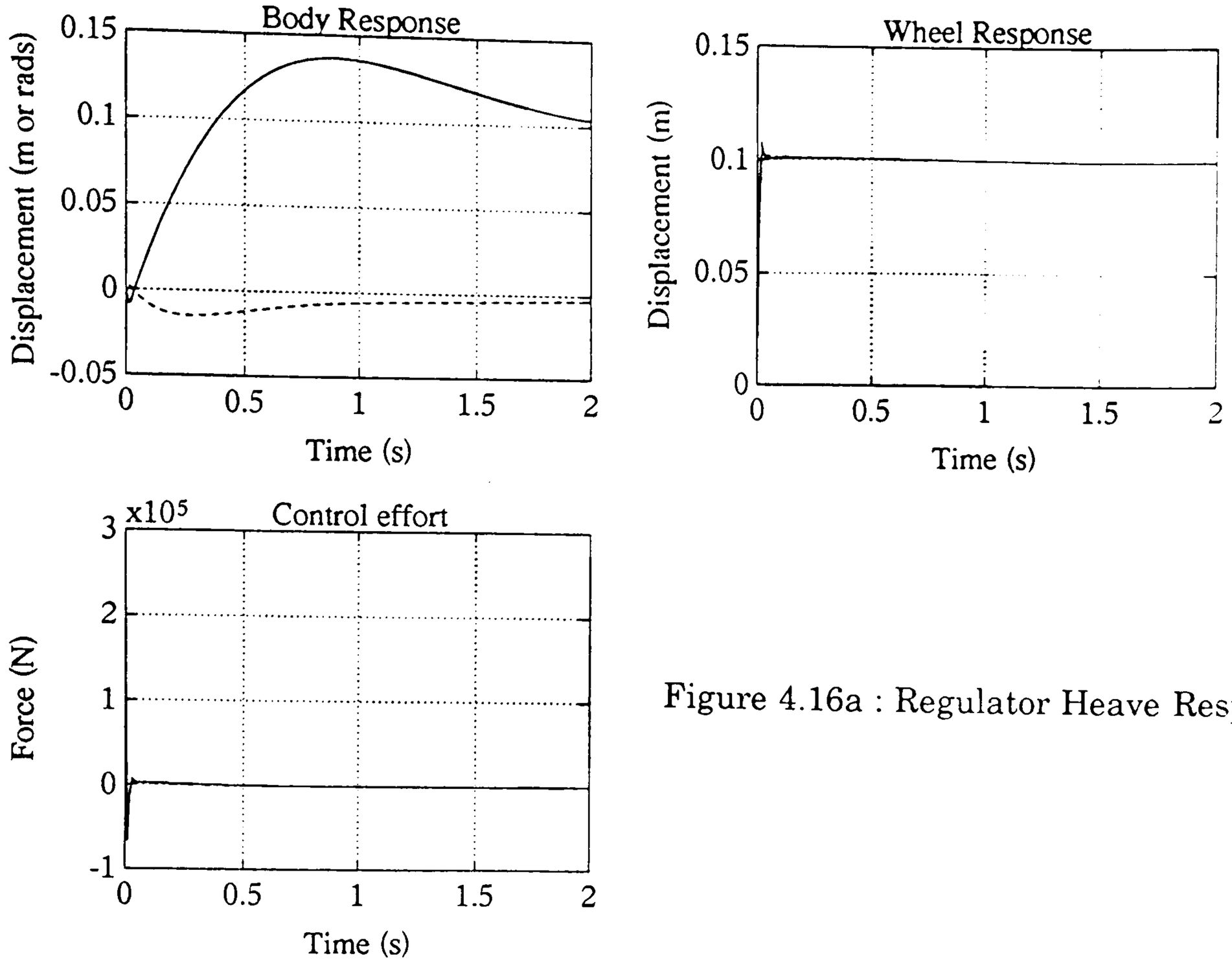


Figure 4.16a : Regulator Heave Response

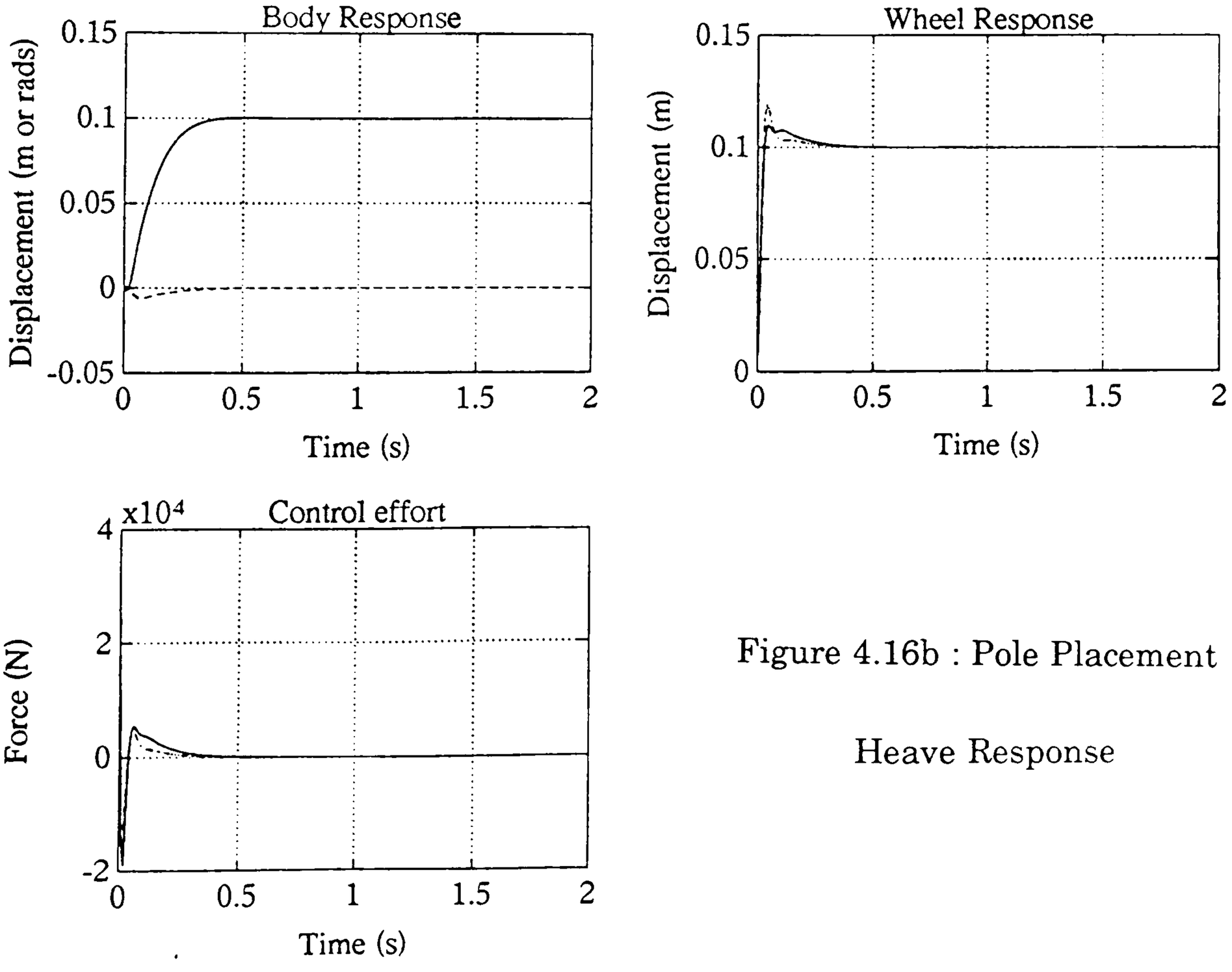


Figure 4.16b : Pole Placement

Heave Response

Figure 4.16 : Comparative Quarter Car Results

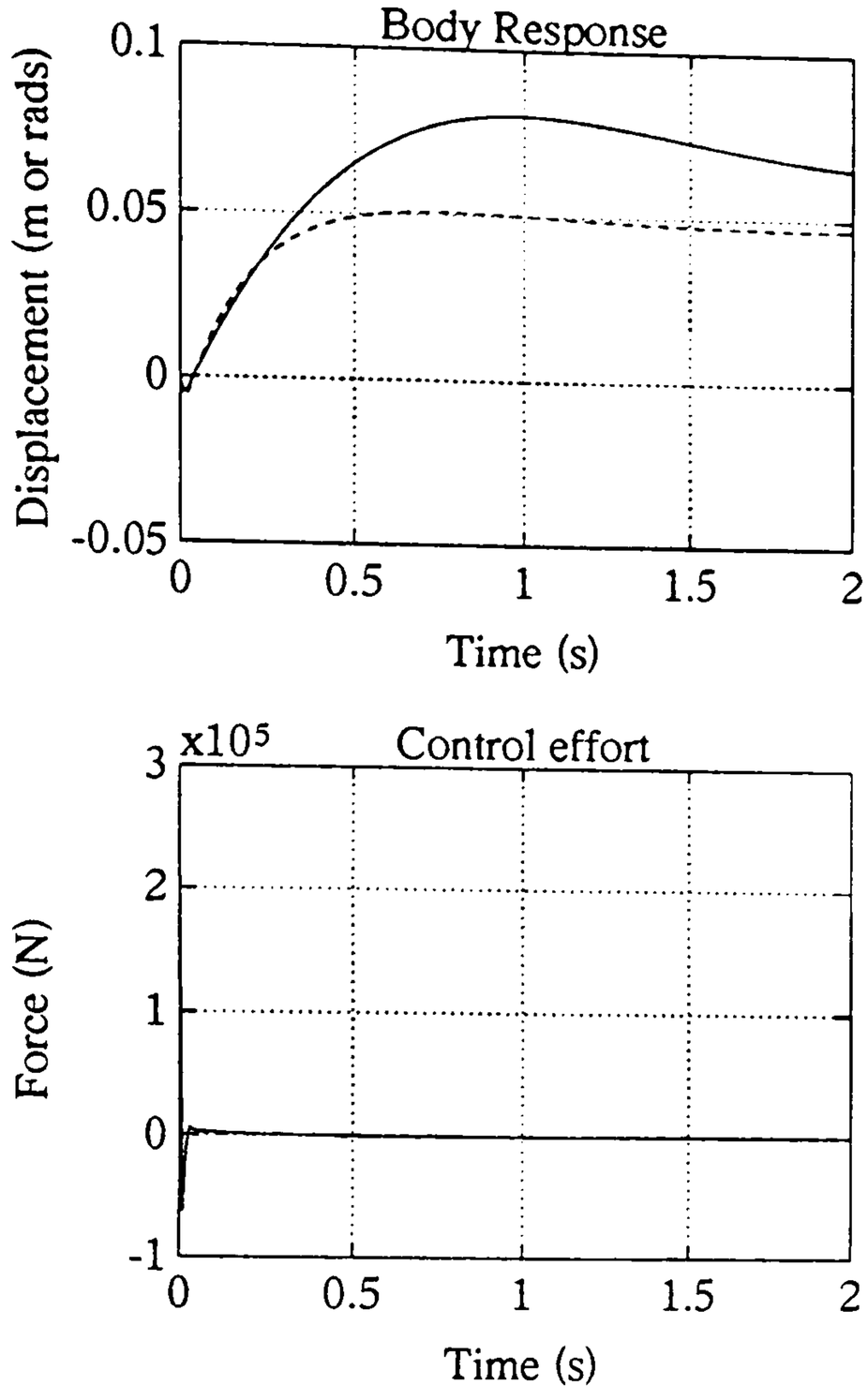


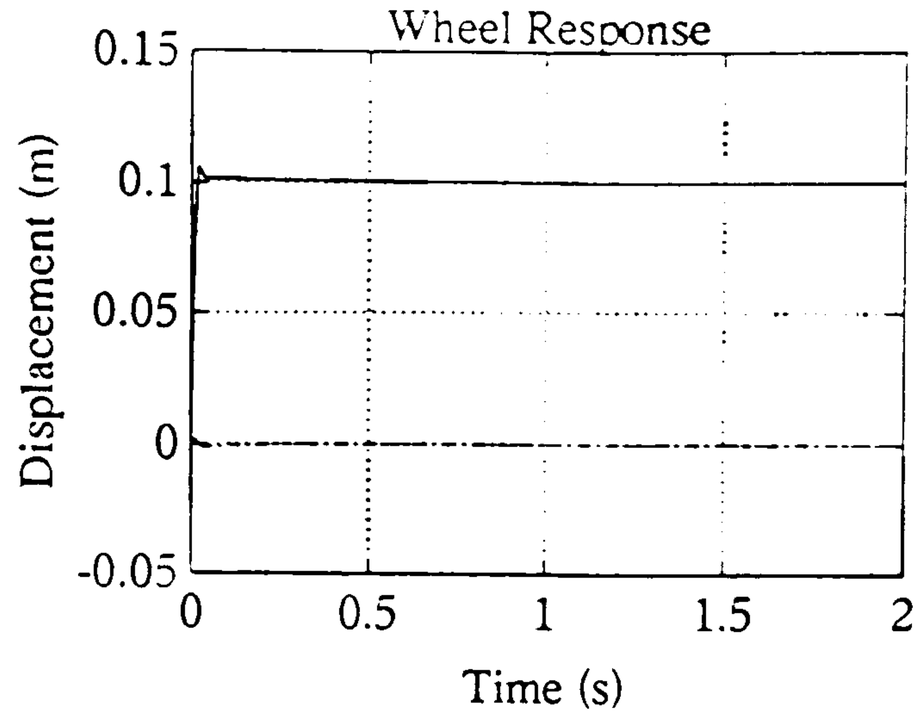


Figure 4.16c : Regulator Pitch Response

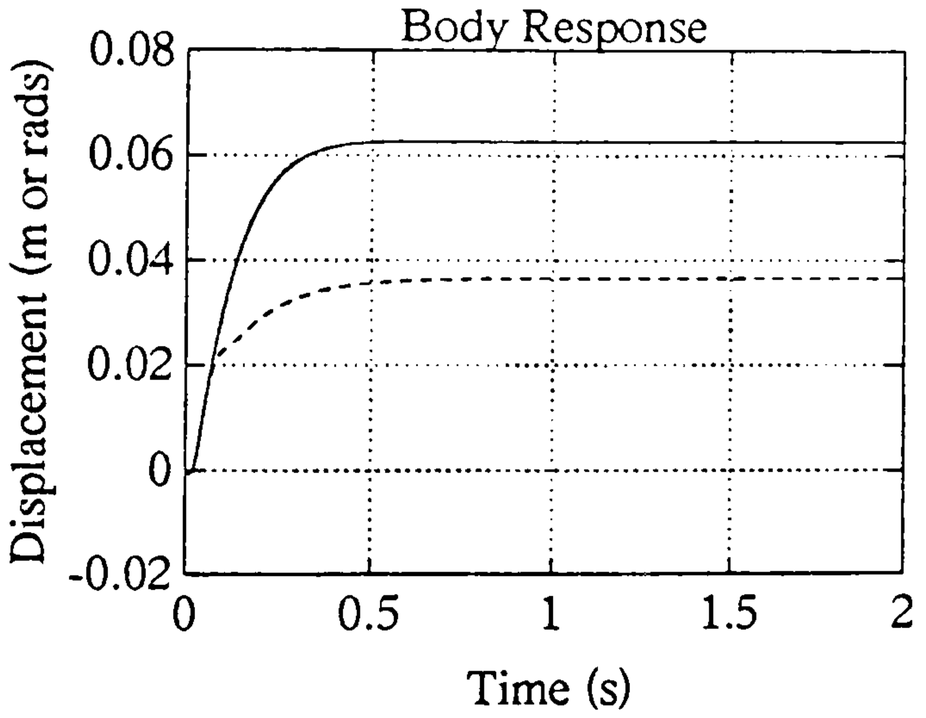


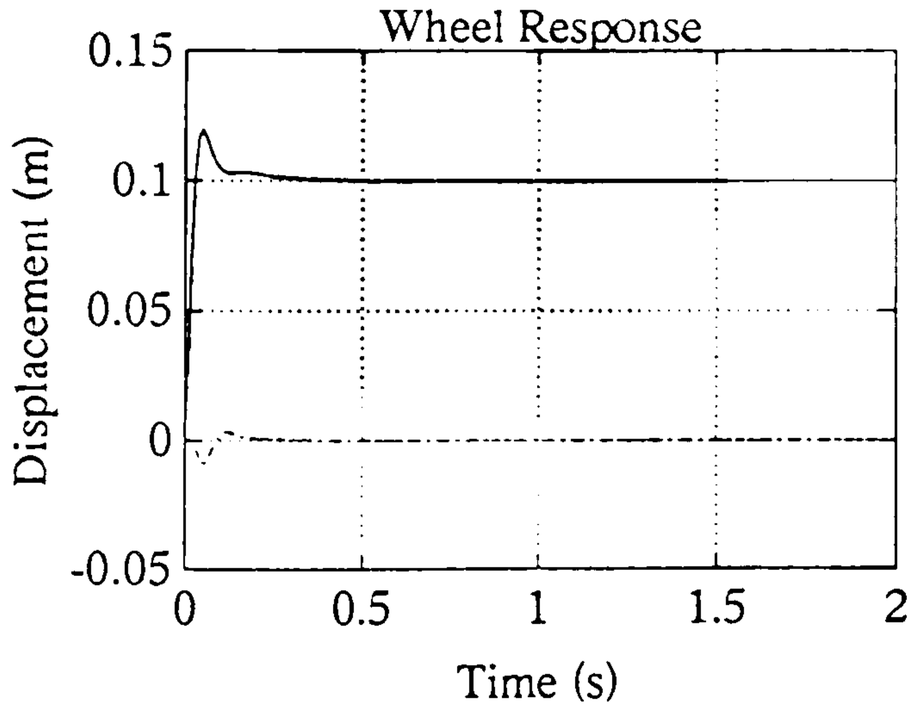


Figure 4.16d : Pole Placement

Pitch Response

Figure 4.16 (continued)

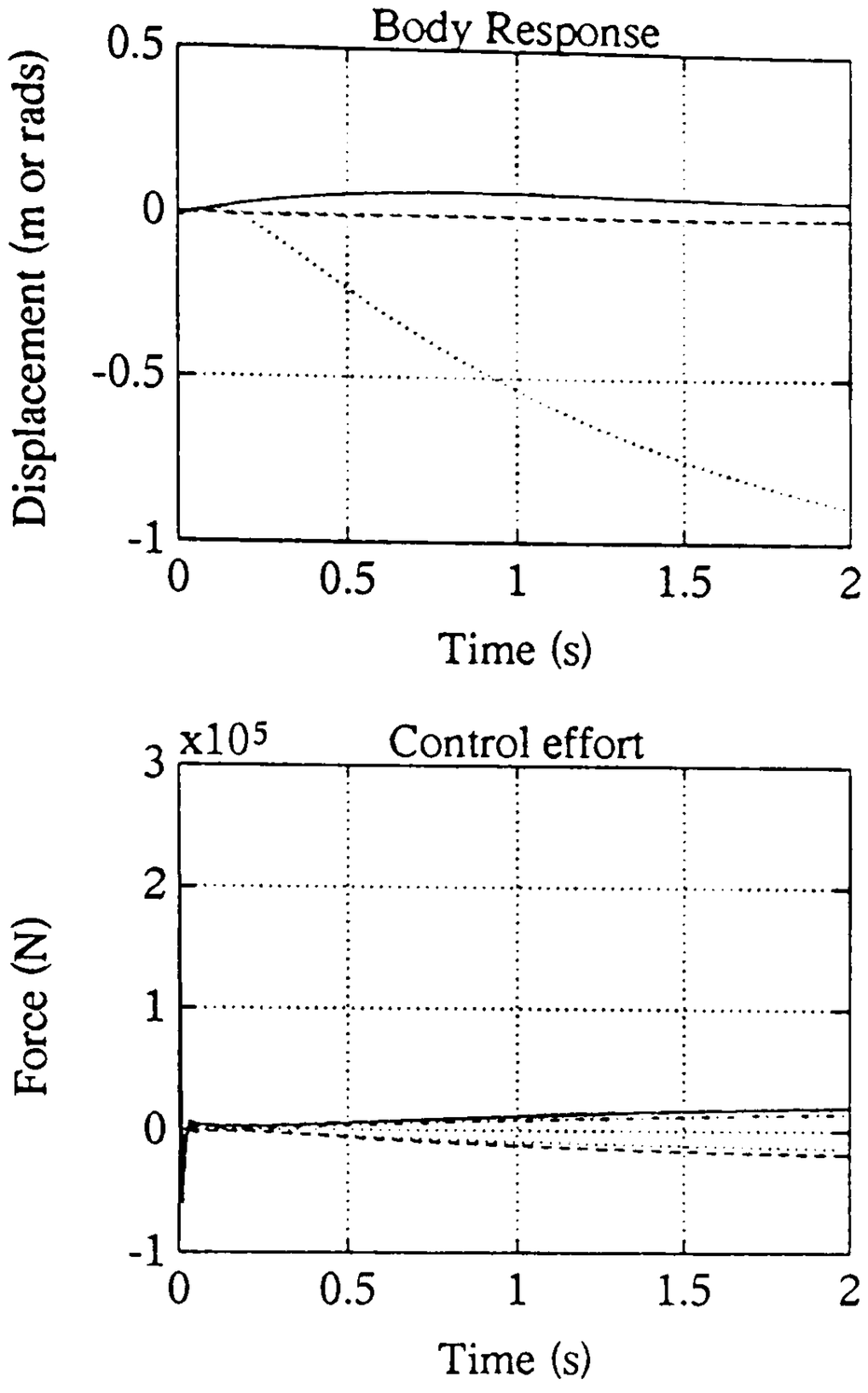


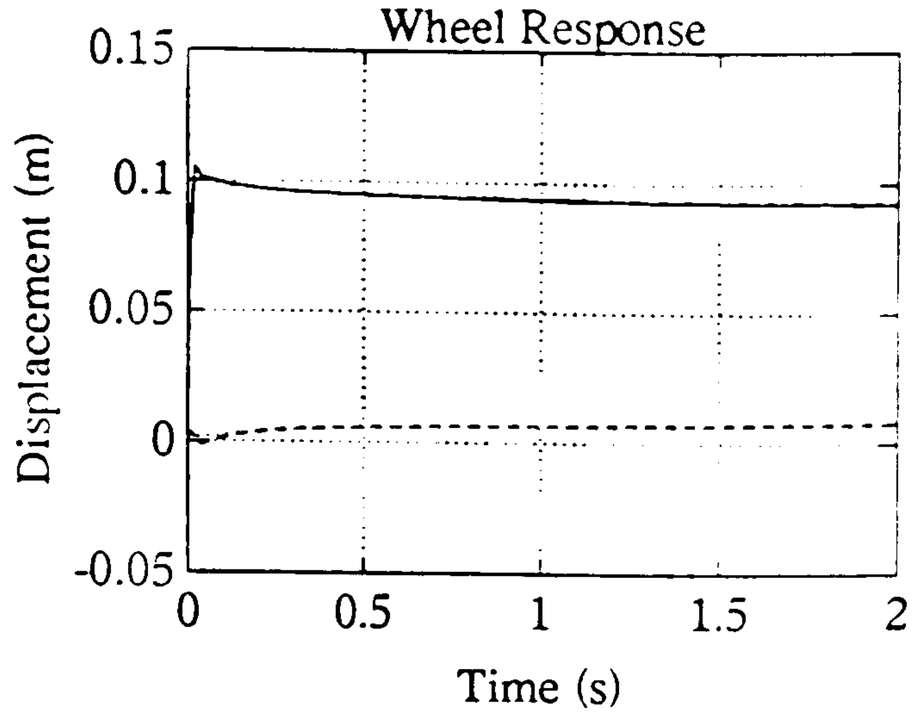


Figure 4.16e : Regulator Roll Response

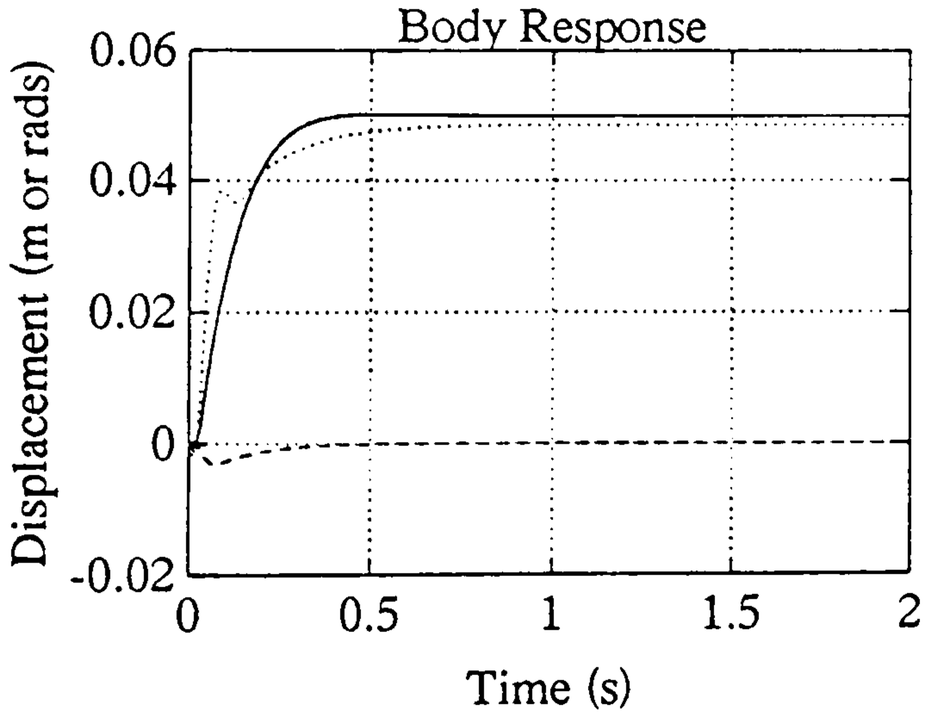


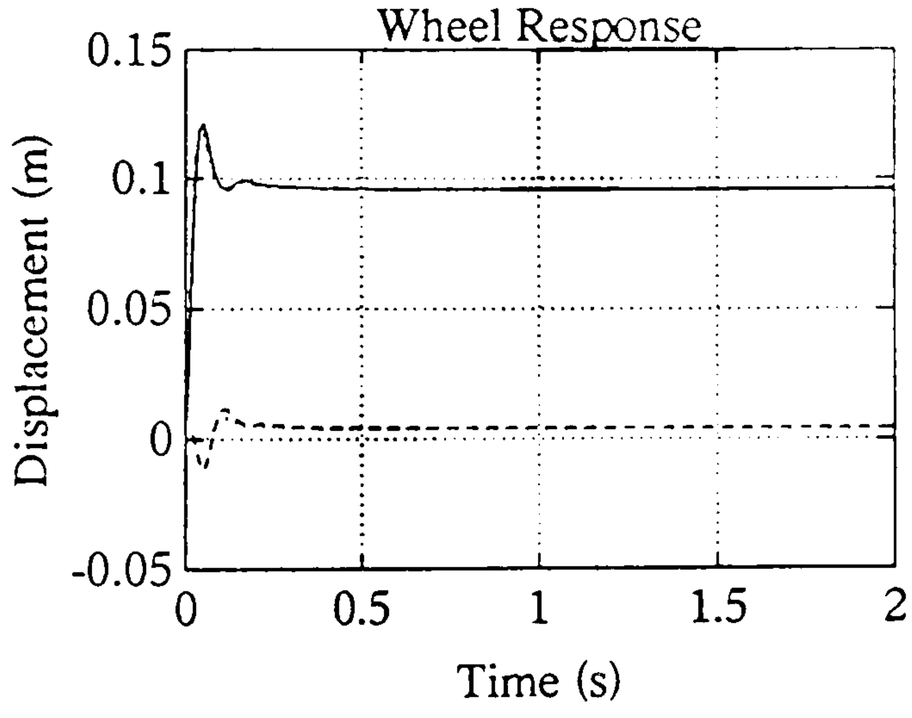


Figure 4.16f : Pole Placement

Roll Response

Figure 4.16 (continued)

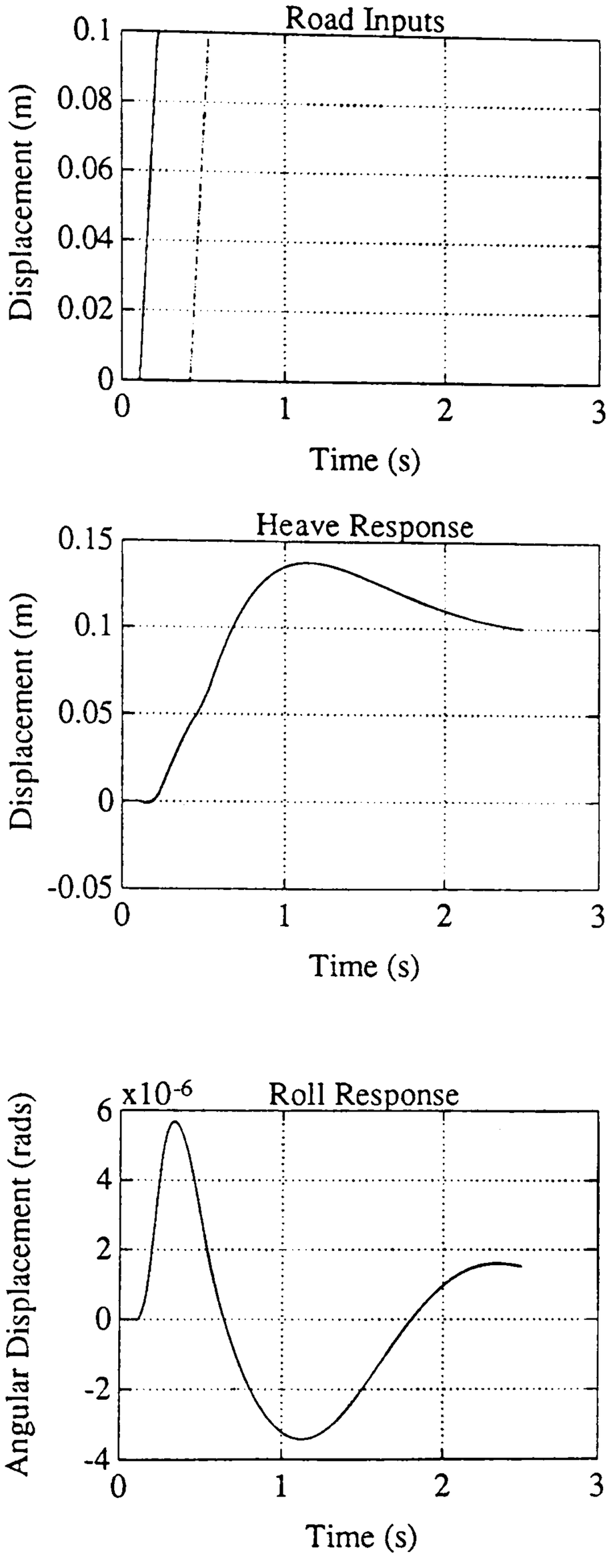


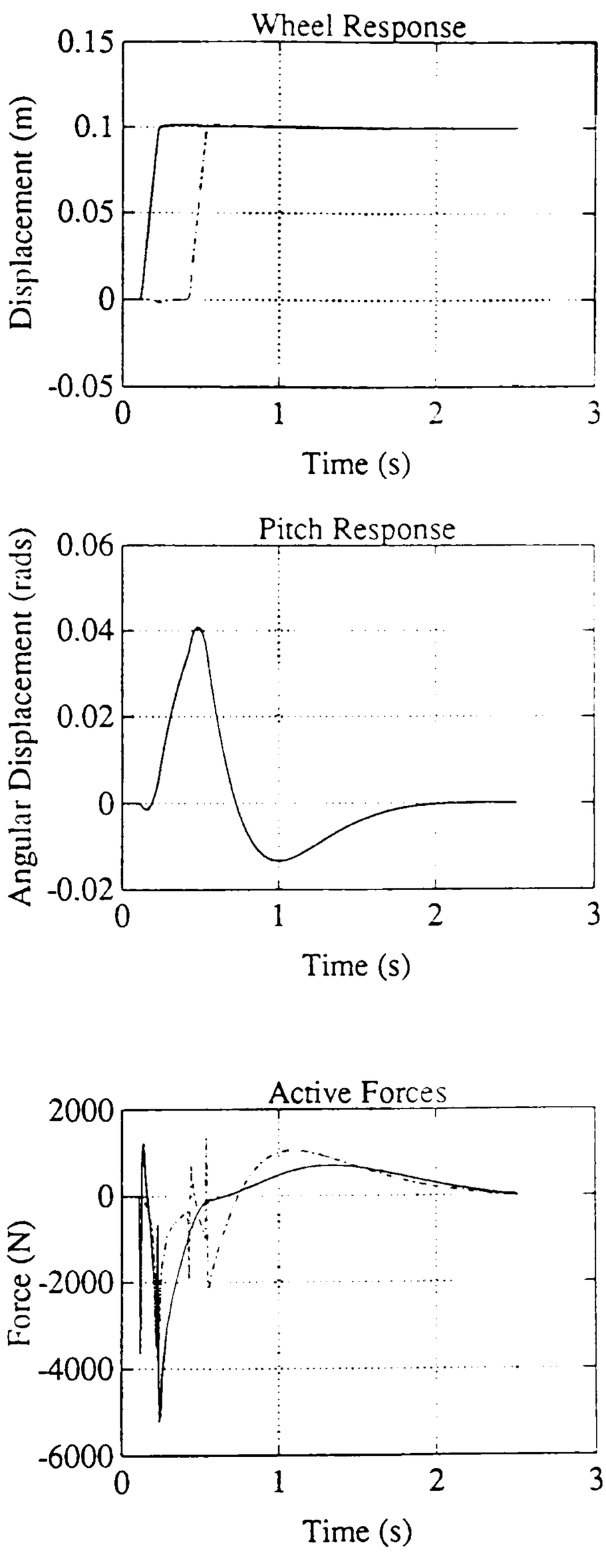














Figure 4.17 : Non-Linear Simulation of Best Regulator Result

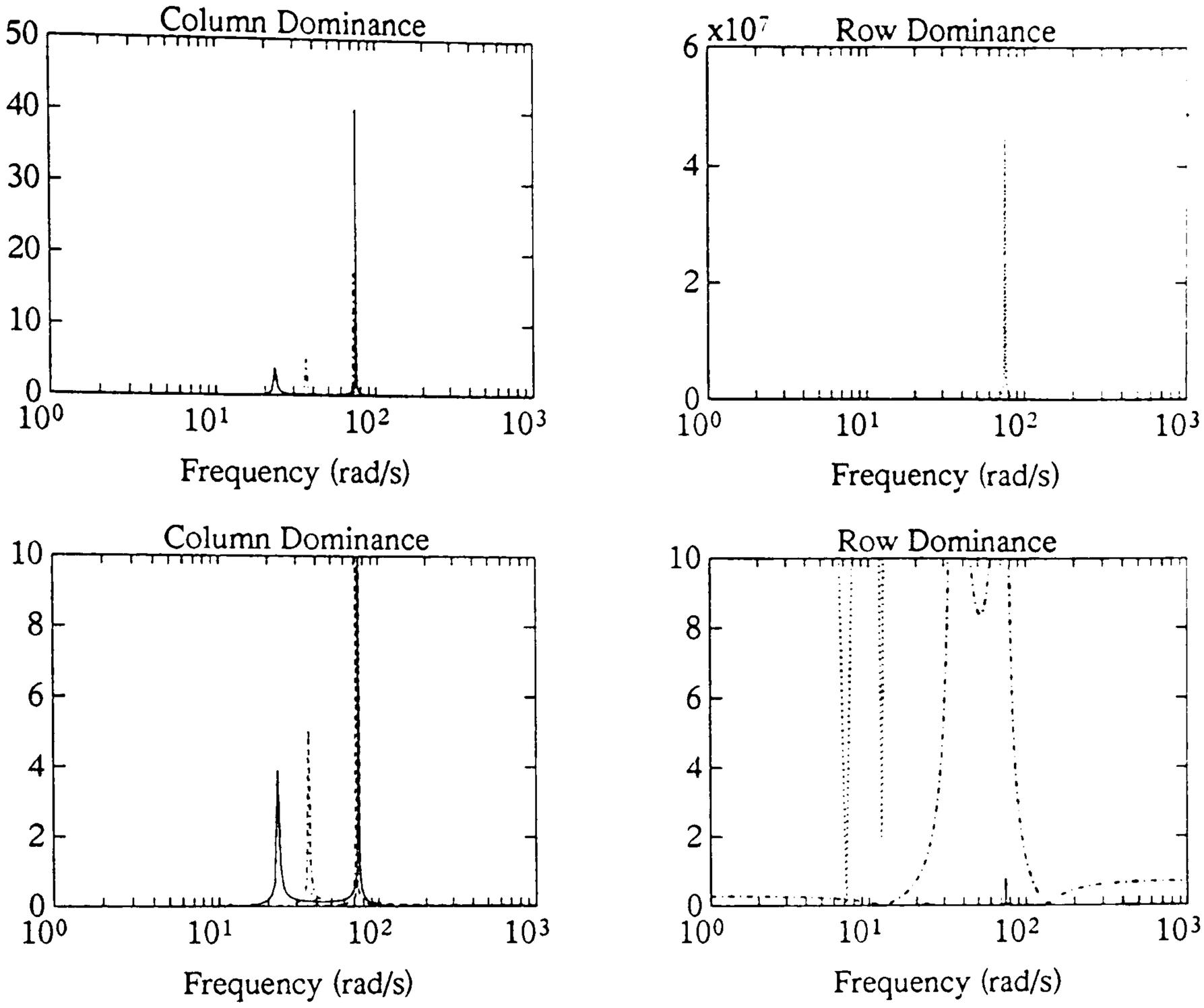


Figure 4.18 : Column and Row Dominance Measures

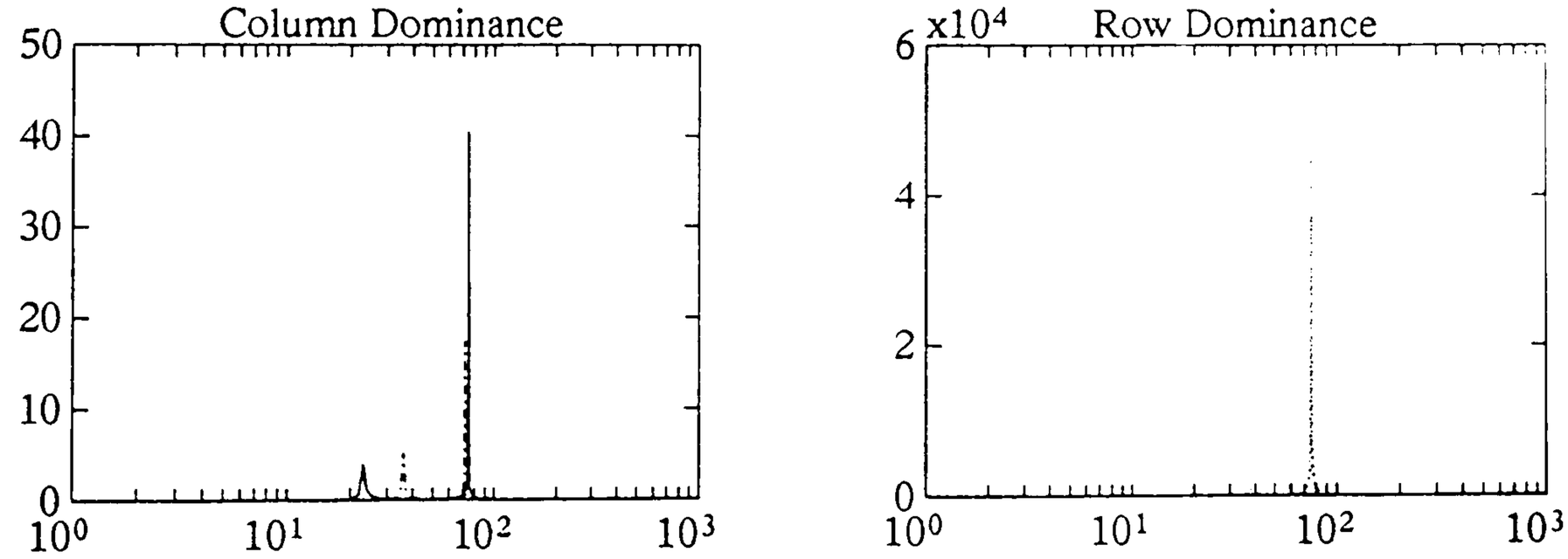


Figure 4.19 : Column and Row Dominance Measures for Scaled System

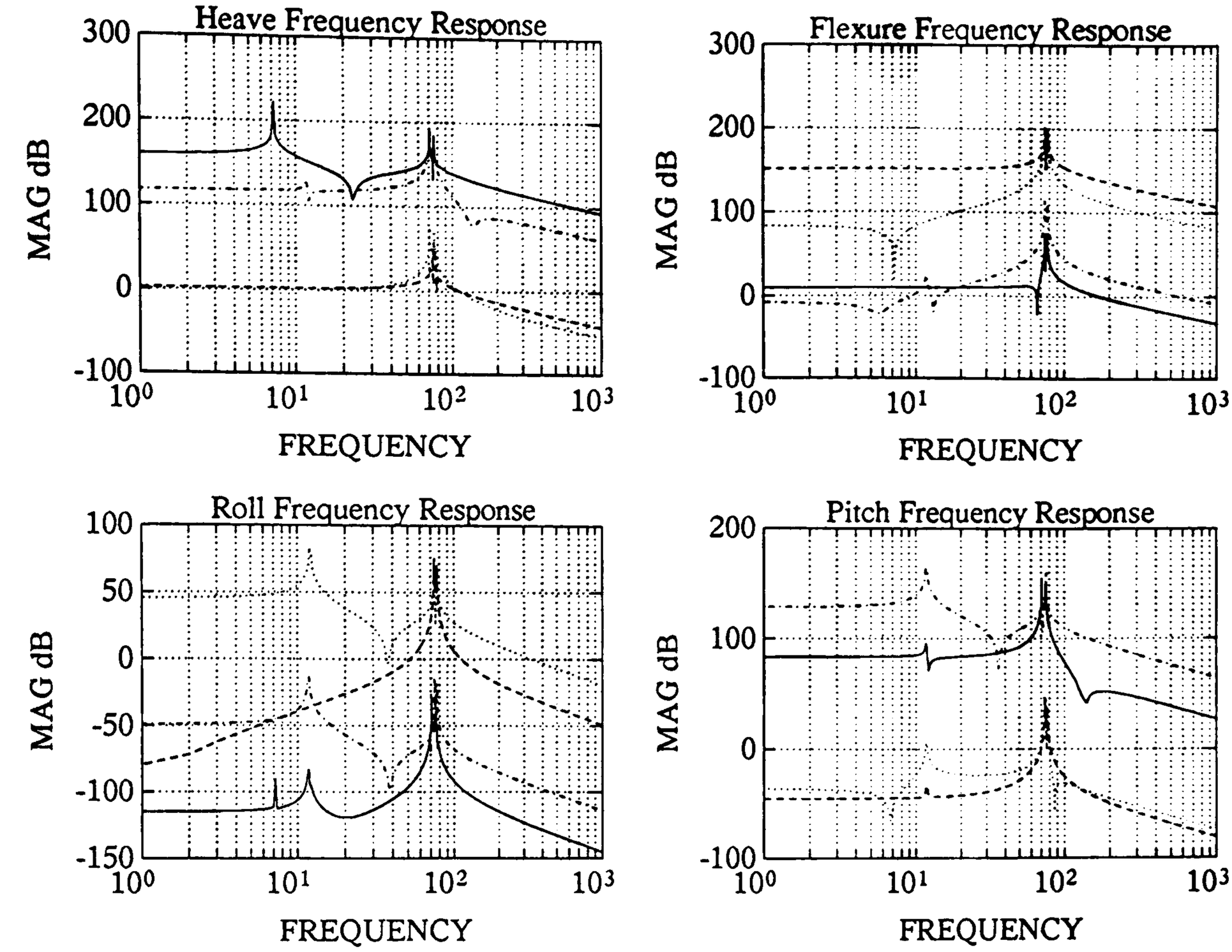


Figure 4.20 : Decoupled System Bode Plots

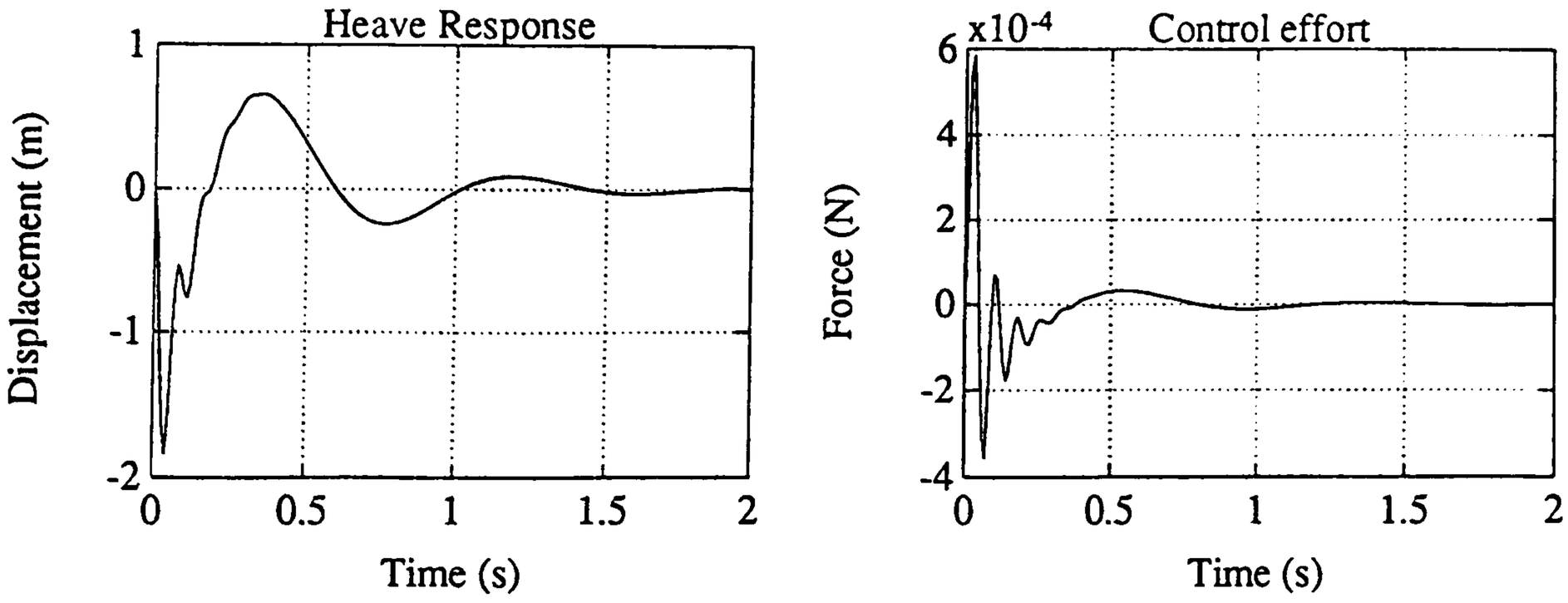


Figure 4.21a : Heave Mode

Figure 4.21 : Frequency Domain Results for Decoupled Systems

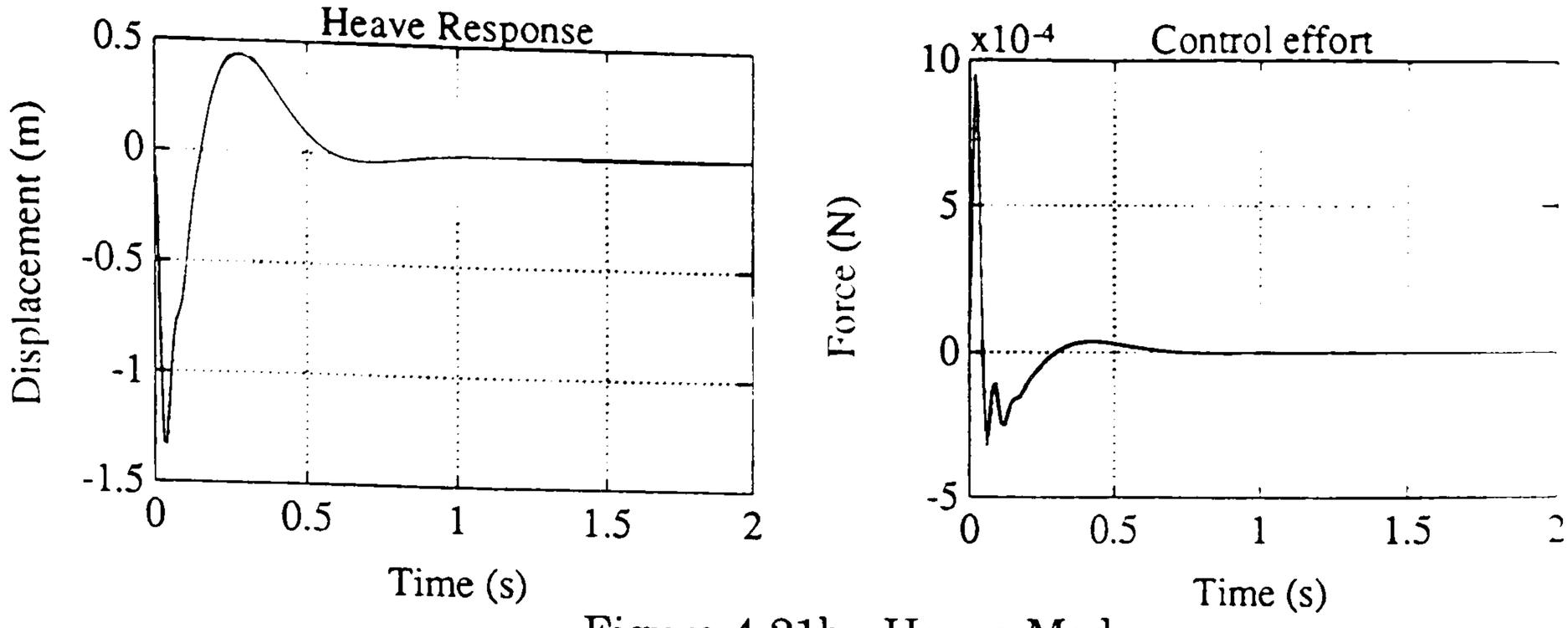


Figure 4.21b : Heave Mode

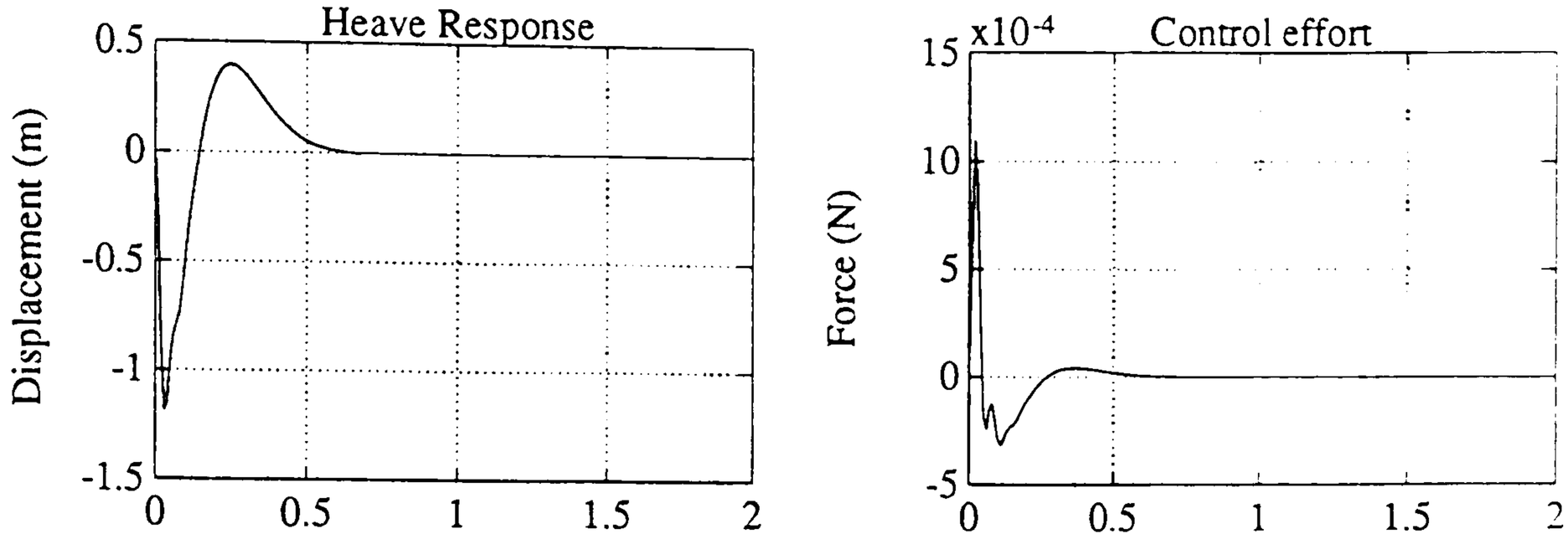


Figure 4.21c : Heave Mode

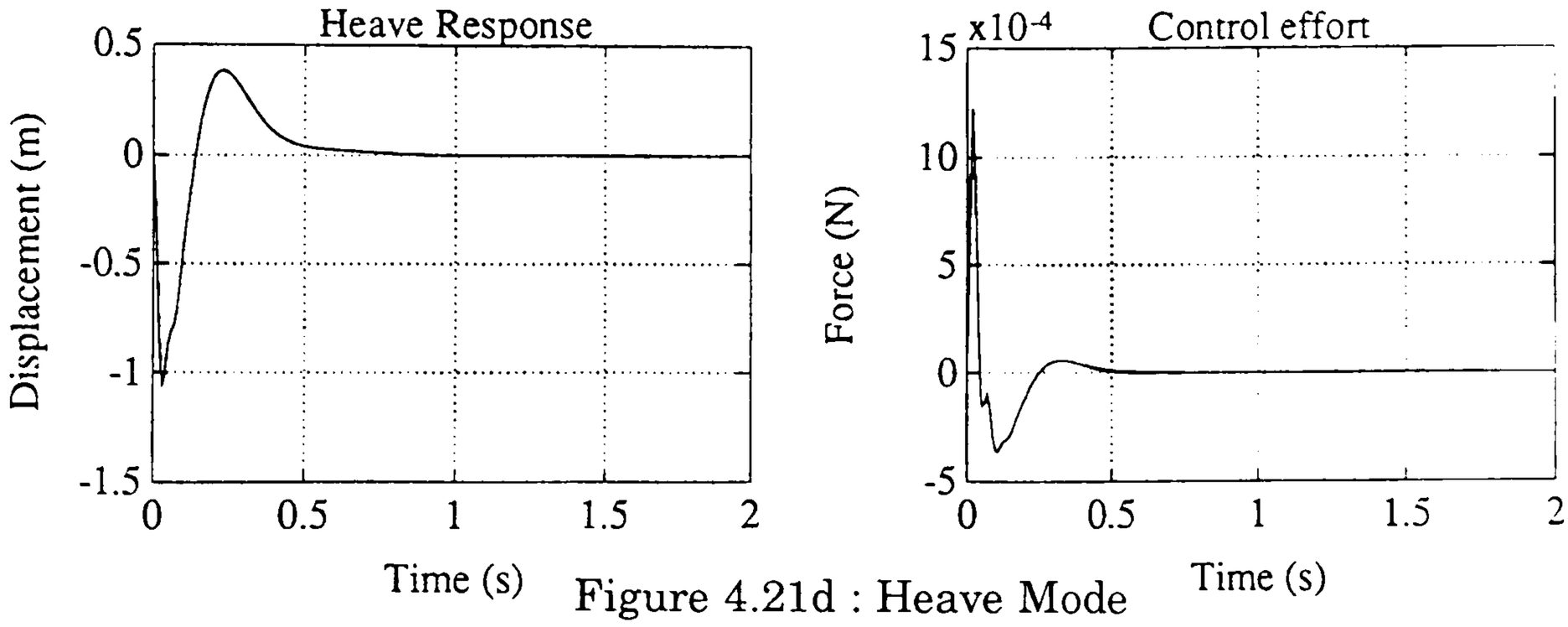


Figure 4.21d : Heave Mode

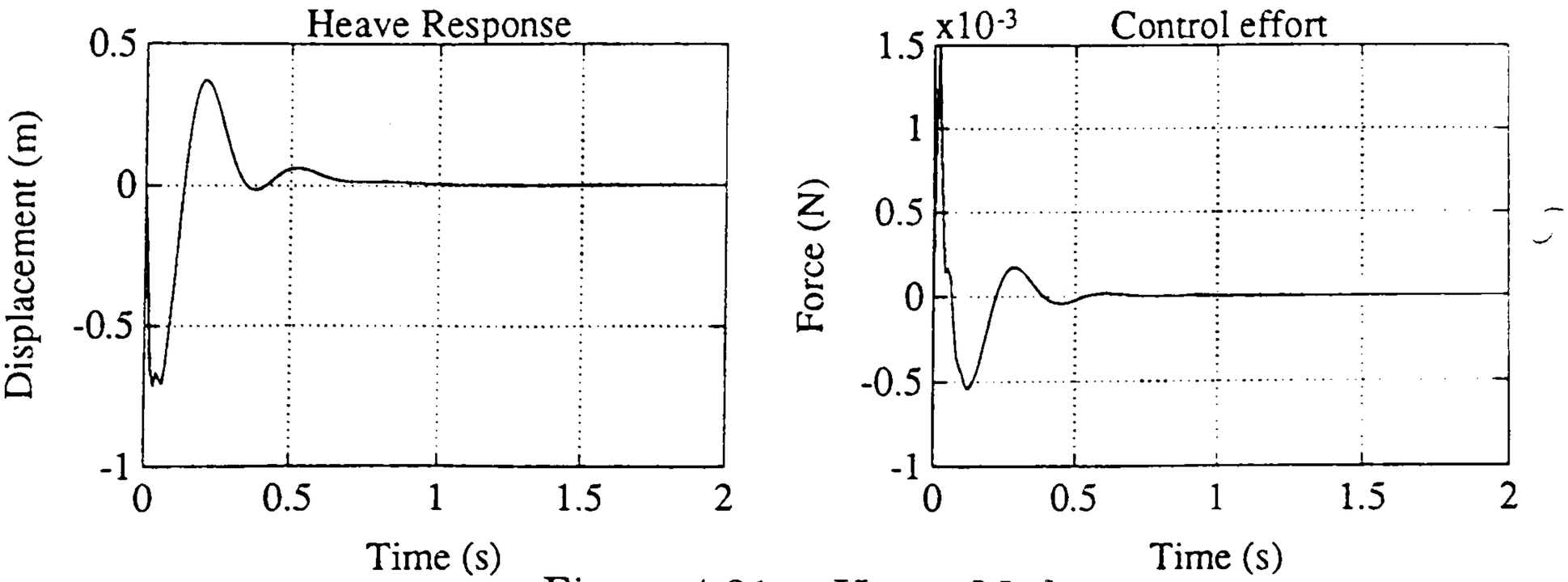


Figure 4.21e : Heave Mode

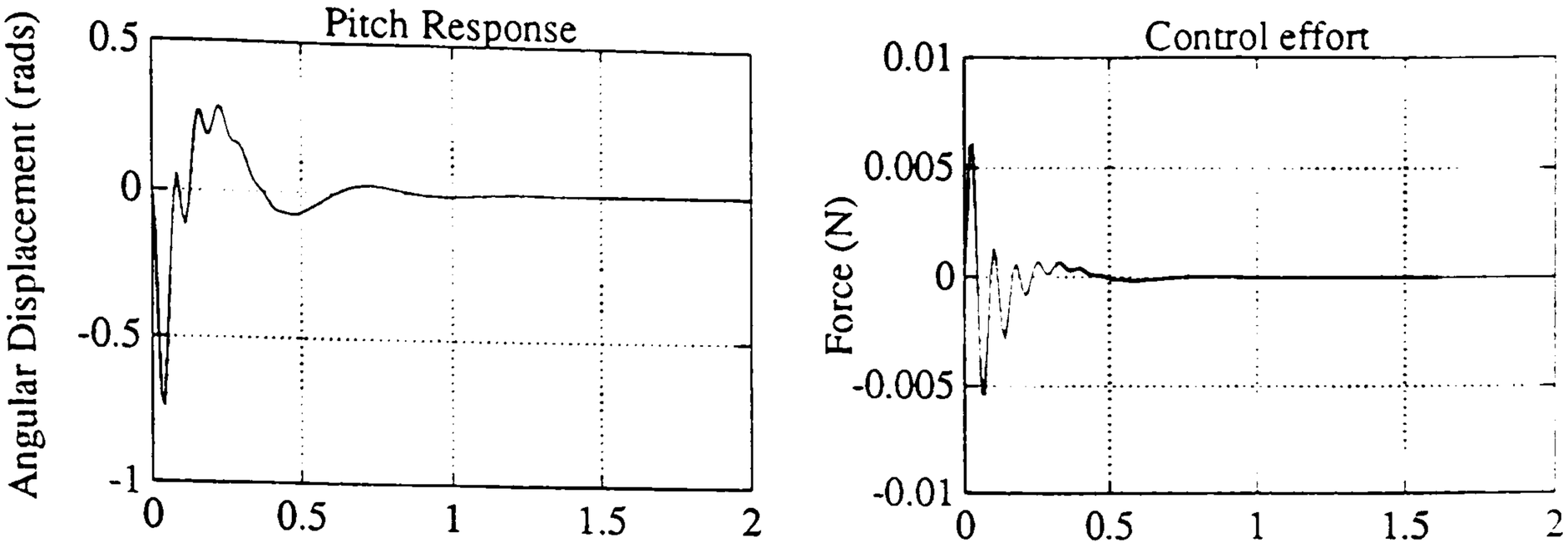


Figure 4.21f : Pitch Mode

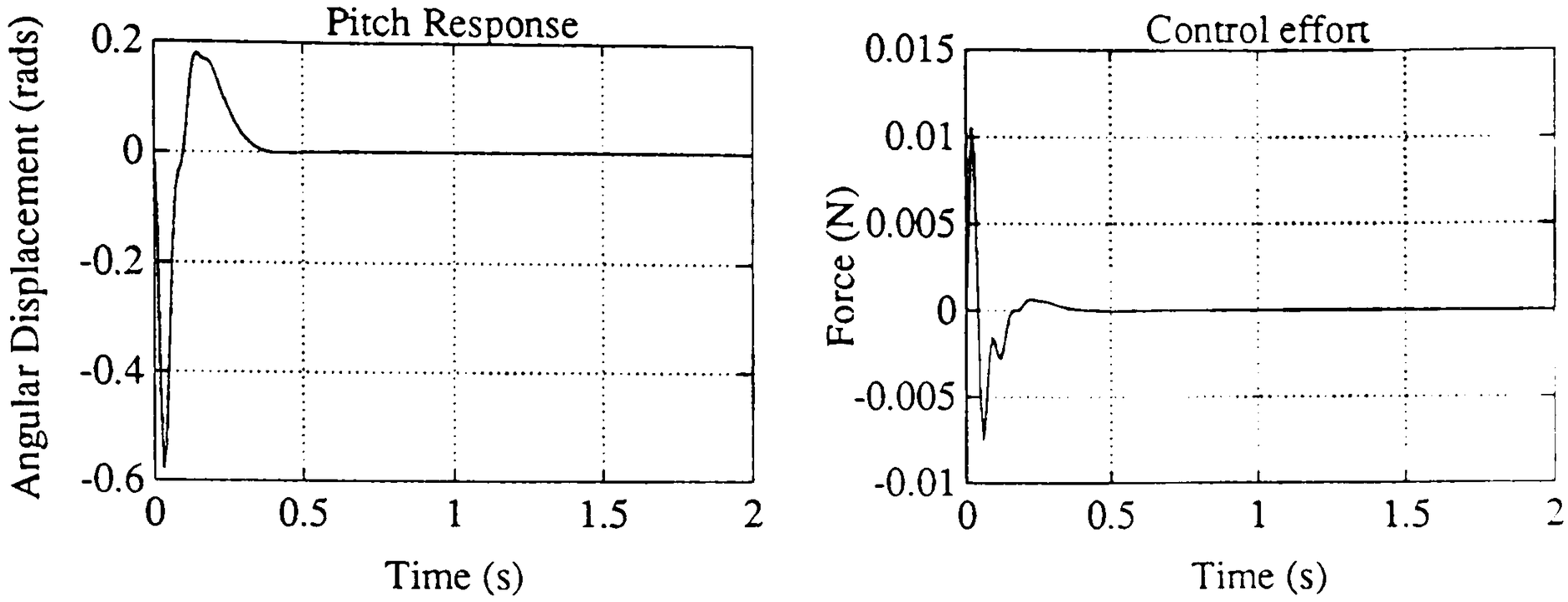


Figure 4.21g : Pitch Mode

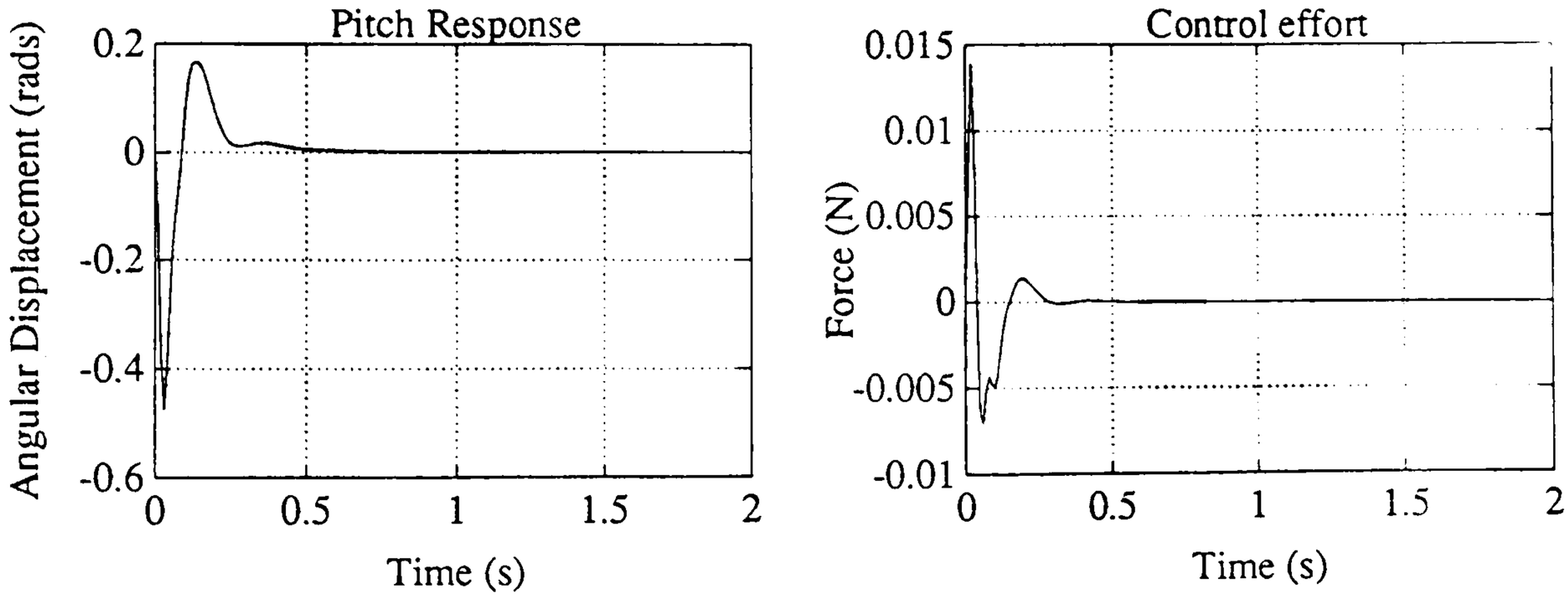


Figure 4.21h : Pitch Mode

Figure 4.21 (continued)

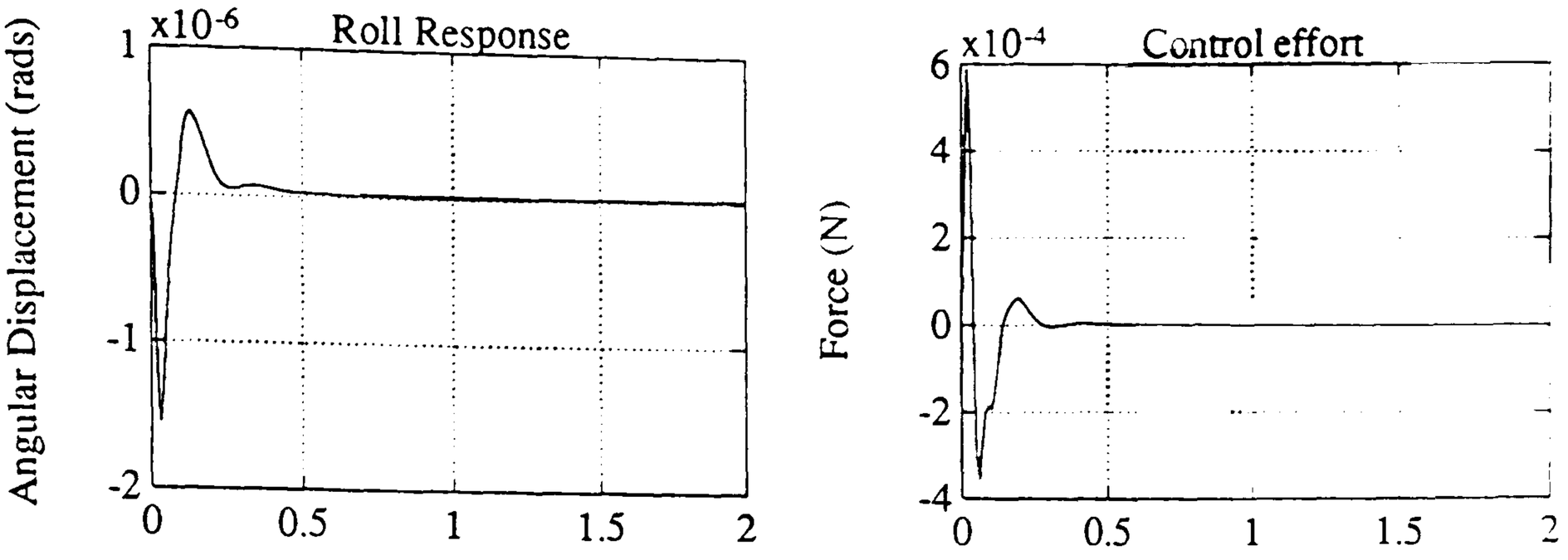


Figure 4.21i : Roll Mode

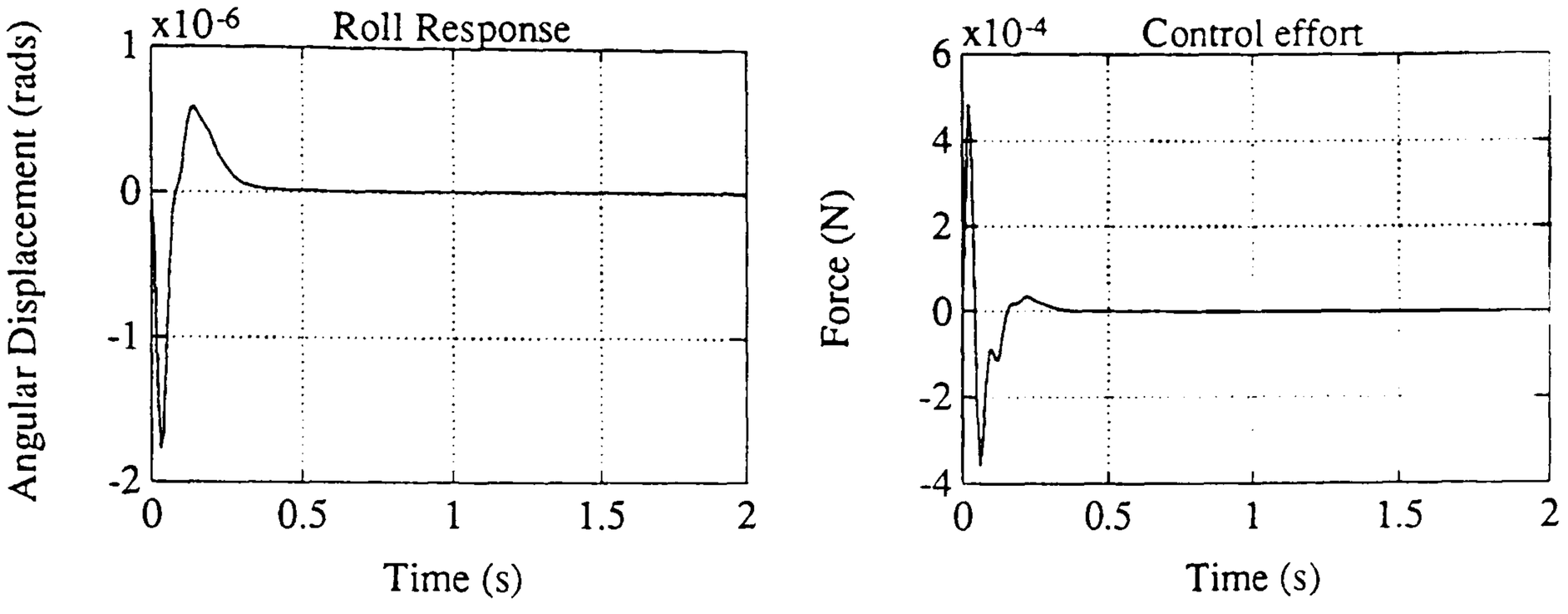


Figure 4.21j : Roll Mode

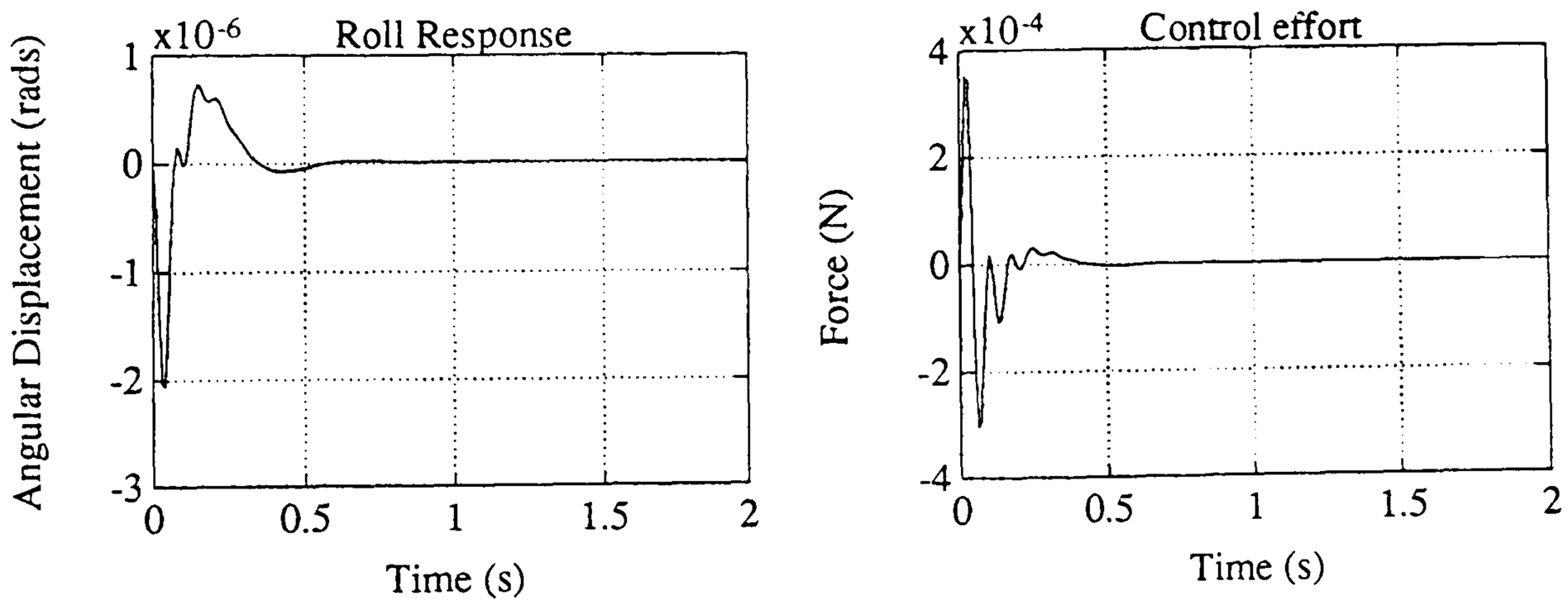


Figure 4.21k : Roll Mode

Figure 4.21 (continued)

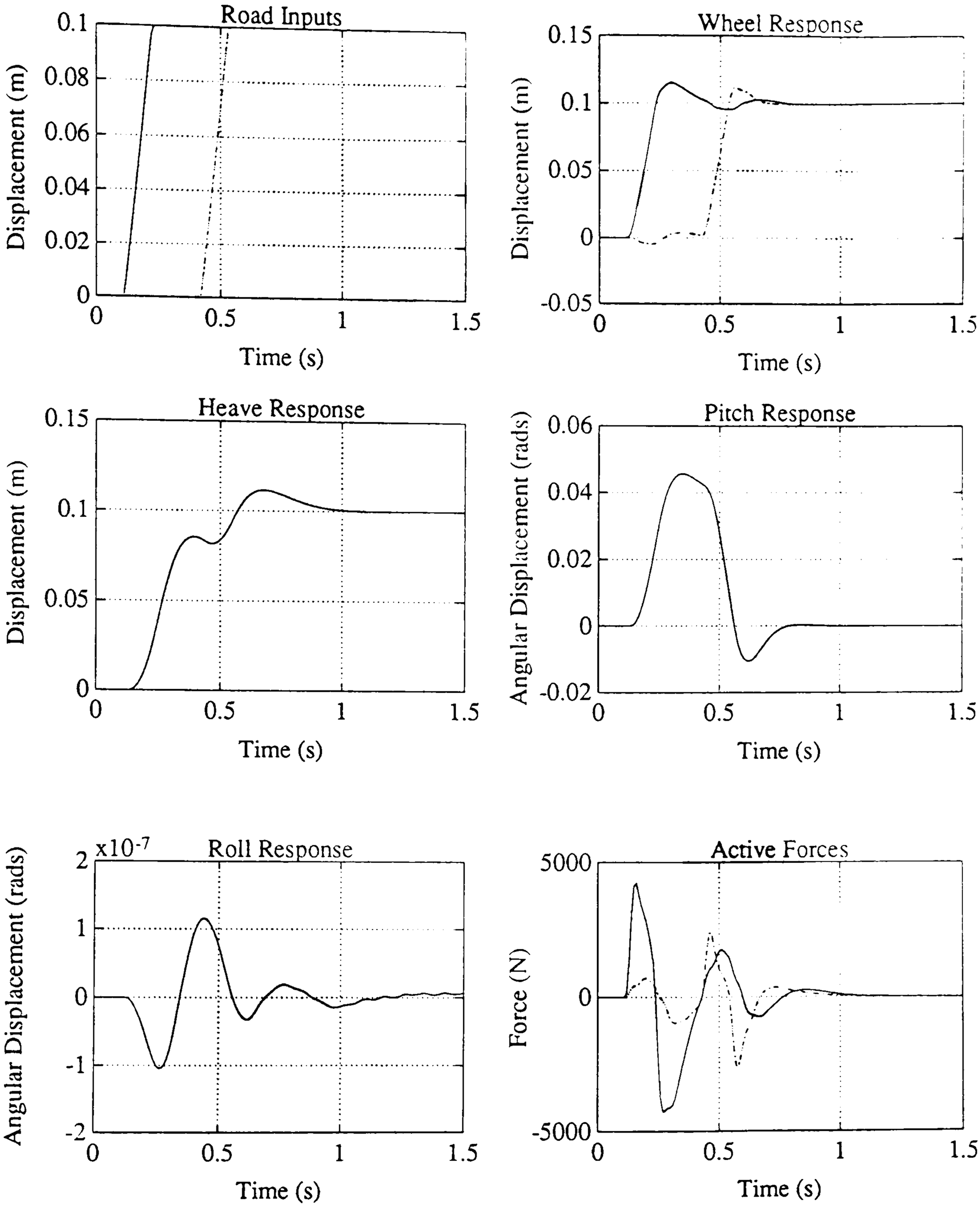


Figure 4.22a : Road Step Input

Figure 4.22 : Non-Linear Simulation of Best Frequency Domain Solution

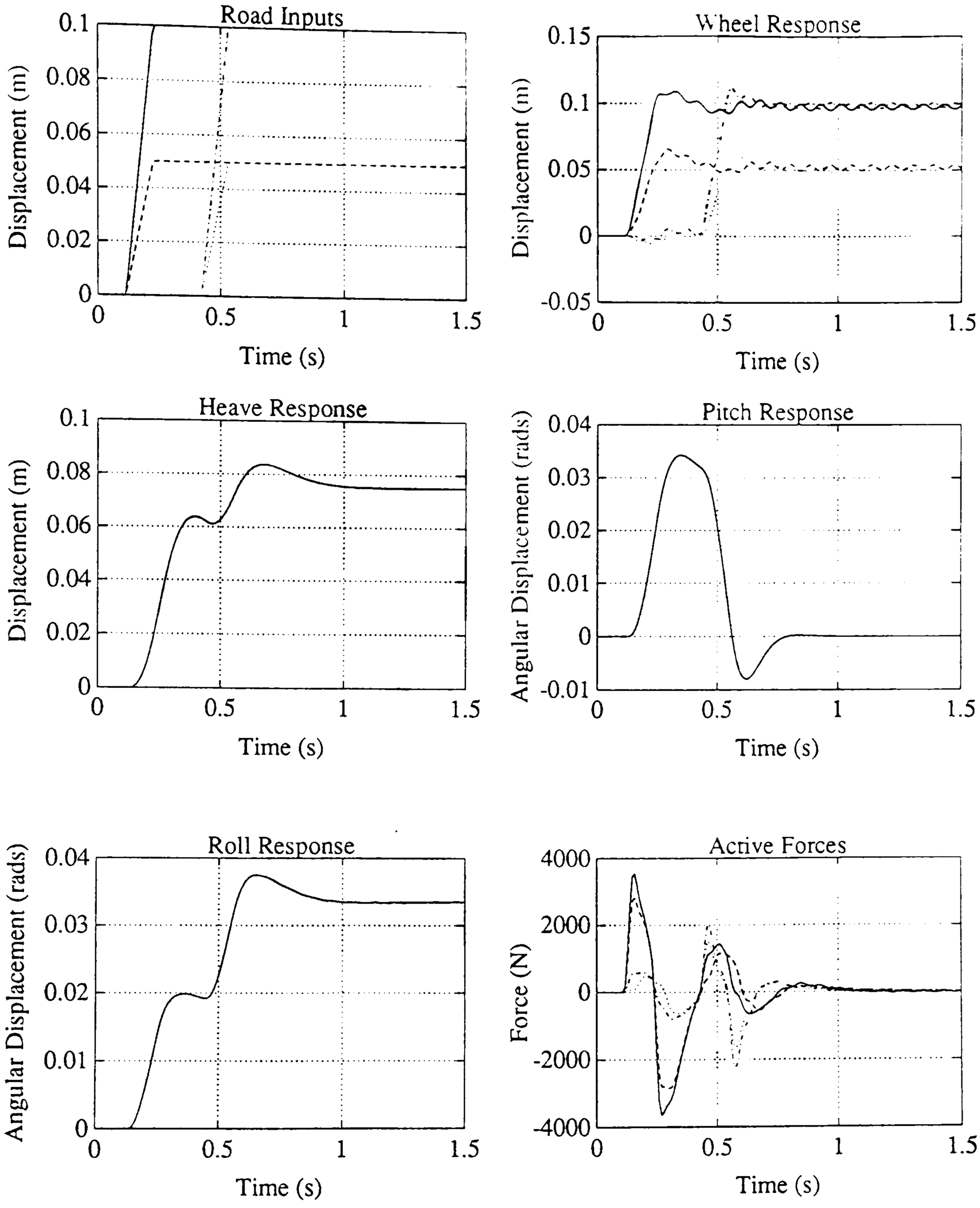


Figure 4.22b : Road Step Input to One Track Only

Figure 4.22 (continued)

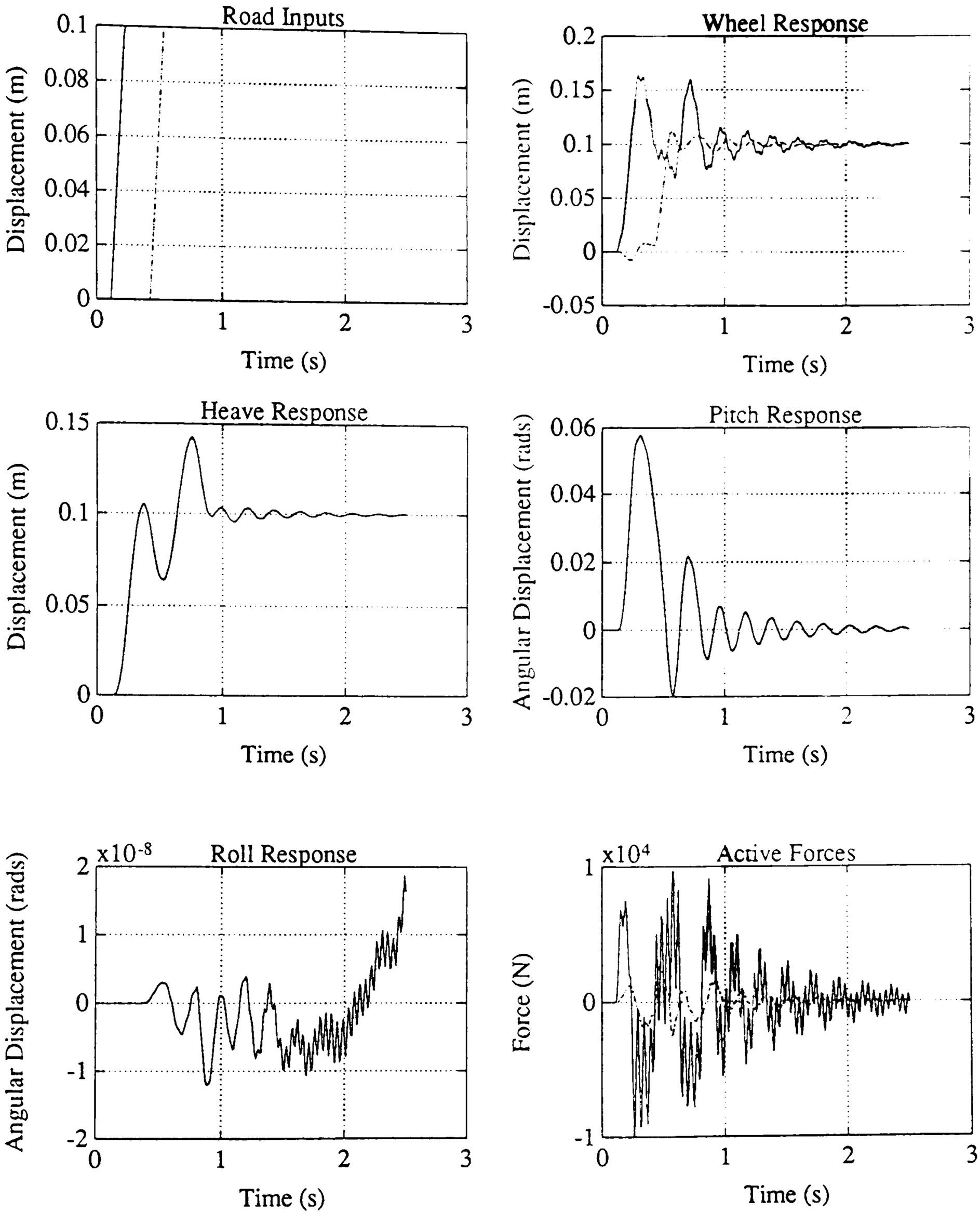


Figure 4.23 : Comparative Quarter Car Results

# Chapter 5 : Control Strategies for Variable Damping Systems

## 5.1 Introduction

Fully active suspension systems have attracted widespread academic interest throughout the past twenty years and have been shown theoretically to produce significant ride performance improvements for automotive vehicles as described in chapter two. In contrast the practical implementation of such systems on production vehicles is a far less attractive proposition, and as a result has been restricted to specialised cases including the Lotus and Citroen systems. The design of such an active system would involve an extensive hydraulic system capable of providing significant levels of power with accuracy and complete safety and reliability. For the majority of automotive manufacturers, this would involve the complete redesign of their suspension systems, with major packaging problems, resulting in prohibitive cost implications.

A simpler approach to advanced suspension systems is achieved by the use of semi-active systems, and theoretical studies have also shown that the ride performance improvements possible for semi-active systems are only marginally inferior to their fully active counterparts. For semi-active systems the actuators are required to dissipate energy from the suspension only, and can be achieved by the use of a combination of variable rate spring and damping elements.

The practical implementation requirements are thus reduced to the

replacement of conventional passive springs and dampers with variable rate equivalents, with the addition of the required sensors and electronic control system. This results in a system involving minimal electrical power requirements, and only minor modifications to the conventional passive suspension system. Consequently semi-active systems can be offered to the customer in cost effective ways including restricting the system to top of the range models, or offering such systems as options. These considerations illustrate the feasibility of practical implementations of semi-active systems, assuming the justification of the additional cost by the improved vehicle ride characteristics.

As previously discussed in chapter three, the design approaches to ride control for semi-active systems have been significantly different for academic studies and practical implementations. The usual approach taken for theoretical studies has been to begin with an ideal active solution, and simply modify the desired control law to fit the system under consideration. For continuously variable semi-active systems, for example, this simply involved setting the semi-active force to equal the desired active force, and to zero when this was not a dissipative force. These studies claimed performance improvements approaching those obtained with fully active systems. However these studies have again assumed ideal semi-active actuators with no consideration of the real practical characteristics of such systems.

In contrast, the control design approach used by automotive manufacturers and their component suppliers has been to apply heuristic design methods directly to the system under consideration. These design methods have involved extensive prototype testing in order to tune the control

algorithm. Due to the availability and cost of variable rate springs and dampers, these practical implementations have used discretely variable dampers with two or three fixed rate settings. The major drawback to this type of approach is concerned with the expensive and time consuming use of prototypes. It would also be relatively complex to apply heuristic control techniques to an advanced suspension system of more complexity than these discretely variable damping systems.

In order to address the drawbacks and limitations of these control design methods, a study of ride control for semi-active systems was undertaken in which analytical modelling and control design techniques were applied to practically realistic systems. This was achieved by the use of realistic vehicle models and by utilising a variety of different control strategies.

For this study the semi-active systems under consideration were variable damping systems, in which the conventional passive dampers are replaced by variable rate dampers, leaving the passive compliance elements in parallel. Both discretely, in which the damping rate can be switched between two or three discrete rates, and continuously, in which the rate can be varied continuously between a maximum and minimum, variable rate dampers were considered.

In order to achieve the aims of this study, the full vehicle model described in chapter four was extended to include steering inputs and lateral dynamics of the vehicle, together with realistic actuator, sensor and controller representations. Both approaches to the control systems design were applied to each system, firstly adapting ideal active controllers to the specific system under consideration, and secondly direct heuristic design techniques. A

discussion of the results achieved will be presented, and the chapter will be completed by some conclusions that were drawn from the study.

## 5.2 Development of the Model

For this study of ride control for variable damping suspension systems, the emphasis was placed on practically realisable systems. In order to achieve this, two major additions were required to the full vehicle model described in chapter four. Firstly for accurate evaluation of variable damping control strategies, realistic representations of the practical characteristics of the systems were essential. The model was therefore extended to include actuator, sensor and controller dynamic characteristics.

The second limitation of the work described so far lies in the design and evaluation of ride control systems for road inputs alone. Automotive vehicle ride incorporates the response, in terms of heave, pitch and roll to driver inputs such as steering, braking and acceleration as well as road inputs. Any practically realisable controller must provide good vehicle response to all road and driving conditions, even if not specifically designed for. In order to allow illustration of the vehicles response to driver inputs, the model was extended to include steering inputs and lateral dynamic behaviour. This involved the inclusion of steering wheel inputs and a representation of lateral tyre dynamics. Due to the control techniques required for the ride control of variable damping systems, this model was not used directly in the control design process. As a result the inclusion of steering inputs and lateral tyre dynamics did not complicate the design process, but merely enlarged the scope of vehicle performance evaluation.

### 5.2.1 Steering Input and Lateral Dynamics

In order to include steering inputs into the full vehicle model described in the previous chapter, the only change required to the SD/FAST model was the addition of a body and joint to represent the steering rack and its motion. Figure 3.4 shows the front suspension topology, and it can be seen that the steering track rods were connected to the sprung mass as outboard bodies by joints and not loop constraints. As a result the required addition was within a direct branch of the tree structure and involved no restructuring of constraint topology. Figure 5.1 illustrates the new connection between the track rods and the sprung mass including the rack. The steering rack was represented by a rigid body connected to the sprung mass by a single translational degree of freedom joint. The two rotational degree of freedom joint previously between the track rods and the sprung mass were used to connect the track rods to the steering rack.

The most suitable method of defining the steering inputs was by the use of prescribed motions on the steering rack translational joint. The SD/FAST input file has to include an indication that the rack joint is to be governed by prescribed motions. The mass and inertia properties of the steering rack rigid body were set to zero as the mass was already included in the sprung mass in the previous model. The centre of mass of the rack body was also set to be at the joint position. Finally the rack joint motion is set to be prescribed in the SD/FAST input file. Table 5.1 gives the centre of mass details for the rack body, and details of the joint positions are included in table 5.2.

The ACSL code then required two additions to accommodate the

steering input. Firstly the prescribed motion for the rack translational joint, in terms of acceleration, velocity and displacement was calculated. In order to specify the steering input in terms of more intuitive variables, a steering ratio relating the rotational input at the steering wheel to the rack motion was used to scale the prescribed motion inputs. In this way the steering wheel rotational input is specified as opposed to the rack translational motion. This steering ratio is given in table 5.3. The resultant prescribed motions for the rack were then applied to the translational rack joint. It is important to ensure the prescribed motion calculations are consistent with each other and with all of the joint initial conditions.

The second addition to the ACSL code involved the extension of the tyre model to include lateral dynamics. Tyre modelling is very complex and the most poorly understood part of vehicle performance prediction, especially lateral dynamics. In this work, tyre modelling was not intended to be a major subject of discussion, with simple tyre representations being used for purely comparative evaluation of suspension systems. As a result, the lateral tyre force, $\boldsymbol{F_{lat}}$, was modelled as a linear function of the tyre slip angle, $\alpha$,

$$F_{lat} = -K_{lat}\,\alpha \tag{5.1}$$

where $\boldsymbol{K_{lat}}$ is the lateral tyre stiffness given in table 5.3. The tyre slip angle, $\alpha$ was calculated from the lateral and longitudinal components of the wheel velocity in the wheel coordinate system, $\boldsymbol{v_{lat}}$ and $\boldsymbol{v_{long}}$ as given by

$$\alpha = \arctan\left(\frac{v_{lat}}{v_{long}}\right) \tag{5.2}$$

and this is illustrated in figure 5.2. The resultant lateral tyre force was then

applied to the unsprung masses as external forces in the lateral direction of the wheel coordinate system. Applying the force to the lateral translational joint between the unsprung masses and ground would be incorrect as the order of these joints means that the lateral joint represents the absolute lateral direction and not the local lateral direction of the wheel.

### 5.2.2 Damper Models

The semi-active actuators under consideration in this study were discretely and continuously variable dampers. In order to realistically evaluate the performance of various control strategies, representative models of the actuator dynamics were included in the full vehicle model described in chapter four. For the case of variable dampers, the force characteristics are essentially the same as a passive damper for each selectable rate, with the addition of switching dynamics. Therefore for both discretely and continuously variable dampers, the damping force was modelled, as for the passive case, as a non-linear function of the strut velocity by a force-velocity characteristic, as shown in equation 3.5. For the variable rate dampers, however, the damping characteristic is dependent on the selected rate as well as the strut velocity.

For the discretely variable case a typical damper with two fixed rate settings was chosen. The damping characteristics used in the model were based on supplier data provided for a set of dampers involved in the implementation study described in appendix A. The force characteristics for the discretely variable damper were modelled as two conventional force velocity curves, one for each of the allowable damper rate settings, firm and soft. Different characteristics were used front to rear, and these are illustrated in figure 5.3.

For the continuously variable case, limited information was available from various component suppliers for typical dampers. The damping characteristics were simply given as two force velocity characteristics for the maximum and minimum allowable damping rates as shown in figure 5.4. These curves are comparative with the rates used in the discretely variable model in that the soft and firm force velocity curves lie between the maximum and minimum variable rate curves. In fact the minimum rate is significantly softer than the discrete soft curve.

Information relating to a realistic method of interpolating between the maximum and minimum rate limits was unavailable. In the absence of relevant information from suppliers, in house experience or published data, linear interpolation was applied to this model. This produced a reasonable approximation to a typical continuously variable damper, suitable for feasibility and comparative studies for various control strategies. However for comparison with the discretely variable system, the absence of a more realistic representation of the force characteristics or any tuning of the rates must be considered.

Therefore the continuously variable damping characteristics were modelled as a map of force against velocity and rate. This map consisted of the maximum and minimum force velocity curves given in figure 5.4, with linear interpolation providing the intermediate rate characteristics. The damper rate selected was indicated by a number from zero to one. Zero represented the minimum damper rate, and one the maximum rate, and the rate was allowed to vary continuously between these limits. These damping characteristics are illustrated by the surface plots given in figure 5.5.

Also included in both variable damper models, was a representation of the switching dynamics, which again was based on supplier information. Figure 5.6 illustrates the typical switching response given for the discretely variable dampers under consideration in this study. The time constants involved in this response would vary depending upon the relative velocity in the damper. For the discretely variable damper this was represented by a time delay between the electrical switching signal initiating the solenoid controlling the damper, and the damping force having changed.

A more accurate model of the switching behaviour would have included a time delay followed by a first order lag. However the time constants involved were small enough that there was negligible difference in the vehicle performance results between a lag and a straight time delay, and so for simplicity the time delay was used. Details are given in table 5.3.

For the continuously variable case supplier data was also provided for a typical damper, with similar switching characteristics as shown in figure 5.6 for the discretely variable damper. However for the continuously variable case, there was large variability in the time constants involved depending on the rates between which switching was occurring as well as the damper velocity. Due to the small time constant involved, a pure time delay was again used to model the damper switching dynamics, and for simplicity the same time delay used for the discretely variable model was used for all switching. This was a reasonable approximation again in the absence of any further information.

### 5.2.3 Sensor and Controller Models

The final model modification required for the study of variable damping

systems included the addition of sensor models and the representation of the discrete controller characteristics. The measurements required for the range of controllers under consideration for the discretely variable case included primary ride sprung mass vertical and lateral accelerations, steering wheel angle and steering rate, relative strut deflections and velocities, and sprung mass velocity at each corner of the vehicle. Experience of the characteristics involved in the first four of these measurements was gained through the study described in appendix A.

However for the measurements used in the control strategies obtained from the literature, no sensor dynamics were available. For all of the measurements excluding the sprung mass accelerations, the sensors were required to cover the complete range of ride frequencies and noise filtering would the be required to remove any sensor noise. As a result the predominant measurement characteristic in terms of the effects on resultant vehicle performance was the restriction of the vertical and lateral sprung mass acceleration measurements to primary ride frequencies. As a result of this importance and the availability of details from component suppliers, a representation of the sprung mass acceleration measurement was included in the model.

The characteristics of the accelerometer and filter combination were provided from the supplier in terms of the measured frequency response as described in appendix A. This analogue sensor and filter combination was approximated in the ACSL model by the continuous transfer function of the form

$$\frac{ks^2}{as^2 + bs + c} \tag{5.3}$$

with coefficients given in table 5.4, and frequency response as shown in figure 5.7. The same model was used for both the vertical and lateral measurements to provide the measured sprung mass primary ride accelerations.

Finally the discrete microprocessor control characteristics were included in the ACSL model by the use of a DISCRETE section. Typical representations in terms of sampling rates and time delays were based on the study described in appendix A. The predominant characteristics were the sampling rate for the controller, calculation times, and other time delays involved with controller flow. The discrete controller model therefore included a typical sampling rate and time delays representing calculation times and the time between the relevant switching flag being set in the controller, to the damper receiving the signal. These timings are given in table 5.5.

To allow direct comparison, all of the controllers evaluated in this variable damping study used the same controller characteristics. Similarly for the continuously variable case, the same sensor and controller models were used as no specific data was available.

## 5.3 Control Strategies

Ride control for active suspension systems can be approximated to a linear control problem as described in chapter three. In contrast, however, variable damping systems provide an inherently non-linear control problem. This can be illustrated by referring to the linear two degree of freedom model described in chapter three with equations of motion given in equation 3.1. For

the variable damping system under consideration in this chapter, the damper rate is the control variable $u$, and the equations of motion become

$$\begin{aligned} m_b\ddot{x}_b &= K_s(x_w - x_b) + u(\dot{x}_w - \dot{x}_b) \\ m_w\ddot{x}_w &= K_t(d - x_w) - K_s(x_w - x_b) - u(\dot{x}_w - \dot{x}_b) \end{aligned} \tag{5.4}$$

This system of equations is then non-linear as it contains terms involving the multiplication of the control variable with part of the state vector. For the discretely variable case the control variable itself will also be non-linear, allowing discontinuities as it switches between two discrete values.

This system non-linearity inherent in variable damping systems precludes the application of linear control techniques and leads to the two basic control design approaches described earlier. The first approach bases the semi-active control on the ideal active linear control law, and then modifies this to suit the variable damping system. The second method involves the direct design of a controller for the specific system under consideration with the use of heuristic techniques.

### 5.3.1 Discretely Variable Damping Control

For the discretely variable damping case, three different ride control strategies were evaluated and compared. The first controller considered was based on the active skyhook damping concept, and has been the most widely reported switching strategy used for theoretical studies [17, 39, 63]. The concept of inertial damping was applied independently to each corner of the vehicle, and thus the four desired damping rates were determined separately. This involved a comparison of the sign of the relative strut velocity with the absolute sprung mass vertical velocity at the relevant corner. The firm damping rate was chosen

when these signs were the same, and soft was selected otherwise. This skyhook damping switching strategy is illustrated in figure 2.9.

The second controller evaluated in this discretely variable damping study has also been described in the literature by Charalambous et al [17]. The switching strategy was designed to minimise the sprung mass acceleration by a comparison of the signs of the strut deflections and velocities. The soft damper rate was chosen when the signs were the same, and firm selected otherwise, as shown in figure 2.10. Again this resulted in four independent controllers acting at each corner of the vehicle. The design concept in this case of minimising the sprung mass acceleration allows this controller to be considered a simplification of the active linear quadratic regulator feedback control.

The third and final discretely variable damping ride controller used the second direct design approach involving heuristic techniques. Similar heuristic rule-based controllers have been the most popular type of control algorithm amongst automotive manufacturers and suppliers to date [39, 45, 63, 77, 89]. These controllers are designed directly for the specific non-linear variable damping systems under consideration by the use of vehicle dynamics expertise and practical experience. The control algorithm consists of a set of logical rules that determine the desired damper rate depending on a combination of measured vehicle response parameters and driver inputs.

The rule-based controller used for this study was based on the system described in detail in appendix A, but chosen to be typical of the majority of heuristic controllers. In contrast to the previous two controllers, all four dampers were switched simultaneously as opposed to individual control at each corner of the vehicle. Four measured inputs were used, vertical and lateral

sprung mass accelerations, relating to the vehicle response, and the driver's steering input in terms of steering wheel angle and rate of change. The control strategy essentially selects the soft damping rate as the default setting. A separate set of rules is then used to process each measured input independently, resulting in a flag being set for any required change in damper rate setting. Basically the firm damper rate setting would be selected to control any excessive primary ride resonant oscillations of the sprung mass and provide stability under any excessive steering manoeuvres.

The rules for each input are then combined by the rule that a single flag only is required for a damper rate change from soft to firm, whereas all rules must indicate soft to be the required rate for it to be selected. This follows the ride criterion requiring soft damping for good ride characteristics, and firm damping to control any primary ride resonant oscillations indicated by severe steering inputs or acceleration measurements. The rule-base for this controller are described in detail in appendix A.

These three ride controllers were then included in the DISCRETE microprocessor section of the ACSL model for the discretely variable damping system, and evaluated.

### 5.3.2 Continuously Variable Damping Control

As discussed earlier, ride control of continuously variable damping systems is a non-linear problem with two distinct methods of design. The first and indirect method bases the control on the equivalent ideal active solution with the practical limitations of the specific system under consideration subsequently imposed [63, 69, 71]. Alternatively heuristic techniques can be

used to design an algorithm directly for the non-linear continuously variable damping system. Theoretical studies have reported successful applications of the indirect linear control method, whereas direct heuristic design techniques have not been applied to the continuously variable damping case.

The major reason for this is related to the availability of variable rate dampers and to the fact that practical implementation studies have tended to favour heuristic techniques. However there are also specific design problems involved in the application of heuristic control techniques to continuously variable damping systems. The extension of a heuristic rule-based controller as previously described to cover the continuously variable case would involve a significant increase in complexity and therefore cost. The rule base required for a heuristic controller with a continuous output would be much larger and more complex than that used for the discrete case. As a result the control performance achieved would be reduced and the task of ensuring vehicle stability and safety would become unmanageable.

As a result the indirect design approach using ideal active control laws was evaluated in this continuously variable damping ride control study. In contrast to the reported studies in the literature, however, the full practical limitations of the system under consideration was incorporated. This included allowing energy dissipation only, and restricting the control force to lie between the maximum and minimum allowable damping forces for the measured strut velocity.

As a starting point, the best solutions to the ideal active ride control problem achieved in the full vehicle study described in chapter four were chosen. In order to compare the results for the different linear control

techniques, the best full vehicle solutions for each of the methods including linear quadratic regulator, pole placement and frequency domain techniques were used. The resultant active feedback laws relating to the solutions chosen are given in tables 4.12, 4.14, 4.19, and their linear heave step responses can be seen in figures 4.14d, 4.15c, with pitch and roll responses in figures 4.14h,i 4.15i,j, with the non-linear results for frequency domain controller in figures 4.22a,b.

These ideal active ride controllers were then modified to produce continuously variable damping algorithms, again controlling each corner of the vehicle independently. The desired active force, $f_{active}$, was first calculated using the required feedback law. The sign of the desired force for each corner of the vehicle was then compared with the sign of the relevant strut velocity. The semi-active force, $f_{semi}$, was then set to equal the desired active force when the signs were opposite, otherwise it was set to zero, as illustrated in figure 2.8 and given by

$$\begin{aligned} f_{semi} &= f_{active} \qquad \textit{if } f_{active} \cdot \dot{x}_s > 0 \\ f_{semi} &= 0 \qquad\qquad \textit{otherwise} \end{aligned} \tag{5.5}$$

This semi-active force replicates that used in the theoretical semi-active studies reported in the literature. In this study, however, this semi-active force was further modified to give a realistic variable damping force. This was achieved by comparing the desired semi-active force with the maximum and minimum allowable damper forces for the measured strut velocity. The continuously variable damper force, $f_{var}$, was then set to equal the desired semi-active force if this falls between the damping force limits, otherwise the relevant limit was chosen, as given by

$$
\begin{aligned}
f_{var} &= \max \qquad \text{if } f_{semi} > \max \\
f_{var} &= f_{semi} \qquad \text{if } \min < f_{semi} < \max \\
f_{var} &= \min \qquad \text{if } f_{semi} < \min
\end{aligned}
\tag{5.6}
$$

These controllers were similarly included in the DISCRETE microprocessor section of the ACSL model for the continuously variable damping system and evaluated.

## 5.4 Simulations

In order to evaluate and compare the variable damping controllers under investigation in this study, a range of simulations were performed with each, using the relevant full vehicle non-linear model. These simulations involved two types of input, road and steering, both of which illustrate ride performance characteristics. For all of the simulations, the road inputs to the rear wheels were simply taken to equal the front wheel inputs with a time delay. The delay between front and rear wheel inputs was determined by the speed of the vehicle together with the wheelbase. Vertical road inputs only were considered in these simulations and therefore the vehicle speed was chosen purely to define the rate of change of the wheel inputs.

The first road input considered was a step input to both left and right wheels simultaneously, providing both heave and pitch input components. This input then consists of a road profile change to be tracked in the long term, with a disturbance to be rejected in terms of the speed and severity of the profile change. A large bump disturbance, equivalent to a sleeping policeman, to both sides was also considered, giving heave and pitch inputs at primary ride resonant frequencies. The amplitude of this input precludes total rejection of the disturbance, however the minimisation of any resonant oscillations is

required. Both of these inputs test the controllers performance under the two conflicting response requirements for road inputs. The two final road inputs considered were small and thus pure disturbances, firstly to both left and right wheels simultaneously, and secondly to just one side of the vehicle. In this final road input simulation the roll mode was also excited.

The steering inputs considered were approximately step inputs at the steering wheel at varying vehicle speeds. The exact prescribed motion consisted of a square acceleration disturbance, which was integrated to give the approximate steering angle step input shown later in the simulation results. All of the steering simulations have used the same steering input in terms of steering wheel angle and rate of input, with variations in the vehicle forward speed.

## 5.5 Discussion of Results

For completeness and as a useful comparison, all of the simulations were first performed using the non-linear model with each of the two discretely variable damper rate settings, soft and firm, fixed throughout. The fixed rate simulation results are shown in figures 5.8a-g, and the controlled system results in figures 5.9-5.11a-g for the discretely variable systems, and figures 5.12-5.14a-g for the continuously variable case. For all of the road input simulations the results plotted show the road inputs, the sprung mass heave, pitch and roll response, together with the four vertical wheel responses. The steering simulation results include the steering angle and sprung mass response in terms of roll, yaw rate and lateral acceleration.

For the discretely variable damping systems all of the simulation results

include plots of the measured outputs used in the switching strategy. For the continuous case the desired active forces used as the basis for the control algorithms are included. Finally the results also include time histories of the selected damper rates for all of the controlled system simulations. For all of the plots that involve a result for each of the four vehicle corners, the solid and dashed lines refer to the front, and the dotted and dashed and dotted to the rear.

### 5.5.1 Discretely Variable Damping Results

The first observation to be made from the simulation results is seen in the vehicle response for the system with fixed soft and firm damper rates given in figures 5.8a-g. The vehicle ride characteristics in terms of sprung mass and unsprung mass responses are not as different for the two rates as expected. In fact for the road input simulations given in figures 5.8a-d, the initial overshoot and speed of response for all of the vehicle parameters are very similar, with a reduction in the subsequent oscillatory behaviour for the firm damper rate. For the steering input simulations, with results shown in figures 5.8e-g, the damper rate selection made a more significant difference to the sprung mass roll response.

The major reason for this can be seen from the force velocity curves for the two discrete damper settings given in figure 5.3. Despite a large variation in damping force for the majority of the velocity range, for low strut velocities the damper rates were very similar. This portion of the damper force velocity curve relates to the practical characteristics of viscous dampers and would therefore not be expected to differ significantly for various damper rates. As a result the

low velocity inputs cause similar responses for both damping rates, thus limiting the potential performance improvements for these variable damping systems.

The first discretely variable controller used the skyhook strategy and the simulation results are included in figures 5.9a-g. For the two large amplitude road inputs illustrated in figures 5.9a,b, the skyhook damping strategy provides very good control of the sprung mass oscillation and initial overshoot and reasonable unsprung mass control. It is interesting to note that the skyhook switching strategy is slow to return the damper setting to soft once the vehicle response has been satisfactorily controlled. This may aggravate any noise or harshness problems unnecessarily. Both simulation results also show frequent damper switching, which is increased by the individual control of each corner of the vehicle, again presenting the possibility of noise problems.

These trends are similarly illustrated in the simulation results for the small amplitude road disturbances given in figures 5.9c,d. Figure 5.9d shows the response to a road input with a roll component resulting in a significant second peak in the roll oscillation. This indicates roll control as the weakest aspect of achievable skyhook damping control.

The steering simulations also show good response results with the firm damper setting being selected for the majority of the simulation. In contrast to the road input simulations, the firm setting was not held excessively following satisfactory sprung mass control.

In comparison, the second controller based on minimum sprung mass acceleration achieved marginally poorer vehicle response characteristics for all of the simulations, as seen in figures 5.10a-g. For the road input simulations

with results in figures 5.10a-d, the minimum acceleration switching strategy gives increased sprung mass overshoot and subsequent oscillation. The roll control performance for road disturbances, however, was marginally better then the skyhook damping results as shown in figure 5.10d. The damper setting is more readily returned to the soft setting following sprung mass control, but again the frequency of damper switching is relatively high.

A similar comparison of the steering simulation results achieved with the minimum acceleration controller in figures 5.10e-g, show very little difference from the skyhook damping results. The minimum acceleration controller did, however, produce marginally more sprung mass overshoot and oscillation.

Finally the rule-based controller with results given in figures 5.11a-g, achieved response characteristics very close to those achieved for the skyhook strategy and marginally better than the minimum acceleration algorithm. For the road input simulations, with results in figures 5.11a-d, the only noticeable difference in vehicle response between the rule-based and skyhook algorithms was marginally increased sprung mass oscillations. Generally the skyhook strategy achieved marginally better heave response, with the rule-based controller giving better pitch response.

The major difference in their respective control performances is seen in the damper switching behaviour. The rule-based control strategy resulted in significantly reduced damper switching frequency due partly to the simultaneous control of all four dampers, and partly to the threshold algorithm. This algorithm also returns the damper to its soft setting more rapidly than the skyhook strategy following satisfactory control. This early return to the soft

setting is the reason for the increase in sprung mass oscillation, however the potential ride improvements with regard to subsequent road irregularities justifies this minor penalty. As a result of this difference in damper switching behaviour the noise and harshness characteristics will be improved.

The steering simulation results given in figures 5.11e-g show no difference in sprung mass response between the rule-based controller and the skyhook damping switching strategy. However again the rule-based controller exhibits preferable damper switching characteristics. It should be noted that the rule-based controller holds the firm damping for a significant time after ride control has been achieved. This could cause a degradation in ride for subsequent road inputs, however this safety bias would provide significant improvements in the vehicle response for a series of steering inputs.

### 5.5.2 Continuously Variable Damping Results

Three controllers were considered in the continuously variable damping study, based on the best solutions achieved with the linear quadratic regulator, pole placement and frequency domain design techniques described for the full vehicle study in chapter four. As previously mentioned the feedback controllers used for these solutions are included in tables 4.12, 4.14, 4.19, with linear response simulation results as given in figures 4.14d, 4.15c for heave and 4.14h,i, 4.15i,j for pitch and roll and non-linear responses for the frequency domain results in figures 4.22a,b. The simulation results achieved for the equivalent continuously variable damping systems are shown in figures 5.12-5.14a-g. It is important to note that the desired active forces were calculated in the discrete controller model, and are therefore discretised in the simulation

results.

The most notable trend appearing in all of these simulation results is seen in the damper rate selections. For the majority of each simulation the maximum or minimum allowable damping rates were selected. This was especially true of both state space controllers, with results shown in figures 5.12,5.13a-g. The frequency domain controller exhibits more intermediate damper rate selection especially for the steering inputs, with results in figures 5.14e-g. However even this controller results in significant selection of the extreme damper rates. Therefore by reducing the ideal active force to fit the practical limitations of the variable rate dampers, the resultant semi-active control algorithm essentially becomes a discrete switching strategy. The simulation results achieved for this control design method would therefore be expected to show only marginal improvements over the discretely variable damping controllers. Closer examination of the simulation results included in figures 5.12-5.14a-g shows this to be the case.

In order to illustrate this the continuously variable damping results were compared to the best discretely variable controllers, using skyhook and rule-based strategies with simulation results given in figures 5.9,5.11a-g. As expected from the damper rate switching behaviour, the continuously variable results were no better, and in some cases worse, than the discrete switching strategies.

For the two large amplitude road inputs, the linear quadratic regulator controller gave increased sprung and unsprung mass oscillation, as shown in figures 5.12a,b, compared with the skyhook strategy with results in figures 5.9a,b. The response to the small road disturbances given in figures 5.12c,d

were very similar to the discretely variable results, with one exception in the pitch response shown in figure 5.12c. This shows an increased negative peak over the skyhook and rule-based controllers, with corresponding results in figures 5.9,5.11c.

In contrast the pole placement controller achieved marginally improved responses to all of the road inputs, as seen in figures 5.13a-d over the corresponding discretely variable damping results, shown in figures 5.9,5.11a-d. Again one notable exception was seen in the roll response for the road input simulations. For road inputs with no roll component the pole placement controller actually induced a sprung mass roll response. This unpredictable vehicle response characteristic would present a significant concern for any proposed practical implementation, and would override any potential benefits.

Finally the continuously variable damping controller based on frequency domain compensation achieved inferior ride performance results for all of the road input simulations. Figures 5.14a-d show increased overshoot and oscillatory behaviour for both sprung and unsprung mass responses compared with the skyhook and rule-based controllers as illustrated in figures 5.9,5.11a-d.

For all of the continuously variable damping controllers considered in this study the vehicle response characteristics to steering inputs were significantly inferior to the discretely variable damper strategies. Figures 5.12-5.14e-g show significant increases in roll overshoot and oscillation over the equivalent skyhook and rule-based results given in figures 5.9,5.11e-g. This can be explained partly by the active feedback design processes consideration of road inputs only, with no account for steering response directly included in the design objectives.

## 5.6 Conclusions

The discretely variable damping study included the investigation of three controllers. The first two were based on active solutions, with a strategy using skyhook damping concepts, and another minimising sprung mass acceleration, thus approximating linear quadratic principles. The third controller utilised heuristic rule-based techniques. The evaluation of these three controllers indicated no conclusively superior control algorithm in terms purely of vehicle response characteristics. However on consideration of other relevant factors for suspension control, the rule-based controller was shown to offer the best overall control.

Both the skyhook and minimum acceleration control strategies provided independent control for each corner of the vehicle, with separate damper switching. This resulted in increased complexity of the overall control system, including four sets of sensors and control calculations. Despite this increase in complexity and cost, no significant performance benefits were gained. The separate damper switching, together with the fact that these controllers produced more frequent damper switching anyway, may lead to obtrusive damper noise and excessive wear.

Another important advantage of the rule-based controller was in the heuristic nature of the design process. This subjective approach to suspension control design suits the conventional automotive design methods. Vehicle expertise is widespread within the automotive industry, whereas control expertise is new and scarce. The penalty for these advantages are also related to the differences in the design procedures. The analytical design methods

follow a well-defined procedure, whereas the rule-based controller requires tuning in order to obtain the thresholds and other controller parameters. The choice of such parameters is not obvious, but can be part of the standard design iterative process involving modelling or testing.

Finally the application of heuristic rule-based methods as opposed to analytical model-based techniques removes the sensitivity to modelling approximations and assumptions required during analytical design processes.

For the study of continuously variable damping systems, ideal active feedback solutions were reduced to fit the practical limitations of the dampers. This involved imposing the energy dissipation only constraint as described in the published academic studies, followed by restricting the semi-active force to lie between the maximum and minimum allowable damping forces. The results achieved fell short of the claims made in the literature.

The controlled damper rate selection for these systems was essentially discrete switching between the minimum and maximum allowable rates, with minimal selection of intermediate rates. As expected from this behaviour, the simulation results for the continuously variable damping systems provided no performance benefits over the discretely variable systems. In fact for steering inputs, the vehicle response was significantly inferior to the discretely variable control strategies.

The continuously variable controllers produced other disadvantages in terms of unpredictable behaviour, especially for the pole placement techniques. As for the discretely variable case, the controllers based on ideal analytical techniques produced high frequency damper switching. For these controllers the four dampers are also controlled separately, thus aggravating the possibility of

noise and harshness problems.

| Body | x coord (m) | y coord (m) | z coord (m) |
|---|---|---|---|
| Rack | 1.145 | 0.0 | 0.196 |

Table 5.1 : Steering Rack Centre of Mass

| Inboard | Outboard | x coord (m) | y coord (m) | z coord (m) |
|---|---|---|---|---|
| Sprung | Rack | 1.145 | 0.0 | 0.196 |
| Rack | Track rod | 1.145 | +/- 0.392 | 0.196 |

Table 5.2 : Steering Rack Joint Positions

| Variable | Value |
|---|---|
| Steering Ratio | 8000 Deg/m |
| $K_{lat}$ | 50000 N/m |
| Switching Delay | 20.0 ms |

Table 5.3 : ACSL Variable Values

| Coefficient | Value |
|---|---|
| K | 62.832 |
| a | 1.0 |
| b | 62.832 |
| c | 39.478 |

Table 5.4 : Filter Coefficients

| Timing | Value |
|---|---|
| Sampling Time | 50 ms |
| Calculation Time | 20 ms |

Table 5.5 : Controller Timings

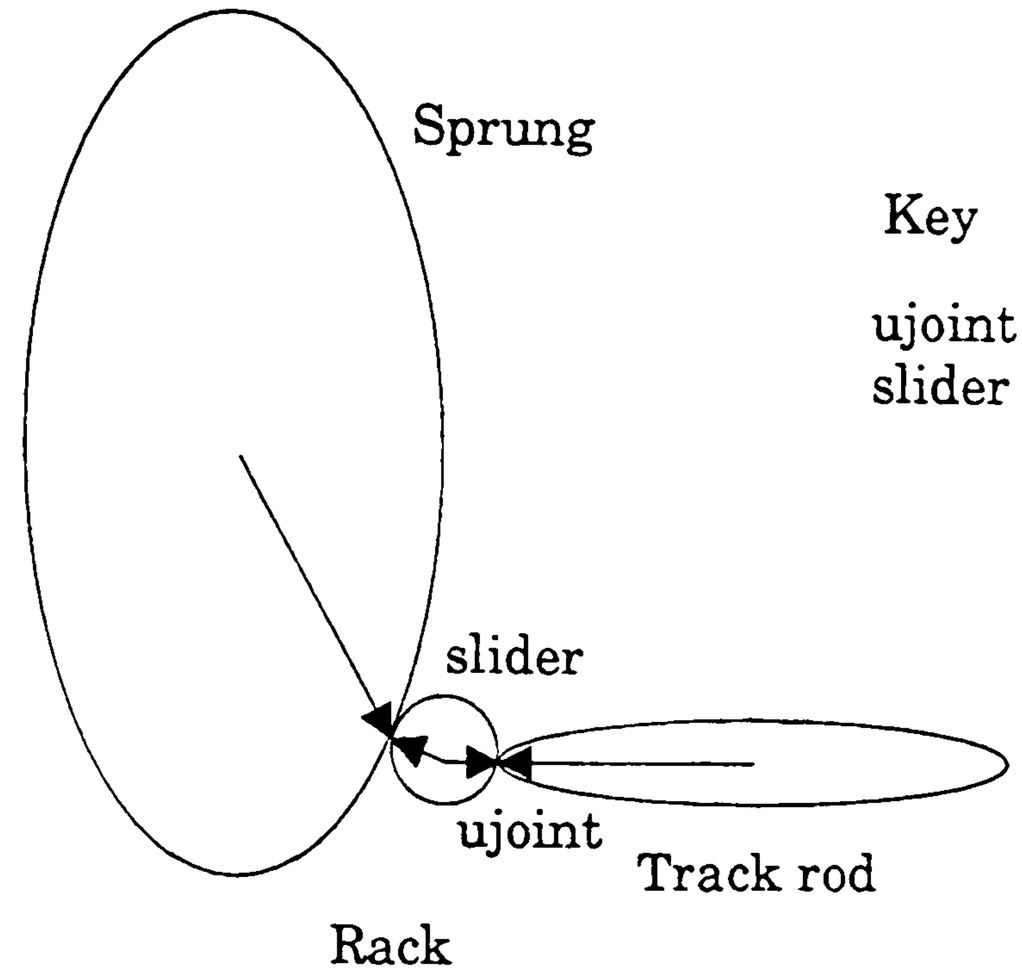


Figure 5.1 : Steering Topology

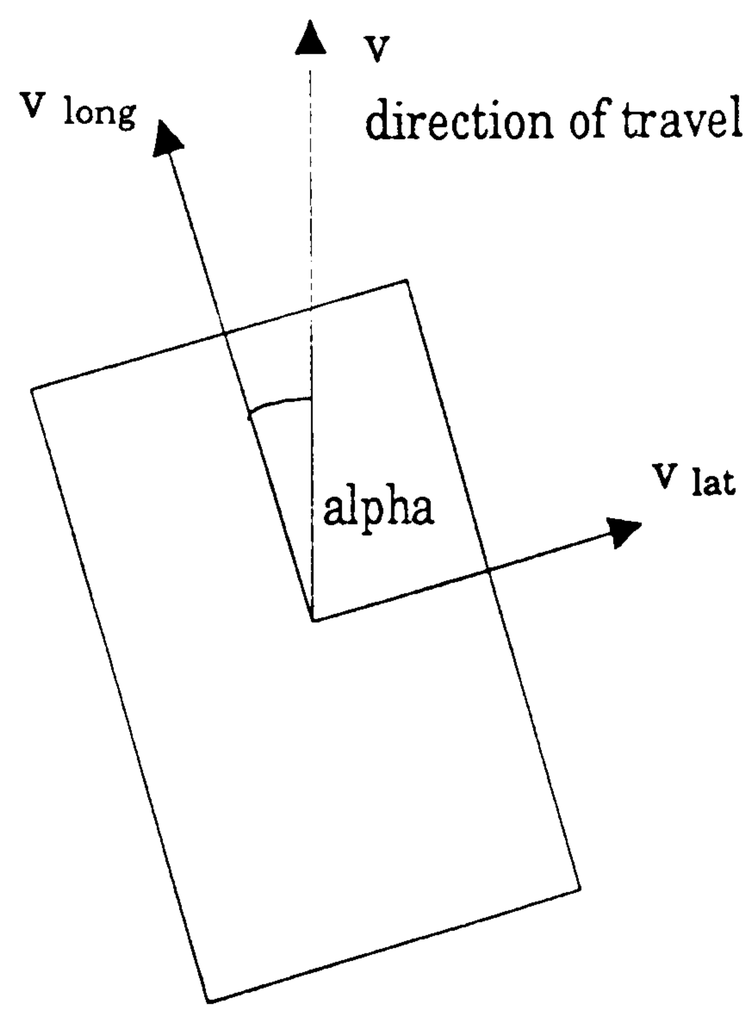


Figure 5.2 : Tyre Slip Angle

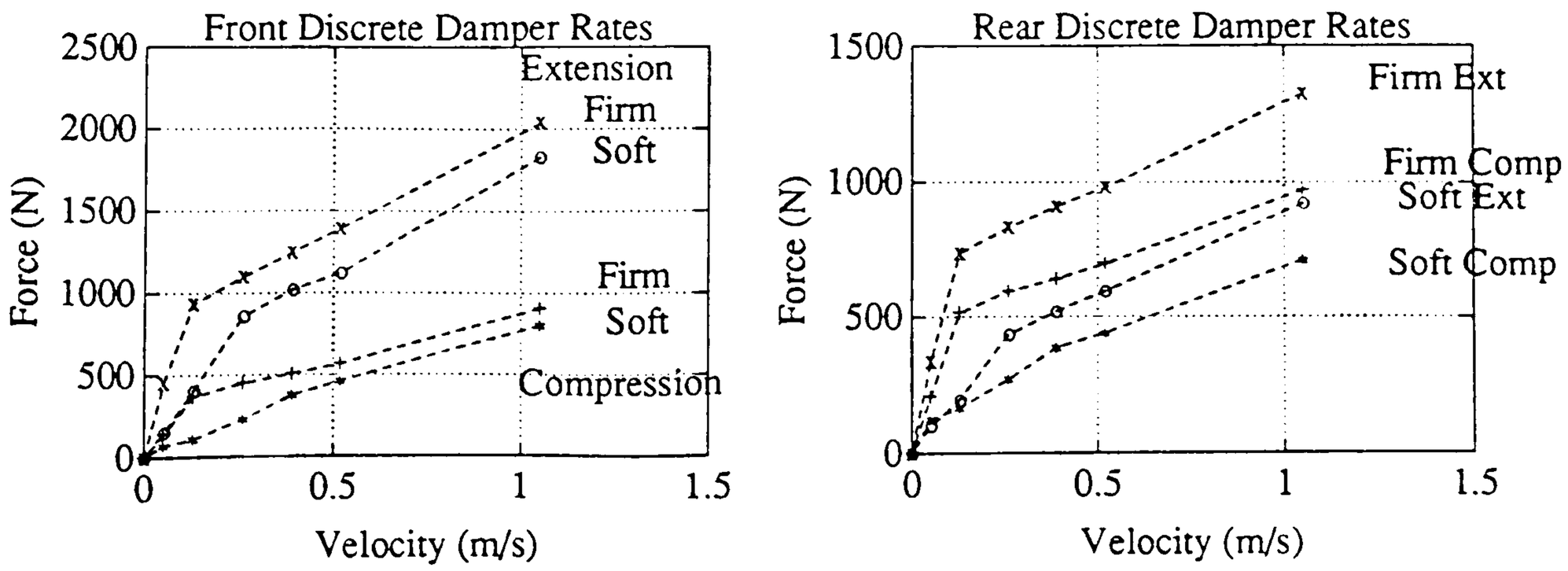


Figure 5.3 : Discretely Variable Damping Characteristics

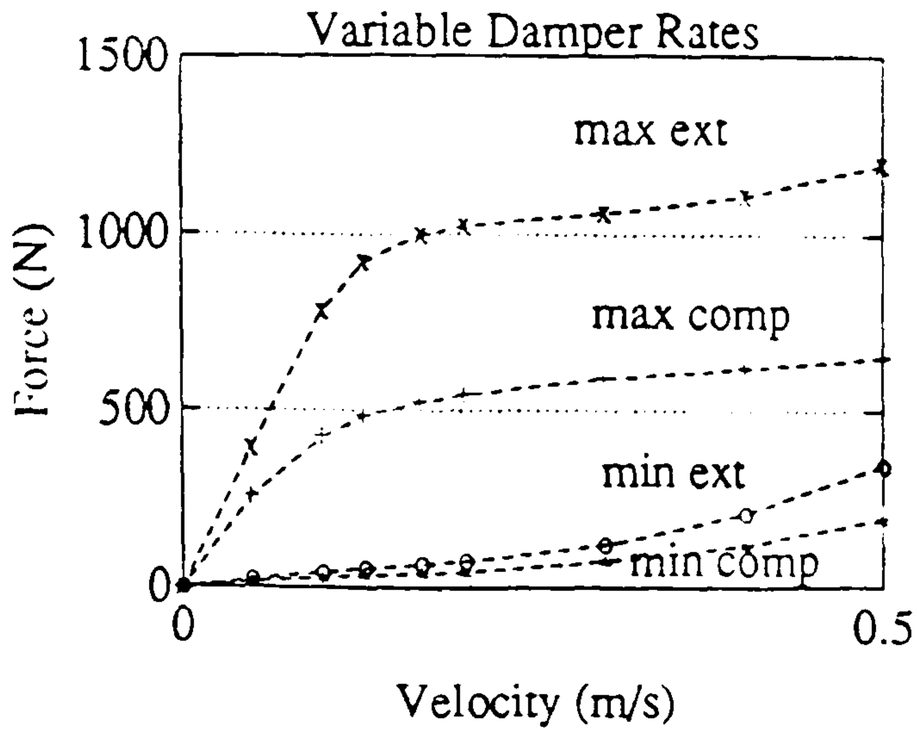


Figure 5.4 : Continuously Variable Damping Limits

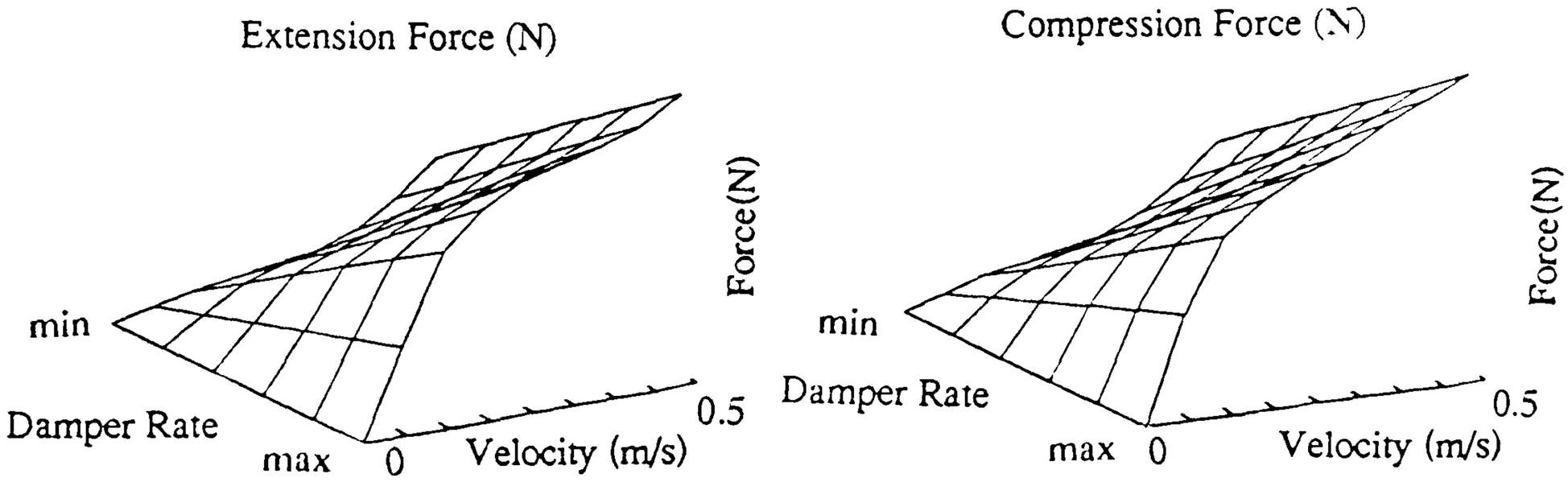


Figure 5.5 : Continuously Variable Damping Characteristics

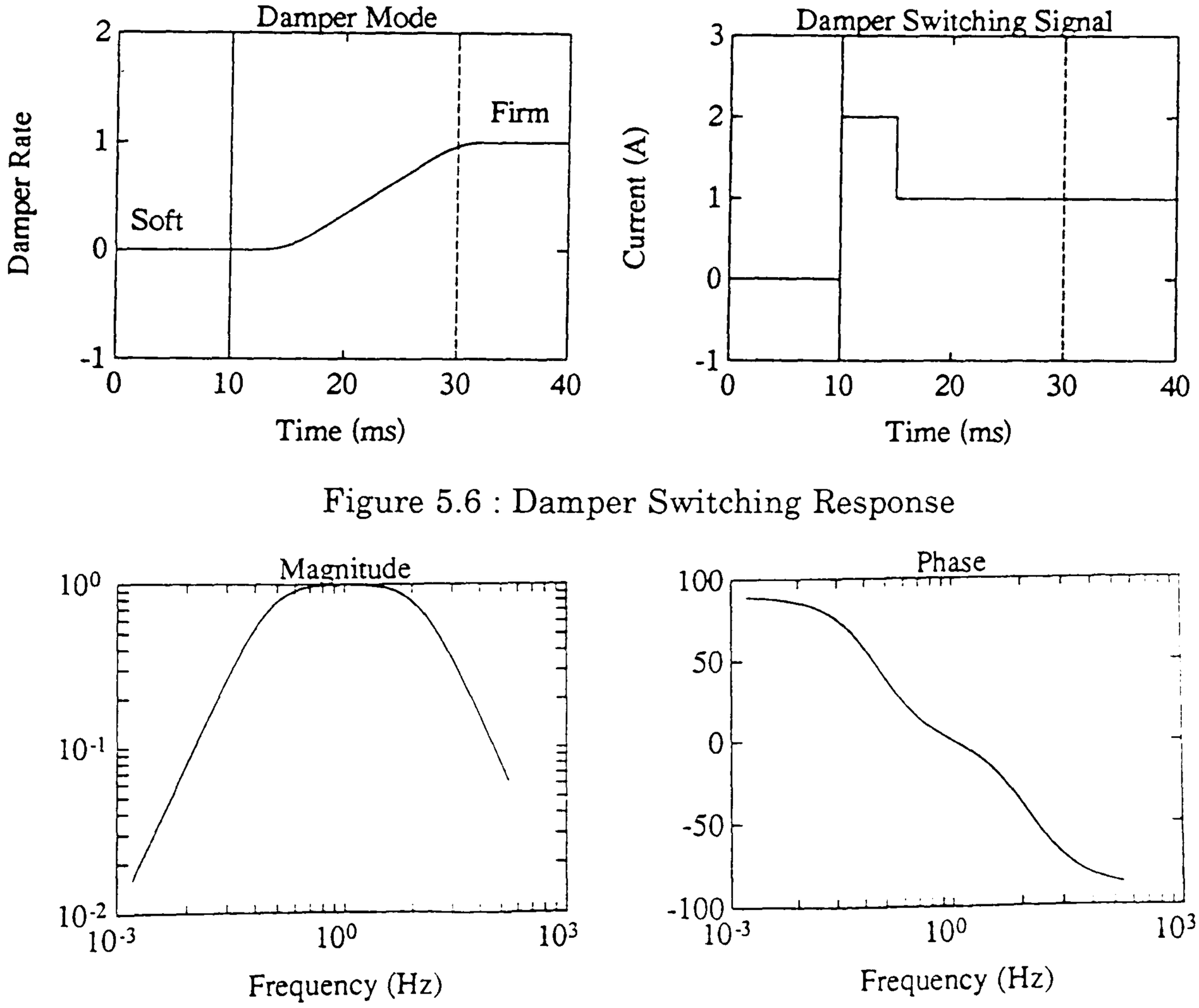


Figure 5.6 : Damper Switching Response




Figure 5.7 : Filter Frequency Response

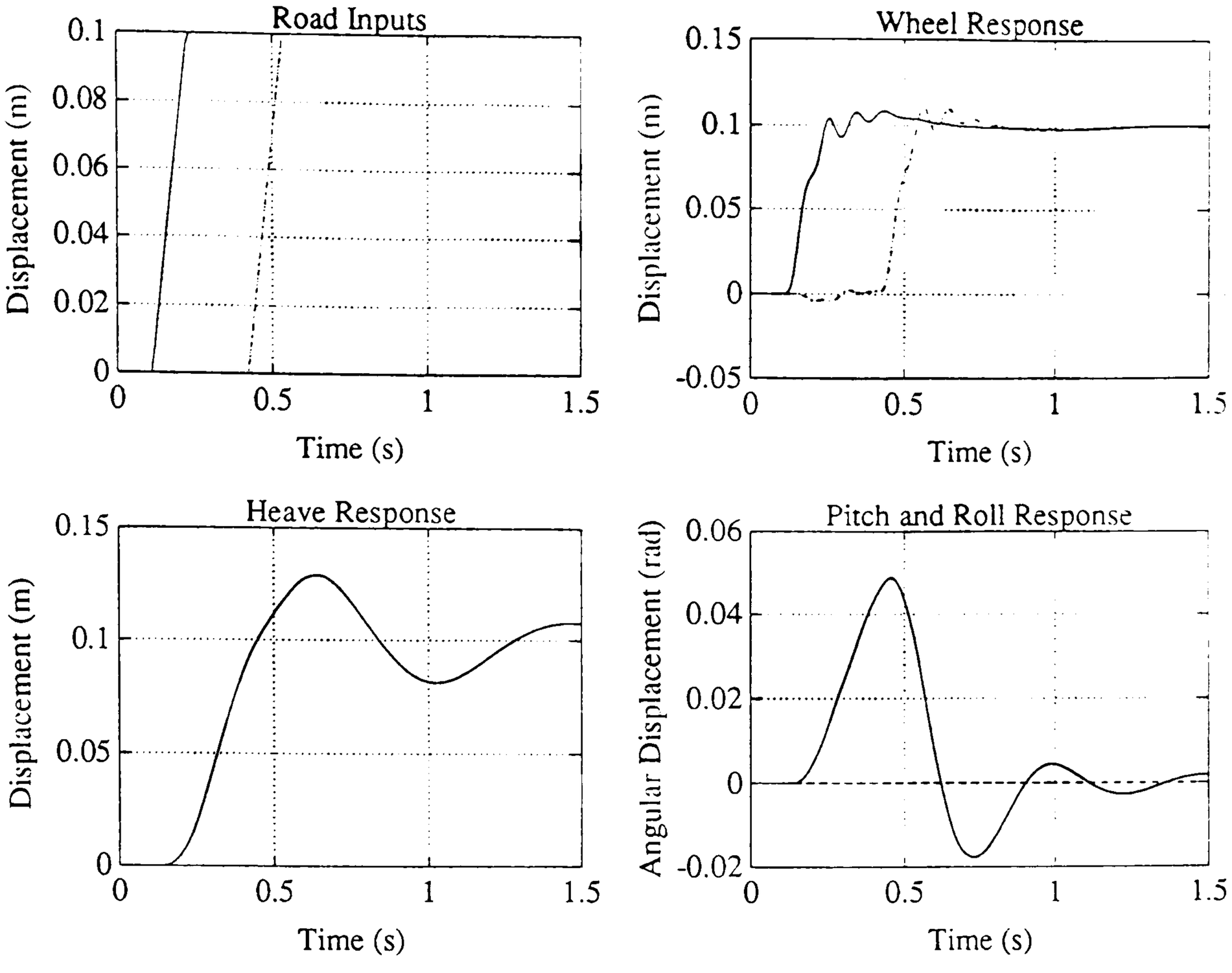


Figure 5.8a : Road Step Input

Figure 5.8 : Soft and Firm Damping Results

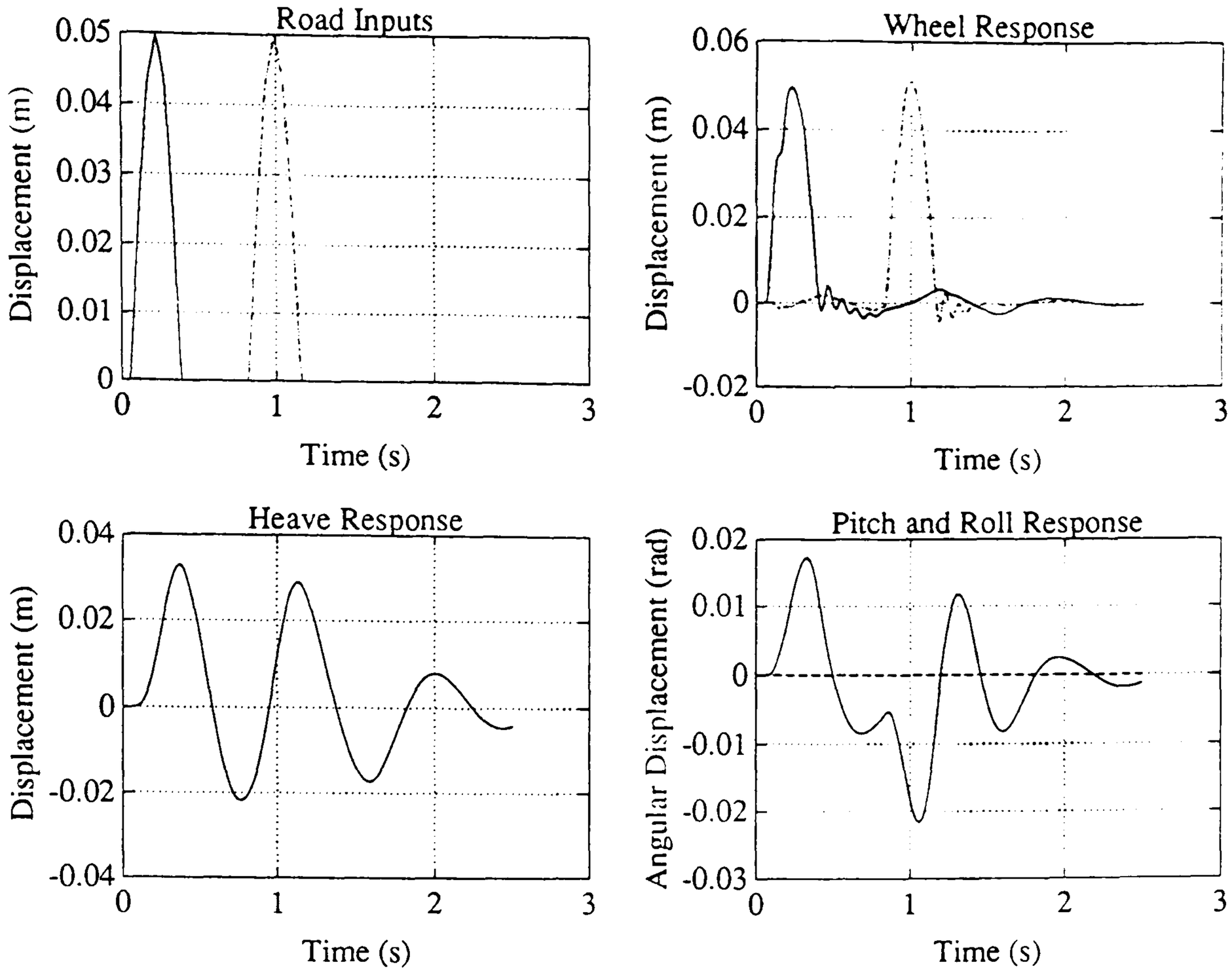


Figure 5.8b : Primary Ride Road Bump Input

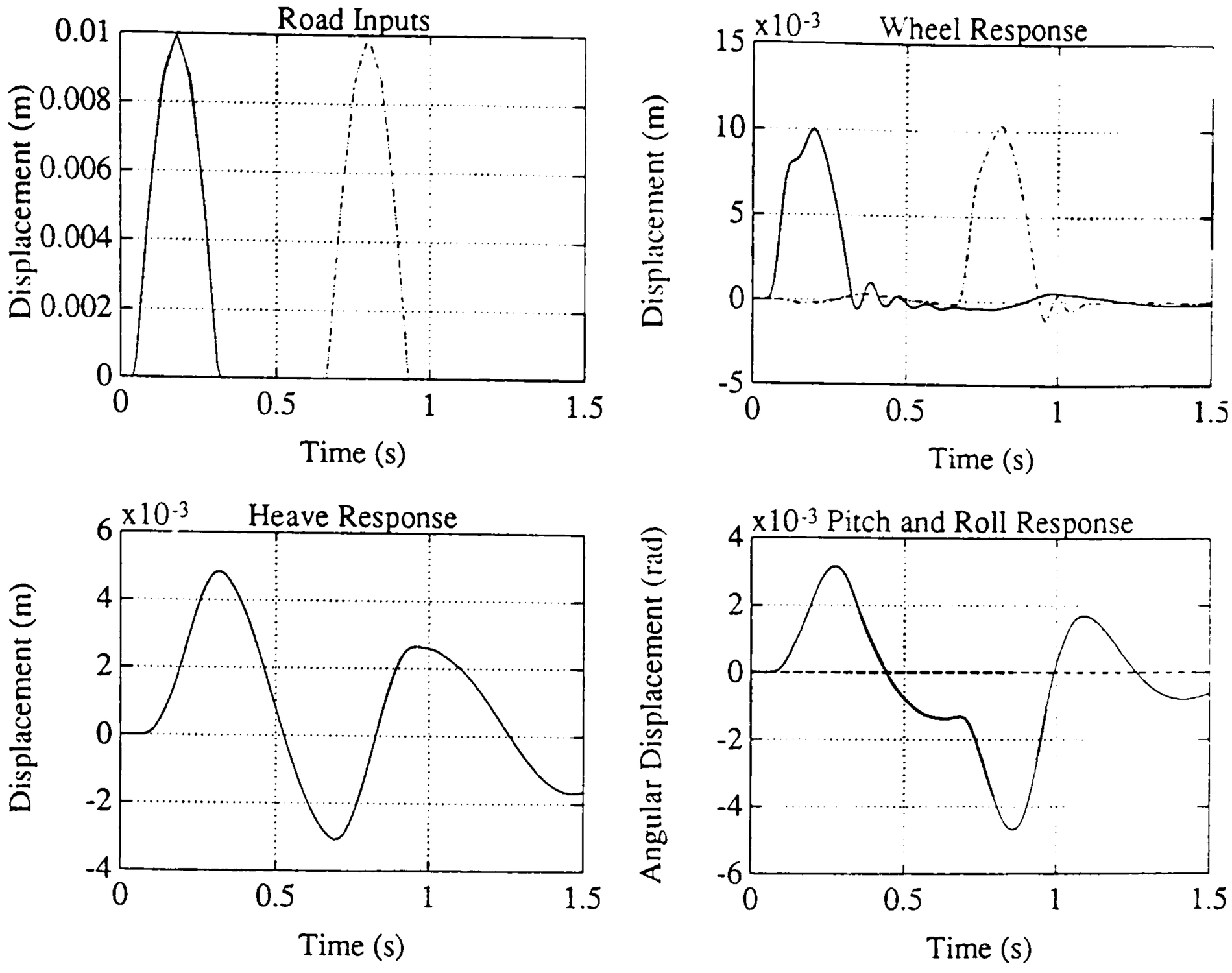


Figure 5.8c : Road Bump Input to Both Tracks

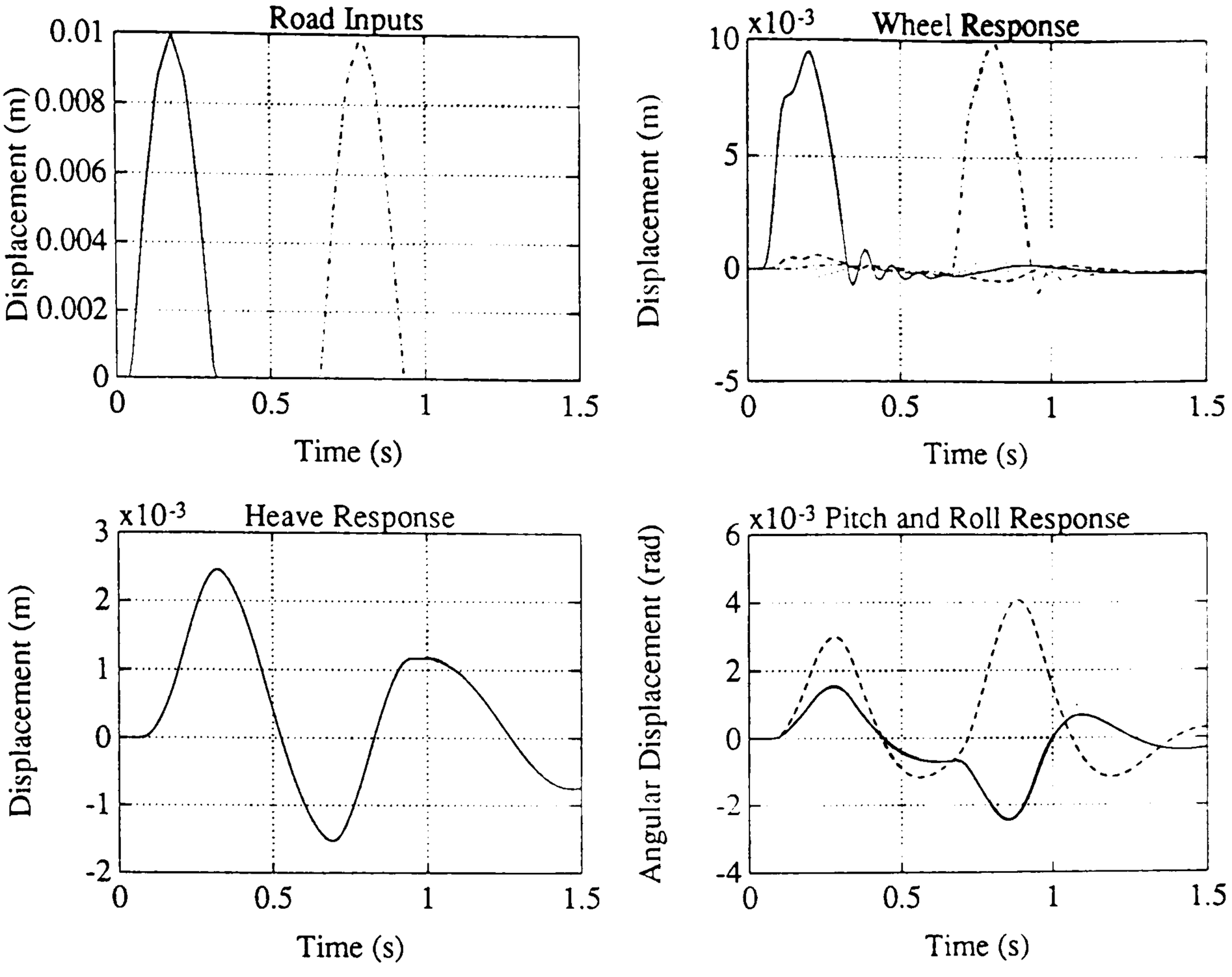


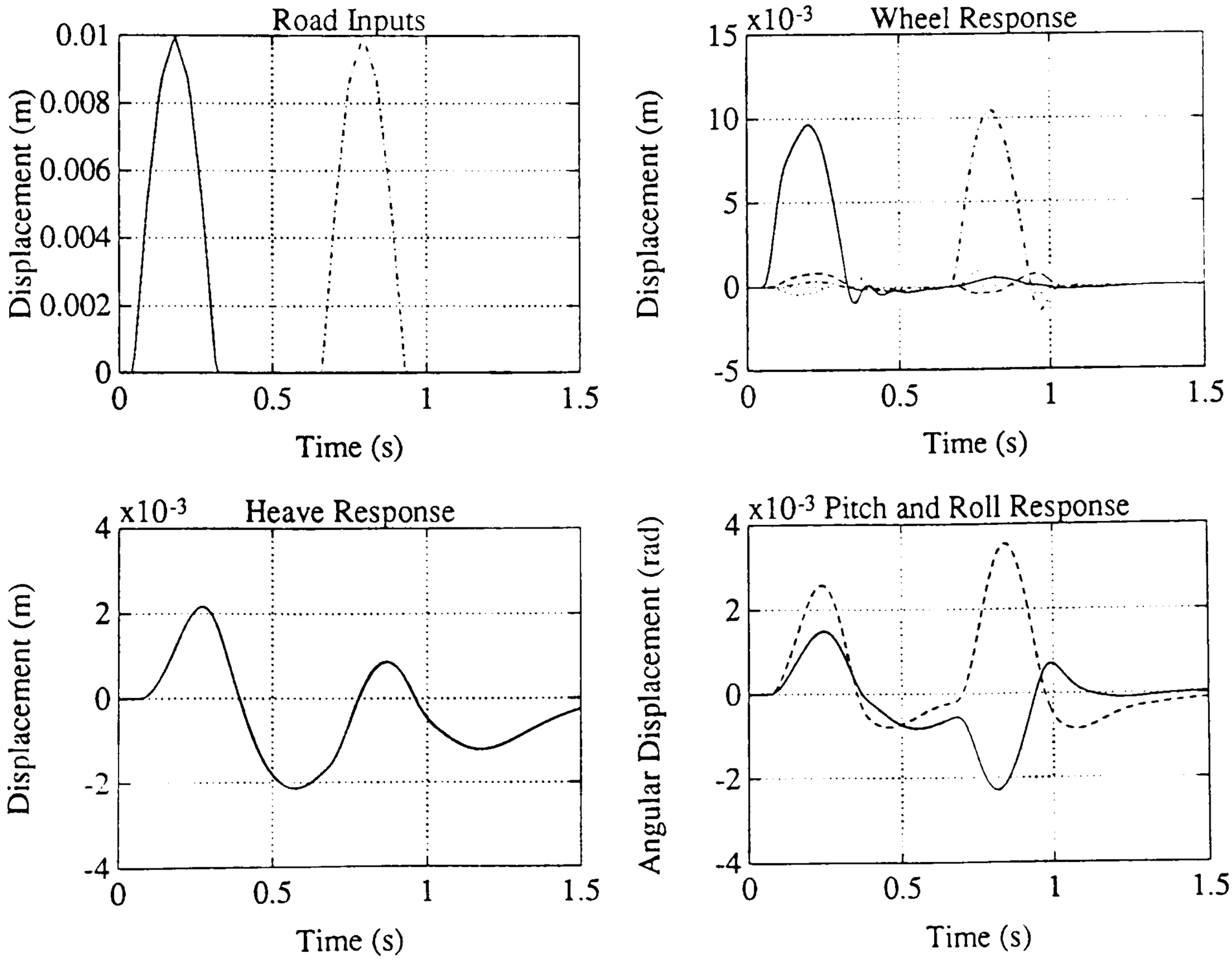


Figure 5.8d : Road Bump Input to One Track Only

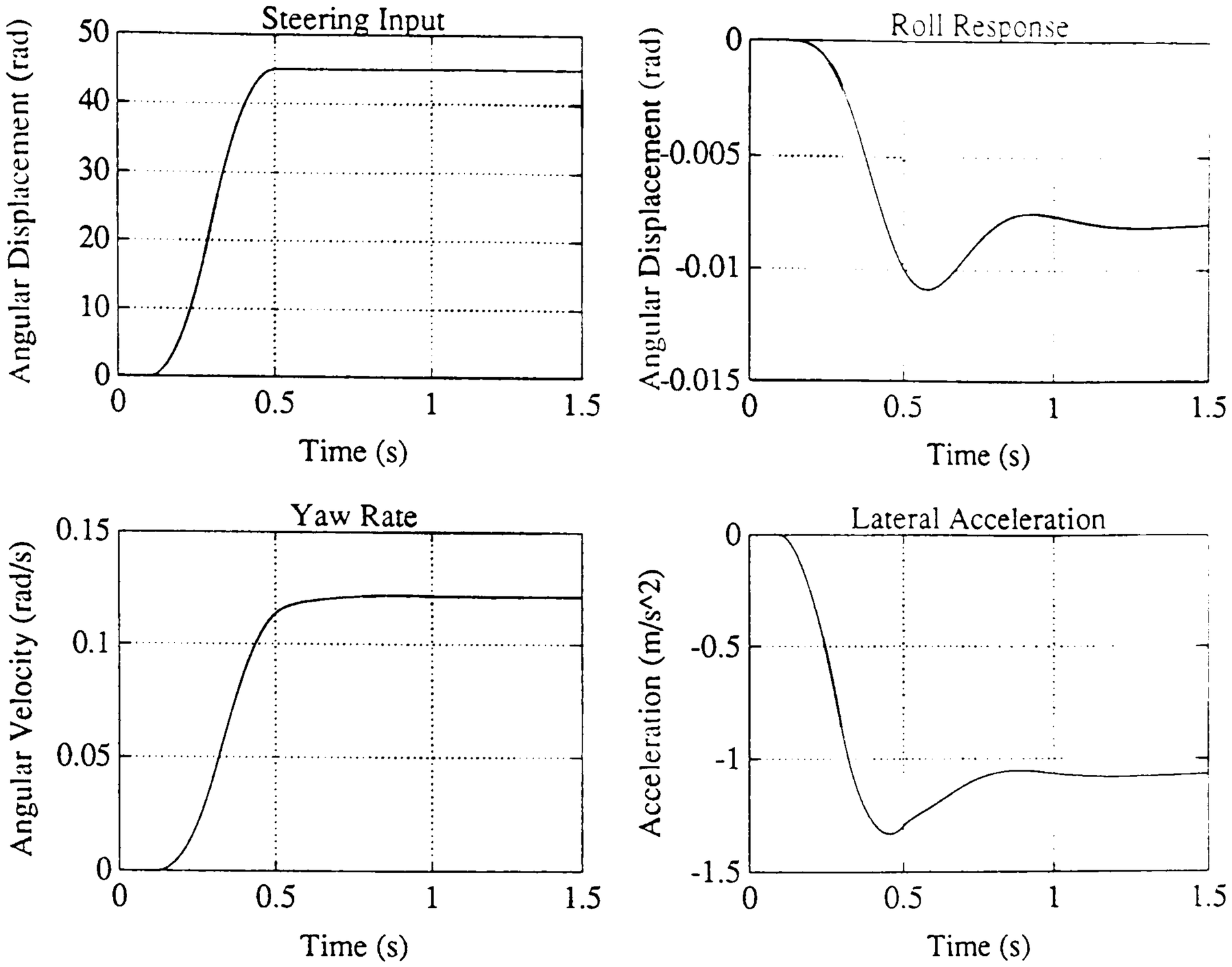





Figure 5.8e : Steering Input at 20 mph

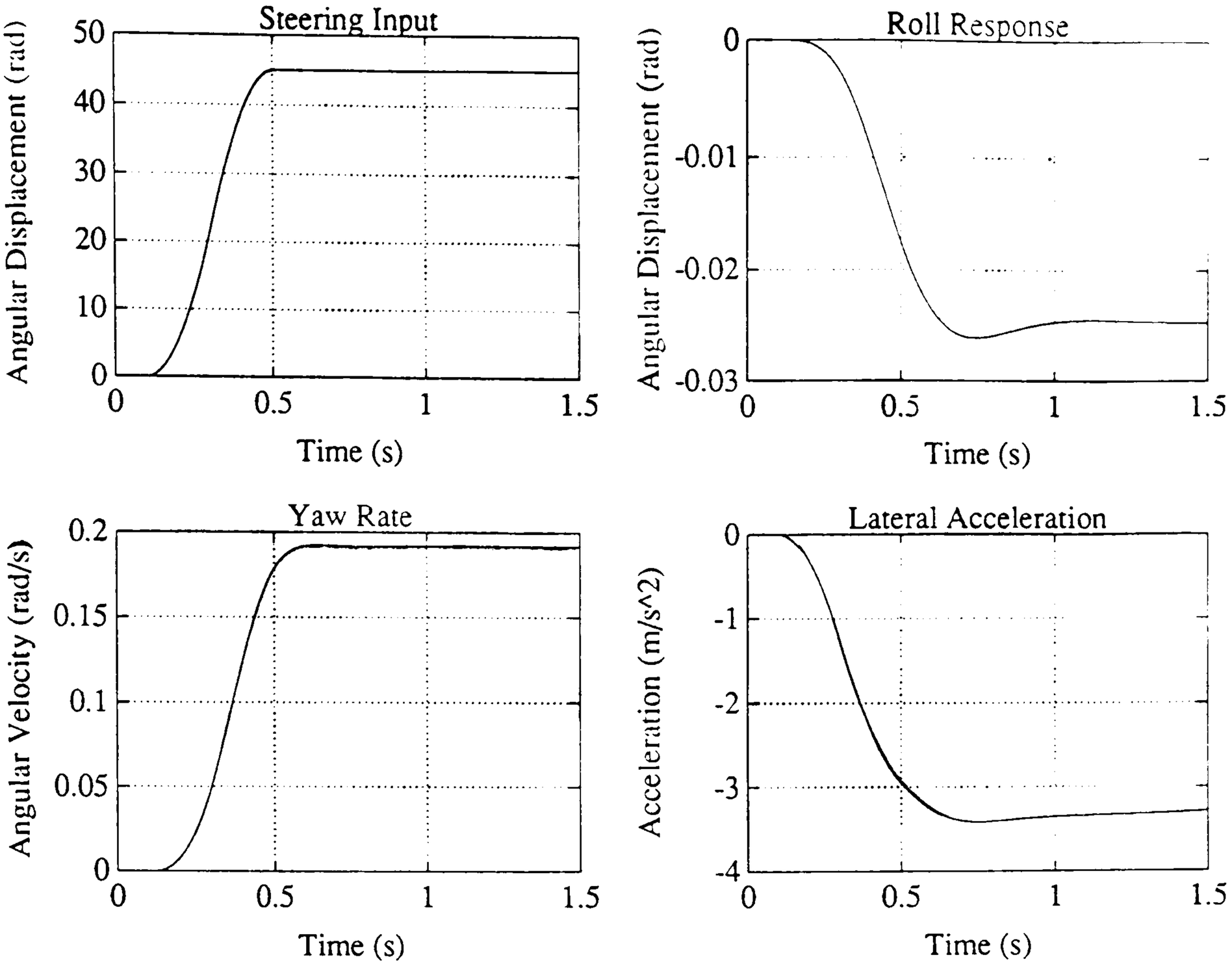


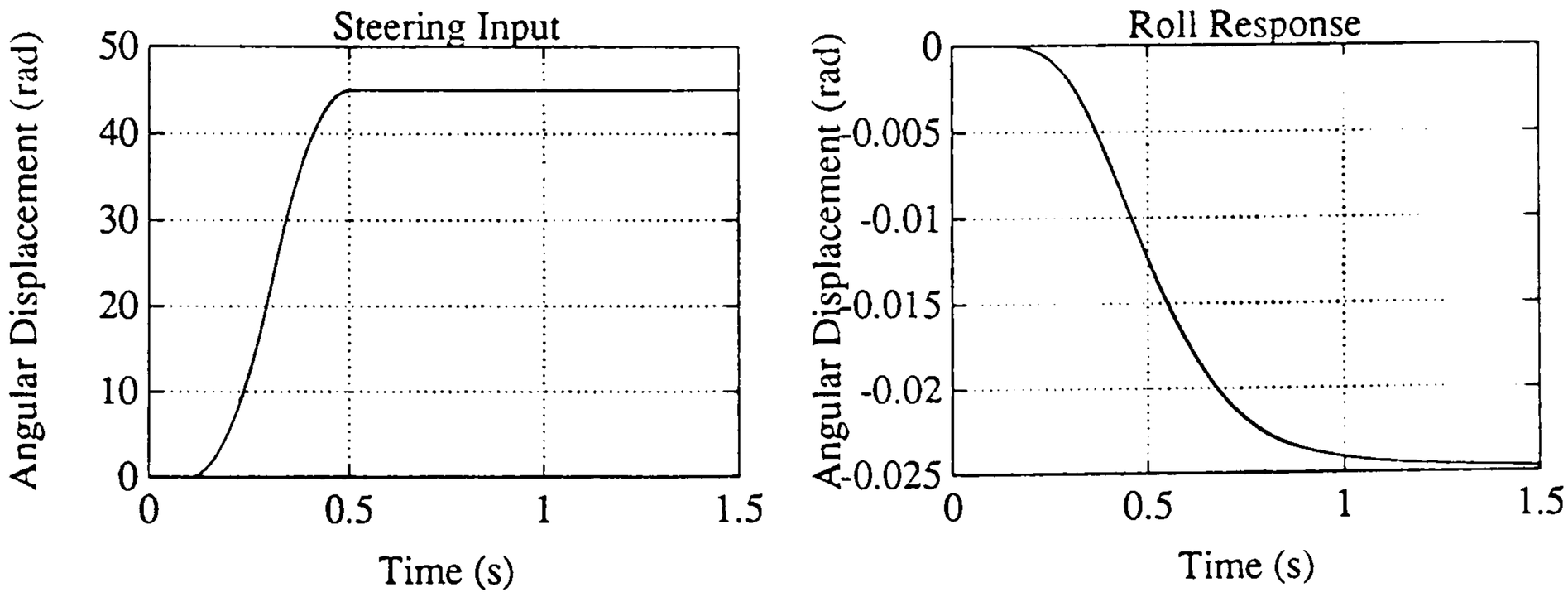


Figure 5.8f : Steering Inupt at 40 mph

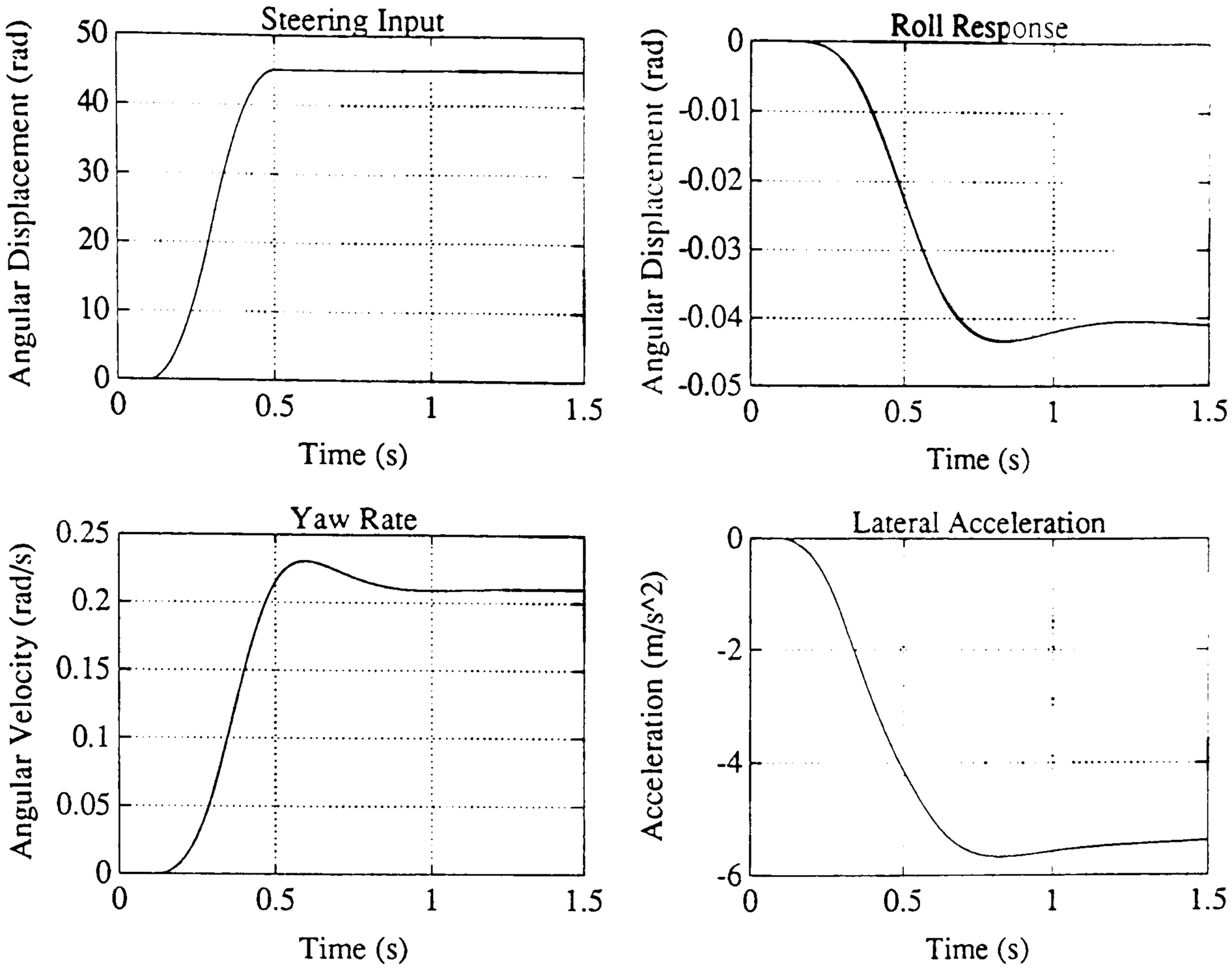


Steering Input
Angular Displacement (rad)
50
40
30
20
10
0
0
0.5
1
1.5
Time (s)
Roll Response
Angular Displacement (rad)
0
-0.01
-0.02
-0.03
-0.04
-0.05
0
0.5
1
1.5
Time (s)
Yaw Rate
Angular Velocity (rad/s)
0.25
0.2
0.15
0.1
0.05
0
0
0.5
1
1.5
Time (s)
Lateral Acceleration
Acceleration (m/s^2)
0
-2
-4
-6
0
0.5
1
1.5
Time (s)

Figure 5.8g : Steering Input at 60 mph

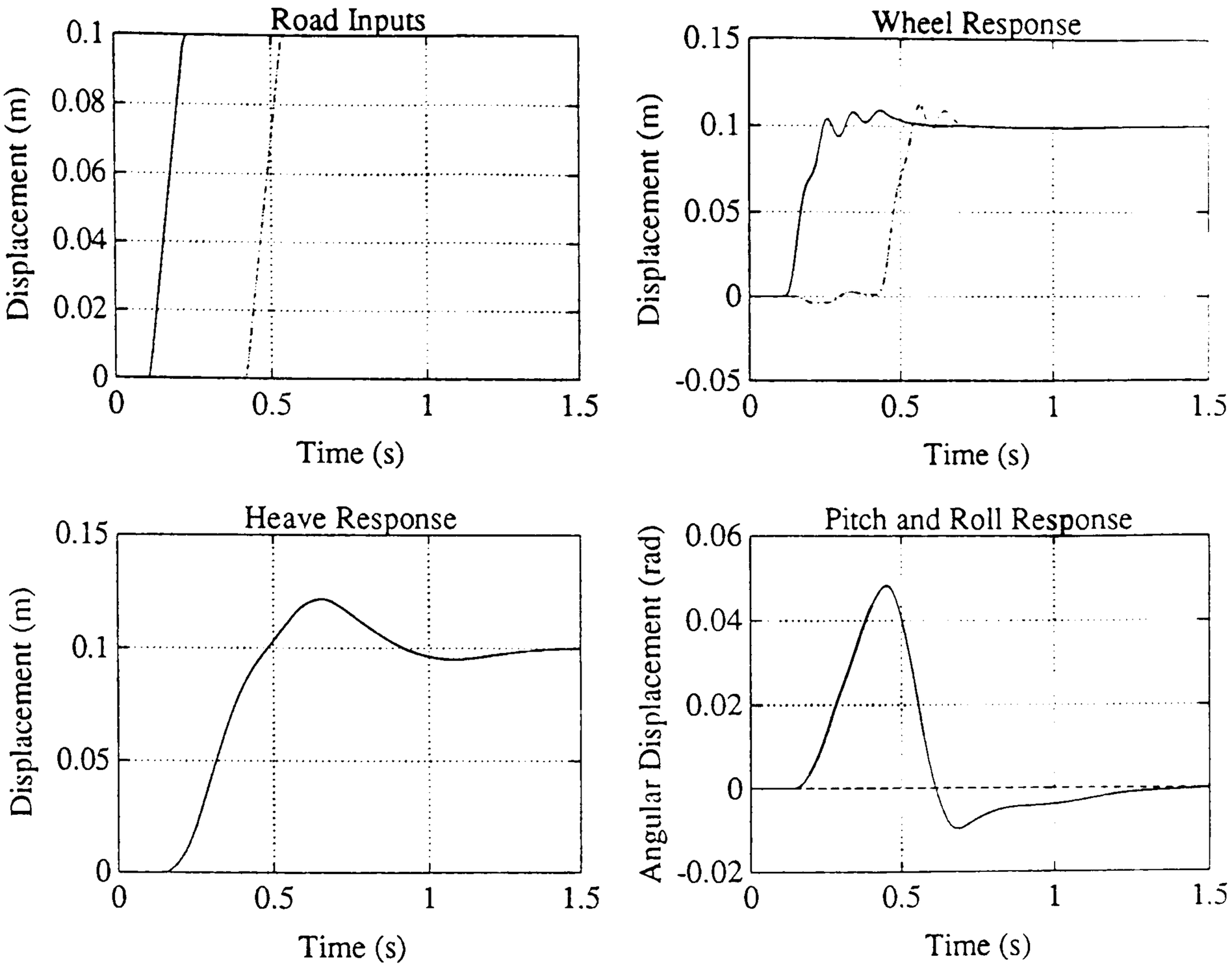


Figure 5.9a : Road Step Input

Figure 5.9 : Skyhook Damping Strategy Results

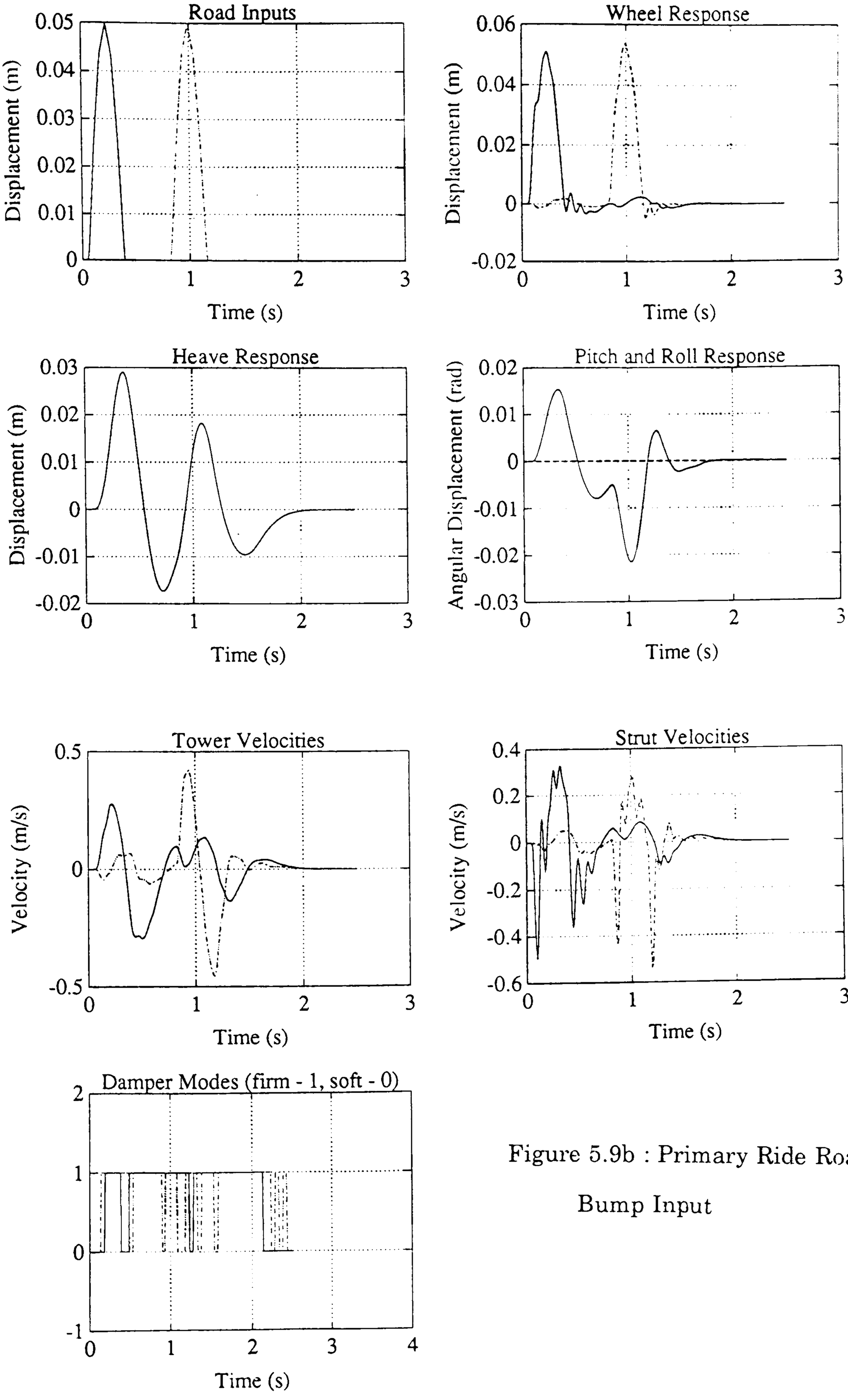


Figure 5.9b : Primary Ride Road Bump Input

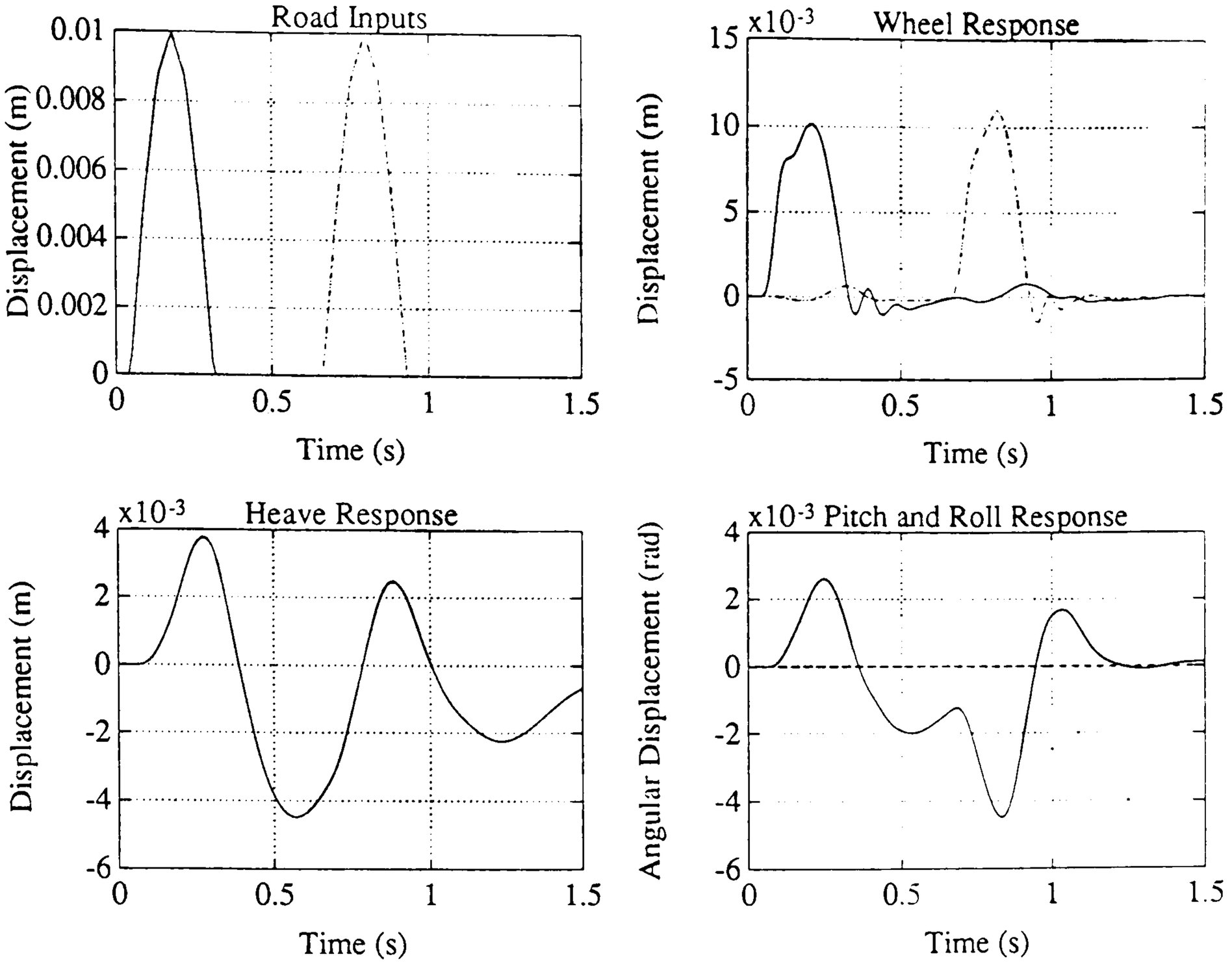


Figure 5.9c : Road Bump Input

to Both Tracks

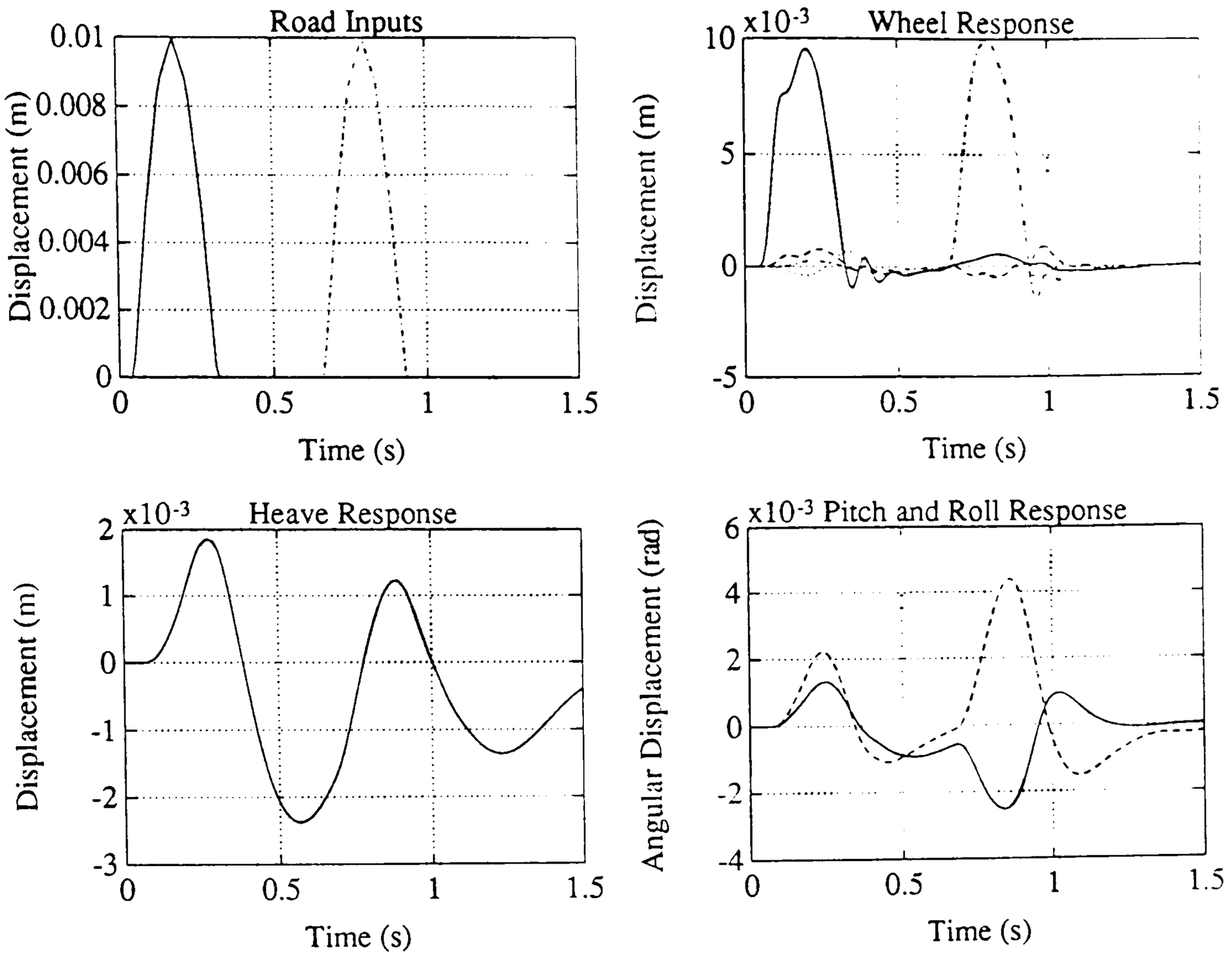


Figure 5.9d : Road Bump Input to One Track Only

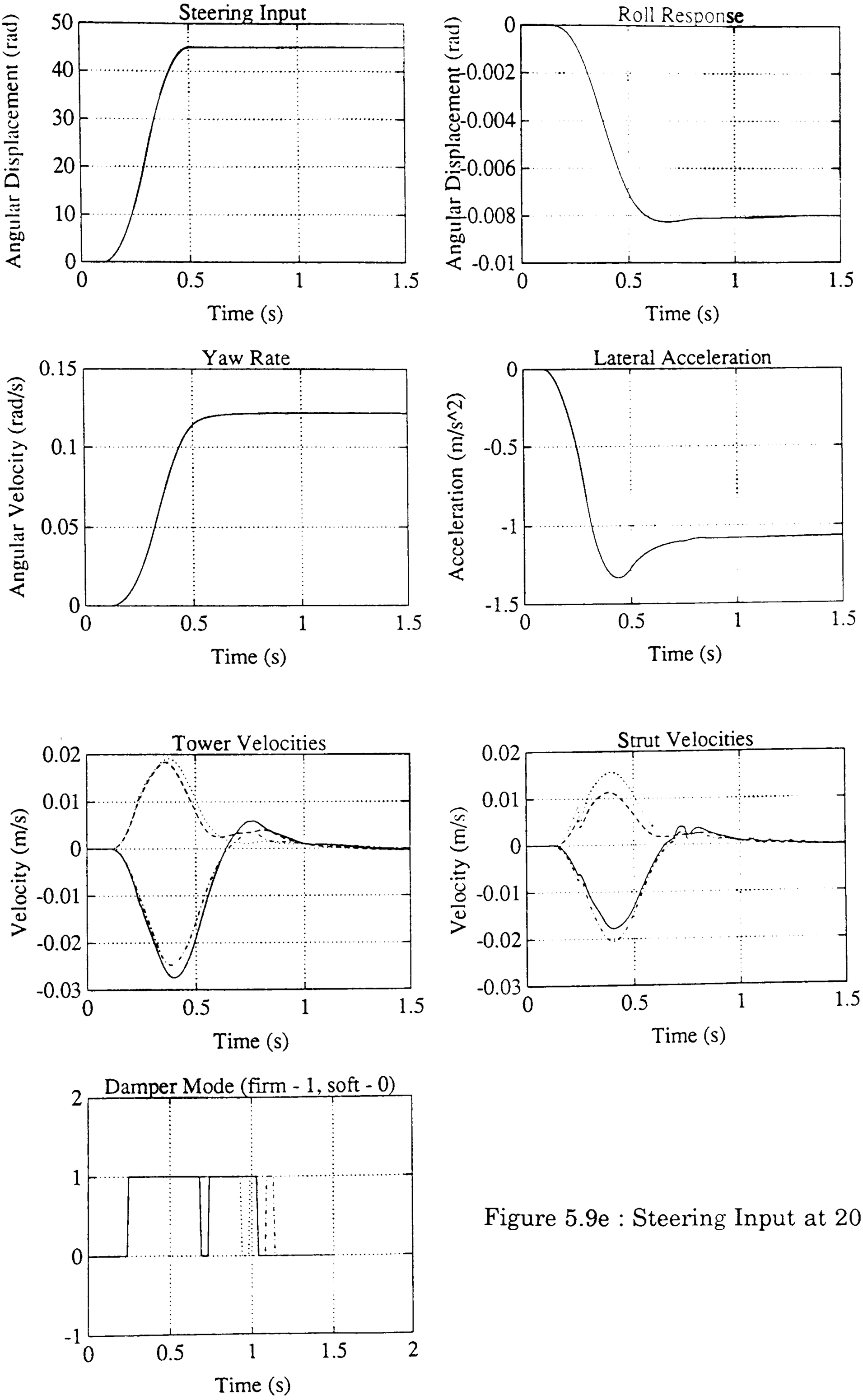


Figure 5.9e : Steering Input at 20 mph

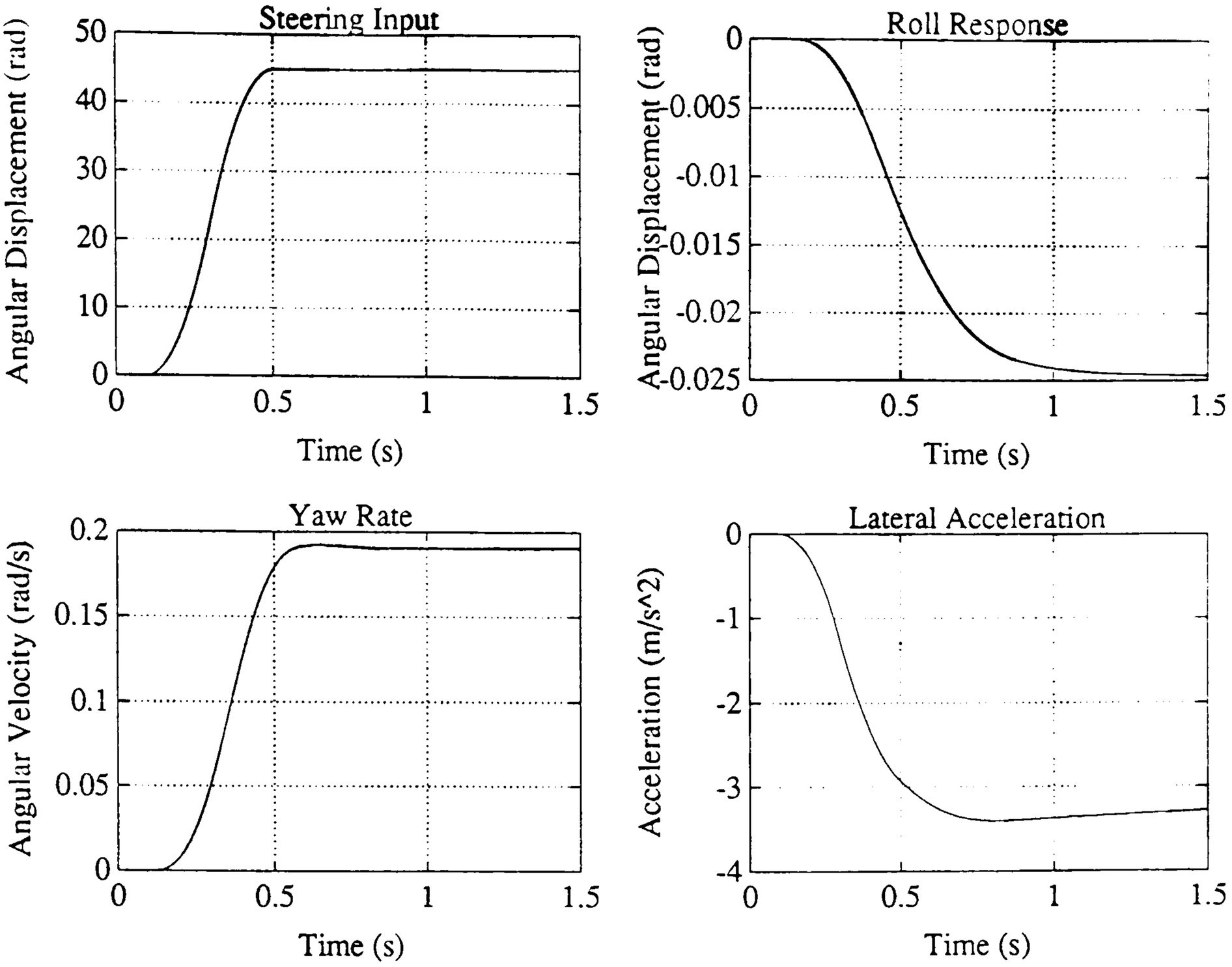


Figure 5.9f : Steering Input at 40 mph

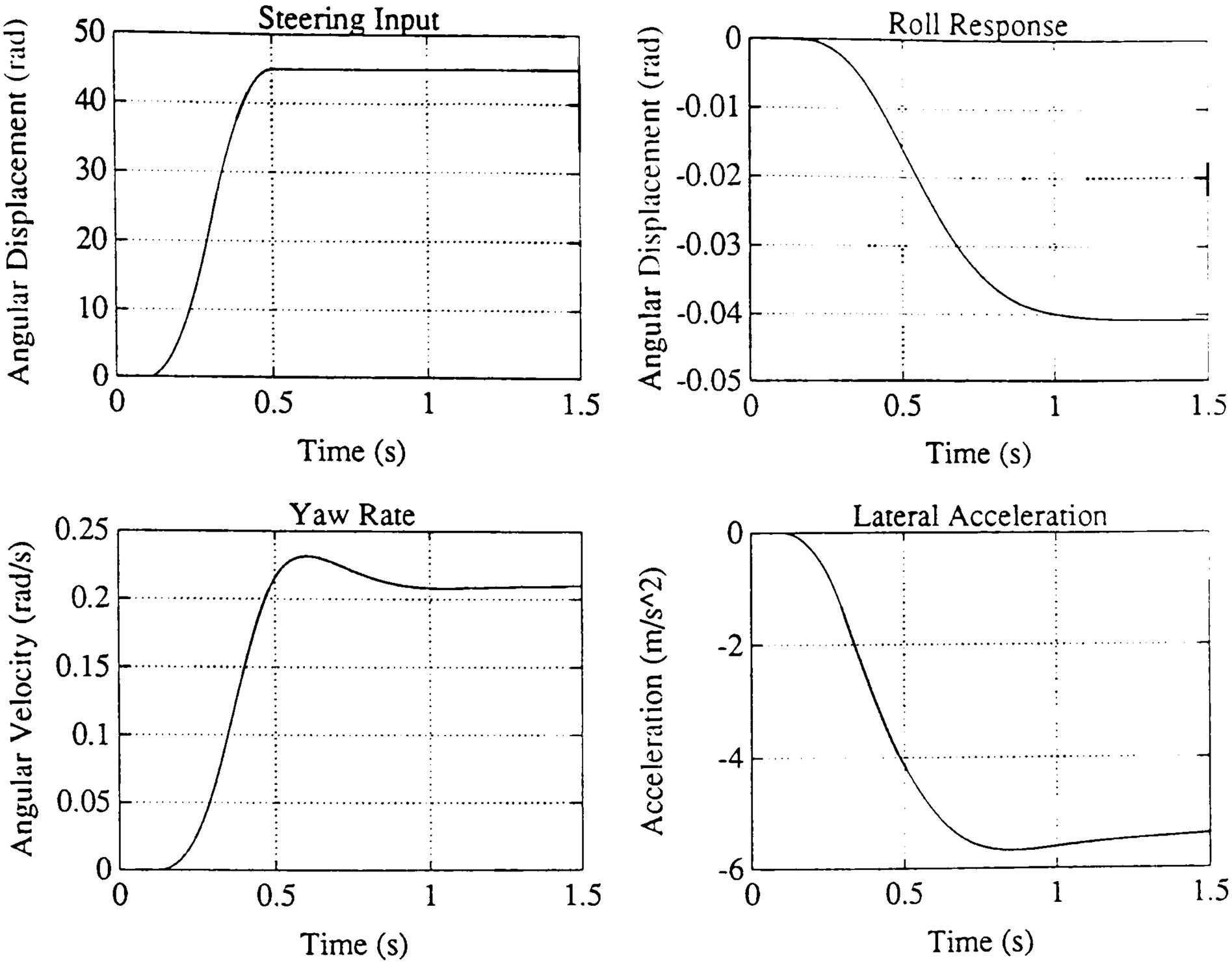


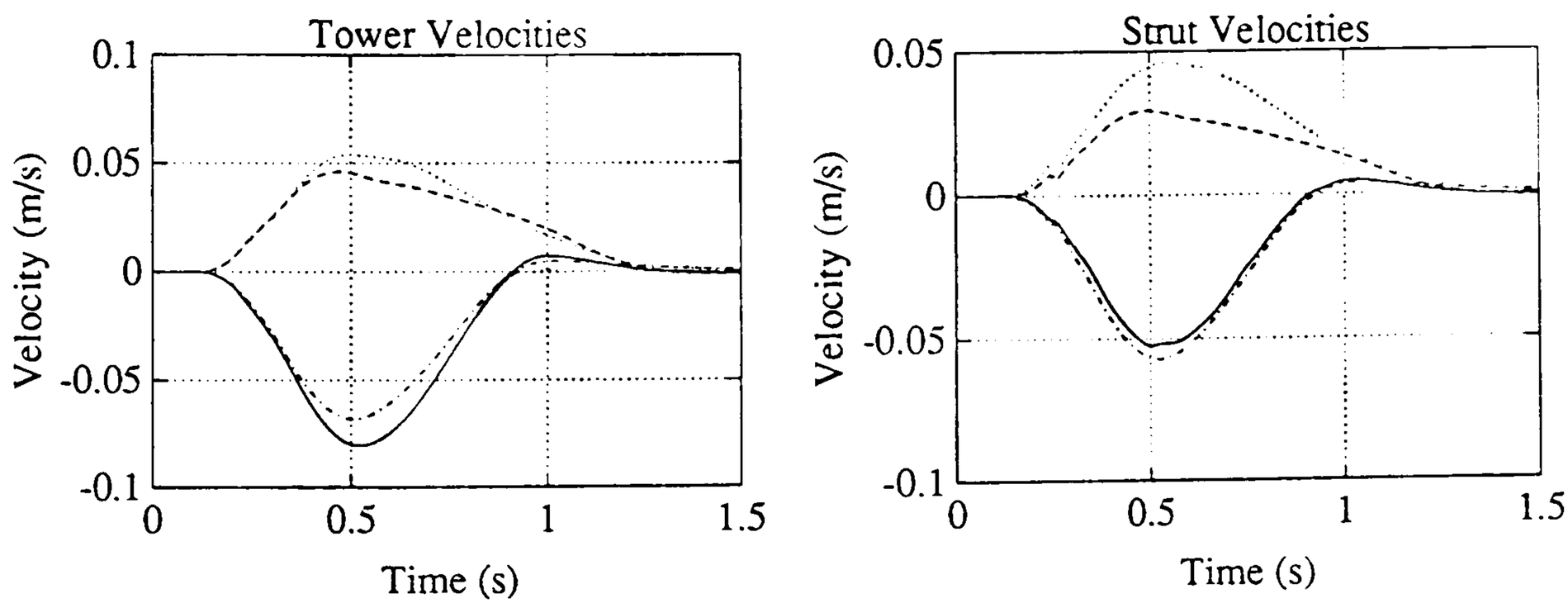


Figure 5.9g : Steering Input at 60 mph

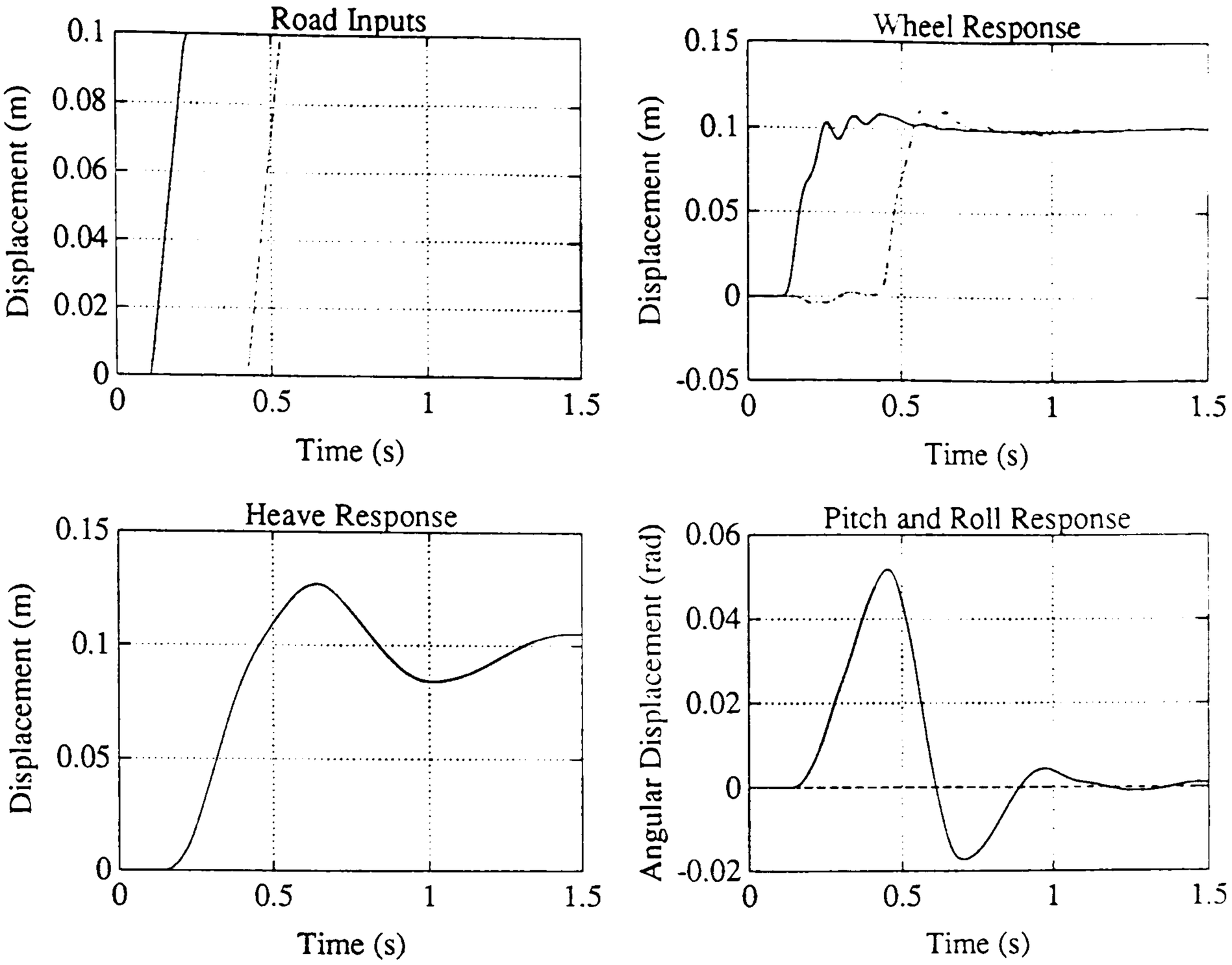


Figure 5.10a : Road Step Input

Figure 5.10 : Minimum Acceleration Strategy Results

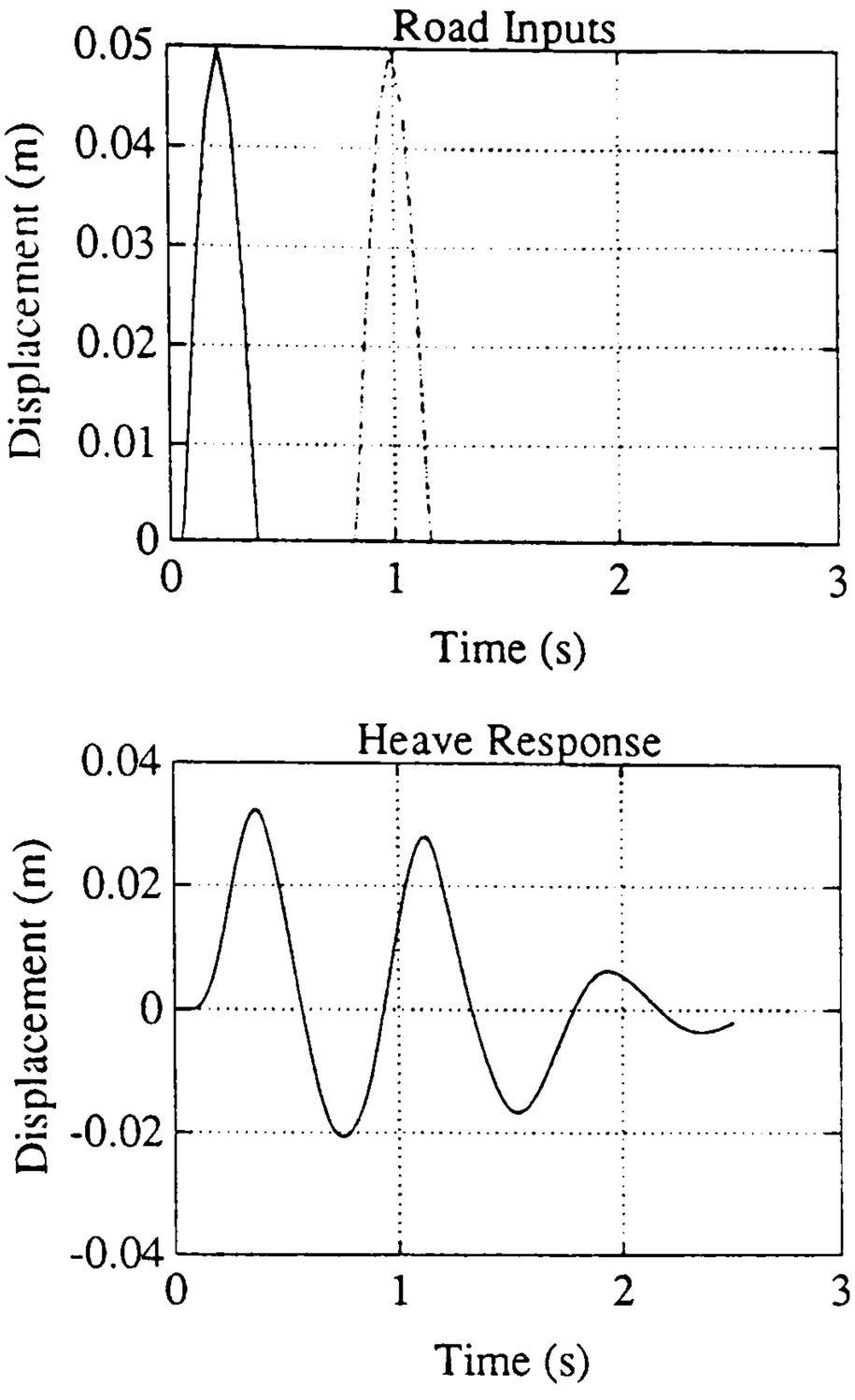


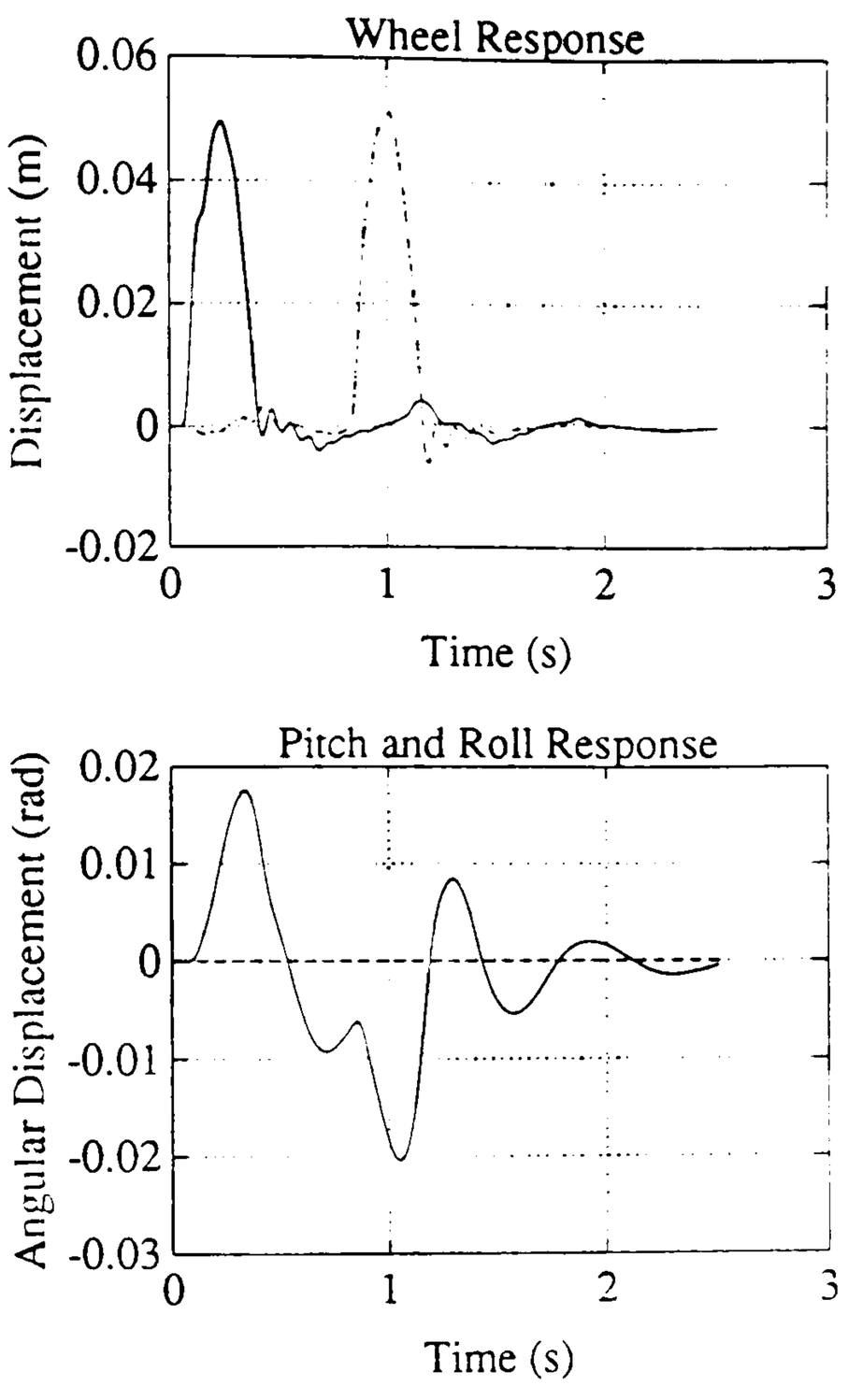


Figure 5.10b : Primary Ride Road Bump Input

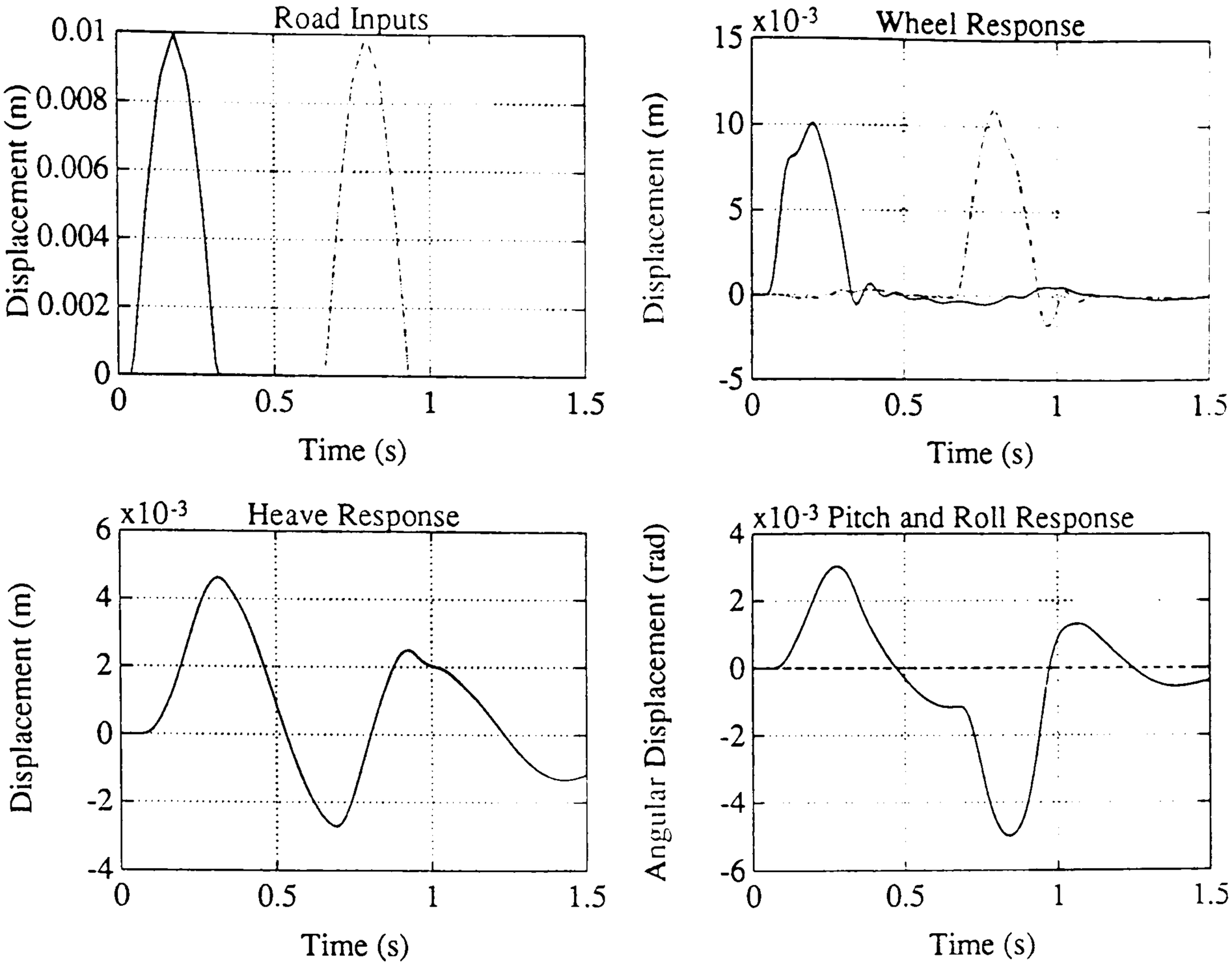


Figure 5.10c : Road Bump Input to Both Tracks

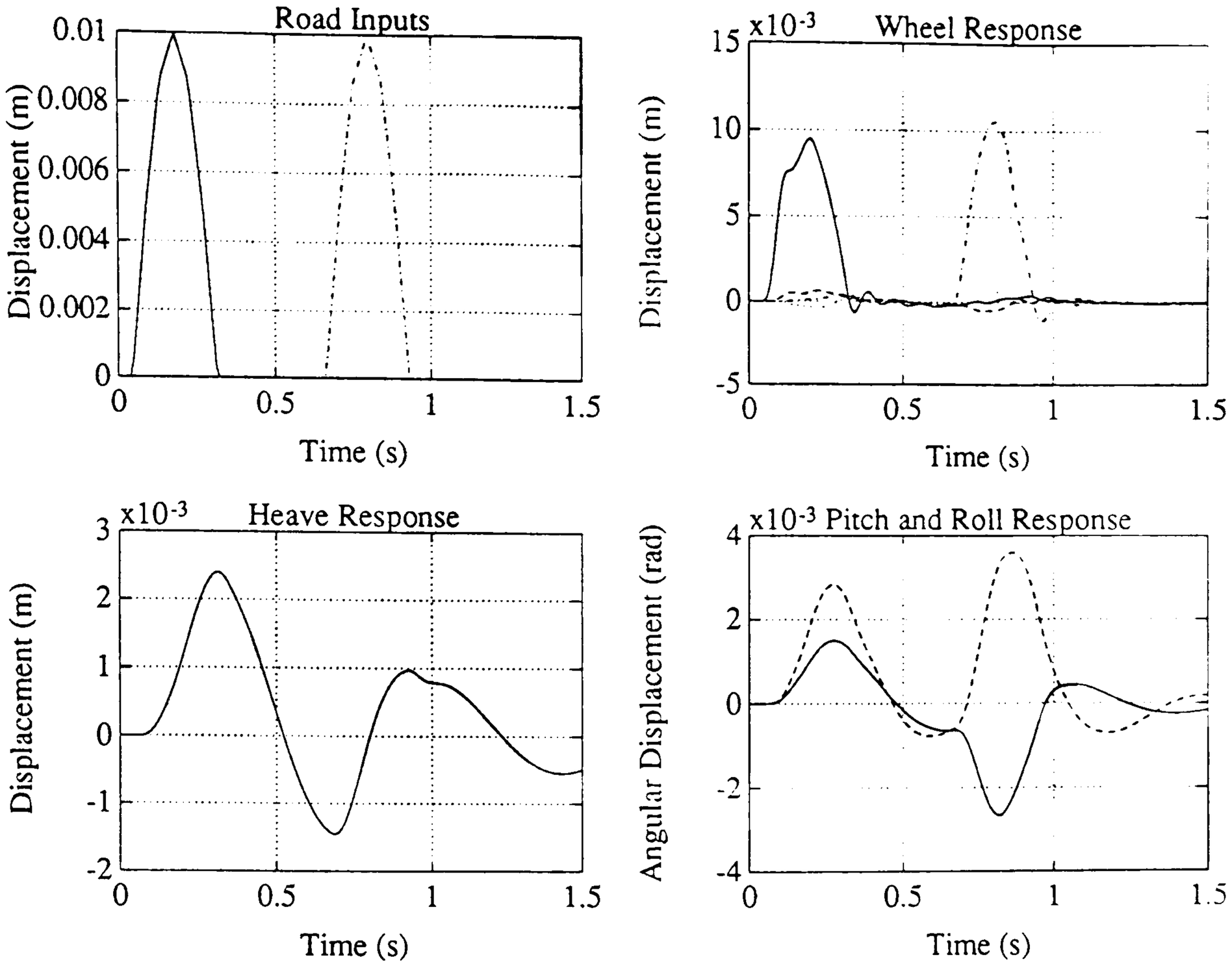


Figure 5.10d : Road Bump Input

to One Track Only

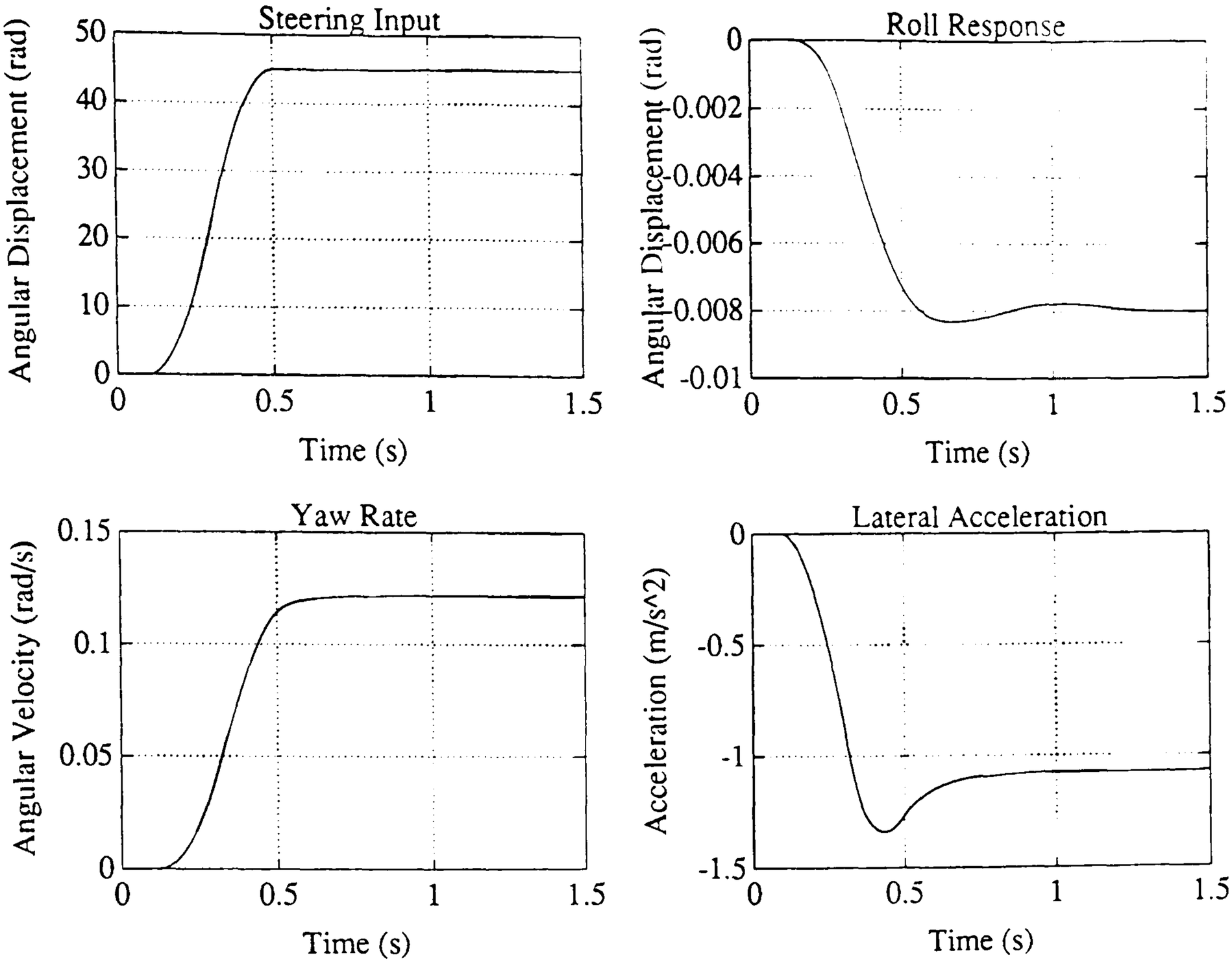


Figure 5.10e : Steering Input at 20 mph

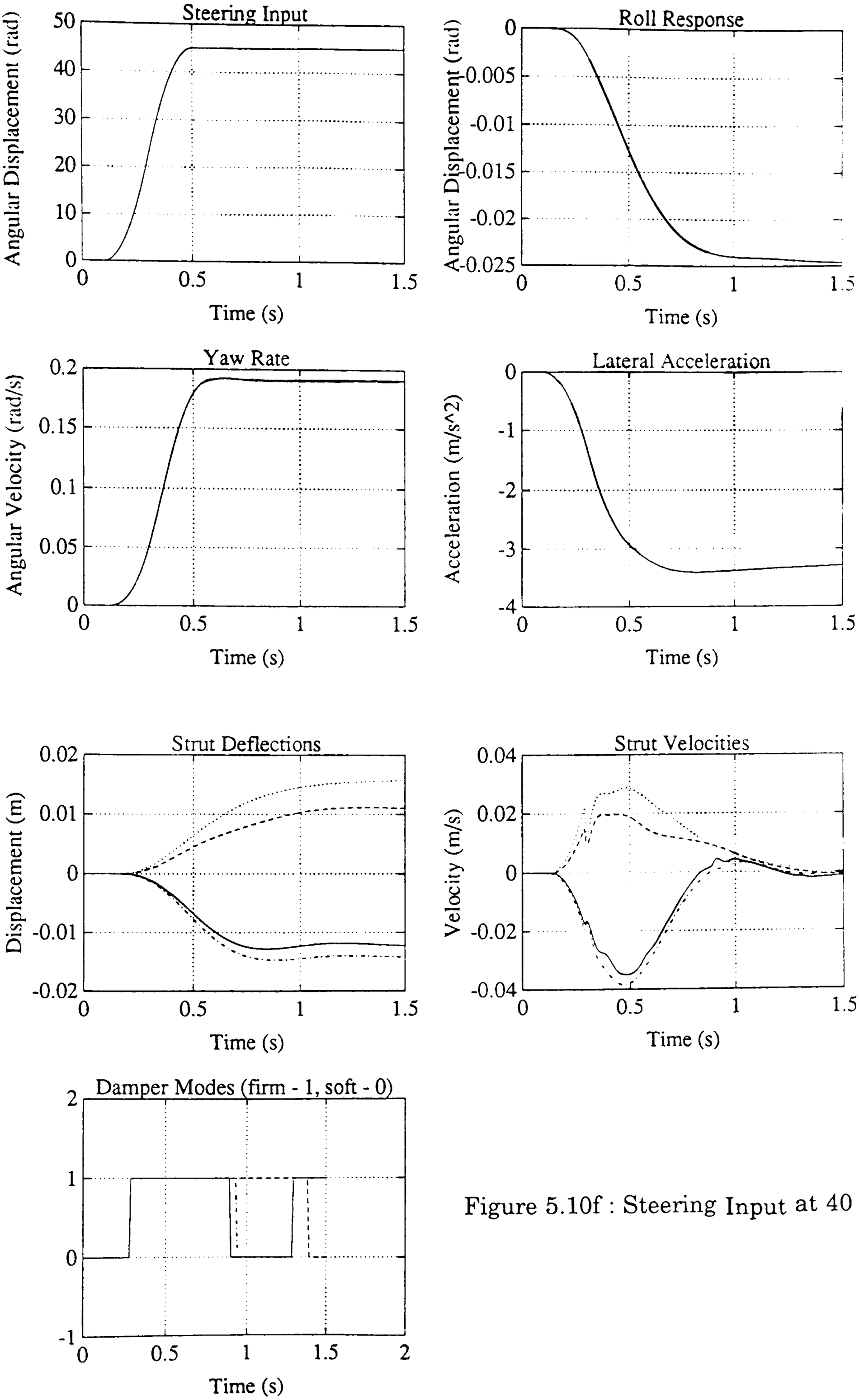


Figure 5.10f : Steering Input at 40 mph

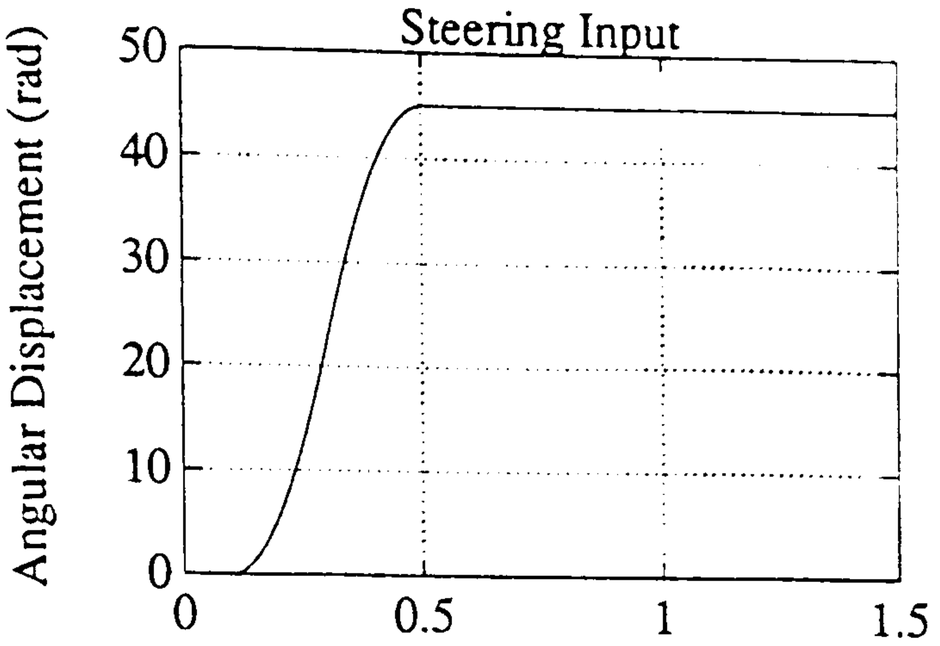


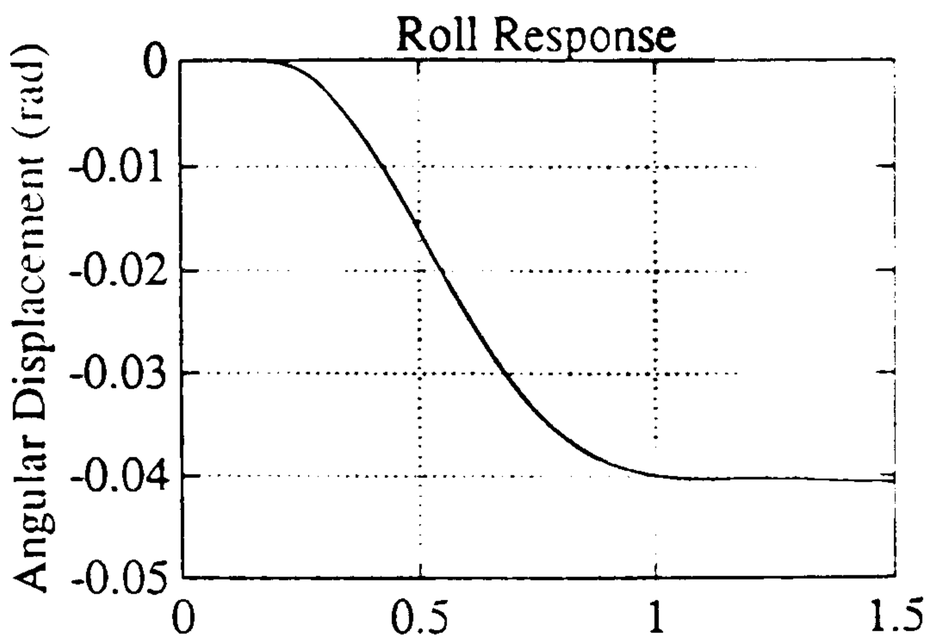


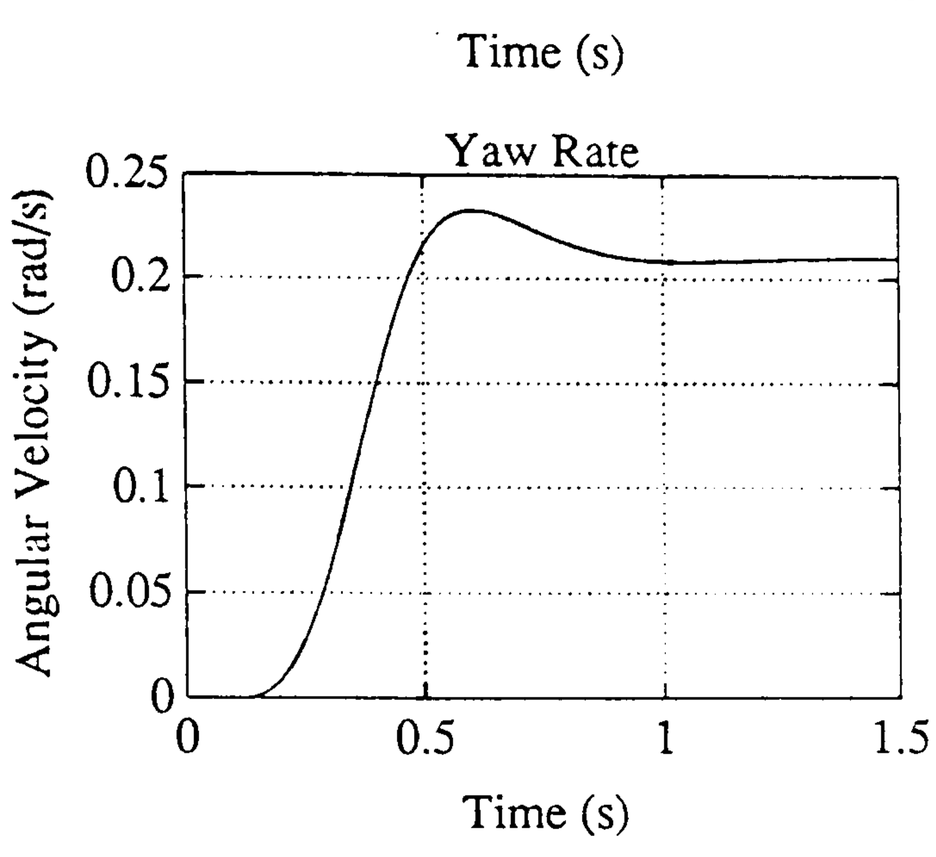


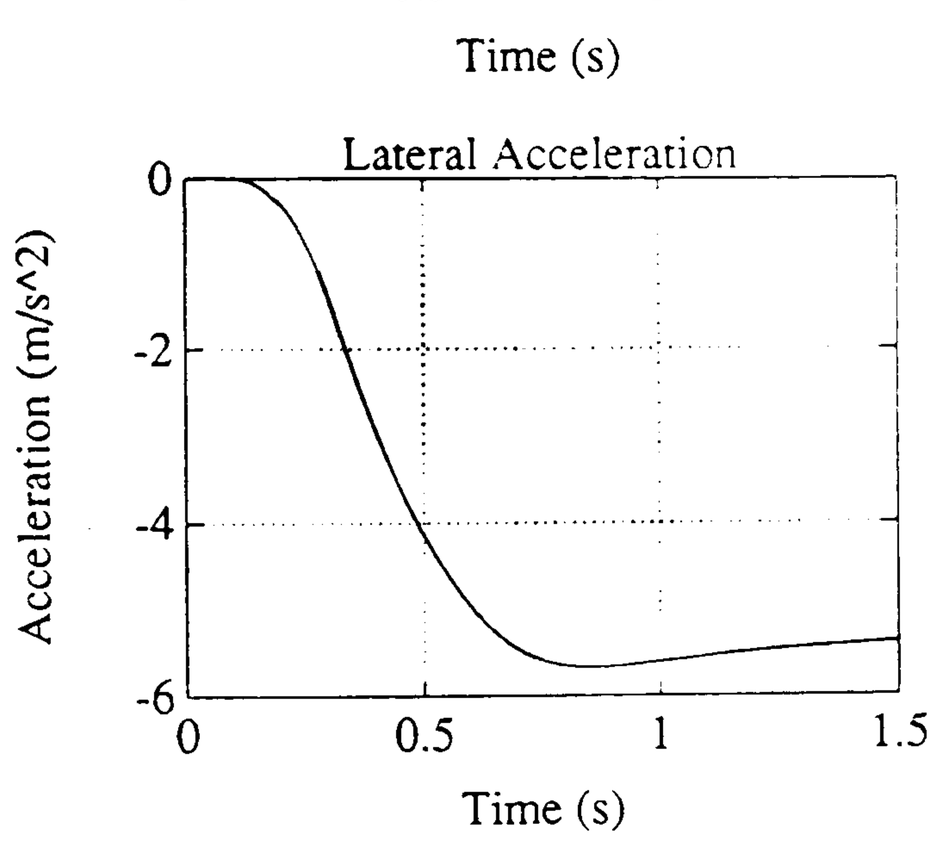


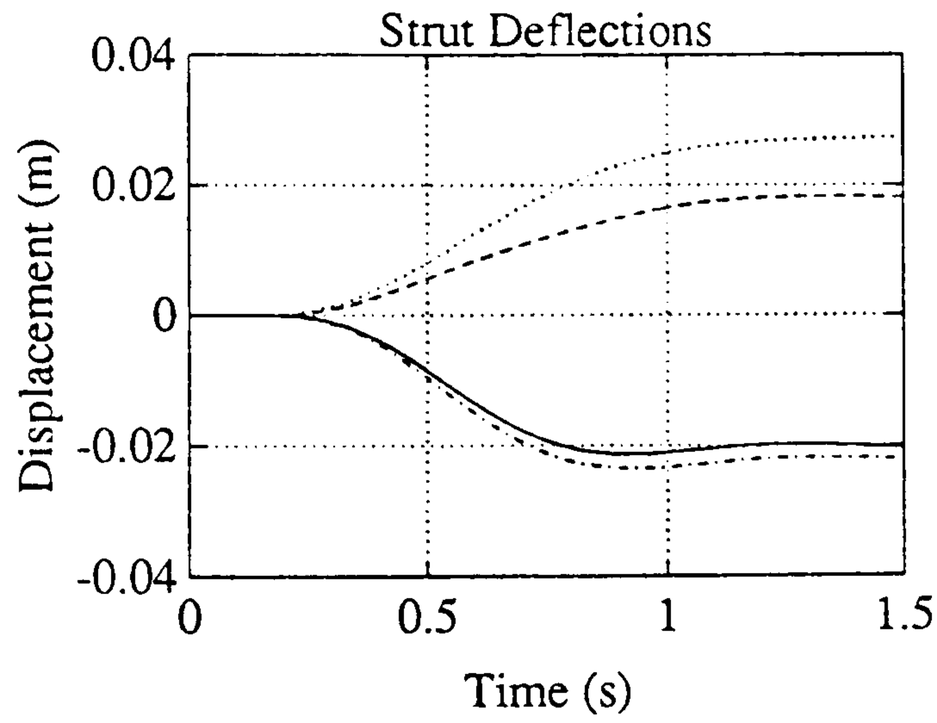


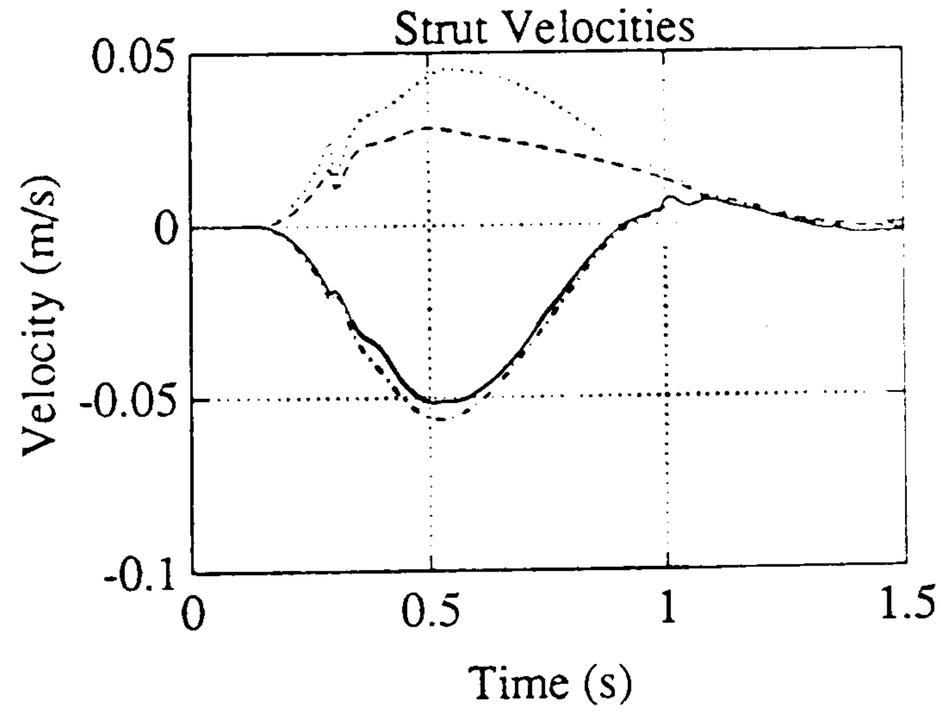


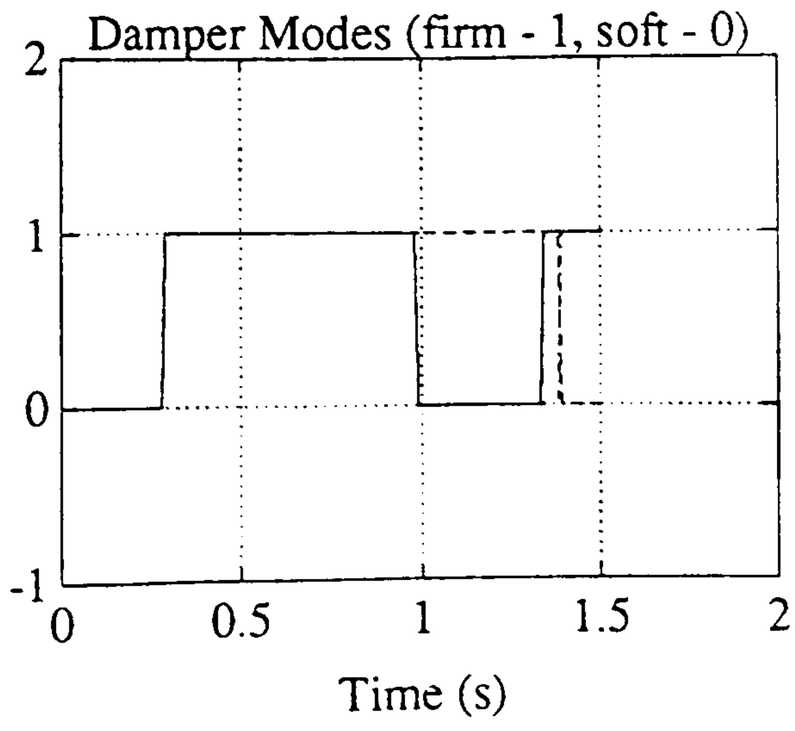


Figure 5.10g : Steering Input at 60 mph

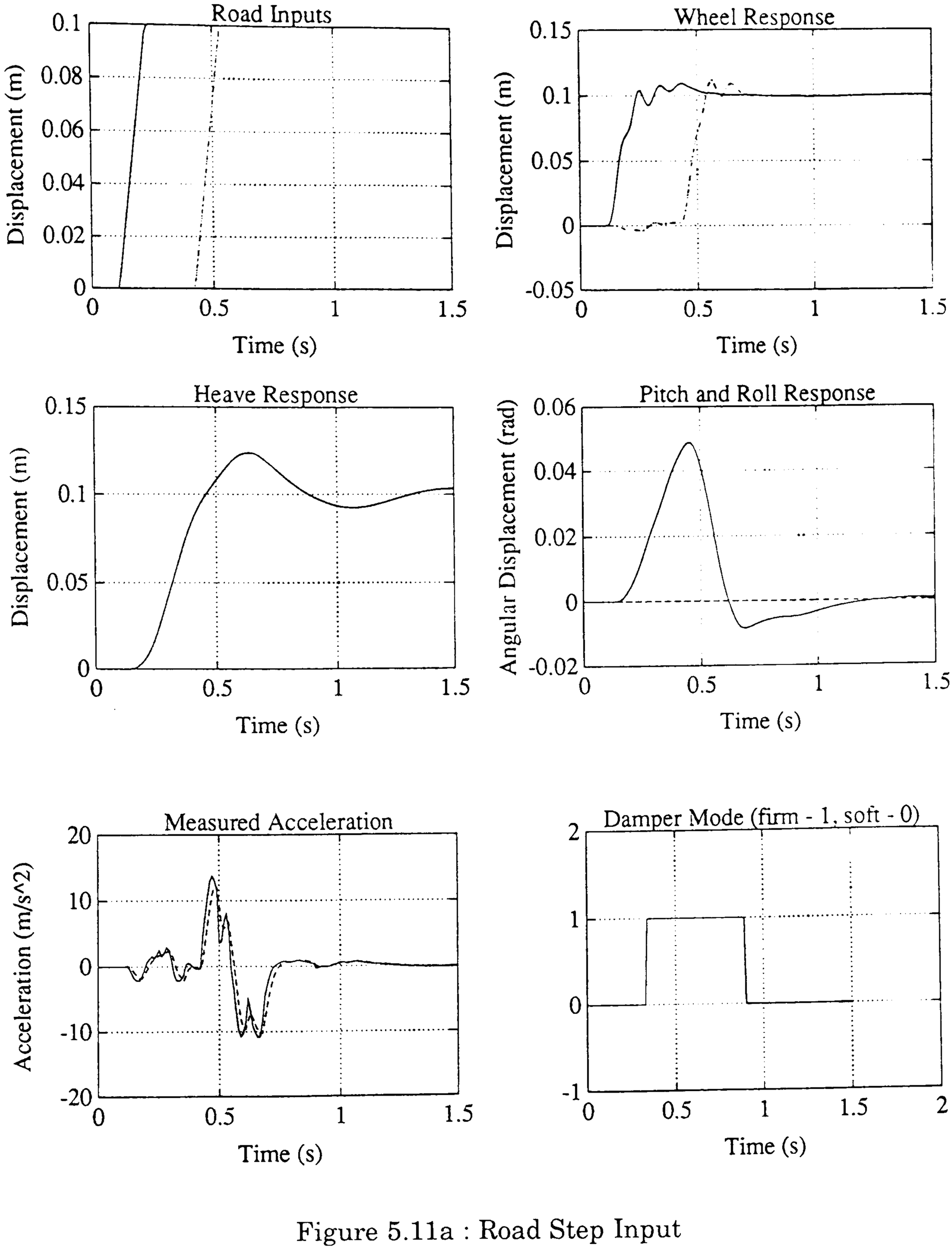


Figure 5.11a : Road Step Input

Figure 5.11 : Rule-Based Controller Results

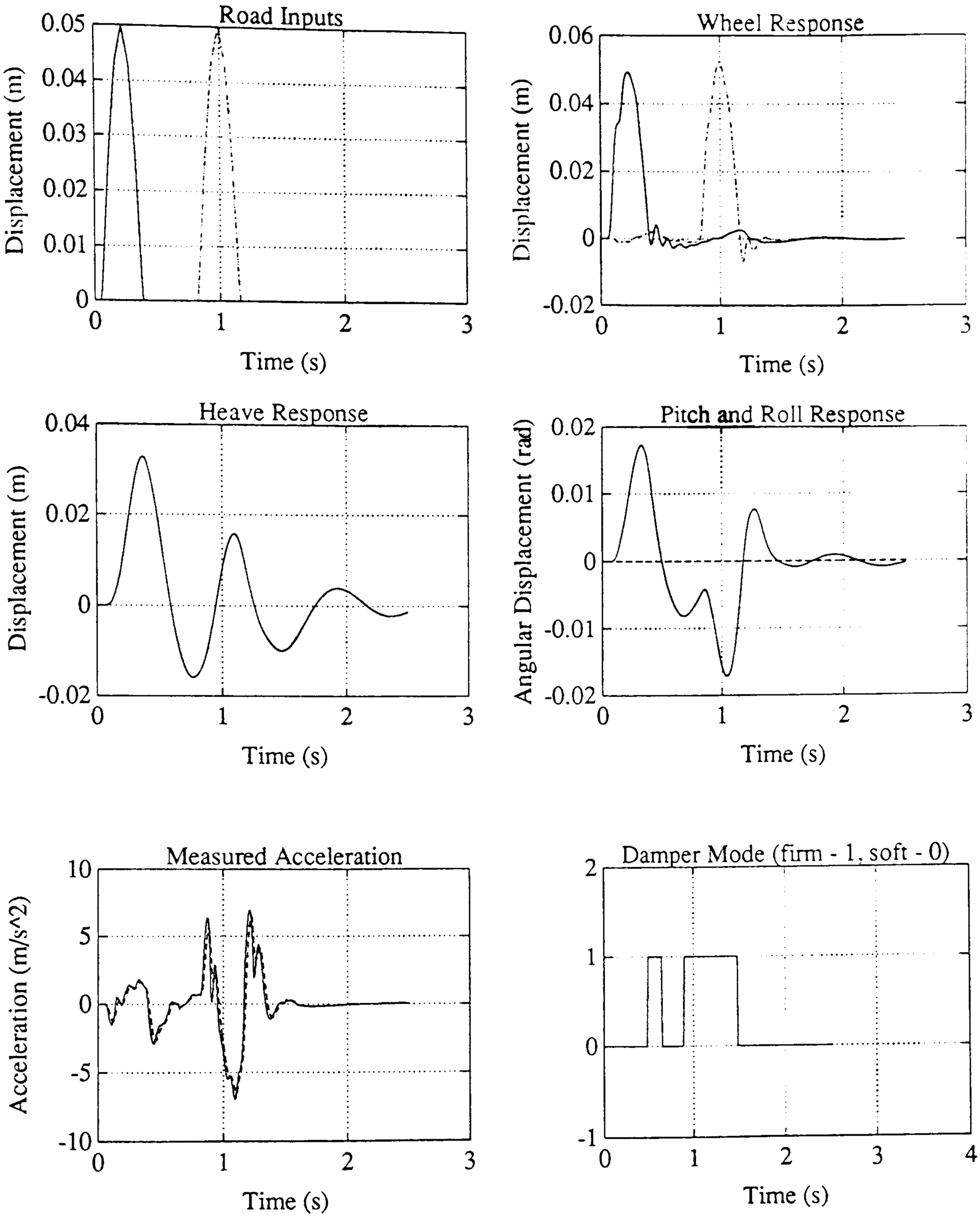


Figure 5.11b : Primary Ride Road Bump Input

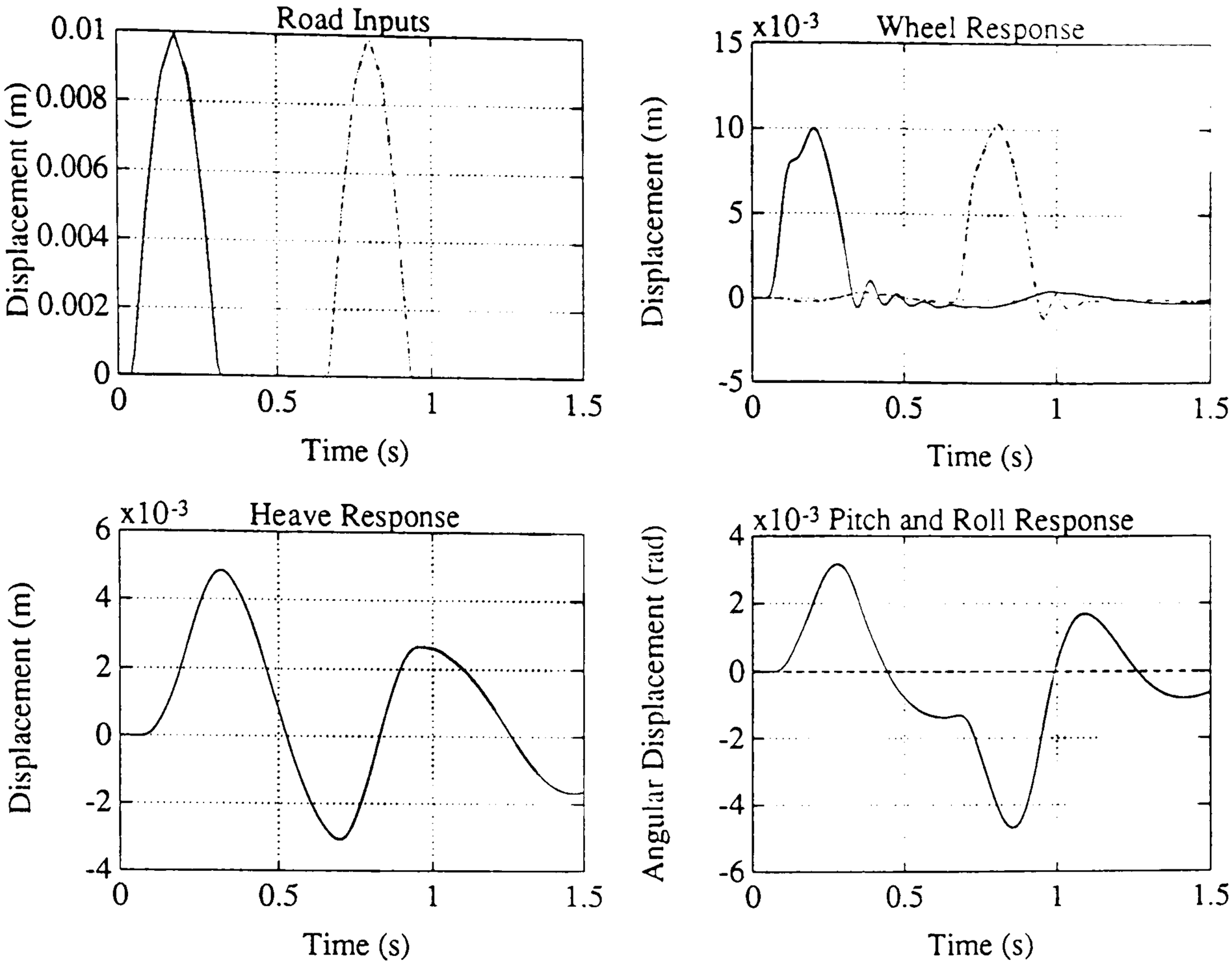


Figure 5.11c : Road Bump Input to Both Tracks

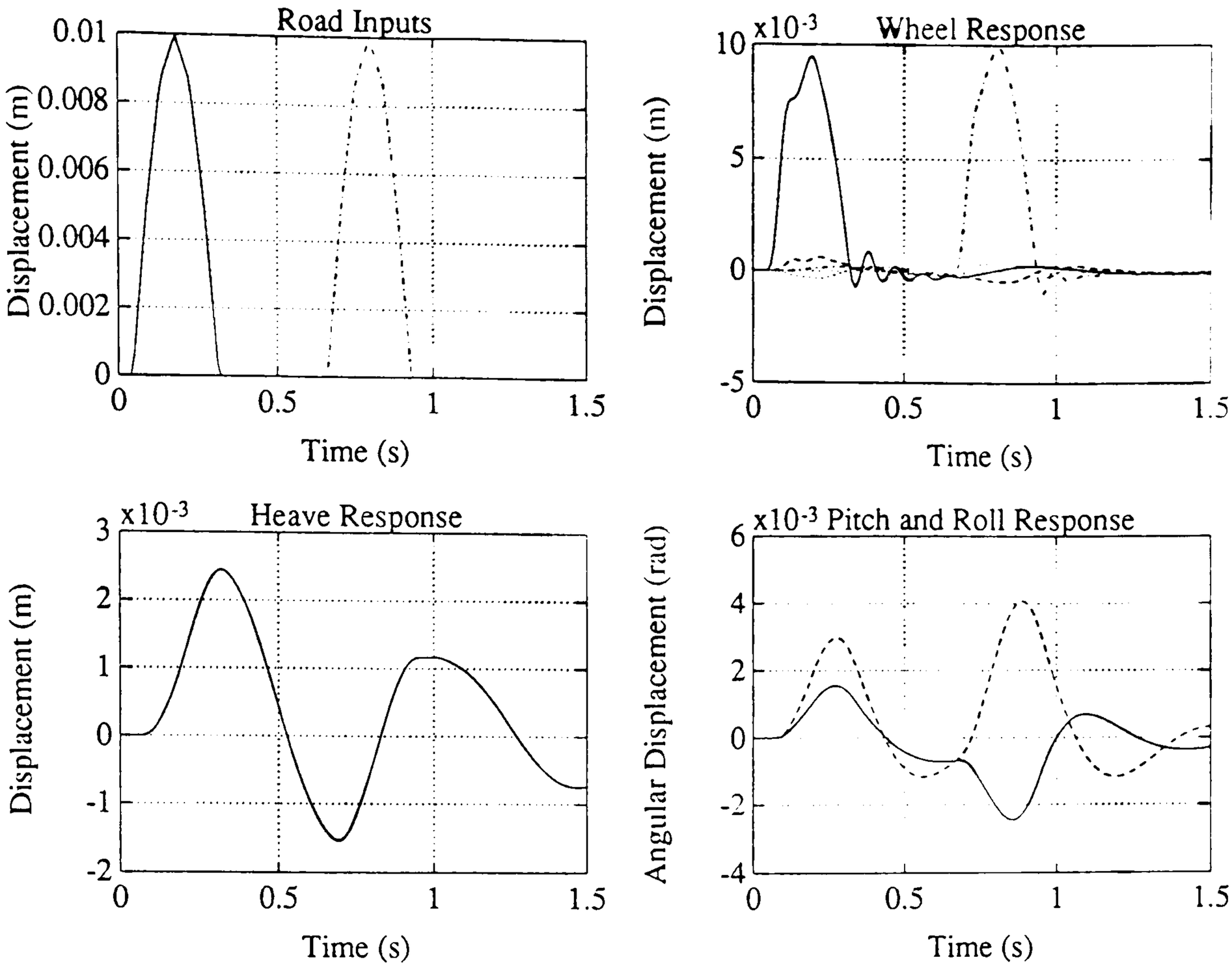


Figure 5.11d : Road Bump Input to One Track Only

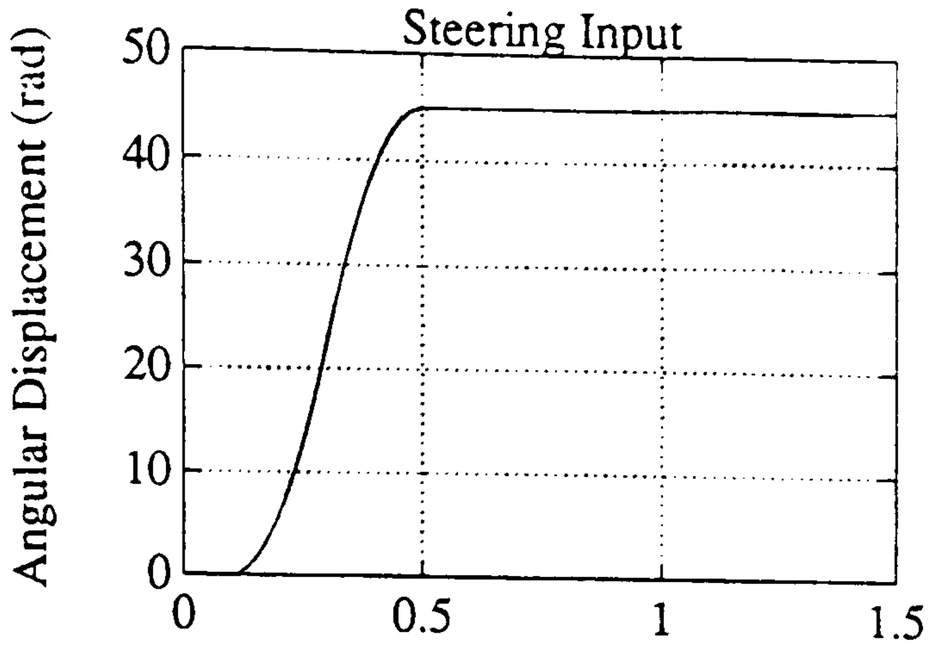


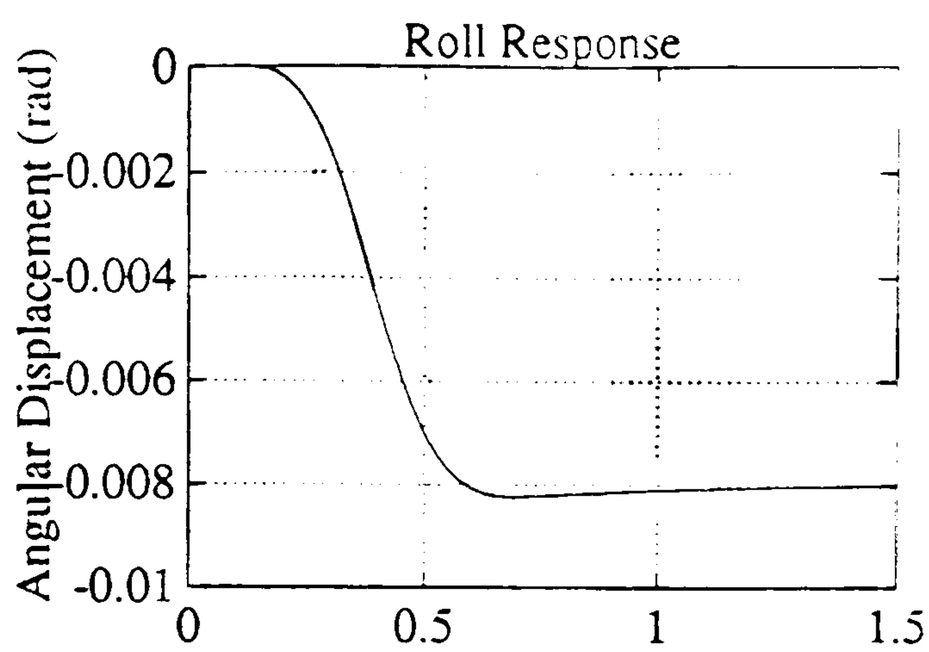


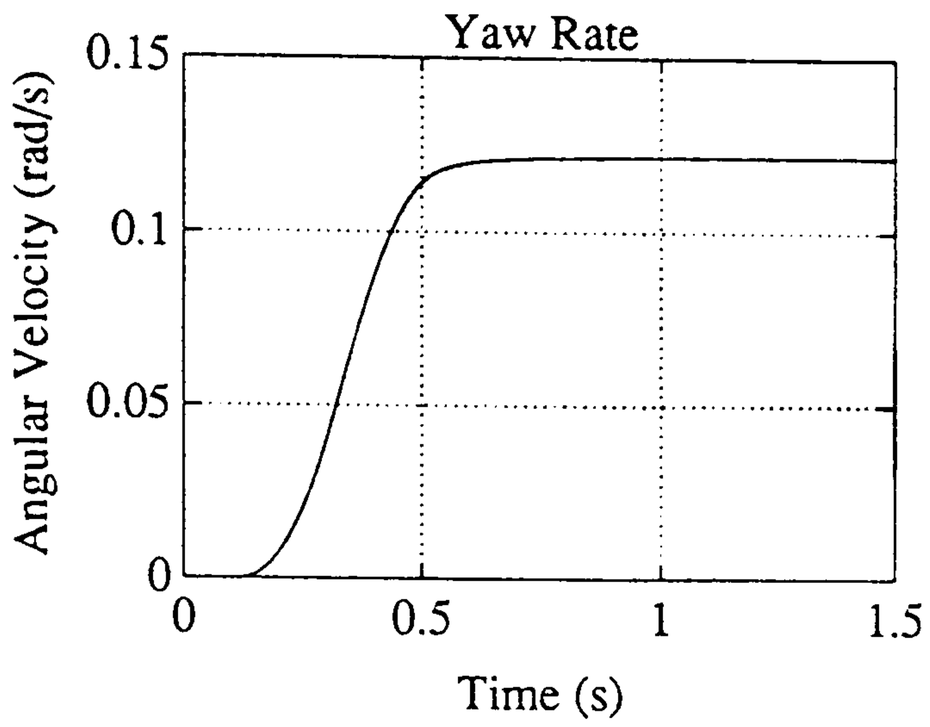


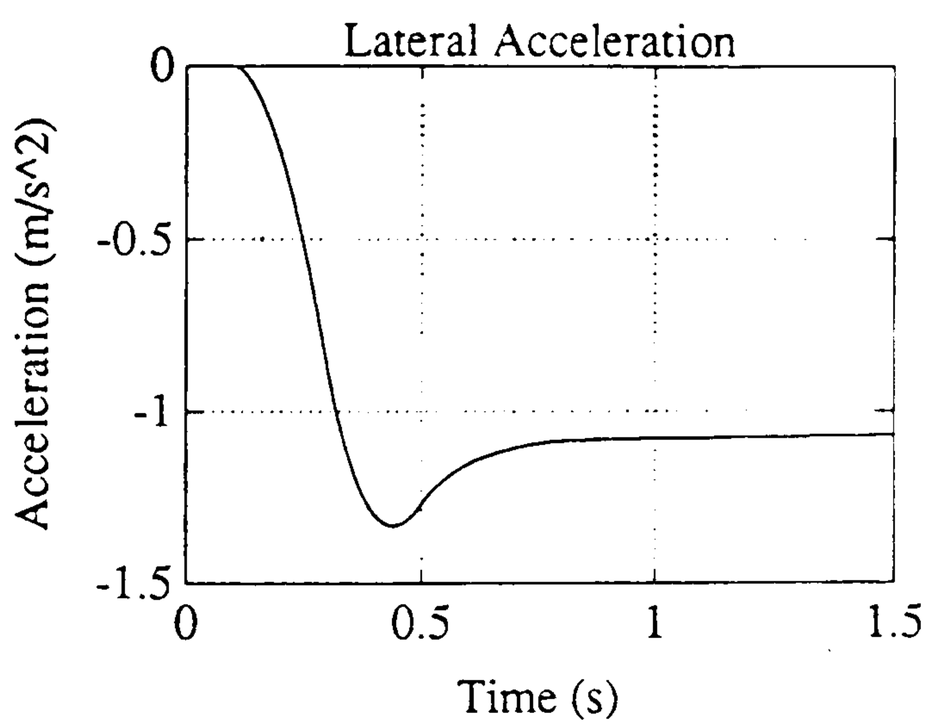


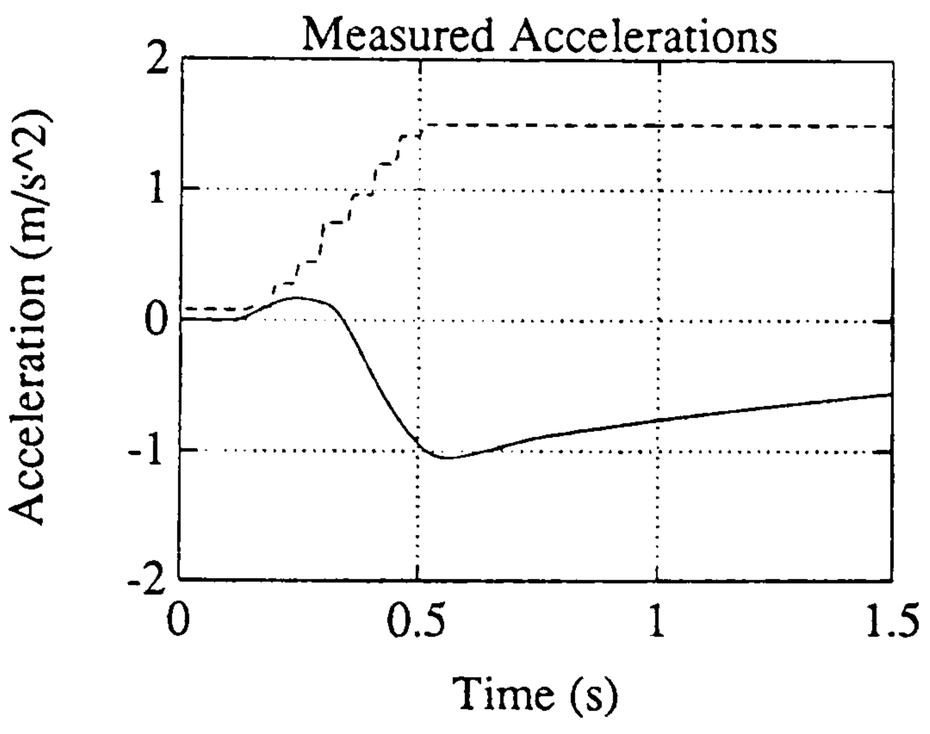


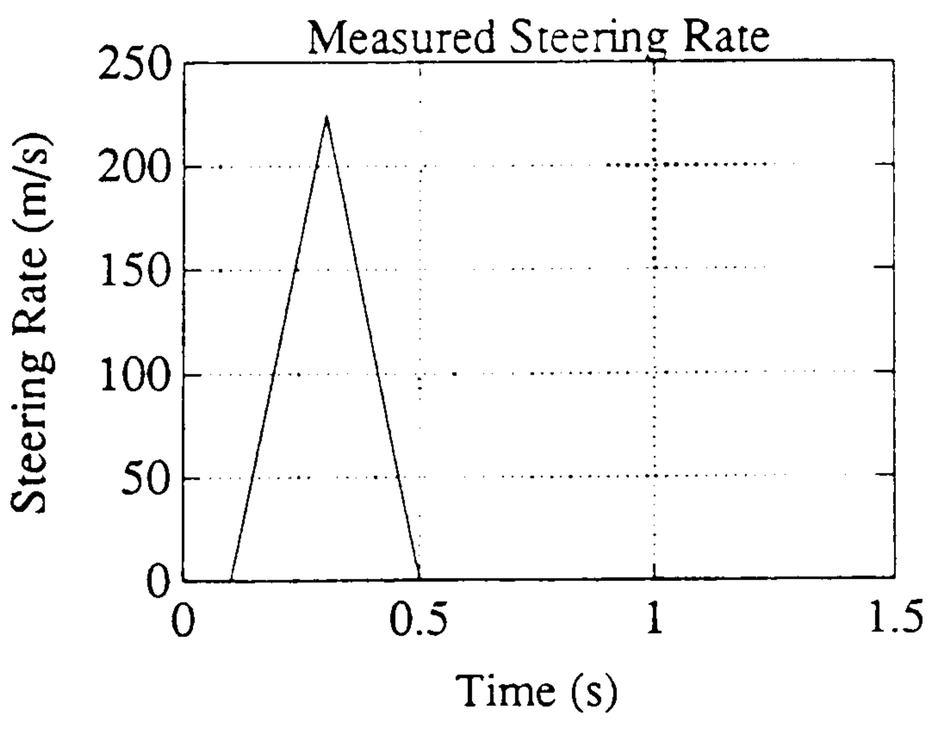


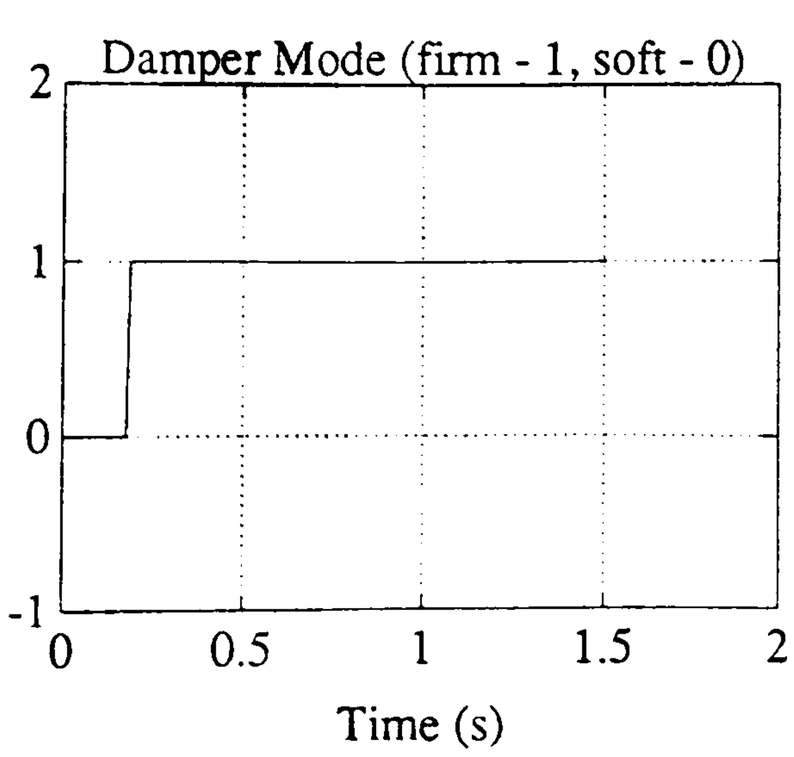


Figure 5.11e : Steering Input at 20 mph

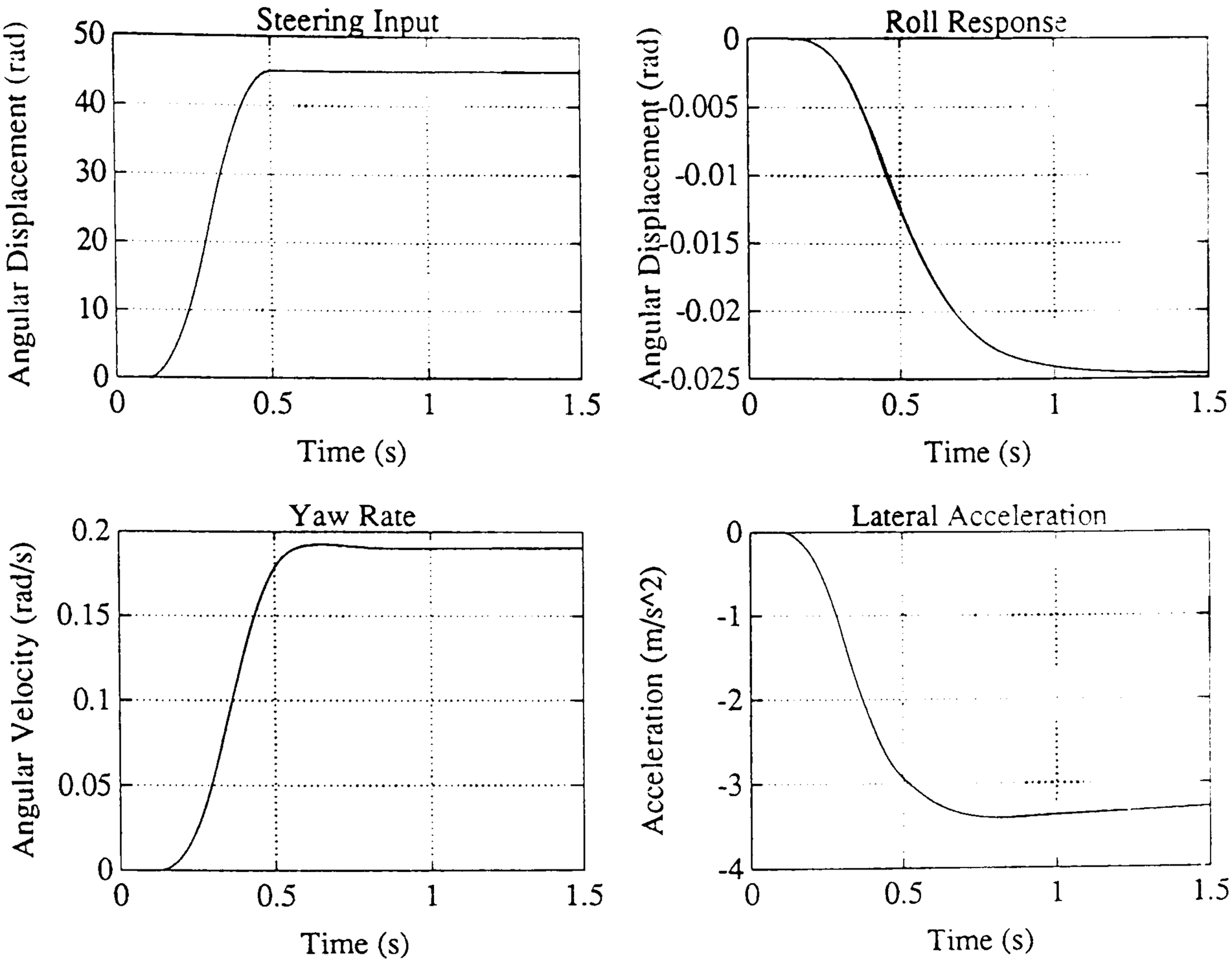


Figure 5.11f : Steering Input at 40 mph

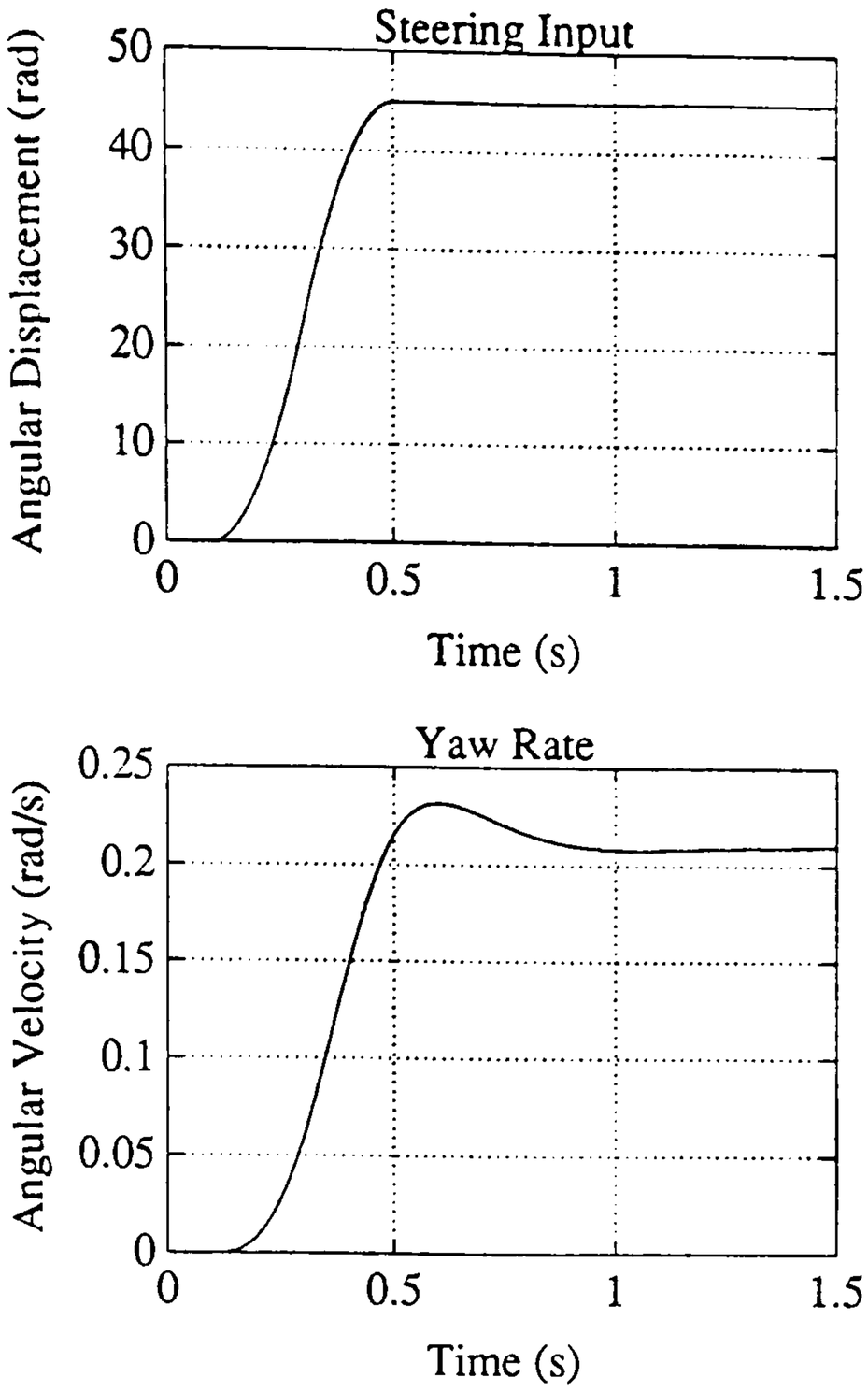


Figure 5.11g : Steering Input at 60 mph

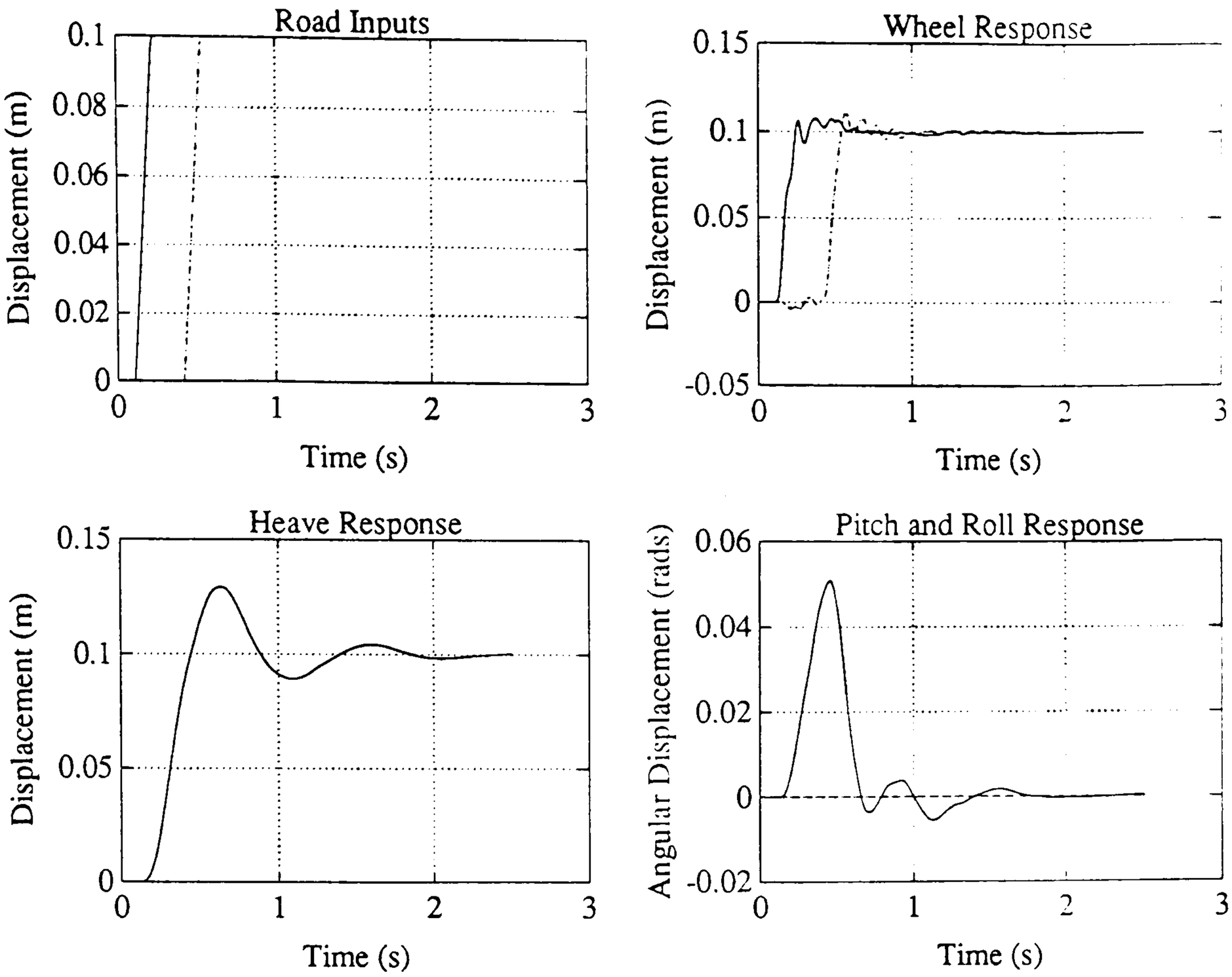


Figure 5.12a : Road Step Input

Figure 5.12 : Linear Quadratic Regulator Based Results

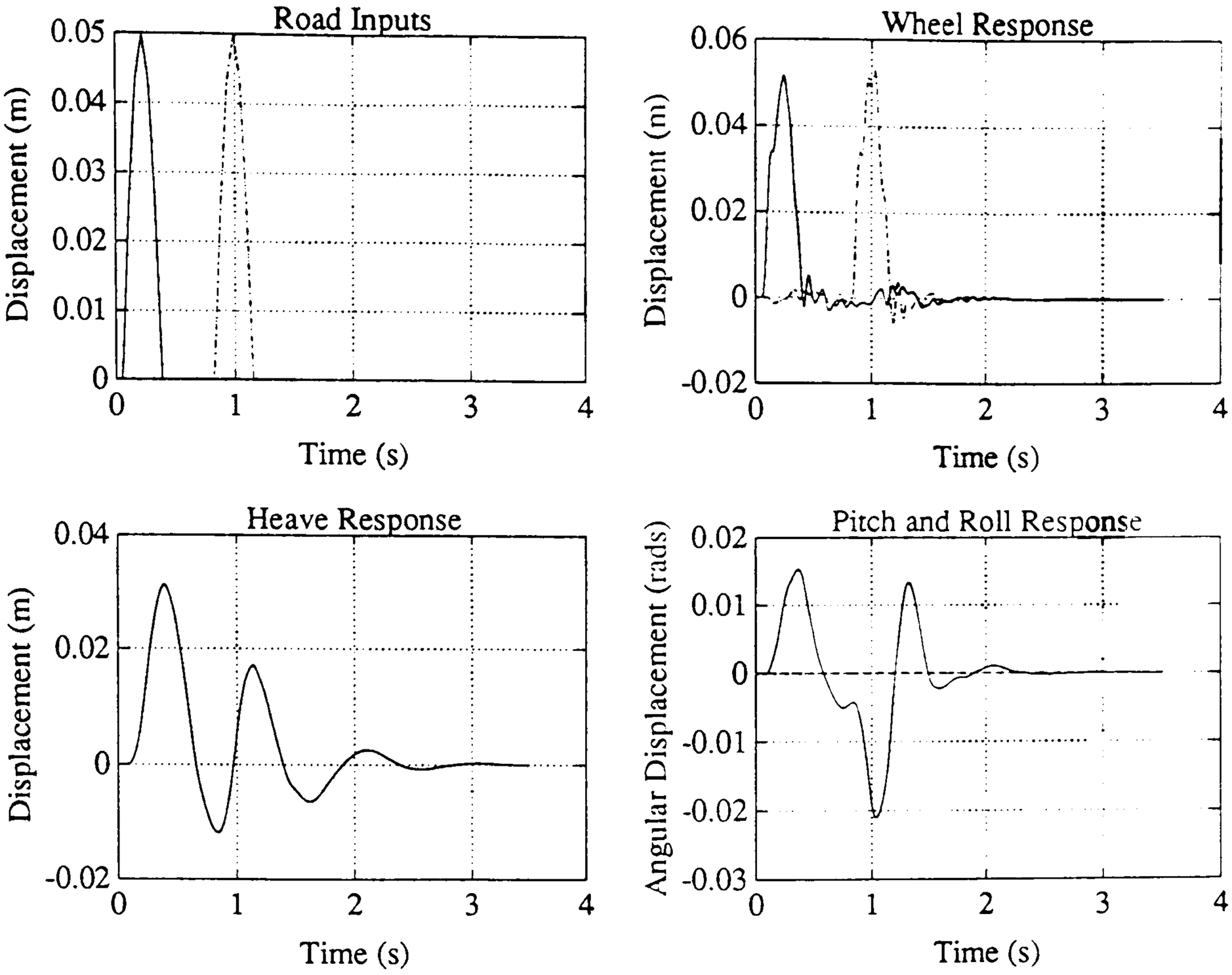


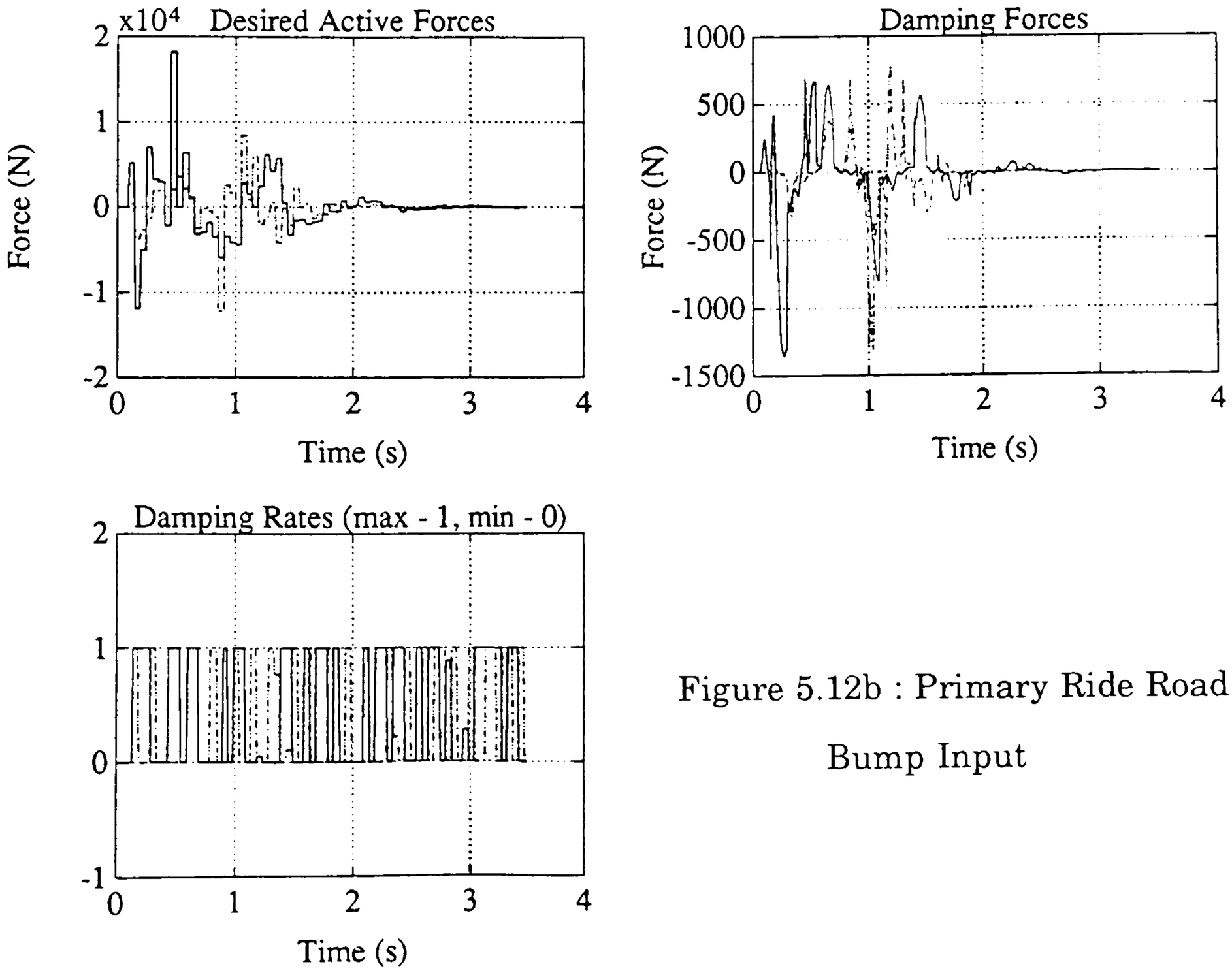


Figure 5.12b : Primary Ride Road Bump Input

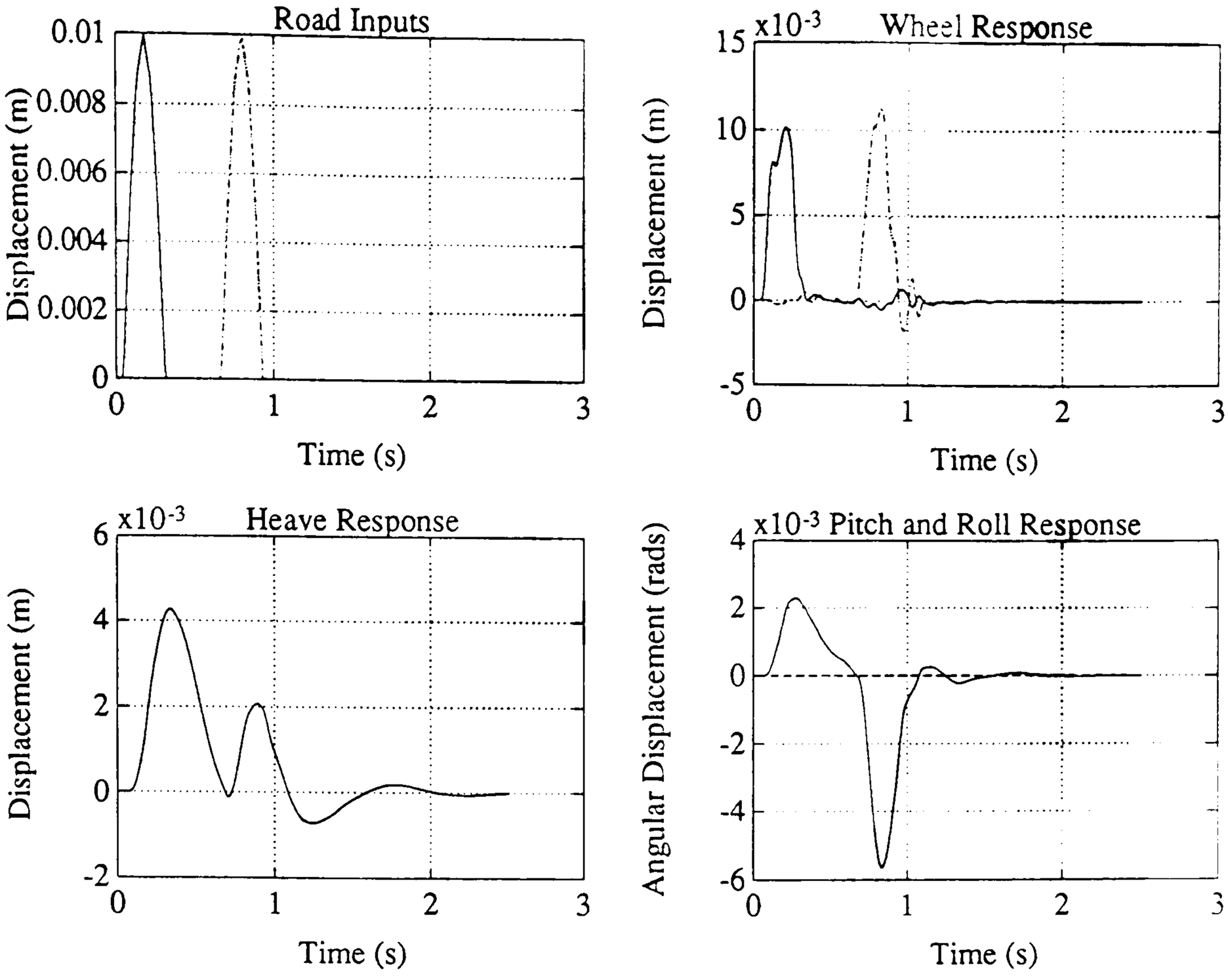


Figure 5.12c : Road Bump Input to Both Tracks

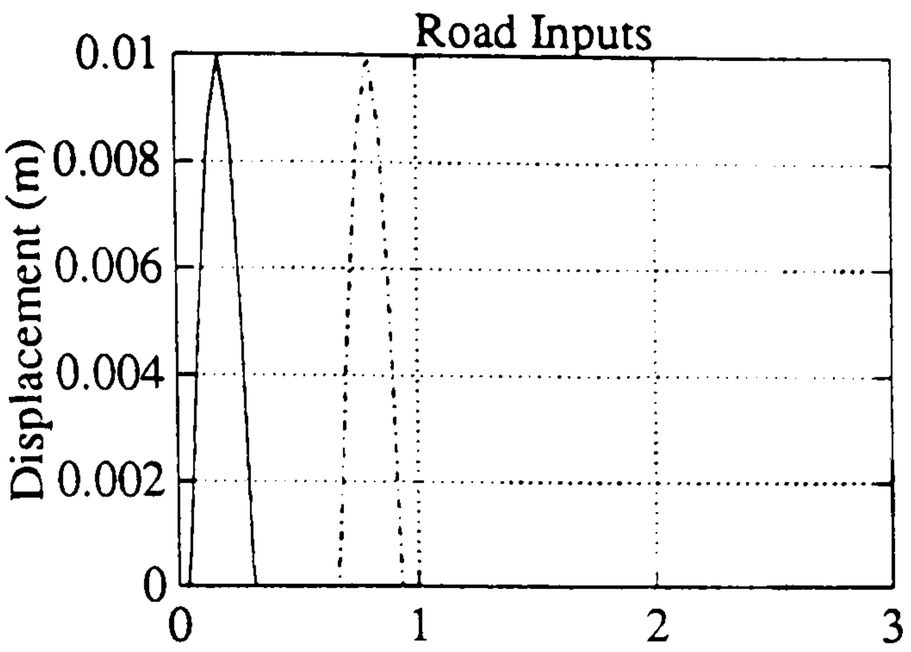


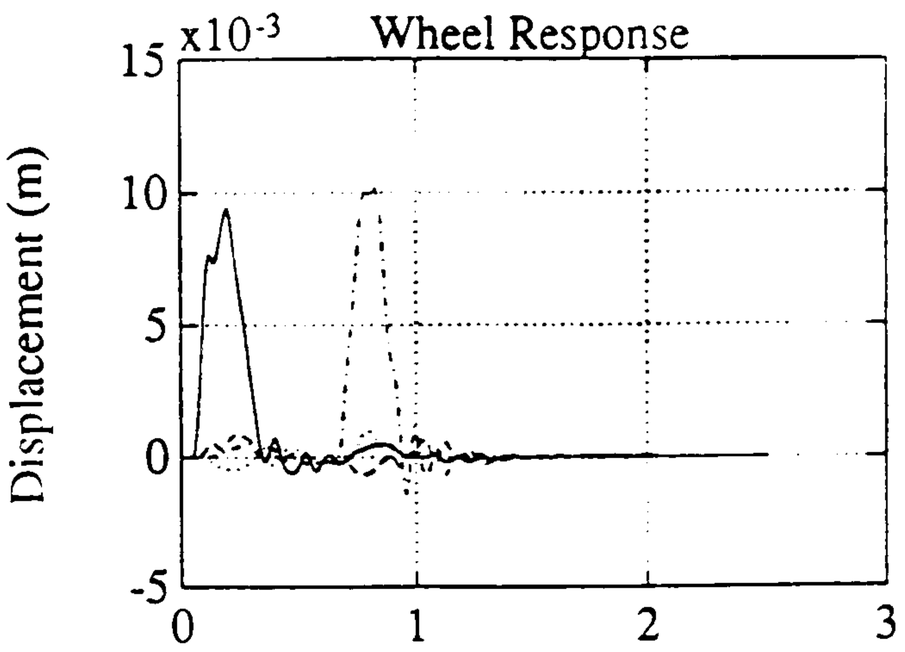


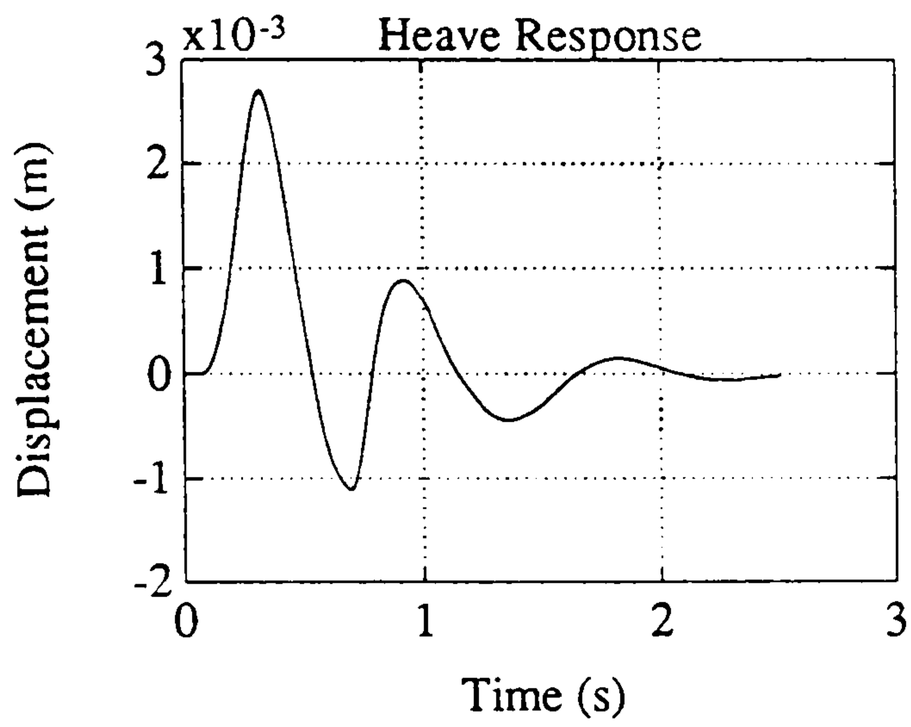


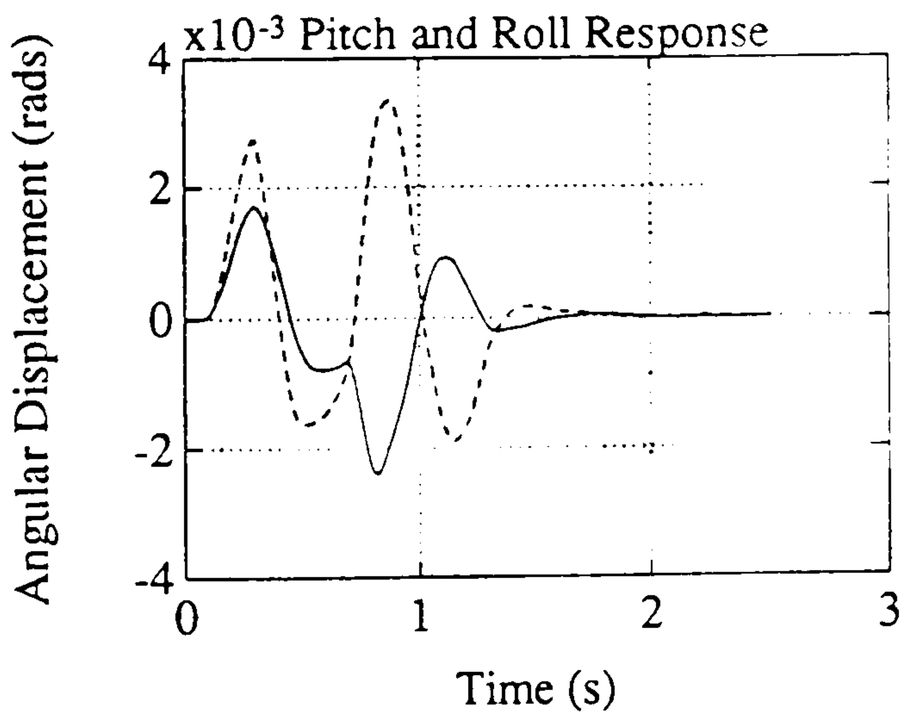


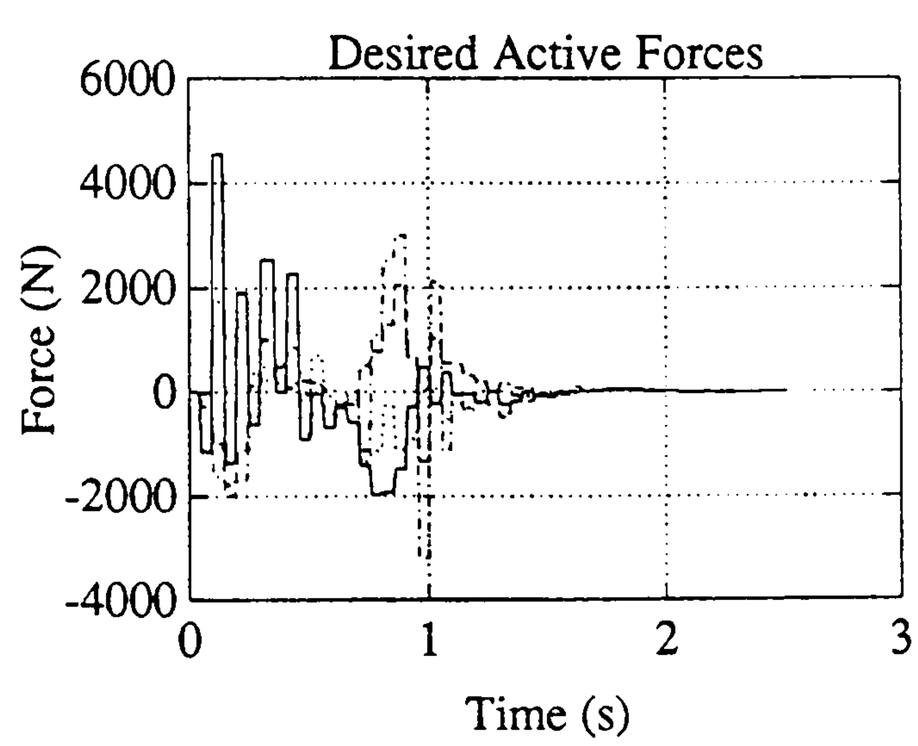


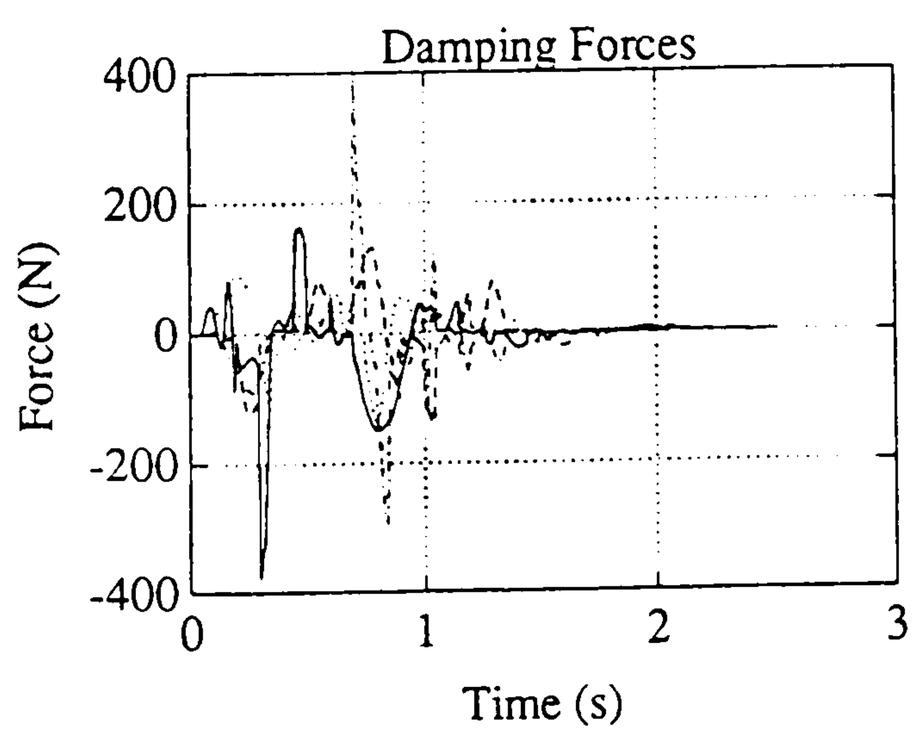


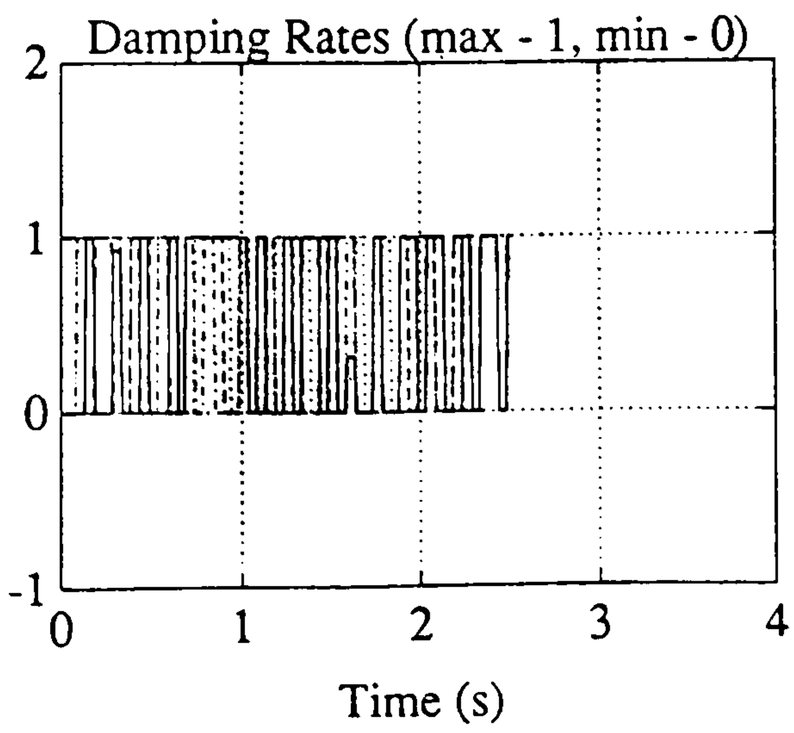


Figure 5.12d : Road Bump Input

to One Track Only

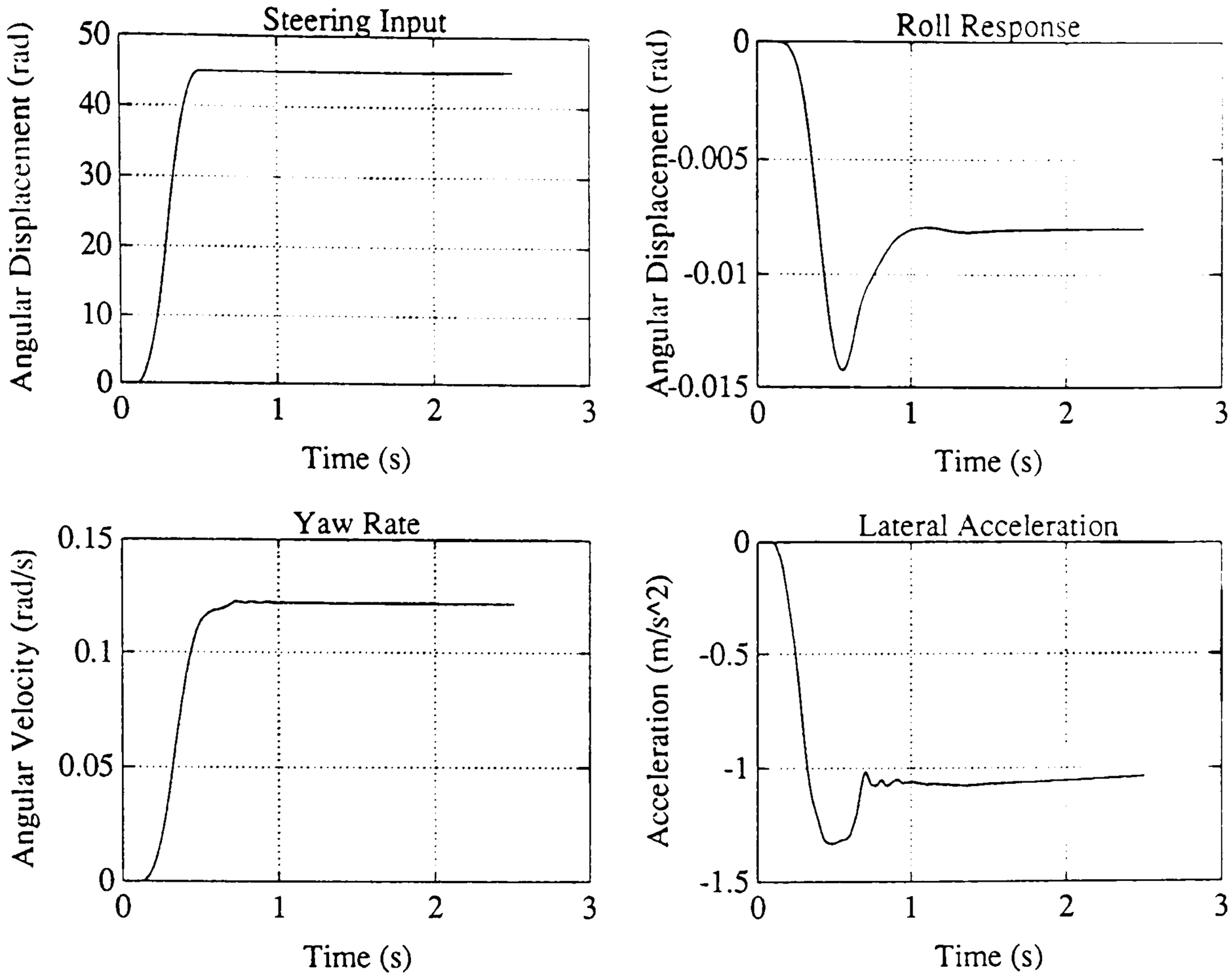


Figure 5.12e : Steering Input at 20 mph

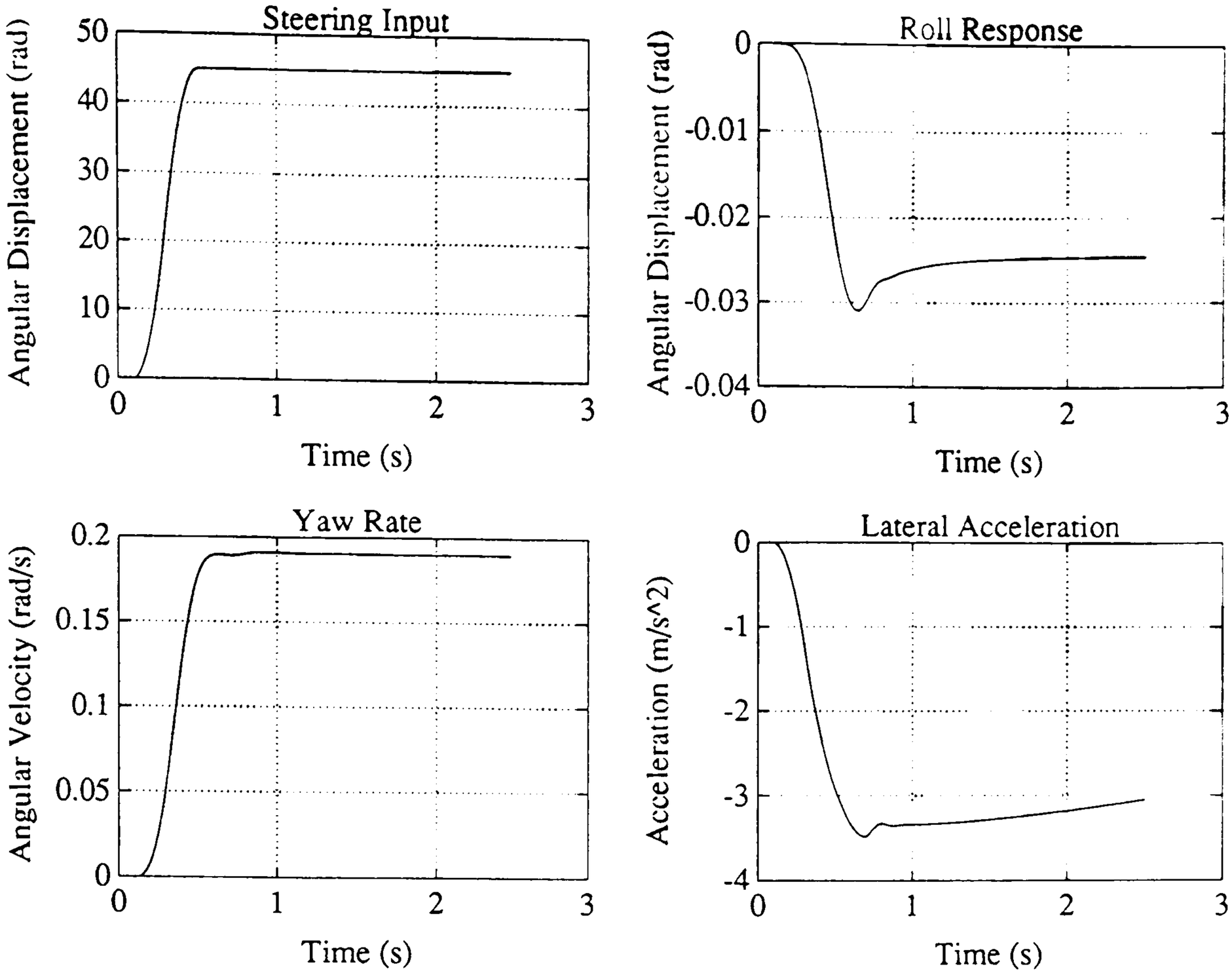


Figure 5.12f : Steering Input at 40 mph

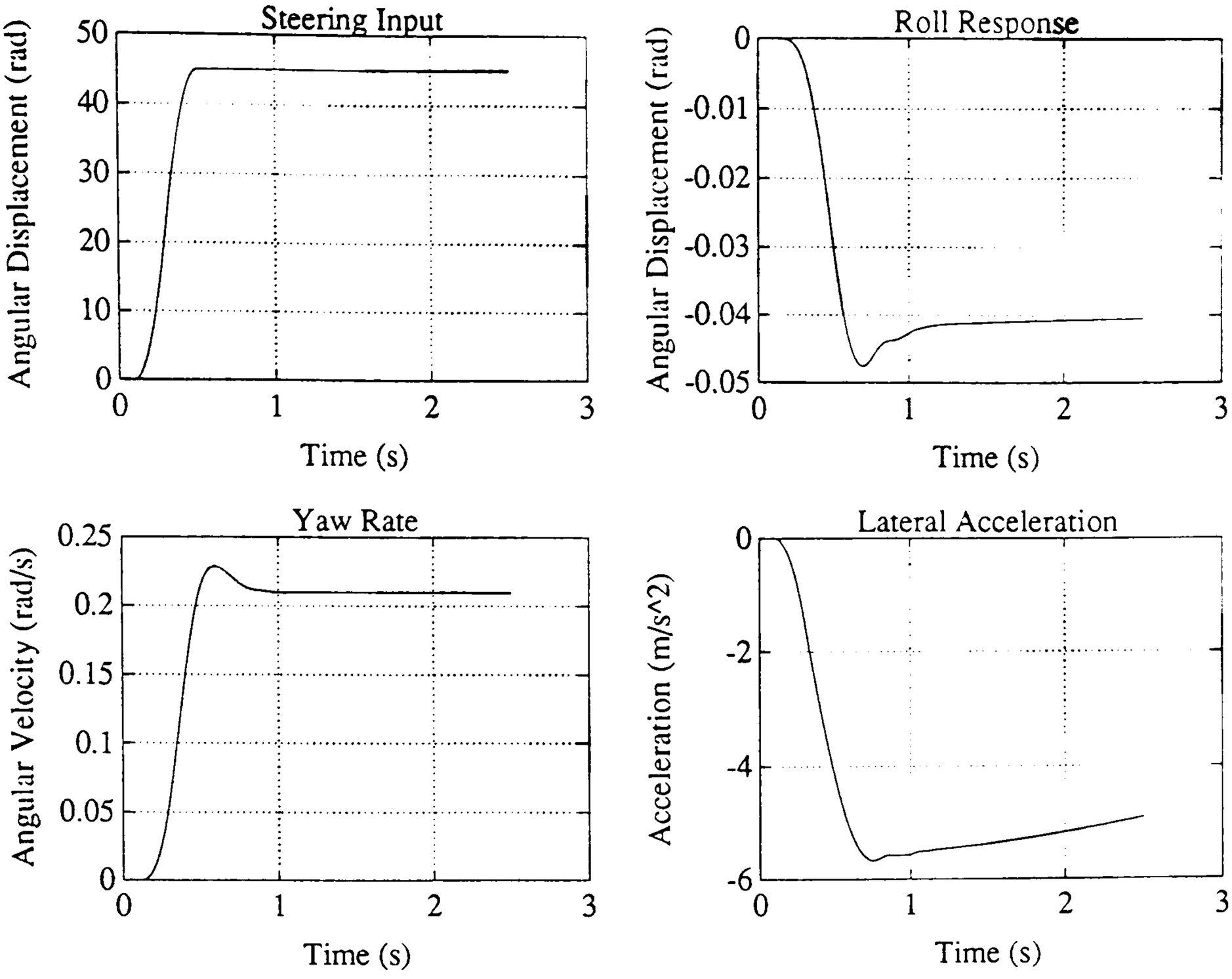


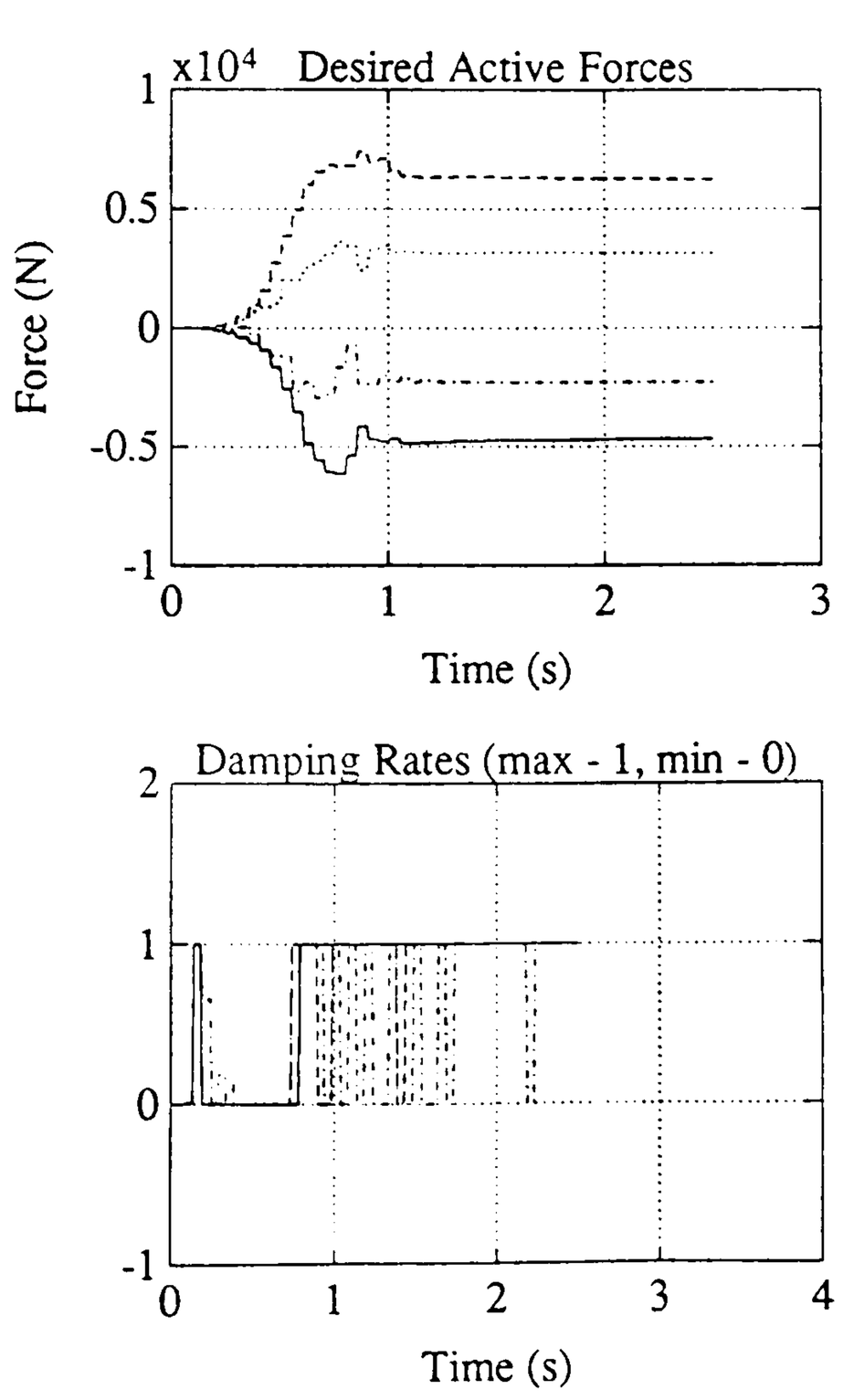


Figure 5.12g : Steering Input at 60 mph

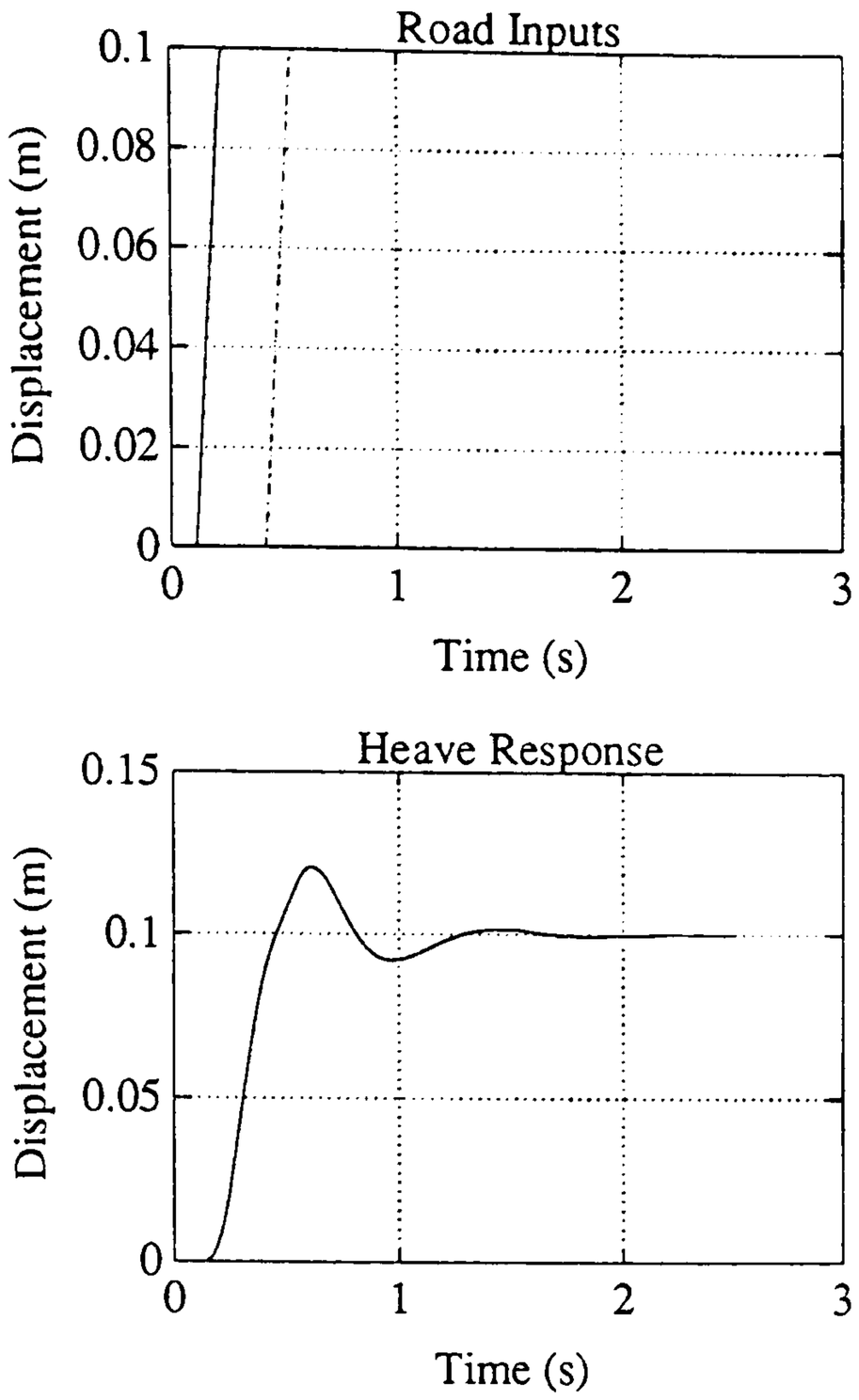


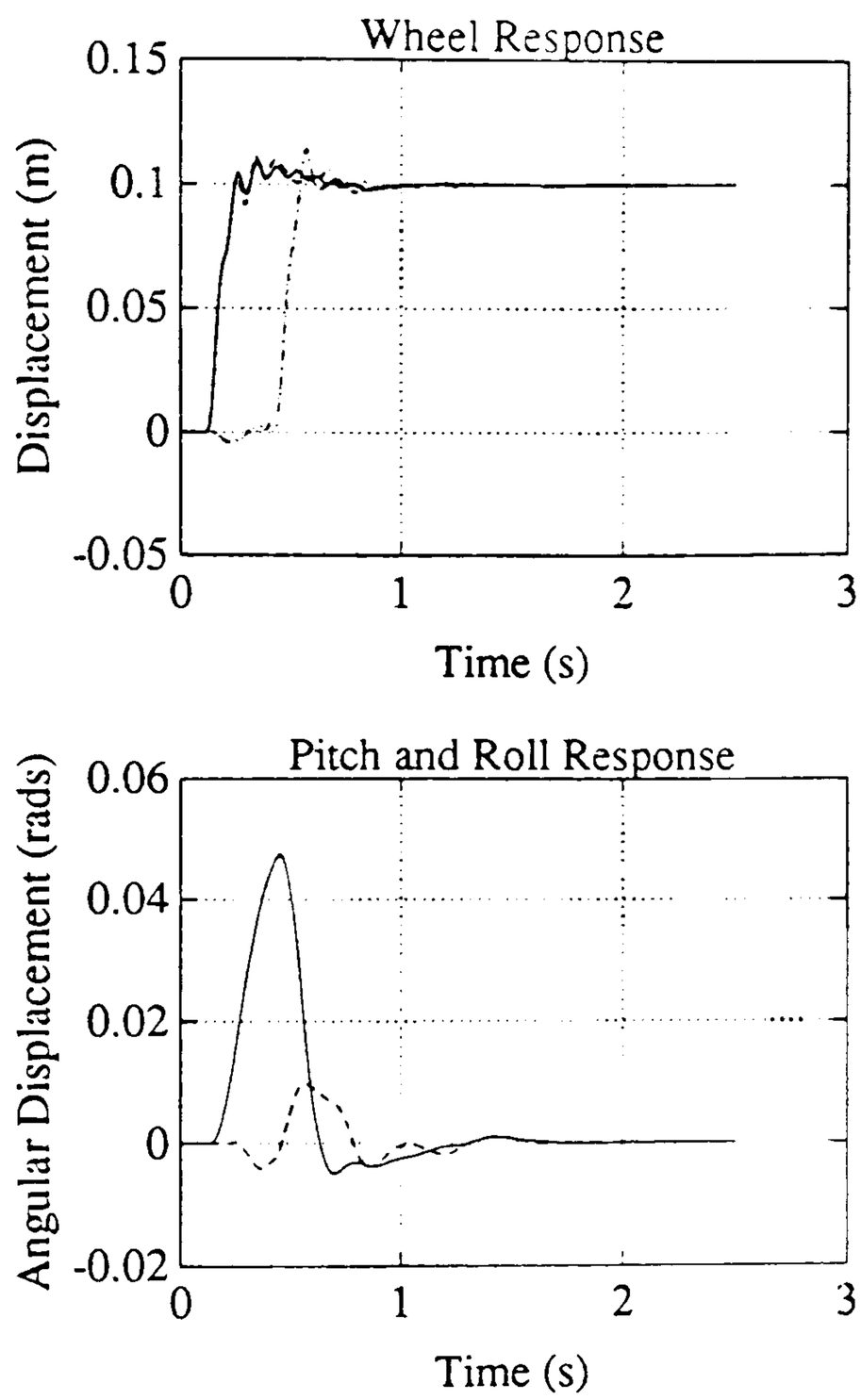








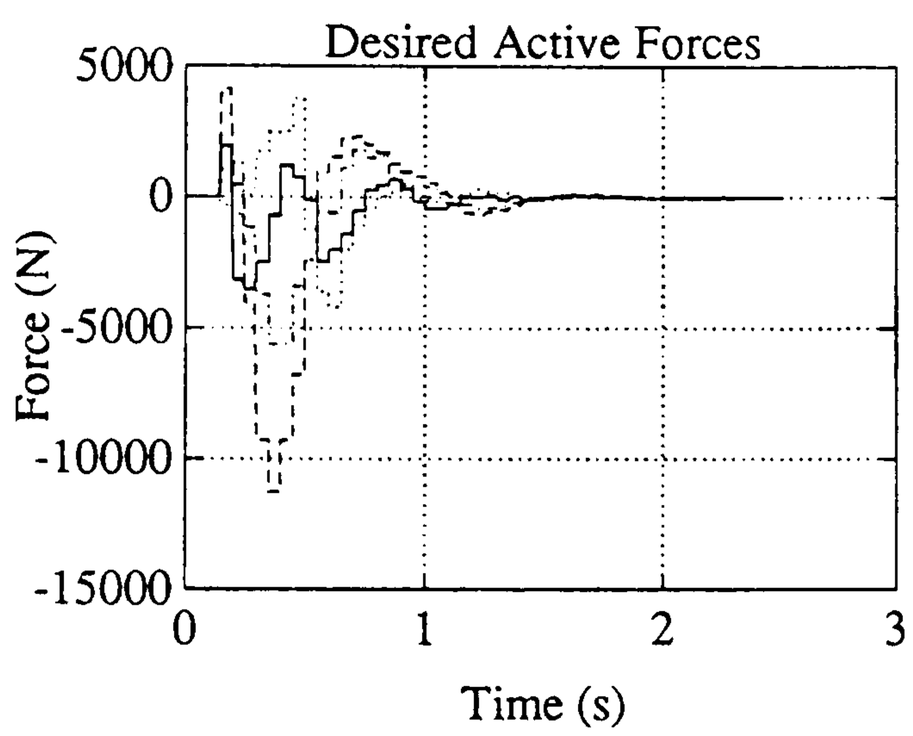


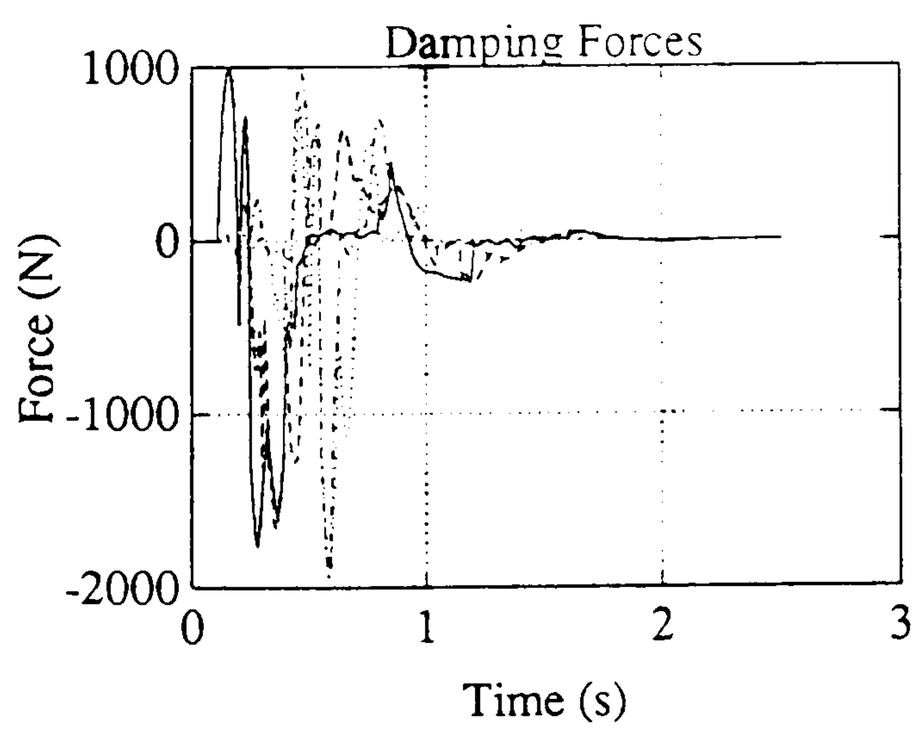


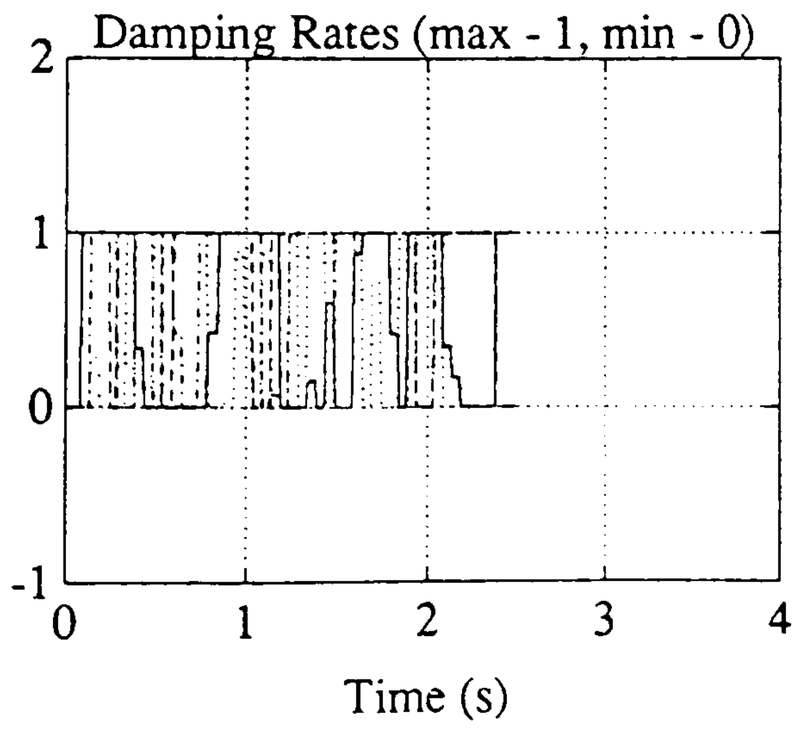


Figure 5.13a : Road Step Input

Figure 5.13 : Pole Placement Based Results

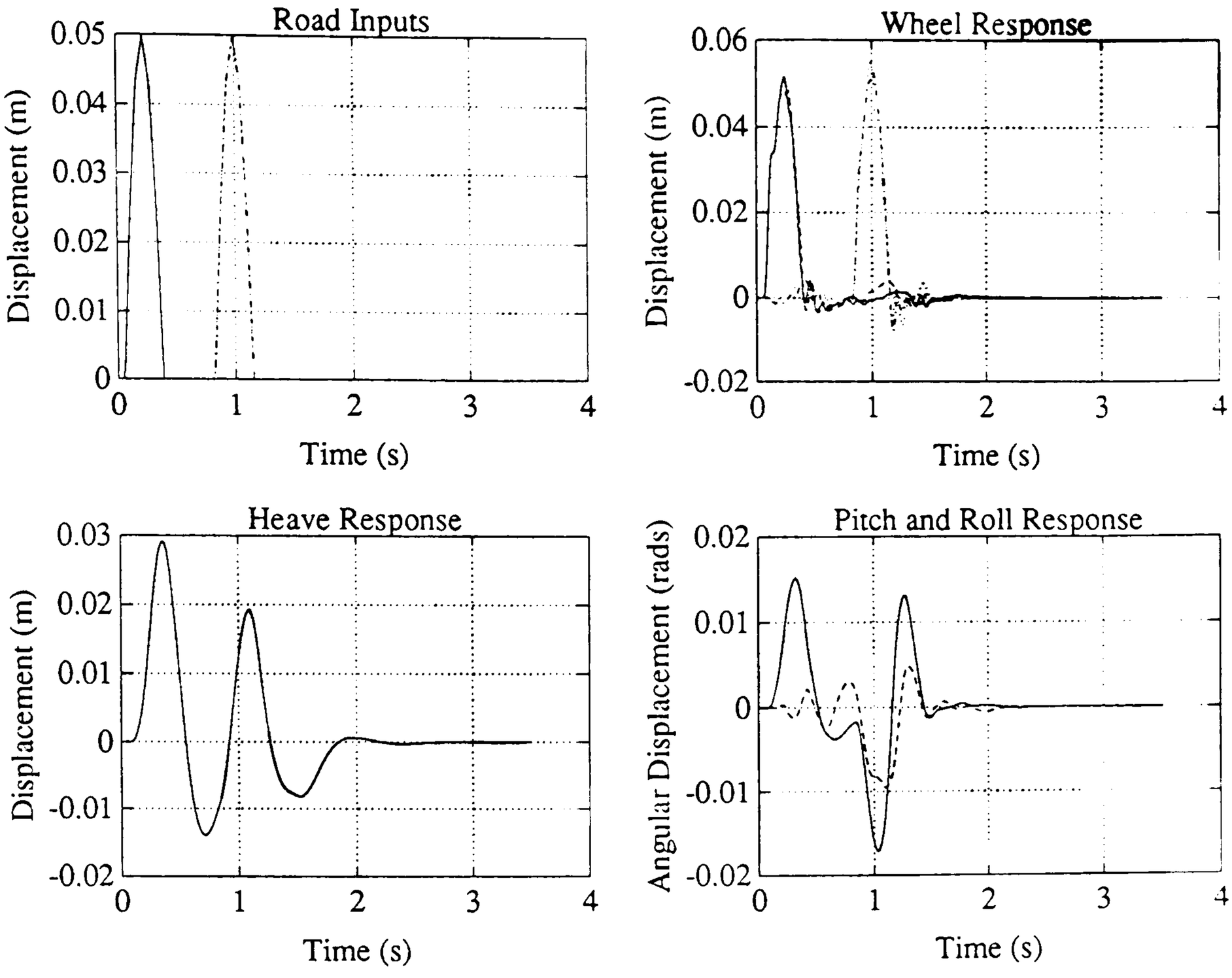


Figure 5.13b : Primary Ride Road Bump Input

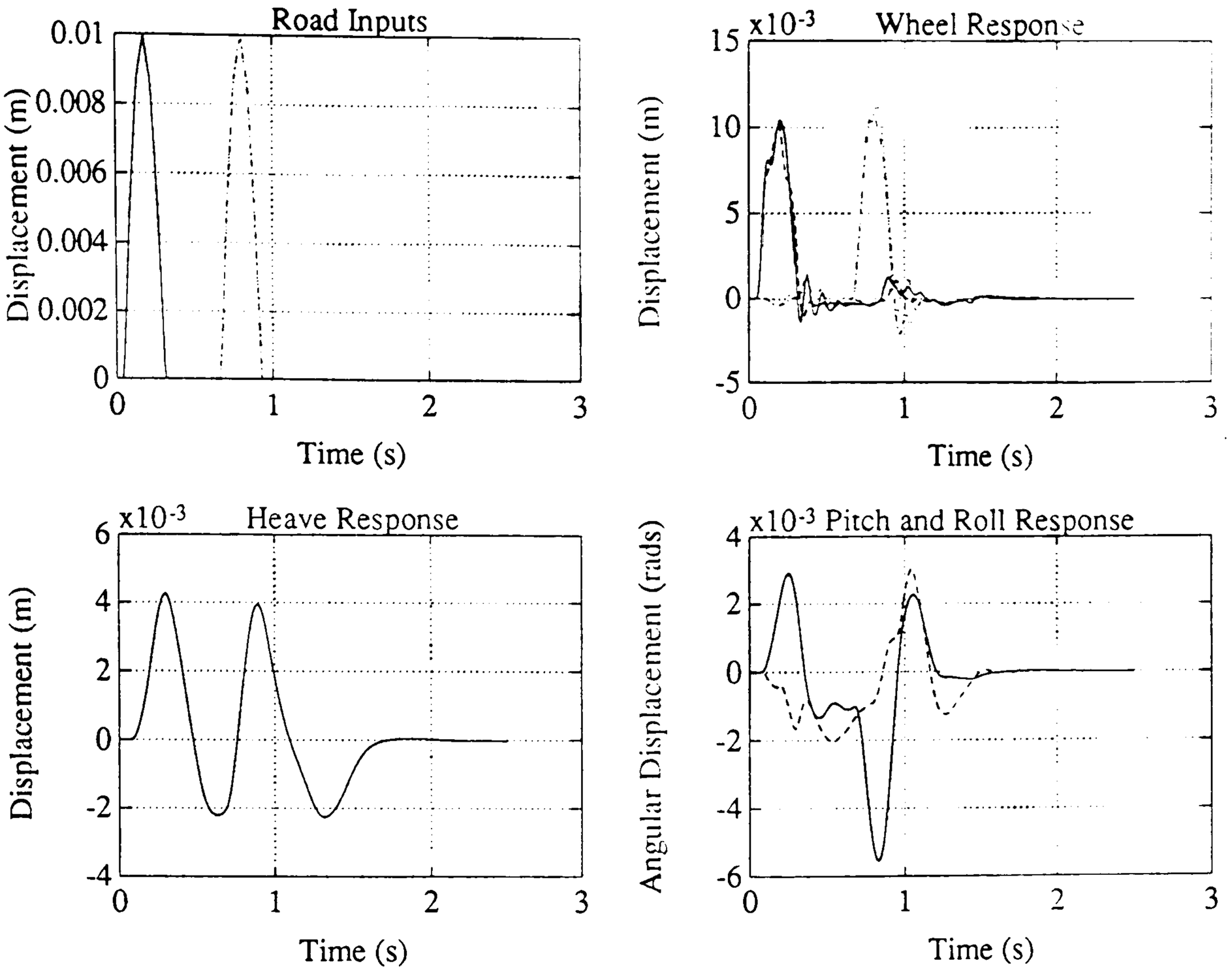


Figure 5.13c : Road Bump Input to Both Tracks

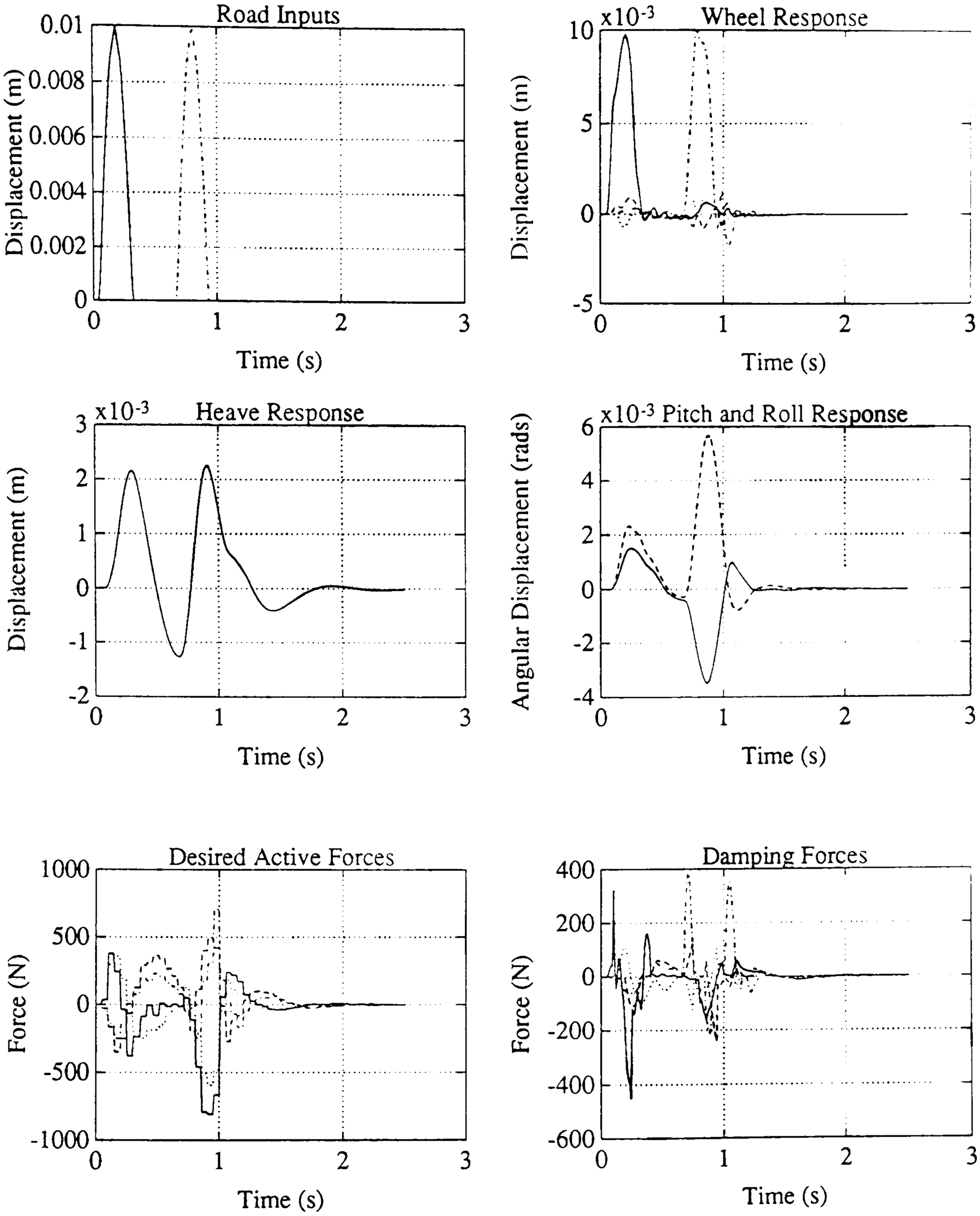


Figure 5.13d : Road Bump Input

to One Track Only

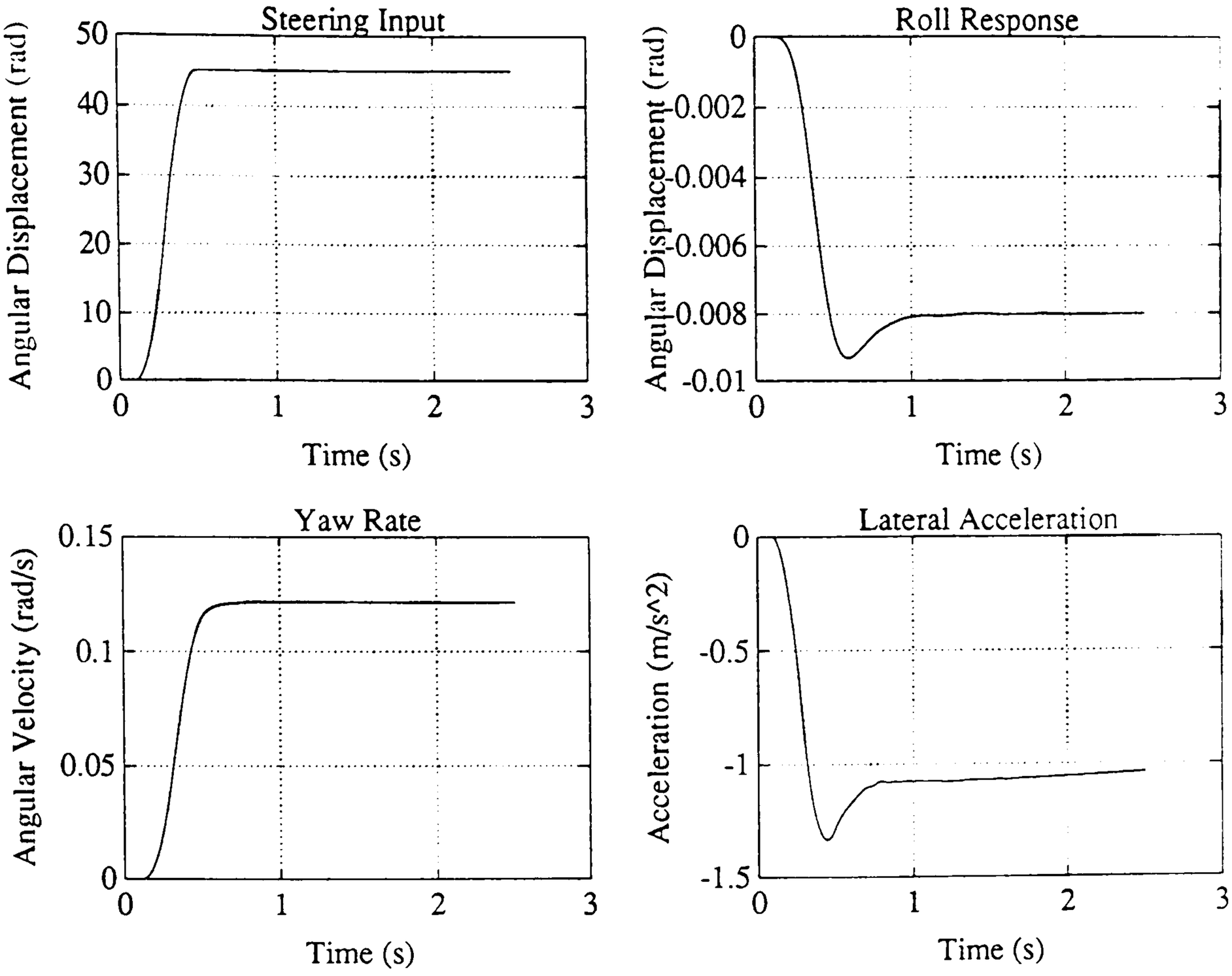


Figure 5.13e : Steering Input at 20 mph

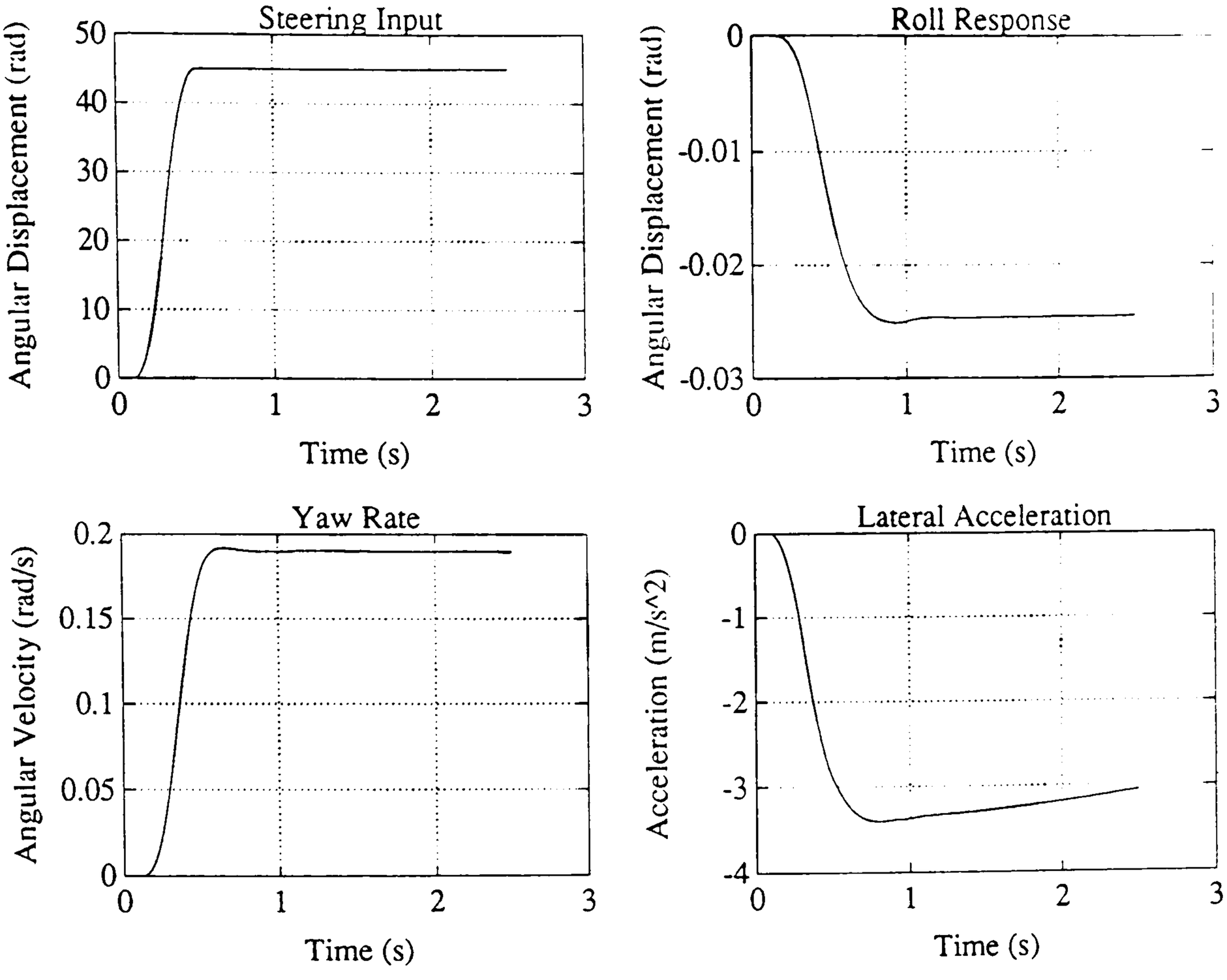


Figure 5.13f : Steering Input at 40 mph

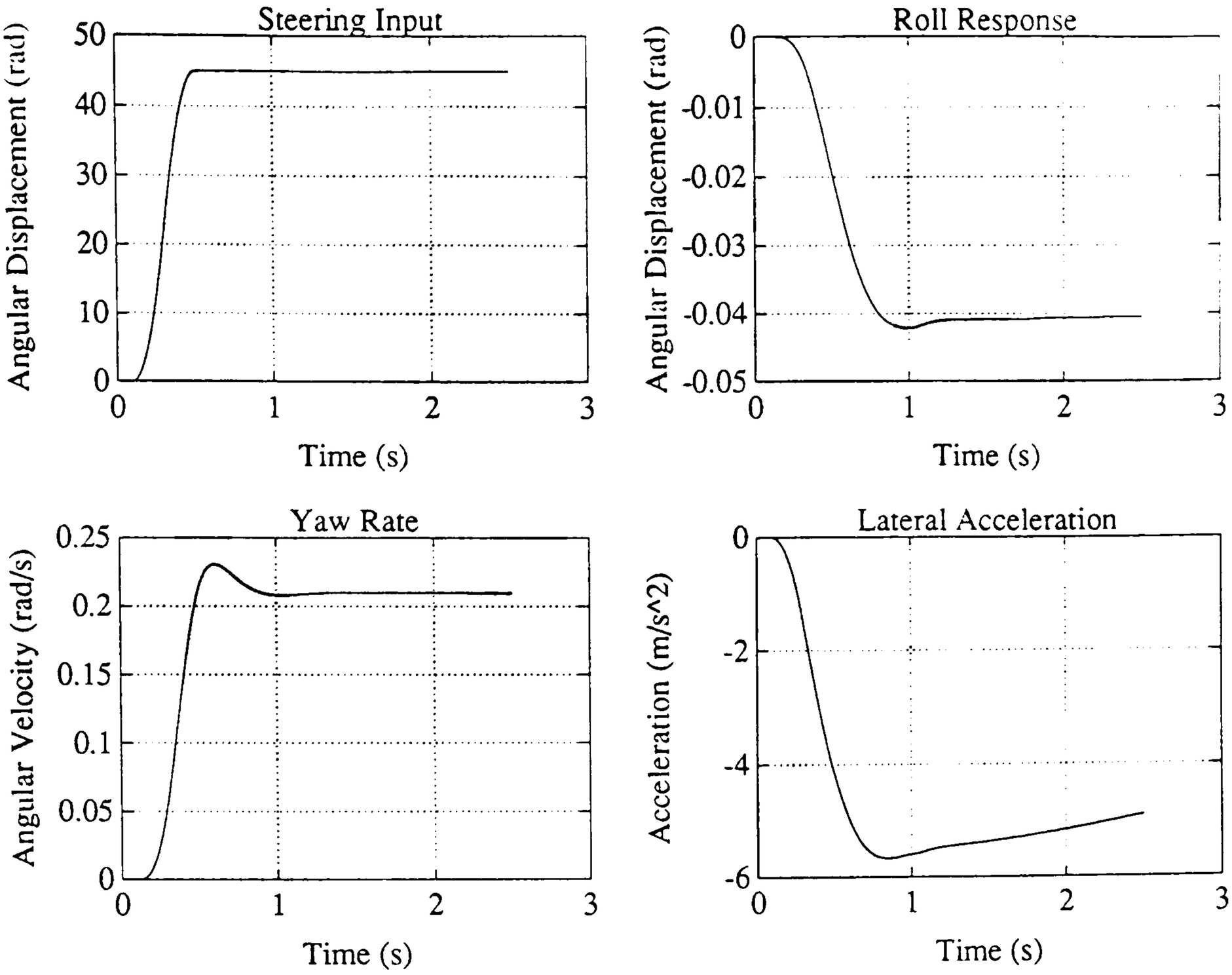


Figure 5.13g : Steering Input at 60 mph

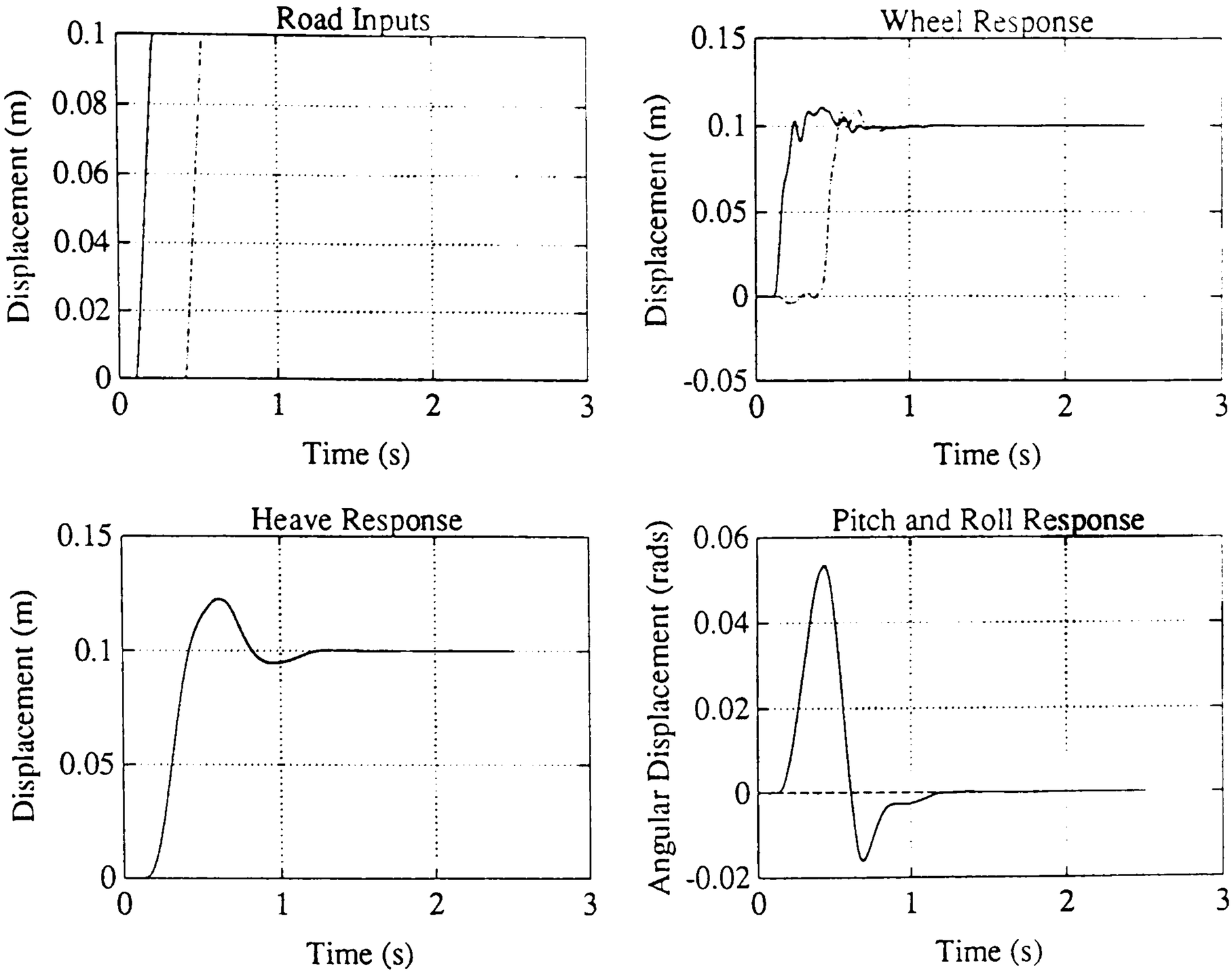


Figure 5.14a : Road Step Input

Figure 5.14 : Frequency Domain Based Results

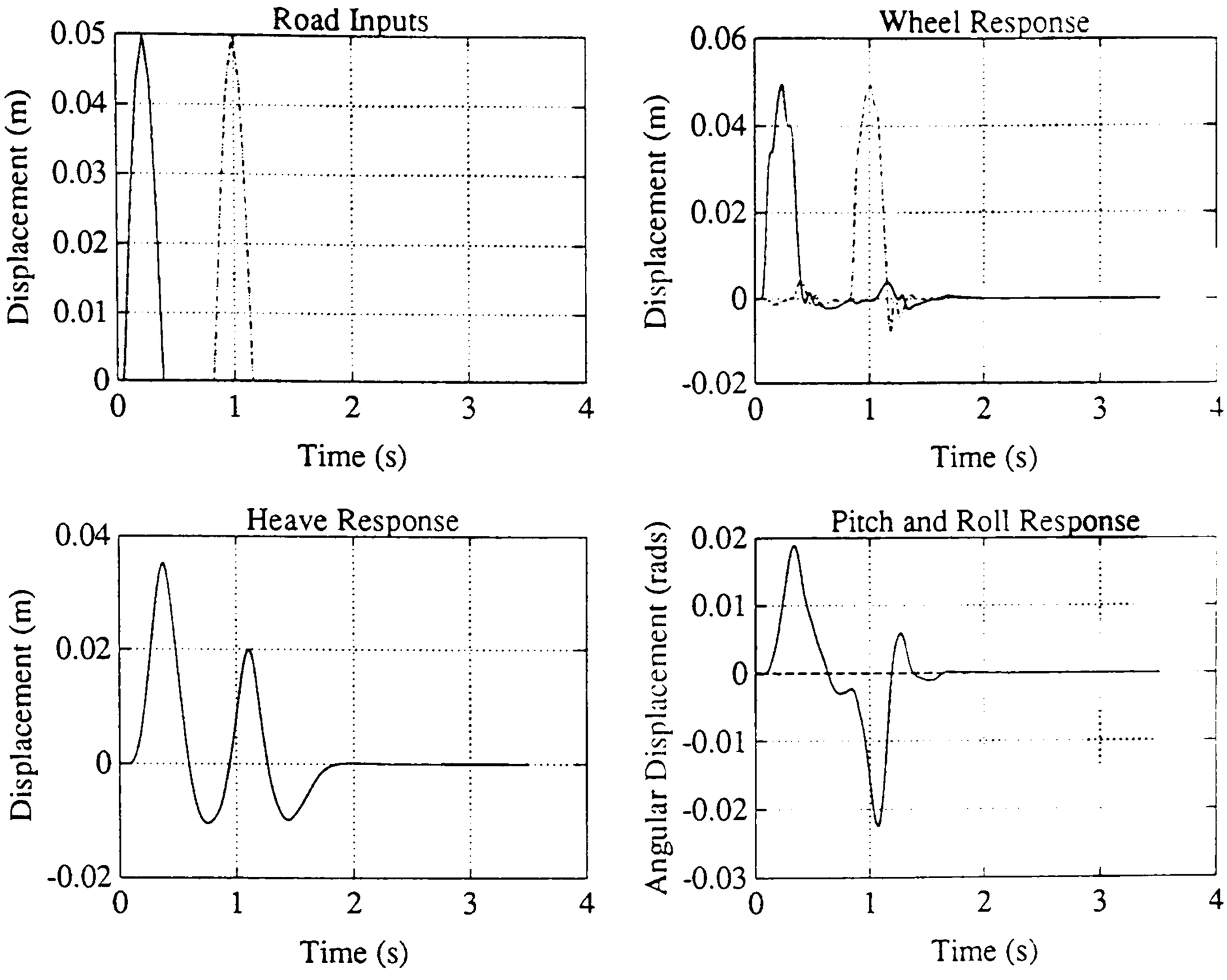


Figure 5.14b : Primary Ride Road Bump Input

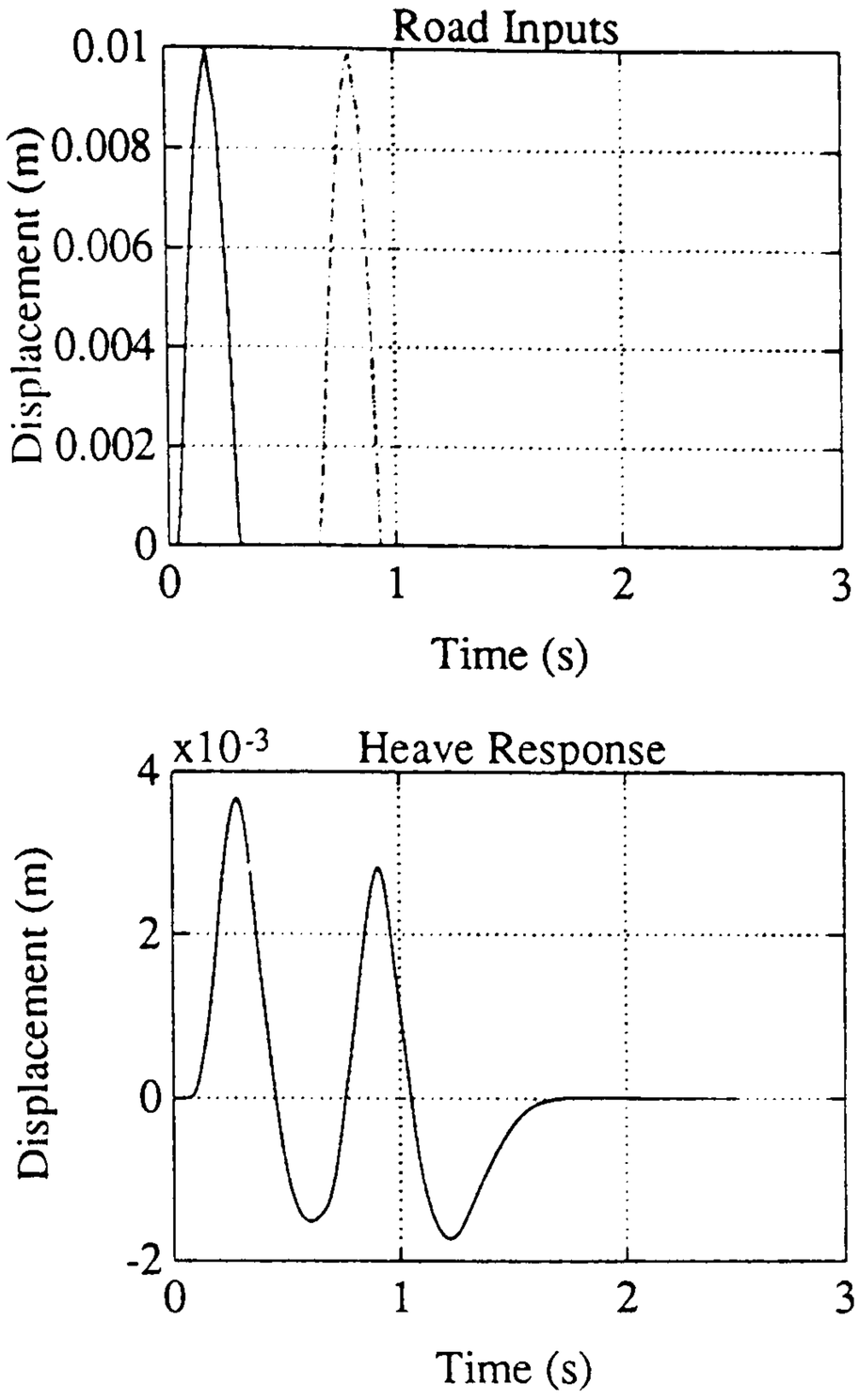


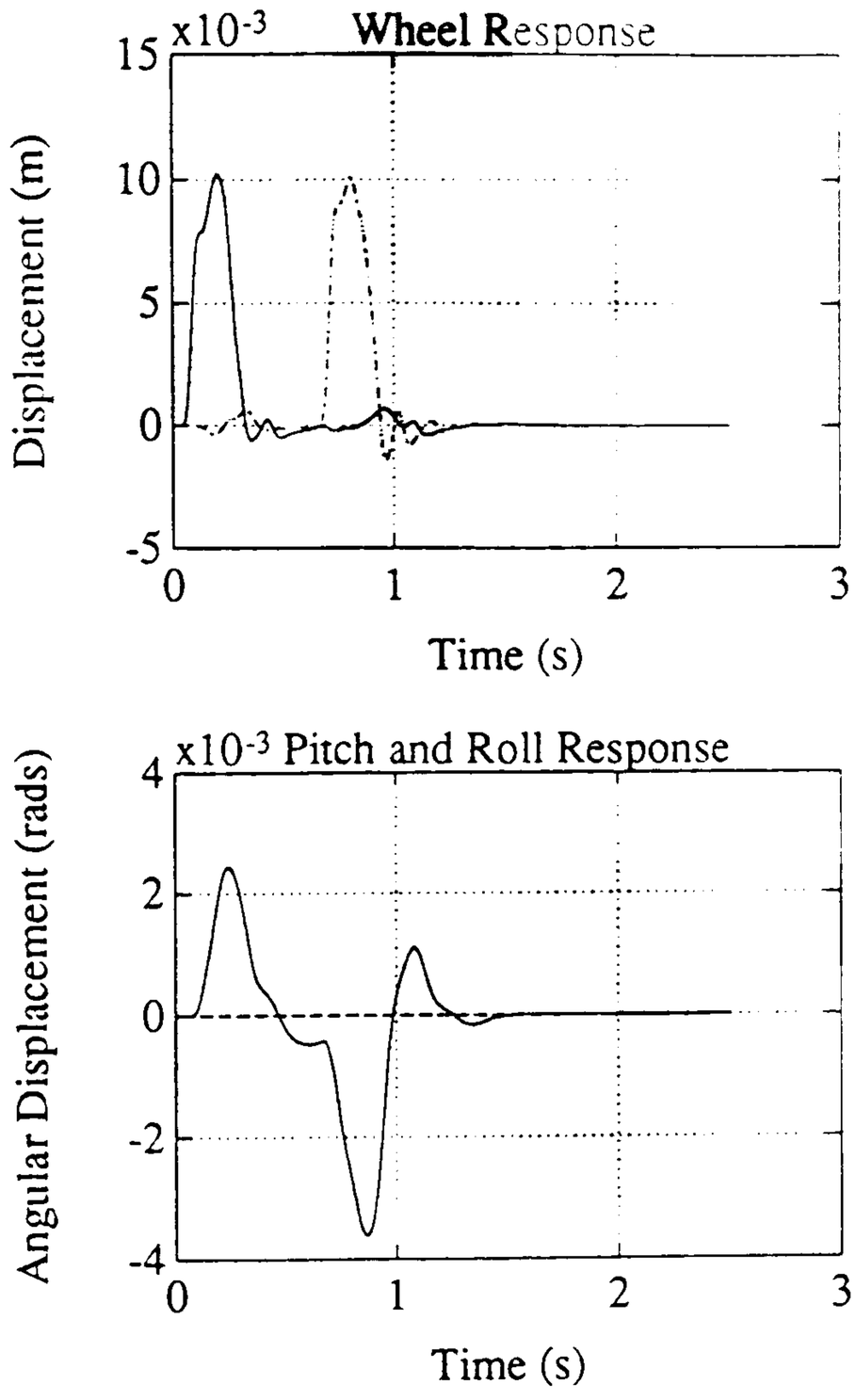








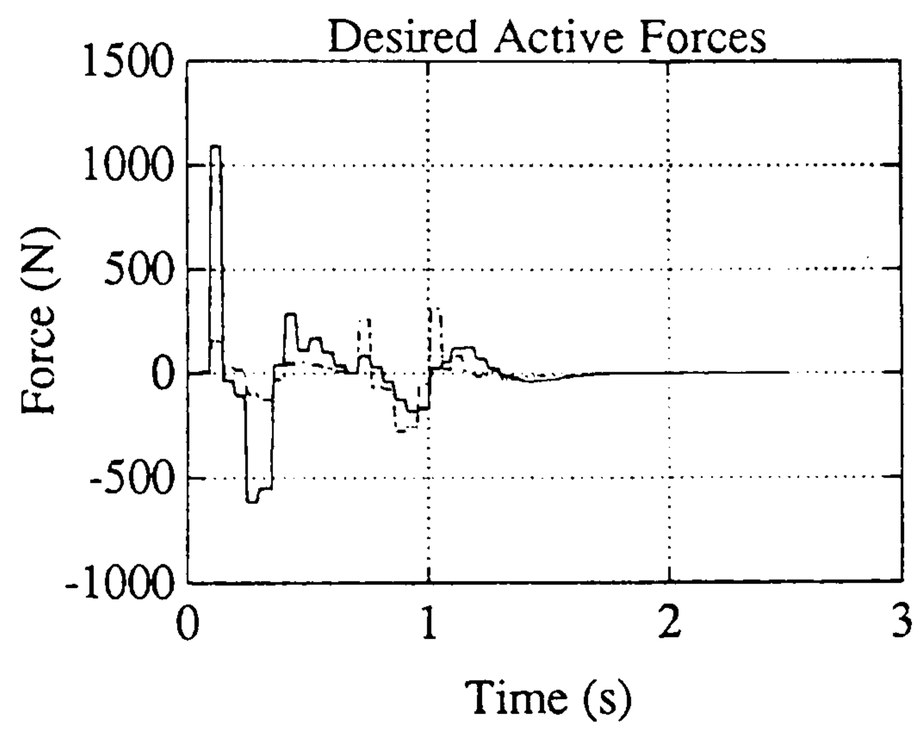


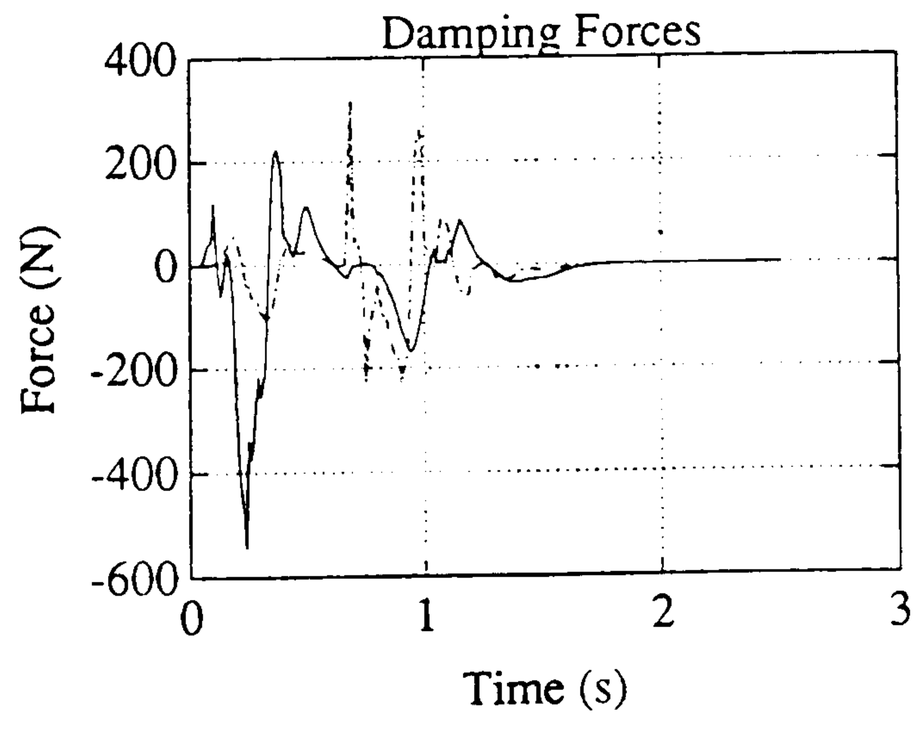


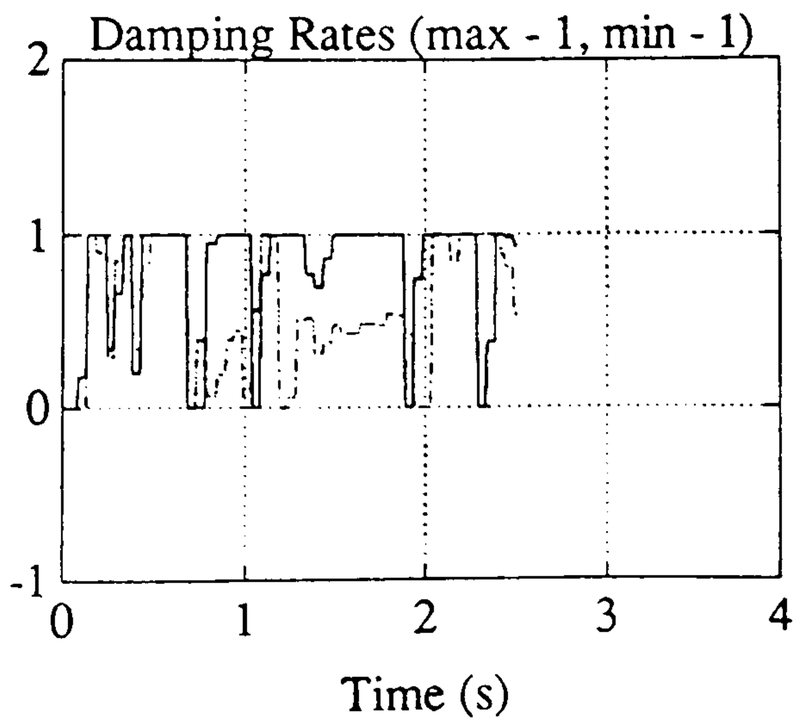


Figure 5.14c : Road Bump Input to Both Tracks

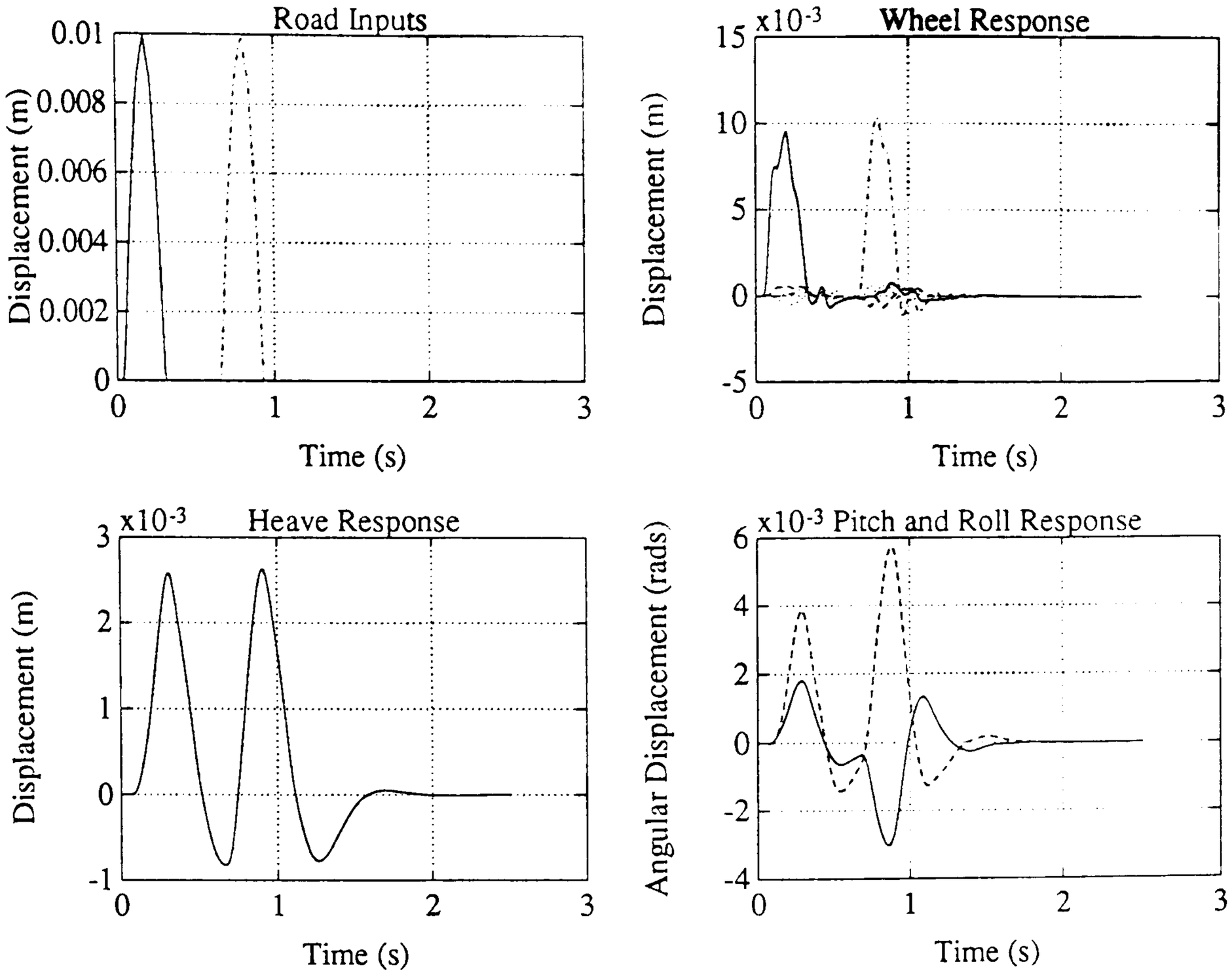


Figure 5.14d : Road Bump Input

to One Track Only

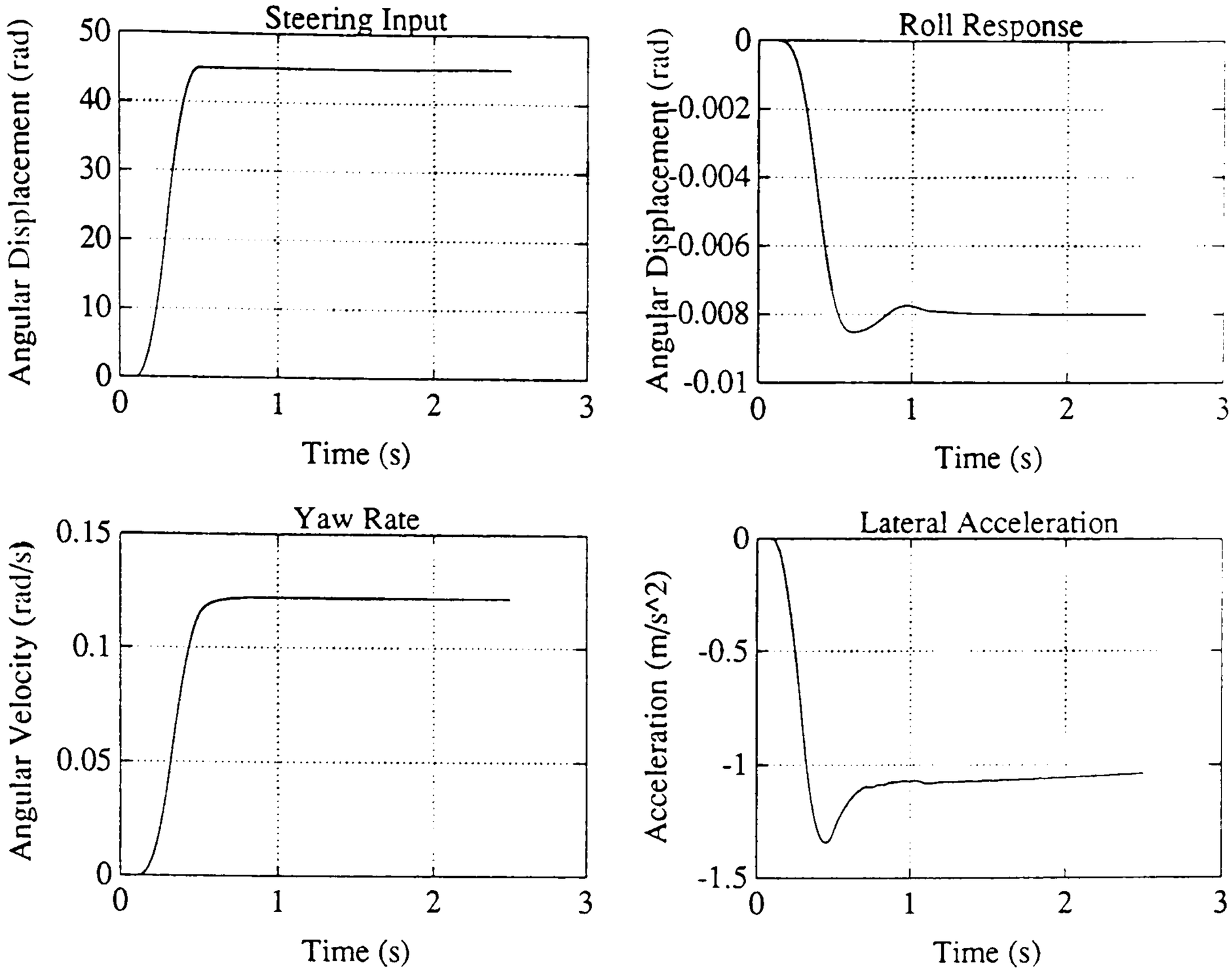


Figure 5.14e : Steering Input at 20 mph

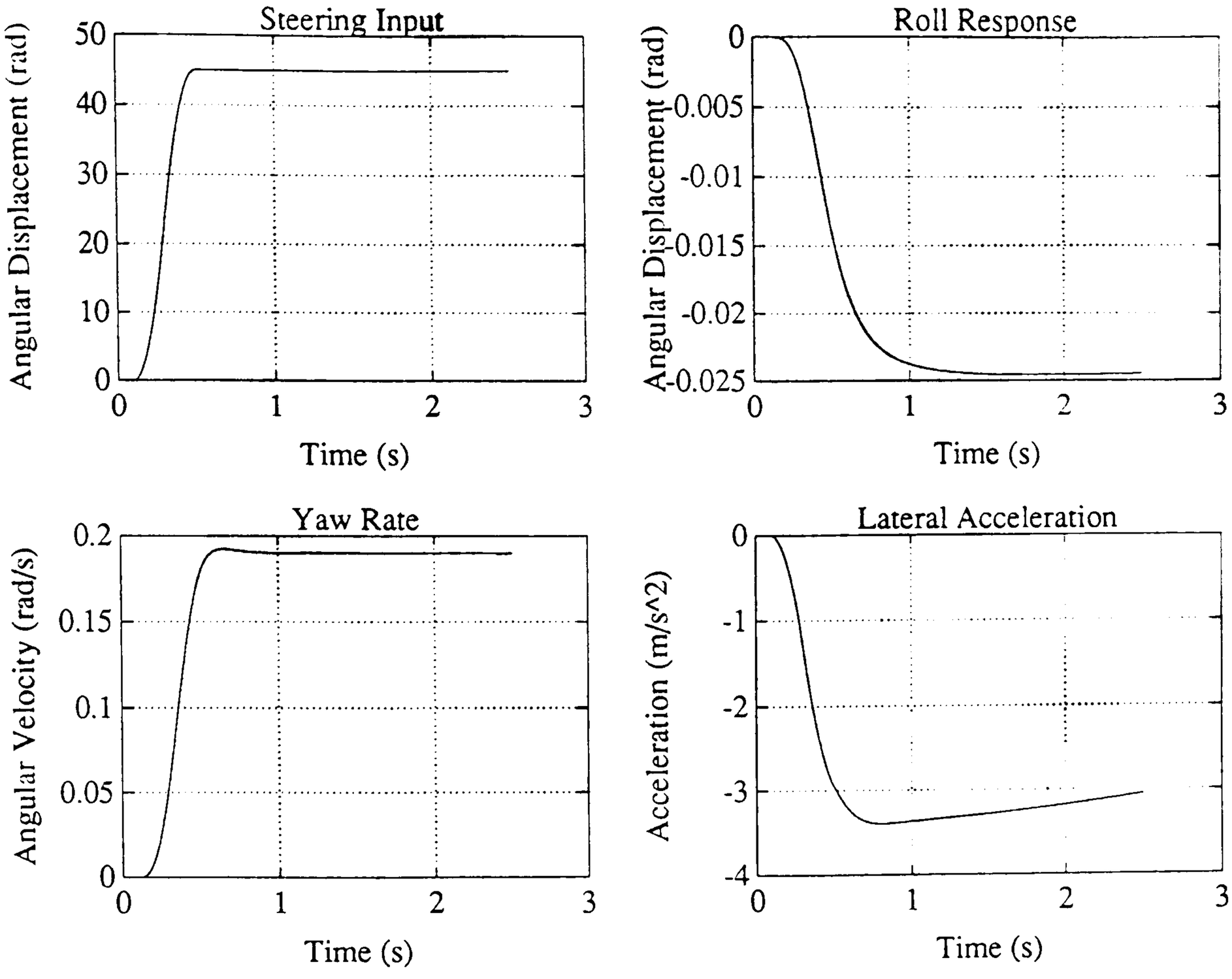


Figure 5.14f : Steering Input at 40 mph

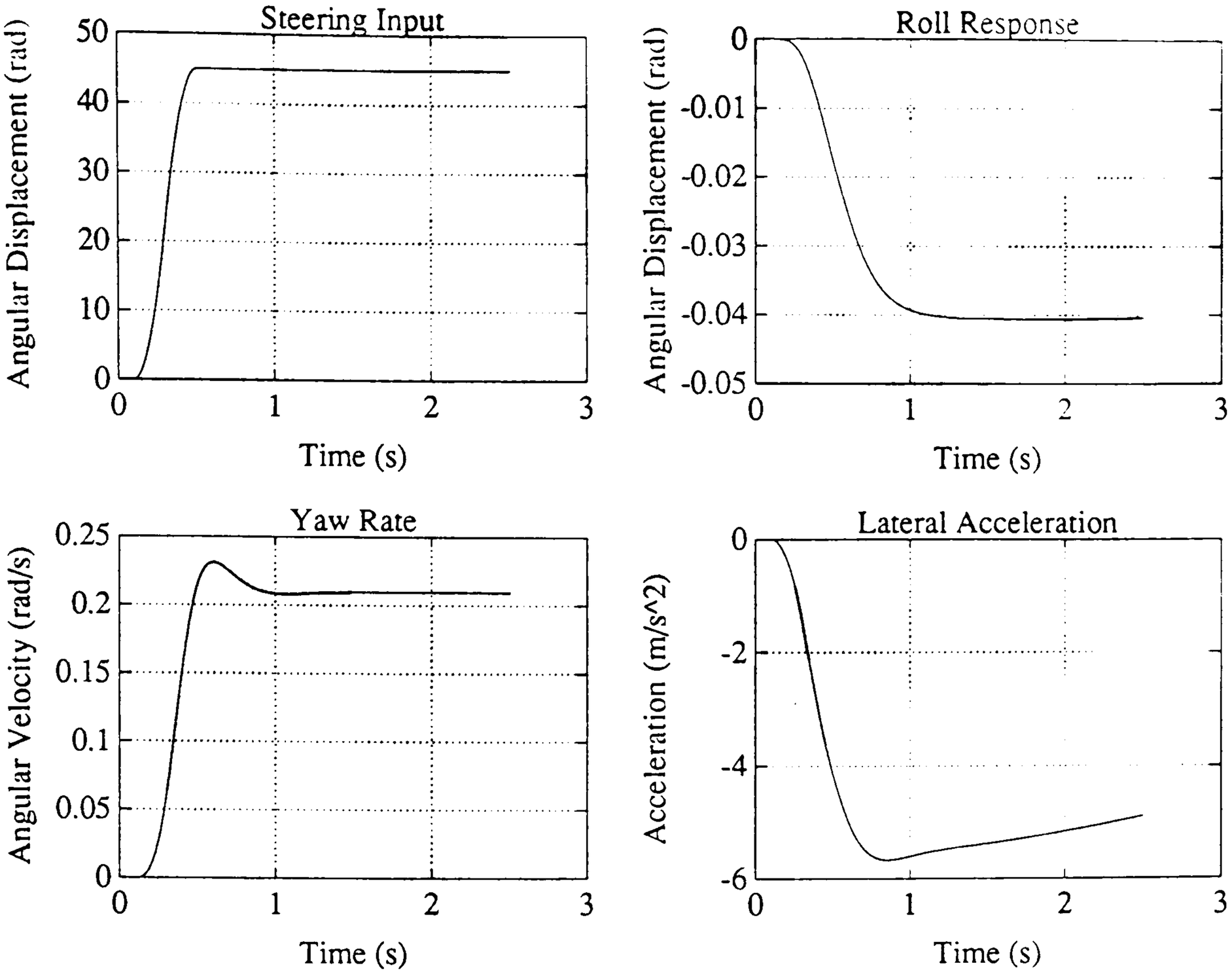


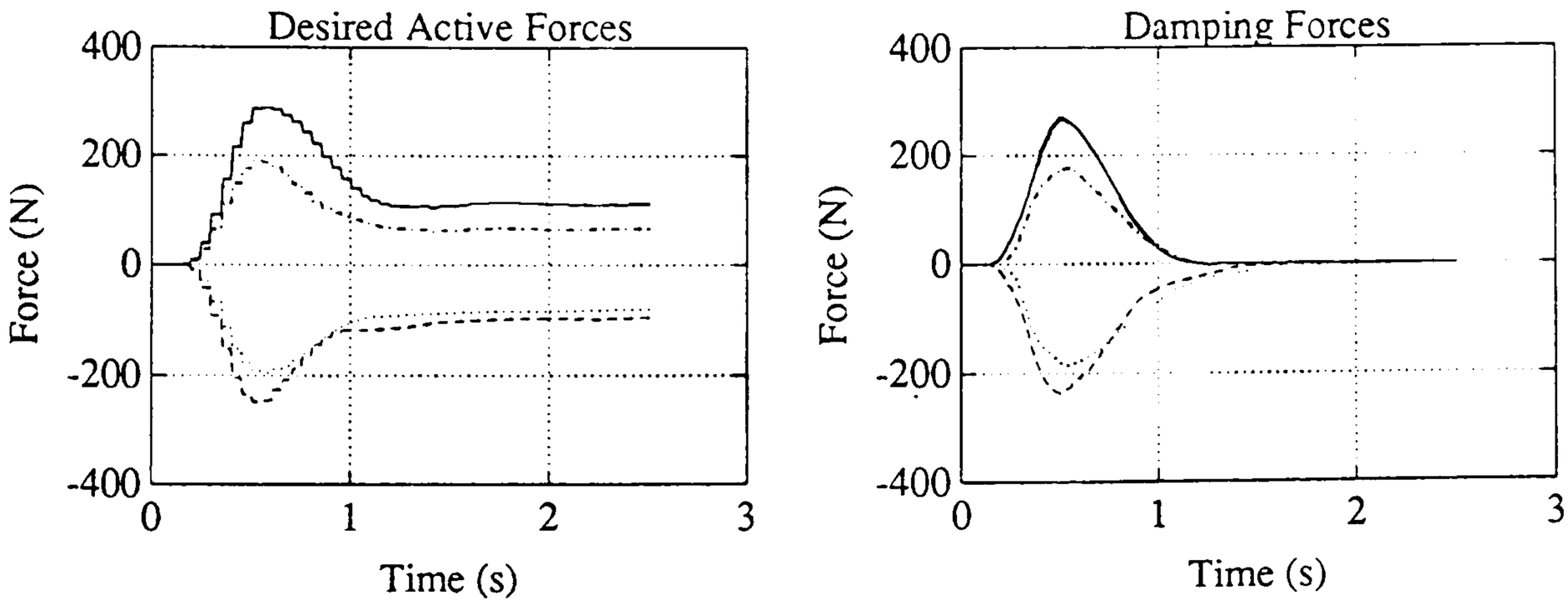


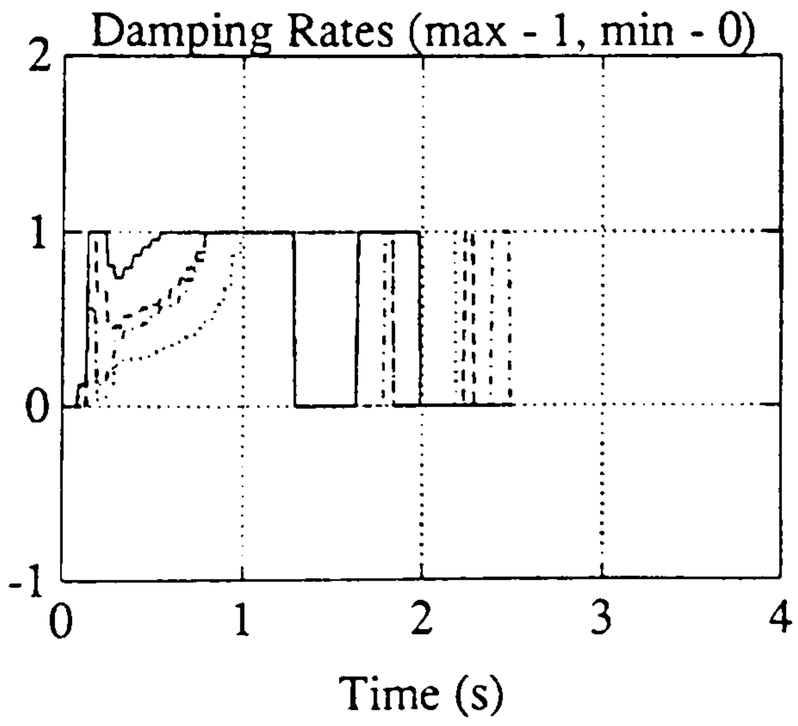


Figure 5.14g : Steering Input at 60 mph

# Chapter 6 : A Fuzzy Logic Approach to Variable Damping Control

## 6.1 Introduction

The study of ride control for variable damping suspension systems described in the previous chapter presented a dilemma regarding the control of continuously variable damping systems. For the discretely variable case, heuristic rule-based controllers were found to produce the best overall vehicle control characteristics. This finding was further corroborated with the poor performance results achieved for the continuously variable damping controller based on the ideal active feedback solutions. As a result, the preferred control strategy for continuously variable damping systems would be based on heuristic rule-based techniques.

The design of such a rule-based controller, however, presents a major problem in terms of complexity and therefore cost. The extension of the heuristic rule-base designed for the discretely variable damping system to give a continuous damper rate output would involve a significant increase in the number of required rules and thus overall complexity of the control strategy. This increase in size and complexity would also lead to significant software development and validation concerns. The resultant prohibitive cost and reliability issues therefore necessitate an alternative control design approach.

The application of fuzzy logic to the ride control problem for continuously variable damping systems offers a potential solution to this dilemma. Fuzzy logic offers a method of interpolating between rules as discussed by Constancis

& Harris [21]. Thus heuristic rule-based techniques could be applied to the variable damping system, with interpolation between the rules facilitated by fuzzy logic to provide the required continuous output.

Fuzzy control involves the application of a theory of vagueness or imprecision to conventional rule-based control techniques. This theory of vagueness is known as fuzzy logic and uses non-precise linguistic descriptions in order to represent human decision processes. A fuzzy control algorithm is based upon a set of rules in which linguistic values are assigned to the system variables, for example ***SPEED is BIG***, or ***ACCELERATION is SMALL***. Fuzzy logic provides a method of handling this non-precise linguistic information in rigorous mathematical manner. It is important to distinguish between uncertainty and the vagueness described here. The imprecision involved in fuzzy logic is due to a lack of sharp definitions and not to randomness.

A conventional rule-based controller consists of a set of precise rules, using Boolean logical functions such as ***AND, OR, NOT*** etc. In the case of rules based upon threshold comparisons as for the discretely variable damping controller, precise numerical variables are also involved. The important feature to note is that for Boolean logic the rule outputs are binary, that is they are either true or false. As a result a conventional rule-based controller can be visualised as a set of switches that select an output depending upon the combination of measured inputs. This process is illustrated in figure 6.1.

In comparison, fuzzy controllers also consist of a set of rules constructed by logical functions such as ***AND, OR, NOT*** etc. In the case of fuzzy controllers, however, the rules are vague and non-precise. The rules involve variables with linguistic values in place of the numerical values used in

traditional rule-based controllers. Also the rule outputs are not simply true or false, as with Boolean logic. Instead they are interpreted using fuzzy logic by assigning a measure of truth to the rule output.

The fuzzy logic controller can be illustrated by the diagram given in figure 6.2, which shows a similar process to the Boolean logic controller illustrated in figure 6.1. The precise inputs are replaced by vague linguistic variables. The rule base has been illustrated as a set of filters that assign a measure of truth to each of the rules depending upon the truth of the input variables. This process then results in vague output variables.

For a real control problem the controller inputs will have precise numerical values, and precise numerical outputs will be required, yet the fuzzy controller illustrated is shown to have vague inputs and outputs. In order to overcome this discrepancy two further steps, known as fuzzification and defuzzification, are added to the process. This revised fuzzy control process is shown in figure 6.3. Fuzzification is the interpretation of a precise numerical input into a fuzzy input, and defuzzification is the selection of a precise output value from the fuzzy controller output.

## 6.2 Historical Survey

The concept of a fuzzy set was first introduced by Zadeh in 1965 [118]. The motivation behind the development of fuzzy control theory was the fact that imprecision and vagueness are inherent in all forms of human thinking, especially in communication, recognition and abstraction. The theory of fuzzy sets provided a way of handling this vagueness and imprecision in a mathematically rigorous manner.

In subsequent work 1968 [119], 1973 [120], Zadeh extended the fuzzy set theory and developed fuzzy logic. This included the use of linguistic values for variables, conditional statements and algorithms to represent relations between fuzzy variables. It was the development of fuzzy logic and algorithms that illustrated the possible potential for the application of fuzzy techniques to system control problems.

Fuzzy control offers the ability to control a plant by means of vague linguistic rules of thumb in place of the usual precise numerical logical controllers. This allows the design of fuzzy controllers that mimic human operators whom in many cases provide better control than traditional automatic controllers. Fuzzy control suits the human understanding of plant dynamics and control objectives, and uses the same linguistic descriptions.

Following Zadeh's introduction of fuzzy control theory, several examples were published using laboratory scale plants or models to illustrate the performance of various fuzzy controllers. The first such application of fuzzy control was reported by Mamdani and Assilian in 1975 [67] and was concerned with the control of a steam engine. Fuzzy logic was used to automate a human operator's heuristic control strategy. The resultant fuzzy controller was compared to a well tuned DDC algorithm and was found to achieve better overall performance and was less sensitive to operating conditions. This study was followed by an investigation into a prescriptive, rather than the usual descriptive, design method for industrial process fuzzy controllers by Mamdani & Baaklini [68]. The starting point is a fuzzy controller containing a universally applicable set of rules and linguistic fuzzy subsets. The rules are then modified until satisfactory control is achieved. The automation of this procedure was

described and thus a self-regulating fuzzy controller is achieved. The results showed very rapid convergence and in cases where convergence was not achieved the control performance was still good.

Kickert and Van Nauta Lemke [56] also reported a successful application of fuzzy control to a warm water plant around the same time. The controller was based on the experience of a human operator, as in Mamdani's steam engine application, and the results were compared to a conventional PI controller. Three different fuzzy controllers were investigated since human operators found difficulty avoiding oscillations around the setpoint. The results again showed significant benefit in using a fuzzy controller in terms of speed of response to set point changes. However only one of the fuzzy controllers managed to reduce the oscillations around the setpoint.

The fuzzy logic traffic junction controller was an application described by Pappis, Ebrahim and Mamdani [86]. This addresses the use of fuzzy control for decision making in switching systems. Again the controller was based upon qualitative knowledge of the system and control instructions used by a human operator. The results were again compared to a conventional effective vehicle-actuated controller, and the fuzzy controller achieved better performance in terms of average delay of vehicles. In this study the improvement in results were not wholly attributed to the fuzzy controller, however the fuzzy theory did facilitate the convenience of linguistic descriptions of decisions.

The world's first reported industrial application of fuzzy control was developed by the Danish cement-plant builder F.L. Smidth with the aid of Jensen & Ostergaard of the Technology University of Denmark [106]. The controller was based on operator control strategies, and modified in subsequent

field trials. The resultant fuzzy controller achieved improved performance and a reduction in fuel consumption. Subsequently Blue Circle also developed a cement kiln fuzzy controller, LINKman [32]. They decided to drop model-based controllers since despite numerous attempts, satisfactory control performances were never achieved. Fuzzy control was attractive due to its ability to mimic an operator. The resultant controller, LINKman has been successfully applied to over twenty cement plants worldwide.

The two most notable industrial applications of fuzzy control in Japan were for a water purification process and for train control. The water purification controller was developed by Fuji Electric [106, 107] and was designed as a man-machine interactive controller allowing modification of the control details by an operator. The system was successfully field tested in 1983, and was shown to provide control equivalent to an experienced operator. The automatic train operating system [106, 107] was developed by Hitachi to control all aspects of acceleration, braking and stopping. This was compared to a conventional PI controller designed simply to minimise the speed error. The resultant fuzzy controller achieved superior control in terms of accuracy and also passenger comfort by reducing the speed changes. The first implementation was on the new Sendai railway in 1987.

Very recent studies include a fuzzy controller that uses voice commands to control a hovering helicopter, being developed by Sugeno [106, 107]. The control of a helicopter is an extremely difficult task due to the non-linearity and instability of the multivariable close-coupled system. Helicopters also have to fly in bad environmental conditions and are highly sensitive to external disturbances. Despite this the fuzzy controller achieved good performance.

In Japan the list of fuzzy control applications is extensive, covering a huge variety of commercially available products including water heaters, washing machines, cameras, as discussed at a recent seminar given by Sugeno [107]. Several papers have reviewed the applications to date [106, 112], and discussed the various design methods that have been used and problems and new areas that should be addressed.

The automotive industry has also shown interest in the use of fuzzy control, especially in Japan, where almost every manufacturer and area of the vehicle is involved. More recently European manufacturers have also become interested, as illustrated at the VW Fuzzy Logic Meeting [1, 14, 18, 78]. The most notable applications include automatic cruise control [106, 107], transmission control [106, 107], automatic braking systems [13, 17, 106, 107] and engine control [1, 106, 107]. Nissan's cruise control [106, 107] unusually shows no significant improvement over conventional controllers, apart from the use of fewer throttle changes. The interesting feature is that it is self-tuning, allowing the same controller to be used on all model variants, and providing adaption to different driving conditions. The new Mitsubishi Gallant has six fuzzy logic controllers on board for transmission control, four wheel drive, four wheel steer, suspension control, air-conditioning and traction control [107].

In the work described here the system under consideration is a continuously variable damping system for a passenger car. The study is aimed as an illustration of the feasibility of fuzzy control for suspension control in general and this system in particular. As a result the controller was an initial design without tuning to provide the best possible performance. Extensive investigations into the most suitable design method were also not carried out.

Instead the most widely reported methods were used for simplicity.

## 6.3 Fuzzy Suspension Control Motivation

The application of fuzzy logic techniques to automotive suspension control overcomes the two major difficulties encountered with traditional control design techniques. The first is a general problem found with all model-based linear control techniques considered in this work. Unlike many other control applications, plant uncertainty is not the most significant difficulty involved in automotive suspension control. In fact the system dynamics are very well understood, although removing the need for accurate yet manageable control analysis models is an obvious advantage. For suspension studies the major obstacle to control design is in the definition of the control objectives.

Historically the performance requirements of an automotive suspension system have tended to be described and assessed in a subjective manner. Vehicle development has been predominantly development led and thus based upon subjective evaluations and not objective measurements. Translating the subjective suspension performance requirements into precise objective criteria is a difficult task.

Consider for example the ride control study using linear state space control techniques described previously. The application of each different technique required the objectives to be restated in various forms. For the quadratic regulator study the ride objectives were expressed in terms of minimising sprung mass accelerations and tyre load variations. Pole placement techniques, however, used frequency and damping criteria to design the ride controller. Although both of these descriptions are reasonable, neither is very

accurate or complete. An objective description of vehicle handling performance objectives is significantly more complex.

This problem of subjective control objectives is easily addressed by the use of fuzzy techniques. In fact fuzzy theory was designed to accommodate the type of vague linguistic descriptions associated with vehicle subjective assessments. This is similar to the use of fuzzy control in order to replicate the control achieved by operators in process control. A subsequent advantage is that system experts, vehicle dynamics and ride and handling experts in this case, design the controller, in place of the usual specialised control engineers. This is especially advantageous for the automotive industry, as control engineering as a discipline is relatively new within the industry, and so control engineering expertise is limited.

The second problem encountered in the suspension control studies discussed so far is specific to the control of variable damping systems. The previous chapter indicated that rule-based controllers were the preferred choice for the discretely variable damping case. However an extension of the rule-based controller to the continuously variable damping case was shown to be prohibitively complex and costly. The reason for this is that the rule-base must include a rule or set of rules covering every combination of inputs giving rise to every possible output value. For a discretely variable damper with two or three rate settings this is a feasible proposition. However in order to realistically represent a continuously variable damper several more possible output values would be required. The result would be a significant increase in the number of rules required. The increase in controller complexity and memory requirements leads to increased costs, which is an important consideration in automotive

design.

Fuzzy logic controllers offer the ability to infer output values for combinations of inputs values that lie 'between' the rules, as described by Harris [21]. The resultant fuzzy controller consists of a relatively small number of rules and yet still offers the full potential benefit of a continuously variable damper.

## 6.4 Fuzzy Continuously Variable Damping Control

In order to design a fuzzy ride controller for the continuously variable damping suspension system the conventional rule-based controller described for the discretely variable system was used as a starting point. The inputs for the fuzzy controller are sprung mass vertical and lateral (maximum of calculated and measured) acceleration, steering rate and vehicle speed. Again the controller output is the continuously variable damper rate taking any real value between zero and one, where zero gives the minimum damper rate and one the maximum.

The first step in designing a fuzzy controller is to write a set of fuzzy rules involving variables with linguistic values, such as ***BIG SPEED***. In many cases the rules will be obtained from an operator with experience of successful plant control, as in many of the studies described [32, 56, 67, 86]. In the case of suspension control, as with many other automotive applications, the rules will be written by the relevant vehicle experts. In the case of suspension control, vehicle ride and handling experts will be involved. For this study the rules were based upon the precise rules used for the discretely variable damping case. Basically the precise thresholds in the traditional rule-based controller were

replaced by vague linguistic values for the inputs. The resultant set of fuzzy rules is given in table 6.1.

The next step in the design process is to define the linguistic terms used as values to the input and output variables, such as ***BIG SPEED***. In fuzzy control we use fuzzy subsets to define the linguistic values for variables, defined as follows.

A **fuzzy subset** ***A*** of a universe of discourse ***U*** is characterised by a **membership function** $\mu_A: U \rightarrow [0,1]$ which associates with each element ***u*** of ***U*** a number $\mu_A(u)$ in the interval [0,1] which represents the **grade of membership** of ***u*** in ***A***.

For the fuzzy ride control example we specify the fuzzy subsets for each of the input and output variables used in the rules, for example ***BIG, MEDIUM*** and ***SMALL*** for the input ***SPEED***. Each fuzzy subset requires a membership functions defined over the range of possible input values. These membership functions can take any shape, and can be described by a continuous function [56] or by discrete points [67, 68, 86]. The membership functions defining the fuzzy subsets required for this example are shown in figures 6.4. In this work the membership functions are described by discrete points over the range of possible values. For simplicity the membership functions are all essentially of the same shape, although they are not all evenly spread along the range of input values.

It should be noted that for the output variable, the fuzzy subsets lying at the extremes of the universe of discourse, ie. ***SMALL and BIG DAMPING***, are extended beyond the range of possible output values. This can be seen from

figure 6.4, showing the output fuzzy subsets for this example. This is a requirement for systems using the centroid method of output selection, and enables the maximum and minimum values of the output to be inferred.

Having defined the variable linguistic values in terms of fuzzy subsets, the interpretation of the fuzzy rules is the next step. The rules given in table 6.1 consist of various fuzzy subsets linked by logical functions similar to those found in Boolean logic. These functions require the following definitions from fuzzy set theory.

The **union** of two fuzzy subsets $A$, $B$ of $U$ is denoted by $AUB$ or $A+B$, and has membership function $\mu_{AUB}(u)$ or $\mu_{A+B}(u)$,defined by,

$$\mu_{A\cup B}(u) = \mu_{A+B}(u) = \max[\mu_a(u),\mu_B(u)] \qquad (6.1)$$

As seen the union corresponds to the connective ***OR***.

Similarly the intersection of $A$, $B$ of $U$ is denoted by $A\cap B$ or $A.B$, and has membership function $\mu_{A\cap B}(u)$ or $\mu_{A.B}(u)$, defined by,

$$\mu_{A\cap B}(u) = \mu_{A.B}(u) = \min[\mu_A(u),\mu_B(u)] \qquad (6.2)$$

and corresponds to the connective ***AND***.

Again these definitions are clarified by a simple example. Consider the two fuzzy sets ***BIG*** and ***MEDIUM*** defined for the fuzzy variable ***SPEED***, shown in figure 6.4. The union and intersection of these fuzzy sets correspond to the fuzzy sets ***BIG or MEDIUM SPEED*** and ***BIG and MEDIUM SPEED*** with membership function shown in figure 6.5.

The most important logical function used in the rules are the ***if*** statements.

**Fuzzy conditional statements**, such as

***if A then B***

are defined as fuzzy relations between fuzzy sets as follows.

A **fuzzy relation** R from a set U to a set V is a fuzzy set on the Cartesian product ***UxV*** characterised by a bivariate membership function $\mu_R(u,v)$, indicating the extent to which the relation is true for ***(u,v)***. The Cartesian product of two fuzzy sets can be defined in many ways, and the definition used in this study is given as follows. For fuzzy subsets ***A*** of ***U*** and ***B*** of ***V*** the Cartesian product is denoted by ***AxB***, with bivariate membership function $\mu_{AxB}(u,v)$, defined by

$$\mu_R(u,v) = \mu_{AxB}(u,v) = \min[\mu_A(u),\mu_B(v)] \qquad \textbf{(6.3)}$$

For example take the simple rule

***if VACC is BIG then DAMP is MED***

with the fuzzy sets as defined in figure 6.4. The resultant fuzzy relation representing this rule then has the bivariate membership function given in figure 6.6.

For a combination of fuzzy conditional statements such as

***if A1 then B1***

***else***

***if A2 then B2***

we define the fuzzy relations ***R1*** and ***R2*** such that the above rules become

***if R1***

***else***

***if R2***

and then use the union operator to define the fuzzy set denoted by ***R1UR2*** with membership function $\mu_{R1UR2}(u,v)$, defined by,

$$\mu_{R1\cup R2}(u,v) = \max[\min[\mu_{A1}(u),\mu_{B1}(v)],\min[\mu_{A2}(u),\mu_{B2}(v)]] \qquad \textbf{(6.4)}$$

Again as an example take the combination of the two rules

***if VACC is BIG then DAMP is MED***

***else***

***if VACC is MED then DAMP is SMALL***

Figures 6.6 and 6.7 give the fuzzy relations representing the individual rules, and figure 6.8 shows the fuzzy representation of the combination of both rules. More complex statements such as those found in the fuzzy rules given in table 6.1 can be interpreted by the use of combinations of these functions.

We now have defined a range of fuzzy subsets for each input and output variable, together with a set of fuzzy rules. In other words we have the complete fuzzy controller description in the form

***if INPUTS then OUTPUT***

Finally we require a method of inference to obtain an output for a given input, ie given input A' what is the corresponding output B'.

The **compositional rule of inference** states that if ***R*** is a fuzzy relation from ***U*** to ***V*** and ***A*** is a fuzzy subset of ***U***, then the fuzzy subset ***B*** of ***V*** which is induced by ***A*** is defined by the **composition** of ***R*** and ***A***, denoted ***AoR*** with membership function $\mu_{AoR}(v)$

$$\mu_B(v) = \mu_{AoR}(v) = \max_u \min[\mu_A(u),\mu_R(u,v)] \qquad \textbf{(6.5)}$$

Take the fuzzy relation with membership function shown in figure 6.8

representing the two rules

***if VACC is BIG then DAMP is MED***

***else***

***if VACC is MED then DAMP is SMALL***

Supposing the input fuzzy set has membership function shown in figure 6.9. The application of the compositional rule of inference gives a fuzzy output set with membership function given in figure 6.9.

This rule of inference completes the description of the fuzzy controller. We now have a method of inferring an output fuzzy set for any given combination of input fuzzy sets. However for real control applications such as the suspension control study under consideration, the controller inputs are precise measurements and not fuzzy subsets. As a result the first step in the control process is fuzzification in which each precise measured input is interpreted as a fuzzy subset. The most obvious and commonly used method is to interpret the input $u_o$ as a fuzzy input set $A$ with all membership function values $\mu_A(u)$ equal to zero except $\mu_A(u_o)$ which is equal to one,

$$\begin{aligned} \mu_A(u) &= 0 \qquad u \in U,\ u \neq u_o \\ \mu_A(u_0) &= 1 \end{aligned} \tag{6.6}$$

Finally for our input $u_o$ we have inferred an output fuzzy subset $B$ of $V$ and a precise output must be obtained. There are several different ways of choosing the output, the two most popular being maximum and centroid. The first method involves choosing the value of the output fuzzy set with the maximum membership value. In the event of an output fuzzy set having a non-unique maximum membership function value, the mean of the maxima is chosen. The second method looks for the centroid of the membership values.

In the literature both methods have been used. All of the early applications used the mean of maximum output selection method [56, 68, 86], whereas later studies have used the centroid method. In recent studies this has been extended to use some form of weighted mean for the output selection [106]. A comparison of the different output selection methods with conventional controllers is discussed by Tong [112]. The mean of maximum method has been compared to a multi-relay, whereas the centroid method is analogous to a PI controller. Constancis & Harris [21] also compared a fuzzy controller to a PI controller.

In this study both options for output selection have been considered, ie maximum and centroid for comparison. As previously mentioned if the centroid output selection method is to be used, the definition of output fuzzy set membership functions must extend the sets beyond the extremes of the range of possible output values to complete the function shapes. This ensures that the extreme values of the output can be achieved. This is illustrated in the previous example with the resultant output fuzzy subset given in figure 6.9. The mean of maximum output selection method would give 0 as the output value, and the centroid method would give 0.18. In the event of a set of inputs lying exactly on a rule whose output is ***SMALL DAMP***, the centroid method would only give the maximum damping rate as its output if the output fuzzy set was defined beyond the range of values to complete the membership function shape.

This description of the inference method used in fuzzy control involves the computation of relation matrices as illustrated in figures 6.6,6.7. The relation matrices are two dimensional as they represent rules with one input and one output. For the specific controller under investigation here all of the

rules involve four inputs and one output, leading to five dimensional relation matrices. This would be very costly in terms of computation and memory requirements. An alternative method is to take the definition of fuzzy input set membership functions for precise measured inputs given in equation 6.6, and use this to simplify the general compositional rule of inference. The membership function derived for a general output fuzzy set was given in equation 6.5, and this would be simplified to

$$\mu_B(v) = \mu_{A \circ R}(v) = \mu_R(u_0, v) \tag{6.7}$$

The application of this method, in contrast, involves the manipulation of fuzzy sets as opposed to fuzzy relation matrices. The reason for this is that instead of calculating the relation matrices representing the rules for a general set of fuzzy inputs, and then inferring the output for specific inputs, the specific inputs are used from the start.

In order to illustrate, again consider the example

***if VACC is BIG then DAMP is BIG***

***else***

***if VACC is MED then DAMP is SMALL***

and suppose the fuzzy subset representing a real input has the membership function given in figure 6.10. Each rule can then be represented by a fuzzy set with a membership function as shown in figures 6.10, in place of the relation matrices with bivariate membership functions as before. The combination of the rules, again involving sets in place of relation matrices, has membership function shown in figure 6.10. This can be checked against the previously described method by using the general compositional rule of inference for the

input set given in figure 6.10, and the relation matrix representing the combination of rules given in figure 6.8.

## 6.5 Simulation

The two fuzzy controllers discussed were included into the full vehicle model with continuously variable damping system as described in the previous chapter. In order to ensure direct comparison between both sets of results, the same controller parameters such as sampling instant and delays were used. The fuzzy controllers were modelled in a similar manner to the conventional rule-based controller.

Once the models for both controllers using different output selection methods were complete, the same road and steering input simulations were performed, and the results are included in figures 6.11, 6.12. Figures 6.11a-g show the results for the fuzzy controller using the mean of maximum output selection method, and figures 6.12a-g for the centroid method.

The same vehicle response parameters have been plotted as for the previous simulation results, together with the simulation inputs. The vehicle response parameters include the wheel vertical responses and the sprung mass heave, pitch and roll response for the road input simulations. Also the measured sprung mass vertical acceleration plus the resultant damper rate output are plotted. For the steering simulation results, the vehicle performance is illustrated by showing the sprung mass roll, yaw rate and lateral acceleration. Again the measured controller inputs of lateral acceleration, steering rate together with the output damper rate are shown.

## 6.6 Discussion of Results

The performance of the fuzzy controllers described will be discussed in terms of their absolute results, and in comparison with the results obtained in the previous chapter, for both types of variable damping system, discrete and continuous.

The first comparison to be discussed was between the two output selection methods used, mean of maximum and centroid. Figures 6.11a-g show the vehicle performance results for the mean of maximum output choice, and figures 6.12a-g show the centroid results. An initial brief comparison of these results shows very little difference between the performance of the controllers for the output selection methods, however there are one or two minor but important variations.

For the road step input the comparison between the output selection methods shows that the mean of maximum choice, figure 6.11a, gives marginally less sprung mass heave and pitch overshoot and significant improvements in subsequent oscillations. The wheel response also has marginally reduced oscillations for the mean of maximum method. A comparison of the damper rate output shows that the mean of maximum output selection choice achieves less variation in the rate than the centroid method, which results in these minor improvements in response. A comparison of the output selection methods for the other three road inputs, given in figures 6.11b-d, 6.12b-d, show negligible differences.

The vehicle response results for the steering simulations also show very similar results for both output selection methods, with the most significant

difference seen in the first steering input, figure 6.11a, 6.12a. In contrast to the road input simulation results, the steering results show that the centroid selection choice is marginally better. This method achieved better vehicle sprung mass response in terms of reduced oscillation in the roll angle and lateral accelerations. A comparison of the damper rate settings selected throughout the simulations illustrated in figures 6.11e,f 6.12e,f show that the major difference between the control strategies relates to the damper rate selected after satisfactory control of the transient response has been achieved. The centroid method, figure 6.12e, returns to a higher damper rate during the cornering manoeuvre, whereas the mean of maximum method, figure 6.11e, returns to the minimum damper rate as soon as the transient is over. This advantage would be greater for a complete cornering simulation in which the vehicle returned to zero steering input, since the controllers would begin the second half of the manoeuvre at different damper rates. Figures 6.11f and 6.12f show the opposite trend, however the difference between the resultant vehicle responses is negligible.

The overall results for this brief illustrative fuzzy control study shows that for this application the output selection methods have minimal effect on the control performance. However the trend shows that the mean of maximum method is advantageous for road inputs and so provides better comfort and isolation performance. In contrast the centroid selection choice puts the emphasis on steering response and therefore stability and handling behaviour.

In the previous chapter, continuously variable damping system controllers were designed from the ideal active solutions as opposed to the direct design method described here. A comparison of these results with the

fuzzy controller results obtained shows that for several reasons the fuzzy control design method is superior. The active results are shown in figures 5.12a-g for the linear quadratic regulator design, 5.13a-g for pole placement , and figures 5.14a-g for frequency domain techniques. For this comparison the best fuzzy control results will be considered, that is the mean of maximum results for the road inputs, and centroid for the steering simulations.

The first obvious difference in the fuzzy control results compared with the previous continuously variable damping results is seen in the damper rate switching behaviour. The fuzzy controllers utilise the full continuous variability of the damper. The damper rates plotted in the fuzzy results shown in figures 6.11, 6.12 are discretely stepping between output values only because the controller is discrete and so the output is updated every sampling instant. There is no actual restriction on the damper rate values allowable between the minimum, zero and the maximum, one. The results from the earlier continuously variable damping study shown in figures 5.12-5.14 gave rapid damper switching between the maximum and minimum damper rates, for the majority of the simulations.

In other words the controller only achieves a discretely switching strategy, despite the complexity involved in the design process and resultant algorithm. The other area of concern regarding the damper switching behaviour is the high frequency of large rate changes leading to the possibility of noise problems.

The resultant vehicle performance characteristics however, do not lead to such definite conclusions. For the first road input, the best fuzzy control result is obtained using the mean of maximum output selection method and is shown

in figure 6.11a. Figures 5.12-5.14a show the simulation results for the controllers based on active linear quadratic regulator, pole placement and frequency domain solutions. A comparison of these results indicates reduced initial heave overshoot for the fuzzy controller, together with increased subsequent oscillations for the wheel and sprung mass responses.

The other road inputs, with results given in figures 6.11b-d for the fuzzy controller, and figures 5.12-5.14b-d for the active results, produce very similar vehicle performance results for both types of controller, with the fuzzy control giving increased oscillations. The fuzzy controller however does provide one response advantage over the active based designs. The results obtained for the designs using linear state space techniques gave some unusual vehicle dynamic characteristics. As an illustration figure 5.12c shows the response of the controller based on a linear quadratic regulator design, and the sprung mass heave and pitch response is unexpected. Despite achieving reduced overshoot and oscillatory behaviour compared with the fuzzy control, unexpected dynamic behaviour may cause driver unease or undesirable reactions. The drivability of the resultant systems is of prime importance in automotive design. The pole placement derived controller also exhibits unusual responses to road inputs. The inputs involved in the first three road input simulations contain heave and pitch constituents. However figures 5.13a-c show that the pole placement derived controller produces vehicle roll response.

A comparison of the steering simulations results indicates the fuzzy controller as the better design reasonably conclusively. Figures 6.12e-g show the fuzzy controller results, and figures 5.12-5.14e-g show the results for the controller based on active solutions. The fuzzy controller produces significantly

less overshoot and oscillatory behaviour in all three sprung mass response characteristics, roll yaw rate and lateral acceleration. For the frequency domain derived controller the results are not so conclusive, however the fuzzy controller does achieve marginally smoother responses.

Overall the fuzzy controller is superior to the control algorithms based on ideal active solutions. The major benefits are in the vehicle response to steering inputs, and in the resultant damper switching behaviour. Also some of the state space derived controller simulation results show unusual dynamic responses which are not desirable.

Finally the fuzzy control results described here were compared to the simulation results obtained for the rule-based control of the discretely variable damping system previously discussed. Figures 5.11a-g show the rule-based control results, and these were compared to the mean of maximum output selection controller for the road inputs, shown in figure 6.11a-d, and the centroid choice controller for the steering simulations, in figures 6.12e-g.

This comparison, however, does not show a significant improvement in the vehicle response as expected, and in some cases the fuzzy controller is worse. For the road step input the fuzzy controller results in figure 6.11a indicate reduced initial heave overshoot, but increased subsequent oscillatory behaviour in the wheel and sprung mass responses compared with the discrete results shown in figure 5.11a. The other three road input simulations also show increased oscillations for the fuzzy controller in all vehicle response parameters, shown in figures 6.11b-d, and 5.11b-d.

For the steering inputs there is very little difference in the controller performance, although there is marginally more oscillation in the fuzzy

controller response for the first steering input, as illustrated in figures 6.12e-g and 5.11e-g.

As a result the rule-based controller for the discretely variable damping system, gave better vehicle performance than the fuzzy control of the continuously variable damping system. The main reason for this is purely the fact that the rule-based controller was fully developed and tuned. The fuzzy controller, in contrast, was designed as a feasibility study of the design method and was not tuned to give the best possible performance.

Tuning this fuzzy control algorithm would be achieved by varying the fuzzy subsets on the input and output variables. In this case the maximum improvement would be achieved by first tuning the output fuzzy subsets. As previously mentioned, the minimum damper rate is very soft, and as a result is only suitable for conditions with no steering or other inputs, and minimal road inputs. This is illustrated by the fact that the fuzzy controller compared badly with the rule-based controller when both algorithms had chosen the softest rate setting. For example the third and fourth road inputs giving the results shown in figures 6.11c,d for the mean of maximum output selection fuzzy controller. Figures 5.11c,d show equivalent results for the rule based controller. For both of these road input simulations the softest rate setting is chosen for the majority of the simulation in both control algorithms, and yet the rule-based control gives superior vehicle performance. This must be due to the softest rate setting for the discretely variable damper being firmer than the minimum setting for the continuously variable damper.

A major improvement in performance for the fuzzy controller would be achieved by moving the small damper rate subset to be centred around a larger

rate, and moving the other subsets accordingly. From the work and results described to date, a significant improvement in vehicle performance would be expected.

## 6.7 Conclusions

Despite the limited experience of one simple example, it is easy to see the potential advantages of fuzzy control techniques for automotive suspension control. The vague linguistic nature of fuzzy algorithms suits the subjective description of suspension performance requirements used within the automotive industry. The heuristic nature also allows the control system specification and design to be undertaken by vehicle dynamics engineers, the system experts in this application. This is a major advantage for the automotive industry since control engineering is a relatively new discipline and so expertise is not prevalent.

Rule-based in contrast to model-based controllers also offer the advantage that the control performance is independent of a representative system model. Although vehicle dynamics are relatively well understood, they are highly non-linear and as a result any control strategy whose performance relies upon linearised or otherwise simplified models will have drawbacks. Full non-linear vehicle models would be used in the fuzzy control design and evaluation process, however the resultant performance would not be compromised by any model limitations. The automotive cost considerations also preclude the use of any controller requiring complex plant models.

Fuzzy control has another major advantage over conventional rule-based control for the specific example considered here. The continuously variable

damping system control would require a significant increase in the number of rules required over the discretely variable case. Fuzzy control provides the ability to infer the control output for a combination of inputs that lie 'between' the rules. The advantage is then reduced complexity and so development time, resulting in a cheaper system.

Since the example described here was a feasibility study of the design method and did not involve extensive algorithm tuning, the vehicle performance results are a little deceptive. However they did show a marked improvement over the previously described continuously variable damping control strategies based upon the ideal active solutions. The response to steering inputs plus the damper switching behaviour were the most significant advantages. Compared with the rule-based control of the discretely variable damping system the fuzzy results did not compare so favourably. However with equivalent levels of algorithm tuning the performance could be improved significantly.

| | |
|---|---|
| *if SPEED is BIG and* | *LATACC is VERY BIG or BIG or MED or SRATE is VERY BIG or BIG or MED* |
| *then DAMP is BIG* | |
| *else* | |
| *if SPEED is BIG and* | *LATACC IS SMALL and SRATE IS SMALL* |
| *then DAMP is MED* | |
| *else* | |
| *if SPEED is MED and* | *LATACC is VERY BIG or BIG or SRATE is VERY BIG or BIG* |
| *then DAMP is BIG* | |
| *else* | |
| *if SPEED is MED and* | *VACC is BIG or LATACC and SRATE are MED or LATACC is MED and SRATE is SMALL or LATACC is SMALL and SRATE is MED* |
| *then DAMP is MED* | |
| *else* | |
| *if SPEED is MED and* | *VACC is SMALL or MED and LATACC is SMALL and SRATE is SMALL* |
| *then DAMP is SMALL* | |
| *else* | |
| *if SPEED is SMALL and* | *LATACC is VERY BIG and SRATE IS VERY BIG* |
| *then DAMP is BIG* | |
| *else* | |
| *if SPEED is SMALL and* | *VACC is BIG or MED or LATACC and SRATE are MED or BIG or LATACC is MED or BIG and SRATE is SMALL or LATACC is SMALL and SRATE is MED or BIG* |
| *then DAMP is MED* | |
| *else* | |
| *if SPEED is SMALL and* | *VACC is SMALL and LATACC is SMALL and SRATE is SMALL* |
| *then DAMP is SMALL* | |

*where*

*LATACC - lateral acceleration*
*VACC - vertical acceleration*
*SRATE - steering rate*

Table 6.1 : Fuzzy Rules

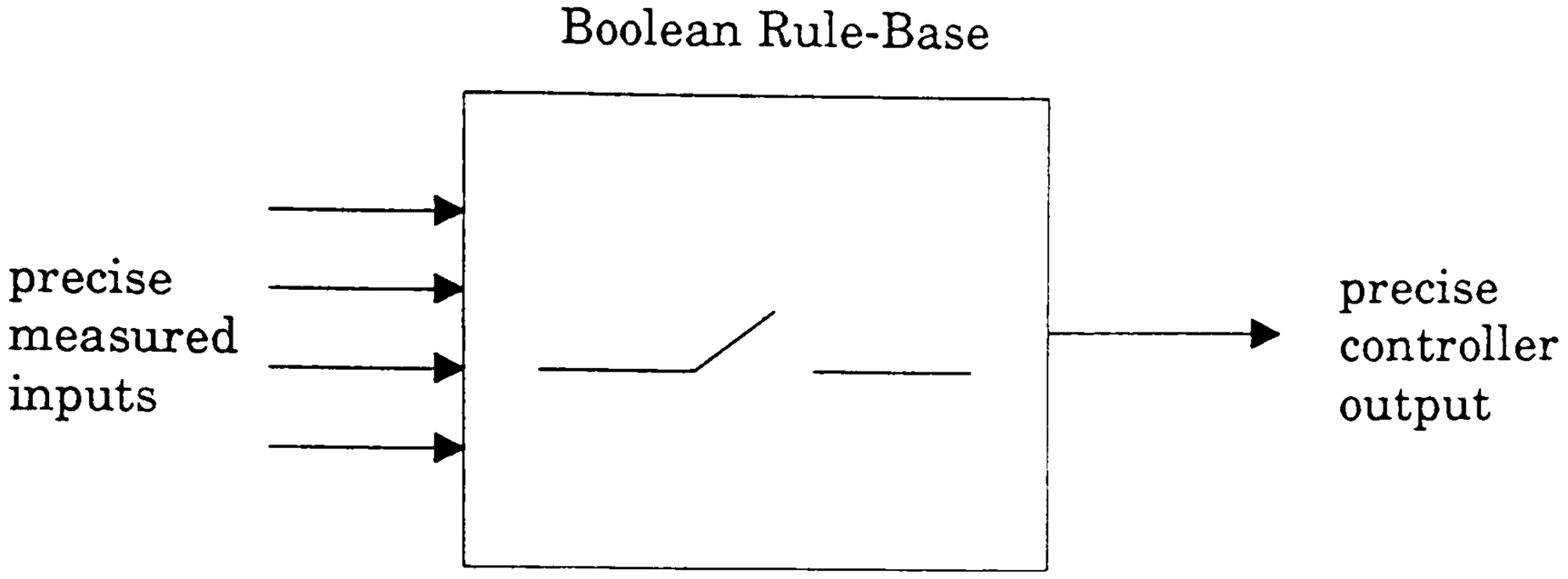


Figure 6.1 : Boolean Logic Representation

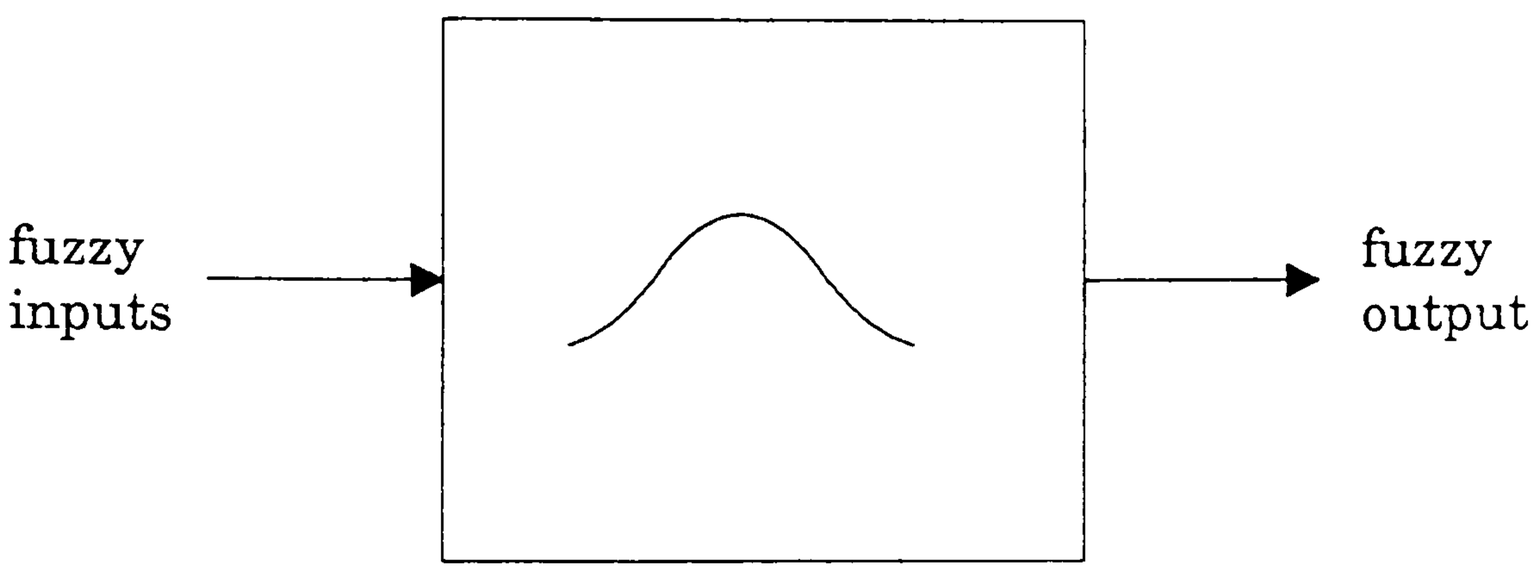


Figure 6.2 : Fuzzy Logic Respresentation

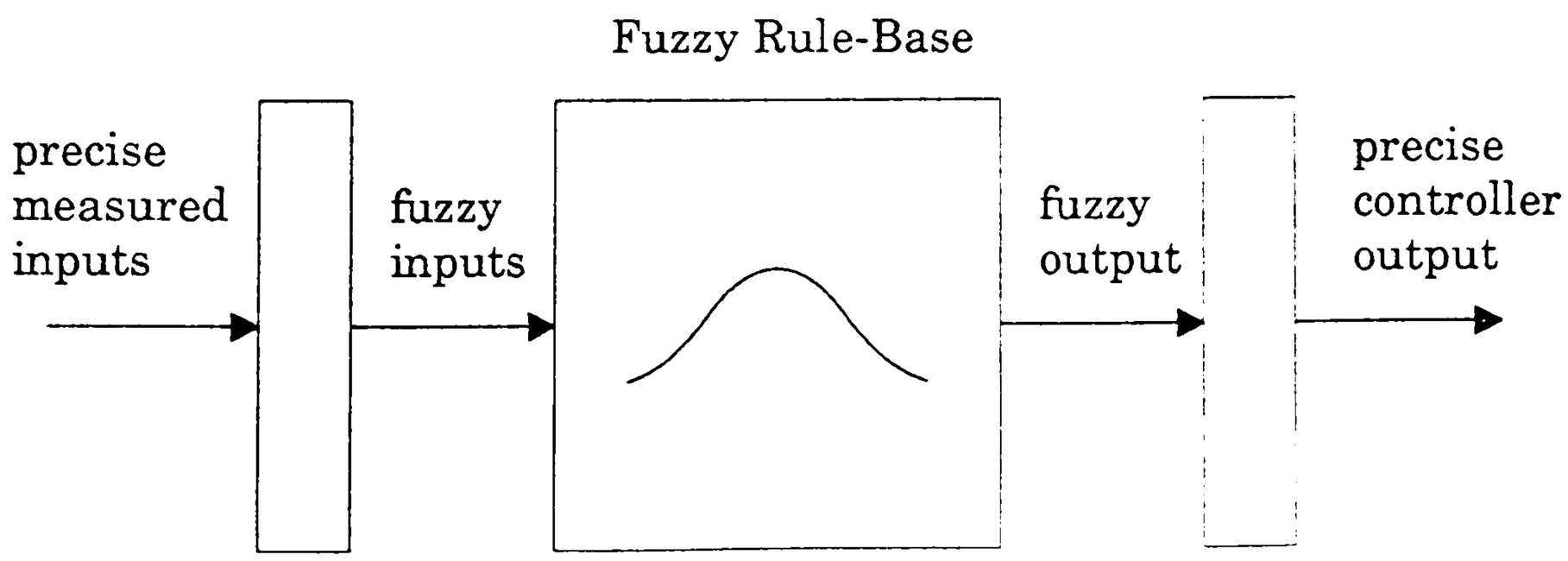


Figure 6.3 : Fuzzy Logic Control with Precise Inputs and Outputs

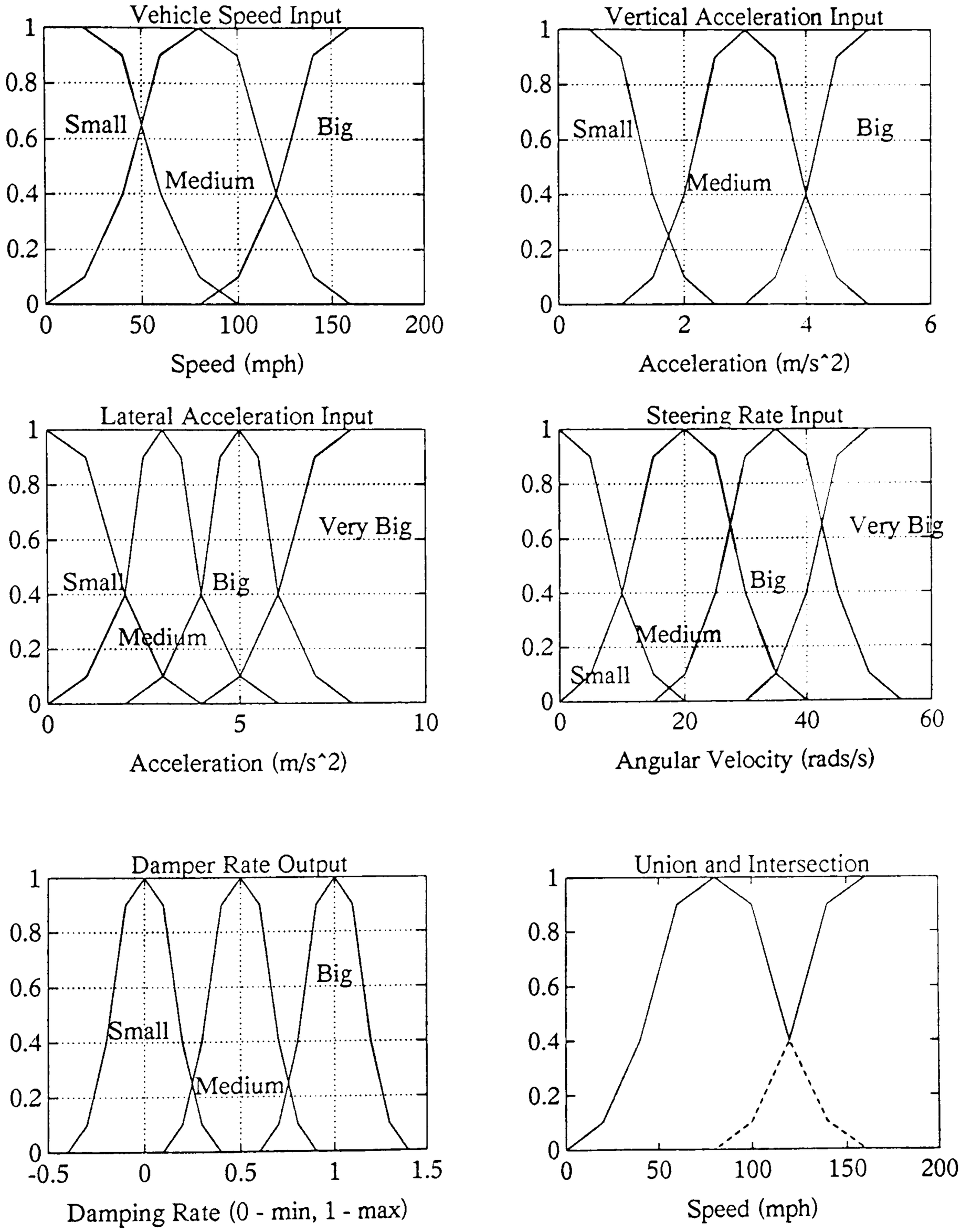


Figure 6.4 : Fuzzy Input and Output Subsets

- : Big or Medium

-- : Big and Medium

Figure 6.5 : Union and Intersetion of Fuzzy Sets

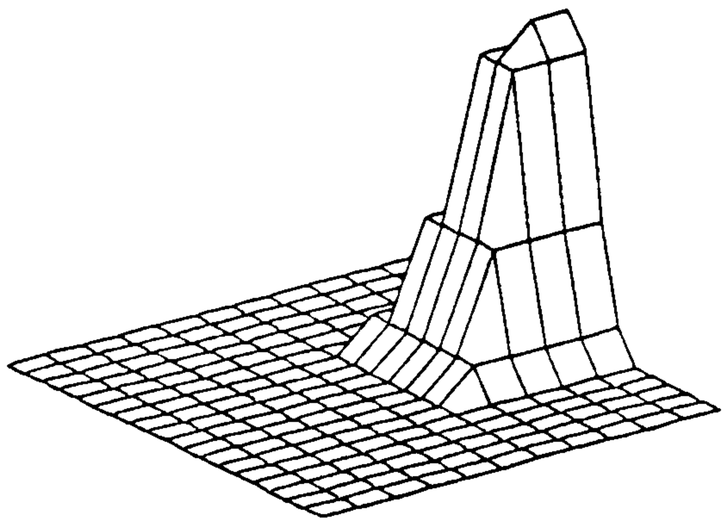

Figure 6.6 : Rule 1 - "if VACC is BIG then DAMP is MEDIUM"

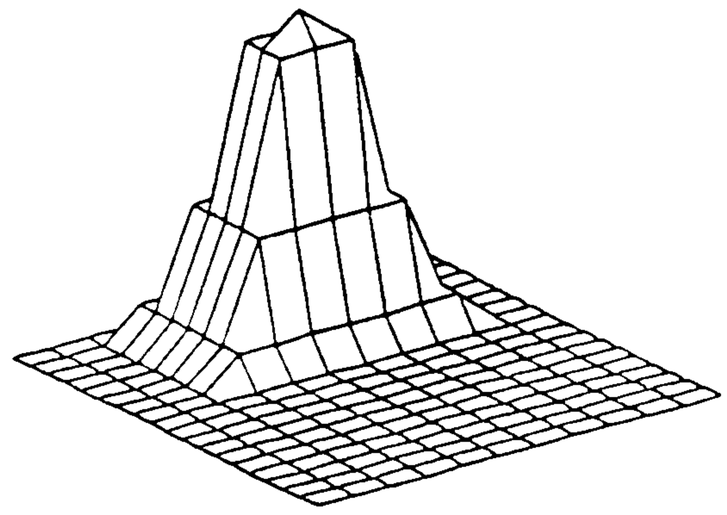

Figure 6.7 : Rule 2 - "if VACC is MEDIUM then DAMP is SMALL"

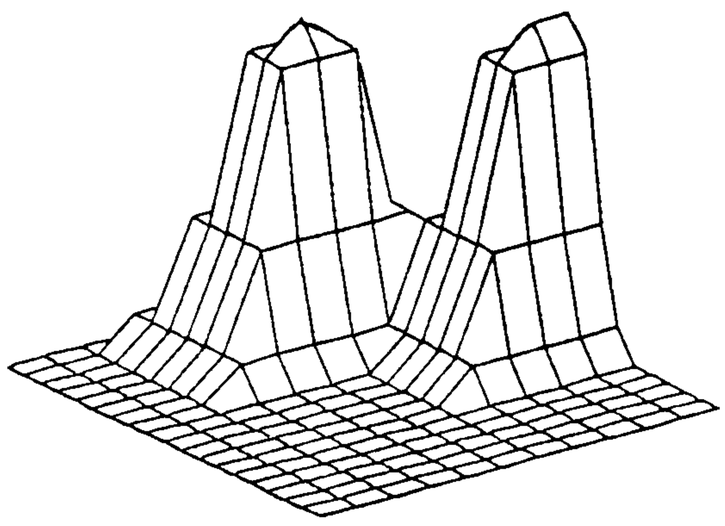

Figure 6.8 : Combination of Rule 1 and 2

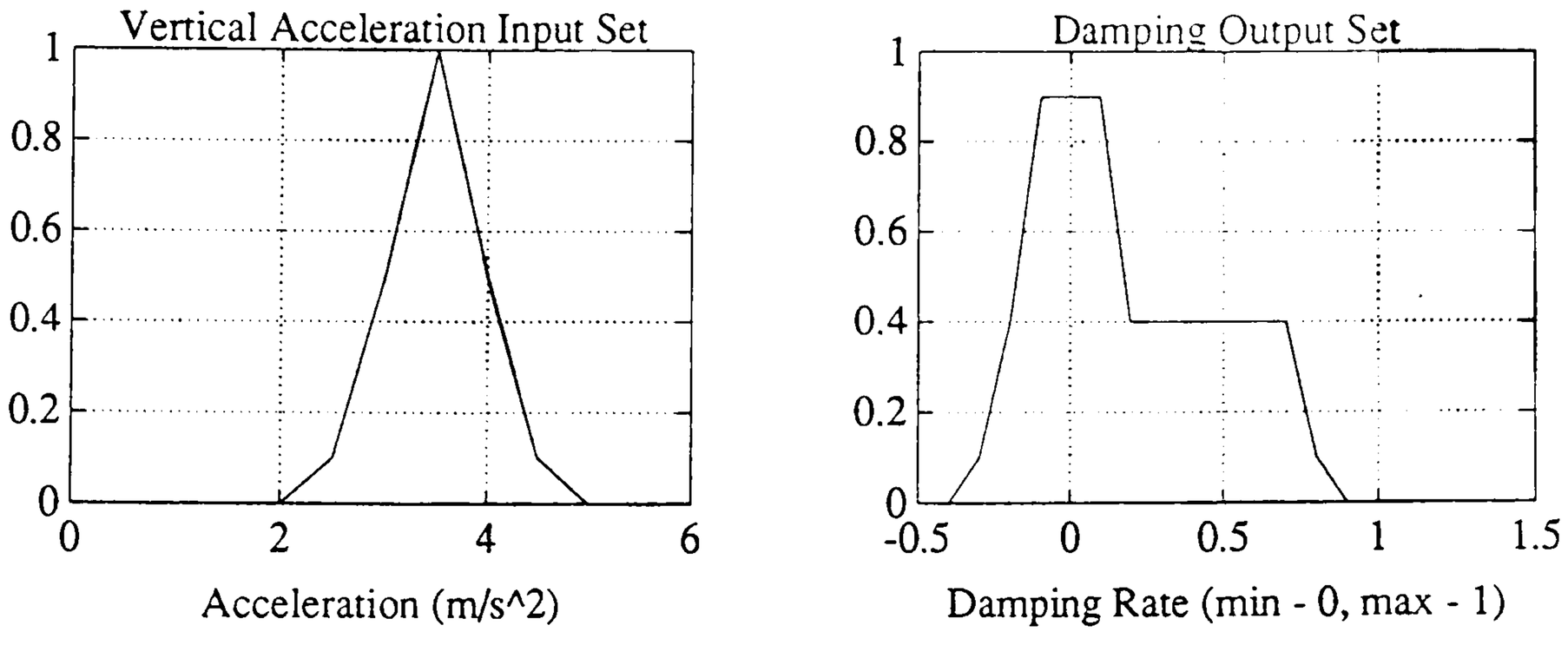


Figure 6.9 : Example Input and Output Fuzzy Sets

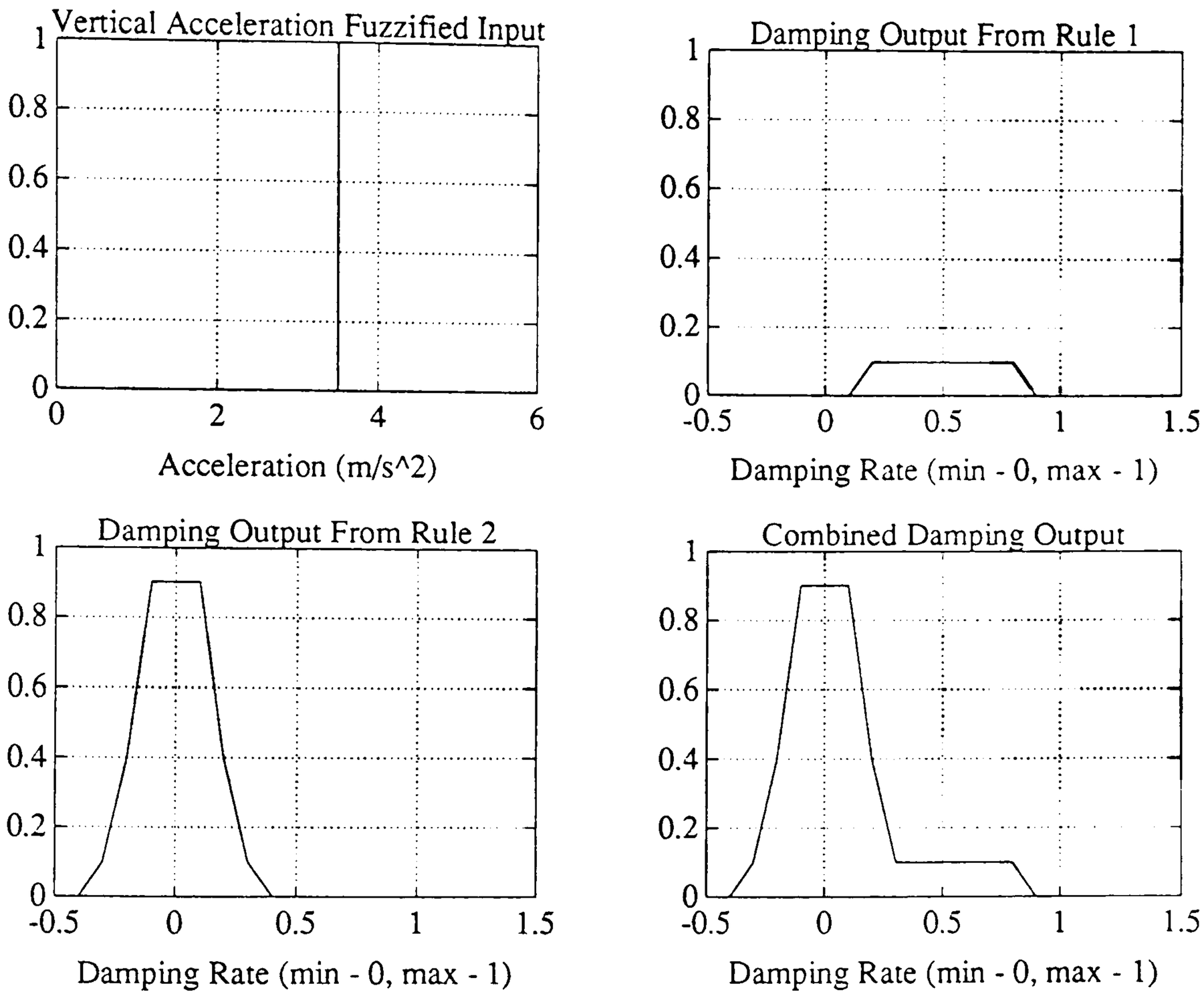


Figure 6.10 : Example with Precise Input

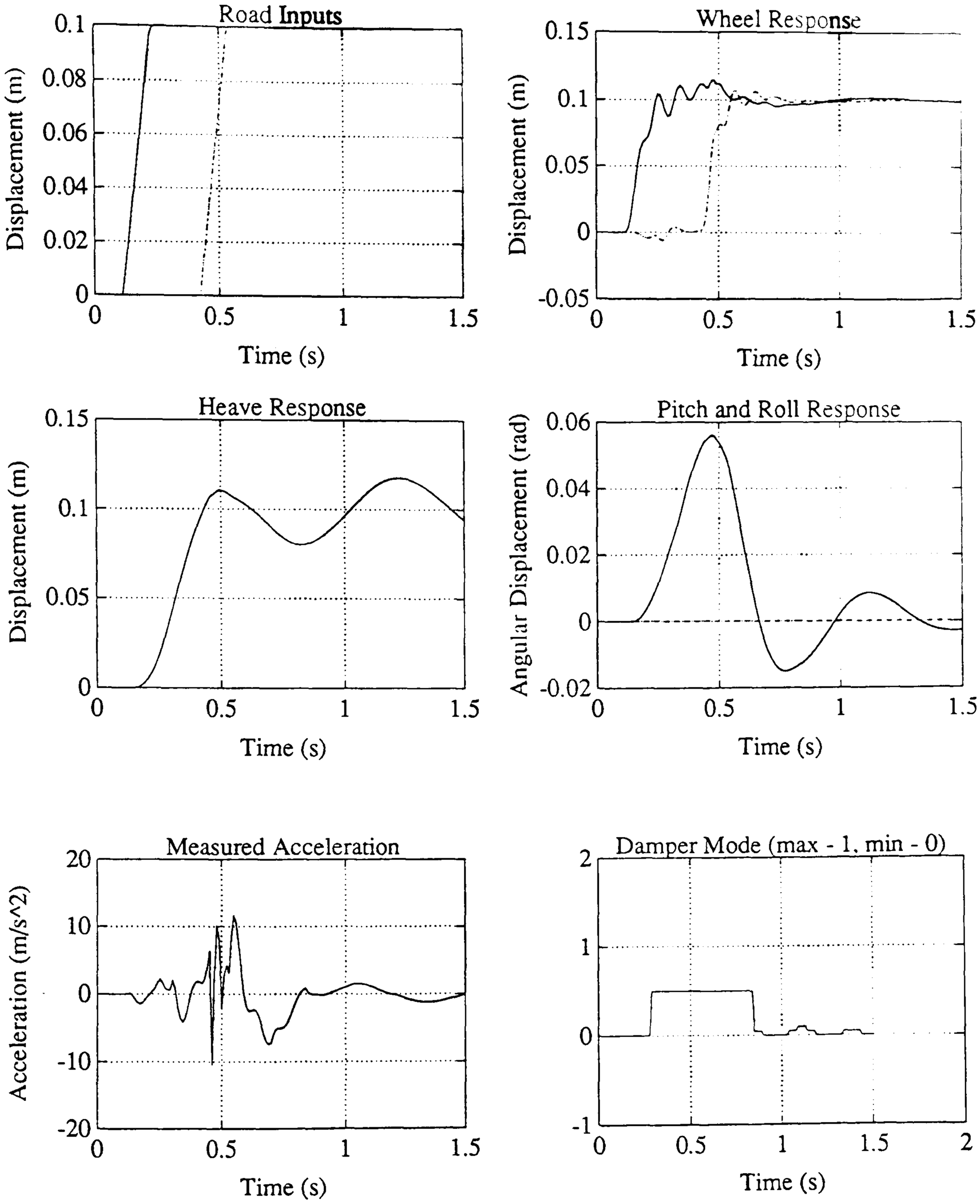


Figure 6.11a : Road Step Input

Figure 6.11 : Mean of Maximum Fuzzy Results

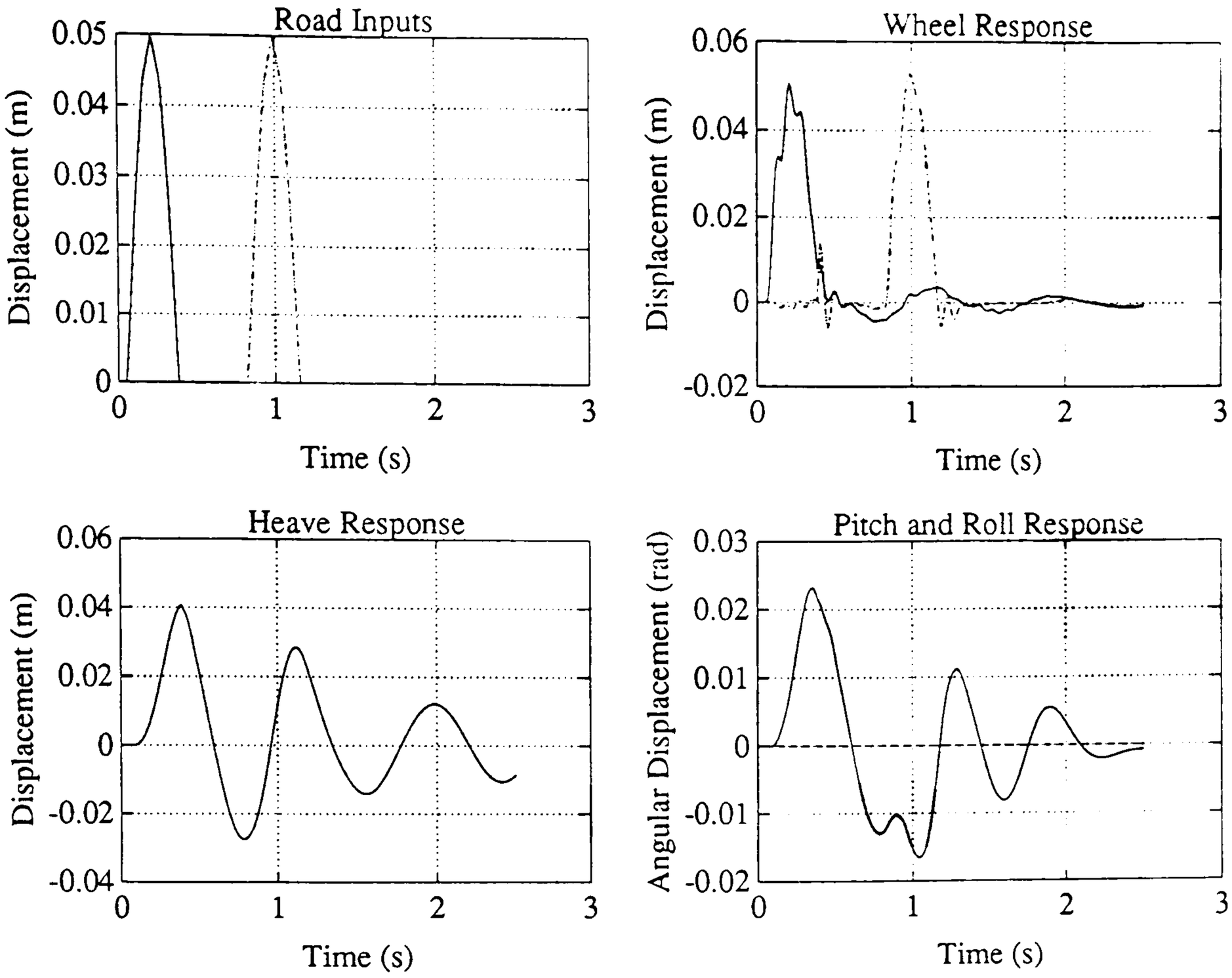


Figure 6.11b : Primary Ride Road Bump Input

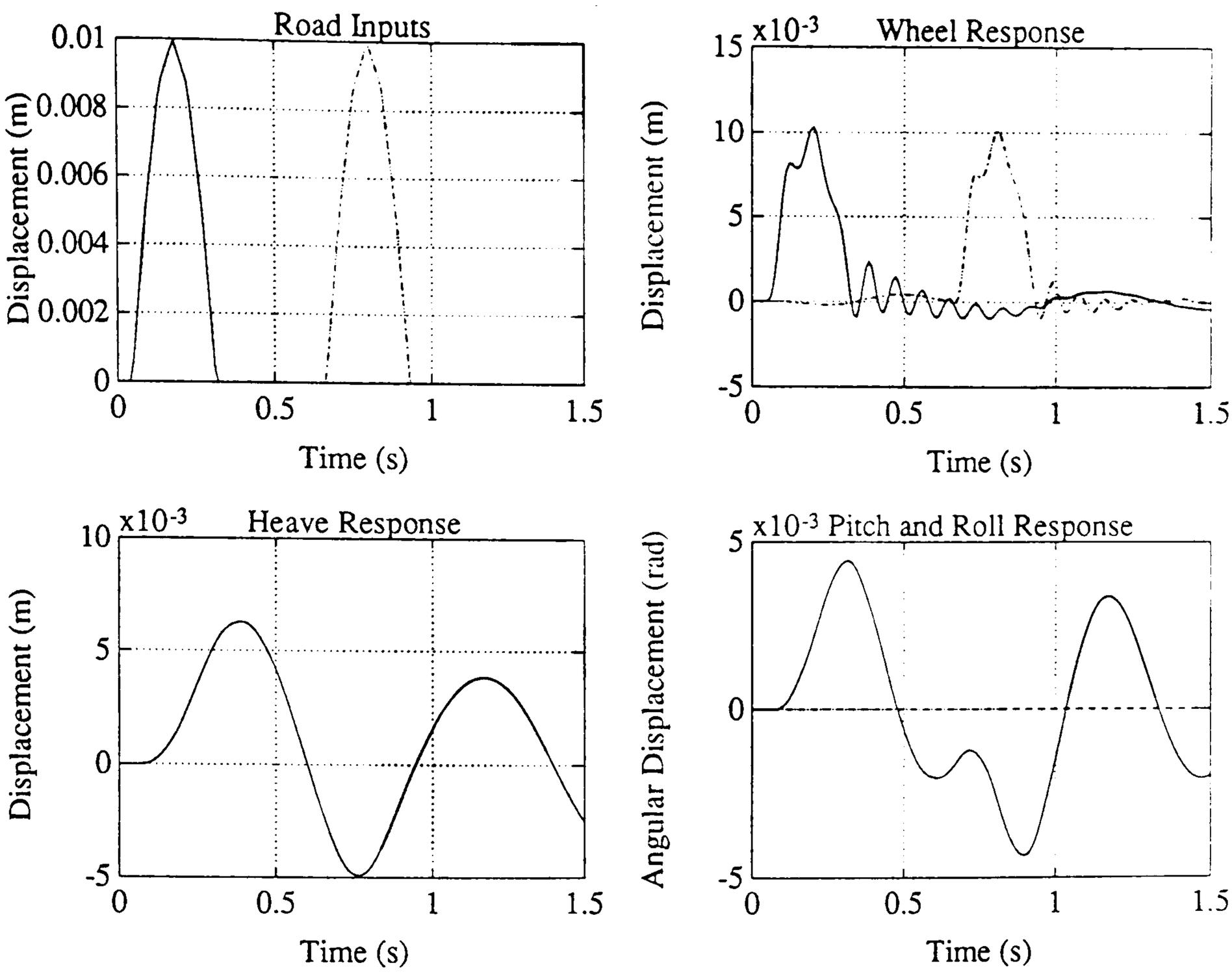


Figure 6.11c : Road Bump Input to Both Tracks

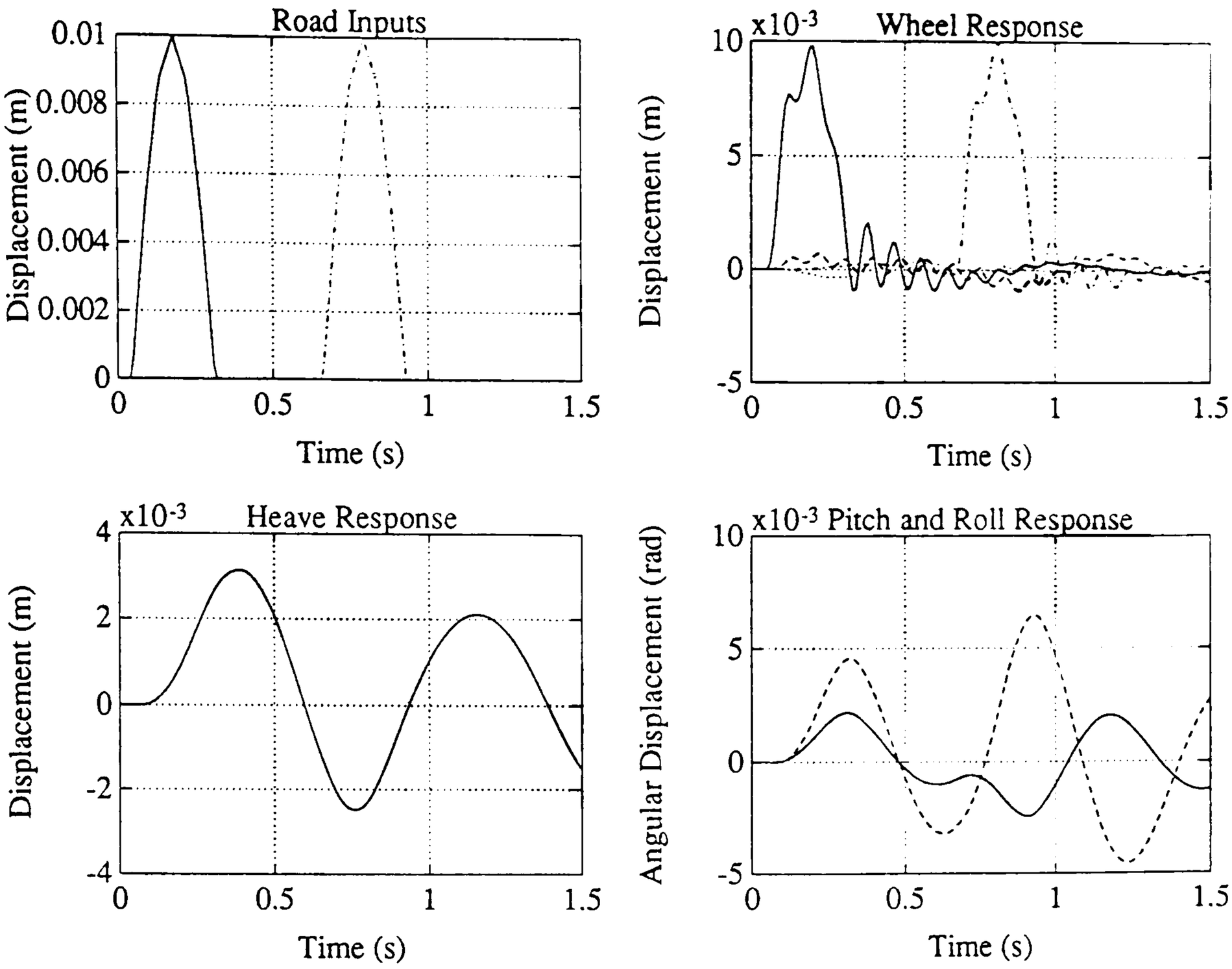


Figure 6.11d : Road Bump Input to One Track Only

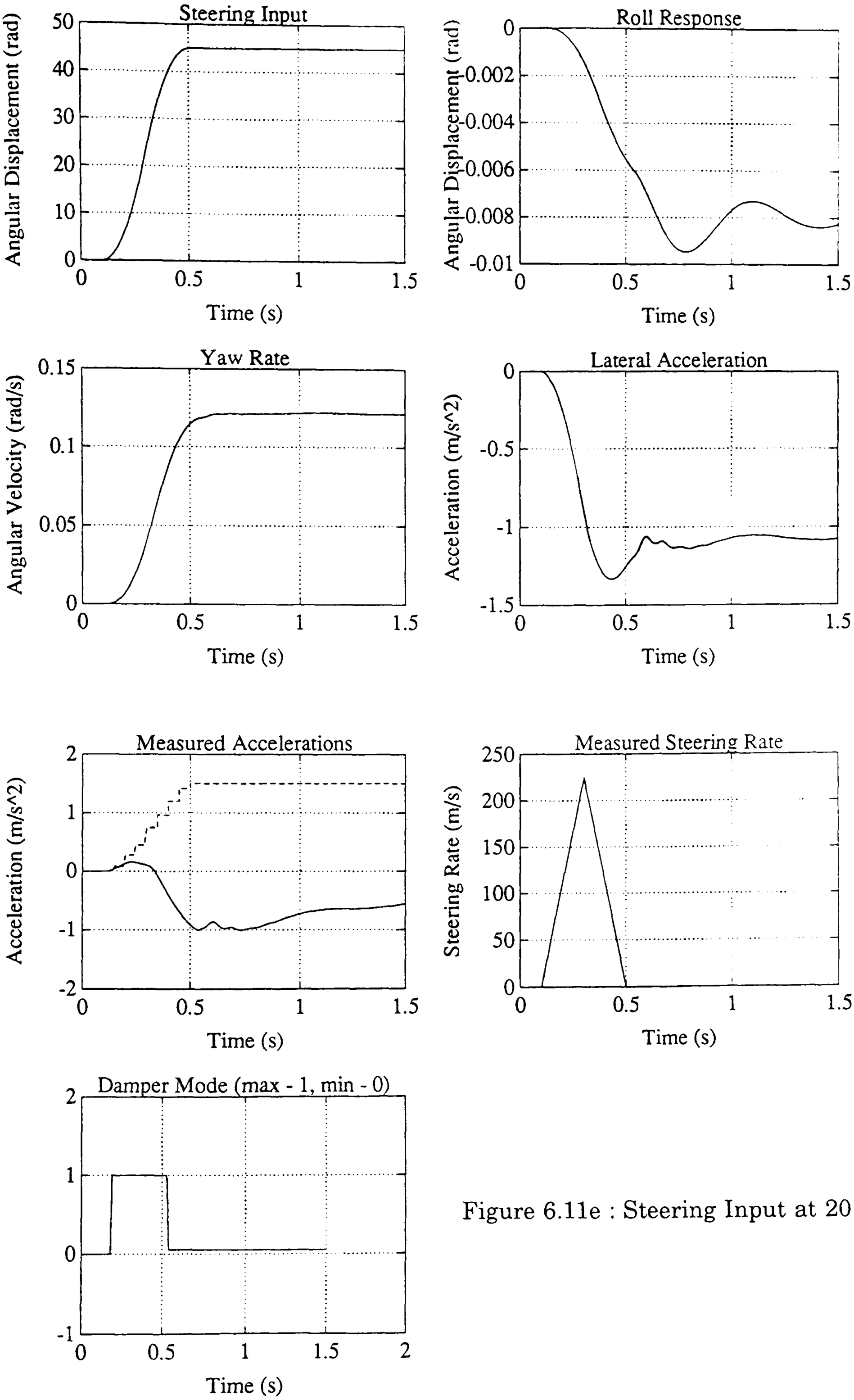


Figure 6.11e : Steering Input at 20 mph

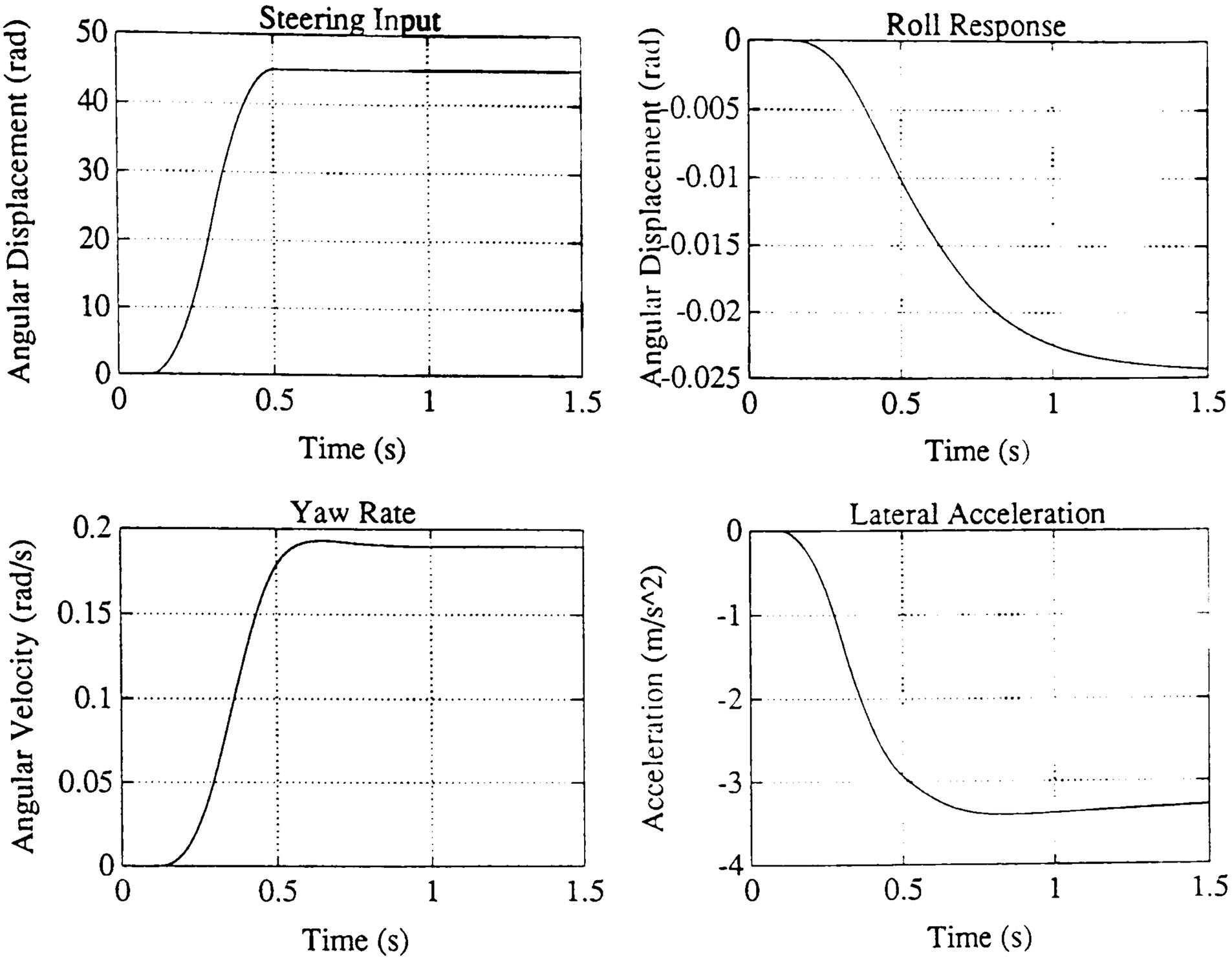


Figure 6.11f : Steering Input at 40 mph

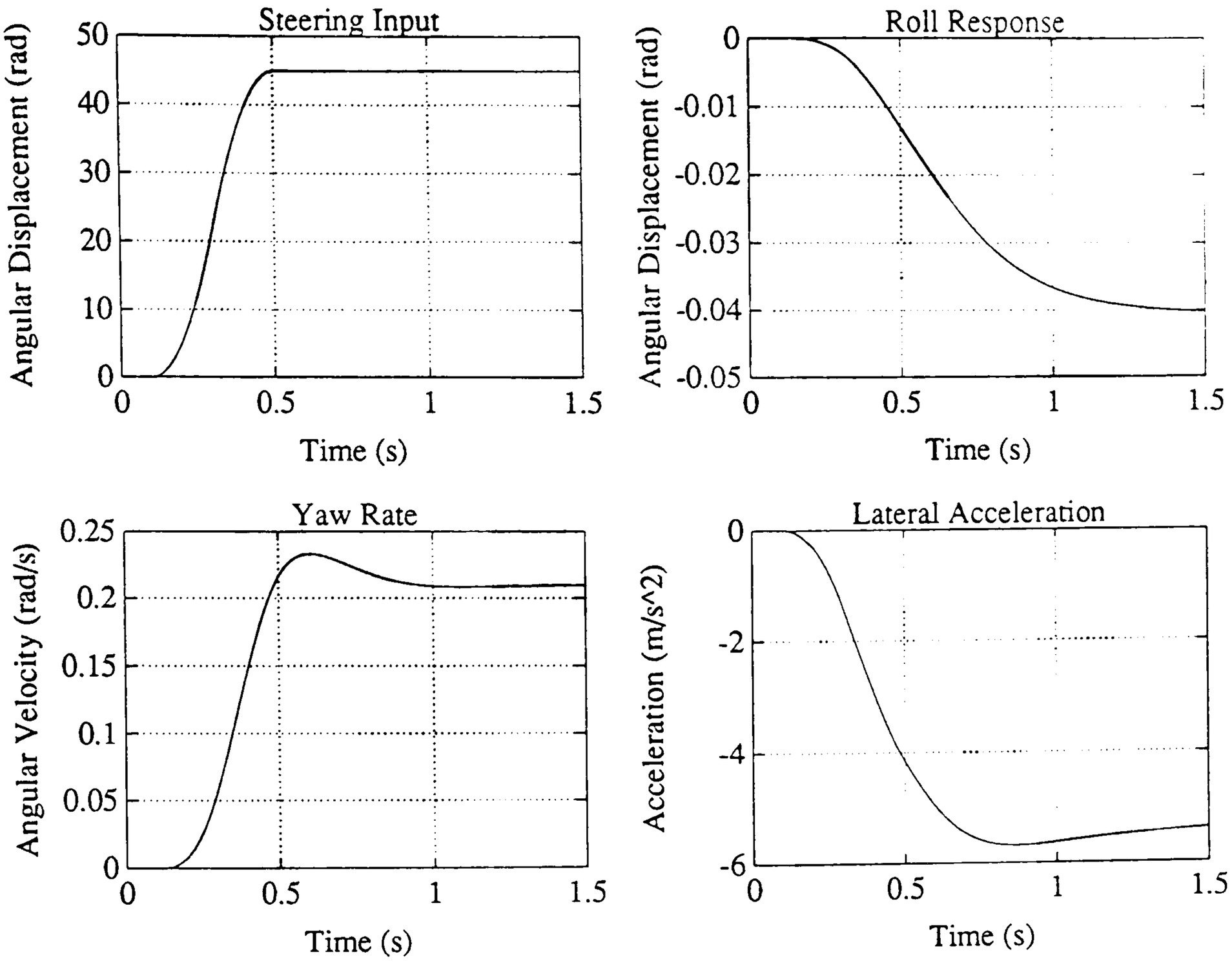


Figure 6.11g : Steering Input at 60 mph

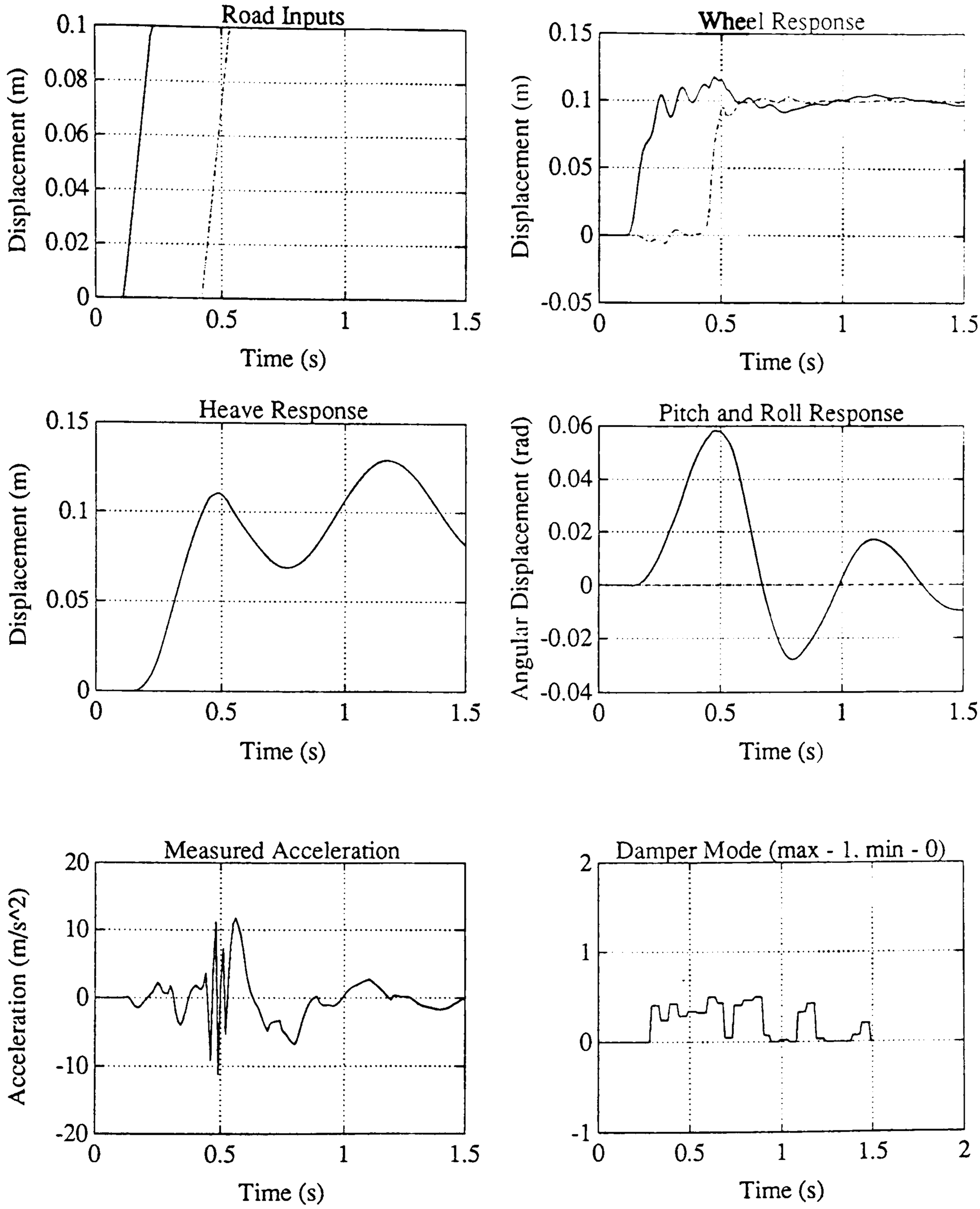


Figure 6.12a : Road Step Input

Figure 6.12 : Centroid Fuzzy Results

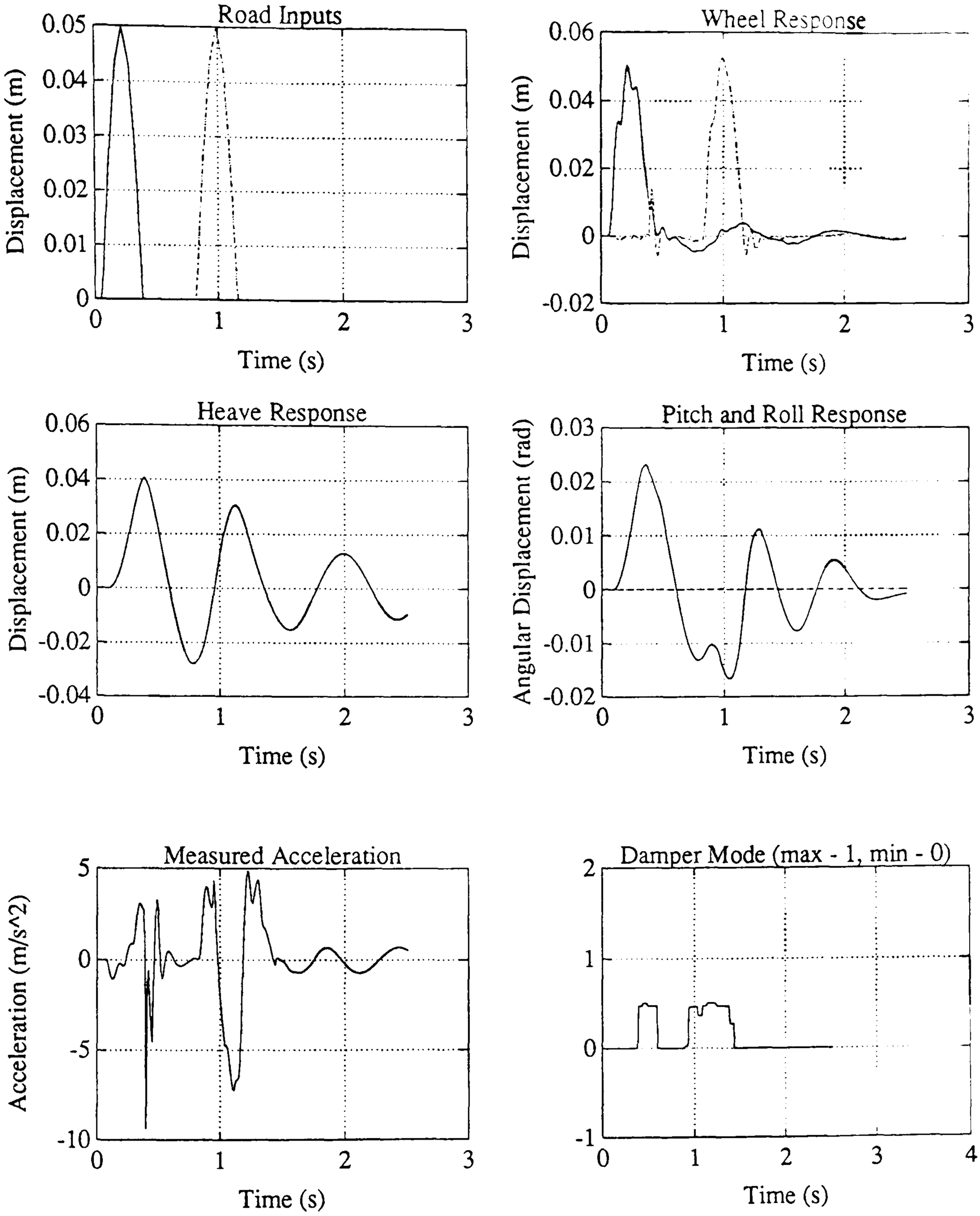


Figure 6.12b : Primary Ride Road Bump Input

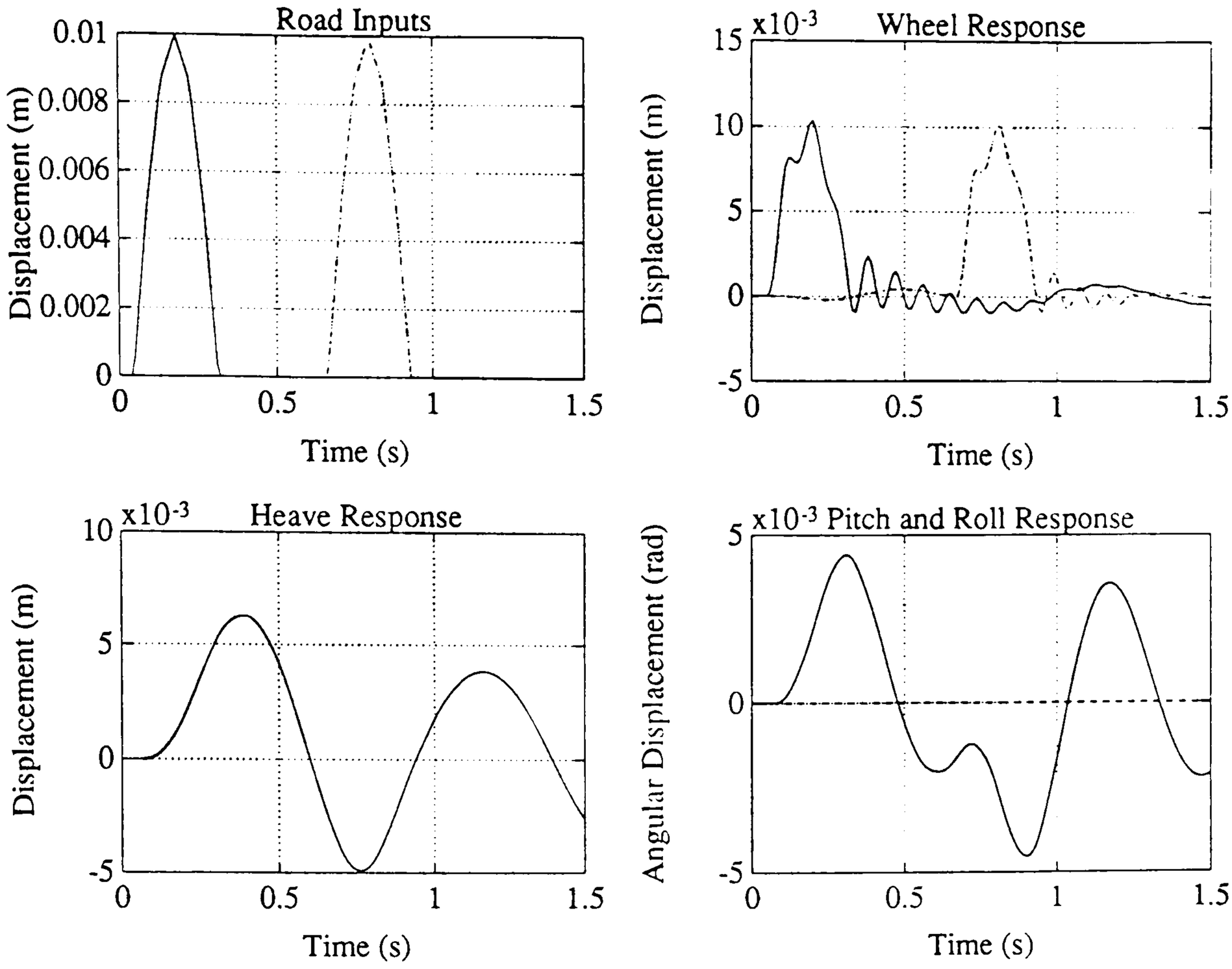


Figure 6.12c : Road Bump Input to Both Tracks

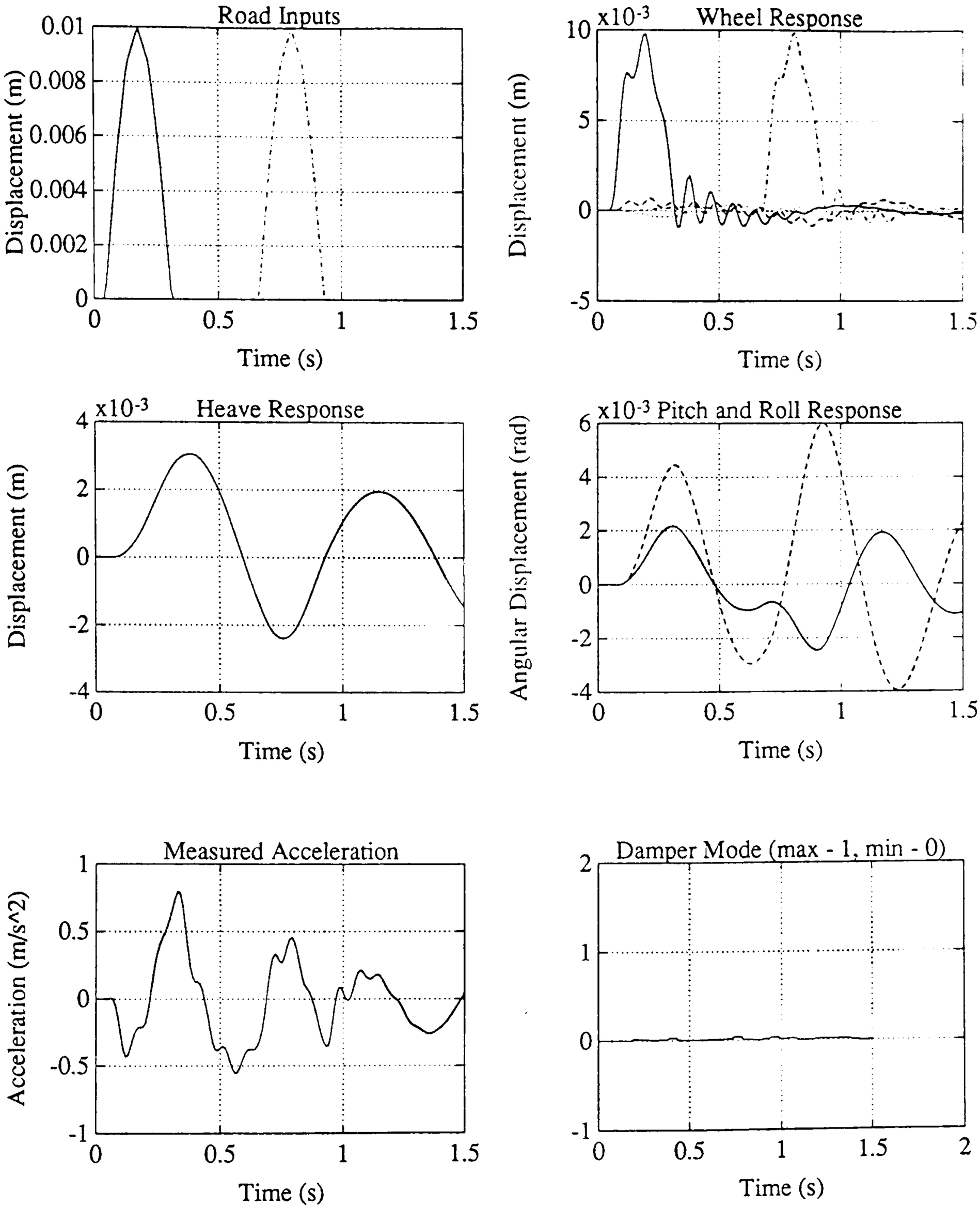


Figure 6.12d : Road Bump Input to One Track Only

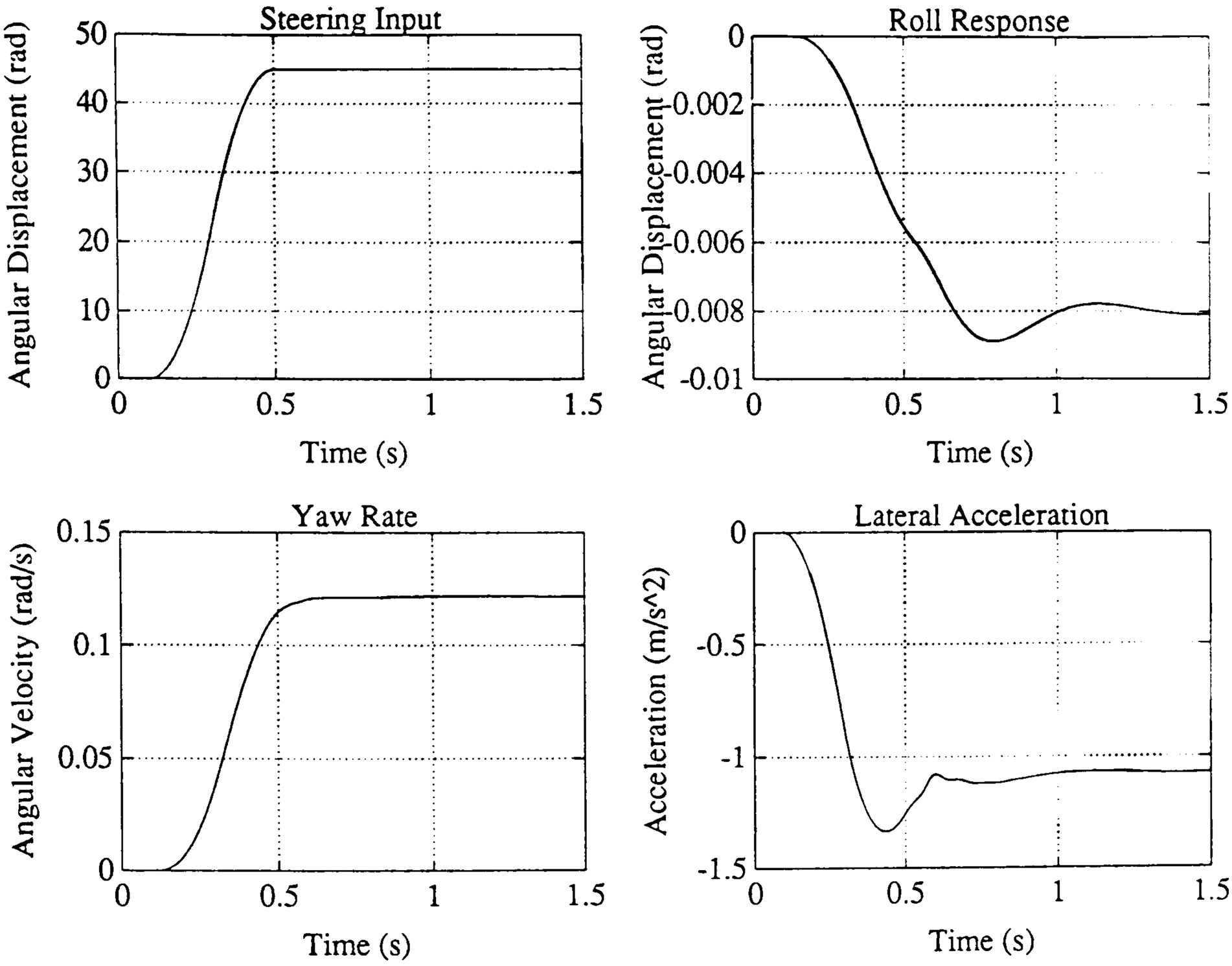


Figure 6.12e : Steering Input at 20 mph

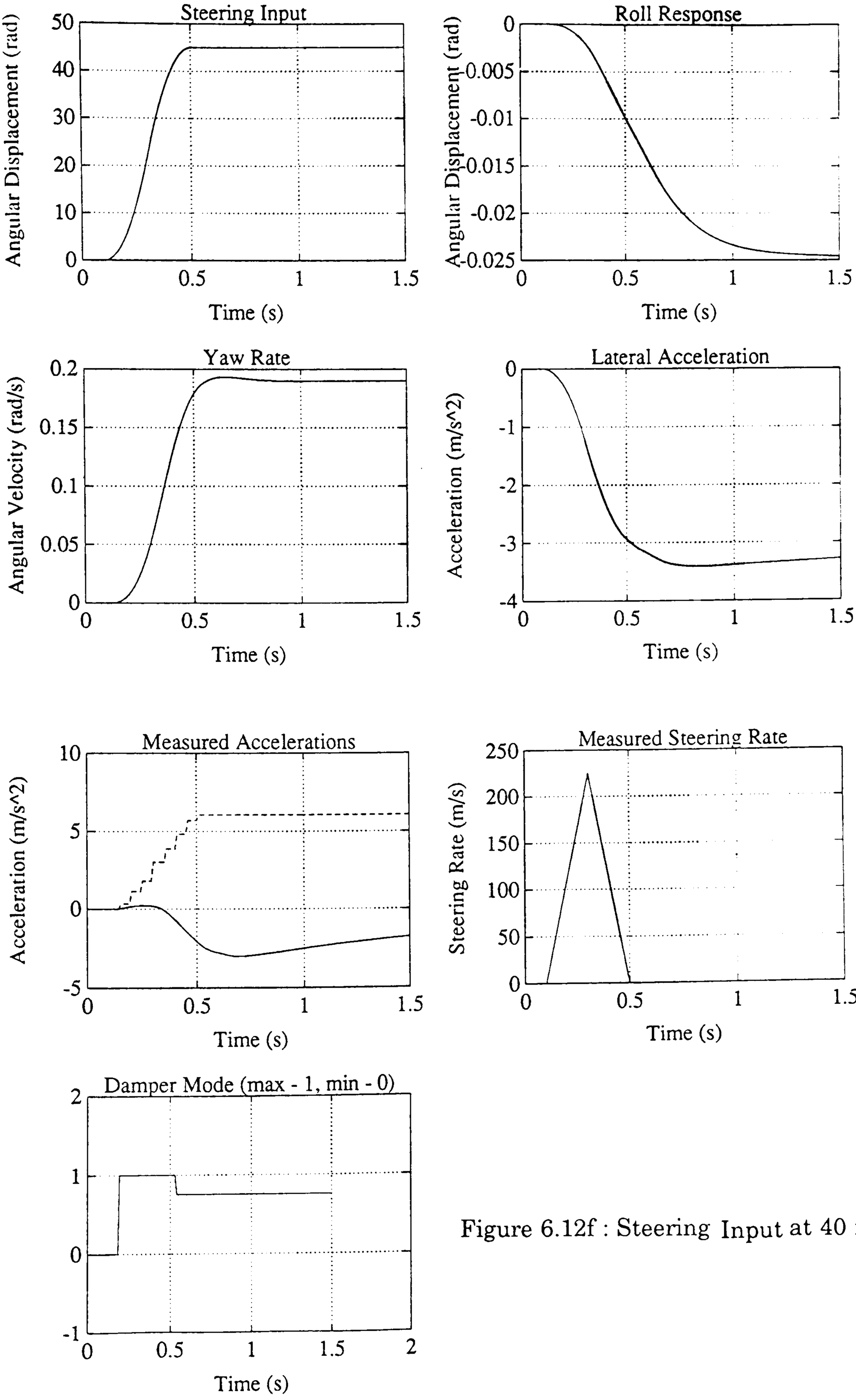


Figure 6.12f : Steering Input at 40 mph

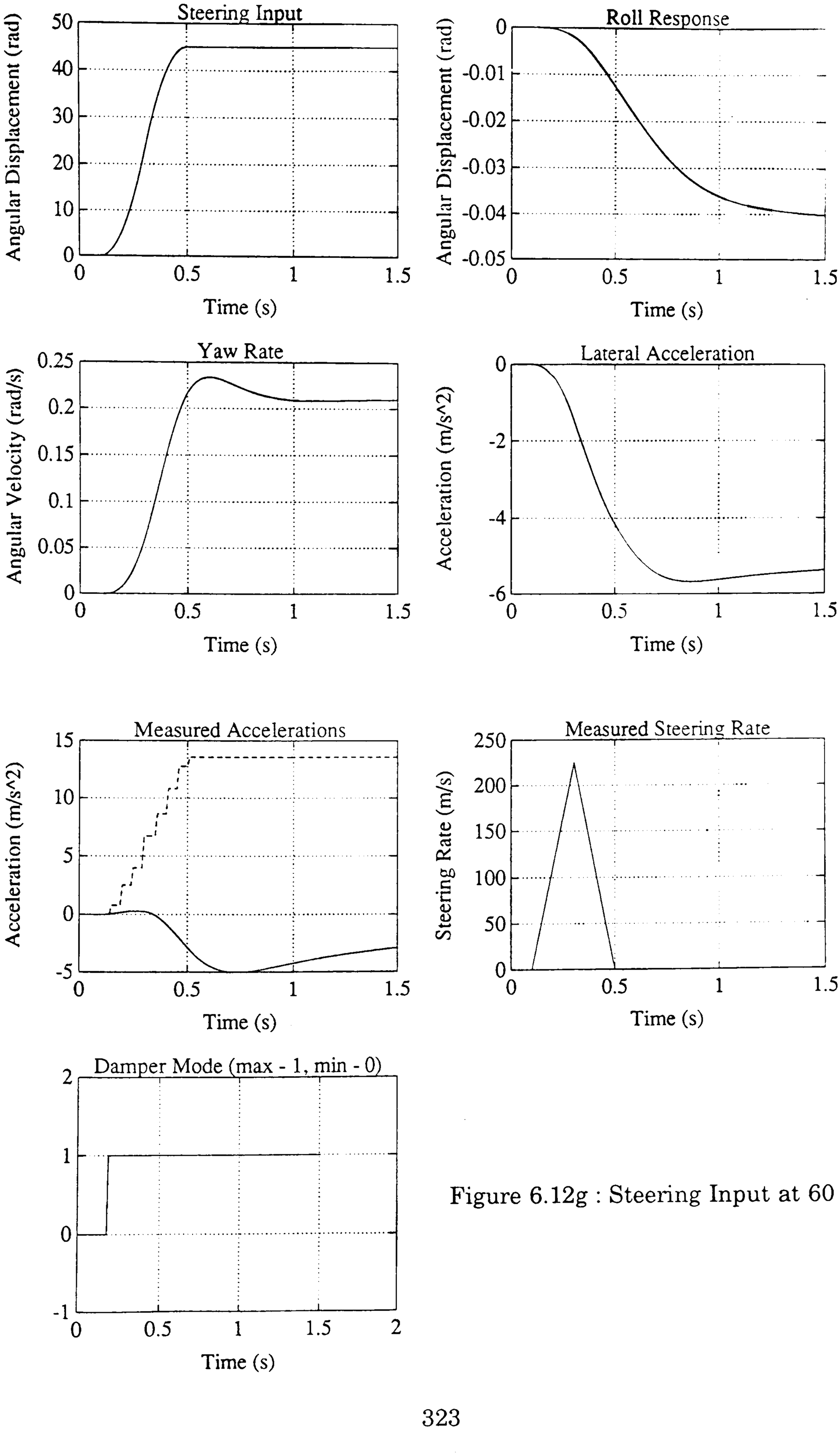


Figure 6.12g : Steering Input at 60 mph

# Chapter 7 : Conclusions

The aims of this thesis were to investigate vehicle modelling and control design analysis techniques applicable to the study of advanced suspension systems involving some form of feedback control. The industrial background of the author led to the emphasis of the work being placed upon practical solutions to realistic design tasks.

The modelling techniques traditionally used for automotive vehicle suspension studies have fallen into two distinct categories. The most widely used approach, especially within industry, has been the use of computer generated code from large generic MBS packages. These models have been used extensively for ride and handling predictions and as a suspension system design tool. The second approach uses hand-derived models from first principles for linear control studies.

The modelling approach used in this work was aimed at bridging this gap, that is using realistic, validated MBS suspension system models for control design studies, and evaluation of the resultant control algorithms. The requirements for this type of modelling were met by the use of a combination of SD/FAST, an MBS modelling package, and ACSL, a simulation language. This combination provides a powerful tool for non-linear vehicle simulations allowing the inclusion of detailed suspension system models and discrete and/or continuous feedback controllers. The linearisation facility of ACSL together with the direct interactive link to MATLAB provided the required capability for control design and analysis.

Alongside the overall modelling and analysis capabilities, this software

combination also provides several other advantages over conventional MBS modelling packages. SD/FAST uses Kane's formulation to generate the equations of motion, together with symbolic algebraic manipulation to simplify the equations for the specific system under consideration. This results in the generation of very efficient code. Another attractive feature is that using SD/FAST effectively splits the simulation task into two separate parts. SD/FAST performs the generation of equations of motion for the geometrical model, and ACSL executes the simulation for the specific force conditions. This feature also increases model efficiency, since the equations of motion are not generated every time the simulation is run. The SD/FAST code is simply accessed every time the ACSL code is executed for a simulation.

This feature also provides flexibility by allowing a wide choice of simulation environment in which the SD/FAST code may be used. Thus the most suitable choice for the application under consideration may be used, including hand written simulation routines. In this work the choice of ACSL allows access to the full control analysis capabilities of MATLAB.

For the purposes of this thesis one specific aspect of advanced suspension system control was addressed, namely ride control. Two basic types of suspension system were considered, ideal active systems and variable damping systems. For each type of system a variety of control system design and analysis methods were used with different levels of success.

The ride control of an ideal active suspension system was addressed using linear state space and frequency domain techniques, based on both quarter car and full vehicle models. The application of state space techniques raised two main difficulties. Numerical problems were the first to be

encountered, especially with the full vehicle model. Scaling the control variable reduced these problems by improving the conditioning of the state space matrices, however care was still required in the specification of the weighting matrices for the linear quadratic regulator study. The second area of difficulty arose in describing the ride control objectives in terms suitable for the specific design method under consideration. The linear quadratic regulator concept of minimising some form of performance index fitted the control objectives best, however the choice of weighting was not obvious. The application of pole placement techniques required the ride control objectives to be specified in terms of frequency and damping levels for the dynamic modes of the system. Although these are intuitive measures, problems were encountered in the interaction between modes, especially with the full vehicle model.

Despite these drawbacks both state space design methods achieved good ride performance improvements, for both the quarter car and full vehicle model. One interesting conclusion drawn from this study was that better ride performance was achieved for the full vehicle by designing the control separately for each corner of the vehicle, as opposed to designing directly for the full vehicle model. The reason for this relates to the number of independent weightings defined for the regulator study and pole locations for the pole placement study.

Both of these state space design methods involved the straight application of standard theory with the relevant functions available in MATLAB. Therefore despite the required numerical care, and the iterative process required to obtain the best results, they both provided a well-defined design process.

The application of frequency domain techniques, in contrast, is a less obvious choice for this ride control problem. In this case the interaction between modes in the quarter car study leads to more significant performance constraints. Feedback compensation on one output does not allow for the separate control of both the body and wheel modes with different response characteristics as required. By trial and error processes some reasonable vehicle performance results were achieved for the quarter car model. In contrast to the state space designs, however, the application of these quarter car results to the full vehicle model caused significant deterioration of ride performance.

In order to apply frequency domain techniques directly to the full vehicle model, specialised multivariable techniques are required. In this study dyadic expansion techniques were shown to achieve diagonal dominance for a range of frequencies including the sprung mass modes. This results in the system being decoupled into four SISO loops, one for each of the four sprung mass modes, heave, pitch, roll and flexure. Frequency domain feedback compensation can then be designed for each loop in turn.

The application of frequency domain techniques to the four decoupled loop avoids the mode interaction problems encountered in the quarter car study since each loop has only one input, one output and one mode to control. The frequency domain design for the full vehicle model using these decoupling techniques achieved some good ride performance results, although these were inferior to those obtained from the state space study.

Overall for an ideal active system, the best vehicle ride control performance was achieved using state space techniques on a representative quarter car model for both front and rear, and applying to each corner of the

full vehicle. This also reduces the complexity of the system and numerical problems encountered in the design process. The major difference between the linear quadratic regulator and pole placement results is due to the regulator design accounting for the level of control effort required. The pole placement results may give better control in terms of sprung mass overshoot, but this is at the cost of more control effort requirements. Frequency domain techniques did not achieve the same level of vehicle performance, however the dyadic expansion techniques provide a valuable tool in their own right. The achievement of diagonal dominance provides insight and understanding of the interactions between modes, and also a method of determining the dominant mode during a manoeuvre from strut measurements, without the need for expensive sensors such as gyros. This decoupling of the system modes could be used in conjunction with any other control techniques, allowing the most suitable type of control for each mode.

The second section of control analysis studies considered in this thesis looked at the control design techniques required for the control of variable damping suspension systems, including both discretely and continuously variable dampers.

For the discretely variable case three types of controller were studied. One based upon the active skyhook damping concept, one based on a minimisation of the sprung mass acceleration, and finally a heuristic rule-based controller. The results showed no obviously superior controller in terms of vehicle ride performance, and thus the added complexity of the first two offered no significant improvement. The rule-based controller offered the advantages of one control strategy switching all four dampers together, and less damper

switching, which can lead to noise problems. The heuristic nature of this type of controller suits the traditional subjective design methods used within the automotive industry. The rule-based approach also offers the advantage of being independent of any model approximations, including non-linearities or unmodelled dynamics, and vehicle variations in mass centre of gravity and manufacturing tolerances. The thresholds and delays involved in the controller are not obvious but are derived as a part of the standard suspension system development process.

For the continuously variable damper, two design approaches were considered, reducing the ideal active controllers to the practical limitations of the specific actuators, and designing a controller directly for the non-linear variable damping system. Despite some of the findings in the literature, the results obtained in this study from reducing the active controllers for the variable damping system show significant performance degradation. The controller also produced high frequency damper switching behaviour, with the damper rate being set to the maximum or minimum rate for the majority of the simulations. The resultant ride performance is no better than achieved for the discretely variable damping system, with a significantly simpler design process.

For the continuously variable case the direct design method took the discretely variable rule-based controller as its starting point, and used fuzzy control techniques to extend it to the continuous case. Two fuzzy controllers were designed and evaluated, using each of the output selection methods. The ride performance results showed that the mean of maximum output selection method gave superior results for road inputs, whereas the centroid method achieved better steering input responses.

The best of the fuzzy controller results were a significant improvement over the designs based on ideal active solutions in terms of steering response and damper switching behaviour. The fuzzy controllers fully utilised the variability of the dampers and led to less frequent damper switching, especially between extreme damper rate settings, reducing any noise problems. The fuzzy control results did not, however, offer any significant improvement over the discretely variable damping system results as expected. The major reason for this was that the controller was designed to show the feasibility of the design method and so a simple controller was designed with little tuning. Further tuning would lead to significant improvements, by redefining the output fuzzy subsets to avoid the softest damper rate settings.

As a control system design method, fuzzy control offers similar advantages to conventional rule-based controllers. The linguistic nature of the rules and variables suits the subjective descriptions of the control requirements that caused the major difficulties in the use of conventional control techniques. Again the rule-based approach reduces the controller sensitivity to modelling approximations and vehicle variations by removing the need for simplified suspension models for control design. For the specific example of continuously variable damping systems the use of fuzzy control techniques allows inferences to be made for combinations of inputs that lie 'between' the rules, thus reducing the required rule-base to the minimum.

There are two main areas for continuing the work described in this thesis. The first is in further applications of the dyadic expansion techniques used to decouple the MIMO full vehicle system model. This provides a useful tool for understanding the interactions, and decoupling the modes for a variety

of applications. One interesting development would be to use the dyadic expansion techniques to decouple the system and then apply separate and different types of control for each mode. This would allow the most suitable control design method to be applied to each mode independently, providing better overall control performance. Rule-based and/or fuzzy logic controllers could be used in conjunction with these decoupling techniques.

The second area for the continuation of this work would be in the field of fuzzy control for all areas of suspension control. The next step would be to fully develop and tune this algorithm and achieve vehicle performance improvements that justify the continuously as opposed to discretely variable damper. Further studies of fuzzy control applications would also provide interesting results, for example for variable rate spring, or for more complex systems such as active anti-roll systems. This could be further extended to cover other vehicle subsystems such as steering or braking.

# Bibliography


[1] Abate, "Application of Fuzzy Logic to the Idle Speed Control of a Petrol Engine", VW Fuzzy Logic Meeting, Wolfsburg, March 1992.

[2] Abdel Hady, M.B.A., Crolla, D.A., "Theoretical Analysis of Active Suspension Performance Using a Four-Wheel Vehicle Model", Proc. IMech.E, vol. 203, 1989.

[3] ACSL - Advanced Continuous Simulation Language. Reference Manual, Mitchell and Gauthier Associates, 1987.

[4] Athans, M., "The Role of Modern Control Theory for Automotive Engine Control", SAE paper 780852, 1978.

[5] Autocar & Motor, pp 44-55, 21 September 1988.

[6] Automotive Handbook, Published by Robert Bosch GmbH, 1986.

[7] Barak, P., Hrovat, D., "Application of the LQG Approach to Design of an Automotive Suspension for Three-Dimensional Vehicle Models", IMech.E, Intl. Conf. Advanced Suspensions, C421/88, 24-25 October 1988.

[8] Barak, P., Sachs, H., "On the Optimal Ride Control of a Dynamic Model for an Automotive Vehicle System", 9th IAVSD Symposium, Switzerland, 1985.

[9] Becker, D., Ertelt, R., Orlamunder, H., "Radio Transmission Based Automobile Driver Guidance System", IMech.E, C183/81, 1981.

[10] Best, A., "Vehicle Ride - Stages in Comprehension", Phys. Technol., Vol 15, pp 205-210, 1984.

[11] Besinger, F.H., Cebon, D., Cole, D.J., "An Experimental Investigation into the Use of Semi-Active Dampers on Heavy Lorries", 12th IAVSD

Symposium, Lyon, France, 1991.

[12] Braess, H.H., Regar, K.N., "Electrically Propelled Vehicles at BMW - Experience to Date and Development Trends", SAE paper 910245, 1991.

[13] Braess, H.H., Thomson, B., "The Motor Vehicle - A Good Example of the Wide Range of Application of Modern Control Engineering", 10th IFAC World Congress, 1987.

[14] Brame, "Fuzzy Logic System Applied to Automatic Braking Control", VW Fuzzy Logic Meeting, Wolfsburg, March 1992.

[15] Brusaglino, G., "Electric Vehicle Development in Fiat", SAE Paper 910244, 1991.

[16] Cech, I., "A Low-Power Active Suspension and its Bounds and Cross Model Performance", IMech.E, Intl. Conf. Advanced Suspensions, C422/88, 24-25 October 1988.

[17] Charalambous, C., Brunning, A., Crawford, I.L., "The Design and Development of a Semi-Active Suspension", IMech.E, Intl. Conf. Advanced Suspensions, C382/058, pp 539-546, 1989.

[18] Chen, "Comparison of Fuzzy Control with Conventional Controls During Braking", VW Fuzzy Logic Meeting, Wolfsburg, March 1992.

[19] Cherry, A.S., "A Fuzzy/Rule-Based Approach to Non-linear Control of an Automotive Suspension System", IEE Colloquium, Digest 1992/193, November 1992.

[20] Christenson, B.C., Frank, A.A., Beachley, N.H., "The Fuel Saving Potential of Cars with Continuously Variable Transmissions and an Optimal Control Algorithm", ASME paper 75-WA/Aut-20, 1975.

[21] Constancis, P., Harris, C.J., "A Comparison Between Fuzzy, PI, and B-

Spline Control", IEEE Intl. Symposium on Intelligent Control, Glasgow, 11-13 August 1992.

[22] Costa, A.N., "Application of Multibody System (MBS) Techniques to Automotive Vehicle Chassis Simulation for Motion Control Studies", PhD thesis, Engineering Department, University of Warwick, 1991.

[23] Costa, A.N., Jones, R.P., "Modelling and Simulation of an Automotive Vehicle Chassis System", CSC Conference, Canada, 1990.

[24] Costa, A.N., Jones, R.P., "Motion Management for Automotive Vehicles", IEE Control Conference, Edinburgh, 1991.

[25] Costa, A.N., "Application of Multibody Systems Techniques to Vehicle Modelling", IEE Colloquium, Group C7, digest 1991/196, Sept. 1991.

[26] Crolla, D.A., Aboul Nour, A.M.A., "Theoretical Comparisons of Various Active Suspension Systems in Terms of Performance and Power Requirements", IMech.E, Intl. Conf. Advanced Suspensions, C420/88, 24-25 October 1988.

[27] Crosby, M.J., Karnopp, D.C., "The Active Damper - A New Concept for Shock and Vibration Control", 43rd Shock and Vibration Bulletin, Part H, June 1973.

[28] Crossley, P.R., Jones, R.P., Howarth, S.I., "Modelling and Simulation of a HGV Powertrain for Transmission Control Studies", Proceedings of ISATA '85, vol. 2, 131-150, 1985.

[29] Crossley, P.R., Cook, J.A., "A Nonlinear Engine Model for Drivetrain System Development", IEE Control '91 Conference, pp 921-925, Scotland, 1991.

[30] Decker, H., Schramm, W., Kallenbach, R., "A Practical Approach

Towards Advanced Semi-Active Suspension Systems", IMech.E, Intl. Conf. Advanced Suspensions, C430/88, 24-25 October 1988.

[31] Doi, S., Yasuda, E., Hayashi, Y., "An Experimental Study of Optimal Vibration Adjustment Using Adaptive Control Methods", IMech.E, Intl. Conf. Advanced Suspensions, C433/88, 24-25 October 1988.

[32] Flintham, T., "Making the Rules", IEE Review, June 1991.

[33] Foag, W., "A Practical Control Concept for Passenger Car Active Suspensions with Preview", IMech.E, Intl. Conf. Advanced Suspensions, C424/88, 24-25 October 1988.

[34] Frommholz, W., "Automatic Temperature Control Systems for Car Heating and Air Conditioning Systems", IMech.E, C209/81, 1981.

[35] Fruhauf, F., Kasper, R., Lueckel,J., "Design of an Active Suspension for a Passenger Vehicle Model Using Input Processes with Time Delays", 9th IAVSD Symposium, Switzerland, 1985.

[36] Goodall, R.M., Kortum, W., "Active Controls in Ground Transportation - A Review of the State-of-the-Art and Future Potential", Vehicle System Dynamics, no. 12, pp 225-257, 1983.

[37] Gordon, T.J., Marsh, C., "Nonlinear Strategies for the Control of Active and Semi-Active Vehicle Suspension Systems", IEE Colloquium, Digest 1992/193, November 1992.

[38] Graves, A., "PROMETHEUS : A New Departure in Automobile R&D?", IMVP Intl. Policy Forum, May 1989.

[39] Guy, Y., Lizell, M.B., Kerastas, M.W., "Advances in Electronic Suspensions - The Monroe View", Automotive Engineering, vol 21.

[40] Hac, A., "Suspension Optimization of a 2-Dof Vehicle Model Using a

Stochastic Optimal Control Technique", Journal of Sound and Vibration, 100(3), pp 343--357, 1985.

[41] Haycock (Cherry), A.S., "Modelling and Control of Automotive Suspension Systems", IEE Control '91 Conference, pp 926-931, Scotland, 1991.

[42] Haynes, N.A., Martin, A.G., Moore, W.R., "Digital Steering Control for Automobiles With Applications for Disabled Drivers", IMech.E, C187/81, 1981.

[43] Hedrick, J.K., Butsuen, T., "Invariant Properties of Automotive Suspensions", IMech.E, Intl. Conf. Advanced Suspensions, C423/88, 24-25 October 1988.

[44] Hennecke, D., Ziegelmeier, F.J., "Frequency Dependent Variable Suspension Damping - Theoretical Background and Practical Success", IMech.E, Intl. Conf. Advanced suspensions, C431/88, 24-25 October, 1988.

[45] Hine, P.J., Pearce, P.T., "A Practical Intelligent Damping System", IMech.E, Intl. Conf. Advanced Suspensions, C436/88, 24-25 October 1988.

[46] Hrovat, D., Powers, W.F., "Power Train Computer Control Systems", 10th IFAC World Congress, 1987.

[47] Ironside, J.M., Stubbs, P.W.R., "Microcomputer Control of an Automotive Perbury Transmission", 3rd IMechE/IEE International Conference on Automotive Electronics, UK, 1981.

[48] International Standard ISO 2631, "Guide for the Evaluation of Human Exposure to Whole-body Vibrations", International Organization for

Standardization, 1974.

[49] Jones R.P., Hughes, M.T.G., Kuriger, I.F., "Computer-Aided Modelling and Simulation of Automotive Powertrains for Control Studies", Intl. Conf. on Computer-Aided Engineering, England, 1986.

[50] Jones, R.P., Kuriger, I.F., Hughes, M.T.G., Holt, M.J., Ironside, J.M., Langley, P.A., "Modelling and Simulation of an Automotive Powertrain Incorporating a Perbury Continuously Variable Transmission", IMech.E, C200/86, 1986.

[51] Kalberlah, A., "Electric Drive Systems for Passenger Cars and Taxis", SAE paper 910247, 1991.

[52] Kane, T.R., Levinson, D.A., "Dynamics: Theory and Applications," McGraw-Hill, New York, 1985.

[53] Kane, T.R., Likins, P.W., "Spacecraft Dynamics", McGraw-Hill, New York, 1983.

[54] Karnopp, D., "Theoretical Limitations in Active Vehicle Suspensions", Vehicle Systems Dynamics, vol. 15, pp 41-54, 1986.

[55] Karnopp, D., Margolis, D., "Adaptive Suspension Concepts for Road Vehicles", Vehicle System Dynamics, vol. 13, pp 145-160, 1984.

[56] Kickert, W.J.M., Van Nauta Lemke, H.R., "Application of a Fuzzy Controller in a Warm Water Plant", Automatica, vol. 12, pp 301-308, 1976.

[57] Kiencke,U., "The role of Automatic Control in Automotive Systems", 10th IFAC World Congress, 1987.

[58] Landman, R.G., Patil, P.B., Burba, J.C., "Control System Architecture, for an Advanced Electric Powertrain", SAE paper 871552, 1988.

[59] Langlois, R.G., Anderson, R.J., Hanna, D.M., "Implementing Preview Control on an off-Road Vehicle with Active Suspension", 12th IAVSD Symposium, Lyon, France, 1991.

[60] Lee, H.Y., Hedrick, J.K., "Dynamic Constraint Equations and Their Impact on Active Suspension Performance", 11th IAVSD Symposium, Ontario, Canada, 1989.

[61] Leiber, H., Czinczel, A., "Antiskid System for Passenger Cars with a Digital Electronic Control Unit", SAE paper 790458, 1979.

[62] Leiber, H., Czinczel, A., "Four Years Experience with 4-Wheel Antiskid Brake System (ABS)", SAE paper 830481, 1983.

[63] Lizell, M., "Semi-Active Damping", IMech.E, Intl. Conf. Advanced Suspensions, C429/88, 24-25 October 1988.

[64] Lizell, M., "Dynamic Levelling a Low Power Active Suspension With Adaptive Control", 12th IAVSD Symposium, Lyon, France, 1991.

[65] Maciejowski, J.M., "Multivariable Feedback Design", Addison-Wesley Publishing Co., 1989.

[66] Malek, K.M., Hedrick, J.K., "Decoupled Active Suspension Design for Improved Automotive Ride Quality/Handling Performance", 9th IAVSD Symposium, Switzerland, 1985.

[67] Mamdani, E.H., Assilian, S., "An Experiment in Linguistic Synthesis with a Fuzzy Logic Controller", Int. J. Man-Machine Studies, vol. 7, pp 1-13, 1975.

[68] Mamdani, E.H., Baaklini, N., "Prescriptive Method for Deriving Control Policy in a Fuzzy-Logic Controller", Electronics Letters, vol. 11 nos 25/26, pp 625-626, December 1975.

[69] Margolis, D.L., "Semi-Active Heave and Pitch Control for Ground Vehicles", Vehicle System Dynamics, 16, pp 167-192, 1982.

[70] Margolis, D.L., "The Response of Active and Semi-Active Suspensions to Realistic Feedback Signals", Vehicle System Dynamics, 11, pp 267-282, 1982.

[71] Margolis, D.L., "Semi-Active Control of Wheel Hop in Ground Vehicles", Vehicle System Dynamics, 12, pp 317-330, 1983.

[72] Margolis, D.L., Goshtasbpour, M., "The Chatter of Semi-Active On-Off Suspensions and its Cure", Vehicle System Dynamics, 13, pp 129-144, 1984.

[73] Mastinu, G., "Passive Automobile Suspension Parameter Adaptation", IMech.E, Intl. Conf. Advanced Suspensions, C425/88, 24-25 October 1988.

[74] Pro-Matlab : User's Guide - For Sun Workstations, The MathWorks Inc., 1987.

[75] Matlab : Control System Toolbox: User's Guide, The Mathworks Inc., 1986.

[76] Matlab: Multivariable Frequency Domain Toolbox: User's Guide, Cambridge Control Ltd., 1990.

[77] Meller, T., Fruhauf, F.J., "Variable Damping - Philosophy and Experiences of a Preferred System", IMech.E, Intl. Conf. Advanced Suspension, C432/88, 24-25 October 1988.

[78] Mergenthaler, M., "Exerience Using Fuzzy Logic in an Expert System for Technical Diagnosis", VW Fuzzy Logic Meeting, Wolfsburg, March 1992.

[79] Metz, D., Maddock, J., "Optimal Ride Height and Pitch Control for

Championship Race Cars", Automatica, vol. 22, no. 5, pp 509-520, 1986.

[80] Miller, L.R., "The Effect of Hardware Limitations on an On/off Semi-Active Suspension", IMech.E, Intl. Conf. Advanced Suspensions, C442/88, 24-25 October 1988.

[81] Motor, "The Works", pp 66-69, w/e 31 October, 1987.

[82] Nagai, M., "Active Four-Wheel-Steering System by Model Following Control", 11th IAVSD Symposium, Ontario, Canada, 1989.

[83] Nakaya, H., Oguchi, Y., "Characteristics of the Four-Wheel Steering Vehicle and its Future Prospects", Int. J. of Vehicle Design, vol. 8, no. 3, pp 314-324, 1987.

[84] Orlandea, N., Chace, M.A., "Simulation of a Vehicle Suspension with the ADAMS Computer Program", 1977 Intl. Automotive Eng. Congress And Exposition, Michigan, SAE paper 770053, 1977.

[85] Owens, D.H., "Feedback and Multivariable Systems", IEE Control Eng. Series 7, Peter Peregrinus Ltd, 1978.

[86] Pappis, C.P., Mamdani, E.H., "A Fuzzy Logic Controller for a Traffic Junction", IEEE Trans. on Systems Man and Cybernetics, vol. SMC-7, no. 10, October 1977.

[87] Pilbeam, C., Sharp, R.S., "Preview, Control of Limited Bandwidth Vehicle Suspension Systems", IEE Colloquium, Digest 1992/193, November 1992.

[88] Polak, P., Burton, R.T., "Improving Suspension Damping", Journal of Automotive Engineering, pp 13-17, February 1971.

[89] Poyser, J., "Development of a Computer Controlled Suspension System", Int. J. of Vehicle Design, vol. 8, no. 1, pp 74-86, 1987.

[90] Rajamani, R., Hedrick, J.K., "Semi-Active Suspensions - A Comparison Between Theory and Experiments", 12th IAVSD Symposium, Lyon, France, 1991.

[91] Rivard, J.G., "The Automobile in 1997", IEEE Spectrum, October 1987.

[92] Rosenthal, D.E., Sherman, M.A., "High Performance Multibody Simulations via Symbolic Equation Manipulation and Kane's Method", J. Astr. Sci., 34, 223-239, 1986.

[93] SAE J670e - Vehicle Dynamics Terminology, Society of Automotive Engineers, 1978.

[94] Sano, S., Furukawa, Y., Shiraishi, S., "Four-Wheel Steering System with Rear Wheel Steer Angle Controlled as a Function of Steering Angle", SAE paper 860625, 1986.

[95] Schwartz, D.G., Klir, G.J., "Fuzzy Logic Flowers in Japan", IEEE Spectrum, July 1992.

[96] SD/FAST User's Manual, version b1.1, pre-release edition, 1990.

[97] Senger, K.H., Kortum, W., "Investigations on State Observers for the Lateral Dynamics of Four-Wheel Steered Vehicles", 11th IAVSD Symposium, Ontario, Canada, 1989.

[98] Sharp, R.S., Crolla, D.A., "Road Vehicle Suspension System Design - A Review", Vehicle System Dynamics, vol. 16, pp 167-192, 1987.

[99] Sharp, R.S., Crolla, D.A., "Intelligent Suspensions for Road Vehicles - Current and Future Developments", EAEC Conf. on New Developments in Power Train and Chassis Eng., Strasbourg, 1987.

[100] Sharp, R.S., Pan, D., "On Active Roll Control for Automobiles", 12th IAVSD Symposium, Lyon, France, 1991.

[101] Sharp, R.S., Hassan, S.A., "The Relative Performance Capabilities of Passive, Active and Semi-Active Car Suspension Systems", IMech.E vol. 200, no. D3, pp 219-228, 1986.

[102] Sharp, R.S., Hassan, S.A., "Performance and Design Considerations for Dissipative Semi-Active Suspension Systems for Automobiles", IMech.E vol. 201, no. D2, pp 149-153, 1987.

[103] Shibahata, Y., Irie, N., Itoh, H., Nakamura, K., "The Development of an Experimental Four-Wheel Steering Vehicle", SAE paper 860623, 1986.

[104] Sohoni, V.N., Duchnowski, L.J., Winkelman, J.R., "Multibody Modelling of Suspension Kinematics for Control Design", American Control Conference 90, 1990.

[105] Stanway, R., Sproston, J.L., "Variable Suspension Damping Using Electro-Rheological Fluids", IMech.E Intl. Conf. Advanced Suspension Systems, C382/034, pp 547-558, 1989.

[106] Sugeno, M., "An Introductory Survey of Fuzzy Control", Information Sciences, 36, pp 59-83, 1985.

[107] Sugeno, M., "The Status of Research on Fuzzy Control and Intelligent Systems in Japan", Seminar, Queen Mary and Westfield College, October 1992.

[108] Sweet, L.M., "Control Systems for Automotive Vehicle Fuel Economy : A Literature Review", J. of Dynamic Systems Measurements and Control, vol. 103 pp 173-180, September 1981.

[109] Sweet, L.M., "Automobile Applications of Modern Control Theory", SAE paper 820913, 1982.

[110] Takiguchi, T., Yasuda, N., Furutani, S., Kanazawa, H., Inoue, H.,

"Improvement of Vehicle Dynamics of Vehicle Speed Sensing Four-Wheel Steering System", SAE paper 860624, 1986.

[111] Thompson, A.G., "Optimum Damping in a Randomly Excited Non-Linear Suspension", IMech.E Intl. Conf., vol. 184, pt. 2A, no. 8, pp 169-178, 1969/70.

[112] Tong, R.M., "A Control Engineering Review of Fuzzy Systems", Automatica, vol. 13, pp 559-569, 1977.

[113] Toyoda, T., Inoue, T., MItsuda, T.,Aoki, K., Yaegashi, T., "Some of the New Control Strategies for Electronic Engine Control Systems", IMech.E, C170/81, 1981.

[114] Truscott, A.J., Wellstead, P.E., "Composite Active Suspension for Automotive Vehicles", IEE Colloquium, Digest 1992/193, November 1992.

[115] Wilson, D.A., Sharp, R.S., Hassan, S.A., "The Application of Linear Optimal Control Theory to the Design of Active Automotive Suspension", Vehicle System Dynamics, vol. 15, pp 105-118, 1986.

[116] Wright, P.G., Williams, D.A., "The Application of Active Suspension to High Performance Road Vehicles", IMech.E, C239/84, 1984.

[117] Yamamoto, M., Harada, H., Matsuo, Y., "A Study on Active Controlled Chassis System for Vehicle Dynamics", 11th IAVSD Symposium, Ontario, Canada, 1989.

[118] Zadeh, L.A., "Fuzzy Sets", Information and Control, 8, pp 338-353, 1965.

[119] Zadeh, L.A., "Fuzzy Algorithms", Information and Control, 12, pp 94-102, 1968.

[120] Zadeh, L.A., "Outline of a New Approach to the Analysis of Complex Systems and Decision Processes", IEE Trans. Systems Man and Cybernetics, SMC-3, pp 28-44, 1973.

# An Investigation of Multibody System Modelling and Control Analysis Techniques for the Development of Advanced Suspension Systems in Passenger Cars

in Two Volumes

Volume 2

**by**

**Ann Susan Cherry**

*A thesis submitted for the degree of Doctor of Philosophy*

*Engineering Department*

*University of Warwick*

*Rover Group Advanced Technology Centre*

*December 1992*

# List of Tables

# List of Figures

# Appendix A : Rule-Base Controller

The rule-based controller applied to the discretely variable damping system studied in this thesis was based on a prototype system developed at Rover. The complete control algorithm was very complex and covered a large selection of measured controller inputs, including both vehicle response parameters and driver inputs. For the study described in chapter five, a simplification of the discretely variable damping system was used with part of the rule-based controller. In this way a typical heuristic rule-based control algorithm was illustrated in a comparative study between other types of control strategy for variable damping systems. The details of the simplifications and the section of the controller used are detailed in this appendix.

The original prototype discretely variable damping system involved the use of switchable dampers with three fixed rate settings to replace the conventional passive dampers. A variety of sensors were then used to measure the vehicle response parameters and driver inputs providing the required controller inputs. These measurements included the sprung mass acceleration in the vertical and lateral directions, and driver inputs relating to braking, accelerating and steering manoeuvres. These measured control inputs were then processed and compared with a separate set of rules for each of a range of vehicle modes, including roll, ride, squat and dive. The required damper rate setting was then selected by a combination of the rule outputs.

The discretely variable damping system with a heuristic rule-based controller used in the study described in chapter five, was based on this prototype system with some simplifications. Firstly the variable rate dampers

used had two fixed rate settings, and the model included a simplified primary ride filter model for the sprung mass acceleration measurements only. The control strategy applied to this system involved two of the modes, namely roll and ride. The controller timings such as sample rate and calculation times were approximated for the study in order to represent a typical yet realistic system.

These simplifications were performed in order to present a typical yet simple rule-based controller for the comparative study of discretely variable damping control strategies.

The section of the control strategy used in the study, as mentioned, was based on the ride and roll modes of the original system. The rules therefore related to the measured controller inputs for sprung mass vertical and lateral accelerations, and steering wheel angle and rate.

The algorithm relating to the measured steering rate, ***SRATE***, lateral and vertical sprung mass accelerations, ***LATACC, VACC***, are illustrated by the flow diagrams given in figures A.1-A.3. The steering angle input is used to calculate an approximate measure of the lateral acceleration of the sprung mass before the vehicle response can be measured, by

$$LATACC = rv^2 \tag{A.1}$$

where $v$ is the vehicle speed and $r$ is the radius of turning circle with values given in table A.1. This calculated lateral acceleration is then processed by the same algorithm as the measured value, as illustrated by the flow diagram in figure A.2.

These flow charts show that the rule-based controller was essentially a threshold comparator for all the inputs, with minor variations for each. The

thresholds are all vehicle speed dependent, with added direction dependency for the vertical acceleration input, as seen in table A.2. For the steering rate mode, a time delay is incorporated before resetting the damper rate to soft once the input value has fallen below the threshold, as shown in figure A.1. A similar time delay is also involved in the vertical acceleration control algorithm given in figure A.3, and the values used for these time delays are given in table A.3. The use of these delays avoids unnecessary frequent or premature damper switching, by ensuring the body motion has been adequately controlled before resetting the damper rate to soft. This is an important addition for vehicle stability and safety as well as for the reduction of noise. For both lateral acceleration inputs, measured and calculated, hysteresis is included in the switching strategy, as opposed to a pure time delay. This is illustrated in figure A.2 and the hysteresis value used in included in table A.3. In this way the complete control of sprung mass roll behaviour is ensured before resetting the soft damper rate, again for stability and safety reasons.

| STANG (Deg) | 22 | 45 | 67 | 90 | 112 | 135 |
|---|---|---|---|---|---|---|
| r (m) | 108 | 53 | 36 | 26 | 21 | 18 |
| | | | | | | |
| STANG (Deg) | 157 | 180 | 300 | 400 | 500 | 630 |
| r (m) | 15 | 13 | 8 | 6.5 | 5.5 | 5 |

Table A.1 : Turning Circles

| Speed (mph) | SRATE (Deg/s) | LATACC ($m/s^2$) | Pos. VACC ($m/s^2$) | Neg. VACC ($m/s^2$) |
|---|---|---|---|---|
| 0 | - | - | 1.962 | 1.962 |
| 20 | 20 | 7.848 | 1.962 | 1.962 |
| 40 | 9 | 5.886 | 1.962 | 2.5506 |
| 60 | 5 | 4.4145 | 3.4335 | 2.5506 |
| 80 | 4 | 34.4145 | 3.4335 | 2.5506 |
| 100 | 4 | 3.924 | 3.4335 | 2.5506 |
| 120 | 3 | 3.4335 | 1.962 | 1.962 |
| 140 | 3 | 2.943 | 1.6677 | 1.1772 |
| 160 | 3 | 2.943 | 1.4715 | 0.981 |
| 200 | - | - | 1.4715 | 0.981 |

Table A.2 : Thresholds

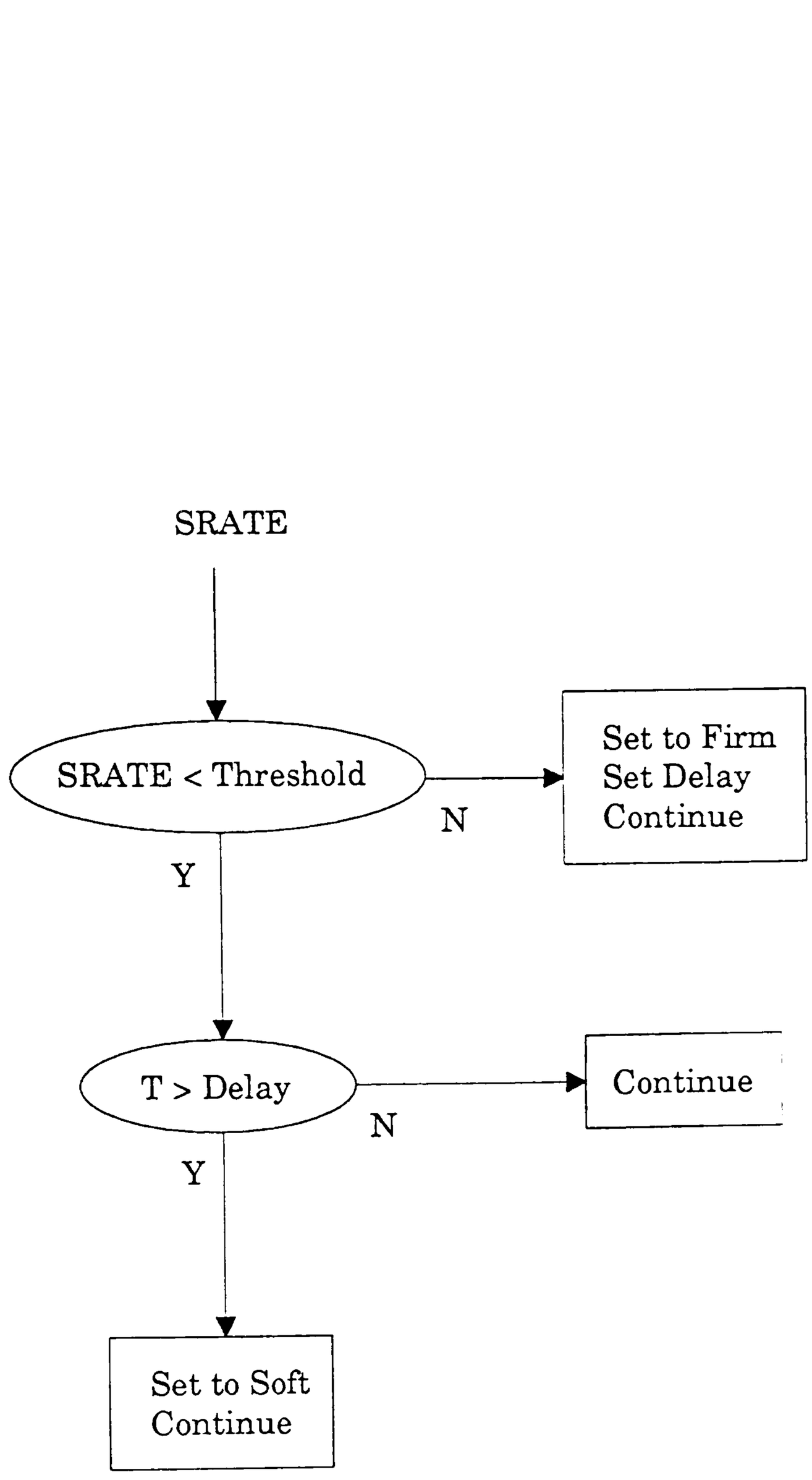


Figure A.1 : Steering Rate Algorithm

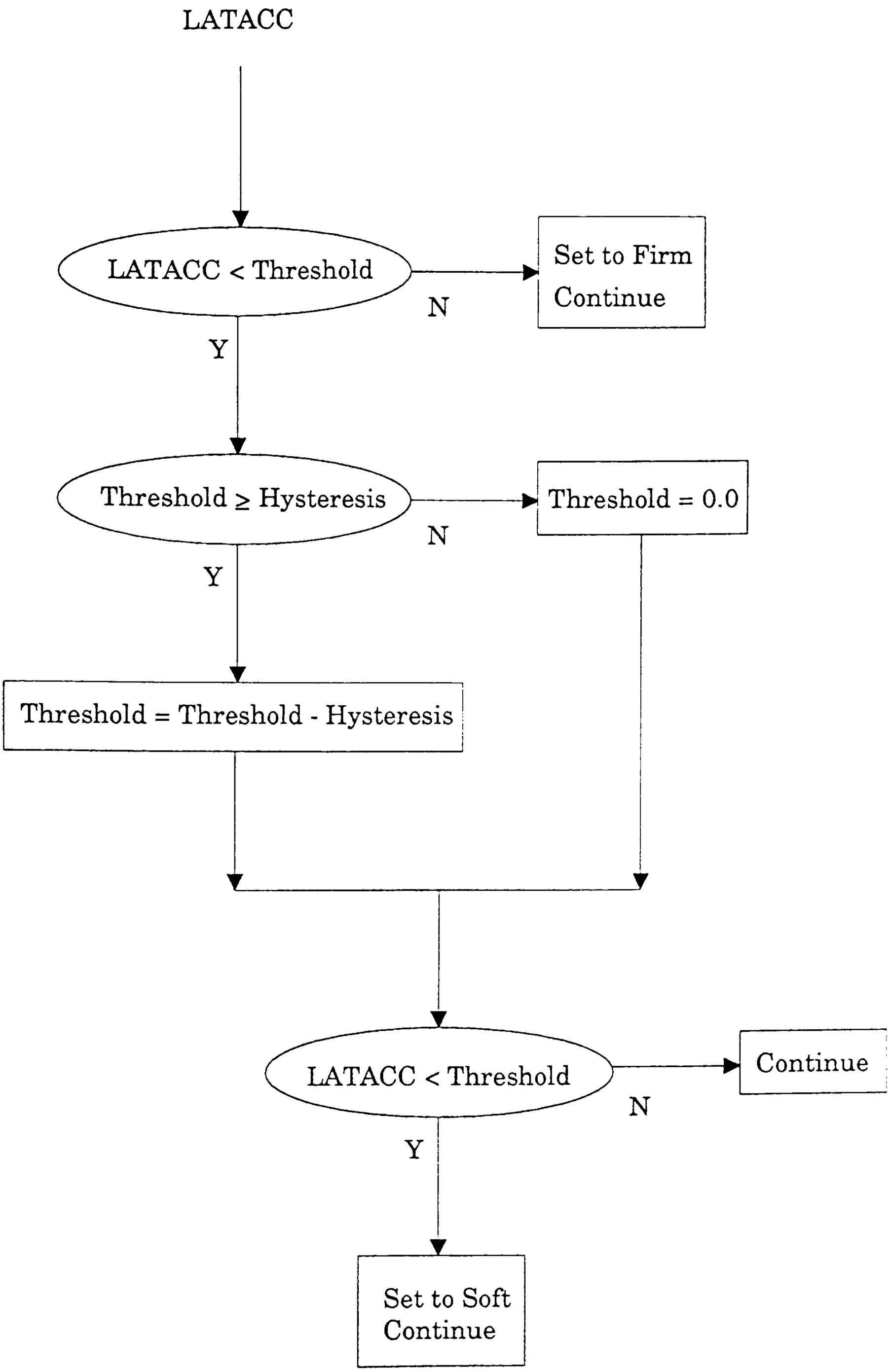


Figure A.2 : Lateral Acceleration Algorithm

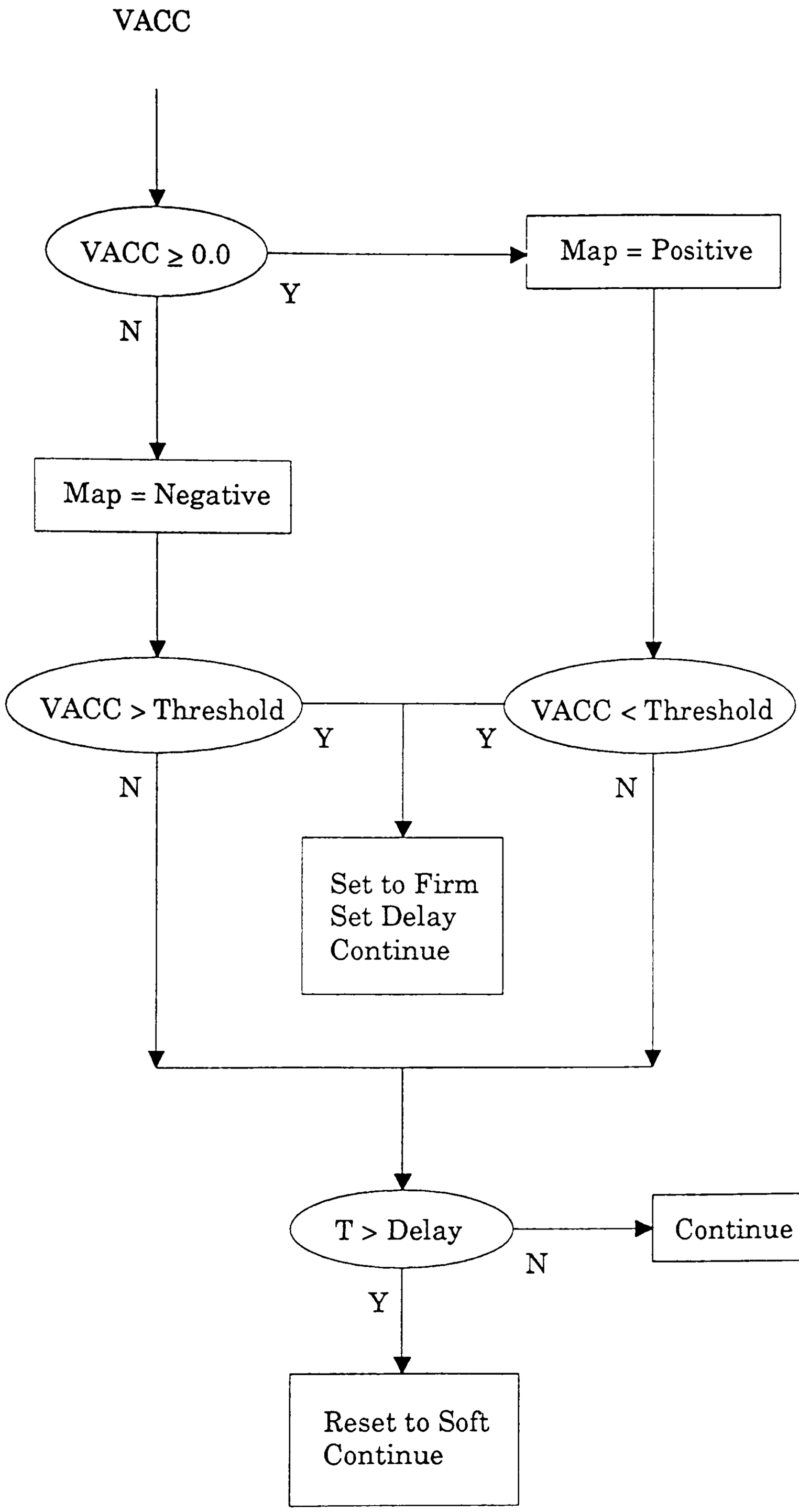


Figure A.3 : Vertical Acceleration Algorithm